

Targeting the SRC/JAK/STAT3 signalling pathway: A novel and promising therapeutic strategy for pancreatic cancer

Author:

Parkin, Ashleigh

Publication Date:

2019

DOI:

<https://doi.org/10.26190/unsworks/2097>

License:

<https://creativecommons.org/licenses/by-nc-nd/3.0/au/>

Link to license to see what you are allowed to do with this resource.

Downloaded from <http://hdl.handle.net/1959.4/65564> in <https://unsworks.unsw.edu.au> on 2024-04-19

Targeting the SRC/JAK/STAT3 signalling pathway: A novel and promising therapeutic strategy for pancreatic cancer

Ashleigh Louise Parkin

A thesis in fulfilment of the requirements for the degree of
Doctor of Philosophy



UNSW
SYDNEY

St Vincent's Clinical School

Faculty of Medicine

November 2019

Thesis/Dissertation Sheet

Surname/Family Name	: Parkin
Given Name/s	: Ashleigh Louise
Abbreviation for degree as give in the University calendar	: PhD
Faculty	: Medicine
School	: St Vincent's Clinical School
Thesis Title	: Targeting the SRC/JAK/STAT3 signalling pathway: A novel and promising therapeutic strategy for pancreatic cancer

Abstract 350 words maximum:

Pancreatic cancer has a 5-year survival of only 8%, and persists as the 4th most common cause of cancer-related death in Western societies. A more tailored treatment approach may be beneficial as the current standard-of-care therapies offer only a modest increase in overall patient survival. Recent large-scale genomic studies have revealed that the SRC/JAK/STAT3 signalling pathway is deregulated in up to 35% of pancreatic cancers, and is yet to be systematically examined in this disease. Consequently, we hypothesized that targeting pancreatic tumours with alterations in the SRC/JAK/STAT3 signalling pathway with JAK and SRC inhibitors represents a promising novel therapeutic strategy for this disease.

In this thesis, we use well-annotated patient-derived cell-line models (ICGC), along with cell-lines generated from the aggressive KPC mouse model, to show that the combination of selected JAK and SRC inhibitors is synergistic in cell lines characterized by high phospho-STAT3 expression and P53 mutations. Using 3D *in vitro* models, including organotypic and organoid models, we show that this therapeutic strategy inhibits the invasive and proliferative capacity of tumour cells, disrupts collagen remodelling and extracellular matrix integrity, interferes with paracrine signalling and has strong immunomodulatory effects. Lastly, we examine the *in vivo* efficacy of SRC and JAK inhibitors using a syngeneic KPC mouse model, as well as patient-derived pancreatic tumour models, characterised by high phospho-STAT3 expression and P53 mutations. From these studies we demonstrate that the combination of SRC and JAK-inhibitors significantly inhibited tumour progression, improved survival, delayed the development of metastasis and significantly improved response to standard of care chemotherapy. Furthermore, tumours treated with SRC and JAK-inhibitors displayed decreased collagen deposition and remodelling, and altered immune cell infiltration.

Our findings demonstrate the potential for tailored therapeutic strategies involving SRC/JAK/STAT3 inhibition in pancreatic cancer, and suggest that therapeutic efficacy may be the result of targeting both tumour cells and the tumour microenvironment, by decreasing fibrosis and overcoming tumour-induced immunosuppression.

Declaration relating to disposition of project thesis/dissertation

I hereby grant to the University of New South Wales or its agents the right to archive and to make available my thesis or dissertation in whole or in part in the University libraries in all forms of media, now or here after known, subject to the provisions of the Copyright Act 1968. I retain all property rights, such as patent rights. I also retain the right to use in future works (such as articles or books) all or part of this thesis or dissertation.

I also authorise University Microfilms to use the 350 word abstract of my thesis in Dissertation Abstracts International (this is applicable to doctoral theses only).

Signature	Witness Signature	Date
-----------	-------------------	------

The University recognises that there may be exceptional circumstances requiring restrictions on copying or conditions on use. Requests for restriction for a period of up to 2 years must be made in writing. Requests for a longer period of restriction may be considered in exceptional circumstances and require the approval of the Dean of Graduate Research.

FOR OFFICE USE ONLY Date of completion of requirements for Award:

ORIGINALITY STATEMENT

'I hereby declare that this submission is my own work and to the best of my knowledge it contains no materials previously published or written by another person, or substantial proportions of material which have been accepted for the award of any other degree or diploma at UNSW or any other educational institution, except where due acknowledgement is made in the thesis. Any contribution made to the research by others, with whom I have worked at UNSW or elsewhere, is explicitly acknowledged in the thesis. I also declare that the intellectual content of this thesis is the product of my own work, except to the extent that assistance from others in the project's design and conception or in style, presentation and linguistic expression is acknowledged.'

Signed

Date

COPYRIGHT STATEMENT

'I hereby grant the University of New South Wales or its agents the right to archive and to make available my thesis or dissertation in whole or part in the University libraries in all forms of media, now or here after known, subject to the provisions of the Copyright Act 1968. I retain all proprietary rights, such as patent rights. I also retain the right to use in future works (such as articles or books) all or part of this thesis or dissertation.

I also authorise University Microfilms to use the 350 word abstract of my thesis in Dissertation Abstract International (this is applicable to doctoral theses only).

I have either used no substantial portions of copyright material in my thesis or I have obtained permission to use copyright material; where permission has not been granted I have applied/will apply for a partial restriction of the digital copy of my thesis or dissertation.'

Signed

Date

AUTHENTICITY STATEMENT

'I certify that the Library deposit digital copy is a direct equivalent of the final officially approved version of my thesis. No emendation of content has occurred and if there are any minor variations in formatting, they are the result of the conversion to digital format.'

Signed

Date

INCLUSION OF PUBLICATIONS STATEMENT

UNSW is supportive of candidates publishing their research results during their candidature as detailed in the UNSW Thesis Examination Procedure.

Publications can be used in their thesis in lieu of a Chapter if:

- The student contributed greater than 50% of the content in the publication and is the "primary author", ie. the student was responsible primarily for the planning, execution and preparation of the work for publication
- The student has approval to include the publication in their thesis in lieu of a Chapter from their supervisor and Postgraduate Coordinator.
- The publication is not subject to any obligations or contractual agreements with a third party that would constrain its inclusion in the thesis

Please indicate whether this thesis contains published material or not.

☐

This thesis contains no publications, either published or submitted for publication

☒

Some of the work described in this thesis has been published and it has been documented in the relevant Chapters with acknowledgement

☐

This thesis has publications (either published or submitted for publication) incorporated into it in lieu of a chapter and the details are presented below

CANDIDATE'S DECLARATION

I declare that:

- I have complied with the Thesis Examination Procedure
- where I have used a publication in lieu of a Chapter, the listed publication(s) below meet(s) the requirements to be included in the thesis.

Name	Signature	Date (11/10/19)
-------------	------------------	------------------------

Parkin, A., et al., *The Evolving Understanding of the Molecular and Therapeutic Landscape of Pancreatic Ductal Adenocarcinoma*. Diseases, 2018. 6(4).

Parkin, A., et al., *Targeting the complexity of Src signalling in the tumour microenvironment of pancreatic cancer: from mechanism to therapy*. The FEBS Journal, 2019. 0(ja).

Acknowledgements

If I were to properly thank every individual who has helped me throughout this PhD journey my acknowledgements section would be longer than the thesis itself, so I will attempt to keep this section as brief as possible.

Firstly I would like to thank my incredible supervisor Dr (and as of 2020, Associate Professor) Marina Pajic. Marina I don't know how I can ever thank you enough for all you have done for me over the past 3.5 years. Thank you for taking a chance on me, and for inviting me into your lab with open arms. Thank you for believing in me, and for encouraging me to always do better and try harder. Thank you for inspiring me, and for igniting my passion for medical research. Thank you for your continued support, care, kindness and understanding. Despite me having to overcome several personal hurdles you never gave up on me, and it is because of you that I never gave up on myself. Thank you for giving me every opportunity to grow and succeed, and lastly, thanks for the memories. I truly consider you more of a friend than a boss, and I am extremely grateful for that friendship. You will always be a *insert Marina's favourite word* legend in my eyes, and I think we make a pretty amazing team.

I would also like to thank my co-supervisor Associate Professor Paul Timpson who provided essential scientific guidance. As well as members of Paul's lab particularly Kendelle Murphy, who taught me many of the techniques used in this thesis. Kendelle you were always available to answer my questions and get me out of trouble in the microscope facility. You are a wealth of knowledge, and also a great shoulder to cry on, and I couldn't imagine going through this journey without you.

Next I would like to thank past and present members of team 'CMP' whom without this project would not have been possible. I particularly need to thank Danielle, Nick, Jen, Payam, Sean and Julia who played a huge role in helping me to generate some of the data for this project and for proof-reading this thesis. I will forever be grateful for the efforts you have put into helping me with this project, and I also thank you for making this experience so much more entertaining. I look forward to continuing our work together.

I also wish to thank Sydney Catalyst for supporting my research by awarding me a top-up research scholarship and a travel award. As well as all our collaborators and funding bodies who have helped make this research possible.

I would like to thank my parents, who have loved, cared and supported me since the very beginning. Mum and Dad I am so grateful for all the love and support you have given me throughout my whole life. You have been my biggest fans and have always encouraged me to do my best and to dream big. You have given me the confidence to believe in myself and to never give up. Honestly you are the reason I am the woman I am today, and I will forever be proud to call myself your daughter. I love you Mum and Dad, to the moon and back times infinity.

This next thank you may seem bizarre, but I truly believe that pets are important companions that often go underappreciated. Thank you to my beautiful puppies Willow and Benson who showered me with sloppy kisses after a long day in the lab, who sat silently and listened while I practiced my presentations, and who kept my lap warm while I typed this thesis. Also thank you Benson for attempting to edit my thesis by slapping your paws on my keyboard.

Lastly I need to thank my amazing husband Tom, who is the reason why I am still sane after writing this thesis. My PhD journey was not your typical PhD experience; it also included getting married, buying land and building a house, and all of that would not have been possible without my incredible husband. Tom I couldn't imagine going through this experience with anyone else but you. You brightened my darkest of days and always knew how to make me smile. Thank you for supporting and caring for me in the most difficult of times. Thank you for believing in me and for encouraging me to achieve my goals and to never give up. Thank you for making me cups of tea whilst I was writing this thesis (and sorry for eating all the biscuits). And lastly, thank you for reminding me to smile, laugh and enjoy the little things in life. I love you forever and always.

Publications arising from PhD studies

Campbell H, *et al.* (**Parkin A mid author**). Δ 133p53 isoform promotes tumour invasion and metastasis via interleukin-6 activation of JAK-STAT and RhoA-ROCK signalling. *Nature Comms* (2017).

Chou A, *et al.* (**Parkin A mid author**). A Tailored first-line and second-line CDK4-targeting treatment combinations in mouse models of pancreatic cancer. *Gut* (2018).

Parkin A, Man J., Chou A., Nagrial A., Samra J., Gill A., Timpson P., Pajic M. The evolving understanding of the molecular and treatment landscape of pancreatic ductal adenocarcinoma. *Diseases* (2018).

Parkin A., Man J., Timpson P., Pajic M. Targeting the complexity of integrin-regulated Src signalling in the tumour microenvironment of pancreatic cancer: from mechanism to therapy. *FEBS Journal* (2019).

Wang K, *et al.* (**Parkin A mid author**) Man J, Baldwin G, Nikfarjam M, He H. PAK inhibition by PF-3758309 enhanced the sensitivity of multiple chemotherapeutic reagents in patient-derived pancreatic cancer cell lines. *Am J Transl Res* (2019).

Vennin C, *et al.* (**Parkin A mid author**). CAF hierarchy driven by pancreatic cancer cell p53-status creates a pro-metastatic and chemoresistant environment via perlecan. *Nat Commun.* (2019).

Castillo L *et al.* (**Parkin A mid author**). MCL-1 antagonism enhances the anti-invasive effects of Dasatinib in pancreatic adenocarcinoma. *Oncogene* (2019).

Lau, M., Ghazanfar, S., **Parkin, A.**, Chou, A., Kuong, T., Yang, J., Pajic, M., Neely, G. Systematic functional identification of cancer multi-drug resistance genes. (Under Review).

Molloy TJ...Parkin A... *et al.* Generation of novel *in vivo* models of acquired chemoresistance provides means for effective targeting of specific pancreatic cancer subtypes. (Manuscript in progress).

Parkin A et al. Integrating tumour microenvironment with cancer molecular signatures to develop a novel targeted therapeutic approach for pancreatic cancer. (Manuscript in progress).

Presentations

The work in this thesis has been presented at the following conferences:

Parkin A, Froio D, Stark R, Drury A, Steinmann A, Timpson P, Pajic M. Examining pancreatic tumours with activated Src/JAK/STAT-3 signalling as a novel and targetable tumour subtype. Sydney Catalyst Post Graduate and Early Career Researcher Symposium (Sydney), April 2016.

- Winner of best 3 minute pet project presentation

Parkin A, Froio D, Stark R, Drury A, Steinmann A, Timpson P, Pajic M. Targeting the Src/JAK/STAT3 signalling pathway: A novel and promising therapeutic strategy for pancreatic cancer. CSTI- Signalling Symposium (Mornington Peninsula, Victoria), May 2017.

- Winner of EMBL best poster prize

Parkin A, Froio D, Stark R, Drury A, Murphy K, Steinmann A, Gill A, Timpson P, Pajic M. Targeting the Src/JAK/STAT3 signalling pathway: A novel and promising therapeutic strategy for pancreatic cancer. Sydney Catalyst International Symposium (Sydney), 2017.

Parkin A, Froio D, Stark R, Drury A, Steinmann A, Man J, Gill A, Timpson P, Pajic M. Targeting the Src/JAK/STAT3 signalling pathway: A novel and promising therapeutic strategy for pancreatic cancer. AACR/EACR Special Conference (Florence, Italy), June 2017.

Parkin A, Froio D, Stark R, Vogel N, Drury A, Steinmann A, Man J, Timpson P, Pajic M. Pancreatic tumours with activated Src/JAK/STAT-3 signalling are a novel and targetable tumour subtype that are yet to be examined. Sydney Catalyst Post-Graduate Researcher Symposium (Sydney), 2017.

- Winner of best T1/T2 talk

Parkin A, Froio D, Stark R, Vogel N, Drury A, Steinmann A, Timpson P, Pajic M. Dual inhibition of JAK and Src: A novel and promising therapeutic combination for pancreatic cancer . EMBL PhD Symposium (Garvan Institute-Sydney), 2017.

Parkin A, Froio D, Vogel N, Man J, Murphy K, Timpson P, Pajic M. Dual inhibition of JAK and Src: A novel and promising therapeutic combination for pancreatic cancer. Lorne Cancer Conference (Lorne, Victoria), 2018.

- Winner of best poster prize

Parkin A, Froio D, Vogel N, Man J, Murphy K, Timpson P, Pajic M. Dual inhibition of JAK and Src: A novel and promising therapeutic combination for pancreatic cancer . EACR25 (Amsterdam, Netherlands), 2018.

Parkin A, Froio D, Vogel N, Man J, Murphy K, Timpson P, Pajic M. Targeting the Src/JAK/STAT3 signalling pathway: A novel and promising therapeutic strategy for pancreatic cancer. Australasian Pancreatic Club (APC) and ASPAN Annual Scientific and Medical Meeting (Brisbane), August 2018.

Parkin A, Froio D, Vogel N, Man J, Murphy K, Timpson P, Pajic M. Dual inhibition of JAK and Src: A novel and promising therapeutic combination for pancreatic cancer . Sydney Cancer Conference (Sydney, Australia), October 2018.

- Best abstract

Parkin A, Froio D, Vogel N, Man J, Murphy K, Timpson P, Pajic M. Dual inhibition of JAK and Src in pancreatic cancer: A novel and synergistic combination to target the tumour and its microenvironment. CSTI- Signalling Symposium (Mornington Peninsula, Victoria), May 2019.

- Winner of FEBS best poster prize

Parkin A, Froio D, Vogel N, Man J, Murphy K, Timpson P, Pajic M. Dual inhibition of JAK and Src in pancreatic cancer: A novel and synergistic combination to target the tumour and its microenvironment. ASMR NSW 27th Annual Scientific Meeting (Sydney), May 2019.

Abstract

Pancreatic cancer has a 5-year survival of only 8%, and persists as the 4th most common cause of cancer-related death in Western societies. A more tailored treatment approach may be beneficial as the current standard-of-care therapies offer only a modest increase in overall patient survival. Recent large-scale genomic studies have revealed that the SRC/JAK/STAT3 signalling pathway is deregulated in up to 35% of pancreatic cancers, and is yet to be systematically examined in this disease. Consequently, we hypothesised that targeting pancreatic tumours with alterations in the SRC/JAK/STAT3 signalling pathway with JAK and SRC inhibitors represents a promising novel therapeutic strategy for this disease.

In this thesis, we use well-annotated patient-derived cell-line models (ICGC), along with cell-lines generated from the aggressive KPC mouse model, to show that the combination of selected JAK and SRC inhibitors is synergistic in cell lines characterised by high phospho-STAT3 expression and P53 mutations. Using 3D *in vitro* models, including organotypic and organoid models, we show that this therapeutic strategy inhibits the invasive and proliferative capacity of tumour cells, disrupts collagen remodelling and extracellular matrix integrity, interferes with paracrine signalling and has strong immunomodulatory effects. Lastly, we examine the *in vivo* efficacy of dasatinib and ruxolitinib using a syngeneic KPC mouse model, as well as patient-derived pancreatic tumour models, characterised by high phospho-STAT3 expression and P53 mutations. From these studies we demonstrate that the combination of dasatinib and ruxolitinib significantly inhibited tumour progression, improved survival, delayed the development of metastasis and significantly improved response to standard of care chemotherapy. Furthermore, tumours treated with dasatinib and ruxolitinib displayed decreased collagen deposition and remodelling, and altered immune cell infiltration in the syngeneic setting.

Our findings demonstrate the potential for tailored therapeutic strategies involving SRC/JAK/STAT3 inhibition in pancreatic cancer, and suggest that therapeutic efficacy may be the result of targeting both tumour cells and the

tumour microenvironment, by decreasing fibrosis and overcoming tumour-induced immunosuppression.

Table of Contents

Acknowledgements	6
Publications arising from PhD studies	8
Presentations	9
Abstract.....	11
List of figures and tables.....	17
List of abbreviations	23
Chapter 1. Introduction.....	26
1.1 The molecular and treatment landscape of pancreatic ductal adenocarcinoma.....	27
1.1.1 Clinical presentation.....	27
1.1.2 Clinico-pathological staging of PDAC	28
1.1.3 Current treatment approaches for operable PDAC	28
1.1.4 Current treatment approaches for advanced PDAC	29
1.1.5 The “omic” diversity of PDAC.....	30
1.1.6 Targeting KRAS	34
1.1.7 G1/S checkpoint as a therapeutic target	35
1.1.8 Targeting DNA damage repair signalling	37
1.1.9 Mismatch repair deficiency.....	39
1.2 The tumour microenvironment of pancreatic cancer	40
1.2.1 Stromal reaction and the extracellular matrix.....	40
1.2.2 The immunosuppressive tumour microenvironment	44
1.2.2.1 Regulatory T cells (T regs).....	46
1.2.2.2 Effector T cells	46
1.2.2.3 Myeloid derived suppressor cells (MDSCs)	46
1.2.2.4 Tumour-associated macrophages (TAMs).....	47
1.2.2.5 Natural killer cells (NK Cells).....	47
1.3 SRC signalling in the tumour microenvironment of pancreatic cancer: from mechanisms to therapy	48
1.3.1 The SRC signalling axis promotes pancreatic cancer progression.....	48
1.3.2 Molecular and genomic aberrations of the SRC signalling axis in Pancreatic Cancer: Implications for therapeutic targeting.....	53
1.3.3 Targeting SRC kinase in pancreatic cancer	56
1.3.4 Modulation of the upstream and downstream SRC-signalling components in pancreatic cancer	63
1.4 JAK/STAT3 signalling in the tumour microenvironment of pancreatic cancer: from mechanisms to therapy	76

1.4.1 JAK/STAT3 signalling promotes pancreatic cancer progression	76
1.4.2 Molecular and genomic alterations of the JAK/STAT3 signalling axis ..	81
1.4.3 Targeting JAK/STAT3 signalling in pancreatic cancer	85
1.4.4 Future perspectives.....	97
Chapter 2. Materials and Methods.....	98
2.1 Tissue culture	98
2.2 Cell lines.....	98
2.3 Cytotoxic drugs and reagents	101
2.4 Proliferation assay (alamarBlue® Cytotoxicity Assay)	101
2.5 Drug synergy screens	102
2.6 Protein isolation and western blot analysis	102
2.7 Generation of stable cell lines expressing GFP-luciferase biosensor	105
2.8 Organotypic assays.....	105
2.9 SHG imaging and analysis.....	106
2.10 Organoid cultures.....	106
2.10.1 Co-culture organoids.....	107
2.10.2 Analysis of cytokine production.....	108
2.10.3 Fixation of organoids.....	108
2.10.4 Single cell sequencing of organoid co-cultures.....	108
2.11 Immunohistochemical and Immunofluorescence staining.....	110
2.12 Picrosirius red staining, polarised light microscopy and analysis.....	112
2.13 Quantification of immunohistochemical and immunofluorescence stains	112
2.13.1 Quantification of various stains on whole tumour sections	112
2.13.2 Quantification of pSTAT3 (Tyr705) on patient-derived xenografts (PDX) tumour microarrays	113
2.14 Animals	113
2.15 Orthotopic injection of cancer cells	113
2.16 <i>In vivo</i> therapeutic studies.....	114
2.17 Whole body IVIS spectrum imaging	117
2.18 Statistical analyses.....	118
Chapter 3. Efficacy of JAK1/2 and SRC inhibitors in two-dimensional <i>in vitro</i> models of pancreatic cancer.....	119
3.1 Introduction	119
3.2 Results	122
3.2.1 SRC/JAK/STAT3 pathway alterations in pancreatic cancer.....	122

3.2.2 Sensitivity of pancreatic cancer cell lines to JAK and SRC inhibitors .	128
3.2.3 Identification of potential biomarkers of <i>in vitro</i> response to ruxolitinib and dasatinib monotherapies	130
3.2.4 Assessing the efficacy of the combined inhibition of JAK and SRC in two-dimensional screens.....	136
3.2.5 Identification of potential biomarkers of <i>in vitro</i> response to the combination of dasatinib and ruxolitinib	138
3.2.6 Assessing SRC/JAK/STAT3 pathway modulation following treatment with dasatinib and ruxolitinib	141
3.3 Discussion	146
Chapter 4. <i>In vitro</i> efficacy of SRC and JAK1/2 inhibitors in 3D models of pancreatic cancer.....	150
4.1 Introduction	150
4.2 Results	154
4.2.1 Assessing the effect of SRC and JAK inhibition on the extracellular matrix in 3D collagen matrices	154
4.2.2 Assessing the anti-invasive potential of the combined inhibition of SRC and JAK in three-dimensional organotypic assays	165
4.2.3 Examining the effect of dasatinib and ruxolitinib treatment on inter-cellular signalling in three-dimensional co-culture organoids.....	177
4.2.4 Identifying transcriptional signatures associated with dasatinib and ruxolitinib treatment in three-dimensional co-culture organoids.....	188
4.2.4.1 Characterising the cellular composition of KPC co-culture organoids using single-cell transcriptomics	188
4.2.4.2 Identifying molecular mechanisms associated with dasatinib and ruxolitinib treatment in KPC organoids using single cell transcriptomics.	198
4.3 Discussion	210
Chapter 5. <i>In vivo</i> efficacy of dasatinib and ruxolitinib in models of pancreatic cancer.....	221
5.1 Introduction	221
5.2 Results	224
5.2.1 Expression of phospho-STAT3 (Tyr705) in selected patient-derived xenograft and KPC models of pancreatic cancer	224
5.2.2 Efficacy of dual dasatinib and ruxolitinib treatment in the immunocompetent (syngeneic) KPC orthotopic model of pancreatic cancer	227
5.2.2.1 Effect of dasatinib and ruxolitinib treatment on tumour growth and metastasis	227
5.2.2.2 Effects of dasatinib and ruxolitinib treatment on cellular proliferation and apoptosis in KPC tumours.....	230

5.2.2.3 Effect of dasatinib and ruxolitinib treatment on regulating pancreatic stellate cell activation <i>in vivo</i>	233
5.2.2.4 Effects of dasatinib and ruxolitinib treatment on remodelling the fibrotic tumour microenvironment.	235
5.2.2.5 Effects of dual SRC/JAK targeting on altering the immunosuppressive tumour microenvironment	238
5.2.2.6 Effect of dasatinib and ruxolitinib treatment on prolonging survival in the highly aggressive and metastatic syngeneic KPC model of pancreatic cancer	241
5.2.3 Efficacy of dual dasatinib and ruxolitinib treatment in immunocompromised, patient-derived, orthotopic models of pancreatic cancer	243
5.2.3.1 Effect of dasatinib and ruxolitinib treatment on tumour growth and metastasis	243
5.2.3.2 Effect of dasatinib and ruxolitinib treatment on cellular proliferation and apoptosis, in patient-derived models of pancreatic cancer	249
5.2.3.3 Effect of dasatinib and ruxolitinib treatment on regulating pancreatic stellate cell activation in patient-derived models of pancreatic cancer.....	252
5.2.3.4 Effects of dasatinib and ruxolitinib treatment on remodelling the fibrotic tumour microenvironment	255
5.2.3.5 Effect of dasatinib and ruxolitinib treatment on prolonging survival in metastatic patient-derived models of pancreatic cancer	258
5.3 Discussion.....	261
Chapter 6. General discussion	265
6.1 Limitations and future studies	268
Appendix.....	273
References.....	282

List of figures and tables

Figure 1.1 Frequently altered signalling pathways that drive pancreatic cancer progression

Figure 1.2 The primary pancreatic tumour microenvironment

Figure 1.3 A model of innate and adaptive immune response during pancreatic tumour progression taken from Wormann *et al.* 2014

Figure 1.4 Schematic of the canonical Integrin/SRC/FAK signalling network

Figure 1.5 Frequency of Integrin, SRC, FAK and PI3K/AKT pathway genetic alterations in publically-available pancreatic cancer genomics datasets

Table 1.1 Clinical trials in pancreatic cancer associated with targeting SRC kinase.

Table 1.2 Clinical trials in pancreatic cancer associated with targeting downstream mediators and interacting partners of SRC kinase

Figure 1.6 Schematic of the JAK/STAT3 signalling pathway

Table 1.3 Downstream effectors of STAT3 reported in pancreatic cancer

Figure 1.7 Frequency of IL-6/JAK/STAT3 genetic alterations in publically-available pancreatic cancer genomics datasets

Table 1.4 Clinical trials in pancreatic cancer associated with targeting STAT3

Table 1.5 Clinical trials in pancreatic cancer associated with targeting IL-6

Figure 1.8 Inhibitors of the IL-6/JAK/STAT3 signalling pathway, taken from Johnson *et al.* 2018

Table 1.6 Clinical trials in pancreatic cancer associated with targeting JAKs

Table 2.1 Pancreatic patient-derived cell lines and their growth conditions

Table 2.2 RPMI media recipe

Table 2.3 HPACmod media recipe

Table 2.4 IMDMrich media recipe

Table 2.5 M199/F12 media recipe

Table 2.6 List of antibodies and associated protocols for western blotting

Table 2.7 Organoid culture media recipe

Table 2.8 Antibody details for immunohistochemistry

Table 2.9 Antibody details for immunofluorescence

Figure 2.1 Preclinical testing pipeline in orthotopic models

Table 2.10 Treatment schedules for immuno-competent model

Table 2.11 Treatment schedules for immunocompromised model

Table 2.12 Drug recipes

Table 2.13 Drug buffer recipes

Table 3.2.1 Alterations in the SRC/JAK/STAT3 molecular pathway in pancreatic cancer

Table 3.2.2 Basic mutation status of selected human and murine pancreatic cancer cell lines

Figure 3.2.1 Western blot for phospho-STAT3 (Tyr705), total STAT3, phospho-SRC (Tyr416), total SRC, phospho-JAK1 (Tyr1022/1023), total JAK1, phospho-JAK2 (Tyr1007/1008), total JAK2 in pancreatic cancer cell lines

Table 3.2.3 Quantification of relative protein expression

Figure 3.2.2 Drug sensitivity of patient-derived cell lines and murine KPC cells

Figure 3.2.3 Correlation of ruxolitinib sensitivity (IC_{50}) and expression of phospho-STAT3 (Tyr705), STAT3, phospho-JAK1 (Tyr1022/1023), JAK1, phospho-JAK2 (Tyr1007/1008), JAK2, phospho-SRC (Tyr416) and SRC in pancreatic cancer cell lines

Figure 3.2.4 Correlation of ruxolitinib sensitivity (IC_{50}) and JAK/STAT3 pathway aberrations, TP53 mutation status, and TGFB/SMAD4 mutations in pancreatic cancer cell lines

Figure 3.2.5 Correlation of phospho-STAT3 (Tyr705) expression or STAT3 expression and JAK/STAT3 pathway aberrations, TP53 mutation status and TGFB/SMAD4 mutations

Figure 3.2.6 Correlation of dasatinib sensitivity (IC_{50}) and expression of phospho-STAT3 (Tyr705), STAT3, phospho-JAK1 (Tyr1022/1023), JAK1, phospho-JAK2 (Tyr1007/1008), JAK2, phospho-SRC (Tyr416) and SRC in pancreatic cancer cell lines

Figure 3.2.7 Correlation of dasatinib sensitivity (IC_{50}) and JAK/STAT3 pathway aberrations, TP53 mutation status, and TGFB/SMAD4 mutations, in pancreatic cancer cell lines

Figure 3.2.8 Drug synergy screens for dasatinib (SRC-inhibitor) and various JAK-inhibitor combinations in pancreatic cancer PDCLs and KPC cells

Figure 3.2.9 Correlation of dasatinib and ruxolitinib synergy with expression of phospho-STAT3 (Tyr705), STAT3, phospho-JAK1 (Tyr1022/1023), JAK1, phospho-JAK2 (Tyr1007/1008), JAK2, phospho-SRC (Tyr416) and SRC in pancreatic cancer cell lines

Figure 3.2.10 Correlation of dasatinib and ruxolitinib synergy with TP53 mutation status JAK/STAT3 pathway aberrations and TGFB/SMAD4 mutation status

Figure 3.2.11 Western blot showing time-dependent effects of dasatinib, ruxolitinib and combination treatment on levels of SRC/STAT3 downstream effectors in KPC cells.

Figure 3.2.12 Densitometry on levels of SRC/STAT3 downstream effectors in KPC cells.

Figure 3.2.13 Densitometry on levels of SRC/STAT3 downstream effectors in TKCC-05 cells.

Figure 4.2.1: Schematic of organotypic invasion assay set-up

Figure 4.2.2 JAK1/2 inhibition disrupts collagen matrix integrity

Figure 4.2.3 JAK1 inhibition disrupts collagen matrix integrity

Figure 4.2.4 JAK2 inhibition does not disrupt collagen matrix integrity

Figure 4.2.5 JAK3 inhibition disrupts collagen matrix integrity

Figure 4.2.6 Dual JAK1/2 inhibition robustly disrupts collagen matrix integrity when compared to JAK1, JAK2 or JAK3 inhibition alone

Figure 4.2.7 JAK1/2 inhibition disrupts collagen remodelling

Figure 4.2.8 The effect of dasatinib and ruxolitinib on the proliferative capacity of fibroblasts in 3D

Figure 4.2.9 Combined dasatinib and ruxolitinib impairs the invasive potential of PDAC cell lines

Figure 4.2.10 Combined SRC and JAK1 inhibition impairs the invasive potential of PDAC cell lines

Figure 4.2.11 Combined SRC and JAK2 inhibition impairs the invasive potential of PDAC cell lines

Figure 4.2.12 Combined SRC and JAK3 inhibition impairs the invasive potential of PDAC cell lines and is no better than dasatinib monotherapy

Figure 4.2.13 JAK1/2 inhibition is the most effective at impairing the invasive potential of PDAC cell lines when compared to JAK1, JAK2 or JAK3 inhibition alone

Figure 4.2.14 SRC inhibition impairs cancer cell proliferation *in vitro* in 3D organotypic assays

Figure 4.2.15 SRC and JAK inhibition does not promote cancer cell apoptosis *in vitro* in 3D organotypic assays

Figure 4.2.16 Schematic of co-culture organoid set-up

Figure 4.2.17 SRC and JAK inhibition alter cytokine profiles in KPC co-culture organoids

Figure 4.2.18 Cytokine profile schematic of KPC co-culture organoids following treatment with dasatinib and ruxolitinib

Figure 4.2.19 SRC and JAK inhibition alter cytokine profiles in TKCC-10 co-culture organoids

Figure 4.2.20 Cytokine profile schematic of TKCC-10 co-culture organoids following treatment with dasatinib and ruxolitinib

Figure 4.2.21 Integrated UMAP plot of KPC co-culture organoids displaying 28355 cells comprising 6 distinct cell populations.

Figure 4.2.22 Cells are classified as malignant and non-malignant based on CNVs.

Figure 4.2.23 Cells are classified as epithelial and non-epithelial based on epithelial marker expression.

Figure 4.2.24 Single cell profiling heatmap of epithelial cancer clusters displaying top differentially expressed genes between each population

Figure 4.2.25 Single cell profiling heatmap of non-epithelial fibroblast clusters displaying top differentially expressed genes between each population

Table 4.2.1 List of most downregulated and upregulated genes in KPC co-culture organoids following treatment with dasatinib.

Figure 4.2.26 Gene ontology (GO) analysis for KPC organoids showing enriched pathways following treatment with dasatinib.

Table 4.2.2 List of most downregulated and upregulated genes in KPC co-culture organoids following treatment with ruxolitinib.

Figure 4.2.27 Gene ontology (GO) analysis for KPC organoids showing enriched pathways following treatment with ruxolitinib.

Table 4.2.3 List of most downregulated and upregulated genes in KPC co-culture organoids following treatment with dasatinib and ruxolitinib.

Figure 4.2.28 Gene ontology (GO) analysis for KPC organoids following treatment with dasatinib + ruxolitinib

Figure 4.2.29 Venn diagrams displaying the number of differentially expressed genes following treatment with dasatinib, ruxolitinib, dasatinib and ruxolitinib in each cluster.

Figure 5.2.1 Expression of phospho-STAT3 (Tyr705) in The Kinghorn Cancer Centre (TKCC) pancreatic cancer patient-derived xenograft cohort

Figure 5.2.2 Expression of phospho-STAT3 (Tyr705) in selected *in vivo* models of pancreatic cancer.

Figure 5.2.3 Effects of dasatinib and ruxolitinib treatment on tumour weight and metastasis in the syngeneic and orthotopic KPC model of pancreatic cancer

Figure 5.2.4 Effects of dasatinib and ruxolitinib treatment on phospho-STAT3 and phospho-SRC protein levels in KPC tumours

Figure 5.2.5 Effects of dasatinib and ruxolitinib treatment on cancer cell apoptosis and proliferation.

Figure 5.2.6 Effects of dasatinib and ruxolitinib treatment on activated cancer-associated fibroblasts

Figure 5.2.7 Effects of dasatinib and ruxolitinib treatment on the extracellular matrix

Figure 5.2.8 Effects of dasatinib and ruxolitinib treatment on additional components of the extracellular matrix and tumour vasculature.

Figure 5.2.9 Effects of dasatinib and ruxolitinib treatment on the immunosuppressive tumour microenvironment.

Figure 5.2.10 Effects of dasatinib and ruxolitinib treatment on tumour-associated macrophages

Figure 5.2.11 Effects of dasatinib and ruxolitinib treatment on survival in the syngeneic and orthotopic KPC model of pancreatic cancer

Figure 5.2.12 Effects of dasatinib and ruxolitinib treatment on tumour weight and metastasis in the immunocompromised, patient-derived TKCC-05 orthotopic model of pancreatic cancer

Figure 5.2.13 Effects of dasatinib and ruxolitinib treatment on tumour weight and metastasis in the immunocompromised, patient-derived TKCC-10 orthotopic model of pancreatic cancer

Figure 5.2.14 Effects of dasatinib and ruxolitinib treatment on metastatic spread using bioluminescence imaging, in the immunocompromised, patient-derived TKCC-05 orthotopic model of pancreatic cancer

Figure 5.2.15 Effects of dasatinib and ruxolitinib treatment on metastatic spread using bioluminescence imaging, in the immunocompromised, patient-derived TKCC-10 orthotopic model of pancreatic cancer

Figure 5.2.16 Effects of dasatinib and ruxolitinib treatment on cancer cell apoptosis and proliferation in the patient-derived TKCC-05 model of pancreatic cancer

Figure 5.2.17 Effects of dasatinib and ruxolitinib treatment on cancer cell apoptosis and proliferation in the patient-derived TKCC-10 model of pancreatic cancer

Figure 5.2.18 Effects of dasatinib and ruxolitinib treatment on activated cancer-associated fibroblasts in TKCC-05 tumours.

Figure 5.2.19 Effects of dasatinib and ruxolitinib treatment on activated cancer-associated fibroblasts in TKCC-10 tumours.

Figure 5.2.20 Effects of dasatinib and ruxolitinib treatment on the extracellular matrix in TKCC-05 tumours.

Figure 5.2.21 Effects of dasatinib and ruxolitinib treatment on the extracellular matrix in TKCC-10 tumours.

Figure 5.2.22 Effects of dasatinib and ruxolitinib treatment on survival in the immunocompromised, patient-derived TKCC-05 orthotopic model of pancreatic cancer

Figure 5.2.23 Effects of dasatinib and ruxolitinib treatment on metastatic spread in the TKCC-05 model.

Table 6.1 Overview of studies focusing on molecular profiling

Figure 6.1 Schematic summary of the effects of dual dasatinib and ruxolitinib treatment on pancreatic tumours and their microenvironment

Appendix A: Luciferin kinetics curve for TKCC-05-eGFP/Luc

Appendix B: Luciferin kinetics curve for TKCC-10-eGFP/Luc

Appendix C: Western blot for phosphorylated STAT3 (phospho-STAT3 Ser727) and beta-actin of pancreatic cancer patient-derived cell lines (TKCC) and cells from the KPC mouse model of PC (KPC R172H).

Appendix D: Protein expression of TKCC-05 cells following treatment with vehicle, dasatinib, ruxolitinib and the combination of dasatinib and ruxolitinib at 24 and 48h.

Appendix E: Principal components analysis (PCA) heatmaps of the most differentially expressed genes in KPC organoids. Elbow plot that ranks the principle components based on the percentage variance of each PC.

Appendix F: UMAP plots for individual replicates showing the same 6 clusters in each replicate.

Appendix G: Cluster tree modelling the phylogenic relationship of different clusters at different clustering resolutions.

Appendix H: Violin plots of the number of unique genes per cell, total number of molecules detected within a cell, and percentage of reads that map to the mitochondrial genome

Appendix I: UMAP plots to visualise the number of unique genes per cell. (B) Total number of molecules detected within a cell. (C) Percentage of reads that map to the mitochondrial genome

Appendix J: Pearson's correlation matrix comparing the association between individual replicates. (Pearson's correlation coefficient of 1.0 indicates a perfect positive relationship).

List of abbreviations

2D: Two-dimensional	FUCCI: Fluorescent ubiquitination-based cell cycle indicator
3D: Three-dimensional	GCSF: Granulocyte-colony stimulating factor
ANOVA: Analysis of variance	GFP: Green fluorescent protein
apCAF: Antigen-presenting cancer associated fibroblast	GLUT1: Glucose transporter 1
APGI: Australian Pancreatic Cancer Genome Initiative	GM-CSF: Granulocyte-macrophage colony-stimulating factor
ATP: Adenosine tri-phosphate	GO: Gene ontology
BCL2: B-cell lymphoma 2	GSK3 β : Glycogen synthase kinase 3 β
CAF: Cancer-associated fibroblast	GTP: Guanosine triphosphate
CCL or CXCL: chemokine	H&E: Hematoxylin and eosin
CCND1: CyclinD1	HA: Hyaluronic acid
CD206: Cluster of differentiation 206	HGF: Hepatocyte growth factor
CD31: Cluster of differentiation 31	HNSCC: Head and neck squamous cell carcinoma
CD68: Cluster of differentiation 68	IC ₅₀ : Inhibitory concentration 50%
CDK4: Cyclin dependent kinase 4	iCAF: Inflammatory cancer-associated fibroblast
CDK6: Cyclin dependent kinase 6	ICGC: International Cancer Genome Consortium
CI: Combination index	IF: Immunofluorescence
CK19: Cytokeratin 19	IFN γ : Interferon gamma
CTLA4: Cytotoxic T-lymphocyte associated protein 4	IFP: Interstitial fluid pressure
Das: Dasatinib	IHC: Immunohistochemistry
DC: Dendritic cell	IL: interleukin
DEG: Differentially expressed gene	ITGA: Integrin α -3
DNA: Deoxyribonucleic acid	JAK: Janus Kinase
DSBR: Double stranded breaks	JNK: Jun kinase
ECM: Extracellular matrix	KRAS: Kirsten rat sarcoma viral oncogene
ED: Effective dose	LAMA: Laminin
EGF: Epidermal growth factor	Lcn2: Lipocalin2
EGFR: Epidermal growth factor receptor	MAPK: Mitogen-activated protein kinase
EMT: Epithelial-mesenchymal transition	MCL1: Myeloid cell leukemia 1
ERK: Extracellular signal-regulated kinase	M-CSF: Macrophage colony-stimulating factor
FAK: Focal adhesion kinase	MDM2: Mouse double minute 2
FBS: Fetal bovine serum	MDSC: Myeloid-derived suppressor cell
FDG: Fluorodeoxyglucose	
FGF: Fibroblast growth factor	
FOLFIRINOX: Folinic acid, fluorouracil, irinotecan, oxaliplatin	
FOV: field of view	
FoxP3: Forkhead box P3	

MEK: Mitogen-activated protein kinase
 MIF: Macrophage migration inhibitory factor
 MLC2: Myosin light chain 2
 MMP: Matrix metalloproteinase
 MMR: Mismatch repair
 mTOR: Mammalian target of rapamycin
 myCAF: myofibroblastic cancer-associated fibroblast
 MYPT1: Myosin phosphatase target subunit 1
 NF2: Neurofibromin 2
 NFkappaB: Nuclear factor kappa-light chain enhancer of activated B cells
 NK: Natural killer cell
 NSCLC: Non small-cell lung cancer
 PALB2: Partner and localizer of BRCA2
 PARP: Poly (ADP-ribose) polymerase
 PBS: Phospho-buffered saline
 PC: Pancreatic cancer
 PCA: Principal components analysis
 PD-L1: Programmed cell death ligand 1
 PDAC: Pancreatic ductal adenocarcinoma
 PDCL: Patient-derived cell line
 PDX: Patient-derived xenograft
 PDX1: Pancreatic and duodenal homeobox 1
 PEGPH20: Pegylated recombinant human hyaluronidase
 PIP: phosphatidylinositol 4,5-bisphosphate
 PSC: Pancreatic stellate cells
 PTEN: Phosphatase and tensin homolog
 PTP-1B: Protein tyrosine phosphatase 1B
 QCMG: Queensland Centre of Medical Genomics
 QM-PDA: Quasi mesenchymal pancreatic ductal adenocarcinoma
 Raf: Rapidly accelerated fibrosarcoma
 Rho: Ras homolog gene family
 RNA: ribonucleic acid
 ROCK: Rho associated coiled-coil containing protein kinase
 ROS: Reactive oxygen species
 Rux: Ruxolitinib
 SE: Standard error
 Ser: Serine
 SHG: Second harmonic generation
 SMA: smooth muscle actin
 SOCS1: Suppressor of cytokine signalling 1
 STAT3: Signal Transducer and Activator of Transcription
 STR: Short tandem repeat
 T-LGL: T-cell large granular lymphocytic leukemia
 TAM: Tumour-associated macrophage
 TCGA: The Cancer Genome Atlas
 TGF- β : transforming growth factor beta
 Th17: T helper 17
 Thr: Threonine
 TIF: Telomerase immortalized fibroblast
 TKCC: The Kinghorn Cancer Centre
 TME: Tumour microenvironment
 TNF-alpha: Tumour necrosis factor alpha
 TNFSF12: Tumour necrosis factor ligand superfamily member 12
 Tofa: Tofacitinib
 TP53: Tumour protein 53
 Treg: T regulatory cell
 TSLP: Thymic stromal lymphopoietin
 Tyr: Tyrosine
 UMAP: Uniform manifold approximation and projection

UTSW: University of Texas South
Western Medical Centre
VEGF: Vascular endothelial
growth factor
UICC: Union for International
Cancer Control
HR: Hazard Ratio
WGS: Whole genome sequencing

XIAP: X-linked inhibitor of
apoptosis
LIF: Leukemia inhibitory factor
CRP: C-reactive protein

Chapter 1. Introduction

Pancreatic ductal adenocarcinoma (PDAC), which constitutes 90% of all pancreatic cancers, is currently the fourth leading cause of all cancer-related deaths [1], presenting a major health issue in the community. This is a highly lethal malignancy, with an overall 5-year survival rate of only 8% [1, 2]. This extremely poor outcome is partly due to the majority of cases being diagnosed when pancreatic cancer has already spread to distant sites, with 5-year survival rates in metastatic disease being only 3% [2].

Moreover, pancreatic cancer appears to be particularly heterogeneous, and apart from a few notable exceptions (P53 and KRAS) [3-7], which have not been successfully targeted, most genetic aberrations occur at a frequency of <5% [3-5]. Hence, even if these mutations are effectively targeted, it is unlikely that an overall benefit would be detected with non-targeted population clinical trial designs, unless combinations are used (for example, combination of chemotherapeutics fluorouracil, leucovorin, irinotecan and oxaliplatin or FOLFIRINOX) [8]. Current standard therapies for patients with advanced pancreatic cancer, in the form of FOLFIRINOX or gemcitabine and nanoparticle albumin-bound paclitaxel (Abraxane®), have shown a significant but modest clinical benefit and a marginal survival advantage of just 4.3 and 1.8 months, respectively, in unselected populations [8, 9].

Adding to the genomic complexity, the desmoplastic stroma that envelops pancreatic cancer cells in growing tumours, not only presents a physical barrier to therapeutic efficacy, but at the same time, presents an environment that actively produces pro-tumourigenic, immunosuppressive signals that further drive pancreatic tumourigenesis, disease progression and treatment resistance [10, 11]. New strategies that involve design of tailored treatments and combinations that target different components of a developing tumour, in smaller, well-defined subgroups of patients are sorely needed. This literature review provides an analysis of the diverse molecular characteristics of pancreatic cancer, challenges with the current treatment landscape, and presents the latest advances in therapeutic targeting, with a particular focus on the as yet unrealised potential of utilising specific modulators of tumour-

stroma signalling as precision medicine strategies for pancreatic cancer. These modulators include inhibitors of the SRC-signalling cascade, and JAK/STAT3 signalling. Key pathways that play a critical role in tumour cell, stromal cell, and immune cell signalling, and drive cancer progression and chemoresistance.

1.1 The molecular and treatment landscape of pancreatic ductal adenocarcinoma

(Published in Parkin, A., et al., The Evolving Understanding of the Molecular and Therapeutic Landscape of Pancreatic Ductal Adenocarcinoma. *Diseases*, 2018. 6(4).)

1.1.1 Clinical presentation

PDAC is a notoriously insidious cancer, frequently presenting with vague, non-specific symptoms that are commonly observed for multiple abdomen or gastrointestinal tract pathologies. The classic presentation is with the triad of epigastric abdominal pain, weight loss and jaundice, which rapidly worsen as disease progresses and lead to a substantial deterioration in quality of life [12]. However, presentation of symptoms varies according to the location of the tumour within the pancreas. Tumours in the head of the pancreas more commonly present with jaundice, steatorrhoea and weight loss [13], with back pain associated with tumours originating in the tail of the pancreas [14]. Adult onset diabetes mellitus presents both an early manifestation and an etiologic factor of PDAC [15]. In metastatic disease, additional symptoms can include an abdominal mass, ascites, lymphadenopathy and bone pain. Diagnosis of pancreatic cancer is performed using a combination of established methodologies involving initially abdominal ultrasonography, followed by more advanced techniques, such as computed tomography and magnetic resonance imaging in combination with endoscopic ultrasonography [16]. Use of invasive methods is necessary to accurately diagnose PDAC, without which there are significant difficulties in differentiating between malignant disease, benign pancreatic lesions, or chronic pancreatitis. Of note, development and future validation of novel blood-based biomarkers that detect somatic mutations or “liquid biopsies” [17, 18], or circulating exosomal biomarkers [19,

20] may present promising new options and a minimally invasive alternative to direct tumour biopsy.

1.1.2 Clinico-pathological staging of PDAC

After a definitive diagnosis of PDAC, clinical staging is utilised to determine the optimal treatment approach for the patient. The American Joint Committee on Cancer TNM staging system is widely utilised worldwide as the most authorised tool for tumour staging assessment. Staging assessment is based on the extent of invasion into the pancreas and surrounding tissue (T), presence or absence of spread to lymph nodes (N), and presence or absence of metastasis (M). In October of 2016, AJCC/UICC released the 8th edition, which incorporated significant changes in the T and N classification of PDAC. In the 8th edition, stages T1-T3 are redefined specifically based on tumour size ($T1 \leq 2 \text{ cm}$; $2 \text{ cm} \leq T2 \leq 4 \text{ cm}$; $T3 > 4 \text{ cm}$). When the tumour invades the celiac axis, common hepatic artery and/or superior mesenteric artery, it is defined as T4, with the classification as “unresectable” (from AJCC 7th edition 2010) now removed. The N classification was further subdivided according to the number of positive lymph nodes as N0, N1 (≥ 1 and ≤ 3) and N2 (> 3). In the 8th edition, T1–3N2M0 was defined as stage III, and the other stages, including Stage IV (metastasised tumours), remain unchanged. Importantly, the system provides useful stratification of patient survival and resectability by stage [21, 22].

1.1.3 Current treatment approaches for operable PDAC

Approximately 15% of patients are eligible for surgical resection based on the American Joint Committee on Cancer (AJCC 7th edition) clinical staging system, and this is often due to the majority of patients having locally invasive or metastatic disease at diagnosis [23]. Total pancreatectomy is rarely performed due to high rates of perioperative mortality and morbidity [24]. However a modified Whipple procedure is often performed on tumours in the head of the pancreas, this surgery is a radical pylorus-preserving pancreaticoduodenectomy. Tumours present in the body or tail of the pancreas rarely present with resectable disease due to late presentation, but can often undergo a pancreatectomy coupled with a splenectomy [25]. In terms of

improvement to survival, complete tumour resection with negative margins (R0) has the most promising 5 year survival rate of up to 27% compared to resected tumours with positive margins (R1) [26, 27]. Overall prognosis for these patients still remains poor with 80% of them developing recurrent disease and 30% dying within one year of surgery [28, 29]. Significant work is now focused on defining preoperative clinical and molecular characteristics to improve patient selection for operative resection. The use of a biomarker-based preoperative nomogram (prognosis prediction tool), that uses the expression of S100A2 and S100A4, pro-metastatic calcium-binding proteins, as prognostic biomarkers has already shown promise in being able to identify those at a higher risk of recurrence [30]. In addition, two single nucleotide polymorphisms (SNP) (*CHI3L2* SNP rs684559 and *CD44* SNP rs353630) may serve as a non-invasive biomarker signature that can identify high-risk patients with very low survival probability post resection, and who may be eligible for inclusion in clinical trials utilising novel therapeutic strategies [31]. The modified combination regiment of 5-fluorouracil, oxaliplatin, and irinotecan (mFOLFIRINOX) is now the preferred adjuvant chemotherapy in the absence of toxicity concerns or intolerance. Alternatively doublet therapy with gemcitabine and capecitabine, or monotherapy with gemcitabine or fluorouracil plus folinic acid can be offered [32, 33]. It is apparent that in order to improve survival we must be able to identify the right patient, perform high-quality surgery at the right time and combine with the best adjuvant therapy [34].

1.1.4 Current treatment approaches for advanced PDAC

Unfortunately, most patients are routinely diagnosed with already advanced, metastatic disease. Gemcitabine monotherapy was established as standard of care treatment for PDAC in 1997 [35], demonstrating superior response rate over 5-fluorouracil. Lack of subsequent further dramatic improvement in patient outcomes is certainly not due to lack of trying. Multiple phase II and III studies have attempted to improve upon gemcitabine efficacy either by modulating its pharmacokinetics [36] or by combining with other agents [37-39].

More recently, two different chemotherapeutic combinations (FOLFIRINOX or gemcitabine plus Abraxane) have been shown to significantly improve survival in advanced disease in well patients (FOLFIRINOX: median overall survival 11.1 vs. 6.8 months for gemcitabine monotherapy, $p < 0.001$; gemcitabine and Abraxane: median overall survival 8.5 vs. 6.7 months for gemcitabine, $p < 0.001$) [8, 9], with recent analyses suggesting comparable real world efficacy [40]. FOLFIRINOX or gemcitabine and Abraxane are both utilised as first-line agents in metastatic PDAC and are administered to well patients, with gemcitabine monotherapy, as a more tolerable treatment, still prescribed for the elderly or patients with a poor performance status [41]. Recent update to the treatment guidelines also recommends immunotherapy pembrolizumab for patients who fail 1st line therapy and whose tumours harbour mismatch repair deficiency/microsatellite instability [42].

New treatment combinations are also on the horizon, with recent data from the Phase IIb PACT-19 trial suggesting that a combination of cisplatin, Abraxane, capecitabine, and gemcitabine increased progression-free survival compared with gemcitabine and Abraxane in the metastatic setting [43]. Validated predictive biomarkers of treatment response to these combinations are currently lacking and needed, to further improve identification of patient subgroups most likely to respond to each regimen.

1.1.5 The “omic” diversity of PDAC

Since the first genomic analysis of PDAC in 2008 [44], with exponential advances in sequencing methodologies and associated bioinformatics approaches, PDAC has been genomically and transcriptomically characterised to an unprecedented depth [3, 4, 6, 7, 45]. Early studies identified the 12 key pathways and processes whose component genes were genetically altered in most pancreatic cancers, including *K-Ras*, transforming growth factor β (*TGF- β*), c-Jun N-terminal kinase, integrin, Wnt/Notch and Hedgehog networks, small GTPase-dependent signalling, G₁/S cell cycle checkpoint regulation, invasion, homophilic cell adhesion, apoptosis and DNA repair pathways [44]. In 2011, using gene expression microarray profiling of resected PDAC specimens, three subtypes of pancreatic cancer were

defined: “quasi-mesenchymal”, which was associated with poor prognosis, “classical”, and “exocrine-like”. These subtypes were found to have differential response to therapeutic agents, with pancreatic cancer cell lines that were of “classical” subtype displaying resistance to gemcitabine, but sensitivity to erlotinib *in vitro*. In contrast, the “quasi-mesenchymal” lines were inversely gemcitabine-sensitive, but erlotinib-resistant [7]. Thus far, these predictive signatures of treatment response have not been translated into clinical application.

In 2015, a comprehensive whole genome sequencing (WGS) analysis of 100 primary operable PDAC cases further stratified pancreatic cancer into four major subtypes based on the extent of structural variation (SV) [4]. PDAC was stratified into:

- (1) “stable” subtype, present in 20% of all patients whose tumour genomes harboured fewer than 50 SV events;
- (2) “locally rearranged” subtype, detected in 30% of the cohort, characterised by a single focal event on one-two chromosomes, breakage-fusion-bridge events, chromothripsis or low prevalence alterations in known oncogenes and therapeutic targets (focal amplifications in *KRAS*, *SOX9*, *GATA6*, *ERBB2*, *MET*, *CDK6*);
- (3) the “scattered” subtype, present in 36% of tumours, showed a range of non-random chromosomal damage with less than 200 structural rearrangements;
- (4) the “unstable” or high SV subtype, present in 14% of PDAC, characterised by a large extent of SV (>200 events), suggesting major defects in DNA maintenance, with associated increased sensitivity to DNA-damaging agents [4]. Deleterious mutations in *BRCA1*, *BRCA2* and *PALB2* genes, essential components of homologous recombination-mediated DNA repair, were associated with the “unstable” PDAC subtype, and similarly, the top quintile of the previously identified BRCA mutational signature [46], was present in the majority (10/14) of unstable genomes [4].

Further comprehensive integrated genomic/transcriptomic analysis of 456 pancreatic cancers [3], defined four PDAC subtypes, based on the differential expression of transcription factors and downstream targets critical during pancreas development, differentiation and regeneration [3]. PDAC was classified into:

- (1) “squamous” subtype, associated with the worst patient prognosis;
- (2) “pancreatic progenitor” subtype, enriched for transcriptional networks containing *PDX1*, *MNX1*, *HNF4G*, *HNF4A*, *HNF1B*, *HNF1A*, *FOXA2*, *FOXA3* and *HES1* genes;
- (3) “aberrantly differentiated endocrine exocrine” (ADEX) subtype, a sub-class of the “pancreatic progenitor” group, defined by transcriptional networks that are essential in later stages of pancreatic development and differentiation. These include upregulation of *NR5A2*, *MIST1*, *RBPJL* and their downstream targets, which regulate acinar cell differentiation and pancreatitis/regeneration;
- (4) “immunogenic” subtype, associated with a significant immune infiltrate, with predominant expression profiles related to infiltrating B and T cells, upregulation of *CTLA4* and *PD1* immuno-suppressive pathways, inferring therapeutic opportunities with immune modulating agents for specific tumours in this class.

Building on these findings, Connor *et al.* [47] subsequently provided further insight into the molecular pathology of PDAC, describing an interesting correlation between signatures that define double-stranded DNA break repair (DSBR) and mismatch repair (MMR) deficiencies and specific immune profiles. Specifically, genes associated with increased cytolytic activity of infiltrating CD8-positive T lymphocytes plus increased expression of immune checkpoint genes (*CTLA-4*, *PD-L1*, *PD-L2*, and indolamine 2,3-dioxygenase 1 (*IDO-1*)) were increased in DSBR and MMR cases within the examined cohort [47], which was similar to the expression patterns observed in melanomas responsive to checkpoint blockade. Importantly, this suggests that similar to other solid cancers [48], pancreatic tumours with a high mutation burden may present a viable target for immune-modulating combination therapies. Despite

the explosion in “omic”- characterisation of pancreatic cancer, which has produced unprecedented insights into the complex mutational and changing landscape of this disease, the established molecular taxonomy is yet to be utilised clinically when establishing effective treatment plans. However, characterisation of major pathways frequently altered in PDAC [3, 44] has already identified numerous opportunities for therapeutic development, [49- 52] (Figure 1.1), with early successes already on the horizon [51, 53, 54], and discussed below.

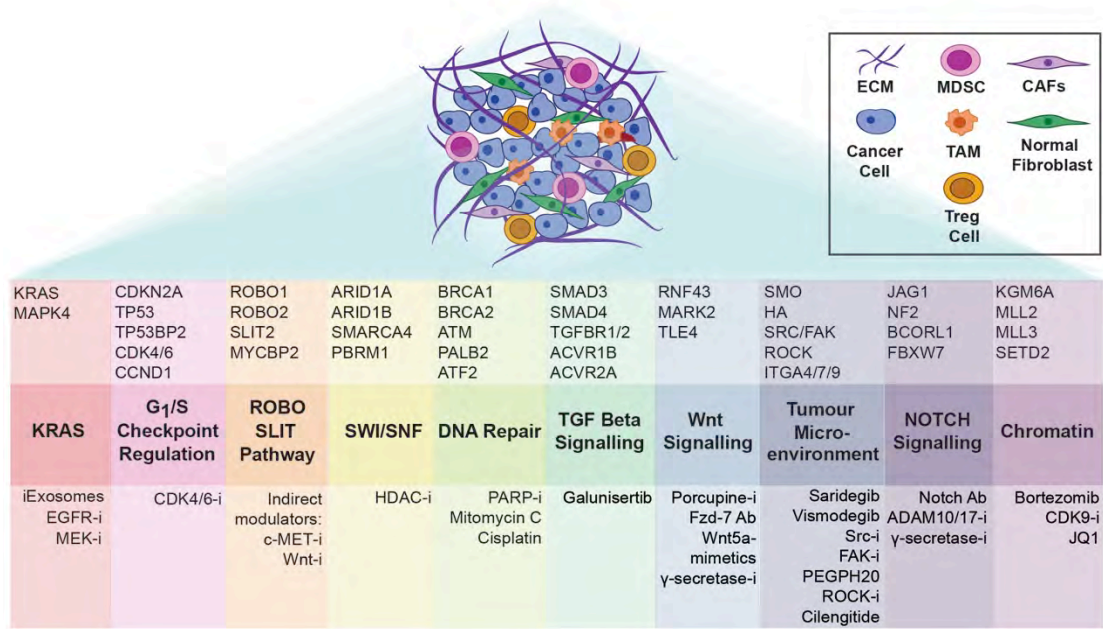


Figure 1.1 Frequently altered signalling pathways that drive pancreatic cancer progression, taken from Parkin *et al.* 2018 [55]. Key aberrations of interest, and associated targeted therapies in pre-clinical/clinical development, including small molecule inhibitors (i), antibodies (Ab) and other agents of interest are depicted. ECM: extracellular matrix; TAM: tumour-associated macrophage; MDSC: myeloid-derived suppressor cell; T-reg: regulatory T cell; CAF: cancer-associated fibroblast.

1.1.6 Targeting KRAS

Mutationally-activated KRAS (Kirsten rat sarcoma viral oncogene homolog) is the most frequently occurring alteration in PDAC (94% of cases; [4, 5, 44]) and a major contributor to therapeutic resistance. Sustained, aberrant activation of KRAS that leads to uncontrolled cell proliferation is largely driven by point mutations at residues G12, G13 and Q61. Moreover, activation of distinct downstream signalling cascades has been linked to specific *KRAS* mutants, where *KRAS*^{G12D} predominantly leads to activation of MAPK and PI3K pathways, whereas *KRAS*^{G12V} activates Ral signalling [56], thus potentially influencing the response to KRAS-driven treatment strategies. The main past and current strategies for developing therapeutics to block mutant *KRAS* function have thus far been largely disappointing [57, 58], with only a few studies into the development of *KRAS*^{G12C} inhibitors for solid cancers showing any real potential, however these specific mutations only occur in 1% of PDAC, making their potential rather limited [59]. With RAS GTPases requiring farnesylation, an essential lipid post-translational modification required for their malignant transforming activity [60], development of farnesyl transferase inhibitors presented a logical next step. Unfortunately, the early promising preclinical findings with these compounds did not translate into meaningful clinical benefit [61, 62]. Of note, recent pre-clinical development of a dual farnesyl and geranylgeranyl transferase inhibitor (FGTI-2734) is promising in terms of overcoming a major hurdle in KRAS resistance, potently inhibiting tumour growth of patient-derived KRAS mutant-driven xenografts from pancreatic cancer patients [63]. Concomitant inhibition of downstream c-RAF and upstream EGFR expression using shRNA-based methodologies was also shown to effectively block tumour progression in select patient-derived xenografts carrying *KRAS* and *TP53* mutations [64]. Both findings warrant further pre-clinical and clinical characterisation. Moreover, recent developments utilising exosomes that were derived from normal mesenchymal cells and packed with short interfering RNA specific to *KRAS*^{G12D} oncogene (iExosomes), suggest that this may present a powerful new approach for targeting *KRAS*-mutant PDAC. Clinical-grade iExosomes have since been produced [54], with a Phase I dose-finding and tolerability

study already underway (NCT03608631). In addition, targeting of *KRAS* effector signalling holds significant promise for clinical translation and has become the focus of numerous studies [65-67].

Conversely, distinct therapeutic options may be available for patients whose pancreatic tumours harbour wild-type *KRAS*. Treatment of advanced PDAC with a combination of gemcitabine and epidermal growth factor receptor (EGFR) inhibitor erlotinib, has led to a marginal therapeutic benefit (median survival of 6.24 months compared with 5.91 months for gemcitabine alone) [68], which lost significance when this combination was examined in all-comers in the adjuvant setting [69]. Further data analyses from trials investigating EGFR inhibitor efficacy, revealed that patients who developed skin rash during erlotinib treatment (an established adverse effect of drugs that target EGFR signalling) had considerably improved prognosis with 1-year survival rates beyond 40%, comparable with previous reports for FOLFIRINOX [68, 70-72]. Moreover, the improvement in survival following combined gemcitabine/EGFR inhibition therapy has also specifically been associated with *KRAS* wild-type tumour status [71, 73, 74], suggesting that this combination may be of considerable benefit in a small, but potentially well-defined subgroup of patients with PDAC.

1.1.7 G₁/S checkpoint as a therapeutic target

Cell cycle checkpoints represent essential control mechanisms in healthy cells that ensure accurate cell division. Apart from p53, the p16-cyclin D-CDK4/6-retinoblastoma protein pathway (CDK4 pathway) is another critical control that promotes the G₁/S-phase cell cycle transition. Under physiological conditions, Cyclin D complexes with its catalytic partners, cyclin-dependent kinases (CDKs) 4 and 6, driving retinoblastoma protein (RB) phosphorylation and G₁ phase progression [75]. Of note, the CDK4 pathway is frequently deregulated in several cancers, including PDAC [3, 44], with the p16INK4A tumour suppressor inactivated in 80-90% of clinical specimens [3, 76].

Early evidence indicating Cyclin D/CDK4 as an oncogene has stimulated research into the development of small-molecule CDK inhibitors as cancer therapeutics. Pan-CDK inhibitors have shown limited efficacy in clinical trials,

however selective CDK4/6 inhibitors, such as PD-0332991 (palbociclib) or LY2835219 (abemaciclib), have emerged as a powerful class of agents with clinical activity in a number of malignancies, firstly demonstrated in the treatment of ER+/HER2- metastatic breast cancer [77, 78], and other solid cancers [79]. As a high proportion of pancreatic tumours carry aberrations in G₁/S checkpoint machinery, targeting PDAC subtypes that are dependent on CDK4/6 signalling may therefore be a reasonable therapeutic approach. Combinations involving dual CDK4/6 and mTOR targeting have shown promise in preclinical studies [80, 81] and were translated into a clinical non-biomarker driven trial (NCT02981342; [82]), however, after the recruitment of the first 80 patients, this specific study was terminated due to significant disease progression, thus reinforcing the need for a clinical biomarker driven trial.

Comprehensive preclinical exploration of the long-term responsiveness to CDK4/6 inhibition and CDK4/6 inhibitor-based combinations, highlights the need for a more personalised approach in the treatment of pancreatic cancer, with RB as a potential companion biomarker that may help enrich for responders to CDK4/6 inhibitor-regimens [83]. Moreover, recent studies in PDAC and other cancers, suggest a considerably more complex mechanism of action for CDK4/6 inhibitors that includes multifaceted global inhibitory effects on tumour cells, stromal cells and extracellular matrix (extracellular matrix) organisation at different stages of PDAC progression [83], inhibition of epithelial-to-mesenchymal transition (EMT) signalling in breast cancer metastasis [84] and improved anti-tumour immunity by enhancing T-cell activation [85, 86]. These new features need to be incorporated into future trial design, and indeed several trials are including a retrospective or prospective analysis of potential companion biomarkers (including tumour RB expression by immunohistochemistry plus *CDK4/6* amplification or *CCND1* amplification) as part of the clinical assessment of PD-0332991 efficacy in PDAC (The MATCH Screening Trial NCT02465060, NCT02501902, Know Your Tumour (KYT) program), and early results of a precision-medicine based approach are promising [87, 88].

1.1.8 Targeting DNA damage repair signalling

Maintenance of cellular genomic integrity is regulated by a complex network of DNA damage response (DDR) proteins, which are readily activated by endogenous and exogenous mitogens, including reactive oxygen species and cytotoxic agents. Importantly, deregulation of this highly organised network, detected in approximately 9-14% of human PDAC [3, 4] could be therapeutically exploited [89].

BRCA1 and *BRCA2* are well-characterised tumour suppressor genes that when heterozygously mutated in the germ line, increase the risk substantially for several malignancies, including breast, ovarian, pancreatic and prostate cancer [90, 91]. Functional *BRCA1* and *BRCA2* proteins are essential for the repair of genotoxic double-stranded DNA breaks through a high fidelity pathway called homologous recombination (HR) [89]. Cancers that arise in individuals with a germline mutation in *BRCA1/2*, frequently acquire a somatic loss-of-function aberration in the corresponding wild-type *BRCA* allele, leading to HR repair deficiency. In addition to *BRCA1/2* mutations, aberrations in other genes (incl *PALB2* [92, 93], *BRCAness* [46] and/or high extent of structural rearrangement [4]), may lead to loss of functional HR, and importantly, may sensitise these cancers to specific DNA-damaging treatments, including poly(ADP-ribose) polymerase (PARP) inhibitors and DNA-intercalating agents (mitomycin C, platinum-based combinations).

Platinum agents have been previously combined with gemcitabine and examined clinically in “all-comers”. Although findings from single trials [94, 95] suggest only trending (but not statistically significant) improvements in overall survival following combination treatment, a pooled analysis of two international multi-centre trials suggests that combining gemcitabine with a platinum analogue may be of significant therapeutic benefit in advanced pancreatic cancer (HR = 0.81; P = 0.031 [96]), and may be further improved upon by adding a companion biomarker. In fact, selected early case studies have already highlighted the potential of personalising these treatment strategies in PDAC. Specifically, addition of cisplatin after progression on gemcitabine monotherapy, led to a complete clinical response in a patient with

a pathogenic germline *BRCA2* (1153insertionT) mutation [97]. Similarly, a patient with a PDAC tumour harbouring biallelic inactivation of the *PALB2* gene, had an exceptional response to mitomycin C [93]. Furthermore, a review on the impact of *BRCA1* and *BRCA2* germline mutations and therapeutic outcome observed superior overall survival in advanced *BRCA*-associated PDAC with platinum exposure ($n=71$ patient study) [98]. Subsequent Phase II trial involving PDAC patients with germline *BRCA* mutations has since confirmed that PARP-inhibitor olaparib offers a clinical benefit [99], particularly as maintenance therapy [100], with similar effects observed with rucaparib in a study of 19 pre-treated patients with *BRCA*-mutant cancer [101], although another PARP-inhibitor veliparib did not elicit a significant response in this setting [102]. Of note, the PARP catalytic inhibitory activities of various PARP inhibitors in clinical testing do not correlate strongly with respect to cytotoxic and trapping potency; for example olaparib has shown greater cytotoxic and PARP-trapping activity than veliparib *in vitro* [103] and this could potentially infer differences in clinical potency between the various PARP-targeting agents.

With growing evidence supporting the clinical development of PARP- or platinum-based regimens (including FOLFIRINOX [92]) in the treatment of *BRCA*-mutated PDAC, the National Comprehensive Cancer Network (NCCN) has recommended consideration of a first-line platinum-based regimen in patients with advanced PDAC and a hereditary cancer syndrome involving a DNA repair mutation [104]. Ongoing clinical studies further aim to assess the tolerability and efficacy of PARP-inhibitor based combinations regimens (NCT01585805), or their utility as maintenance monotherapy after first-line platinum-based chemotherapy in *BRCA1*, *BRCA2* or *PALB2*-mutant pancreatic cancer (POLO trial: NCT02184195, NCT03140670). The POLO trial has already shown promising results with a significant improvement in progression-free survival (PFS) following treatment with olaparib, (median PFS was 7.4 vs 3.8 months; olaparib vs placebo) [105].

1.1.9 Mismatch repair deficiency

During the malignant transformation process, pancreatic cancer cells acquire multiple mechanisms to evade the immune response. Antibodies that target these inhibitory signals called immune checkpoint inhibitors, although highly successful in the treatment of certain solid cancers [106, 107], have thus far not demonstrated significant activity in PDAC, when examined without a companion biomarker [108-110]. More recently, deficiency in mismatch repair has been effectively utilised to predict response to immunotherapy agents in the treatment of metastatic colorectal and other cancers [111]. Mismatch repair (MMR) is another highly conserved mechanism for the repair of DNA lesions, which recognises and repairs small loops within the duplex DNA that arise from nucleotide misincorporation either by base–base mismatches or by insertion/deletion loops [112]. Defects in MMR lead to genome-wide instability, particularly in simple repetitive sequences, known as microsatellite instability.

MMR deficiency is rare in PDAC and accounts for approximately 1% of cases [3], however as these patients present with a significantly higher burden of mutations that may lead to higher immunogenicity, there is strong rationale for the use of checkpoint inhibitors in this setting. The recently published, expanded Phase II study by Le *et al.* [48] demonstrated that significant responses to immune checkpoint inhibitor pembrolizumab were observed only in patients with MMR-deficient tumours. A pancreatic cancer-focussed study revealed that 57% of the MMR-deficient patients (7/833, 0.8% frequency of MMR-deficiency) treated with immune checkpoint blockade had treatment benefit (1 complete response, 2 partial responses, 1 stable disease) [113]. These promising results have since led to the first ever cancer-agnostic FDA approval of pembrolizumab for biomarker-defined disease, (MMR-deficient malignancies, including PDAC) [51].

1.2 The tumour microenvironment of pancreatic cancer

1.2.1 Stromal reaction and the extracellular matrix

The pancreatic tumour microenvironment (TME) comprises both cellular elements and marked desmoplasia, that collectively not only form an effective physical barrier leading to limited drug penetration, but also through dynamic cancer cell-stromal cell crosstalk, directly promote cancer growth, survival and treatment failure (Figure 1.2) [114]. The cellular components within the tumour microenvironment are incredibly diverse, and include myofibroblasts, immune cells, adipose cells, the blood and lymphatic vascular networks, all of which are embedded in a dense extracellular matrix, rich in hyaluronic acid (HA), collagens, fibronectin, laminin and proteoglycans [114].

The extracellular matrix is a key regulator of cellular and tissue function in the body, with dynamic and tightly controlled extracellular matrix remodelling essential during development, wound healing and normal organ homeostasis [115]. The extracellular matrix is a major component of the tumour microenvironment and provides mechanical and structural support to cells, aids in cell migration, whilst also coordinating important signalling processes [116]. The extracellular matrix is made up of a complex interlocking mesh of specialised protein families, including fibrillar and non-fibrillar collagens (comprising up to 90% of the extracellular matrix), fibronectins, laminins and glycosaminoglycan (GAG)-containing non-collagenous glycoproteins (hyaluronan and proteoglycans) [117].

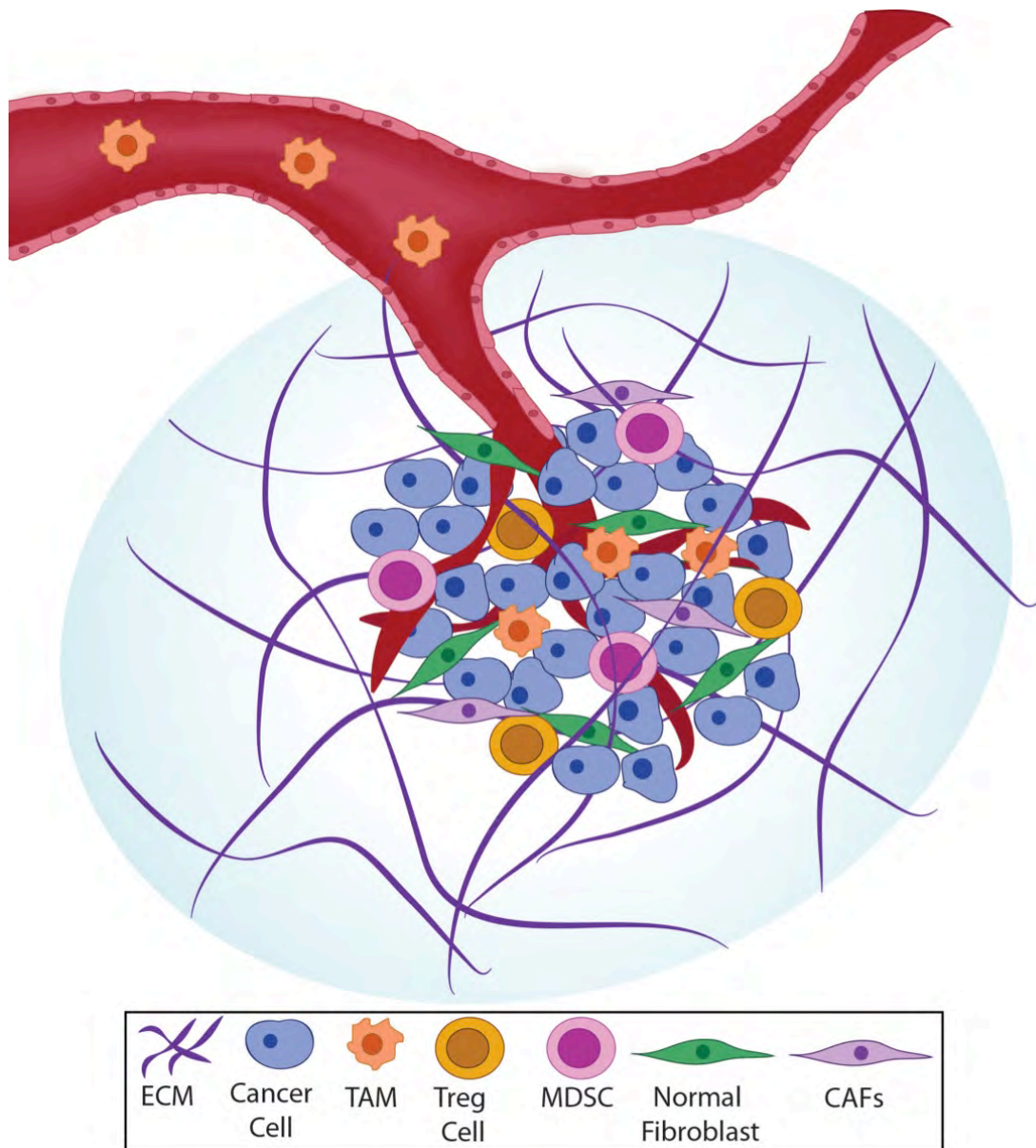


Figure 1.2: The primary pancreatic tumour microenvironment. Pancreatic cancer cells are surrounded by a profuse desmoplastic stroma (ECM) that consists of numerous cell types including fibroblasts, pancreatic cancer-associated fibroblasts (CAFs, also known as pancreatic stellate cells), blood vessels, and several different classes of immune cells including tumour-associated macrophages (TAM), myeloid-derived suppressor cells (MDSC), and T cells, including the regulatory T cells (Treg).

Sustained and extensive remodelling and deposition of multiple extracellular matrix components has been shown to lead to enhanced interstitial fluid pressure (IFP), increased tissue stiffness, and can mechanically induce intracellular signalling that drives tissue fibrosis and inflammation [118-120]. In pancreatic cancer the extracellular matrix encompasses up to 70% of the tumour microenvironment [115]. Recent assessments of collagen abundance and extracellular matrix stiffness in normal pancreas material and pancreatic tissues harbouring early neoplastic and advanced PDAC lesions revealed that pancreatic cancer progression is accompanied by increased collagen crosslinking and extracellular matrix-driven stiffening of the tumour tissue, driving epithelial-to-mesenchymal (EMT) transition in pancreatic cancer cells and chemoresistance [121]. Moreover, recent work indicates that extracellular matrix de-regulation is spatially regulated, with local site-specific remodelling of extracellular matrix components, rather than global and uniform changes across the tumour tissue, promoting disease progression in PDAC [122]. Laklai *et al.* also revealed that cellular tension 'tunes' the pancreatic stroma, in a JAK-STAT3-ROCK-dependent manner, to further promote pro-tumourigenic signalling, cancer growth and disease progression.

The transformation of the pancreatic tumour microenvironment is largely due to the activation of mesenchymal cells, called pancreatic stellate cells (PSCs) into cancer-associated fibroblasts (CAFs) [123]. CAFs are the dominant cell type within the stromal compartment, and are the primary source of extracellular matrix components such as collagen, fibronectin and laminin. They also regulate the synthesis, deposition and remodelling of the extracellular matrix [124-126]. Due to complex signalling networks, and the ability of these cells to provide growth factors, matrix remodelling enzymes, inflammatory cytokines and reactive oxygen species, CAFs have the ability to influence cancer cell function, and in turn, cancer progression [124, 127-134]. This symbiotic interaction allows CAFs and cancer cells to influence each other's behaviour through paracrine signalling [135, 136]. Treating PSCs with cancer cell-conditioned media resulted in the activation of PSCs [124]. Whilst co-culturing CAFs with PDAC cancer cells up-regulated genes from the CXC/CC chemokine family such as *CCL2*, *CXCL1*, *CXCL2* and *IL8*, which

play a role in invasion, metastasis and angiogenesis [137]. In pancreatic cancer, CAFs, can be identified by their expression of desmin, glial fibrillary acidic protein, nestin, neural cell adhesion molecule and α -smooth muscle actin [124, 138]. Following internal or external tissue injury (which may include external injury to the pancreas, chronic pancreatitis or aberrant cell death), the release of inflammatory cytokines, chemokines and growth factors (TGF- β , VEGF, PDGF, angiotensin), facilitates the accumulation of CAFs [115, 139], which results in increased accumulation of extracellular matrix proteins, increased inflammation, changes in blood vasculature, and changes to the extracellular matrix biochemical and structural properties. These modifications provide a favourable environment for cancer cells to survive and proliferate, and the resulting physical changes to the microenvironment impairs drug delivery and may contribute to drug resistance [140-144].

However, the traditional view of a uniform tumour stroma has recently been redefined by the concept of intratumoural CAF heterogeneity. Papers by Ohlund *et al.* [141] and Elyada *et al.* [145] have identified three spatially separated, reversible and mutually exclusive CAF subtypes. The 'inflammatory CAFs (iCAFs)' are a population that express inflammatory markers such interleukin-6 and leukemia inhibitory factor (LIF), (which are known to induce cell survival and chemotherapy resistance [146]), and iCAFs are located farther away within the dense stroma. Whilst the 'myofibroblastic CAFs (myCAFs)', are a population that express myofibroblast markers such as α -smooth muscle actin, and fibroblast activation protein (FAP), and are associated with extensive extracellular matrix deposition [141, 147]. MyCAFs are located adjacent to tumour cells due to their formation being dependent on juxtacrine interactions with cancer cells. TGF- β and IL-1/JAK/STAT signalling have been identified as the major signalling pathways responsible for myCAF and iCAF formation. Tumour-secreted IL-1 induces LIF expression and JAK/STAT activation to generate iCAFs, whilst TGF- β antagonizes IL-1 activity and JAK/STAT signalling to promote differentiation into myofibroblasts [141, 147]. Antigen-presenting CAFs (apCAFs), are another population of CAFs defined by their expression of MHCII molecules, and their ability to present a model antigen to CD4⁺ T cells [145]. These findings support a new

model of the pancreatic tumour stroma that describes the symbiotic relationship between cancer cells and CAFs, as well as the plasticity between heterogeneous CAF subtypes. Moreover, this new model reveals the potential for selective therapeutic targeting of each population.

Since the mechanical microenvironment is a potent contributor to pancreatic cancer progression, investigation of extracellular matrix components as viable therapeutic targets in cancer is an exponentially growing area of research [148]. Examples include the use of fasudil as a priming agent before chemotherapy to reduce fibrosis and improve tissue perfusion [149], as well as targeting hyaluronic acid (HA), a critical component of the extracellular matrix, with PEGPH20 which is already showing promise in clinical trials [143, 144]. Collectively, these findings highlight the potential utility of extracellular matrix-based stratification, where high amounts of fibrillar collagen could serve as a companion biomarker to identify patients who will most benefit from extracellular matrix manipulation prior to chemotherapy.

1.2.2 The immunosuppressive tumour microenvironment

Pancreatic tumours are defined by their highly immunosuppressive microenvironment [150]. Immune and inflammatory cells such as lymphocytes, dendritic cells, neutrophils, macrophages and mast cells accumulate in the pancreatic tumour microenvironment during cancer progression (Figure 1.3) [151]. Pancreatic cancer cells over-activate pro-inflammatory signalling networks which results in cytokine release (including IL-6, IL-10, IL-13, VEGF, TGF- β) [152], subsequently recruiting and activating tumour-associated macrophages (TAMs), neutrophils and regulatory T cells (T_{reg}) [153]. Consequently, activated immune cells create an immunosuppressive tumour microenvironment, which contributes to immune evasion and tumour progression [154]. In addition, the unique microenvironment of PDAC confers resistance to therapeutic agents including immunotherapy, with numerous studies concluding that checkpoint inhibition alone is insufficient for PDAC patients [106, 155].

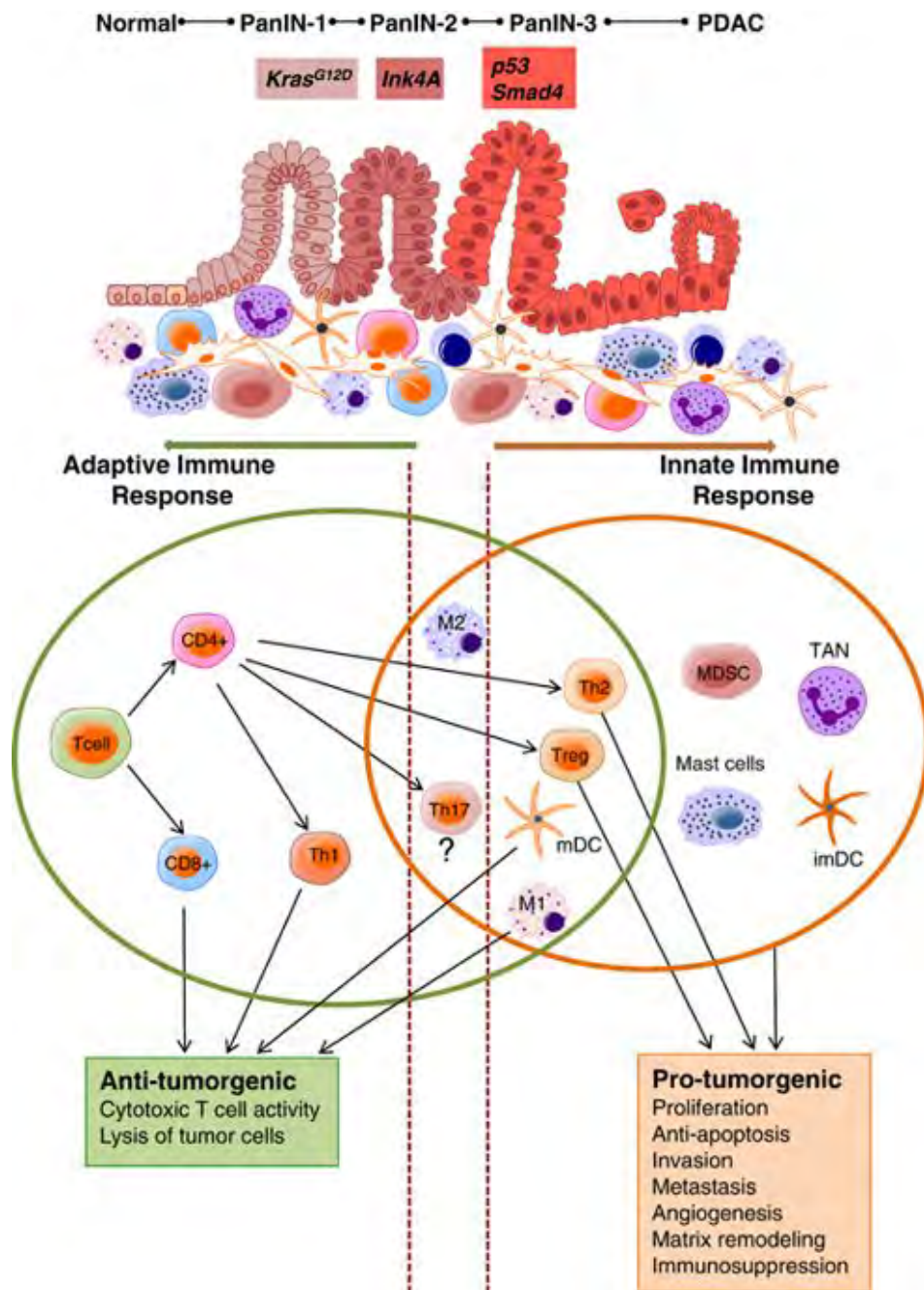


Figure 1.3: A model of innate and adaptive immune response during pancreatic tumour progression taken from Wormann *et al.* 2014 [156]. The immune response is activated during early PDAC development, causing anti- and pro-tumourigenic effects. The innate immune response is complemented with activation of adaptive immune cells. These activated immune cells release cytokines and chemokines that promote proliferation of neoplastic cells, as well as stromal remodelling and neoangiogenesis. Macrophages (M1, M2), myeloid derived suppressor cell (MDSC), immature dendritic cell (imDC), mature dendritic cell (mDC), tumour-associated neutrophil (TAN).

1.2.2.1 Regulatory T cells (T regs)

Regulatory T cells (CD4⁺ CD25⁺ FoxP3⁺) suppress the adaptive immune response promoting progression from the premalignant stage to established cancer and are also associated with tumour progression and a poorer prognosis of PDAC patients, while infiltration of effector or cytotoxic (CD8⁺) T cells is inversely correlated [157, 158]. PDAC is associated with increased production of CCL5, which encourages the migration of T regs into the tumour microenvironment due to their CCR5 expression [159]. Regulatory T cells are then able to suppress the anti-tumour immune response by inhibiting effector T cell functions [160]. Expression of CTLA4 competes for co-stimulatory ligands (CD80 and CD86), preventing CD28 binding, a necessary process for effector T cell activation [159].

1.2.2.2 Effector T cells

Effector or Cytotoxic CD8⁺ T cells are the predominant T cell subset and are associated with favourable clinical outcomes and prolonged survival [156]. They work by eliminating tumour cells via IFN- γ -mediated direct tumouricidal activity, and via induction of macrophage tumouricidal activity. However it is thought that pancreatic cancer cells may escape the effects of CD8⁺ T cells by promoting their aggregation in fibrous tissue, and that down regulation of activation markers on CD8⁺ T cells can decrease their cytotoxic activity [156].

1.2.2.3 Myeloid derived suppressor cells (MDSCs)

Myeloid-derived suppressor cells are systemically expanded and are recruited to PDAC tumours following induction by GM-CSF (produced by pancreatic cancer cells) or CXCL12 (produced by fibroblasts) [160]. MDSCs promote primary tumour growth and invasion through a number of mechanisms including inducible nitric oxide synthase, ROS upregulation, T cell recruitment and neoangiogenesis promotion [156]. They can suppress the anti-tumour activity of CD8⁺ and CD4⁺ T cells, as well as the expansion and differentiation of regulatory T cells following secretion of immunosuppressive cytokines such as IL-6, IL-10 and TGF- β [161]. They can also block innate immunity by transforming M1 macrophages (anti-tumourigenic phenotype) to M2 macrophages (pro-tumourigenic) [162], and can suppress natural killer

(NK) cells anti-tumour cytotoxicity [163]. Disruption of the paracrine signalling that occurs between MDSCs and tumour cells has been shown to lead to inhibition of MDSC accumulation, restoration of CD8⁺ T cell immunity and overcomes the immunosuppressive effects on local cytotoxic T cells [156].

1.2.2.4 Tumour-associated macrophages (TAMs)

Tumour-associated macrophages can be recruited to the PDAC microenvironment via CCL2, CCL5 and CXCL12 [164]. However cytokines such as IL-4, IL-10, IL-13 and GM-CSF regulate recruitment, maturation and differentiation of macrophages into the M2-activated macrophage state, which is defined by an immunosuppressive and pro-tumourigenic phenotype [165]. These macrophages are present in both pre-invasive pancreatic lesions and persist into invasive PDAC, particularly in the invasive front of the tumour [156]. They secrete a series of matrix proteins and proteases that modify the extracellular matrix, such as serine proteases, cathepsins and metalloproteinases (MMPs) [160]. TAMs can also secrete angiogenic factors (thymidine phosphorylase, VEGF, MMPs, COX-2, CXCL12, CCL2) as well as FAP, a serine proteinase that stimulates fibroblasts to promote angiogenesis and metastasis, and IL-6, which initiates STAT3 signalling and promotes cancer development [166-168]. In addition, pancreatic TAMs promote cancer cells to produce cytidine deaminase, which can metabolize gemcitabine, promoting chemoresistance [169].

1.2.2.5 Natural killer cells (NK Cells)

Natural killer cells are a subset of innate lymphoid cells that make up approximately 5-15% of the circulating cell population. These cells are able to recognize and kill tumour cells specifically due to their killer-cell immunoglobulin-like receptors (KIRs) [170]. Once activated they secrete numerous cytokines and chemokines including IFN- γ , TNF α , GM-CSF, CCL1, CCL2, CCL3, CCL4, CCL5, and CXCL8, all of which can recruit and activate other innate and adaptive immune cells [171]. In PDAC, loss of NK cells was shown to promote pancreatic cancer in LSL-KrasG12D/+ driven mouse models [172], with a positive correlation between the number of circulating NK cells and overall patient survival [173]. However the cytotoxic capacity of NK

cells in PDAC patients is frequently reduced, including their capacity to secrete immune-activating cytokines such as TNF α and IFN- γ [171].

1.3 SRC signalling in the tumour microenvironment of pancreatic cancer: from mechanisms to therapy

(Published in Parkin, A., et al., Targeting the complexity of Src signalling in the tumour microenvironment of pancreatic cancer: from mechanism to therapy. The FEBS Journal, 2019. 0(ja).)

1.3.1 The SRC signalling axis promotes pancreatic cancer progression

The proto-oncogene tyrosine-protein kinase SRC or cellular SRC (c-SRC) belongs to a family of nine non-receptor tyrosine kinases that share similar structure and function [174]. SRC kinase localizes at cell-matrix adhesions, and is readily activated by positive migratory growth factor signalling, including, but not limited to, epidermal growth factor (EGF), hepatocyte growth factor (HGF), platelet-derived growth factor (PDGF), vascular endothelial growth factor (VEGF) and integrin [175] and Eph receptor (EphA2) activation [176]. In turn, SRC can phosphorylate substrates from numerous molecular pathways and consequently promotes tumour cell survival, proliferation, cell-adhesion, migration, invasion and angiogenesis, key hallmarks of cancer (Figure 1.4) [177-184]. The roles of SRC in tumourigenesis and metastasis are well established, with constitutive activation of SRC being observed in a variety of cancers including breast, lung, colon, prostate and pancreas [177, 182, 185].

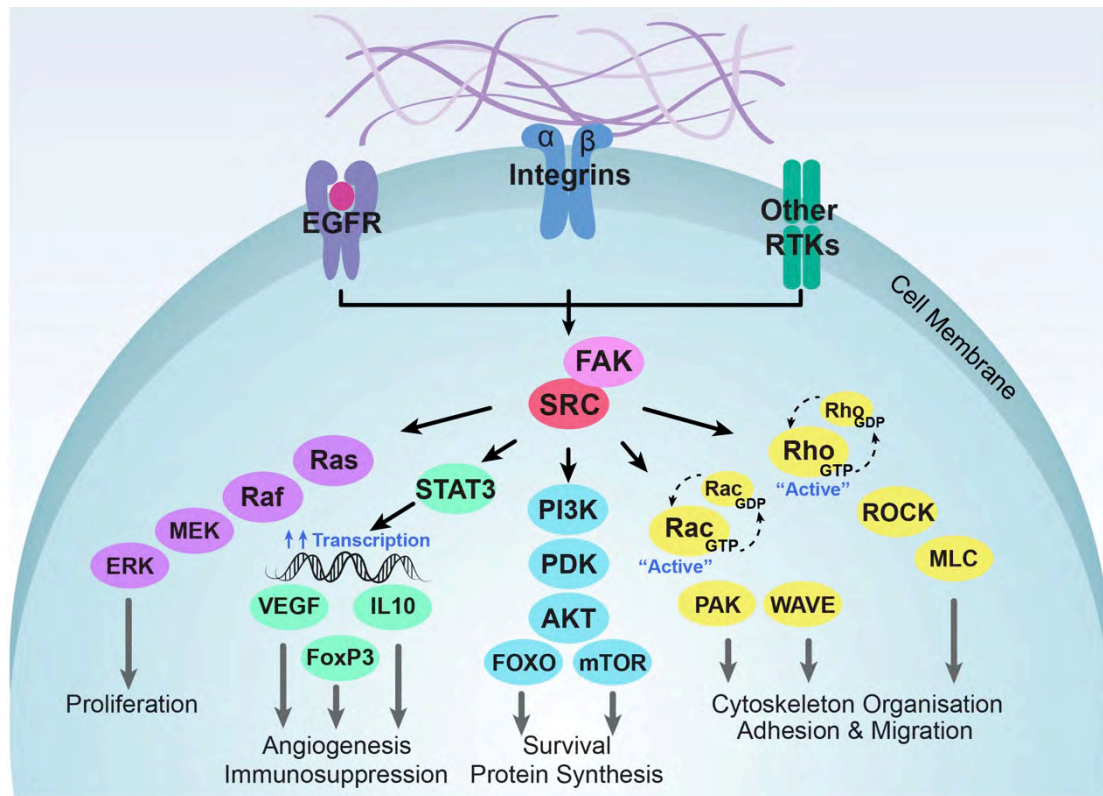


Figure 1.4 Schematic of the canonical Integrin/SRC/FAK signalling network taken from Parkin *et al.* 2019 [186]. SRC and FAK interact with numerous receptor tyrosine kinases (RTKs), including epidermal growth factor receptor (EGFR), vascular endothelial growth factor receptor (VEGFR), fibroblast growth factor receptor (FGFR), and platelet-derived growth factor receptor (PDGFR), as well as the ‘matrix receptor’ integrins, which all facilitate their downstream signalling. (i) Phosphorylation and activation of RAS, RAF, MEK1/2 and ERK1/2 leads to the transcriptional regulation of genes associated with cell growth and proliferation. (ii) Phosphorylation of signal transducer and activator of transcription 3 (STAT3), regulates gene expression of VEGF, IL-10 and FoxP3 leading to angiogenesis and immunosuppression. (iii) PI3K recruits Akt, where it is phosphorylated by PDK1/2. Akt inhibits the family of forkhead transcription factors (FOXO), leading to cell survival, and activation of the mTORC complex which leads to RNA translation and protein synthesis. (iv) Activation of Rho GTPases results in actin cytoskeleton remodelling and cell motility, while activation of Rac GTPases affects actin dynamics and lamellipodia formation.

SRC modulates integrin adhesions, cadherin-mediated cell-cell adhesions and metalloproteinase expression, and it is this disruption of intercellular adhesion that results in the detachment of tumour cells from the tumour mass, allowing them to invade through the extracellular matrix, penetrate the blood vessels and metastasize to other sites [183]. Furthermore, SRC kinase activity is required for mesenchymal invasion (involving integrin and protease-dependent stromal remodelling) as it controls the turnover of integrin-based adhesions [187]. In addition, SRC has been suggested as a mechanistic link between inflammation and cancer [188]. Specifically, SRC activation in tumour-associated macrophages, leads to their increased motility and infiltration into the tumour, a process which is driven by the secretion of pro-inflammatory cytokines within the tumour microenvironment [188-190]. SRC also plays a role in the metabolic reprogramming of cancers by promoting the Warburg effect. This involves activation of hexokinases and upregulation of glycolysis, which in turn promotes tumourigenesis [185].

The significance of SRC in PDAC tumourigenesis is also well established [177, 189, 191]. SRC kinase expression and activity is up-regulated in PDAC, increased further during progression to invasive and metastatic (advanced) PDAC and is associated with poor survival [177, 191, 192]. SRC also plays a role in the progression of pancreatitis, an inflammatory condition that presents a risk for development of pancreatic cancer [193]. Similarly to other cancers, SRC inhibition has been shown to reduce proliferation, migration and invasion in PDAC cell lines, as well as inhibit tumour progression and metastasis *in vivo* [183, 194-198]. SRC can also promote the progression of PDAC by reducing tumour response to gemcitabine, one of the current standard-of-care chemotherapies for this cancer [199].

In addition to SRC, the integrin-focal adhesion signalling-mediated modulation of extracellular matrix mechanics and cytoskeleton stability involves several important sensor proteins that are also frequently deregulated in cancer, including integrins, FAK and downstream Akt/PI 3-kinase, LIM kinase, and Rho/ROCK activation [200-203] (Figure 1.4). Integrins are composed of two non-covalently associated transmembrane glycoprotein subunits, and can be divided into several subtypes [204]. These molecules can signal

bidirectionally: through the recruitment of adaptor proteins the integrin receptor becomes activated and has a high affinity for extracellular matrix ligands, which in turn leads to the recruitment of signalling proteins and the assembly of focal adhesions [204]. Integrins bind to, and remodel extracellular matrix components such as vitronectin, laminin, fibronectin and collagen, thereby providing the traction required for tumour cell motility and invasion. Increased deposition and cross-linking of extracellular matrix proteins can also further promote tumour progression via mechanical force-induced clustering of integrin receptors [205].

The crosstalk between integrins, growth factor receptors, and SRC oncogene are readily exploited by cancer cells during both tumour initiation and disease progression [200]. Furthermore, integrins also play a role in angiogenesis, by providing a docking site for several cell types, including endothelial cells, endothelial stem cells and inflammatory cells, at the site of angiogenesis [206]. Upregulation of $\alpha\text{v}\beta\text{6}$ -integrins occurs in a variety of tumours, including PDAC, where it has been shown to activate TGF- β , stimulating tumour cell epithelial-to-mesenchymal transition (EMT) and stromal myofibroblast differentiation [207], which has in turn been shown to either promote [208] or restrict tumour growth and progression [209]. The association between $\alpha\text{v}\beta\text{6}$ -integrins and increased migration, invasion, and cell survival is partly due to the regulation of proteases (MMPs), and urokinase-type plasminogen activator (uPA) [204, 207, 210-212]. In PDAC specifically, overexpression of integrin $\alpha\text{v}\beta\text{3}/\alpha\text{v}\beta\text{6}$ has been previously shown to associate with poor survival of patients as well as lymph node metastasis [200, 213], and recent findings indicate that the stromal localization and levels of active $\alpha\text{5}\beta\text{1}$ -integrin and FAK can identify two readily distinguishable desmoplastic phenotypes in pancreatic cancer. Tumours with high stromal pSMAD2/3 levels were found to be prognostic of poor outcome, whilst increased stromal levels of active $\alpha\text{,}\beta$ -integrin constituted a patient-protective PDAC-associated desmoplastic phenotype [214]. In addition, integrins also play a role in regulating cancer stem cell properties leading to metastasis as well as resistance to tyrosine kinase inhibitors in PDAC [215].

Focal adhesion kinase (FAK) is a ubiquitously expressed non-receptor tyrosine kinase that regulates integrin-mediated cell-extracellular matrix signalling, and its phosphorylation and activation is dependent on SRC. The SRC-FAK multi-protein complex localises at cell-matrix attachment sites and influences several downstream pathways including cell motility, migration, invasion, survival, immunosuppression and apoptosis [177, 216-218]. The mechanisms involved are complex but often include the regulation of downstream effectors, including TGF- β , as well as regulators of ERK, Jun kinase (JNK) and Rho signalling pathways [182, 219-223]. FAK is overexpressed in a variety of cancers including PDAC, and overexpression is associated with poor prognosis [218, 224]. It has recently been shown that FAK plays an important role in regulating pro-inflammatory pathway activation and cytokine production during wound healing [184, 217, 224-227]. In PDAC specifically, FAK activity has been shown to correlate with high levels of fibrosis and poor CD8+ cytotoxic T-cell infiltration, making it a promising target to overcome the highly fibrotic and immunosuppressive nature of PDAC [217, 228].

SRC-family kinases (SFKs) not only promote cell-matrix adhesion turnover through FAK, but also regulate Rho family of small GTPases, in particular RhoA and Rac1 activation [229, 230]. Rho GTPases are often hijacked by cancers because they regulate diverse cellular processes that are important for tumour growth and metastasis including cytoskeletal dynamics, motility, contractility, cell polarity, membrane transport, gene transcription, as well as regulating the interaction between stromal cells and cancer cells [149, 231-236]. SFKs control the regulatory molecules of Rho GTPases (guanine nucleotide exchange factors (GEFs), GTPase-activating proteins (GAPs) and guanine dissociation inhibitors (GDIs), and it is the tight regulation and extensive crosstalk between SRC/FAK and SRC/RhoA/Rac1 that controls integrin-mediated cell-adhesion and migration [237-239]. We have recently reviewed the role of Rho-associated kinase signalling in cancers including PDAC [231, 232].

PI 3-kinase (PI3K) signalling is another relevant, tumour-promoting and potentially druggable effector network activated through FAK/SFK [240-242].

Activated PI3K phosphorylates phosphatidylinositol 4,5-bisphosphate (PIP₂) to produce PIP₃, and this process is negatively regulated by PTEN [243]. Activation of PIP₃ can then further activate Akt (Akt activation occurs in ~59% PDAC samples [244]) and additional downstream targets such as Bcl-2, Mdm2, GSK3 β , NF- κ B and mTOR [240, 245], ultimately promoting cancer cell survival, growth, and motility and inhibiting apoptosis [240, 243, 246, 247]. The PI3K-Akt-mTOR pathway is also responsible for controlling cellular metabolism. Oncogenic K-Ras can enhance the activity of the metabolic enzyme ATP citrate lyase in an Akt-dependent manner leading to histone acetylation and alteration of the acetyl-CoA pool, subsequently leading to changes in gene expression, DNA damage response and DNA replication [248]. The PI3K/Akt pathway can also inhibit glucose metabolism by blocking glycogen synthase kinase 3 β and can alter glucose uptake by mediating expression of glucose transporters such as GLUT1 [248, 249]. Furthermore, Akt signalling is present in preneoplastic lesions during pancreatic carcinogenesis induced by mutated Kras, and is associated with progression towards higher grade tumours and poorer patient survival [242, 250-252].

1.3.2 Molecular and genomic aberrations of the SRC signalling axis in Pancreatic Cancer: Implications for therapeutic targeting

Historically, the documented cases of activating SRC mutations are rare, with only one major study in colon cancer documenting 12% of cases with a truncating mutation at codon 531 [253], which when functionally validated, was shown to lead to increased SRC specificity and transformation of NIH 3T3 cells. Despite this, other studies using larger colon cancer populations document no such mutations [254, 255]. In addition, no such mutations have been documented for SRC-implicated cancers, such as haematological malignancies [256]. In PDAC specifically, examination of multidimensional publically-available cancer genomics datasets (TCGA, PanCan Atlas and QCMG cohorts) revealed that SRC mutations occur at a frequency of less than 2% (Figure 1.5B) [257, 258], indicating that aberrant intra-tumoural SRC activity occurs through constitutive activation of SRC, or by changes in the levels of regulators of SRC and amplification of downstream signalling

pathways [256, 259-261]. Importantly frequency differences between datasets are due to limited data availability.

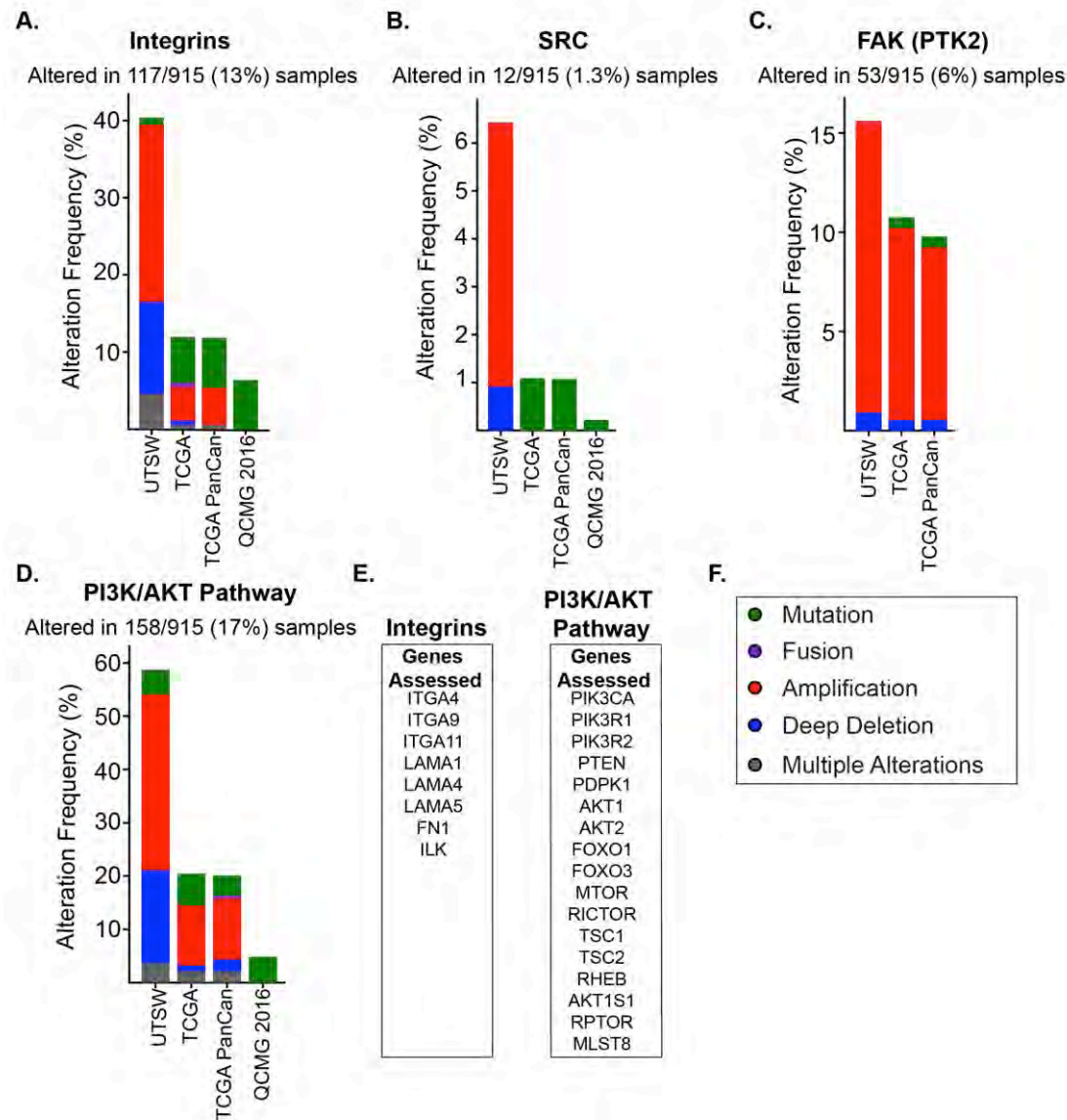


Figure 1.5 Frequency of (A) Integrin, (B) SRC, (C) FAK and (D) PI3K/AKT pathway genetic alterations in publically-available pancreatic cancer genomics datasets (The Cancer Genome Atlas (TCGA), PanCan Atlas, University of Texas South Western Medical Centre (UTSW) and Queensland Centre for Medical Genomics (QCMG) cohorts) [257, 258]. (E + F) Genes used to define the integrin and PI3K/AKT pathways, respectively. (F) Alterations include mutations (green), fusions (purple), amplifications (red), deep deletions (blue) and multiple alterations (grey). Taken from Parkin *et al.* 2019 [186].

Integrins are key regulators of SRC signalling, and are also deregulated in cancers, but are rarely mutated. Several cancers including glioblastoma, show modifications of the integrin pattern to be associated with tumour progression and poor patient survival, including $\alpha 6\beta 4$, $\alpha 6\beta 1$, $\alpha v\beta 6$ and $\alpha v\beta 3$ [262]. An early sequencing study demonstrated a positive association between mutations in subunit $\alpha 7$ (encoded by *ITGA7* gene), identified in 57% of prostate cancers, and increased cancer recurrence [263]. The mutation also occurred in 21% of hepatocellular carcinomas and 83% of glioblastomas, as well as leiomyosarcomas [263]. Decreased integrin expression has also been correlated to cancer progression. In mesothelioma reduced expression of *ITGA7* associated with promoter methylation and was identified as an important mechanism for the aggressive migratory transformation of mesothelioma [264, 265]. Similar results have also been seen with $\alpha 2\beta 1$ in breast cancer, and $\alpha 6\beta 4$ / $\alpha 6\beta 1$ in esophageal carcinoma [200]. In PDAC, early sequencing studies identified genetic alterations in the integrin signalling pathway (*ITGA4*, *ITGA9*, *ITGA11*, *LAMA1*, *LAMA4*, *LAMA5*, *FN1* and *ILK*) in 67% of tumours [44]. However, these alterations appear less frequent (67% versus 13%) when compared to the findings of the TCGA, UTSW, ICGC and QCMG [257, 258, 266] (Figure 1.5A). This inconsistency may be explained through the study design of Jones *et al.* where only small cohorts derived from cell lines (commercial and patient-derived; $n=24$), and xenograft models ($n=90$) were used to analyse the mutational cancer landscape. Recent findings suggest that molecular landscapes of patient-derived models may diverge from their parental tumours during long-term propagation [267]. More recently, the integrin $\beta 4$ subunit was found to be commonly over-expressed in PDAC and is an adverse prognostic marker, however isn't commonly mutated [268]. An alternate mechanism involving a mutation in *TP53* is thought to promote integrin $\alpha 6\beta 4$ -mediated tumour cell survival [268].

In addition, recent large-scale, pan-cancer proteogenomic studies have identified molecular alterations in several SRC effector networks including PI3K/Akt/mTOR and FAK [224, 269-271]. Of the >7000 tumours examined, 63% harboured non-silent somatic mutations or copy number alterations within the PI3K/AKT/mTOR pathway [270]. In PDAC specifically, ~17% of

tumours carried alterations, the majority of which involved gene amplification, and this finding is consistent across multiple cohorts [257, 258] (Figure 1.5D). The *PI3KCA* gene mutations present in 3–5% of pancreatic cancer patients can act as activating mutations initiating pancreatic tumour formation [272]. Further, inactivating aberrations in PTEN (negative regulator of PI3K/PI3K pathway) occur in up to 70% of human PDAC, and have been shown to activate the tumour-promoting stromal and immune cell components that shape the PDAC tumour microenvironment [273]. FAK is also frequently overexpressed and deregulated in PDAC, with genomics alterations occurring at a frequency of ~6%, the majority of which are gene amplifications (Figure 1.5C) [257, 258]. FAK inhibitor monotherapy has shown mixed clinical efficacy in mesothelioma tumours that harbour loss of specific tumour suppressive signals, such as merlin (encoded by *NF2* gene; [274]). Although mutations at the *NF2* locus are rare (~10%) in human PDAC [3, 47], merlin expression is lost in >40% of PDAC, and is negatively correlated with tumour stage, regional lymph node metastasis and differentiation [275]. Assessment into the efficacy of FAK-inhibition in the context of Merlin loss, and combined with additional biomarkers, in PDAC may be of interest.

A personalised treatment strategy using pharmacological inhibition of SRC, SRC-associated regulators or downstream targets, in tumour subtypes carrying these aberrations, could be beneficial and remains to be examined. Currently there are no FDA-approved prognostic or predictive biomarkers for PDAC [276]. Importantly, moving forward, the integration of DNA copy-number alterations, methylome, mRNA and protein, metabolomics and clinical information may help to further delineate the extent of SRC signalling deregulation in pancreatic and other cancers, and could potentially lay the foundation for more accurate and rapid implementation of therapeutic inhibitors of SRC as personalised cancer therapeutics.

1.3.3 Targeting SRC kinase in pancreatic cancer

Recognising the established role of SRC in cancer initiation and progression led to the rapid development of several small molecule inhibitors (Table 1.1) [277]. Inhibitors including bosutinib, saracatinib and dasatinib have shown

measurable anti-tumour activity in several *in vitro* and *in vivo* models of cancer [188, 194, 197, 278-280]. Dasatinib is a potent adenosine triphosphate-competitive inhibitor of SRC and Abl kinases, as well as c-KIT, PDGFR and ephrin-A2, which works by competitive inhibition of the ATP binding site. Its activity results in inhibition of cell proliferation (causing G₀/G₁ arrest), as well as inhibition of cell adhesion, migration, invasion and tumour metastasis [184, 194, 281-285]. These results were particularly promising in models of advanced PDAC, presenting dasatinib as an encouraging anti-metastatic agent for this disease [177, 197, 286]. Despite the encouraging clinical results for the use of dasatinib as a standalone therapy in CML, clinical findings with dasatinib or alternative SRC/ABL-kinase inhibitors (saracatinib, bosutinib) [287, 288] in PDAC were predominately negative, partially due to poor drug tolerance, but also due to the highly aggressive and adaptable nature of this disease to single-agent targeted therapies and rapid onset of resistance [194, 280, 289-298]. Moreover, the presumption that these biologic agents would significantly improve survival in non-stratified cohorts, particularly in PDAC, is inconsistent with prior preclinical data, which suggests that therapeutic response may correlate with biological markers. For example, Saracatinib effectively inhibited growth of three patient-derived pancreatic xenografts characterised by decreased FAK, paxillin and STAT3 signalling [278]. In addition Bosutinib sensitivity was shown to correlate with caveolin 1 expression [280], and clinical trial data indicate that selected individuals experienced durable and sustained responses to dasatinib treatment [245, 292, 293]. Collectively, these data highlight the need for further investigation into the biological 'omics' of patients prior to treatment in order to identify the mechanistic rationale that can predict which patients may most optimally respond to SRC-based therapies.

Given that in pancreatic (and other) cancers, multiple mechanisms often work in synchrony to lead to chemoresistance, considering more tailored treatment combinations that involve inhibition of SRC, other molecular targets, plus tumour-debulking cytotoxic agents may present a more effective approach. The rationale behind this includes the finding that SRC is associated with increased chemoresistance in PDAC, and that inhibition of SRC can

overcome resistance to gemcitabine [199, 279, 285]. Furthermore SRC-inhibition is associated with decreased thymidylate synthase, which in turn is associated with the reversal of 5-fluorouracil resistance [279]. Recent data indicate that SRC inhibition can further lead to the reversal of epithelial-to-mesenchymal transition (EMT) in drug-sensitive PDAC cells through repression of Slug [299]. SRC inhibition can also increase oxaliplatin activity, and inhibit oxaliplatin-induced SRC activation [279]. When dasatinib was combined with gemcitabine in locally advanced pancreatic cancer, there was no improvement in progression-free or overall survival (NCT01395017) (Table 1.1) [300]. However, newer combination chemotherapy regimens, such as FOLFIRINOX [8], lead to significantly higher response rates and disease control in patients with metastatic disease. Hence, a potentially more appropriate future study design may involve sequential administration of dasatinib as “maintenance” therapy, after optimal disease control is achieved with this highly active chemotherapy regimen (similar to successful previous studies utilising sunitinib [294]), or alternatively a ‘priming regimen’ could be applied [149], thus limiting toxicity associated with chronic dosing.

The SRC signalling network is also known to play an important role in the movement and infiltration of immune cells into the tumour. In addition SRC activation is mediated by inflammatory cytokines within the tumour microenvironment, whilst also being involved in inter-cellular communication [188]. Although there is minimal evidence in pancreatic cancer, research into other solid cancers including melanoma, sarcoma, colon and breast cancer demonstrates that tyrosine kinase inhibitors such as dasatinib (a pan-Src/Bcr-Abl kinase inhibitor) have potent immunomodulatory functions [301], and consequently may present a promising adjunct to immunotherapy. Dasatinib may enhance cellular immunity through a number of mechanisms including T cell immunomodulation, whereby treatment has been shown to reduce the number of intra-tumoural regulatory T cells, in various solid tumour mouse models and haematological malignancies, promoting natural killer (NK) cell expansion and differentiation [301-303]. In chronic myeloid leukaemia (CML) cancer models, dasatinib may increase the number of Granzyme B (GrB) expressing memory CD4⁺ T cells (GrB+CD4⁺ T cells) and promote their

differentiation into Th1-type T cells, which in turn produce interferon-gamma, a powerful tumour-suppressive cytokine [304]. Moreover, in CML and head and neck cancers, dasatinib has been shown to reduce the number of myeloid-derived suppressor cells (MDSCs), and induce anti-inflammatory macrophages (defined by increased production of IL-10, decreased production of IL-6, IL-12p40 and TNF- α , and high expression of LIGHT, SPHK1 and arginase 1), via the inhibition of salt-inducible kinases [303, 305, 306]. Surprisingly, the potential in combining the immunomodulatory effects of SRC-inhibitors with other immunomodulatory therapies hasn't been extensively studied. Pre-clinical data in head and neck squamous cell carcinoma (HNSCC) showed inhibition of tumour growth, suggesting that combining dasatinib with anti-CTLA4 immunotherapy may be a viable treatment approach [307]. However in a clinical study of gastrointestinal stromal tumours (GIST), dasatinib and anti-CTLA4 antibody ipilimumab, were well tolerated yet the combination was not synergistic, potentially due to the lack of a biomarker-driven approach [308]. At present there is only one phase II trial underway examining the combination of dasatinib and anti-PD-1 therapy nivolumab in non-small cell lung cancer (NCT02750514). However due to the strong immunomodulatory effects of SRC inhibition seen *in vivo*, assessment of synergistic combinatorial therapies including dasatinib and other immunomodulatory drugs is warranted. This could be particularly relevant in pancreatic cancer where immunotherapy provides no therapeutic benefit as a result of the immunosuppressive microenvironment that defines these tumours [309].

Combining SRC-inhibition with additional targeted therapies is another potentially beneficial approach aimed at enhancing anti-tumour efficacy, while minimizing inherent and acquired resistance. This strategy has already shown promise in several cancers [310]. Almost 30 years ago, SRC tyrosine kinase and EGFR were found to synergistically stimulate EGF-induced mitogenic cellular responses in fibroblast cultures [311]. Since then, SRC has been shown to directly phosphorylate EGFR and may also mediate transactivation of EGFR by other receptor signalling pathways [175, 312, 313]. The EGF-mediated RAS/RAF/MEK/ERK pathway (Figure 1.4) is one of the major

players in the regulation of tumour growth, survival, proliferation, inhibition of apoptosis and autophagy [314, 315], with deregulated activation associated with poor prognosis in solid tumours [316], including PDAC [317].

Targeting this key pro-tumourigenic molecular pathway has been explored in PDAC with the combination of standard therapy gemcitabine and small molecule EGFR inhibitor erlotinib revealing a modest but significant improvement in patient survival in advanced disease [71, 318], particularly in KRAS wild-type tumours [73, 74]. Dasatinib has also been combined with the EGFR inhibitor, erlotinib in NSCLC, resulting in two partial responses, and a disease control rate of 63% [319]. Collectively, these studies highlight the potential utility of this treatment combination when applied in small, but potentially well-defined subgroups of patients with pancreatic cancer. Moreover, the combination of dasatinib, erlotinib and gemcitabine showed significant synergy in preclinical studies, with potent inhibition of cancer cell proliferation, viability and xenograft tumour growth [320]. The triple combination was also shown to overcome constitutive activation of STAT3-mediated signalling, a key player in PDAC chemoresistance [147, 196, 320, 321], and was shown to be well tolerated, with promising preliminary clinical activity in advanced pancreatic cancer [322]. The potential of this therapeutic combination also provides support for the development of a novel multikinase inhibitor (SKLB261) that potently inhibits EGFR, SRC and VEGFR2 kinases. In the context of PDAC, this inhibitor effectively inhibited cancer cell proliferation, migration, invasion, and induced apoptosis *in vitro*, and demonstrated potent anti-angiogenic effects in pancreatic cancer xenografts, with stronger anti-tumour activity when compared to dasatinib, erlotinib and gemcitabine monotherapies [323].

Dual SRC/MEK blockade using saracatinib/selumetinib presents another interesting therapeutic strategy shown to induce apoptosis of dormant cancer cells and limit tumour recurrence in breast cancer models [324] that may potentially be applied to other solid cancers, including PDAC. Dual targeting of SRC and the protein tyrosine phosphatase SHP-2, required for full activation of the RAS/ERK1/ERK2 pathway, has also shown promise in *in vitro* and *in vivo* models of pancreatic cancer. Combined SRC/SHP-2

inhibition resulted in a supra-additive loss of phosphorylation of Akt and ERK-1/2, and led to an increase in apoptotic marker expression in L3.6pl and PANC-1 pancreatic cancer cells. The combination also led to a reduction in cell viability, adhesion, migration and invasion *in vitro* and reduction in pancreatic tumour formation *in vivo*, using the L3.6pl orthotopic model [325]. The central role for SHP-2 in oncogenic KRAS-driven tumours has been therapeutically exploited in other contexts, with most recent data demonstrating potent synergistic anti-tumour effects of combined SHP-2 and MEK inhibition in multiple cancer types [326], including genetically-engineered models of KRAS-mutant lung and pancreatic cancer [65]. Further exploration of these targeted therapeutic combinations, particularly in molecularly enriched patient subsets, is warranted, with early dose-finding clinical studies underway (NCT03114319, NCT03634982; Table 1.1).

Table 1.1: Clinical trials in pancreatic cancer associated with targeting SRC kinase.

Signalling Pathway	Agent	Molecular Target	Cancer Type	Phase	Combination Therapy	Findings/Status	Protocol ID	Reference
SRC	Dasatinib	SRC, Abl, PDGFR	Metastatic Pancreatic Cancer	II (Single Arm)	Monotherapy	Completed: No significant clinical activity measured ($n=34$); 1 durable sustained response on therapy (>20 months), plus 6 long-term survivors noted (>20 months)	NCT00474812	[292]
			Metastatic Pancreatic Cancer	II (Single Arm)	Monotherapy	Terminated: Due to toxicity ($n=7$)	NCT00544908	
			Molecular Analysis for Therapy Choice (MATCH), Multiple Solid Cancers incl Metastatic or Recurrent Pancreatic Cancer	II (Personalised)	Monotherapy-Targeted against <i>DDR2</i> mutations	Recruiting	NCT02465060	
			Metastatic Pancreatic Cancer	I	Gemcitabine	Terminated: Due to low accrual	NCT00598091	
			Locally-Advanced Pancreatic Cancer	II (Randomised)	Gemcitabine	Completed: No significant improvement in PFS, OS in unselected patient cohort ($n=202$). High dose regimen utilised leading to significant adverse events	NCT01395017	[297]
			Resected Pancreatic Cancer (Adjuvant)	II (Randomised)	Gemcitabine	Completed: Awaiting results	NCT01234935	
			Advanced Pancreatic Cancer	I	Erlotinib + Gemcitabine	Active, not recruiting. Well tolerated. Early clinical activity with reported OS 8 months and disease control rate 69% vs historical control OS 5.9 months and 58% respectively. Small patient cohort ($n=19$)	NCT01660971	[322]
			Metastatic Pancreatic Cancer	II (Single Arm)	mFOLFOX6	Active, not recruiting ($n=38$)	NCT01652976	[279]
	Bosutinib	SRC, Abl	Advanced Solid Cancers (incl Pancreatic)	I	Monotherapy	Completed: MTD determined; no significant efficacy observed	NCT00195260	[296]
			Resected Pancreatic Cancer	I	Gemcitabine	Terminated: Due to slow accrual	NCT01025570	
			Locally Advanced/Metastatic Solid Cancers (incl Pancreatic)	I/II	Capecitabine	Terminated: Tolerated, limited efficacy overall ($n=5$ pancreatic cancer patients)	NCT00959946	[298]
	Saracatinib (AZD0530)	SRC	Recurrent Metastatic Pancreatic Cancer	II (Single Arm)	Monotherapy	Completed: No objective response observed in unselected cohort ($n=19$)	NCT00735917	[280]
			Advanced Pancreatic Cancer	I/II (Single Arm)	Gemcitabine	Completed: Well tolerated but no improvement in efficacy over Gemcitabine alone	NCT00265876	[295]
			Advanced Solid Cancers (incl Pancreatic)	I	Cediranib (VEGFR1 inhibitor)	Completed: Tolerated. Demonstrated stable disease as best response in 22/35 evaluable patients	NCT00475956	[327]
	TNO155	SHP-2	Advanced Solid Cancers	I	Monotherapy	Recruiting	NCT03114319	
	RMC-4630		Advanced Refractory Solid Cancers	I	Monotherapy	Recruiting	NCT03634982	

1.3.4 Modulation of the upstream and downstream SRC-signalling components in pancreatic cancer

Modulation of the downstream mediators and interacting partners of SRC represents another potentially viable therapeutic approach that is increasingly being investigated (Table 1.2). Inhibition of FAK decreased PDAC cell growth and migration *in vitro* [328, 329], and limited pancreatic tumour progression *in vivo*, doubling the survival in the p48-Cre;LSL-KrasG12D;Trp53flox/+ (KPC) mouse model of PDAC [217, 330, 331]. FAK inhibitor VS-4718 treatment further reduced tumour fibrosis and numbers of infiltrating immunosuppressive populations of myeloid-derived suppressor cells (MDSCs), tumour-associated macrophages (TAMs) and regulatory T cells, sensitising the KPC mouse model to checkpoint immunotherapy [217]. Most recent work already points to potential mechanisms of treatment resistance associated with prolonged FAK inhibition, mediated through a feedback loop involving decreased stromal TGF- β and activation of STAT3 signalling, which after a period of disease stabilisation, leads to enhanced PDAC cell proliferation and tumour growth [332]. Nonetheless, with significant promising pre-clinical data, several trials are now focused on combining FAK-inhibition with immunotherapies such as trametinib, and pembrolizumab in PDAC (NCT02428270 [333], NCT02758587) (Table 1.2). In addition, FAK inhibitors such as PF-00562271 are well tolerated and hence show significant promise for the treatment of PDAC [274, 334]. Promising pre-clinical data in malignant pleural mesothelioma, ovarian and other solid tumours suggests that therapeutic responsiveness to FAK inhibition may be guided by Merlin loss [274, 335, 336], or E-cadherin levels [337]. This is supported by positive data from two phase I studies (NCT01138033, NCT01938443) in advanced solid tumours, where improved response to the FAK inhibitor GSK2256098 was observed in Merlin-negative mesothelioma [274, 338]. However, findings of a recent prospective phase II trial in malignant pleural mesothelioma (MPM; COMMAND study), has since failed to confirm merlin expression as a predictive biomarker of efficacy to a different FAK inhibitor, defactinib [339]. The observed discordance in the findings of these studies could potentially be due to a substantial difference in the cut-offs utilised to define Merlin-negative

or Merlin-low tumour status, with the Soria *et al.* [274] and Mak *et al.* [338] trials more stringently defining Merlin-negative cancers. These studies also differ in terms of their patient selection and cohort size, with the larger COMMAND trial [339] being a prospective study examining defactinib efficacy as a maintenance therapy in chemo-responsive advanced MPM, whereas the smaller phase I and Ib studies of the GSK2256098 compound examined efficacy in advanced chemo-resistant solid tumours, including mesothelioma. Moreover, as defactinib targets both FAK and Pyk2 [340] while GSK2256098 is selective for FAK alone, this difference in target selectivity between the two compounds may potentially lead to divergent antitumour activity, and mechanism of action on tumour cells, as well as the distinct components of the tumour microenvironment. Further assessment into the efficacy of FAK-inhibition in the context of Merlin loss may still be of interest, particularly in pancreatic cancer where it has yet to be examined. Future trials would however need to consider standardisation of the biomarker analysis and interpretation of Merlin-loss, sampling of multiple tumour areas where possible to account for potential intra-tumoural heterogeneity of molecular marker(s) of interest, and incorporation of additional promising biomarkers to aid identification of clinical responders to FAK-inhibitor based treatment regimens.

Several inhibitors that target Rho GTPase or its downstream effectors including Rho-associated kinases (ROCK) have shown anti-tumour activity in preclinical models, which we have reviewed previously [231, 232]. Most recently, fasudil, an inexpensive, off-patent ROCK inhibitor, may present a promising new treatment approach for PDAC. It has recently been shown that using a short-term 'priming' treatment approach to inhibit ROCK signalling can reduce tissue stiffness, improve vascular patency, increase tumour perfusion, decrease *in vivo* primary tumour growth, metastasis and improve response to standard of care therapy [114, 149], similarly to chronic fasudil treatment [233]. Newer ROCK inhibitors (such as ripasudil, CCT129254 or AT13148), are currently being trialled, and utilise a similar 'priming' [149, 236] or intermittent regime [341]. The rationale behind this novel treatment scheduling involves modulating or "loosening" the extracellular matrix, without completely ablating the stroma, via ROCK inhibition, prior to chemotherapy administration

in order to improve chemotherapy drug perfusion and reduce toxicity [149]. Potentially, this regime could be applied for the use of other stromal-based therapies in PDAC as well as other stromal-driven cancers.

Furthermore, there has been significant research dedicated to targeting the PI3K/AKT signalling pathway in PDAC due to its role in cell metabolism, cell cycle, protein synthesis and apoptosis [342]. Rapamycin, an mTORC1 inhibitor showed promising preclinical results in PDAC, significantly halting disease progression in PI3K/AKT-activated tumours [343]. However clinical data failed to demonstrate a benefit, particularly when administered as monotherapy (Table 1.2) [344]. This may further be explained by mTORC1 being involved in complex negative feedback loops that restrain upstream signalling. For example, inhibition of mTORC1 drives activation of PI3K-, AKT- or ERK pathways [345], which in turn limits the efficacy of mTORC-inhibitors as targeted therapies [346]. More recently developed dual ATP-competitive agents that target mTORC1/mTORC2 have shown favourable results [347, 348] with AZD2014 effectively inhibiting PDAC cell division (G1 arrest), proliferation, and invasion *in vitro* (159, 161) and prolonging survival in the KPC mouse model of PDAC [252, 348, 349]. However there is still some debate as to whether blocking mTORC1/2 leads to the adaptive activation of the PI3K-AKT pathway [349], and consequently whether multiple targeting of this network is required to effectively interfere with both branches of adaptive signalling and to elicit a durable therapeutic response.

The combination of cyclin-dependent kinase (CDK) inhibitors with PI3K pathway inhibition has been shown to inhibit tumour growth and metastasis in a variety of cancers including PDAC [5, 350], with a need for molecular stratification into responsive subtypes [83]. Furthermore, multi-target, unique formulations, including SM-88, a combination of a tyrosine derivative (D,L-alpha-metyrosine), mTOR inhibitor (sirolimus), CYP3a4 inducer (phenytoin) and oxidative stress catalyst (methoxsalen), are showing encouraging efficacy in early-stage trials, particularly in patients with advanced pancreatic cancer (Table 1.2) [351, 352], who have frequently exhausted all options. There is also ample evidence supporting the combination of PI3K/AKT/mTOR inhibitors with tyrosine kinase inhibitors (TKIs). Cancers with

active/overexpressed TKIs often display resistance to TKIs through PI3K signalling [353]. In addition, targeting RAS/RAF/MEK/ERK pathway in combination with PI3K/AKT/mTOR inhibitors is another promising strategy because there is significant stimulatory cross-talk [353]. Synergy has previously been shown between a MEK-inhibitor and PI3K/mTOR-inhibitor in a lung cancer model, where inhibition of MEK/ERK was shown to stabilise BIM, and PI3K/AKT inhibition upregulated PUMA via FOXO, all of which are key mediators of apoptosis [354, 355]. Inhibition of the MAPK pathway has also been shown to associate with increased PI3K pathway activity [356, 357]. This therapeutic combination could also be beneficial in PDAC, as an alternative approach for inhibiting oncogenic Kras, which is located upstream of MEK/ERK and PI3K. Whilst combining MEK inhibitors with alternative pathway modulators such as PI3K or SRC has shown early promise [357-359], these combinations, including addition of chemotherapies, may require an alternative, intermittent dosing regimen design due to issues with chronic administration [360-362], and are yet to be systematically examined in PDAC. Preclinical data suggest that therapeutic efficacy may be dependent on PDAC subtype, as well as MEK activity and expression [155], with further investigation, including determination of biologically effective dose(s) of targeted therapies, testing and implementation of alternative dosing regimens, warranted.

Given the importance of integrin/SRC/FAK signalling in diverse cancer types, significant research has also gone into targeting molecules upstream of SRC, including integrins, which critically modulate extracellular matrix mechanics and cytoskeleton stability, stellate cell activation [363], cancer cell survival and angiogenesis [200] and most recently, production of tumour-promoting cytokines and chemokines [364]. With each integrin comprising an α and β transmembrane subunit, most studies have focused on testing $\alpha v \beta 1$, $\alpha v \beta 3$, $\alpha v \beta 5$ integrin antagonists, the most promising of which is cilengitide. Cilengitide is an RGD (arginine-glycine-aspartic acid) peptide which is selective against $\alpha v \beta 3$, $\alpha v \beta 5$ integrins [365]. Cilengitide was shown to have anti-tumour activity in recurrent and newly diagnosed glioblastoma [366-369], however further phase III studies showed no significant differences in median

overall survival [368], with similar negative findings in PDAC when examined in all-comers [370]. In contrast, results from a phase I study suggest promising early signals of activity with cilengitide and chemoradiotherapy combination in advanced non-small cell lung cancer [371]. Clinical trials of further integrin antagonists including intetumumab, volociximab, ATN-161 (Ac-PHSCN-NH₂ peptide), abituzumab and etaracizumab, all of which are antibodies or peptide mimetics, has largely yielded no improvements in patient progression-free or overall survival (Table 1.2) [372, 373], however specific studies in colon cancer suggest that their anti-tumour activity may be linked to the presence of a biomarker [374], and alternatively, may specifically inhibit progression of bone-associated metastases in prostate cancer [375]. Adding to the complexity, anti-integrin compounds may increase intra-tumoural hypoxia, leading to increased tumour growth, metastasis and chemoresistance in certain settings [376, 377], process that is dose and/or tumour type dependent [206, 378]. Reynolds et al. showed that in fact, low (nanomolar) concentrations of $\alpha_v\beta_3$, $\alpha_v\beta_5$ inhibitors can paradoxically promote VEGF-mediated angiogenesis by altering $\alpha_v\beta_3$ integrin and VEGFR-2 trafficking, stimulating cancer growth [378].

Hence, more recent research efforts have focussed on utilising these agents as part of 'vascular normalisation', whereby improved tumour blood flow increases drug delivery [379]. However as this approach is highly time- and dose-dependent, its clinical implementation may be challenging [380]. Specifically, in pancreatic cancer, cilengitide has been effectively applied in combination with chemotherapy using a strategy called 'vascular promotion', aimed at improving delivery of chemotherapy to the tumour [381]. Although the combination has yet to be trialled in the clinic, pre-clinical evidence is positive. Co-administration of low dose therapy regimen of cilengitide and verapamil increased tumour blood flow and perfusion, promoted gemcitabine delivery inside growing pancreatic tumours, ultimately leading to reduced primary tumour growth, metastasis and significantly improved survival in multiple models of PDAC with minimal side effects [381]. This dual therapy also increased levels of proteins involved in active transport of gemcitabine into cells, and production of active metabolites, further enhancing gemcitabine

potency. Vascular promotion is also associated with reduced hypoxia and desmoplasia, salient features of PDAC [381]. In addition, volociximab, an integrin $\alpha 5\beta 1$ blocking antibody, has completed phase II trials in combination with gemcitabine in metastatic pancreatic cancer, with results pending (NCT00401570). Of note, mutant P53 has been shown to regulate $\alpha 5\beta 1$ signalling and EGFR, which suggests there may also be potential for molecular stratification [382].

Another major advance in extracellular matrix-targeting is the development of agents that break down hyaluronic acid (HA). HA is a large, linear, glycosaminoglycan that plays an important structural role in the extracellular matrix, and accumulates in conditions involving rapid and invasive cell division, including cancer. HA regulates interstitial gel fluid pressure within tumours, often impacting on drug delivery. Pegylated recombinant human hyaluronidase (PEGPH20) and 4-methylumbelliferone are two key examples of compounds that inhibit and/or break down HA. Of note, PEGPH20 has already shown significant promise in PDAC. HA degradation following PEGPH20 treatment has been shown to normalise interstitial fluid pressures and re-expand the microvasculature by increasing the diameter but not the total number of blood vessels within PDAC tumours [143]. This in turn significantly improved chemotherapeutic response in the KPC murine model of PDAC, resulting in a near doubling of overall survival [143, 144]. Clinical studies of PEGPH20 are also promising with Phase II data already demonstrating significant efficacy of this agent when combined with chemotherapy, effect particularly prominent in patients with HA-high tumours [53], highlighting the potential utility of intratumoural HA as a predictive biomarker of response [53, 383, 384]. Favorable results are particularly observed when PEGPH20 is combined with gemcitabine and Abraxane [53, 385, 386], whereas FOLFIRINOX in contrast, may be better utilised in other settings [387, 388]. Development of a liquid biopsy-based companion diagnostic for selecting potential PEGPH20 responders is also underway [389], along with innovative MRI-based imaging methodologies to detect early responders to stroma-directed drugs [390]. Consequently several Phase II/III clinical trials are now investigating further the clinical efficacy of PEGPH20, in

combination with standard of care chemotherapies (Table 1.2) (NCT02487277, NCT02715804), or immune checkpoint inhibition (NCT03481920; NCT03634332, NCT03193190) in HA-high molecular subgroups of PDAC [53, 391]. These encouraging early clinical findings highlight the potential of stromal components as viable therapeutic targets, supporting further clinical development of PEGPH20 as well as detailed exploration of new biomarker-driven therapeutic combinations utilising this agent.

Table 1.2: Clinical trials in pancreatic cancer associated with targeting downstream mediators and interacting partners of SRC kinase.

Signalling Pathway	Agent	Molecular Target	Cancer Type	Phase	Combination Therapy	Findings/Status	Protocol ID	Reference
EGFR	Erlotinib	EGFR	Advanced Pancreatic Cancer	III	Gemcitabine	Completed: Modest significant improvement in OS (0.33 months) ($n=569$). Association between rash and a better outcome was observed.	NCT00026338	[318]
			Locally Advanced Pancreatic Cancer	III	Gemcitabine	Completed: No significant improvement in OS in combination arm (1.7 months; $P=0.09$; $n=449$)	NCT00634725	[392]
			Advanced Pancreatic Cancer	II (Single Arm)	Gemcitabine	Completed: Well tolerated, no significant improvement in PFS as primary measure in unselected cohort ($n=30$)	NCT00810719	[393]
			Advanced Pancreatic Cancer	III	Cross-over design (Gemcitabine vs Capecitabine)	Completed: Well tolerated, comparable efficacy between the two Erlotinib-based regimens ($n=274$). KRAS wild-type status was associated with an improved overall survival (HR 1.68, $P=0.005$).	NCT00440167	[71, 394]
			Resected Pancreatic Cancer (Adjuvant)	III (Open label)	Gemcitabine	Completed: No improvement in patient survival observed ($n=436$) and occurrence of rash was not associated with response	CONKO-005	[69]
			Metastatic Pancreatic Cancer	II (Single Arm)	Gemcitabine	Completed: Improved survival in rash-positive patients, comparable 1% survival rate to FOLFIRINOX	NCT0172948	[72]
	Cetuximab	Chimeric monoclonal IgG ₁ antibody against extracellular III domain of EGFR	Advanced Pancreatic Cancer	III	Gemcitabine	Completed: No significant improvement in survival ($n=745$) and no association with EGFR IHC	NCT00075686	[395]
	Nimotuzumab	Humanized IgG ₂ mAb against extracellular III domain of EGFR	Advanced Pancreatic Cancer	IIb (Randomised)	Gemcitabine	Completed: Safe and well tolerated. One-year OS and PFS were significantly improved ($n=192$). Particularly of benefit in KRAS wild-type patients	NCT00561990	[396]
FAK	PF-00562271	FAK	Advanced Solid Cancers (incl Pancreatic)	I	Monotherapy	Completed: Tolerated, MTD established. ($n=99$; 14% pancreatic)	NCT00666926	[334]
	VS-4718		Advanced Pancreatic Cancer	I	Gemcitabine/ Nab-paclitaxel	Terminated: Company de-prioritized drug development	NCT02651727	
	Defactinib		Molecular Analysis for Therapy Choice (MATCH), Multiple Solid Cancers (incl Metastatic/ Recurrent Pancreatic Cancer)	II (Personalised)	Monotherapy- Targeted against NF2 inactivation	Recruiting	NCT02465060	

	GSK2256098		Advanced Solid Cancers (incl Pancreatic)	I/II	Pembrolizumab (anti-PD1)	Recruiting	NCT02758587	
			Advanced Solid Cancers (incl Pancreatic)	I	Pembrolizumab and Gemcitabine	Phase I Completed (<i>n</i> =17). Well tolerated. Recruiting: Expansion cohort	NCT02546531	[397]
			Recurrent Pancreatic Cancer	II (Single Arm)	Trametinib (MEK1/2 inhibitor)	Completed: No objective response measured in unselected cohort (<i>n</i> =16). 1 patient with <i>KRAS</i> amplification showed stable disease for 5 months after rapid progression on 1st line FOLFIRINOX; Correlative biomarker studies ongoing from collected material	NCT02428270	[333]
Integrin	Cilengitide	Cyclic peptide inhibitor of $\alpha v\beta 3/\alpha v\beta 5$ integrins	Advanced Pancreatic Cancer	II (Randomised, Open label)	Gemcitabine	Completed: Well tolerated, no improvements in OS, PFS and response rate in unselected cohort (<i>n</i> =89)	EMD 121974	[370]
	Volociximab (M200)	Chimeric mAb against human $\alpha 5\beta 1$ integrin	Metastatic Pancreatic Cancer	II (Single Arm, Open label)	Gemcitabine	Completed: Well tolerated, awaiting further results	NCT00401570	[373]
	IMGN388	Human IgG1 anti-integrin Ab conjugated to maytansinoid (DM4)	Advanced Solid Cancers	I	Monotherapy	Completed: Well tolerated, safety data reported on 26 patients; awaiting final results	NCT00721669	[398]
Hyaluronan	PEGPH20	Hyaluronan	Metastatic Pancreatic Cancer	Ib/II (Randomised)	Gemcitabine	Completed: Tolerated combination therapy, with promising early clinical activity, particularly in patients with HA-high tumours (IHC). Phase II terminated due to change in standard-of-care chemotherapy treatment	NCT01453153	[399]
			Metastatic Pancreatic Cancer	II (Randomised, Open Label)	Gemcitabine/ Nab-paclitaxel	Completed: Improved PFS as primary endpoint in the overall cohort (<i>n</i> =279), with the greatest improvement in PFS observed in patients with HA-high tumours (prevalence of 34%)	NCT01839487	[53]
			Advanced Pancreatic Cancer	NA (Non-randomised, Open Label)	Gemcitabine/ Nab-paclitaxel	Recruiting: Interim results indicate adding Rivaroxaban is safe and effectively controls thromboembolic events, with PEGPH20-combination therapy showing encouraging early responses (<i>n</i> =28)	NCT02921022	[386]
			Borderline Resectable Pancreatic Cancer (Neoadjuvant)	II (Single Arm, Open label)	Gemcitabine/ Nab-paclitaxel	Recruiting	NCT02487277	[400]
			Metastatic Pancreatic Cancer	III (Randomised)	Gemcitabine/ Nab-paclitaxel	Recruiting	NCT02715804	
			Locally-Advanced Pancreatic Cancer	II (Single Arm, Open label)	Gemcitabine and radiation	No longer recruiting, no results posted	NCT02910882	

			Metastatic Pancreatic Cancer	I/II	modified (m) FOLFIRINOX	Phase II closed as PEGPH20 with mFFOX caused significantly increased toxicity and decreased treatment duration compared to mFFOX alone	NCT01959139	[387]
			Resectable Pancreatic Cancer (Neoadjuvant)	NA	Cetuximab	Study closed due to slow accrual.	NCT02241187	[401]
			Advanced (Chemotherapy Resistant) Pancreatic Cancer	I	Avelumab	Recruiting	NCT03481920	
			Advanced (Chemotherapy Resistant) Pancreatic Cancer: HA high	II (Single Arm, Open Label)	Pembrolizumab	Not yet recruiting	NCT03634332	
			Metastatic Pancreatic Cancer	Ib/II (Randomised, Open Label)	Atezolizumab	Recruiting	NCT03193190	
Rho/ROCK	AT13148	AGC Kinase	Advanced Solid Cancers	I	Monotherapy	Completed: Tolerable, dose escalation ongoing (n=30), awaiting final results	NCT01585701	[341]
PI3K/Akt Pathway	MK2206	Akt (pan)	Advanced Pancreatic Cancer	I/Ib (Randomised, Open Label)	Dinaciclib (CDK inhibitor)	Completed: results pending	NCT01783171	
			Recurrent Metastatic Pancreatic Cancer	II (Randomised, Open label)	Selumetinib (MEK1/2 inhibitor)	Completed: No improvement in OS, and increased rate of adverse events in experimental arm, compared to mFOLFOX standard therapy (n=137)	NCT01658943	[361]
	Afuresertib (GSK2110183)	Akt (pan)	Advanced Solid Cancers (incl Pancreatic)	I/II (Open Label)	Trametinib (MEK1/2 inhibitor)	Completed: Poor tolerability with daily dosing. Potential for intermittent administration discussed within study	NCT01476137	[362]
	Uprosertib (GSK2141795)	Akt (pan)	Advanced Solid Cancers (incl Pancreatic)	I	Trametinib (MEK1/2 inhibitor)	Completed: results pending	NCT01138085	
	Oleandrin (PBI-05204)	Akt (pan)	Metastatic Pancreatic Cancer	II (Single Arm, Open label)	Monotherapy	Active, not recruiting	NCT02329717	
	AZD5363	Akt (pan)	Molecular Analysis for Therapy Choice (MATCH), Multiple Solid Cancers (incl Metastatic/ Recurrent Pancreatic Cancer)	II (Personalised)	Monotherapy targeted against Akt mutations	Recruiting	NCT02465060	
	Perifosine	Akt (pan)	Advanced Pancreatic Cancer	II (Single Arm, Open label)	Monotherapy	Completed: No results posted	NCT00053924	
			Advanced Pancreatic Cancer	II (Single Arm, Open label)	Monotherapy	Terminated: Significant treatment-related toxicity (n=10). Disease progression noted.	NCT00059982	[402]

	Alpelisib (BYL719)	PI3K α	Advanced Solid Cancers (incl Pancreatic Neuroendocrine Neoplasms)	Ib	Everolimus (mTOR) + Exemestane (Aromatase)	Active, not recruiting	NCT02077933	
			Advanced Pancreatic Cancer	I/Ib (Single Arm, Open Label)	Gemcitabine/ Nab-paclitaxel	Active, not recruiting	NCT02155088	
	Buparlisib (BKM120)	PI3K (pan)	Metastatic Pancreatic Cancer	I (Single Arm, Open Label)	mFOLFOX6	Completed: results pending	NCT01571024	
			Advanced Solid Cancers (incl Pancreatic)	Ib (Single Arm, Open Label)	Trametinib (MEK1/2 inhibitor)	Completed: Long-term tolerability of the combination was challenging, with promising efficacy in select tumour types (ovarian) ($n=113$; 47 patients in the expansion cohort).	NCT01155453	[360]
			Advanced Solid Cancers (incl Pancreatic)	Ib (Single Arm, Open Label)	MEK162 (MEK1/2 inhibitor)	Completed: results pending	NCT01363232	
	Sirolimus (Rapamycin)	mTORC1	Advanced (Gemcitabine resistant) Pancreatic Cancer	II (Single Arm, Open label)	Monotherapy	Completed: well tolerated, marginal efficacy, examined biomarker (p70S6K IHC) did not correlate with activity ($n=31$)	NCT00499486	[344]
			Advanced Pancreatic Cancer	II (Single Arm, Open label)	Monotherapy	Recruiting	NCT03662412	
			Advanced Solid Cancers (incl Pancreatic Ductal and Acinar Adenocarcinoma)	I	Vismodegib (Hedgehog inhibitor)	Suspended: results pending	NCT01537107	
			Advanced Solid Cancers	I	Sunitinib (RTK inhibitor)	Completed: results pending	NCT00583063	
			Advanced Solid Cancers	I	Sorafenib (Raf, VEGFR inhibitor)	Completed: results pending	NCT00449280	
			Metastatic Pancreatic Cancer	I/II (Randomised, Open label)	Metformin	Active, not recruiting	NCT02048384	
	SM-88	Combination: metyrosine-derivative + low-dose sirolimus, phenytoin + methoxsalen	Metastatic (Chemotherapy Resistant) Pancreatic Cancer	II (Randomised)	Monotherapy	Recruiting: Preliminary results are promising, with therapy well tolerated ($n=28$), with a median of 4.3 months of follow-up after treatment initiation, 67.8% still alive (trial ongoing), promising compared with historical data	NCT03512756	[351]

	Temsirrolimus	mTORC1	Metastatic Pancreatic Cancer	II (Single Arm, Open label)	Gemcitabine	Terminated	NCT00593008	
			Advanced Solid Cancers (incl Pancreatic)	I/II (Single Arm, Open label)	Nivolumab	Terminated: Investigator no longer at site to enrol patients or write up data	NCT02423954	
			Advanced Pancreatic Cancer	II (Single Arm, Open label)	Monotherapy	Terminated: Study closed due to significant treatment-related toxicity (n=5). Disease progression noted in 2 patients	NCT00075647	[403]
	Everolimus (RAD001)	mTORC1	Advanced or Metastatic Pancreatic Cancer	II (Single Arm, Open label)	Erlotinib	Terminated: Study closed due to significant treatment-related toxicity (n=15). Lack of objective responses noted. Study suggests activation of negative feedback loops following mTOR inhibition may explain lack of efficacy, and which may require simultaneous inhibition of multiple PI3K pathway components to elicit response	NCT00640978	[403]
			Metastatic (Gemcitabine resistant) Pancreatic Cancer	II (Single Arm, Open label)	Monotherapy	Completed: well tolerated, minimal clinical activity as monotherapy in unselected cohort (n=33)	NCT00409292	[404]
			Advanced or Metastatic Pancreatic Cancer	I/II (Randomised, Open label)	Irinotecan and Cetuximab	Terminated: emergence of FOLFIRINOX and slow recruitment. Triple combination showed similar PFS but increased OS compared to Capecitabine + Oxaliplatin (7.7 vs 4.5 months $P=0.04$) (n=26)	NCT01042028	[405]
			Metastatic Pancreatic Cancer	II (Non-randomised, Open label)	Capecitabine and Cetuximab	Completed: MTD determined; partial response documented in 2 patients (6.5%), and 5 (16.1%) had stable disease. Considerable epidermal and mucosal toxicities.	NCT01077986	[406]
			Metastatic (Gemcitabine Refractory) Pancreatic Cancer	I/II (Single Arm, Open Label)	Sorafenib	Completed: Awaiting results	NCT00981162	
			Advanced and/or Metastatic Pancreatic Cancer	I/II (Single Arm, Open Label)	Gemcitabine	Completed: MTD determined. Clinical benefit (CR, PR or stable disease) observed in 78% patients (n=21).	NCT00560963	[407]
			Pancreatic Neuroendocrine Tumours	I/II (Open Label)	X-82 (VEGFR/PDGFR inhibitor)	Active, not recruiting. Prolonged stable disease (3-23 months) (n=10)	NCT01784861	[408]
			Advanced GI Neuroendocrine Tumours (incl Pancreatic)	II (Single Arm, Open label)	Monotherapy	Active, recruitment complete (n=25). Early data indicate therapy is well tolerated with signs of efficacy (high rate of PR)	NCT01648465	[409]
	Vistusertib	mTORC1/2	Advanced Solid Cancers (incl Pancreatic)	II (Personalised, Single Arm)	Monotherapy-targeted against RICTOR amplifications	Not yet recruiting	NCT03166904	

			Advanced Solid Cancers (incl Pancreatic)	II (Personalised, Single Arm)	Monotherapy-targeted against TSC1/2 mutations	Not yet recruiting	NCT03166176	
	Dactolisib	PI3K/mTOR	Advanced Solid Cancers (incl Pancreatic)	Ib (Open Label)	MEK162 (MEK1/2 inhibitor)	Completed: results pending	NCT01337765	
	Gedatolisib	PI3K/mTOR	Advanced Solid Cancers (incl Pancreatic)	I (Single Arm, Open label)	Palbociclib	Recruiting	NCT03065062	

1.4 JAK/STAT3 signalling in the tumour microenvironment of pancreatic cancer: from mechanisms to therapy

1.4.1 JAK/STAT3 signalling promotes pancreatic cancer progression

The JAK/STAT3 pathway plays a key role in tumour growth and progression and is associated with poor patient outcomes in a wide variety of malignancies including acute myeloid leukaemia, multiple myeloma, as well as solid tumours of the pancreas, lung, liver, ovary, breast, stomach and prostate [410, 411]. STAT3 is a transcription factor directly inducible by cytokines including IL-6, IL-11 and IL-10 through their shared receptor subunits gp130 [412-414] and IL-10R β respectively [415]; as well as growth factor receptors (EGFR, HER2, FGFR, IGFR, PDGFR, VEGFR), G-protein coupled receptors, toll-like receptors, and it is also indirectly activated by non-receptor tyrosine kinases such as SRC and Abl (Figure 1.6) [416-418]. Activation of STAT3 signalling occurs via the constitutive association between JAK proteins and receptor chains. In terms of IL-6-directed STAT3 signalling, IL-6 can form hexameric complexes with IL-11 or alternatively can form trimeric complexes, which associate with JAK molecules. The resulting complex triggers trans-phosphorylation of associated JAK kinases (JAK1, JAK2 and TYK2), and subsequently phosphorylates tyrosine residues on IL6 receptor subunit gp130, which serve as binding sites for STAT3 [411]. Canonical STAT3 activation occurs via the phosphorylation of tyrosine residue 705, which allows for its homo- and hetero-dimerisation leading to STAT3 nuclear translocation and DNA binding at consensus response elements in the promoters of a range of target genes that regulate fundamental biological processes [411]. These include, but are not limited to, regulators of apoptosis (BCL-XL), cell proliferation (c-MYC and cyclin-D1), angiogenesis (VEGF), tumour cell survival (MCL1 and survivin), immunosuppressive growth factors and cytokines (IL-6), as well as numerous genes associated with tumour cell invasion and metastasis [419-429]. Moreover, as a central intra-cellular node, STAT3 also integrates signals from EGFR [111][112][113], RAS-RAF-

mitogen-activated protein kinase [111][113], SRC [114], Wnt [115], c-MET [116], and TGF- β pathways [117][118], thereby enabling cross-talk with most signalling pathways that are instrumental for cancer growth.

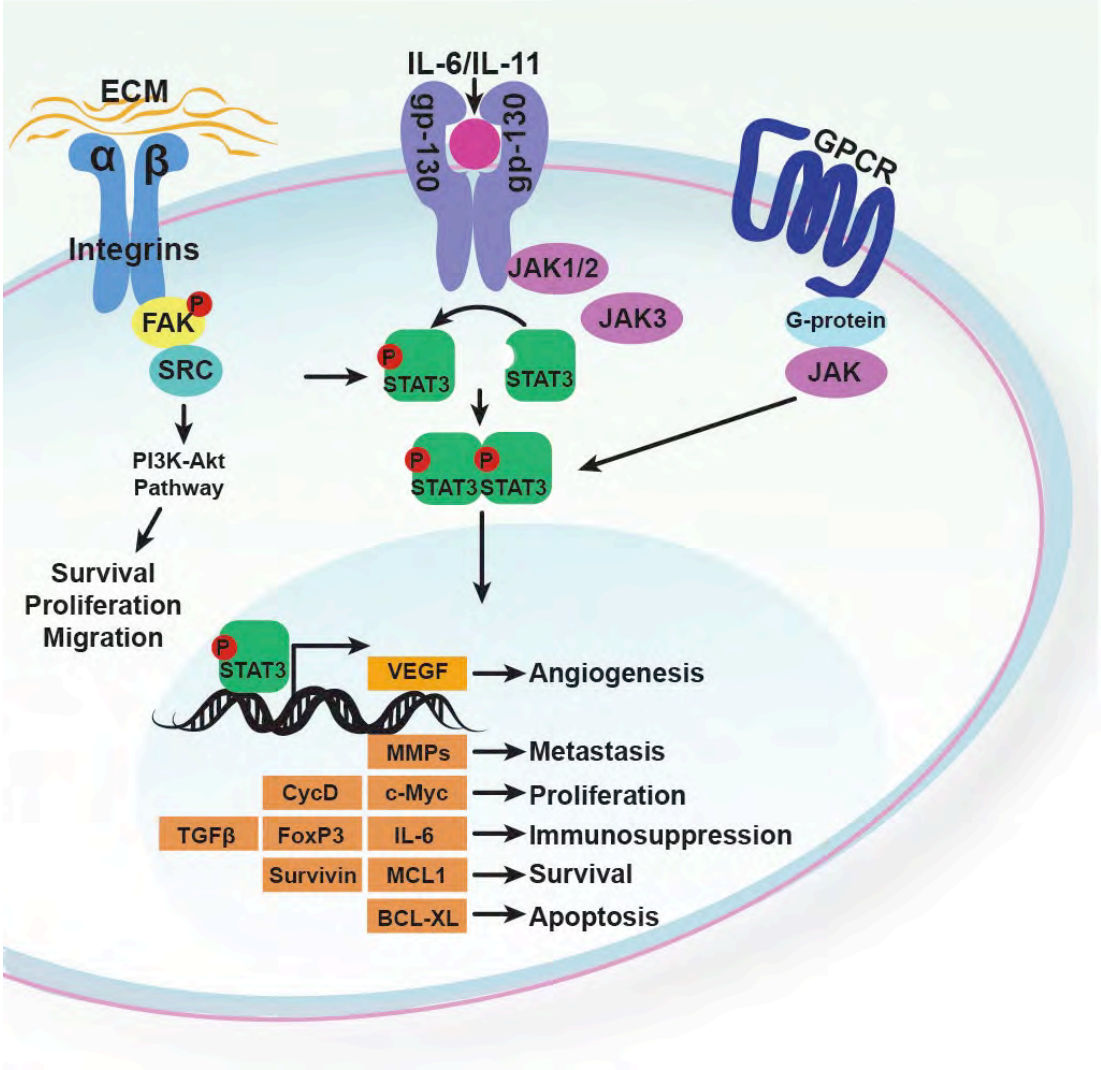


Figure 1.6: Schematic of the JAK/STAT3 signalling pathway

STAT3 can also be activated via a trans-signalling pathway, whereby soluble IL-6R binds to IL-6 forming a complex, which interacts with gp130 leading to its dimerisation and activation of downstream signalling pathways [411, 430, 431]. This form of signalling enables IL-6 to act on cells that have limited IL-6R expression such as cells in the tumour microenvironment [432-434]. STAT3 can also be phosphorylated at a serine residue 727, which leads to mitochondrial translocation, and aids in functions independent of gene transcription including cell metabolism and electron transport [20, 435]. Thus STAT3 is a master regulator and potential oncogene in several molecular pathways involved in the progression of a variety of cancers.

The significance of aberrant JAK/STAT3 signalling in pancreatic cancer is emerging; evidence indicates that the pathway plays a role in regulating PDAC development and progression from early stage acinar-to-ductal metaplasia (ADM) in both a spontaneous and pancreatitis-accelerated manner [166, 410, 428, 436-440]. Further, activation of STAT3 is associated with increased pancreatic cancer cell proliferation and viability, angiogenesis and metastasis [441, 442]. This is supported by comprehensive studies using genetically engineered mouse models of PDAC, where up-regulation of STAT3 was found to be associated with tumour and stromal cell proliferation [443]. Several studies have also shown a link between STAT3 activation and resistance to gemcitabine chemotherapy, however the associated mechanisms are still disputed [321, 410, 444, 445]. Zhang *et al.* suggests that STAT3 mediates gemcitabine-induced cancer stem-cell properties [445]. Whilst Wormann *et al.* propose that loss of P53 function activates JAK2/STAT3 signalling leading to desmoplasia of the tumour stroma and decreased chemotherapy efficacy [321]. Nagathihalli *et al.* support this proposal, and have shown that combined STAT3-inhibition with gemcitabine enhances drug delivery via stromal remodelling as well as downregulation of cytidine deaminase [443].

The downstream effectors of the JAK/STAT3 pathway that have been reported in pancreatic cancer are detailed further in Table 1.3. Constitutive activation of STAT3 in pancreatic cancer prevents apoptosis via the upregulation of anti-apoptotic proteins, including BCL-XL (B-cell lymphoma-2-

like 1) and Survivin/ BIRC5 [446]. Expression of these proteins correlated with pancreatic cancer cell apoptosis and is also involved in pancreatic duct cell tumour development [370, 447]. In addition, overexpression of Cyclin D1, a key protein involved in the progression of the cell cycle, and a known STAT3 target gene [448], was reported to correlate with poor prognosis in PDAC [449], and is down-regulated following STAT3 blockade *in vitro* [410]. STAT3 can also accelerate G1/S-phase progression via inhibition of cyclin-dependent kinase 2 activity [438]. Moreover, blockade of STAT3 has been shown to induce apoptosis and inhibit cell viability, confirming the critical role of STAT3 in pancreatic cancer cell survival [410, 446].

Table 1.3: Downstream effectors of STAT3 reported in pancreatic cancer

Function	STAT3-regulated gene products in PDAC	Reference
Proliferation and Survival	MYC ↑	[450]
	Cyclin D1 ↑	[448]
	BCL-XL ↑	[446]
	MCL1 ↑	[451]
	Survivin ↑	[446]
Angiogenesis	VEGF ↑	[410]
	HGF ↑	[452]
	HIF-1 α ↑	[453]
	MMP2 ↑	[454]
	MMP9 ↑	[455]
	IFN- β ↓	[456]
	IFN- γ ↓	[457]
	CXCL10 ↓	[458]
	AKT ↓	[459]
Immunosuppression	IL-6 ↑	[460]
	IL-10 ↑	[461]
	TGF- β ↑	[462]
	VEGF ↑	[410]
	IFN- β ↓	[456]
	IFN- γ ↓	[457]
	IL-12 ↓	[463]
	TNF ↓	[464]
	CXCL10 ↓	[458]
	CCL5 ↓	[465]
	CD80 ↓	[466]

Angiogenesis is another fundamental biological process regulated by STAT3. VEGF is a potent mitogen for endothelial cells, and is one of the most effective pro-angiogenic growth factors [467]. Autocrine VEGF promotes tumour cell migration and invasion, and upregulation of STAT3 has been shown to increase VEGF expression and selected MMPs, which promote angiogenesis and/or metastasis in pancreatic cancer cells [428]. Consequently, STAT3 has been accepted as a key contributor to oncogenesis and is a promising target for cancer therapy in pancreatic cancer.

In addition to the intrinsic effects on tumour cells, the JAK/STAT3 signalling pathway has important extrinsic effects on the surrounding tumour microenvironment. In particular, STAT3 has been shown to coordinate the molecular cross-talk between tumour cells and immune cells, and can induce and maintain a procarcinogenic inflammatory microenvironment. Recent studies in pancreatic cancer suggest that there is an association between the presence of tumour-associated macrophages (TAMs) and pSTAT3 positive epithelial cells, and that this association correlates with poorer patient outcomes [151, 468]. Further, epithelial STAT3 activity has been shown to protect pancreatic tumour cells from chemotherapy when co-cultured with macrophages [151], and can modulate the function of M2 macrophages (immunosuppressive phenotype) and their polarisation [469, 470]. STAT3 is also able to mediate crosstalk between macrophages and myeloid-derived suppressor cells (MDSCs), as well as drive the differentiation and expansion of MDSCs [471, 472]. In addition, STAT3 up-regulates FoxP3, a transcriptional regulator needed for T regulatory cell differentiation [473], and can repress CD8⁺ T cell chemotaxis and activation [474]. Moreover STAT3 negatively regulates T helper 1-cell-mediated inflammation, and can induce expression of factors (VEGF, IL-10, TGF- β) that suppress immune cell activity through inhibiting dendritic cell maturation [475-477]. Consequently STAT3 signalling actively promotes immune evasion by tumour cells, and maintains this procarcinogenic inflammatory microenvironment; a key hallmark of cancer [421, 478].

The role of JAK/STAT3 activation in pancreatic cancer desmoplasia is further exemplified by its ability to transform human fibroblasts into cancer-associated

fibroblasts (CAFs) [415, 416]. CAFs facilitate the growth and spread of tumours by secreting pro-survival and pro-angiogenic factors such as IL-6, TGF- β and VEGF into the tumour stroma, which consequently promotes the accumulation of MDSCs via a STAT3-dependent mechanism, and contributes to immunosuppression [134, 415, 479]. As discussed in 1.2.1, there are three distinct CAF subtypes in pancreatic cancer, which are characterised by myofibroblastic or inflammatory phenotypes [141, 147], and the JAK/STAT3 pathway plays a key role in the establishment of these distinct fibroblast niches. Upstream IL-1 was shown to induce LIF expression and downstream JAK/STAT3 activation, consequently driving the invasive inflammatory CAF phenotype [147]. CAFs dynamically interact with other cell types within the microenvironment, particularly pancreatic cancer cells, an interaction frequently mediated by IL-6 [479], or via secreted TGF- β [480]. However they also contribute to the extracellular matrix deposition and stromal remodelling. STAT3 signalling has been shown to promote tumour progression by increasing matricellular fibrosis and tissue tension. In addition, STAT3 ablation has been shown to reverse this, by reducing stromal stiffening and epithelial contractility via loss of TGF- β signalling [122].

1.4.2 Molecular and genomic alterations of the JAK/STAT3 signalling axis

Activation of the JAK/STAT3 pathway has been documented in a variety of malignancies including solid cancers, and is known to be associated with poorer outcomes in gastric, lung, glioma, hepatic, osteosarcoma, prostate and pancreatic cancers [481]. In PDAC specifically, activation of STAT3 has been reported in 30-100% of human PDAC tumour samples and 80% of PDAC cell lines, while the pathway is inactive in normal pancreas [436] [410, 428]. In addition, expression of IL-6R, phospho-JAK1 and phospho-STAT3 have been shown to correlate with reduced survival in resected PDAC [482]. Although several potential causes of STAT3 activation have been identified for other cancers, there is limited research in pancreas [421].

Examination of multidimensional publically-available cancer genomics datasets (TCGA, PanCan Atlas and QCMG cohorts) revealed that alterations

in the JAK/STAT3 pathway occur at a frequency of ~6% (54/934), with mutations only occurring in less than 1% of patients (Figure 1.7A) [257, 258]. This is supported by research into other solid tumours where it has been found that activating mutations in STATs are generally rare [483]. STAT3 is predominantly mutated in hematopoietic neoplasms such as T-cell large granular lymphocytic leukemia (T-LGL), where 30-40% patients have STAT3 mutations [484]. Data collected from the Catalogue of Somatic Mutations in Cancer study (COSMIC) identified the frequency of somatic STAT3 mutations in various cancer types (skin cancers, melanoma, gastrointestinal neoplasms, neural tumours, hematopoietic neoplasms), and found STAT3 to be the most frequently mutated STAT family gene in hematopoietic cancers, however STAT family genes were not significantly mutated in other cancers [484]. In terms of hematopoietic neoplasms, STAT3 mutations often occur on exon 21, which encodes the SRC homology 2 (SH2) domain, whereby the introduction of hydrophobic residues stabilises STAT dimers and leads to increased STAT-responsive transcription [483, 485, 486].

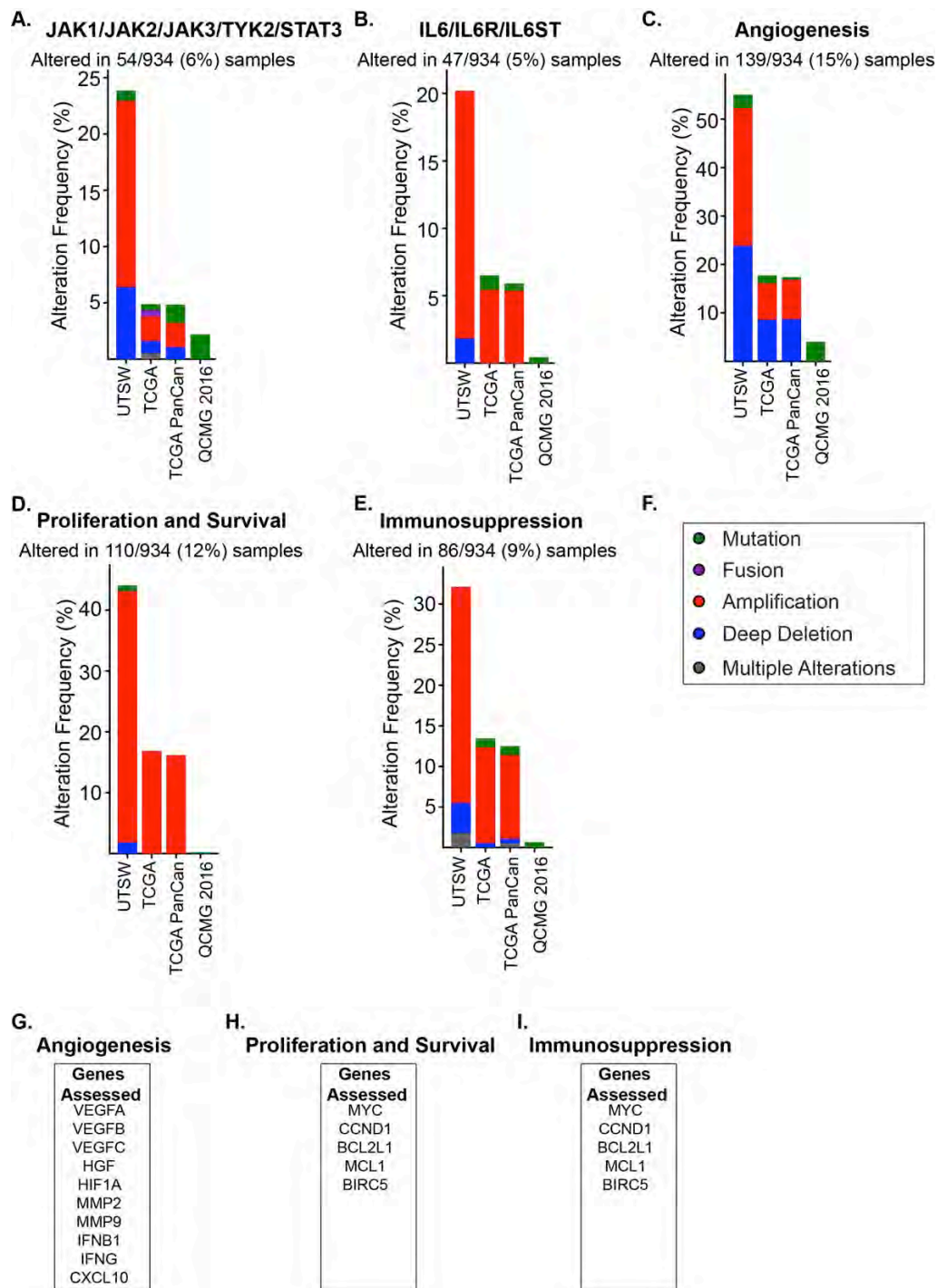


Figure 1.7: Frequency of genetic alterations in publically-available pancreatic cancer genomics datasets (TCGA, PanCan Atlas, UTSW QCMG) [257, 258]. (A) Alterations in *JAK1*, *JAK2*, *JAK3*, *TYK2*, *STAT3*, (B) *IL-6*, *IL-6R*, *IL-6ST*. Genes associated with (C) angiogenesis (D) proliferation and survival, (E) immunosuppression. (G, H + I) Genes used to define STAT3-driven angiogenesis, proliferation and survival, and immunosuppression, respectively. (F) Alterations include mutations (green), fusions (purple), amplifications (red), deep deletions (blue) and multiple alterations (grey).

In hematological malignancies activation of STAT3 is frequently associated with somatic mutations in *JAK2* (*JAK2*^{V617F}), as well as *JAK1* and *JAK3*. Somatic mutations have also been identified in the SH2 domain of *JAK1* in acute myeloid leukemia, acute lymphoblastic leukemia, breast ductal carcinoma and NSCLC [487, 488]. While these mutations are commonly found in haematological malignancies, they rarely occur in solid tumours [484, 489, 490], and have not been documented in PDAC. Whole genome sequencing studies have identified *JAK1* somatic missense mutations in around 10% of hepatitis B-associated hepatocellular carcinoma, activating mutations have been identified in hepatocellular carcinoma [491], and amplification of *JAK2* has been described in gastric cancer [492]. Despite the lack of mutations in PDAC, amplification of the pathway is seen in 2-17% of patients (Figure 1.7A), indicating that alternate mechanisms lead to hyperactive STAT3 signalling. Most studies suggest that aberrant intra-tumoural JAK and STAT3 activity occurs through hyperactive growth factor receptors, cytokine signalling or amplification of downstream signalling pathways [493-495].

Elevated levels of IL-6 are observed in a large proportion of patients with haematopoietic malignancies as well as solid tumours [496], and elevated IL-6 can stimulate the hyperactivation of JAK/STAT3 signalling in both tumour cells and the tumour microenvironment due to paracrine and autocrine feed-forward loops [411, 491]. Although 5% (47/934) of PDAC cases show alterations to the *IL-6*, *IL-6R* and *GP130* (*IL-6ST*) genes (the majority of which involve gene amplification) (Figure 1.7B), no clinically relevant genomic alterations have been detected in any of the tumour types analysed by The Cancer Genome Atlas (TCGA) [411]. In pancreatic cancer, Wormann *et al.* suggest that P53 mediates persistent STAT3 activation which is initiated by autocrine or paracrine effects of IL-6, but isn't further dependent on IL-6 signalling, trans-signalling or gp130 ligands [321]. Conversely, activating mutations of *GP130* occur in ~60% of hepatocellular adenoma surgical specimens [497], and a single nucleotide polymorphism in the IL-6 promoter has been shown to increase IL-6 expression in inflammatory disease [498]. It has also been suggested that epigenetic alterations play a role in activation of

the IL-6/JAK/STAT3 pathway [411]. Consequently there are still discrepancies in the mechanisms underlying IL-6-related persistent STAT3 activation.

Alterations in negative regulators of STAT3 can also contribute to activation of the JAK/STAT3 pathway. Loss of SOCS1 and SOCS3 expression, due to promoter hypermethylation, has been observed in several cancers including PDAC [491]. Further, mutation and inhibition of the SHP1 and SHP2 phosphatases, and loss of expression of PIAS family members has been reported in solid cancers and haematopoietic malignancies [491, 499]. As mentioned previously, modifications in the downstream effectors of STAT3 may also explain aberrant pathway activity. In PDAC specifically, STAT3-regulated genes associated with angiogenesis are altered in 15% (139/934) of cases (Figure 1.7C), genes associated with proliferation and survival are altered in 12% (110/934) of cases (Figure 1.7D), and genes associated with immunosuppression are altered in 9% (86/934) of cases (Figure 1.7E), the majority of which are gene amplifications. Despite these findings, the exact nature of STAT3 activation in PDAC remains to be elucidated, and further work in this field is warranted.

1.4.3 Targeting JAK/STAT3 signalling in pancreatic cancer

In normal cells activation of STAT3 is rapid and transient, it is also not required for normal cell proliferation and normal cells are tolerant to STAT3 loss [446]. In addition, STAT3 has well-established tumour promoting properties, is overexpressed in the majority of human cancers and is often associated with a poor prognosis, making it an ideal therapeutic target for cancers such as PDAC. However, due to STAT3's complex biology and lack of enzymatic activity, there is a lack of efficacious therapies. Numerous studies have been aimed at developing chemical inhibitors targeting the STAT3 SH2 domain, the DNA-binding domain, and the N-terminal domain of STAT3 [411]. Although these compounds demonstrate pro-apoptotic and anti-tumour effects, most compounds have struggled to reach clinical development due to issues with selectivity, specificity, stability, permeability, potential immunogenicity and low biological activity [500], and very few have entered clinical trials for use in PDAC (Table 1.4).

Table 1.4 Clinical trials in pancreatic cancer associated with targeting STAT3

Agent	Molecular Target	Cancer Type	Phase	Combination Therapy	Findings/Status	Protocol ID	Reference
AZD9150	STAT3 (STAT3 antisense oligonucleotide)	Advanced solid cancers, metastatic HNSCC	I/II (Randomised, open label)	MEDI4736 (PD-L1 monoclonal antibody)	Recruiting	NCT02499328	
		Advanced pancreatic cancer, NSCLC, and CRC	II (Non-randomised)		Recruiting	NCT02983578	
TTI-101	STAT3 SH2 binding domain	Advanced cancers	I (Single arm, open label)		Recruiting	NCT03195699	
OPB-31121	STAT3 SH2 binding domain	Advanced solid cancers	I (Non-randomised, open label)		Stable disease in 8/18 patients, however only 1 pancreatic cancer patient. MTD determined	NCT00657176	[501]
OPB 51602	STAT3 SH2 binding domain	Advanced cancers	I (Non-randomised, open label)		Completed: awaiting results	NCT01423903	
		Advanced solid cancers	I (Single arm, open label)		Completed: Poor tolerability and poor half-life. Less frequent dosing should be explored. Only 1 PDAC patient	NCT01184807	[502]
Napabucasin	STAT3	Metastatic pancreatic cancer	III (Randomised, open label)	Gemcitabine and nab-paclitaxel	Recruiting	NCT03721744	
		Metastatic pancreatic cancer	Ib (Non-randomised)	Gemcitabine, nab-paclitaxel, FOLFIRINOX, MM-398	Active not recruiting	NCT02231723	
		Metastatic pancreatic cancer	III (Randomised open label)	Gemcitabine and nab-paclitaxel	Active not recruiting	NCT02993731	

Table 1.5 Clinical trials in pancreatic cancer associated with targeting IL-6

Agent	Molecular Target	Cancer Type	Phase	Combination Therapy	Findings/Status	Protocol ID	Reference
Siltuximab	IL-6	Pancreatic neoplasms	I/II (Non-randomised, open label)		Completed: well tolerated but no clinical activity	NCT00841191	[503]
Tocilizumab	IL-6R	Unresectable pancreatic cancer	II (Randomised, open label)	Gemcitabine, nab-paclitaxel	Recruiting	NCT02767557	

Non-peptide STAT3-SH2 domain antagonists (OPB-31121, OPB-51602, and C188-9) have been evaluated in phase I clinical trials [411] for hepatocellular carcinoma and advanced stage solid cancers (Figure 1.8). Anti-tumour activity has been reported for several of these compounds, however these studies showed tolerability-related difficulties including drug-induced pneumonitis and peripheral neuropathy [501, 502, 504]. Double-stranded decoy oligonucleotides have been developed as an alternative method to inhibit STAT3. A STAT3 decoy corresponding to the STAT3 response element in the FOS promoter competitively inhibits the interactions between STAT3 and FOS, resulting in decreased tumour growth in various preclinical cancer models including brain, lung, ovarian and skin cancer [411]. A cyclic STAT3 decoy has also been developed which has increased anti-tumour activity, increased heat and nuclease resistance and no apparent toxicity in xenograft tumour models [505, 506]. Moreover, antisense oligonucleotides are another approach that have shown success in various pre-clinical cancer models as well as promising clinical activity [507-509]. AZD9150 has been shown to reduce STAT3 protein expression, inhibit the growth of lymphoma and NSCLC xenografts, and has shown limited toxicity in the clinic [508]. AZD9150 has also shown significant single agent anti-tumour activity in patients with treatment-refractory lymphoma and non-small cell lung cancer [508], with further trials underway in pancreatic cancer with use as a monotherapy (NCT02983578) and in combination with immunotherapy (NCT02499328). The small molecule inhibitor Napabucasin (BBI608), is another promising compound that blocks the transcription of STAT3 target genes, subsequently decreasing cancer stemness properties [510]. Napabucasin blocks survival and self-renewal of cancer stem cells and has been shown to inhibit cancer relapse and metastasis in preclinical mouse models [510, 511]. In 2016, following promising phase I/II clinical trials, the FDA approved Napabucasin as an orphan drug for gastric and pancreatic cancer. Currently there are three active clinical trials looking at combination Napabucasin and chemotherapies including gemcitabine and nab-paclitaxel, FOLFIRINOX and MM-398 (a nanoliposomal version of irinotecan), in advanced pancreatic cancer (NCT03721744, NCT02231723, NCT02993731).

Pending results from these various trials will help identify if further evaluation is required. Importantly, there is a lack of molecular stratification in these clinical trials, hence there is the potential to misidentify true responders to these therapies. Accordingly, future trials may have more success when molecular stratification is implemented.

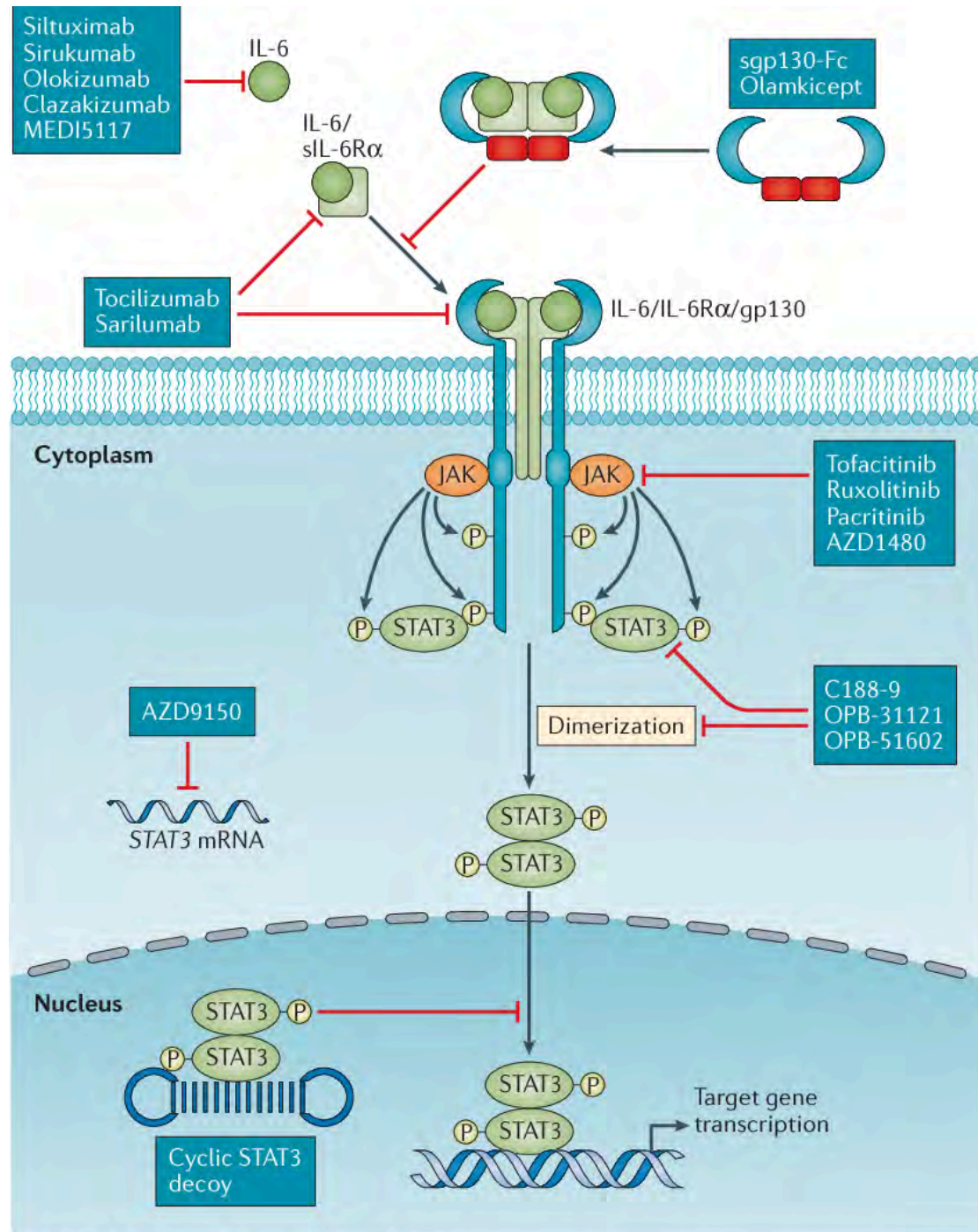


Figure 1.8: Inhibitors of the IL-6/JAK/STAT3 signalling pathway, taken from Johnson *et al.* 2018 [411].

Significant research has also gone into targeting molecules upstream of STAT3 including IL-6. There are three main methods of inhibiting IL-6: directly with antibodies (siltuximab), indirectly via IL-6R with antibodies (tocilizumab), and targeting the IL-6/IL-6R complex using fusion proteins incorporating gp130 [411, 430, 512] (Table 1.5). Siltuximab is a chimeric mouse-human antibody that has shown positive results in clinical trials for the treatment of a multicentric rare lymphoproliferative disorder Castleman disease [513-515]. Preclinically in solid tumours, siltuximab has displayed considerable anti-tumour efficacy against ovarian, prostate and lung cancers [516-518]. However while there have been promising preclinical results, evidence demonstrating clinical activity in solid cancers has been limited, with no clinical activity being observed in phase I/II trials in patients with advanced stage cancers including PDAC [503]. Tocilizumab is a humanized monoclonal antibody recognising IL-6R, that has shown promising preclinical results in solid cancers including pancreatic, where it was shown to decrease tumour weight and metastatic spread *in vivo* [519]. Consequently phase I/II trials are currently ongoing to explore safety and efficacy in combination with Trastuzumab and Pertuzumab for breast cancers (NCT03135171), and in combination with gemcitabine and nab-paclitaxel for pancreatic cancers (NCT02767557). Taken together, these studies suggest that in PDAC, targeting IL-6 signalling alone has limited efficacy. Future studies may need to consider more effective combination therapies or the identification of biomarkers to predict response to treatment. Furthermore, some caution needs to be taken when targeting IL-6, due to its ability to also activate STAT1 which is known to have tumour-suppressive properties [411, 520, 521].

Tyrosine kinases are a more promising therapeutic target due to the ability to inhibit their catalytic activity, and/or block their dimerization, therefore preventing activation [522]. Several inhibitors have been developed to target the JAK proteins and their clinical application has been heavily focused on conditions involving chronic inflammation and myeloproliferative neoplasms [523, 524], with little evaluation in solid tumours. Pyridine 6 was the first *bona fide* JAK inhibitor that was shown to have nanomolar activity against all JAK family members, however it had a poor pharmacokinetic profile, which

prevented its use *in vivo* [525]. Currently, ruxolitinib, tofacitinib and pacritinib are the most extensively investigated JAK inhibitors.

Ruxolitinib inhibits phosphorylation of JAK1 and JAK2, and has proven successful for the treatment of patients with myelofibrosis. Phase I/II trials have indicated that the drug was well tolerated, reduced splenomegaly, improved quality of life, and reduced levels of pro-inflammatory cytokines [526]. In addition, two phase III studies in myelofibrosis (COMFORT-I/II) were conducted, and found that after a three year follow up, treatment improved survival in both intermediate and high-risk disease, with 78% of patients surviving 144 weeks compared to 31% in the control [527]. Consequently, in November 2011, the U.S. Food and Drug Administration approved ruxolitinib for the treatment of myelofibrosis and polycythaemia vera [528]. Interestingly, ruxolitinib efficacy in myelofibrosis patients was not dependent on the JAK2 (V617F) mutation [529].

The potential for repurposing JAK inhibitors in solid cancers emerged after several preclinical studies reported efficacy of pan-JAK1/2 inhibitors in several cancers including NSCLC, ovarian and gastric cancers [530-532]. In a pancreatic cancer mouse model that expresses mutated Kras and lacks RB (KRC), ruxolitinib was shown to inhibit tumour angiogenesis, control disease progression and improve overall survival [533]. Moreover, ruxolitinib treatment blocked tumour growth in a syngeneic PAN02 pancreatic mouse model [534]. Similar results have been seen with other JAK inhibitors including the JAK2 inhibitor BMS-911543, which was shown to improve survival in the aggressive KPC-Brca1 genetically engineered PDAC mouse model [535]. In addition, ruxolitinib has been reported to modulate the stromal reaction, with treatment resulting in reduced phospho-STAT3 expression, cell proliferation and alpha-smooth muscle actin expression in pancreatic stellate cells [536]. Moreover, JAK inhibition has been shown to promote a shift in the CAF population from an iCAF phenotype towards a more myofibroblastic state, which has been previously suggested to restrain tumour progression [147, 537, 538]. Furthermore, targeting LIF, a paracrine factor that activates JAK/STAT3 in iCAFs is also effective at slowing tumour progression [539, 540]. Due to the high molecular heterogeneity and highly aggressive nature of PDAC, these

therapies are most likely to succeed as part of combination treatment, discussed further below.

Tofacitinib is a selective JAK3 inhibitor [541, 542], and a clinically approved therapy for rheumatoid arthritis. It is currently being tested in the pre-clinical setting for sensitizing lymphoproliferative disease to chemotherapy, and may have potential in treating primary mediastinal large B-cell lymphoma [543, 544]. JAK3/1 signalling is known to play a role in the development of inflammatory disease, and tofacitinib is thought to inhibit the production of inflammatory mediators and suppress the IL-6/JAK/STAT3 pathway. In line with this, tofacitinib has shown greater anti-proliferative and pro-apoptotic activity in JAK2-mutated cell lines compared to JAK2-wildtype cell lines [545]. Although tofacitinib is a potent JAK3 inhibitor, enzymatic assays indicate that both JAK1 and JAK2 are 100- and 20-fold less sensitive to inhibition by tofacitinib. At a 50% inhibitory concentration of 20nM for JAK2 tofacitinib has significant pro-apoptotic and anti-proliferative effect in cells carrying JAK2^{V617F} mutations [546]. Pancreatic cancer development is thought to occur through several inflammatory processes including the desmoplastic reaction, which provides a source of inflammatory mediators [547, 548]. Consequently these findings suggest that there is potential for tofacitinib to be re-purposed as a cancer therapeutic, however it has yet to be tested in this setting. The potential of tofacitinib is exemplified in a recent lymphoma case study. A 14-year old girl was diagnosed with refractory, primary mediastinal large B-cell lymphoma, with a JAK3 activating mutation. After unsuccessful first and second-line therapies, a third-line therapy of gemcitabine and oxaliplatin, ofatumumab and tofacitinib was administered, to which she had a partial response, with a reduction in disease size and FDG avidity [541]. Moreover, recent data suggest that tofacitinib treatment can alter the TME in models of pancreatic and triple negative breast cancers through depletion of tumour-associated inflammatory cells and inhibition of chemokine signalling, which in turn may improve the treatment efficacy of antibody-based anticancer therapeutics [549]. These findings illustrate the potential for a JAK3 inhibitor to be re-purposed as a cancer therapeutic in specific settings, an approach which has yet to be examined in pancreatic cancer.

Several other JAK inhibitors have been developed however results have been discouraging compared to ruxolitinib, including a selective JAK2 and FLT3 inhibitor, pacritinib [529, 550, 551], and JAK2-selective (and to a lower extent JAK1) inhibitor AZD1480, which was associated with severe adverse events including anxiety, ataxia, hallucinations and memory loss in Phase I studies [552]. Because these events do not occur with all JAK inhibitors, they are unlikely to be caused from specific, on-target toxicity. Also, differences in drug permeability across the blood brain barrier may also explain these disparate central nervous system effects [491].

Combining JAK-inhibition with chemotherapy is another potentially beneficial approach aimed at enhancing anti-tumour efficacy, while minimizing therapeutic resistance. In pancreatic cancer there is evidence to suggest that JAK inhibitors may improve the efficacy of current chemotherapies. Ruxolitinib combined with gemcitabine has been reported to inhibit tumour growth, increase microvessel density and enhance drug delivery via stromal remodelling and downregulation of cytidine deaminase (Cda) in orthotopic and PKT mouse models of PDAC [443, 553, 554]. Similar findings were seen with fedratinib (JAK2 inhibitor) and gemcitabine, which was found to reduce pancreatic tumour growth *in vivo* and improve overall survival compared to chemotherapy alone [555]. Tumours treated with fedratinib and gemcitabine also showed fewer activated pancreatic stellate cells, lower levels of periostin, decreased collagen production and changes to collagen organisation [321]. Suggesting that JAK2 inhibition is efficacious in remodelling the tumour stroma, and thus increases chemotherapeutic efficacy. These findings led to a phase Ib study looking at safety and tolerability of ruxolitinib and gemcitabine with or without nab-paclitaxel in advanced pancreatic cancer (NCT01822756). Unfortunately the sponsor terminated the trial after interim results from the JANUS 1 trial combining ruxolitinib and capecitabine in CRP high patients showed no additional benefit (Table 1.6) [555-557]. Despite being terminated early, the combination of ruxolitinib, gemcitabine and nab-paclitaxel saw an objective response rate of 23.5% (of 34 patients). Indicating that this therapy may have potential when molecular stratification is implemented. This rationale is currently being tested in a phase Ib study (NCT03878524) for

pancreatic cancer. Ruxolitinib has also shown promising results when combined with other chemotherapies including paclitaxel and azacytidine in haematologic disease [558, 559], which supports the potential of JAK inhibition to improve chemotherapeutic efficacy.

Given that in pancreatic cancer, multiple mechanisms often work in synchrony to promote tumour progression and metastasis, considering more tailored treatment combinations that involve inhibition of JAK and other molecular targets is a promising therapeutic strategy. In myeloproliferative disease combining a JAK2 inhibitor (TG101209) with an inhibitor of heat shock protein 90 (Hsp90) induced apoptosis in a synergistic manner [560], and JAK inhibitor CYT387 synergized (pro-apoptotic) with the proteasome inhibitor bortezomib [561]. Synergistic anti-proliferative effects have also been seen with histone deacetylase inhibitors *in vitro* for myeloproliferative neoplasms and Hodgkin Lymphoma [562, 563], and combining ruxolitinib with panobinostat (pan-deacetylase inhibitor) revealed cooperative effects in mouse models of myeloproliferative neoplasms [564]. Others have found that dual JAK, ERK and MEK inhibition have a synergistic anti-proliferative effect in acute lymphoblastic leukemia xenografts models [565], with targeted inhibition of MEK and STAT3 aggressive PDAC cell phenotypes [480]. Strong synergy has also been observed between JAK and PI3K inhibitors in haematological malignancies, owing to a mechanism where STAT5 interacts with the regulatory p85 subunit of PI3K [566, 567]. When JAK inhibitors were combined with BH3 mimetics in lymphoma it was found that STAT3 dependent expression of anti-apoptotic proteins (BCL-2, BCL-XL, Survivin and XIAP) was reduced [562, 568]. Another report determined that the combination of JAK2 inhibition (AG490) and methylsulfonylmethane reduces the DNA binding activity of STAT3 and STAT5B [569]. Moreover, combined inhibition of JAK and FAK signalling shows suppression of cell proliferation *in vitro*, and durable efficacy in PDAC animal models [332]. Of specific relevance to this thesis, combination of ruxolitinib and dasatinib (SRC and BCR-ABL inhibitor) has shown significant therapeutic potential in a mouse model of Ph+ acute lymphoblastic leukemia [570]. Ruxolitinib and dasatinib have also been reported to overcome bone marrow stroma-related tyrosine kinase inhibitor

resistance [571]. Moreover, the combination of SRC and JAK1/2 inhibitors has shown synergism in renal cell carcinoma xenografts, where it was reported to reduce proliferation, increase apoptosis and improve survival [572]. Currently the combination of ruxolitinib and dasatinib is undergoing phase I trials for acute lymphoblastic leukemia (NCT02494882) and phase II trials for chronic myelogenous leukemia (NCT03654768). Consequently, combining JAK inhibitors with compounds that target commonly deregulated signalling pathways in solid cancers or pathways that alter the tumour microenvironment may also show synergistic potential and this may be a beneficial, as yet unexplored, therapeutic strategy for pancreatic cancer.

Table 1.6 Clinical trials in pancreatic cancer associated with targeting JAKs

Agent	Molecular Target	Cancer Type	Phase	Combination Therapy	Findings/Status	Protocol ID	Reference
Ruxolitinib	JAK1/2	Recurrent or metastatic pancreatic cancer	II (Randomised, parallel assignment)	Capecitabine	Completed: Well tolerated and prolonged survival following ruxolitinib treatment, particularly in CRP-positive patients	NCT01423604	[556]
		Advanced pancreatic cancer	III (Randomised, parallel assignment)	Capecitabine	Terminated: No safety concerns however sponsor terminated due to lack of efficacy in a similar trial	NCT02119663	[573]
		Advanced pancreatic cancer	III (Randomised, parallel assignment)	Capecitabine	Terminated: Due to no efficacy in interim analysis	NCT02117479	[573]
		Advanced pancreatic cancer	I (Non-randomised, single arm)	Gemcitabine and/or nab-paclitaxel	Terminated: No safety concerns however sponsor terminated due to lack of efficacy in a similar trial	NCT01822756	[555]
		Advanced pancreatic cancer	II (Non-randomised, open label)	Capecitabine	Enrolling by invitation: for patients that were enrolled in initial Incyte study	NCT02955940	
		Advanced pancreatic cancer	I (Sequential assignment, open label)	Personalised medicine approach based on DNA mutation, RNA and protein expression data	Not yet recruiting	NCT03878524	
		Solid cancers	I/II (Non-randomised, open label)	Chemotherapies: Gemcitabine, paclitaxel, rucaparib, abiraterone, azacitidine	Terminated due to safety issues	NCT02711137	
BMS-911543	JAK2	Cancer	I/II (Non-randomised, open label)		Terminated: due to business decisions made by the sponsor	NCT01236352	
AZD1480	JAK2	Solid cancers	I (Non-randomised, open label)		Terminated: Decision to stop development of AZD1480	NCT01112397	
		Advanced solid cancers	I (Non-randomised, open label)		Terminated: Decision to stop development of AZD1480	NCT01219543	
Mometotinib (CYT387)	JAK1/2	Refractory or metastatic pancreatic cancer	I (Non-randomised, open label)		Terminated: no reason provided	NCT02244489	
		Metastatic pancreatic cancer	III (Non-randomised, parallel assignment)	Gemcitabine and nab-paclitaxel	Terminated: Due to no efficacy in interim analysis	NCT02101021	
Itacitinib	JAK1	Advanced solid cancers	I (Non-randomised, open label)	Pembrolizumab	Active, not yet recruiting	NCT02646748	

1.4.4 Future perspectives

The extraordinary and constantly expanding understanding of the role of SRC signalling and IL-6/JAK/STAT3 signalling in pancreatic cancer biology and treatment supports the foundation for the specific inhibition of these complex networks in PDAC. However, the presumption that a single targeted therapy will improve survival in such an aggressive disease is unrealistic. Unfortunately, most targeted therapies are at best only transiently effective, with cancer cells rapidly acquiring resistance, often leading to more rapid disease progression. This is supported by the numerous unsuccessful non-biomarker driven clinical trials that have been summarised in this review.

Further understanding of the intricacies of these signalling pathways in the various tumour compartments will determine whether the inhibitors of these complex networks may serve as effective treatments for newly diagnosed or recurrent tumours and will establish optimal combinations with radiation, cytotoxic chemotherapy, and other targeted molecular compounds. Given the need for co-targeting of multiple cancer capabilities to overcome the high therapeutic resistance of pancreatic tumours, future clinical applications of multi-modality treatment plans, will likely require a more innovative approach to dosing, including use of biologically effective doses of targeted agents, and alternative dosing schedules such as 'priming' or 'maintenance therapy' to ensure maximal benefit to the patient [294]. Finally, the emerging efficacy of SRC pathway inhibitors, and JAK/STAT3 pathway inhibitors in combination with other targeted and/or cytotoxic therapies, when examined in a molecular subtype-specific context [53, 383], and with longitudinal tracking of long-term therapeutic responsiveness, reveals significant potential as a personalised medicine strategy for pancreatic cancer, and provides real hope for patients in the future.

Chapter 2. Materials and Methods

2.1 Tissue culture

Twenty-five pancreatic cancer patient-derived cell lines (TKCC cell lines) were generated by Dr Marina Pajic using methods previously described [574, 575]. Briefly, patient-derived xenograft tumours (from immunocompromised mice) were mechanically and enzymatically digested using collagenase and hyaluronidase (Stem Cell Technologies USA), and plated onto 0.2mg/mL rat-tail collagen coated flasks (BD Biosciences, USA). Once established, mouse fibroblasts were removed via single-cell sorting (FACS Aria III Cell Sorter (BD Biosciences, USA), using a biotinylated anti-mouse MHC I antibody (1:200, eBiosciences, USA), coupled with a Streptavidin AlexaFluor 647 secondary (1:1000, BD Biosciences, USA), and an anti-mouse CD140a-PE antibody (1:300, BD Biosciences, USA) to remove mouse stroma. Dead cells were also removed using propidium iodide (Sigma-Aldrich, Australia).

All TKCC cell lines have been characterised by whole genome sequencing [3, 4], and have been profiled by short tandem repeat (STR) DNA analysis by Cell Bank Australia. The TKCC cell lines are all *Mycoplasma* spp free, and free from contamination. Cell culture conditions can be found in (Table 2.1), whilst media recipes can be found in (Tables 2.2-2.5).

2.2 Cell lines

Pancreatic patient-derived cell lines were isolated as previously described [4]. These cell lines and their culture conditions are listed in (Table 2.1).

Primary syngeneic KPC cancer cells were isolated from *Pdx1-Cre*, *LSL-KRasG12D/+*, *LSL-TrP53R172H/+* tumours [331], while telomerase-immortalised fibroblasts (TIFs) were generated as previously described [576]. Both KPC cells and TIFs were cultured in DMEM with 10% filtered FBS and 50 U/mL penicillin/streptomycin in 20% oxygen.

Table 2.1: Pancreatic patient-derived cell lines and their growth conditions

Cell Line	Oxygen Level	Media
TKCC-01	5%	RPMI
TKCC-2.1	5%	RPMI
TKCC-03	20%	RPMI
TKCC-04	20%	RPMI
TKCC-05	20%	HPAC mod
TKCC-06	20%	HPAC mod
TKCC-07	20%	M199/F12
TKCC-08	20%	M199/F12
TKCC-09	20%	M199/F12
TKCC-10	5%	M199/F12
TKCC-12	20%	M199/F12
TKCC-14	20%	M199/F12
TKCC-15	5%	M199/F12
TKCC-16	5%	M199/F12
TKCC-17	5%	M199/F12
TKCC-18	5%	IMDM
TKCC-19	5%	IMDM
TKCC-22	5%	IMDM
TKCC-23	5%	M199/F12
TKCC-25	5%	IMDM
TKCC-26	5%	M199/F12
TKCC-27	5%	M199/F12
TKCC-29	5%	M199/F12

Table 2.2: RPMI media recipe

Component	Volume to add	Final Concentration
RPMI (Gibco™)	500 mL	-
Fetal Bovine Serum (filtered) (Gibco™)	56 mL	10%
hEGF 0.1 mg/mL (Gibco™)	112 µL	20 ng/mL
Penicillin/Streptomycin 5000 U/mL (Gibco™)	5.6 mL	50 U/mL
Gentamicin 40 mg/mL (Pfizer, AUS)	280 µL	20 µg/mL

Table 2.3: HPACmod media recipe

Component	Volume to add	Final Concentration
DMEM/F12 (Gibco™)	500 mL	-
HEPES 1M (Gibco™)	8.4 mL	15 mM
Fetal Bovine Serum (filtered) (Gibco™)	42 mL	7.5%
hEGF 0.1 mg/mL (Gibco™)	56 µL	10 ng/µL
Hydrocortisone (1 mg/mL in 100% Ethanol) (Sigma-Aldrich, AUS)	22 µL	40 ng/mL
Insulin 100 IU/mL (Novo Nordisk, AUS)	560 µL	0.1 IU/mL
Glucose solution (10%) (Gibco™)	6.7 mL	0.12%
Penicillin/Streptomycin 5000 U/mL (Gibco™)	5.6 mL	50 U/mL
Gentamicin 40 mg/mL (Pfizer, AUS)	280 µL	20 µg/mL

Table 2.4: IMDMrich media recipe

Component	Volume to add	Final Concentration
IMDM (Gibco™)	500 mL	-
Fetal Bovine Serum (filtered) (Gibco™)	128 mL	20%
hEGF 0.1 mg/mL (Gibco™)	128 µL	20 ng/mL
apo-transferrin (2.5 mg/mL) (Sigma-Aldrich, AUS)	3.2 mL	12.5 µg/mL
Insulin 100 IU/mL (Novo Nordisk, AUS)	1.28 mL	0.2 IU/mL
MEM vitamins 100x (Gibco™)	3.2 mL	0.5x
Penicillin/Streptomycin 5000 U/mL (Gibco™)	6.4 mL	50 U/mL
Gentamicin 40 mg/mL (Pfizer, AUS)	320 µL	20 µg/mL

Table 2.5: M199/F12 media recipe

Component	Volume to add	Final Concentration
M199 (Gibco™)	250 mL	-
F12 (Gibco™)	250 mL	-
HEPES (Gibco™)	8.7 mL	15 mM
FBS (filtered) (Gibco™)	43.5 mL	7.5%
Glutamine 2mM (Gibco™)	5.8 mL	20 nM
hEGF 0.1 mg/mL (Gibco™)	116 µL	20 ng/mL
Hydrocortisone (1 mg/mL in 100% Ethanol) (Sigma-Aldrich, AUS)	23 µL	40 ng/mL
apo-transferrin 2.5 mg/mL (Sigma-Aldrich, AUS)	5.8 mL	25 µg/mL
Insulin 100 IU/mL (Novo Nordisk, AUS)	1.2 mL	0.2 IU/mL
Glucose solution (10%) (Gibco™)	3.5 mL	0.06%
Tri-iodothyronine (0.1 µg/mL) (Sigma-Aldrich, AUS)	2.9 µL	0.5 pg/mL
MEM vitamins (100x) (Gibco™)	5.8 mL	1 x
O-phosphoryl ethanolamine (20 mg/mL) (Sigma-Aldrich, AUS)	58 µL	2 µg/mL
Penicillin/Streptomycin (5000 U/mL) (Gibco™)	5.8 mL	50 U/mL
Gentamicin 40 mg/mL (Pfizer, AUS)	290 µL	20 µg/mL

2.3 Cytotoxic drugs and reagents

Gemcitabine HCl (catalogue number S1149), ruxolitinib (catalogue number S1378) tofacitinib (catalogue number S2789), and dasatinib (catalogue number S1021) were purchased from Selleck Chemicals (Houston TX USA). AZD1480 (catalogue number A-1135) was purchased from Active Biochem LTD (Hong Kong, China). Nab-paclitaxel (Abraxane®) was gifted from our oncology collaborators at the Garvan Institute/ The Kinghorn Cancer Centre. AZD289 was gifted from our collaborators at ONJCRI (Professor Matthias Ernst). AlamarBlue® for fluorometric analysis of cell viability was purchased from Thermo Scientific™ (VIC AUS).

2.4 Proliferation assay (alamarBlue® Cytotoxicity Assay)

Cells for proliferation assays were seeded in sterile 96-well flat-bottom plates (Corning from Sigma-Aldrich NSW, AUS). Optimal seeding density was

previously optimized by Dr Marina Pajic. Cells were left for 24h, following which dasatinib, ruxolitinib, AZD289, AZD1480 or tofacitinib were added. A serial dilution was prepared and 20 μ L of drug was added per well. Cell viability was measured at 72 h with alamarBlue® (Ex 530-560 nm, Em 590 nm; Invitrogen™, AUS), using a multi-well plate reader. Fluorescence data was expressed as percentage cell viability (fluorescent intensity of treated wells/ control wells). Sigmoidal dose response curves and IC₅₀ (drug concentration that inhibits cell growth by 50%) values were calculated using GraphPad Prism (V7.0.1, GraphPad, USA).

2.5 Drug synergy screens

For combination drug treatments, dasatinib and ruxolitinib, or dasatinib and AZD289, or dasatinib and AZD1480, were added at the same time and left for 72 h, at a fixed drug-ratio determined from the IC₅₀ concentration of the drugs for each cell line. Drug interactions were analysed using CompuSyn (V3.0.1, ComboSyn, USA) to generate a combination index (CI) value, where CI<1 indicates synergy, CI=1 additive effect and CI>1 indicates antagonism.

2.6 Protein isolation and western blot analysis

Monolayers of cells in log-phase growth, both untreated and treated with 4 μ M of ruxolitinib, or 50nM dasatinib for 24 hours were harvested by washing twice with cold PBS and subsequent scraping of cells into ice-cold normal lysis buffer [Glycerol (10%), MgCl₂ (0.03%), HEPES (1.2%), SAPP (1%), Triton (1%), NaCl (0.8%), NaF (0.4%), EGTA (0.04%)] supplemented with protease inhibitors [MG132 (10 μ g/mL), Aprotinin (10 μ g/mL), DTT (1 μ M), Leupeptin (10 μ g/mL), Sodium Vanadate (1 mM), PMSF (1 μ M)]. Cell debris was removed via centrifugation and protein concentration quantified using a Pierce™ BCA assay kit (Thermo Fisher Scientific, AUS).

Samples were prepared for gel loading to a total amount of 15-20 μ g of protein per lane, which consisted of 3.5 μ L sample buffer (NuPage, Invitrogen™, AUS), 1.4 μ L of reducing agent (NuPage, Invitrogen™, AUS), and the remainder made up with normal lysis buffer 15 μ L total volume. The samples were then heated at 70°C for 10 minutes and resolved by SDS-PAGE on a Bis-Tris gel (4-12%) (Invitrogen™, AUS), using 1x MOPS buffer.

A SeeBlue® Plus 2 (Invitrogen™, AUS) protein molecular weight marker was also used. Resolved gels were transferred to a PVDF (0.45 µM) membrane (Thermo Scientific™, AUS). Membranes were blocked in 5% non-fat milk in TBS-T [NaCl (0.87%), Tris (0.12%), Tween®20 (0.1%)] followed by overnight primary antibody incubation at 4°C. A list of antibodies and their conditions can be found in (Table 2.6). Horseradish peroxidase-conjugated secondary antibodies (GE Healthcare, UK) were prepared in 5% skim milk/TBS-tween at 1:5000 and incubated for 1 h at room temperature. Detection was performed using a HRP-conjugated enhanced chemiluminescence-based system (Plus-ECL, Perkin-Elmer, AUS) and relative protein expression was quantified using Image J2 Software (V1.51, NIH, USA).

Table 2.6: List of antibodies and associated protocols for western blotting

Antibody Name	Supplier/ company	Catalog ue No.	Host	Dilution and incubation time
Phospho-STAT3 (Ser 727)	Cell Signaling	9134S	Rabbit	1:1000 TBS/BSA, ON incubation
STAT3 (79D7)	Cell Signaling	4904S	Rabbit	1:2000 TBS/BSA, ON incubation
JAK1	Cell Signaling	3332S	Rabbit	1:900 TBS/BSA, ON incubation
JAK2 (D2E12) XP	Cell Signaling	3230S	Rabbit	1:900 TBS/BSA, ON incubation
JAK3	Cell Signaling	3775S	Rabbit	1:900 TBS/BSA, ON incubation
pJAK2 (Tyr1007/1008)	Millipore	07-606	Rabbit	1:500 in milk ON incubation
pJAK1 (Tyr1022/1023)	Millipore	07-849-I	Rabbit	1:100 in milk ON incubation
pJAK3 (B-12)	Santa Cruz	Sc-16567	Goat	1:200 in TBA/BSA, ON incubation
Phospho-STAT3 (Tyr705)	Cell Signaling	9131S	Rabbit	1:1000 TBS/BSA, ON incubation
SRC	Cell Signaling	2108S	Rabbit	1:1000 TBS/BSA, ON incubation
pSRC (Tyr416)	Cell Signaling	2101S	Rabbit	1:200 in Milk, ON incubation
STAT5A	Millipore	06-553	Rabbit	1:1000 TBS/BSA, ON incubation
pSTAT5 (Tyr 694)	Cell Signaling	9351	Rabbit	1:1000 TBS/BSA, ON Incubation
VEGFC	abcam	ab9546	Rabbit	1:500 (2-5ug/ml) milk, ON incubation,
VEGFA [VG-1]	abcam	ab1316	Mouse	1:200 (5-10ug/ml) TBST, ON incubation
VEGFR1 [Y103]	abcam	ab32152	Rabbit	1:1000-1:5000, ON incubation
Alpha Smooth Muscle Actin	abcam	ab5694	Rabbit	1:500, ON incubation

2.7 Generation of stable cell lines expressing GFP-luciferase biosensor

Stable cell lines were generated as described previously [83]. Briefly, lentiviral particles were generated by transient transfection of HEK293T cells utilising a third generation packaging system, as previously described [83, 577]. To summarise, HEK293T cells were transfected with a mixture of construct plasmids [pMD.G (2.8 µg), pMDLg/pRRE (4.5 µg), pRSV-Rev (6.4 µg)], and 15 µg of a transfer plasmid, eGFP-luciferase for luciferase-expressing cells, and Lipofectamine 2000®. 24 h post-transfection, HEK293T media was replenished and 24 h later viral particles were harvested by filtration through a 0.45 µm filter. KPC cells and PDCLs were infected by adding an optimized lentivirus dilution to culture media for 48 h. Cells were harvested, washed extensively and positive cells were selected via cell sorting on a FACS Aria III (BD Biosciences, USA) [83].

2.8 Organotypic assays

Organotypic assays were conducted as previously described (Figure 4.2.1) [221, 578, 579]. Briefly, rat tail collagen I solution was prepared from the extraction of rat tendons with 0.5 mol/L acetic acid to a concentration of 2 mg/ml. Telomerase immortalised fibroblasts (TIFs) (8.3×10^4 cells) were embedded in a mix of 2.5 ml of rat tail collagen I. Once polymerised the matrices were allowed to contract in complete media for 14 days (until matrices reached ~1.5 cm in diameter). Subsequently, 1×10^5 luciferase-labeled TKCC-05 cells or TKCC-10 cells, or 80,000 KPC cells were seeded on top of the matrix and allowed to grow to confluence for 4 days. Matrices were then transferred onto metal grids and raised to an air-liquid interface, where cell invasion occurred for 21 days (TKCC-05 and TKCC-10 cells), or 14 days (KPC cells), with media being replaced every 2 days. For drug treatments, 10 nM (TKCC-05 or TKCC-10) or 50 nM dasatinib, 4 µM ruxolitinib, 4 µM AZD289, 4 µM AZD1480 or 4 µM tofacitinib was added for the entire invasion period, and was replenished every 2-3 days. Concentrations were selected based on the highest non-toxic concentration for each cell line. Following invasion, the matrices were fixed in 10% formalin

and processed for histochemical analysis. Cell invasion was determined by counting GFP-positive cells, or multi-cytokeratin positive cells between 100 μm (site of obvious invasion) and 400 μm within the matrix. 12 independent images were taken per condition for analysis (n=3 independent biological experiments).

2.9 SHG imaging and analysis

Second Harmonic Generation (SHG) analysis was conducted as previously described [83], on both formalin-fixed organotypic matrices and 8 μm thick sections for orthotopic tumour sections. Briefly, 3 or 4 representative regions of interest (respectively) were imaged over a 3D z-stack (80 μm depth for organotypic matrix with z-step size of 2.52 μm ; 8 μm depth for tumour tissue with z-step size of 1.51 μm). SHG signal was acquired using a 25x 0.95NA water objective on an inverted Leica DMI 6000 SP8 confocal microscope. Excitation source was a Ti:Sapphire femtosecond laser cavity (Coherent Chameleon Ultra II), operating at 80 MHz tuned to a wavelength of 890 nm for organotypic matrices or 880 nm for tumour sections. RLD HyD detectors (440/20 and 435/40, respectively) were used to detect SHG signal intensity. SHG signal intensity was calculated in MATLAB (MathWorks, USA) for each image or stack and the maximum for each treatment was plotted.

2.10 Organoid cultures

Organoid culture was performed as described by Ohlund *et al.* [141]. Briefly, tumour tissue (*Pdx1-Cre*, *LSL-KRasG12D/+*, *LSL-TrP53R172H/+* tumours) was mechanically and enzymatically digested using collagenase and hyaluronidase (Stem Cell Technologies, USA) for ~1 h at 37°C. The digested tumour material was embedded in 80% BD Matrigel™ Matrix GFR (Cat # 356230, BD Biosciences, USA.) (diluted in culture media, see Section 2.2) and seeded into wells of 12-well plate (50 μl droplet per well). Matrigel was left to set for 5 minutes, following which culture media containing 5% FCS was added to cover the Matrigel™.

The patient-derived cell line TKCC-10 was also used to generate organoid cultures. Tumour cells (60,000 cells per organoid) were seeded in 80% MatriGel™ (diluted in organoid culture media, Table 7), and seeded into wells

of a 12-well plate (50 µl droplet per well). Matrigel™ was left to set for 5 minutes, following which organoid culture media (Table 7) was added to cover the Matrigel™.

Organoids were passaged using TrypLE™ (Gibco™, AUS) for 5-10 minutes at 37°C with gentle agitation.

Table 2.7 Organoid culture media recipe

Component	Volume to add	Final Concentration
Advanced DMEM/F12 (Gibco™, AUS)	42 mL	
R-spondin/Noggin conditioned media (generated from the L-WRN cell line, ATCC, USA)	5 mL	10%
Penicillin/Streptomycin (Gibco™, AUS)	0.5 mL	1x
GlutaMAX (Gibco™, AUS)	0.5 mL	1x
HEPES (Gibco™, AUS)	0.5 mL	10 mM
Nicotinamide (Sigma-Aldrich, AUS)	2.5 µL	10 nM
N-Acetylcysteine (Sigma-Aldrich, AUS)	416 µL	1.25 mM
Gastrin (Sigma-Aldrich, AUS)	2.5 µL	10 nM
hEGF (Invitrogen™)	25 µL	50 ng/mL
FGF10 (PeproTech, USA)	50 µL	100 ng/mL
B27(Gibco™, AUS)	1 mL	1x

2.10.1 Co-culture organoids

Organoid cultures were set up as described in 2.10, with the addition of KPC cancer-associated fibroblasts (for KPC organoids) or Telomerase immortalized fibroblasts (TIFs) (for TKCC-10-LO organoids). CAFs/TIFs and cancer-cell organoids were filtered through a 75 µM filter prior to seeding. For KPC co-culture organoids, KPC organoids and CAFs were combined at a ratio of 3:2 (CAF: KPC cells), with a total cell count of 40,000 cells per organoid. For TKCC-10-LO co-culture organoids, TKCC-10-LO and TIFs were combined at a ratio of 85:15 (TKCC-10-LO: TIFs) with a total cell count of 60000 cells per organoid.

2.10.2 Analysis of cytokine production

Co-culture organoids were set up as described in 2.10.1, and were left to grow for 7 days (Figure 4.2.16). On Day 7, media was changed and drug was added (ruxolitinib 4 μ M, dasatinib 50 nM). Organoids were left for 24 h and 48 h following which supernatants were collected. Supernatants were centrifuged at 1200 rpm for 5 minutes to pellet any debris. Supernatants were then transferred to a clean microcentrifuge tube and were assessed for cytokine production using Bio-Rad Bio-Plex Pro™ multiplexed cytokine arrays (MD000000EL Bio-Plex Pro™ Mouse Cytokine 9-Plex Assay, M60009RDPD Bio-Plex Pro™ Mouse Cytokine 23-plex Assay, 171AK99MR2 Bio-Plex Pro™ Human Chemokine Panel 40-plex Assay, 171AL001M Bio-Plex Pro™ Human Inflammation Panel 1 37-plex Assay), method as per manufacturer's instructions.

2.10.3 Fixation of organoids

Organoids were washed in 1X PBS, and fixed in 4% PFA for 4 minutes at room temperature. Following fixation, organoids were washed with 1X PBS and embedded in HistoGel™ (Thermo Scientific™, AUS). Once the HistoGel™ had solidified it was transferred into 70% ethanol and then processed by The Kinghorn Cancer Centre histopathology laboratory to form a PFA fixed, paraffin embedded organoid block.

2.10.4 Single cell sequencing of organoid co-cultures

Co-culture organoids were set up as described in 2.10.1. On Day 7, media was changed, drug was added (ruxolitinib 4 μ M, dasatinib 50 nM) and organoids were left to grow for 24 h. Organoids were then collected, washed in 1X PBS and dissociated using TrypLE™ (Gibco™), for 5-10 minutes at 37°C. Dissociated organoids were then filtered through a 40 μ m and 100 μ m filter to obtain a single cell suspension. Cells were then centrifuged at 1300 rpm for 4 minutes, and then resuspended in 2% FCS/PBS ready for capture.

Single cell suspensions were counted using a haemocytometer, diluted to 1.0×10^6 cells/mL in 10% FCS (v/v), DMEM (Thermo Fisher™, AUS) and subsequently loaded onto a 10x Chromium Single Cell A Chip to target

capture of 5000 cells per lane. Single cell capture, GEM generation, sample barcoding and library construction were performed according to the manufacturers Single Cell 3' Protocol (V2; CG00052; 10x Genomics, USA) at the GWCCG (Garvan Institute). 13 cycles were used for cDNA amplification and 12 cycles for library amplification. Libraries were sequenced to an average depth of 60,000 reads per cell on a S4 flow cell on a NovaSeq 6000 sequencer (Illumina, USA) at the Ramaciotti Centre for Genomics (UNSW, AUS).

The Garvan-Weizmann Centre for Cellular Genomics processed and mapped the raw bcl files using Cell Ranger v3.1.0 (10x Genomics, USA). Reads were mapped to the mouse reference genome (mm10). Seurat v3.1.0's [580, 581] SCTransform integration workflow was used to integrate the datasets. Default parameters were used unless otherwise stated. Low quality or dying cells (less than 500 genes per cell, more than 8500 genes per cell, less than 3 cells per gene and over 12.5% mitochondrial counts) were excluded. Principal Component Analysis (PCA) was performed using highly variable genes. Significant principle components (1 to 16) were selected using visualisation via elbow plot and heatmaps for clustering analysis and Uniform Manifold Approximation and Projection (UMAP) projection [582]. Differentially expressed genes in each cluster, across control and treated samples were identified by running FindMarkers function in the Seurat package using the MAST framework [583]. DEGs were filtered by $FDR < 0.05$ (Bonferroni correction) and $|\text{average log fold change}| > 0.1$. Preranked gene set enrichment analysis was completed using fgsea v1.9.7 [584] using Broad's Molecular Signatures Database using the curated gene set c2. Gene Ontology (GO) enrichment analysis was completed using clusterProfiler v3.10.1 [585] and filtered for $p\text{-value} < 0.01$ and $q\text{-value} < 0.05$. Copy number variants (CNV) were inferred using CONICS v0.0.01 [586]. All analyses were conducted on R v3.5.1 unless otherwise specified.

2.11 Immunohistochemical and Immunofluorescence staining

Tissues were fixed in 10% buffered formalin and embedded in paraffin. Tissues were cut into 4 µm sections and mounted on SuperFrost slides (Menzel-Glaser, Braunschweig, Germany). Haematoxylin and eosin (H&E) staining was performed using Leica Autostainer.

The immunohistochemical stains used, preparation, retrieval and antibody dilutions are outlined in table 2.8. Briefly, post de-paraffinisation and rehydration (Leica ST5010 Autostainer; Leica, DEU), antigen retrieval was performed using target retrieval solution (either pH 6 or pH 9) at (93°C for organotypic matrices, and 100°C for tumour tissue). Slides were quenched in 3% H₂O₂ before addition of a Protein Block (Dako or Leica). Slides were then incubated with primary antibodies followed by secondary antibodies coupled to HRP (Dako Envision System or Leica Bond Polymer Refined). Detection was attained with diaminobenzidine (DAB). Counterstaining was then performed on a Leica Autostainer (Leica, DEU). The Leica Autostainer was also used for haematoxylin and eosin (H & E) staining.

The immunofluorescence stains used, preparation, retrieval and antibody dilutions are outlined in (Table 2.9). Briefly, antigen retrieval was performed using the S1699 target retrieval solution (pH 6; Dako Corporation, AU) by boiling in a water bath for 20 minutes. Slides were blocked in 3%-BSA-PBST (0.3% Triton-X-100/PBS, with 0.04% glycine) for 1.5 h at room temperature (RT). All antibodies were diluted in 3%-BSA-PBST and slides were incubated overnight for 16 h at 4°C. Following 3x PBST washes, slides were incubated with 488- (cat#A-11008), Cy3- (cat#A10520) or 647-Alexa-Fluor (cat#A32733) secondary antibodies (Thermo Scientific™, AUS), diluted 1:200 in 3%-BSA-PBST, for 1 h at RT. Slides were washed 3x in PBST and stained with DAPI (1 µg/ml, Thermo Scientific™, AUS) for 2 minutes at RT. Slides were then mounted using ProLong Gold antifade reagent (#P36934, Invitrogen™, AUS) and imaged at 20x on a Leica DM5500 microscope.

Table 2.8: Antibody details for immunohistochemistry

Antibody Name	Supplier/ company	Catalogue No.	Antibody dilution	Staining System	Retrieval
Anti-alpha smooth muscle actin	abcam	ab5694	1:800	Dako envision rabbit	pH 6 20 min
Cleaved Caspase-3 (D175)	Cell Signaling	9661L	1:300	Leica BOND IHCF	pH 9 20 min
Ki-67	Thermo Scientific™	RM-9106-S1	1:500	Dako envision rabbit	pH 9 25min
GFP	Life technologies	A-11122	1:800	Dako envision rabbit	pH 9 30min
pSTAT3 (Tyr705)	Cell Signaling	9131S	1:100	Leica BOND IHCF	pH 9 30min
CD4	Cell Signaling	25229	1:100	Leica BOND IHCF	pH 9 20min
CD8	Cell Signaling	98941	1:200	Leica BOND IHCF	pH 9 30min
FoxP3	Cell Signaling	12653	1:400	Leica BOND IHCF	pH 9 20min
F4/80	Cell Signaling	70076	1:400	Dako envision rabbit + signal stain	pH 6 20min
Multi-Cytokeratin	Thermo Scientific™	MS-149-P	1:200	Leica BOND IHCF	pH 9 30min

Table 2.9: Antibody details for immunofluorescence

Antibody Name	Supplier/ company	Catalogue No. or clone	Antibody dilution	Retrieval
Periostin	abcam	ab14041	1:200	pH6 20 min
Fibronectin	BD Transduction Labs	610077	1:1000	pH6 20 min
CD31	Dianova	DIA-310	1:100	pH6 20 min
CK19	DSHB	Troma-III	1:100	pH6 20 min
F4/80	Cell-Signaling	D4C8V	1:300	pH6 20 min
CD68	Bio-Rad	FA-11	1:100	pH6 20 min
CD206	Bio-Rad	MR5D3	1:200	pH6 20 min

2.12 Picrosirius red staining, polarised light microscopy and analysis

Picrosirius red staining, polarised light microscopy and analysis was performed as described in [83]. Briefly, Picrosirius Red staining was performed as per manufacturers instructions (Polysciences). Briefly, 4 μ m tissue sections underwent de-paraffinisation and rehydration using a Leica Autostainer (Leica, DEU). Haematoxylin was added for 30 seconds following which sections were rinsed in running water for 2 minutes. 2% Phosphomolybdic acid was added for 2 minutes and then sections were rinsed in running water. 0.1% Picrosirius Red stain (Polysciences) was then added for 1 hour, following which the sections were rinsed with acidified water (0.5% acetic acid). Sections were then dehydrated using graded ethanol washes and coverslipped.

Polarised light images were then taken using an Olympus U-POT polarizer in combination with an Olympus U-ANT transmitted light analyser fitted to the microscope. Quantitative intensity measurements of fibrillar collagen and birefringent signal were performed on polarised light images using ImageJ. For each polarised light image, Hue-Saturation-Balance thresholding was applied. For red-orange, high birefringent fibers ($1 \geq H \leq 27$ | $0 \geq S \leq 255$ | $7 \geq B \leq 255$), for yellow, medium birefringent fibers ($28 \geq H \leq 54$ | $0 \geq S \leq 255$ | $7 \geq B \leq 255$), and for green, low birefringent fibers ($1 \geq H \leq 100$ | $0 \geq S \leq 255$ | $7 \geq B \leq 255$). The relative area (% total fibres ($(1 \geq H \leq 100$ | $0 \geq S \leq 255$ | $7 \geq B \leq 255)$)) was then calculated.

2.13 Quantification of immunohistochemical and immunofluorescence stains

2.13.1 Quantification of various stains on whole tumour sections

Immunohistochemical and immunofluorescence analyses were performed using 'Andy's Algorithms', a series of automated image analysis pipelines for FIJI, which can be publicly accessed at <https://github.com/andlaw1841/Andy-s-Algorithm> [587]. This program was used to calculate area coverage or the proportion of DAB positive cells per field of view (FOV).

2.13.2 Quantification of pSTAT3 (Tyr705) on patient-derived xenografts (PDX) tumour microarrays

The Kinghorn Cancer Centre (TKCC) patient-derived xenograft cohort (n=54) was analysed for pSTAT3 (Tyr705) expression using two scoring methods: semi-quantitative scoring and H-score. For semi-quantitative scoring, complete absent nuclear staining was scored a 0, the presence of weak positive nuclear staining in any percentage of tumour cells was scored as 1+, and the presence of moderate to strong staining in any percentage of tumour cells was scored as 2+. The H-score was calculated using the following formula $[0 \times (\% \text{ cells } 0) + 1 \times (\% \text{ cells } 1+) + 2 \times (\% \text{ cells } 2+)]$ [588].

2.14 Animals

Animal experiments were conducted in accordance with the Australian code of practice for the care and use of animals for scientific purposes and in compliance with Garvan Ethics Committee guidelines (16/35, 14/11, 14/12, 18/28, 17/15 and 17/18 Animal Research Authorities). C57BL6 and NOD/SCID/ILR2 γ mice were purchased from Australian BioResources (Mossvale, AUS) and were housed at the Biological Testing Facility (Garvan Institute, AUS) for the duration of the project.

2.15 Orthotopic injection of cancer cells

For the immunocompetent model, luciferase-labelled syngeneic KPC cells were injected orthotopically into the pancreas of C57BL6 mice (anesthetised with isoflurane 3L oxygen 1L/min, vacuum was used to remove excess oxygen). For survival studies, 500 KPC cells in 30 μ L of 1:1 PBS:Matrigel™ (BD Biosciences, USA) were injected during an open laparotomy.

For the immunocompromised model, luciferase labelled TKCC-05 and TKCC-10 patient-derived cell lines were injected orthotopically into the pancreas of NOD/SCID/ILR2 γ mice. For survival studies, 15,000 TKCC-05 cells or 1,000,000 TKCC-10 cells in 30 μ L of 1:1 PBS:Matrigel™ (BD Biosciences, US) were injected during an open laparotomy.

2.16 *In vivo* therapeutic studies

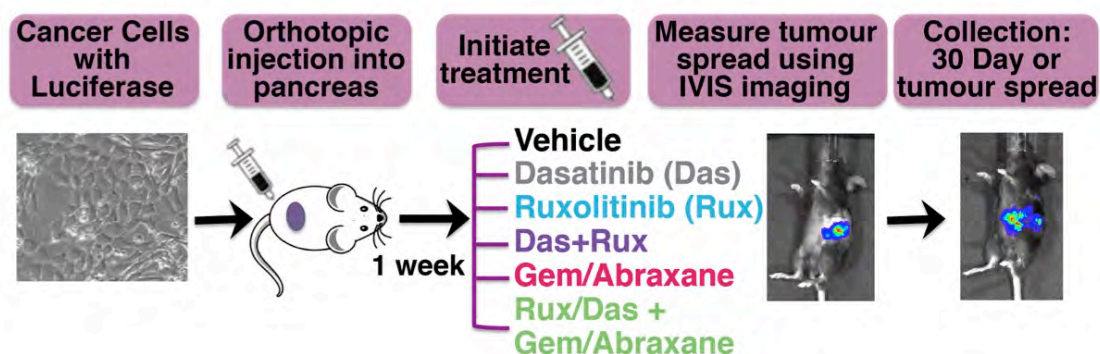


Figure 2.1: Preclinical testing pipeline in orthotopic models.

For syngeneic orthotopic models, one week post orthotopic injection of cancer cells (2.16), mice were randomised into different treatment groups (Figure 2.1). For immunocompromised orthotopic models, following palpable primary tumour development using bioluminescence imaging (outlined in 2.18), TKCC-05-eGFP-Luc or TKCC-10-eGFP-Luc tumour-bearing mice were randomised into various treatment groups. These treatment groups, dosages and schedules are summarised in (Table 2.10) for the syngeneic model, and (Table 2.11) for the immunocompromised model. Clinically-applicable once weekly dosing for gemcitabine/Abraxane (nab-paclitaxel) was used for the immunocompromised models, and due to the highly aggressive nature of KPC PDAC the chemotherapy schedule was increased to twice weekly dosing. Preparation of drugs is outlined in (Table 2.12), and drug buffer/solution recipes are outlined in (Table 2.13).

Bioluminescent live imaging (IVIS Spectrum, Perkin-Elmer, USA) (outlined in 2.18) was performed weekly, and was used to measure tumour burden post orthotopic injection of cancer cells. Endpoint was defined by a timepoint (30 days), or for survival studies endpoint was defined by metastatic spread (as evident from IVIS) and ascites. At endpoint mice were euthanised, tumours were weighed, and organs were fixed in formalin for further histological analysis.

Table 2.10: Treatment schedules for immunocompetent model

Treatment Group	Dose	Schedule	Cycle
Saline Control		Twice weekly: DAY1, DAY4	4 weeks treatment followed by 1 week break
Gemcitabine + Abraxane	Gemcitabine: 60mg/kg [83] Abraxane: 30mg/kg [83]	Twice weekly: DAY1, DAY4	4 weeks treatment followed by 1 week break
Gemcitabine	120mg/kg [83]	Twice weekly: DAY1, DAY4	4 weeks treatment followed by 1 week break
Dasatinib	10mg/kg [177]	Twice daily: Day1-5	4 weeks treatment followed by 1 week break
Ruxolitinib	60mg/kg [443]	Once daily: Day1-5	4 weeks treatment followed by 1 week break
Dasatinib + Ruxolitinib	Dasatinib: 10mg/kg Ruxolitinib: 60mg/kg	Dasatinib: Twice daily, Ruxolitinib: Once daily, DAY1-5	4 weeks treatment followed by 1 week break
Dasatinib + Ruxolitinib + Gemcitabine	Dasatinib: 10mg/kg Ruxolitinib: 60mg/kg Gemcitabine 120mg/kg	Dasatinib: Twice daily, Ruxolitinib: Once daily, DAY1-5 Gemcitabine: Twice weekly: DAY1, DAY4	4 weeks treatment followed by 1 week break
Dasatinib + Ruxolitinib + Gemcitabine + Abraxane	Dasatinib: 10mg/kg Ruxolitinib: 60mg/kg Gemcitabine 60mg/kg Abraxane: 30mg/kg	Dasatinib: Twice daily, Ruxolitinib: Once daily, DAY1-5 Gemcitabine+ Abraxane: Twice weekly: DAY1, DAY4	4 weeks treatment followed by 1 week break

Table 2.11: Treatment schedules for immunocompromised model

Treatment Group	Dose	Schedule	Cycle
Saline Control		Once weekly: DAY1	4 weeks treatment followed by 1 week break
Gemcitabine + Abraxane	Gemcitabine: 100mg/kg [83] Abraxane: 30mg/kg [83]	Once weekly: DAY4	4 weeks treatment followed by 1 week break
Gemcitabine	Gemcitabine: 120mg/kg [83]	Twice weekly: DAY1, DAY4	4 weeks treatment followed by 1 week break
Dasatinib	10mg/kg [177]	Twice daily: Day1-5	4 weeks treatment followed by 1 week break
Ruxolitinib	60mg/kg [443]	Once daily: Day1-5	4 weeks treatment followed by 1 week break
Dasatinib + Ruxolitinib	Dasatinib: 10mg/kg Ruxolitinib: 60mg/kg	Dasatinib: Twice daily, Ruxolitinib: Once daily, DAY1-5	4 weeks treatment followed by 1 week break
Dasatinib + Ruxolitinib + Gemcitabine	Dasatinib: 10mg/kg Ruxolitinib: 60mg/kg Gemcitabine 120mg/kg	Dasatinib: Twice daily, Ruxolitinib: Once daily, DAY1-5 Gemcitabine: Twice weekly: DAY1, DAY4	4 weeks treatment followed by 1 week break
Dasatinib + Ruxolitinib + Gemcitabine + Abraxane	Dasatinib: 10mg/kg Ruxolitinib: 60mg/kg Gemcitabine 120mg/kg Abraxane: 30mg/kg	Dasatinib: Twice daily, Ruxolitinib: Once daily, DAY1-5 Gemcitabine+ Abraxane: Once weekly: DAY4	4 weeks treatment followed by 1 week break

Table 2.12: Drug recipes

Drug	Administration	Dose	Buffer
Gemcitabine	IP	10 μ L/g	NaCl
Abraxane	IP	10 μ L/g	NaCl
Dasatinib	Gavage	5 μ L/g	Citric acid buffer pH 3
Ruxolitinib	Gavage	10 μ L/g	5% dimethylacetamide (DMA), 0.5% methylcellulose

Table 2.13: Drug buffer recipes

Buffer	Recipe
80 mM CITRIC ACID BUFFER (pH 2.1, 3.0)	0.615 g citric acid monohydrate (C1909). 40 mL autoclaved water. Check pH and adjust accordingly
0.5% (w/v) METHYL CELLULOSE	250 mg methyl cellulose. 50 mL autoclaved water at 90°C. Shake until dissolved

2.17 Whole body IVIS spectrum imaging

Luciferase signal was imaged using the IVIS Spectrum, (Perkin-Elmer, USA), to determine orthotopic tumour growth and spread weekly. Luciferin was administered by IP injection (150 mg/kg, Gold Biotechnology, USA). Mice were then anaesthetized (with isoflurane 3L oxygen 1L/min, vacuum was used to remove excess oxygen), and positioned on the IVIS stage so that the left flank (pancreas site) was exposed.

The bioluminescent signal was then acquired using open filters and small binning. The total flux of each tumour was measured using the Region of Interest Tool in the IVIS software (Living Image Software, Perkin-Elmer, US), and the threshold was set to 25%. Total flux was used as a measure of tumour burden, and metastatic spread was evident from the location of the signal.

To determine the timepoint to image the mice post luciferin injection a kinetics curve for luciferin expression was produced for each cell-line model prior to experimental studies. Following isoflurane induction, mice were imaged

every minute for up to 40 minutes. Once the curve was established a timepoint was selected based on the stabilisation of the curve. For TKCC-05-eGFP-Luc, 9 minutes was selected, and for TKCC-10-eGFP-Luc 13 minutes was selected (Appendix A and B).

2.18 Statistical analyses

Statistical analyses were performed using GraphPad Prism (GraphPad Prism Software, Version 8, GraphPad, USA). To assess statistical significance between three or more variables a one-way ANOVA test with a Tukey correction for multiple comparisons was used to avoid Type I errors inherent in performing multiple t-tests. To assess statistical significance between two variables a non-parametric t-test was used.

Survival curves were generated using Kaplan-Meier method and comparisons of outcome between subgroups were performed using the log-rank test for univariate comparisons. Significance was defined as $p^* < 0.05$, $p^{**} < 0.01$, $p^{***} < 0.001$, $p^{****} < 0.0001$.

Chapter 3. Efficacy of JAK1/2 and SRC inhibitors in two-dimensional *in vitro* models of pancreatic cancer

3.1 Introduction

The widespread molecular heterogeneity, the lack of effective therapies and the almost uniform mortality, make pancreatic cancer a prime model for advancing personalised medicine strategies. Modern chemotherapy regimens for PDAC patients include gemcitabine and Abraxane (albumin-bound paclitaxel) or 4-drug chemotherapy FOLFIRINOX (for younger, fitter patients), or gemcitabine monotherapy; therapies that have only a modest clinical benefit and a modest survival advantage in unselected populations [8, 9]. Consequently there is a clear need for a fundamental shift in clinical oncology to utilise molecular taxonomy, where individual cancers are selected for optimal therapy depending on their molecular phenotype.

The SRC/JAK/STAT3 pathway is a major oncogenic signalling cascade [478], which is known to play an important role in pancreatic carcinogenesis, from development of the earliest pre-malignant pancreatic lesions, acinar-to-ductal metaplasia and pancreatic intraepithelial neoplasia, to promoting cancer progression and metastasis in established pancreatic ductal adenocarcinoma [321]. Key components of this dynamic pathway have been shown to be frequently altered in pancreatic cancer and associate with poor patient prognosis [122, 177, 321], making this network an attractive target for the development of tailored treatment strategies. Early evidence of the potential role of SRC and STAT3 as oncogenes has fuelled the development of small-molecule inhibitors as cancer therapeutics. SRC inhibition has been shown to reduce proliferation, migration and invasion in PDAC cell lines, as well as inhibit tumour progression and metastasis *in vivo* [183, 194-198]. Furthermore, JAK/STAT3 inhibition reduced tumourigenicity in several *in vivo* models of different cancers including pancreas [530-534]

In addition, there is strong evidence to suggest that combining JAK inhibitors with compounds that target commonly deregulated signalling pathways, or pathways that alter the tumour microenvironment may show synergistic potential [560-562, 564, 566]. One such combination is ruxolitinib (JAK1/2-

inhibitor) and dasatinib (SRC-inhibitor), a combination which has shown significant efficacy in pre-clinical models of acute lymphoblastic leukaemia [570], and is currently in clinical testing in this setting (NCT02494882). However, this therapeutic combination has not been examined in pancreatic cancer.

Thus it is reasonable to hypothesise that dual targeting of SRC and JAK/STAT3 signals in tumours harbouring aberrations in this network may represent a promising and novel treatment strategy. Currently, the limited *in vitro* findings on the efficacy of SRC or JAK/STAT3 targeted agents as monotherapies in PDAC has utilised commercial cell lines, and genetically engineered models; models which lack the molecular heterogeneity that defines PDAC. Previous work from our lab has attempted to deal with this issue by developing a bank of genomically-characterised patient-derived cell lines (PDCLs) [3, 4, 83], which have also been histopathologically verified to be representative of the primary tumour [3, 4, 6, 589]. As a result of their molecular diversity, these cell lines enable the personalised testing of novel therapeutics, and allow for detailed analysis of the biological mechanisms behind therapeutic response. The personalised testing of various JAK and SRC inhibitors has not been previously examined, and hence requires systematic investigation.

This chapter aims to:

- Identify SRC/JAK/STAT3 pathway alterations in the APGI/ICGC patient cohort and in pancreatic patient-derived cell lines (PDCLs).
- Assess the therapeutic efficacy of various JAK and SRC inhibitors in PDCLs of PDAC, and primary murine PDAC cells from the genetically engineered Pdx1-Cre, LSL-KrasG12D/+, LSL-TrP53R172H/+ (KPC) model [331], using two-dimensional drug screens.
- Assess the dual therapeutic efficacy of combined JAK and SRC inhibition in two-dimensional drug screens.
- Identify potential biomarkers of response to JAK and SRC inhibition.

3.2 Results

3.2.1 SRC/JAK/STAT3 pathway alterations in pancreatic cancer

To assess the prevalence of SRC/JAK/STAT3 pathway alterations in pancreatic cancer, publicly available sequencing data from clinical cohorts (ICGC, UTSW, TCGA) was accessed from cBioportal [257]. Of the 392 PDAC tumours that were sequenced as part of the APGI/ICGC effort, 12.5% (49/392) displayed somatic mutations in the SRC/JAK/STAT3 molecular pathway (Table 3.2.1). In addition, whole exome sequencing data from UTSW reported 26.8% (29/108) of pancreatic tumours harboured copy number variations (27.52% of which were gene amplifications). Similarly, TCGA data indicate that 27.4% (51/185) of pancreatic tumours showed either copy number alterations or mutations in the SRC/JAK/STAT3 pathway, suggesting that this network is aberrantly activated in a measurable proportion of PDACs.

For the preclinical testing of inhibitors of the SRC/JAK/STAT3 pathway, patient-derived cell lines (PDCLs) available from the APGI/ICGC cohort were utilised along with cells from the KPC (Pdx1-Cre, LSL-KRasG12D/+, LSL-Trp53R172H/+) mouse model of PDAC. The basic mutation status of 16 cell lines, is summarised in table 3.2.2. The frequency of key commonly occurring mutations in PDAC [3] is faithfully mirrored in these models, with mutations in *KRAS* occurring in 94% (15/16) of PDCLs, and *TP53* and *SMAD4/TGFB* alterations present in 69% (11/16) and 38% (6/16) of lines, respectively.

With regard to SRC and JAK/STAT3 pathway aberrations, 5/16 cell lines (31%) displayed copy number alterations, mutations or structural rearrangements, the majority of which were gene amplifications (Table 3.2.1 and Table 3.2.2). One PDCL (TKCC-15) harboured amplification of SRC, IL-6, STAT3-target genes *SOCS3* and *BCL2L1* and JAK2 copy number loss. Interesting aberrations were further observed in TKCC-05 (JAK3 mutation (R431W)), TKCC-06 (JAK3 copy number loss), TKCC-12 (JAK2 copy number loss), and TKCC-17 (intrachromosomal rearrangement of *STAT3* gene), with substantial “omic” diversity represented in the PDCL panel, as a potentially attractive tool for further therapeutic screening.

Table 3.2.1 Alterations in the SRC/JAK/STAT3 molecular pathway in pancreatic cancer samples from the International Cancer Genome Consortium (ICGC), University of Texas Southwestern (UTSW) and The Cancer Genome Atlas (TCGA) clinical cohorts. WGS= whole genome sequencing, CNV= Copy number variation, WES= whole exome sequencing, RNAseq= RNA sequencing. Data was obtained from cBioportal [257, 258]

Molecular Characterisation	Number per Total (Method)	Overall Prevalence
JAK/STAT3 aberrations:		12.5-31%
(ICGC Nat. 2012)		
Pathway mutations (substitution/indels)	49/392 (WGS)	12.5%
IL6/SRC/JAK/STAT3 CNV/mutations	5/16 (WGS CNV)	31%
(UTSW Nat Comm. 2015)		
SRC/JAK/STAT3 CNV	29/108 (WES)	26.8%
(TCGA Provisional)		
SRC/JAK/STAT3 CNV/ mutations	51/185 (WES/ RNASeq)	27.4%

Table 3.2.2 Basic mutation status of selected human and murine pancreatic cancer cell lines

Cell line	Structural variant classification (Waddell <i>et al.</i> Nature 2015)	KRAS mutations	TP53 mutations	JAK/STAT3 pathway aberrations	SMAD4/TGFB mutations
TKCC-03	Scattered	c.227C>T p.G12D	c.517 C>T p.V173M	wild-type	wild-type
TKCC-05	Scattered	c.227C>A p.G12V	c.733C>T p.G245S	JAK3 c.1391G>A p.R431W	wild-type
TKCC-06	Stable	c.227C>A p.G12V	wild-type	TYK2 CN loss, SOCS3 CN loss, JAK3 CN loss	SMAD4 (nonsense) c.1591C>T p.R445
TKCC-07	Focal	c.227C>A p.G12V	c.493G>A p.Q165	wild-type	wild-type
TKCC-10	Unstable	c.227C>A p.G12V	c.455->G (Frame_Shift_Ins) p.P59P	wild-type	TGFBR2 c1783A>- (Frame_Shift_Del) p.V467V
TKCC-12	Stable	c.227C>A p.G12V	c.586G>A p.R196	JAK2 CN loss, SOCS1 CN loss,	TGFBR2 c1790TA>- (Frame_Shift_Del) p.Y470Y
TKCC-14	Focal	c.227C>A p.G12V	c.527C>G p.C176S	wild-type	wild-type
TKCC-15	Scattered	c.227C>T p.G12D	wild-type	JAK2 CN loss, IL6 CN gain, SRC CN gain, SOCS3 CN gain, BCL2L1 CN gain	TGFBR2 c1719A>T p.D446V
TKCC-17	Scattered	c.183T> A p.Q61H	c.377T>C p.Y126C	STAT3 Dup/Ins/Itx (Intrachromosomal)	SMAD4 c.537TAATA>- (Frame_Shift_Del) p.LI57LI
TKCC-19	Scattered	c.227C>A p.G12V	wild-type	wild-type	wild-type
TKCC-22	Unstable	c.227C>A p.G12V	wild-type	wild-type	TGFBR2 Del/Itx (intrachromosomal). YAP1 loss of function Del (intrachromosomal)
TKCC-23	Stable	wild type	wild-type	wild-type	wild-type
TKCC-25	Scattered	c.227C>A p.G12V	c.578T>- (Frame_Shift_Del) p.H193H	wild-type	wild-type
TKCC-26	Focal	c.226C>G p.G12R	c.372G>T p.C124	wild-type	wild-type
TKCC-27	Unstable	c.227C>T p.G12D	c.485A>T p.I162N	wild-type	wild-type
KPC	-	LSL/G12D+	R172H	wild-type	wild-type

To examine pathway activation at the protein level, protein lysates were generated from a panel of 15 PDCLs, and primary murine cells from the KPC (Pdx1-Cre, LSL-KRasG12D/+, LSL-TrP53R172H/+) mouse model of pancreatic cancer. Protein levels for JAK1, JAK2, STAT3 and SRC, as well as activation of these proteins (as indicated by phosphorylation) were assessed using western blotting (Figure 3.2.1). Expression values (determined by densitometry) were normalised relative to beta-actin (Table 3.2.3), and showed that there is variation in expression of all proteins assessed across the various pancreatic cancer cell lines. Higher than average phospho-STAT3 (Tyr705) levels were defined as values greater than or equal to the average expression detected across the examined panel (mean relative expression=1.2), and higher than average expression was present in 50% (8/16) of cell lines. Utilising the same approach as above to define higher than average expression, phospho-JAK2 (Tyr1007/1008; mean relative expression= 1) and phospho-SRC (Tyr416; mean relative expression= 0.2) were measured in 44% (7/16) and 75% (12/16) of pancreatic cancer lines, respectively.

Activation of JAK1 (analysed as 'negative' or 'positive') was less frequent, with phospho-JAK1 (Tyr1022/1023) detected in 13% (2/16) of cell lines. STAT3, SRC, JAK1 and JAK2 were expressed in all cell lines, with variable levels across the panel.

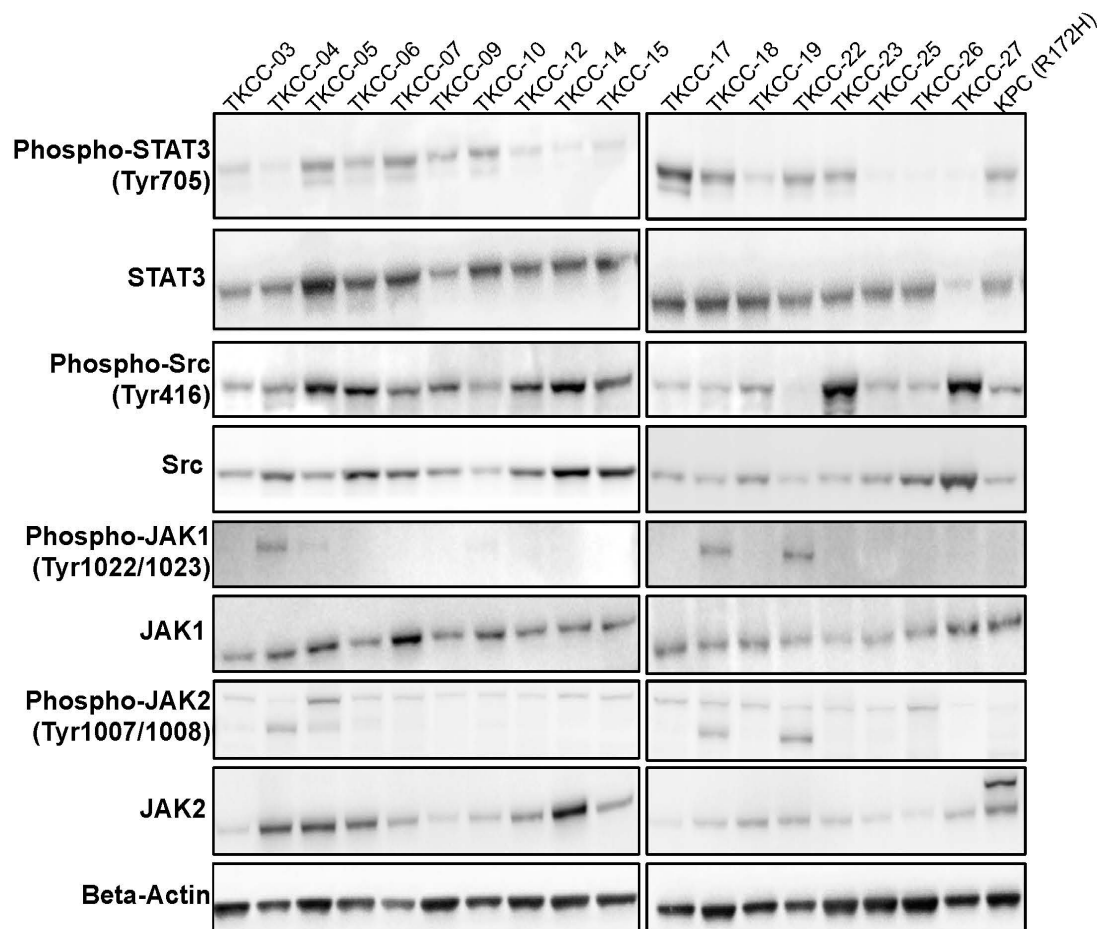


Figure 3.2.1 Western blot for phosphorylated STAT3 (phospho-STAT3; Tyr705), total STAT3, phospho-SRC (Tyr416), total SRC, phospho-JAK1 (Tyr1022/1023), total JAK1, phospho-JAK2 (Tyr1007/1008), total JAK2 and beta-actin of pancreatic cancer patient-derived cell lines (TKCC), and cells from the KPC mouse model of pancreatic cancer (KPC R172H) Data presented as representative images (n=3 independent experiments performed).

Table 3.2.3 Quantification of relative protein expression for phosphorylated STAT3 (phospho-STAT3; Tyr705), total STAT3, phospho-SRC (Tyr416), total SRC, phospho-JAK1 (Tyr1022/1023), total JAK1, phospho-JAK2 (Tyr1007/1008), total JAK2 and beta-actin of 15 pancreatic cancer patient-derived cell lines (TKCC), and primary murine cells from the KPC mouse model of pancreatic cancer (KPC R172H). Expression of target proteins was normalised to beta-actin. Green boxes indicate 'Higher than average' expression, and red boxes indicate 'Lower than average' expression. Higher than average expression was defined as expression \geq mean expression of all lines. Data presented as mean (n=3 independent experiments performed).

Relative protein expression								
Cell line	Phospho-JAK1	JAK1	Phospho-JAK2	JAK2	Phospho-STAT3	STAT3	Phospho-SRC	SRC
TKCC-03	0	0.6	1	0.3	1.2	0.3	0.1	0.7
TKCC-05	0.9	0.7	1.2	0.5	2	0.5	0.3	0.6
TKCC-06	0	0.5	0.9	0.4	1	0.4	0.2	0.8
TKCC-07	0	0.7	0.9	0.3	1.2	0.4	0.3	0.6
TKCC-10	0	0.7	0.8	0.3	1.2	0.4	0.1	0.5
TKCC-12	0	0.7	0.7	0.4	0.7	0.3	0.2	0.7
TKCC-14	0	0.7	0.7	0.5	0.9	0.4	0.2	1.1
TKCC-15	0	0.8	0.8	0.3	1	0.3	0.2	0.9
TKCC-17	0	0.7	0.4	0.3	1.8	0.5	0.1	0.8
TKCC-19	0	0.7	0.5	0.4	1	0.5	0.2	0.8
TKCC-22	0.3	0.7	1	0.5	1.1	0.5	0.1	0.6
TKCC-23	0	0.5	0.5	0.3	1	0.4	0.4	0.6
TKCC-25	0	0.6	0.7	0.3	1	0.5	0.2	0.8
TKCC-26	0	0.6	0.6	0.3	1.2	0.4	0.2	0.8
TKCC-27	0	0.6	0.5	0.3	1.1	0.3	0.4	1
KPC (R172H)	0	0.8	0.6	0.5	1.2	0.4	0.2	0.5

3.2.2 Sensitivity of pancreatic cancer cell lines to JAK and SRC inhibitors

To systematically examine whether SRC-inhibitors and JAK-inhibitors are efficacious in specific subtypes of PDAC, 15 PDCLs suitable for screening in a 96-well format and murine KPC cells were tested for their sensitivity to dasatinib (SRC-inhibitor) (Figure 3.2.2E), ruxolitinib (JAK1/2-inhibitor) (Figure 3.2.2A), and tofacitinib (JAK3/1-inhibitor) (Figure 3.2.2B), using a standard 72-hour cell viability assay. For comparison purposes therapeutic response to JAK1-selective inhibitor AZD289 (Figure 3.2.2C) and JAK2-selective inhibitor AZD1480 (Figure 3.2.2D) was further examined in 3 candidate PDCLs and the KPC cells. Pancreatic cancer cell lines exhibited a range of sensitivities to ruxolitinib (IC_{50} range of 20 μ M to 97 μ M), with a subset of 2/16 cell lines (13%) being relatively sensitive to JAK1/2 inhibition ($IC_{50} < 30 \mu$ M), and 4/16 cell lines (25%) being resistant ($IC_{50} > 60 \mu$ M).

In contrast, all pancreatic cancer cell lines were resistant to JAK3-selective inhibitor tofacitinib ($IC_{50} > 80 \mu$ M; Figures 3.2.2B). Interestingly, examined candidate cell lines were more resistant to JAK1-selective inhibitor AZD289 compared to ruxolitinib, except for KPC cells which had similar IC_{50} s for both compounds (38 μ M AZD289 and 36 μ M ruxolitinib). These same lines were found to be even more resistant to JAK2-selective inhibitor AZD1480 when compared to AZD289 and ruxolitinib ($IC_{50} > 85 \mu$ M for all lines tested). TKCC-22 was highly resistant to treatment with all four JAK inhibitors (AZD289, AZD1480, ruxolitinib and tofacitinib). Overall, the 2D *in vitro* sensitivity data suggest that pancreatic tumour cell lines are most sensitive to dual inhibition of JAK1 and JAK2 kinases.

Pancreatic cancer cell lines also displayed a broad range of sensitivities to SRC inhibitor dasatinib (IC_{50} range of 3 nM to 7.5 μ M) (Figure 3.2.2E), with a subset of 11/16 cell lines (69%) being highly sensitive to SRC-inhibition ($IC_{50} < 150$ nM), and 5/16 cell lines (31%) showing resistance to this agent ($IC_{50} > 1.2 \mu$ M).

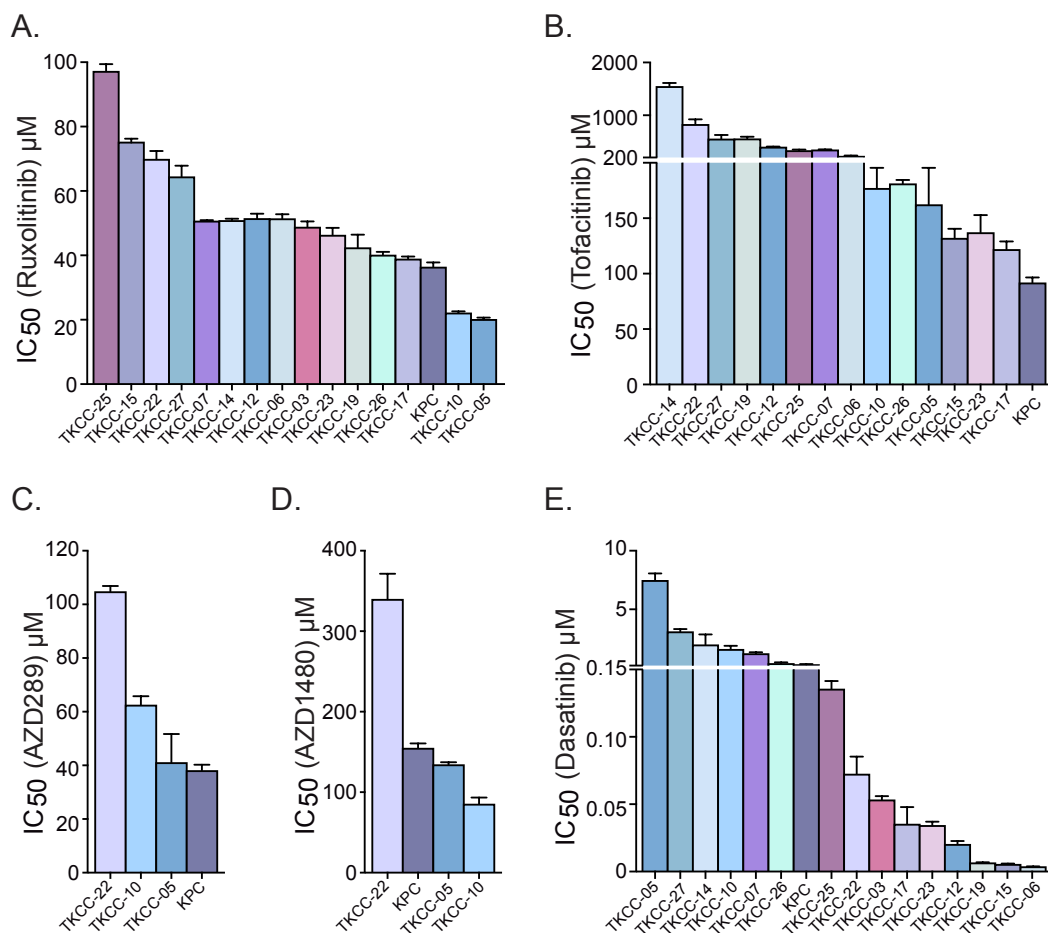


Figure 3.2.2 Drug sensitivity of patient-derived cell lines and murine KPC cells to (A) JAK1/2 inhibitor ruxolitinib, (B) JAK3 inhibitor tofacitinib, (C) JAK1 inhibitor AZD289, (D) JAK2 inhibitor AZD1480 and (E) SRC inhibitor dasatinib. Data presented as mean \pm SE (n=3 independent experiments performed in quadruplicate).

3.2.3 Identification of potential biomarkers of *in vitro* response to ruxolitinib and dasatinib monotherapies

To identify potential molecular correlates of treatment response to key candidate agents (ruxolitinib and dasatinib monotherapies), *in vitro* drug sensitivity data was first correlated with protein expression of various components of the SRC/JAK/STAT3 networks and the SRC/JAK/STAT3 genomic alteration data. As loss of P53 function [321] and inactivation of TGF- β /SMAD4 signalling [122] have previously been shown to directly activate STAT3 signalling in pancreatic tumour cells, therapeutic response was further correlated with *TP53* and *TGFB/SMAD4* mutations.

Of note, higher than average phospho-STAT3 (Tyr705) levels in pancreatic cancer lines were significantly associated with *in vitro* sensitivity to ruxolitinib ($P=0.01$; Figure 3.2.3A), and this correlation remained significant when specific lines with the lowest and highest phospho-STAT3 expression were compared ($P=0.02$; Figure 3.2.3B). Levels of other key proteins within this network (as per Figure 3.2.1), did not correlate with ruxolitinib sensitivity (Figure 3.2.3C-I). Ruxolitinib sensitivity in PDAC lines did not correlate with SRC/JAK/STAT3 pathway aberrations (Figure 3.2.4A), *TP53* mutations (Figure 3.2.4B), or *TGFB/SMAD4* mutations (Figure 3.2.4C). Moreover, subsequent correlation of the levels of phospho-STAT3 (Tyr705) (Figure 3.2.5A-C) or total STAT3 (Figure 3.2.5D-F) proteins with the above-described genomic alterations was not significant.

In contrast with the observed significant association of phospho-STAT3 and ruxolitinib sensitivity, no significant correlates with dasatinib response were found by examining the protein expression (Figure 3.2.6) and mutation data (Figure 3.2.7).

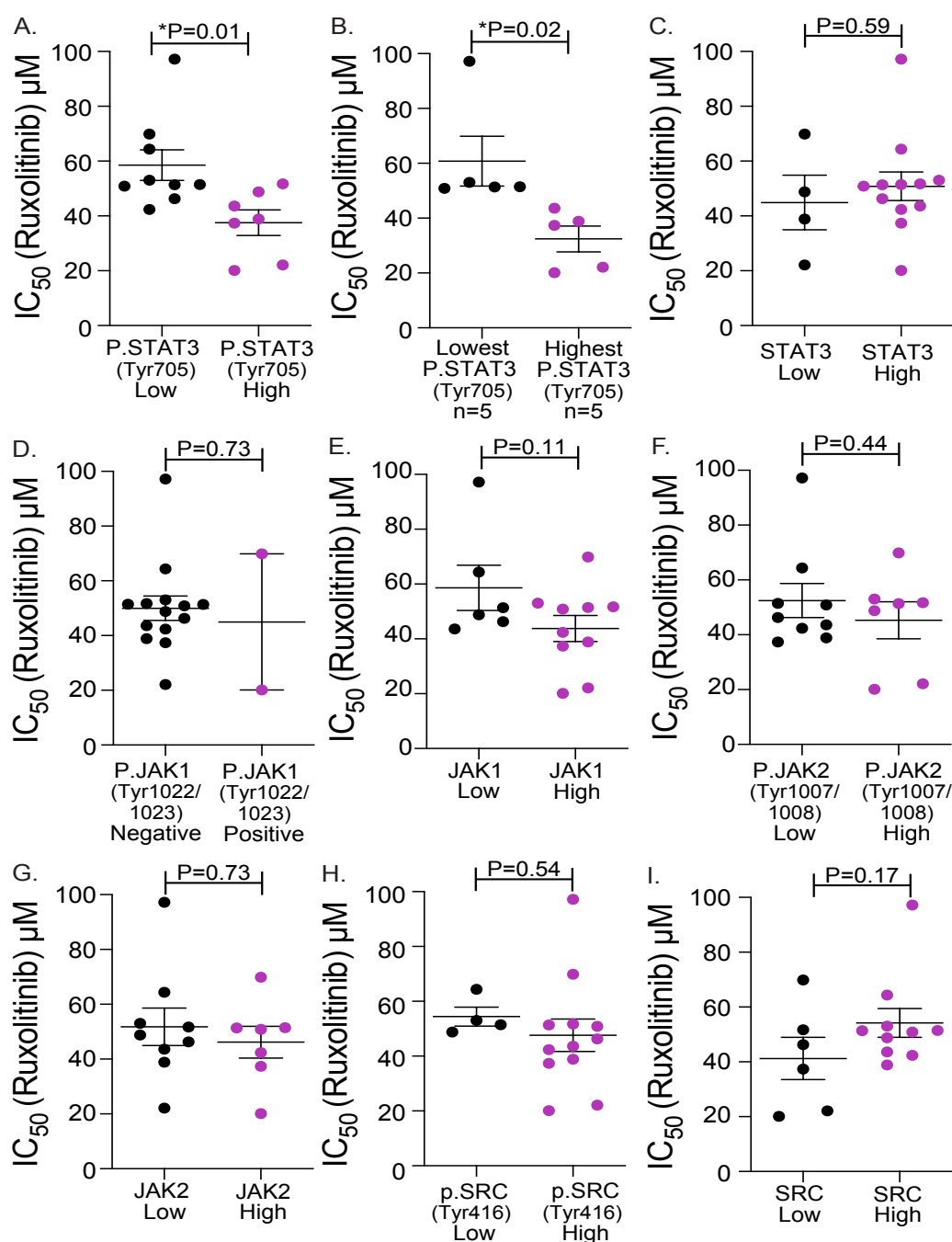


Figure 3.2.3 Correlation of ruxolitinib sensitivity (IC_{50}) and (A) pSTAT3 (Tyr705) expression, (B) lowest (n=5) and highest (n=5) pSTAT3 expressing cell lines, (C) STAT3 expression, (D) pJAK1 (Tyr1022/1023) positivity, (E) JAK1 expression, (F) pJAK2 (Tyr1007/1008) expression, (G) JAK2 expression (H) pSRC (Tyr416) expression, and (F) SRC expression in pancreatic cancer cell lines. 'High' is defined as higher than average expression (expression \geq mean expression of all lines). Data presented as mean \pm SE (n=3 independent experiments). Significance was determined by an unpaired, two-tailed t-test, where * $p < 0.05$, ** $p < 0.01$, *** $p < 0.001$ and **** $p < 0.0001$.

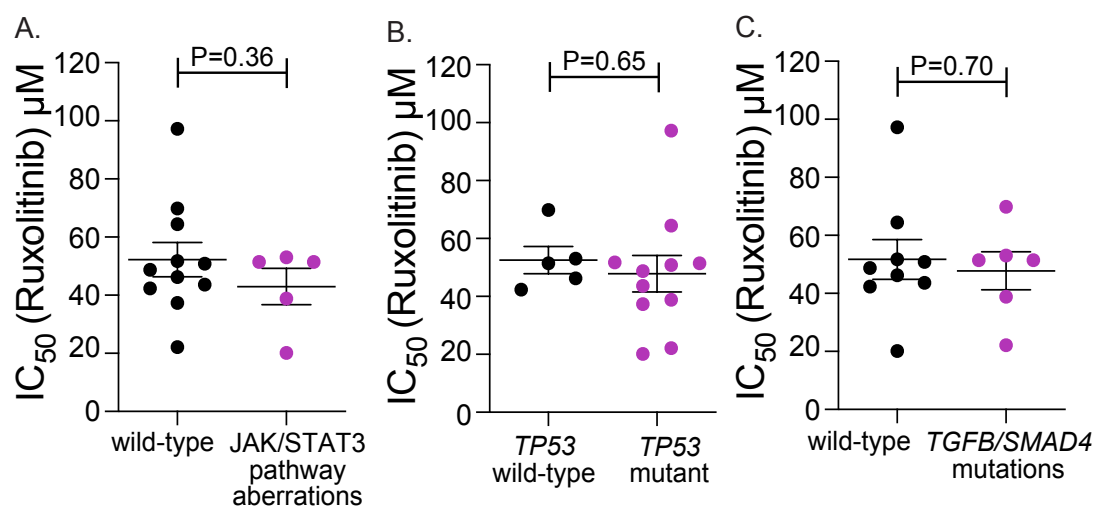


Figure 3.2.4 Correlation of ruxolitinib sensitivity (IC_{50}) and (A) JAK/STAT3 pathway aberrations, (B) *TP53* mutation status, and (C) *TGFB/SMAD4* mutations in pancreatic cancer cell lines. Data presented as mean \pm SE (n=3 independent experiments). Significance was determined by an unpaired, two-tailed t-test, where * $p < 0.05$, ** $p < 0.01$, *** $p < 0.001$ and **** $p < 0.0001$.

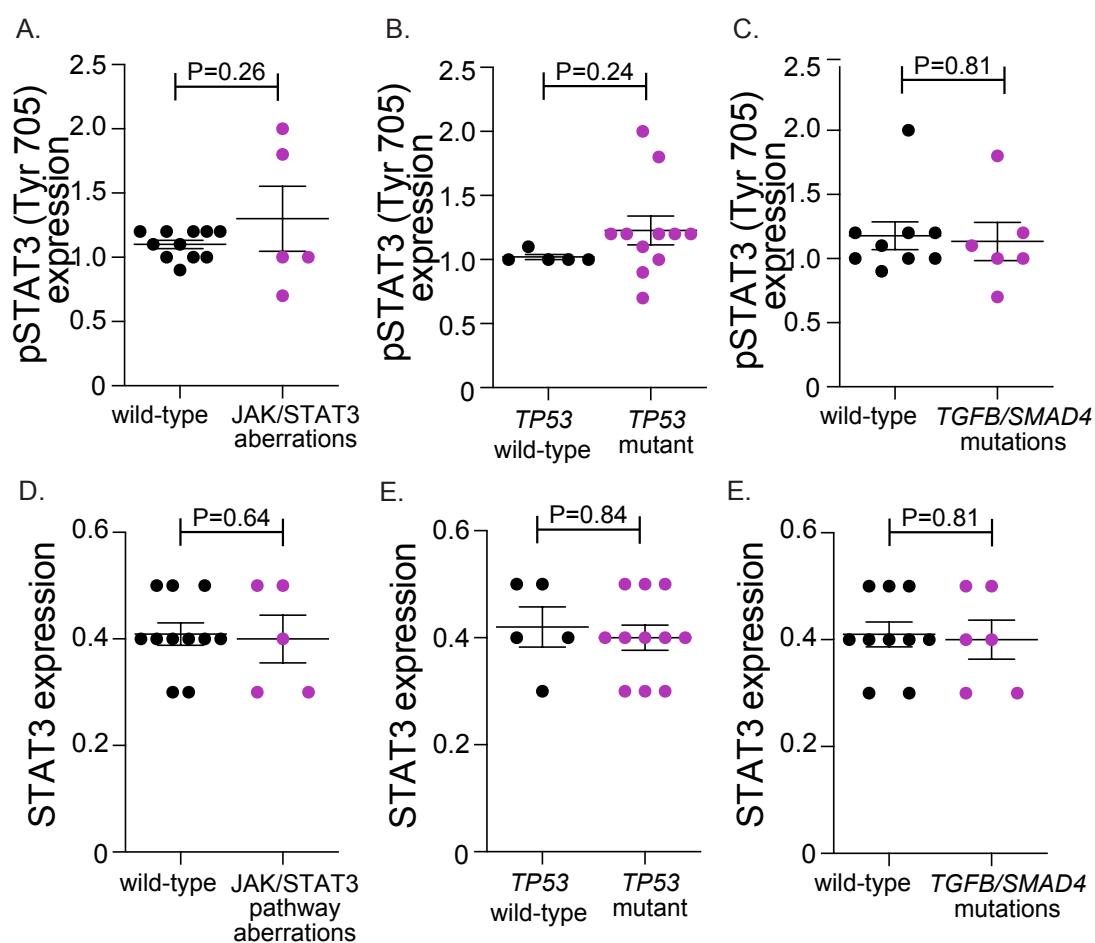


Figure 3.2.5 Correlation of phospho-STAT3 (Tyr705) expression and (A) JAK/STAT3 pathway aberrations, (B) *TP53* mutation status and (C) *TGFB/SMAD4* mutations. Correlation of STAT3 expression and (D) JAK/STAT3 pathway aberrations, (E) *TP53* mutation status and (F) *TGFB/SMAD4* mutations in pancreatic cancer cell lines. Data presented as mean \pm SE (n=3 independent experiments). Significance was determined by an unpaired, two-tailed t-test, where *p<0.05, **p<0.01, ***p<0.001 and ****p<0.0001.

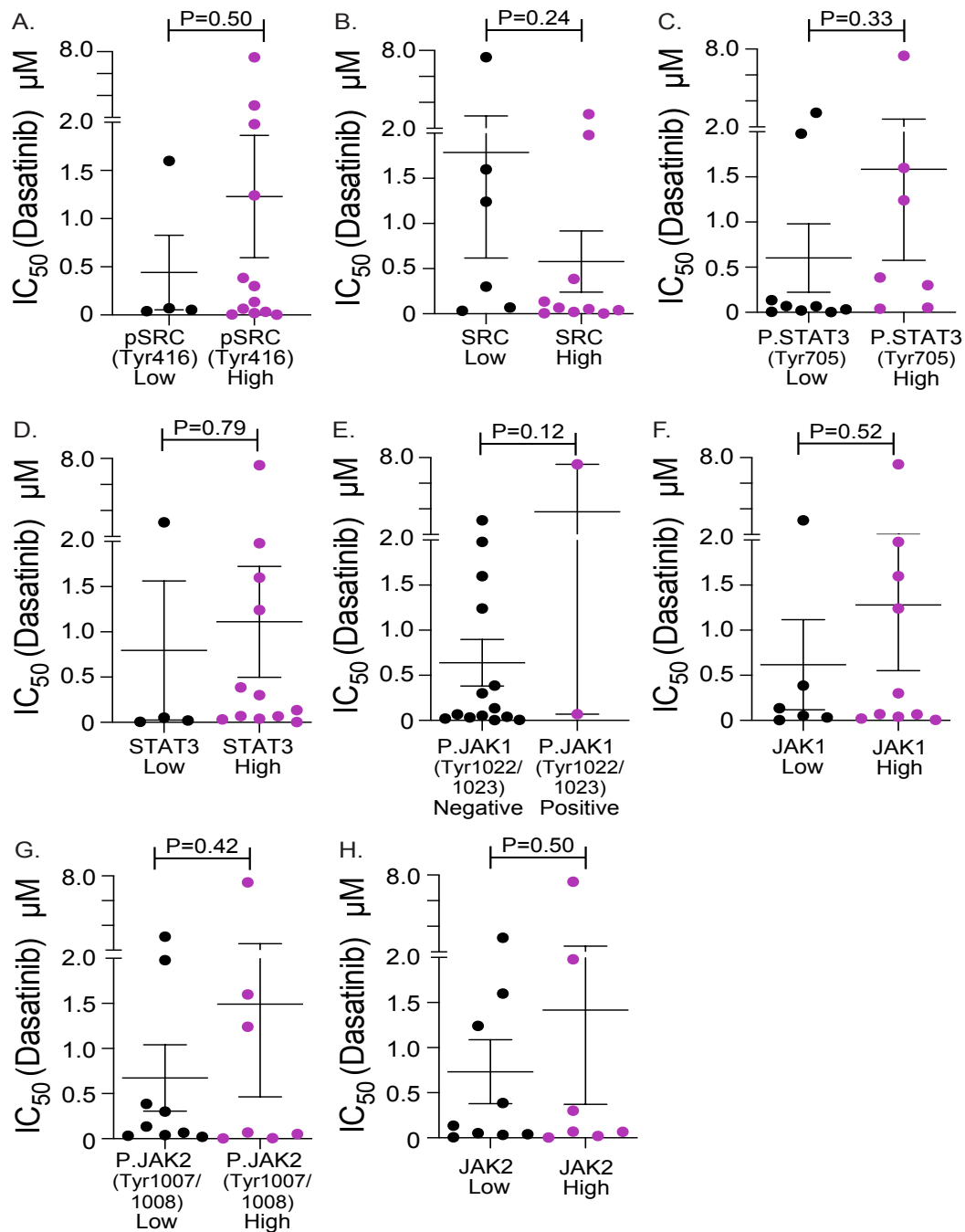


Figure 3.2.6 Correlation of dasatinib sensitivity (IC_{50}) and (A) pSRC (Tyr416) expression, (B) SRC expression, (C) pSTAT3 (Tyr705) expression, (D) STAT3 expression, (E) pJAK1 (Tyr1022/1023) positivity, (F) JAK1 expression, (G) pJAK2 (Tyr1007/1008) expression, and (H) JAK2 expression in pancreatic cancer cell lines. 'High' expression was defined as expression \geq mean expression of all lines. Data presented as mean \pm SE (n=3 independent experiments). Significance was determined by an unpaired, two-tailed t-test, where * $p < 0.05$, ** $p < 0.01$, *** $p < 0.001$ and **** $p < 0.0001$.

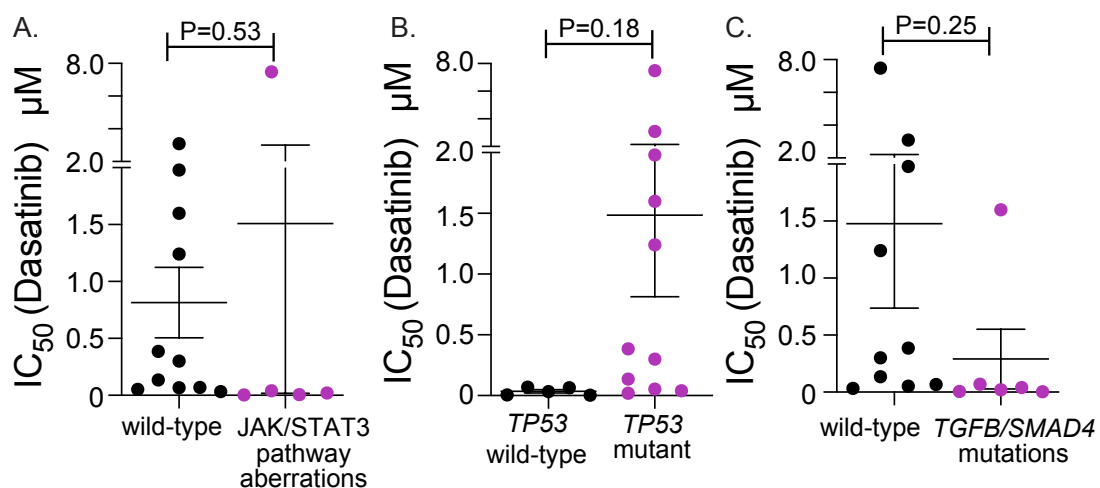


Figure 3.2.7 Correlation of dasatinib sensitivity (IC_{50}) and (A) JAK/STAT3 pathway aberrations, (B) *TP53* mutation status, and (C) *TGFB/SMAD4* mutations, in pancreatic cancer cell lines. Data presented as mean \pm SE (n=3 independent experiments). Significance was determined by an unpaired, two-tailed t-test, where * $p < 0.05$, ** $p < 0.01$, *** $p < 0.001$ and **** $p < 0.0001$.

3.2.4 Assessing the efficacy of the combined inhibition of JAK and SRC in two-dimensional screens

To determine if dual JAK and SRC inhibition potently kills pancreatic cancer cells *in vitro*, dasatinib and ruxolitinib were combined for drug synergy analysis in 12 PDCLs and KPC cells. Drug synergy analysis involves conducting a two-drug combination cell viability assay, and using the combination index method, also known as the 'Chou-Talalay' method for data interpretation [590]. Using this method, a combination index (CI) is calculated at various effective doses (EDs). A combination index (CI) < 1 indicates synergy, CI = 1 indicates an additive effect, and CI > 1 indicates antagonism. Combining dasatinib and ruxolitinib showed strong synergy in 46% (6/13) of the pancreatic cancer cell lines tested (Figure 3.2.8A), these included PDCLs TKCC-05, TKCC-07, TKCC-10, TKCC-17, and TKCC-26, as well as the primary murine KPC cells. In contrast, antagonism was present in 38% (5/13) of cell lines tested (Figure 3.2.8B), including TKCC-06, TKCC-23, TKCC-27, TKCC-22 and TKCC-19. The remaining 15% (2/13 cell lines) exhibited an additive effect, and these cell lines included TKCC-29 and TKCC-14 (Figure 3.2.8C).

To determine if synergy is a likely result of dual JAK1 and JAK2 targeting, two, more selective inhibitors of the JAK family of kinases were included in the synergy screens for comparison (Figure 3.2.8 D-G). The response of the combination of JAK1-selective inhibitor (AZD289) and dasatinib closely mirrored the efficacy observed when dasatinib was combined with ruxolitinib (synergy: TKCC-05, TKCC-10 and KPC (Figure 3.2.8D); antagonism: TKCC-22 (Figure 3.2.8E)).

The JAK2-specific inhibitor (AZD1480) combined with dasatinib resulted in synergy in two of the same cell lines as the ruxolitinib/dasatinib combination (TKCC-10 and KPC; Figure 3.2.8F), and antagonism in one of the same cell lines (TKCC-22; Figure 3.2.8G), highlighting potential differences in response.

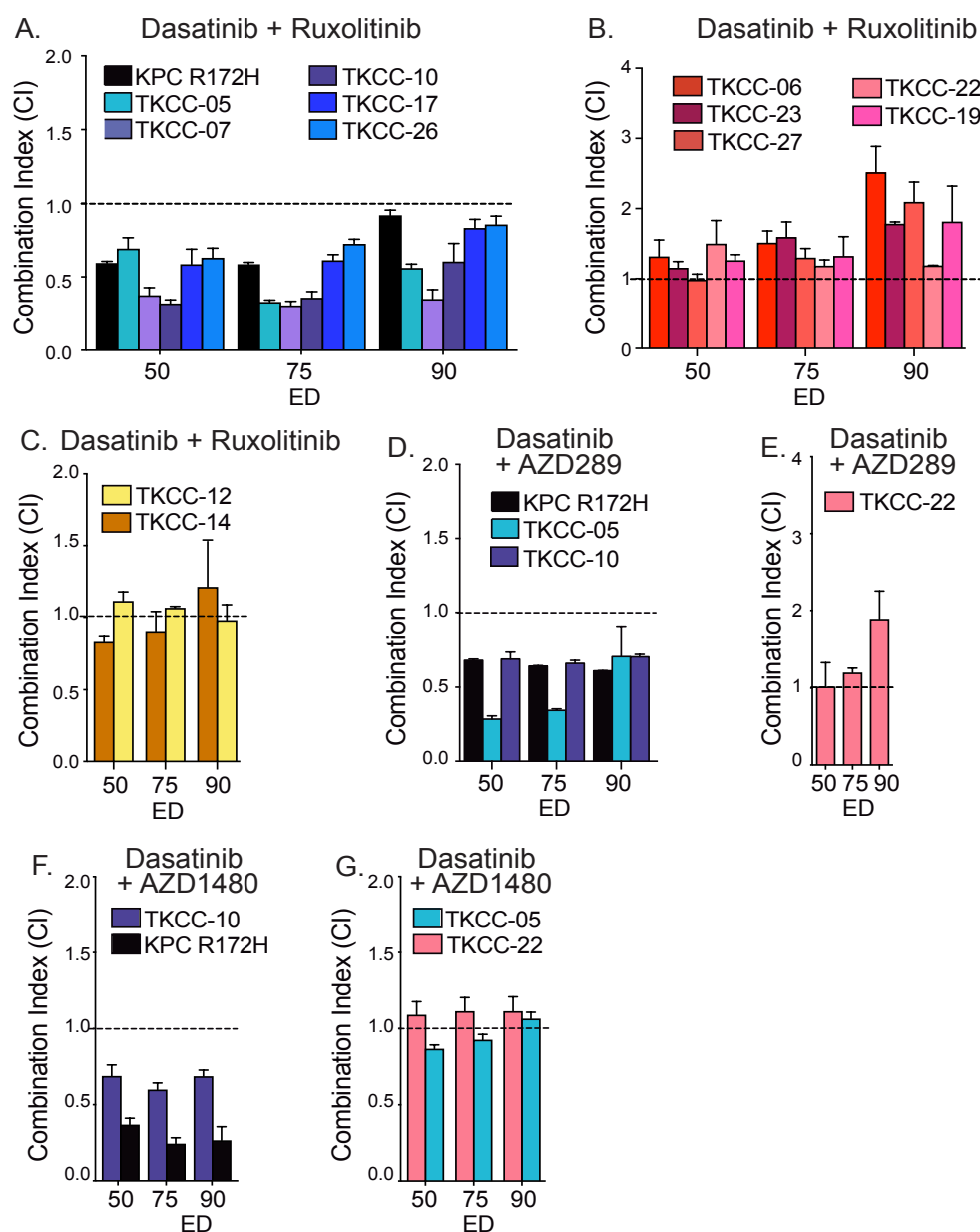


Figure 3.2.8 Drug synergy screens for dasatinib (SRC-inhibitor) and various JAK-inhibitor combinations in pancreatic cancer PDCLs and KPC cells. Combination index (CI) values are calculated using CompuSyn program. CI<1 indicates synergy, CI>1 indicates antagonism, C=1 indicates additive effect, (broken line at CI=1). CI of dasatinib and ruxolitinib (JAK1/2 inhibitor) at various effective doses (ED) in (A) synergistic (B) antagonistic and (C) additive cell lines. CI of dasatinib and AZD289 (JAK1-inhibitor) in (D) synergistic and (E) antagonistic cell lines. CI of dasatinib and AZD1480 (JAK2 inhibitor) in (F) synergistic and (G) antagonistic cell lines. Data presented as mean \pm SE (n=3 independent experiments performed in quadruplicate).

3.2.5 Identification of potential biomarkers of *in vitro* response to the combination of dasatinib and ruxolitinib

As significant correlates of *in vitro* sensitivity of PDAC lines to ruxolitinib have been identified (Figure 3.2.3), the next logical step involved correlation of the combination treatment efficacy data with protein expression of the key SRC/JAK/STAT3 network components (Figure 3.2.9), including the genomic aberrations (SRC/JAK/STAT3, *TP53*, *TGFB/SMAD4*; Figure 3.2.10).

Interestingly, high levels of phospho-STAT3 (Tyr705) as a measure of STAT3 activation were significantly associated with dasatinib and ruxolitinib synergy ($P=0.04$; Figure 3.2.9A), with low phospho-STAT3 levels prevalent in lines where the two-drug combination displayed antagonistic or additive effects. Moreover, *TP53* mutations were significantly associated with sensitivity to the dasatinib/ruxolitinib combination ($P= 0.0098$; Figure 3.2.10A), with 6/9 *TP53* mutant cell lines displaying synergy, and 2/9 cell lines displaying additive effects to this treatment approach (Figure 3.2.9A). In comparison, dasatinib/ruxolitinib combination was antagonistic in all 4 *TP53* wildtype cell lines. *TGFB/SMAD4* mutation status and JAK/STAT3 pathway aberrations did not correlate with response to dasatinib and ruxolitinib combination (Figure 3.2.10B,C).

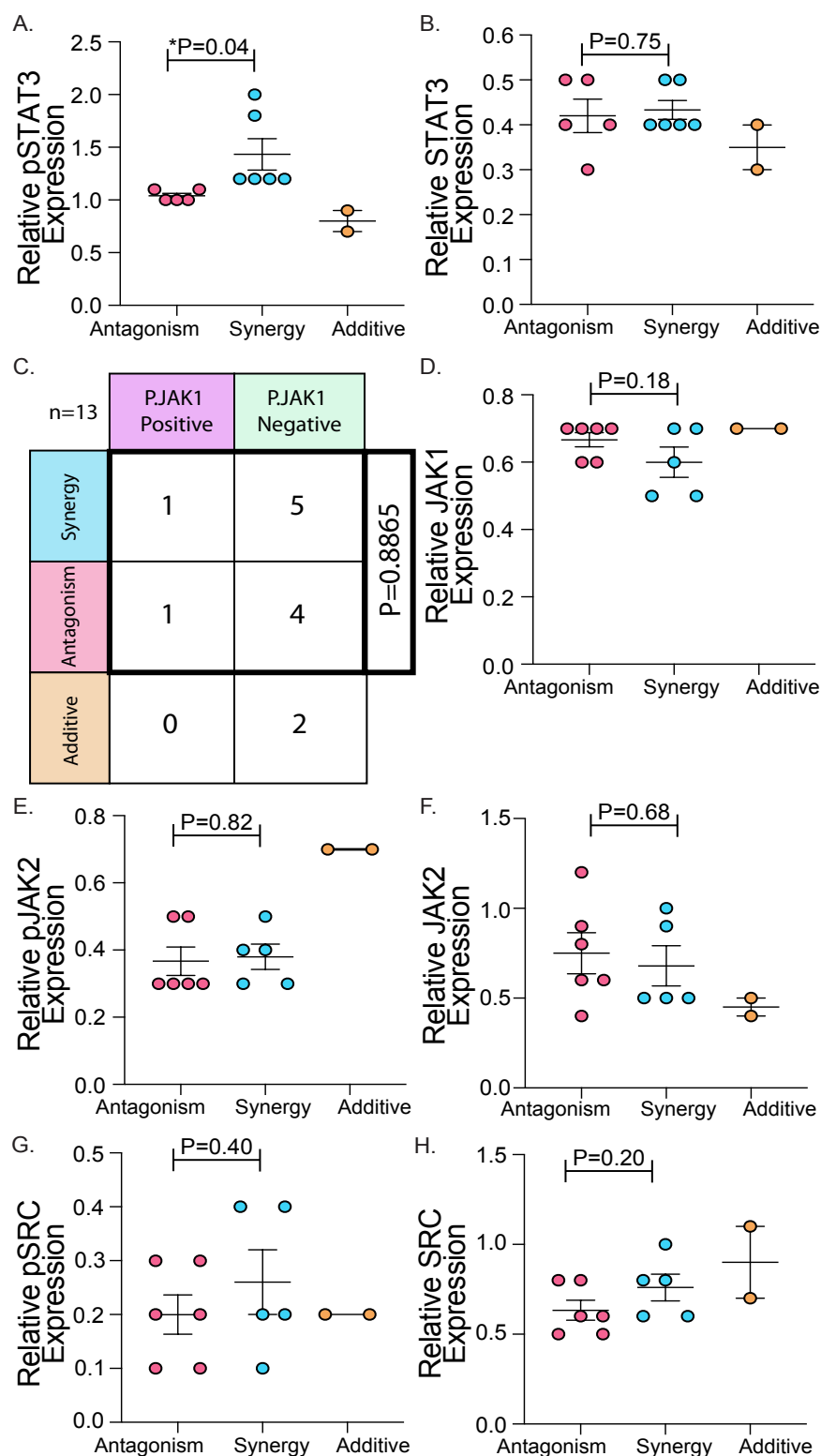


Figure 3.2.9 Correlation of dasatinib and ruxolitinib synergy with (A) pSTAT3 (Tyr705), (B) STAT3, (C) pJAK1 (Tyr1022/1023), (D) JAK1, (E) pJAK2 (Tyr1007/1008), (F) JAK2, (G) pSRC (Tyr416) and (H) SRC expression, in PDAC lines. Data shown as mean \pm SE (n=3). Significance was determined by an unpaired, two-tailed t-test, or a Fisher's exact test for categorical data, *p<0.05, **p<0.01, ***p<0.001 and ****p<0.0001.

A.			
n=13			
	TP53 Mutant	TP53 Wildtype	
Synergy	6	0	**P=0.0098
Antagonism	1	4	
Additive	2	0	

B.			
n=13			
	JAK/STAT3 Pathway Aberrations	JAK/STAT3 Wildtype	
Synergy	2	4	P=0.999
Antagonism	1	4	
Additive	1	1	

C.			
n=13			
	TGFB/SMAD4 Mutant	TGFB/SMAD4 Wildtype	
Synergy	2	4	P=0.567
Antagonism	3	2	
Additive	1	1	

Figure 3.2.10 Correlation of dasatinib and ruxolitinib synergy with (A) *TP53* mutations (B) JAK/STAT3 pathway aberrations and (C) *TGFB/SMAD4* mutation status. Significance was determined by a Fisher's exact test, *p<0.05, **p<0.01, ***p<0.0001 and ****p<0.0001.

3.2.6 Assessing SRC/JAK/STAT3 pathway modulation following treatment with dasatinib and ruxolitinib

Given that the proposed treatment combination of dasatinib and ruxolitinib showed considerable *in vitro* efficacy, particularly in PDAC lines characterised by STAT3 activation (phospho-STAT3 high) and *TP53* mutations (P53 mutant), the next step was to confirm target modulation following treatment and to assess the effects on the downstream signalling. To this end, key candidate patient-derived (TKCC-05) and murine (KPC) pancreatic cancer lines were treated with vehicle, dasatinib, ruxolitinib or the combination of dasatinib and ruxolitinib for 24 and 48 hours. Protein lysates were collected and protein expression was assessed using western blotting (Figure 3.2.11 and Figure 3.2.13). Densitometry was used to quantify the protein expression of various JAK/STAT3 pathway components for KPC cells (Figure 3.2.12) and TKCC-05 cells (Figure 3.2.14).

In the phospho-STAT3 high, P53 mutant (R172H) KPC cells, treatment with ruxolitinib monotherapy, as well as the dasatinib/ruxolitinib combination resulted in a significant and robust inhibition of STAT3 phosphorylation (Tyr705), with no change in levels of total STAT3 (Figure 3.2.11 and Figure 3.2.12A). Phosphorylation status of STAT3 at Ser727, which has previously been shown to have a different role in mitochondrial translocation, cell metabolism and electron transport [20, 435], remained unchanged following treatment with ruxolitinib, but was slightly decreased following combination treatment ($P=0.02$; 24 hours; $P=0.01$; 48 hours) (Figure 3.2.12B), although the overall levels of phospho-STAT3 (Ser727) were low (Appendix C) and required substantial over-exposure of the membrane during the western blot procedure. Dasatinib and the dasatinib/ ruxolitinib combination both effectively inhibited SRC phosphorylation (Tyr416) (Figure 3.2.12D), at the same time leading to a small increase in SRC levels (0.2-fold), indicating an accumulation of unphosphorylated SRC (Figure 3.2.12E). The combination of dasatinib and ruxolitinib further effectively modulated selected downstream effectors of the SRC/JAK/STAT3 pathway, specifically inhibiting AKT phosphorylation (Ser473 and Thr696) as well as phosphorylation of ROCK-

effectors MLC2 (Ser19) and MYPT1 (Thr696). No change in ROCK2, MMP2 and BCL2 levels was measured (Figure 3.2.12F-L).

In the second candidate, pSTAT3-high, P53-mutant (G245S), patient-derived TKCC-05 cell line, similar modulation of the SRC/JAK/STAT3 pathway was observed following treatment with dasatinib, ruxolitinib and dasatinib/ruxolitinib combination. Namely, both ruxolitinib and combination treatment potently blocked STAT3 phosphorylation (Tyr705), with no change in the levels of total STAT3 protein (Figure 3.2.13 A+C and Appendix D). Ser727 phosphorylation, which was present at very low levels (Appendix C), remained unchanged following treatment (Figure 3.2.13B). Again, both dasatinib and dasatinib/ruxolitinib treatment effectively blocked SRC phosphorylation (Tyr416), leading to a small increase in SRC levels (0.2-fold; $P=0.02$; Figure 3.2.13E). As in the KPC model, the combination of dasatinib and ruxolitinib significantly inhibited phosphorylation of AKT (Ser473 and Thr208), MLC2 (Ser19) and MYPT1 (Thr696), with no change in the levels of ROCK2, MMP2 and BCL2 measured (Figure 3.2.13F-L). Collectively, these studies suggest that dasatinib and ruxolitinib effectively modulate key targets SRC and STAT3, as well as the downstream Akt and ROCK signalling components.

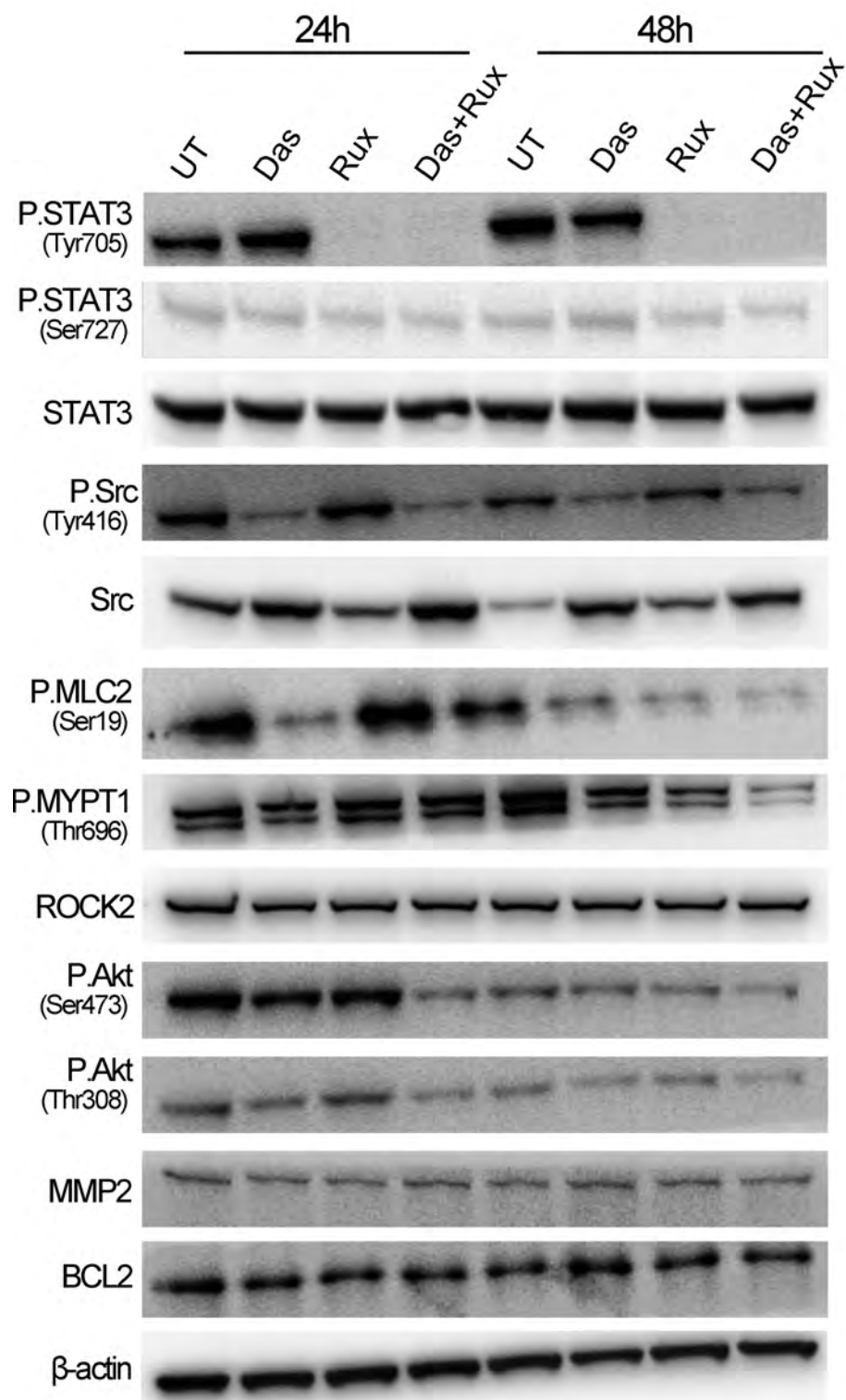


Figure 3.2.11 Western blot showing time-dependent effects of dasatinib, ruxolitinib and combination treatment on levels of SRC/STAT3 downstream effectors in KPC cells.

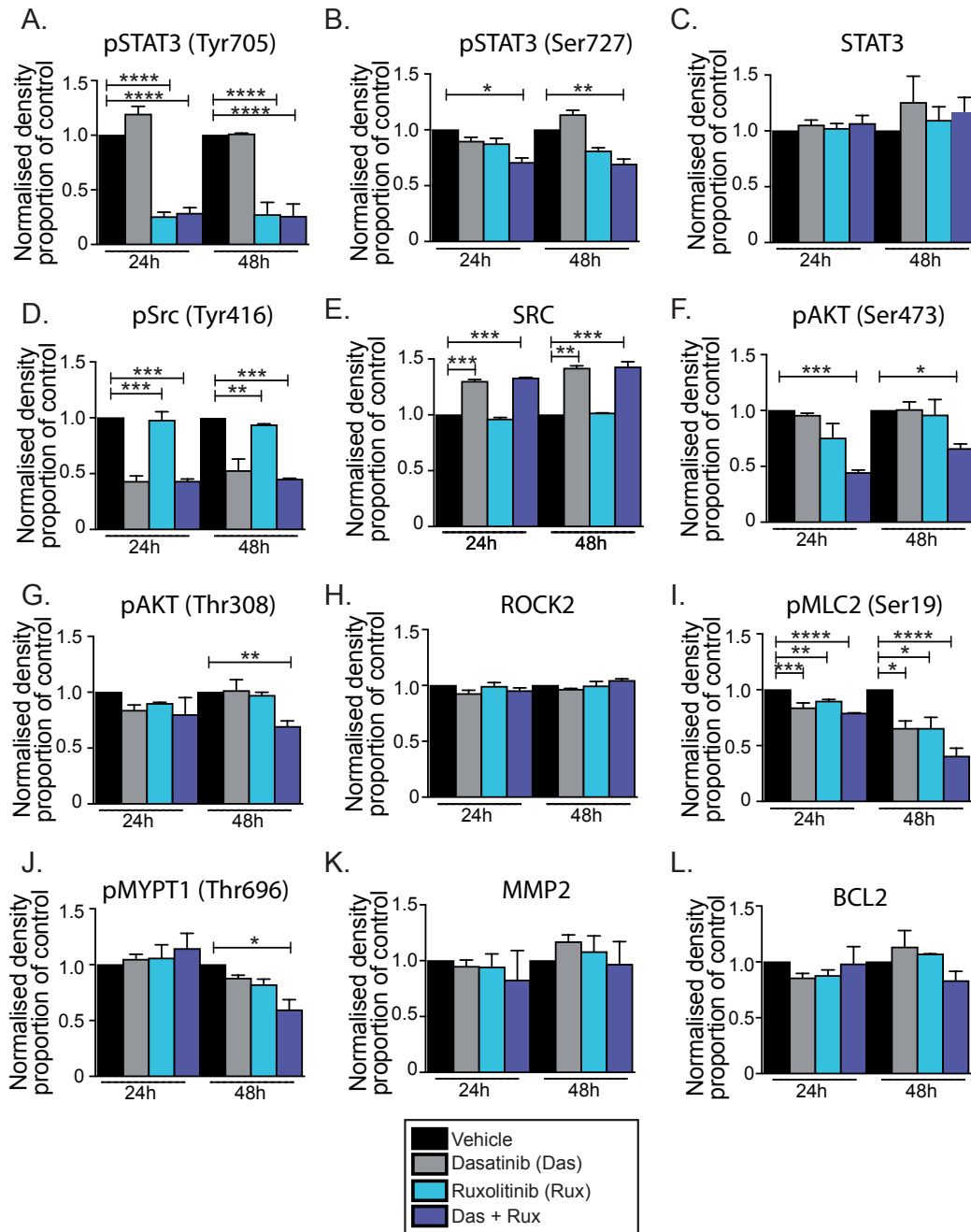


Figure 3.2.12 Densitometry on levels of SRC/STAT3 downstream effectors in KPC cells, assessed for: (A) pSTAT3 (Tyr705), (B) pSTAT3 (Ser727), (C) STAT3, (D) pSRC (Tyr416), (E) SRC, (F) pAKT (Ser473), (G) pAKT (Thr308), (H) ROCK2, (I) pMLC2 (Ser19), (J) pMYPT1 (Thr696), (K) MMP2, (L) BCL2. Data presented as mean \pm SE (n=3 independent experiments). Significance was determined using nonparametric ANOVA test with a Tukey multiple comparisons test where *p<0.05, **p<0.01, ***p<0.001 and ****p<0.0001.

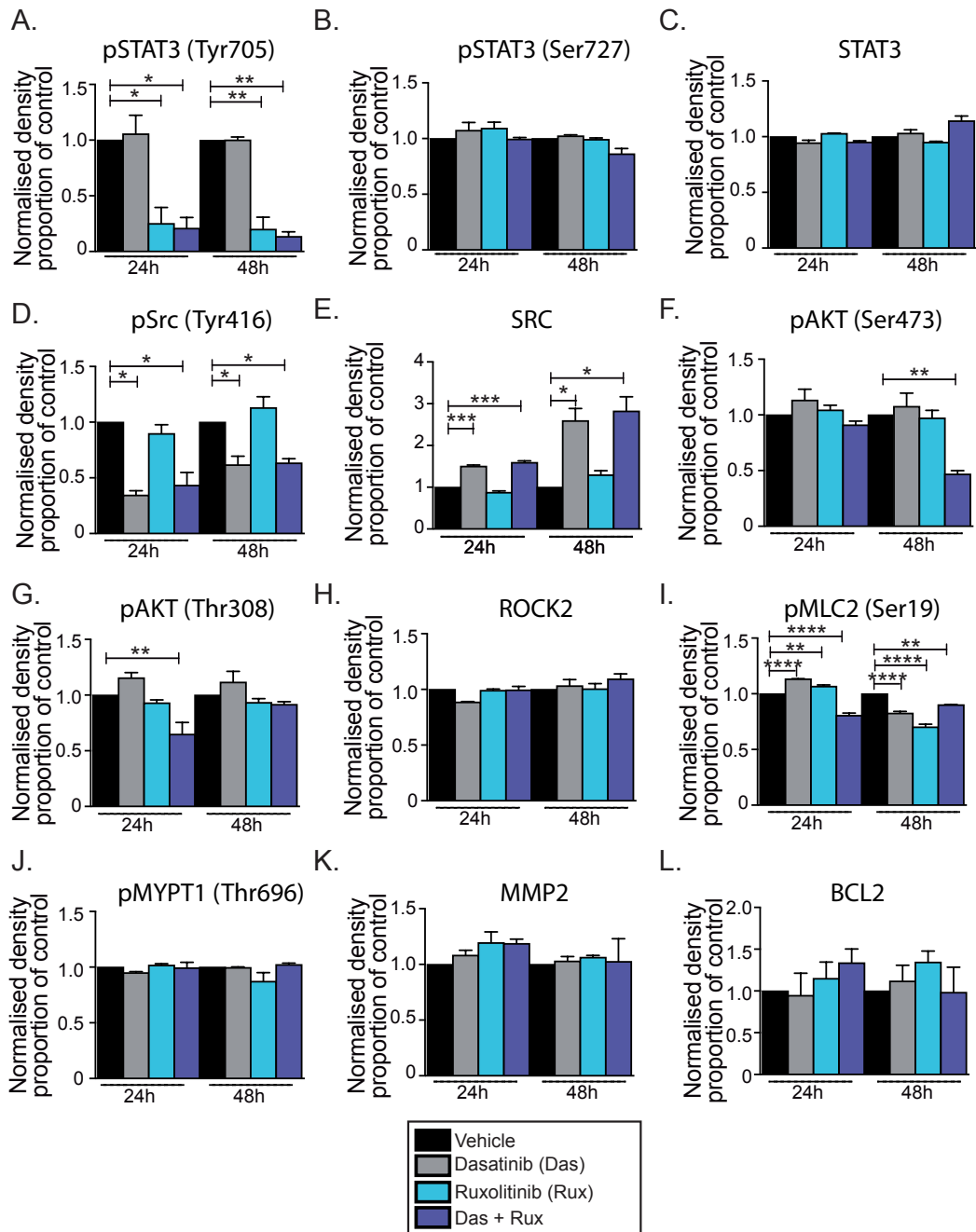


Figure 3.2.13 Densitometry on levels of SRC/STAT3 downstream effectors in TKCC-05 cells, assessed for: (A) pSTAT3 (Tyr705), (B) pSTAT3 (Ser727), (C) STAT3, (D) pSRC (Tyr416), (E) SRC, (F) pAKT (Ser473), (G) pAKT (Thr308), (H) ROCK2, (I) pMLC2 (Ser19), (J) pMYPT1 (Thr696), (K) MMP2, (L) BCL2. Significance was determined using nonparametric ANOVA test with a Tukey multiple comparisons test where * $p < 0.05$, ** $p < 0.01$, *** $p < 0.001$ and **** $p < 0.0001$.

3.3 Discussion

The SRC/JAK/STAT3 pathway is a major oncogenic signalling cascade that plays a role in pancreatic carcinogenesis from the development of early pre-malignant pancreatic lesions to promoting cancer progression and metastasis in established PDAC [321]. Key components of this dynamic pathway have been shown to be frequently altered in pancreatic cancer and can promote a pro-tumourigenic pancreatic tumour microenvironment. Moreover STAT3 is a target of SRC, that drives invasive tumour cell behaviour [177]. Earlier immunohistochemical (IHC) analyses in human PDAC have identified SRC to be expressed in all PDAC tumours assessed [177, 191]. High expression (grade 3) of activated (phosphorylated) SRC was present in 26% (23/90) of resection-margin positive PDAC tumours, and was significantly correlated with reduced survival [177]. Moreover, IHC studies have identified activated (phosphorylated) STAT3 to be highly expressed in 52% of PDAC tumours [321], and high STAT3 activation levels together with P53 accumulation were associated significantly with reduced overall survival [321]. Following these findings, we have utilised the sequencing data from three separate clinical cohorts (ICGC, UTSW, TCGA) and have identified the SRC/JAK/STAT3 pathway to be altered in approximately one third of pancreatic cancer patients. Consistent with previous reports very few of these changes were somatic mutations, and the majority of pancreatic tumours exhibited copy number alterations [489]. Consequently the SRC/JAK/STAT3 pathway presents an interesting signalling network for therapeutic targeting in PDAC.

Given the role that the SRC/JAK/STAT3 pathway plays in cellular proliferation and viability, angiogenesis and metastasis of pancreatic cancer [441, 442], we hypothesised that dual inhibition of this pathway with SRC and JAK small-molecule inhibitors may lead to significant sensitisation of PDAC cell lines, in a subtype-specific context. Our *in vitro* results demonstrate that the effects of SRC inhibition and JAK inhibition on cellular proliferation are heterogenous, and are relevant to what has been previously published in pancreatic cancer cell lines (ruxolitinib IC_{50} = 5-191 μ M; dasatinib IC_{50} = 0.04-254 μ M) [591]. Moreover we have shown that levels of STAT3 phosphorylation (a measure of STAT3 activation) can predict for ruxolitinib sensitivity ($P=0.01$; Figure 3.2.3).

It is important to note that these ruxolitinib-sensitive cell lines had IC₅₀ values in excess of 20 µM, and some off-target activity may have contributed to the anti-proliferative activity. Importantly, no biomarkers of therapeutic response have previously been identified for ruxolitinib, and this may explain the poor clinical efficacy of ruxolitinib when examined in unselected populations in PDAC [555, 573]. Furthermore, we are the first to demonstrate that candidate pancreatic cancer cell lines are more sensitive to combined JAK1 and JAK2 inhibition compared to selective targeting of JAK1, JAK2 kinases, and were resistant to JAK3 kinase inhibition. Prior studies have examined efficacy of JAK and SRC inhibitors as monotherapies on cancer cell proliferation using genetically engineered and commercial pancreatic cancer cell lines [177, 533, 534], but have never examined the proliferative effects on a genomically diverse panel of cell lines, and have never assessed these inhibitors as a combination treatment regimen.

The widespread molecular heterogeneity and the lack of effective therapies make pancreatic cancer an ideal disease for advancing personalised medicine strategies, and there is strong evidence to suggest that the use of biomarkers and molecular stratification is successful in pancreatic cancer [4, 7, 592, 593]. Building on the promising preclinical and early clinical data on the robust efficacy of JAK and SRC-inhibitor combinations in specific haematological malignancies [570, 571, 594], the observed strong synergy between dasatinib and ruxolitinib in a substantial number of PDAC lines, as described in this chapter, is of significant interest. Our findings provide the first direct evidence of synergy between JAK and SRC inhibition in pancreatic cancer and moreover, this efficacy appears to be subtype-specific. Namely, PDAC lines characterised by high levels of phospho-STAT3 (Tyr705) and *TP53* mutations were highly sensitive to combined JAK1/2 and SRC inhibition (P=0.04, phospho-STAT3, Figure 3.2.9A; P=0.0098, P53, Figure 3.2.10A). In concordance, dual JAK/SRC targeting was ineffective in phospho-STAT3 low PDCLs, that do not harbour genetic alterations in P53 (4/5; Figure 3.2.10A).

The use of a large genomically-characterised panel of PDCLs in this study has enabled us to characterise the broad range of responsiveness to the proposed treatment approach. The cause of constitutive STAT3 activation in

pancreatic cancer is complex and numerous mechanisms have been described including persistent PDX-1 expression [437], changes in the tumour mutational landscape [122, 321], tumour microenvironment (non-cell autonomous activation) [595], and persistent expression of IL-6, IL-11 [166]. It has also been shown that mutated or biallelic loss of P53 contributes to STAT3 activation in both murine and human pancreatic cancer [321]. The mechanism behind *TP53* mutations leading to STAT3 activation in this context is yet to be elucidated, however the relationship between P53 and STAT3 is known to be complex, and many have attempted to discover its intricacies. Wormann *et al.* reported loss of P53 shifting transient STAT3 activation to persistent STAT3 activation, a process which is mediated by intracellular reactive oxygen species (ROS) accumulation, Shp2 inactivation, and prolonged JAK2 phosphorylation [321]. Mutations in *TP53* have also been shown to disrupt the balance of protein tyrosine phosphatase 1-B (PTP-1B) and its target JAK2, leading to upregulation of phospho-STAT3 in ovarian carcinoma [596]. Furthermore, wildtype P53 has been demonstrated to reduce expression of phosphorylated STAT3 and inhibit STAT3 DNA binding activity in prostate cancer cell lines that have constitutively activated STAT3 [597]. Interestingly, the two cell lines where dasatinib and ruxolitinib combination displayed an additive effect had *TP53* mutations (TKCC-12: c.586G>A p.R196; TKCC-14: c.527C>G p.C176S), but expressed low phospho-STAT3. In addition, TKCC-25 (P53: c.578T>- p.H193H; low phospho-STAT3) and TKCC-27 (P53: c.485A>T p.I162N; low phospho-STAT3), were both found to be highly resistant to ruxolitinib, suggesting that other mechanisms may further contribute to STAT3 activation, at the same time helping explain the lack of association between ruxolitinib sensitivity or phospho-STAT3 levels with *TP53* mutation status.

We further observed no correlation between *TGFB/SMAD4* mutations and phospho-STAT3 levels despite previous reports describing the contribution of impaired TGF β signalling to elevated epithelial STAT3 activity in PDAC models [122]. These discrepancies may be further explained by the non-cell autonomous mechanisms behind STAT3 activation, including stromal signalling [166] present in the human PDAC tumours analysed in the

Wormann *et al.* [321] and Laklai *et al.* [122] studies, but absent in the two-dimensional *in vitro* cultures utilised in this chapter.

Our findings also demonstrate that synergy isn't dependent on JAK1 or JAK2 inhibition alone, and that the strength of synergy may be cell-line dependent. Moreover, we observed potent target modulation in phospho-STAT3 high, P53-mutant pancreatic cancer cell lines of interest, following JAK, SRC inhibition as well as dual JAK/SRC targeting. Only the combination therapy effectively blocked the downstream Rho/ROCK and PI3K/Akt effector pathways at the selected 24 hour and 48 hour timepoints, however these findings need further examination to determine exact downstream mechanisms via investigation of additional downstream proteins. Although downregulation of some of the other known downstream effectors including MMP2 was not observed post-treatment, this could potentially be attributed to the lack of tumour microenvironment and extracellular matrix in the two-dimensional *in vitro* cultures here, which is necessary for MMP-mediated effects [177, 598]. Our data thus indicate that dual-inhibition of STAT3 and SRC is effective at modulating the SRC/JAK/STAT3 pathway.

In summary, these *in vitro* studies are the first to establish that the combination of JAK and SRC inhibition is synergistic in specific pancreatic cancer cell types, in particular lines that harbour *TP53* mutation and activated STAT3, and that this therapeutic combination is more effective at modulating the SRC/JAK/STAT3 pathway than either therapy alone. Due to limitations of two-dimensional proliferation assays, which do not fully recapitulate the complex tumour ecosystem and do not consider the important role the microenvironment plays in SRC/JAK/STAT3 pathway regulation [186, 599], as well as in drug pharmacodynamics and tissue perfusion [600], the remaining chapters of this thesis will assess the efficacy of this therapeutic combination in the context of a more complex tumour microenvironment using three-dimensional *in vitro* assays, as well as *in vivo* studies.

Chapter 4. *In vitro* efficacy of SRC and JAK1/2 inhibitors in 3D models of pancreatic cancer

4.1 Introduction

The pancreatic tumour microenvironment comprises both cellular elements and significant desmoplasia that collectively form an effective physical barrier leading to limited drug penetration. In addition, dynamic cancer cell-stromal cell crosstalk directly promotes cancer growth, survival and treatment failure [114]. The extracellular matrix is a major component of the tumour microenvironment that provides mechanical and structural support to cells, aids in cell migration and coordinates important signalling processes (as outlined in chapter 1.2) [116]. The highly remodelled extracellular matrix and resultant tumour stiffening in PDAC [321, 540] actively promotes pancreatic cancer cell invasion into the surrounding tissues, increases propensity for metastasis, and drives disease progression [201, 205, 321, 540, 601], simultaneously impeding chemotherapy penetration and ultimately leading to chemoresistance [443]. Consequently, therapeutic targeting of extracellular matrix remodelling and aspects of pancreatic tumour desmoplasia is an interesting and highly active area of research.

The SRC/JAK/STAT3 pathway has been previously demonstrated to promote matricellular fibrosis and increased tissue tension in PDAC, leading to decreased chemotherapeutic efficacy [321]. In addition, downstream Rho/ROCK signalling regulates the actomyosin cytoskeleton during PDAC progression, and can ‘tune’ the desmoplastic stroma to further promote pro-tumourigenic signalling, cancer growth and disease spread [122, 201, 602, 603]. Furthermore, STAT3 ablation combined with chemotherapy can enhance drug delivery by reducing stromal stiffening and epithelial contractility via loss of TGF- β signalling and downregulation of cytidine deaminase [122] [443]. Therefore targeted inhibition of this pathway has significant potential to decrease fibrosis and may improve chemotherapeutic efficacy, particularly if the treatment approach is coupled with a biomarker.

In this chapter, firstly, we assessed the effects of dual SRC and JAK inhibition on the structural and mechanical properties of the extracellular matrix, using

3D fibroblast-driven contraction assays. This assay recreates the structural properties of PDAC that cannot be examined using 2D cultures, and has been extensively used to assess extracellular matrix remodelling in PDAC [602, 604-606].

Cancer cell invasion is the first step towards tumour cell spread and metastasis, and this process can be regulated by various cell-autonomous mechanisms [607, 608], as well as mechanical and biomechanical cues from the surrounding microenvironment [607, 609]. Extracellular matrix integrity can directly promote cell migration and invasion, and intercellular signalling via integrins is also essential [610, 611]. Furthermore, stromal fibroblasts play a role in the formation of matrix 'tracks' to guide the movement of cancer cells [608], and the dynamic cancer cell-stromal cell crosstalk directly promotes cancer cell invasion, growth and survival [114]. Due to the role the SRC/JAK/STAT3 pathway plays in this crosstalk and in extracellular matrix remodelling, we assessed the effect of SRC and JAK inhibition on PDAC cellular invasion in a molecular subtype-specific context, using key candidate P53 mutant and phospho-STAT3 "high" cell lines, in 3D organotypic assays. These assays recreate the structural and mechanical properties of the extracellular matrix as well as the interactions that occur between cancer cells and fibroblasts. This methodology has been used extensively to assess the mechanisms of cell invasion and for therapeutic efficacy studies [83, 149, 604, 605, 612].

The cellular elements of the pancreatic tumour microenvironment are diverse, and include a heterogeneous population of activated cancer-associated fibroblasts (including inflammatory CAFs (iCAFs) and myofibroblasts (myCAFs)) as well as different subsets of immune cells [114, 141]. iCAFs express inflammatory markers such as *IL-6* and *Lif*, while myCAFs are a population that express myofibroblast and matrix-associated markers such as collagens (*Col1a1*, *Col15a1*, *Col12a1*, *Col8a1*), actin (*Acta2*), and *Sparc*, as well as *Tgfb1*. TGF- β and IL-1/JAK/STAT3 signalling are responsible for the formation and plasticity of these different CAF populations [141]. Furthermore, complex intercellular signalling networks that occur between the cellular elements of the tumour microenvironment drive cancer progression

[124, 127-134]. Specifically, paracrine signalling between cancer cells and CAFs provides growth factors, matrix remodelling enzymes and inflammatory cytokines, that influence cancer cell behaviour and promote tumour cell invasion, metastasis and survival, resulting in a cooperative relationship [135, 136]. Over-activation of these pro-inflammatory signalling networks is largely driven by the JAK/STAT3 pathway [188, 416], and results in cytokine release and subsequent recruitment and activation of various immune cells including tumour-associated macrophages (TAMs), myeloid-derived suppressor cells (MDSCs), and regulatory T cells (T regs) [153]. The resulting immunosuppressive tumour microenvironment is a defining characteristic of PDAC.

The potent immunomodulatory functions of SRC and JAK/STAT3 pathway inhibition has been previously demonstrated in cancers including pancreas [301, 321], however the assessment of synergistic combinatorial therapies involving immunomodulatory drugs such as dasatinib and ruxolitinib has not been studied. Therefore, in this chapter, we established 3D co-culture organoids and utilised multiplex cytokine arrays to determine if dual targeting of SRC and JAK/STAT3 may effectively modulate pro-inflammatory, pro-fibrotic and pro-tumourigenic signalling networks. Finally, using a highly-parallel single-cell RNA-sequencing approach, we identified important transcriptional changes following treatment with dasatinib and ruxolitinib in distinct cellular populations within the co-culture organoids. Of note, single-cell analyses provides a high level of resolution when studying tumour heterogeneity and therapeutic mechanism of action [613], and may reveal the potential for selective therapeutic targeting of individual cell populations.

This chapter aims to:

- Examine the effects of SRC and JAK inhibition on fibroblast contractility and extracellular matrix integrity using *in vitro* 3D contraction assays.
- Assess the anti-invasive effects of SRC and JAK inhibition using 3D organotypic invasion assays.
- Examine the effects of SRC and JAK inhibition on intercellular crosstalk using 3D co-culture organoids.
- Identify transcriptional signatures associated with SRC and JAK inhibition in various cell populations of 3D co-culture organoids.

4.2 Results

4.2.1 Assessing the effect of SRC and JAK inhibition on the extracellular matrix in 3D collagen matrices

To examine the effects of SRC and JAK inhibition on extracellular matrix remodelling *ex vivo*, and specifically, collagen contraction, telomerase-immortalised fibroblasts (TIFs) were embedded in rat-tail collagen I, and allowed to remodel the collagen matrix over 12 days in the presence or absence of targeted therapies of interest (Figure 4.2.1; described in methods section 2.8, and published by Timpson *et al.* [614]). Measurement of the surface area of the collagen matrix at day 12 indicated that ruxolitinib (JAK1/2-inhibitor) significantly impaired the ability of fibroblasts to contract native, fibrillar collagen, with similar effects when ruxolitinib and dasatinib were combined (Figure 4.2.2A). To assess the effects of JAK1/2 inhibition on the physical and mechanical properties of the extracellular matrix, collagen matrices were examined using Second Harmonic Generation imaging (SHG) (Figure 4.2.2B) [615], and Picrosirius Red-staining (Figure 4.2.2C) [616]. Maximum intensity of the SHG signal acquired throughout the section was significantly decreased upon treatment with ruxolitinib mono- and combination therapy, compared to control. These findings were confirmed by brightfield imaging of Picrosirius Red-stained sections (Figure 4.2.2C), where collagen I and III density was significantly decreased following ruxolitinib treatment and the combination of dasatinib and ruxolitinib. In contrast, dasatinib treatment led to a more modest decrease in collagen content (measured using SHG imaging). These data indicate that JAK1/2 inhibition with ruxolitinib leads to decreased levels of fibrillar collagen, reducing the ability of fibroblasts to contract the matrix.

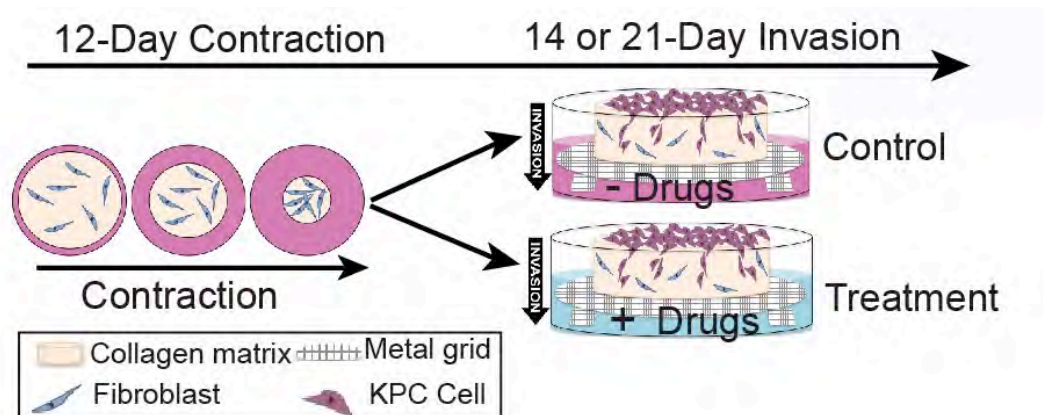


Figure 4.2.1 Schematic of organotypic invasion assay set-up. Collagen-fibroblast plugs are allowed to contract for 12 days, following which cancer cells are seeded on top and allowed to attach for 4 days. The plugs are then transferred on top of a metal grid, and an air-liquid interface is created to promote cells to invade through the collagen matrix.

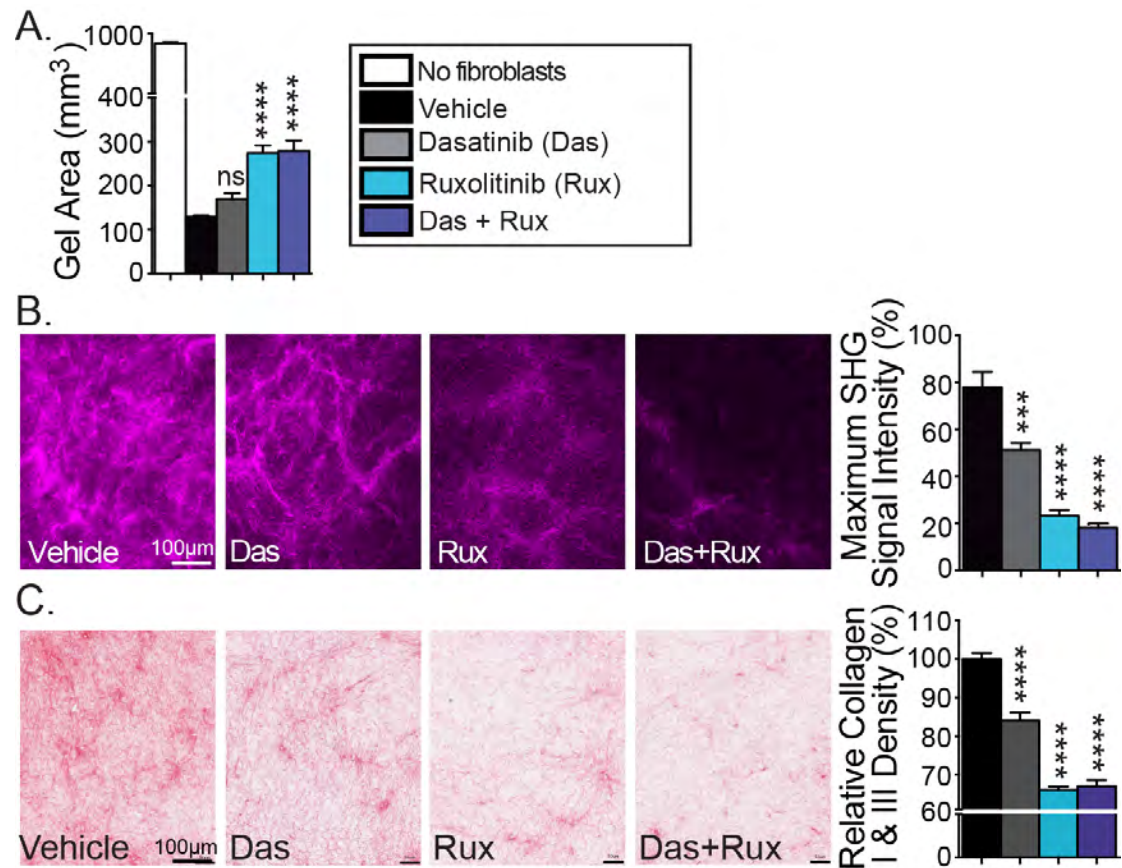


Figure 4.2.2 JAK1/2 inhibition disrupts collagen matrix integrity. (A) Quantification of TIF-collagen matrix area following treatment with dasatinib, ruxolitinib and the combination of dasatinib and ruxolitinib at endpoint (12 days). (B) Quantification and representative maximum intensity projections of second harmonic generation (SHG) signal intensity at peak in matrices after 12 days of contraction. (C) Quantification and bright-field images of Picrosirius Red-stained collagen matrices treated with dasatinib and ruxolitinib. Data are presented as mean \pm SEM (n=3 independent experiments, performed in triplicate matrices per condition, per repeat). Significance was determined using nonparametric ANOVA test with a Tukey multiple comparisons test where *p<0.05, **p<0.01, ***p<0.001 and ****p<0.0001. Unless indicated, significance is compared against vehicle. Das: dasatinib; Rux: ruxolitinib; Das+Rux: dasatinib and ruxolitinib.

To determine if the effects seen on the extracellular matrix are likely the result of dual JAK1 and JAK2 targeting, three additional more selective inhibitors of the JAK family of kinases were assessed for their ability to remodel the extracellular matrix *in vitro*. The findings for AZD289 (JAK1-selective inhibitor), AZD1480 (JAK2-inhibitor) and tofacitinib (JAK3-selective inhibitor) are summarised in Figures 4.2.3, 4.2.4 and 4.2.5, respectively. JAK1 and JAK3 inhibitors (AZD289 and tofacitinib), significantly inhibited the ability of fibroblasts to contract the matrix (Figure 4.2.3A and Figure 4.2.5A), and blocked collagen deposition *in vitro* (Figure 4.2.3B+C and Figure 4.2.5B+C; SHG imaging and Picrosirius Red staining). These effects were predominantly modulated through targeting of JAK kinases, and were not further improved by the addition of SRC inhibitor, dasatinib. In contrast, targeting JAK2 with AZD1480 did not alter fibroblast contractility (Figure 4.2.4A), and showed no effect on collagen deposition (Figure 4.2.4B+C; SHG imaging and Picrosirius Red staining).

To directly compare the efficacy of JAK1/2 inhibition versus more selective JAK-inhibition, data were normalised to the vehicle control of each individual experiment (Figure 4.2.6). Interestingly, ruxolitinib (JAK1/2-inhibitor) and AZD289 (JAK1-inhibitor) were equally effective at inhibiting fibroblast contractility (Figure 4.2.6A) and collagen deposition in 3D matrices, when compared to tofacitinib (JAK3-inhibitor) treatment (Figure 4.2.6B+C). Collectively, these data demonstrate that inhibition of JAK1 and JAK3, but not JAK2, decreases fibroblast contractility and alters collagen levels in a three-dimensional setting.

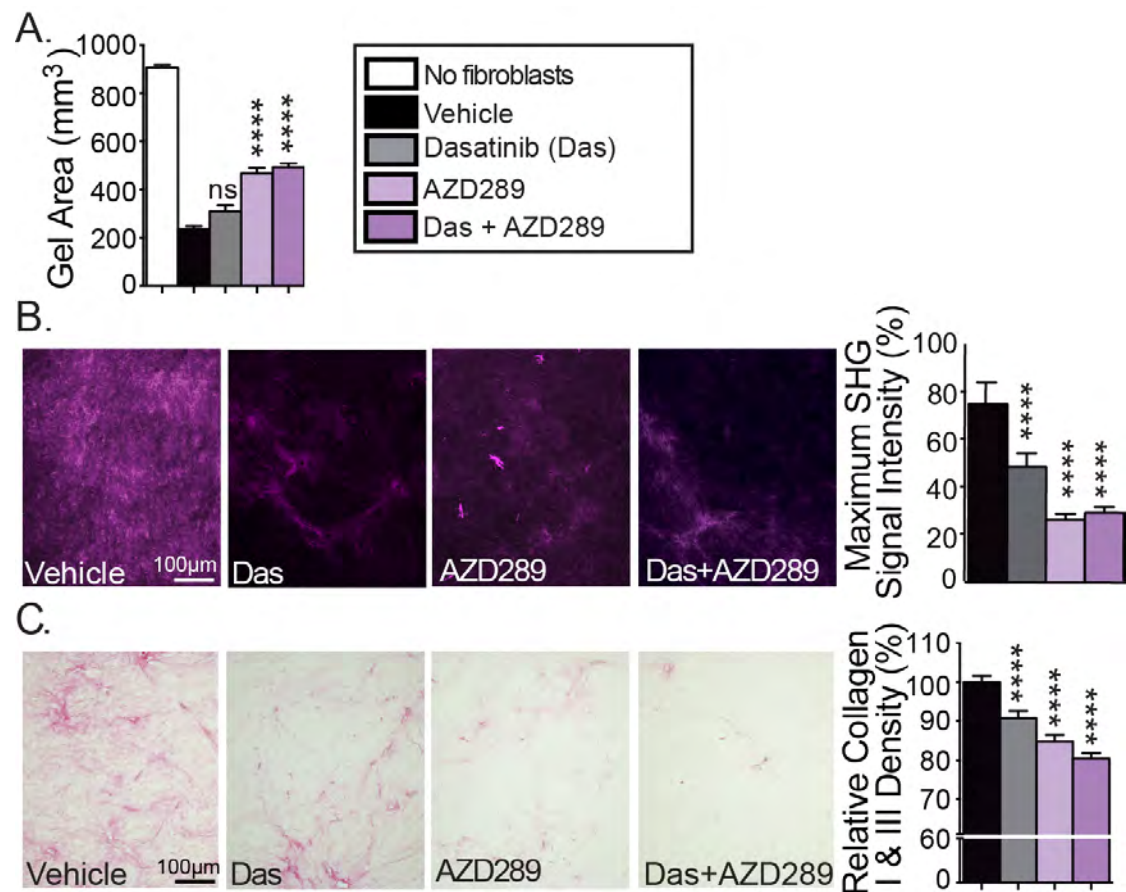


Figure 4.2.3 JAK1 inhibition disrupts collagen matrix integrity. (A) Quantification of TIF-collagen matrix area following treatment with dasatinib, AZD289 and the combination of dasatinib and AZD289 at endpoint (12 days). (B) Quantification and representative maximum intensity projections of second harmonic generation (SHG) signal intensity at peak in matrices after 12 days of contraction. (C) Quantification and bright-field images of Picrosirius Red-stained collagen matrices treated with dasatinib and AD289. Data are presented as mean \pm SEM (n=3 independent experiments, performed in triplicate matrices per condition, per repeat). Significance was determined using nonparametric ANOVA test with a Tukey multiple comparisons test where *p<0.05, **p<0.01, ***p<0.001 and ****p<0.0001. Unless indicated, significance is compared against vehicle. Das: dasatinib; Das+AZD289: dasatinib and AZD289.

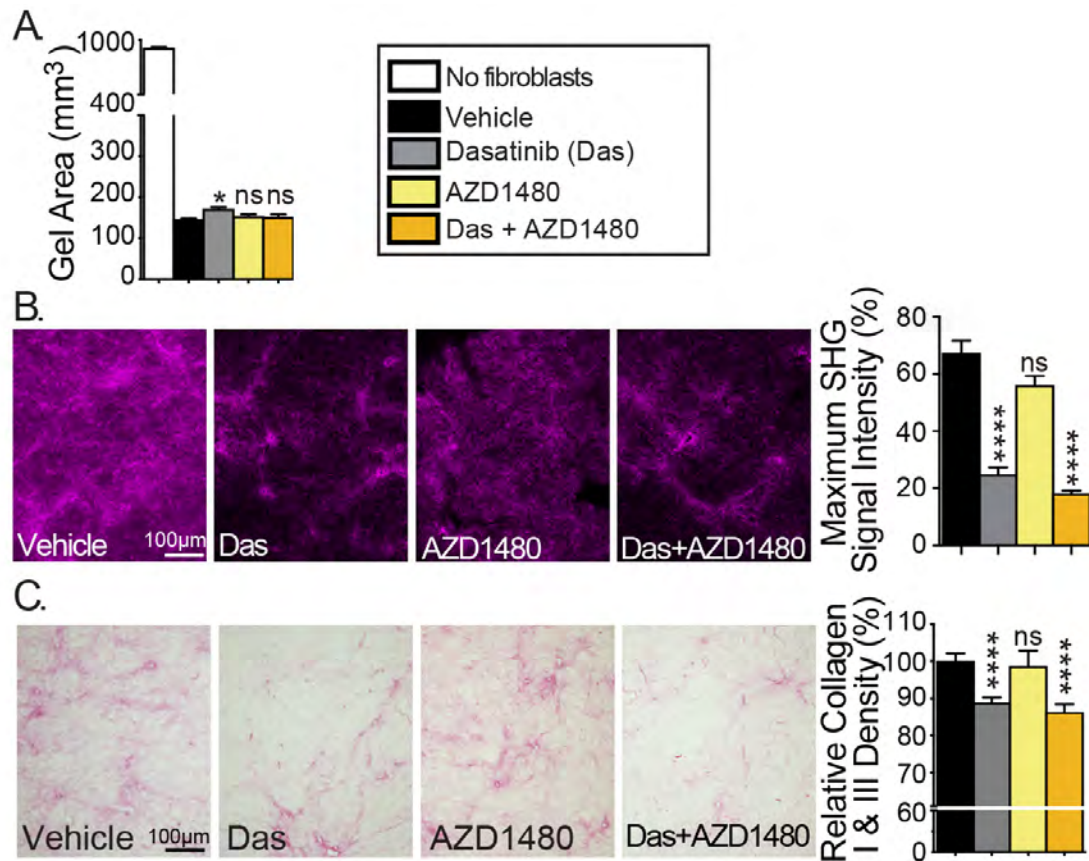


Figure 4.2.4 JAK2 inhibition does not disrupt collagen matrix integrity. (A) Quantification of TIF-collagen matrix area following treatment with dasatinib, AZD1480 and the combination of dasatinib and AZD1480 at endpoint (12 days). (B) Quantification and representative maximum intensity projections of second harmonic generation (SHG) signal intensity at peak in matrices after 12 days of contraction. (C) Quantification and bright-field images of Picrosirius Red-stained collagen matrices treated with dasatinib and AD1480. Data are presented as mean \pm SEM (n=3 independent experiments, performed in triplicate matrices per condition, per repeat). Significance was determined using nonparametric ANOVA test with a Tukey multiple comparisons test where *p<0.05, **p<0.01, ***p<0.001 and ****p<0.0001. Unless indicated, significance is compared against vehicle. Das: dasatinib; Das+AZD1480: dasatinib and AZD1480.

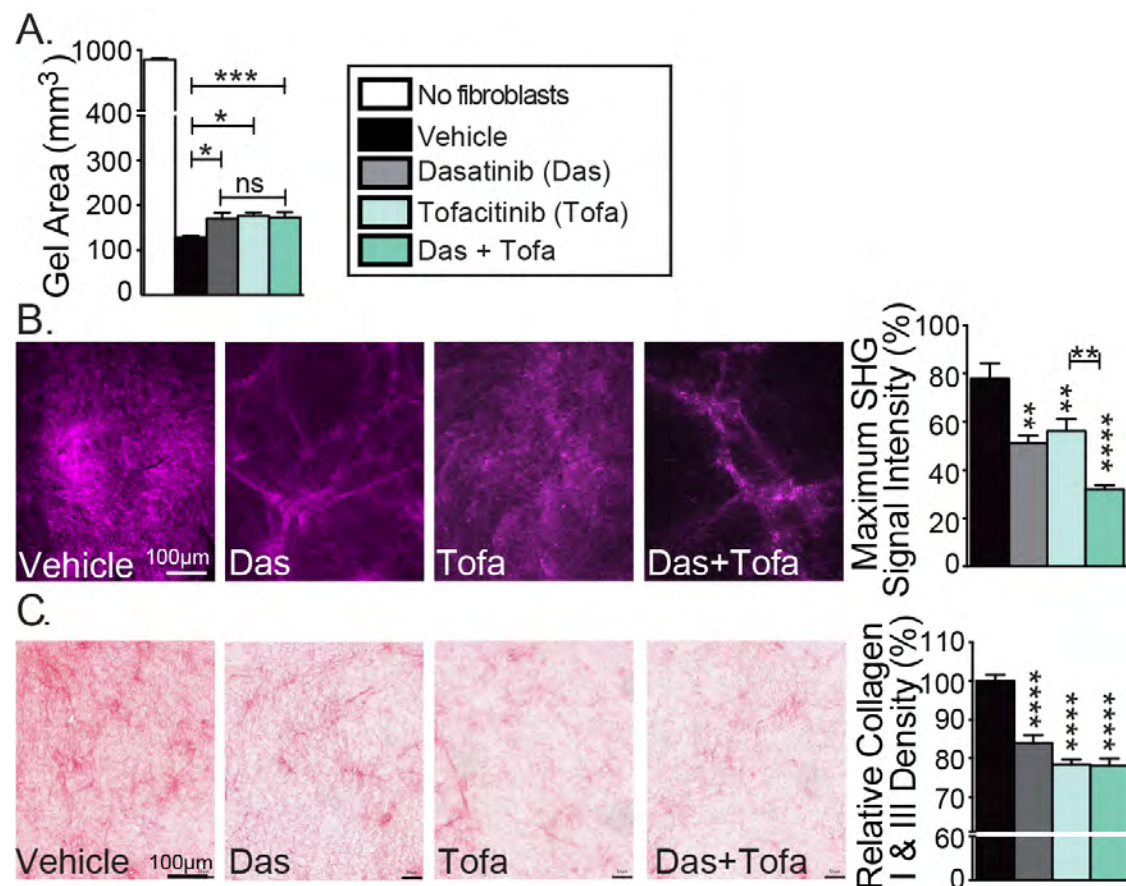


Figure 4.2.5 JAK3 inhibition disrupts collagen matrix integrity. (A) Quantification of TIF-collagen matrix area following treatment with dasatinib, tofacitinib and the combination of dasatinib and tofacitinib at endpoint (12 days). (B) Quantification and representative maximum intensity projections of second harmonic generation (SHG) signal intensity at peak in matrices after 12 days of contraction. (C) Quantification and bright-field images of Picrosirius Red-stained collagen matrices treated with dasatinib and tofacitinib. Data are presented as mean \pm SEM (n=3 independent experiments, performed in triplicate matrices per condition, per repeat). Significance was determined using nonparametric ANOVA test with a Tukey multiple comparisons test where *p<0.05, **p<0.01, ***p<0.001 and ****p<0.0001. Unless indicated, significance is compared against vehicle. Das: dasatinib; Tofa: tofacitinib; das+tofa: dasatinib and tofacitinib.

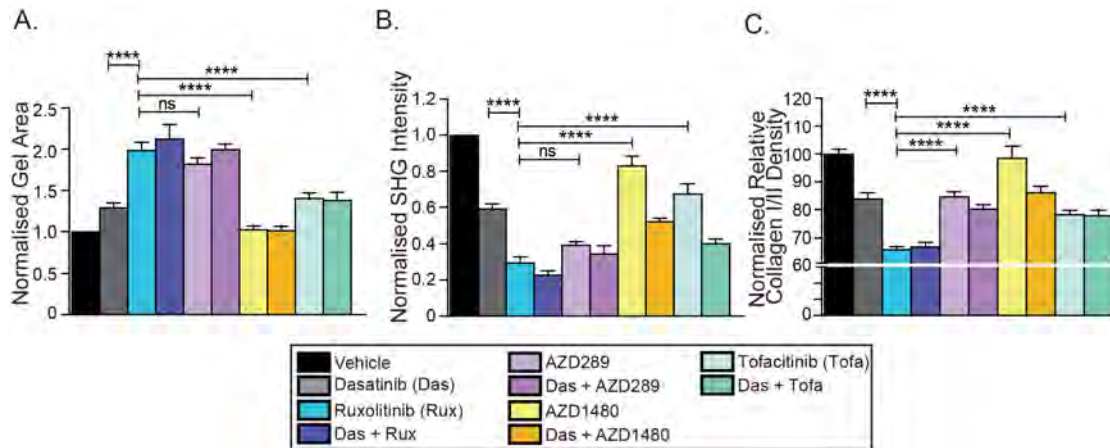


Figure 4.2.6 Dual JAK1/2 inhibition robustly disrupts collagen matrix integrity when compared to JAK1, JAK2 or JAK3 inhibition alone. (A) Normalised quantification of TIF-collagen matrix area following treatment with dasatinib, ruxolitinib, AZD289, AZD1480 or tofacitinib monotherapies, and combinations of dasatinib and JAK-inhibitors (B) Normalised quantification of second harmonic generation (SHG) signal intensity at peak in matrices after 12 days of contraction following treatment (C) Normalised quantification of Picrosirius Red-stained collagen matrices following treatment. Data are presented as mean \pm SEM ($n=3$ independent experiments, performed in triplicate matrices per condition, per repeat). Significance was determined using nonparametric ANOVA test with a Tukey multiple comparisons test where * $p<0.05$, ** $p<0.01$, *** $p<0.001$ and **** $p<0.0001$.

To further understand the contribution of dual JAK1/2 or JAK1-selective targeting in extracellular matrix remodelling, we next assessed the effect of ruxolitinib and AZD289 on extracellular matrix organisation, using birefringence analysis. Polarised light imaging of Picrosirius Red-stained sections revealed that the total birefringent signal was significantly decreased in ruxolitinib treated (Figure 4.2.7A), and AZD289 treated conditions (Figure 4.2.7D), compared to control (collaboration Dr Thomas Cox, Garvan Institute). Of note, quantification of the contribution to total signal of collagen fibres with different birefringence properties showed that ruxolitinib treatment reduced the proportion of highly crosslinked collagen fibres with high and medium birefringence, and this was associated with an increase in less remodelled collagen fibres with low birefringence (Figure 4.2.7B+C), suggesting a significantly looser matrix. In comparison, AZD289 treatment did not significantly change the proportion of highly crosslinked collagen fibres (Figure 4.2.7E+F). Impairment of matrix contraction and alterations in extracellular matrix integrity following treatment with SRC and JAK inhibitors were independent of changes in fibroblast proliferation (Figure 4.2.8), as indicated by immunohistochemical analyses of Ki67 on contracted-matrices. Collectively, these data suggest that only dual targeting of the JAK1/2 kinases promotes a significantly disorganised extracellular matrix network.

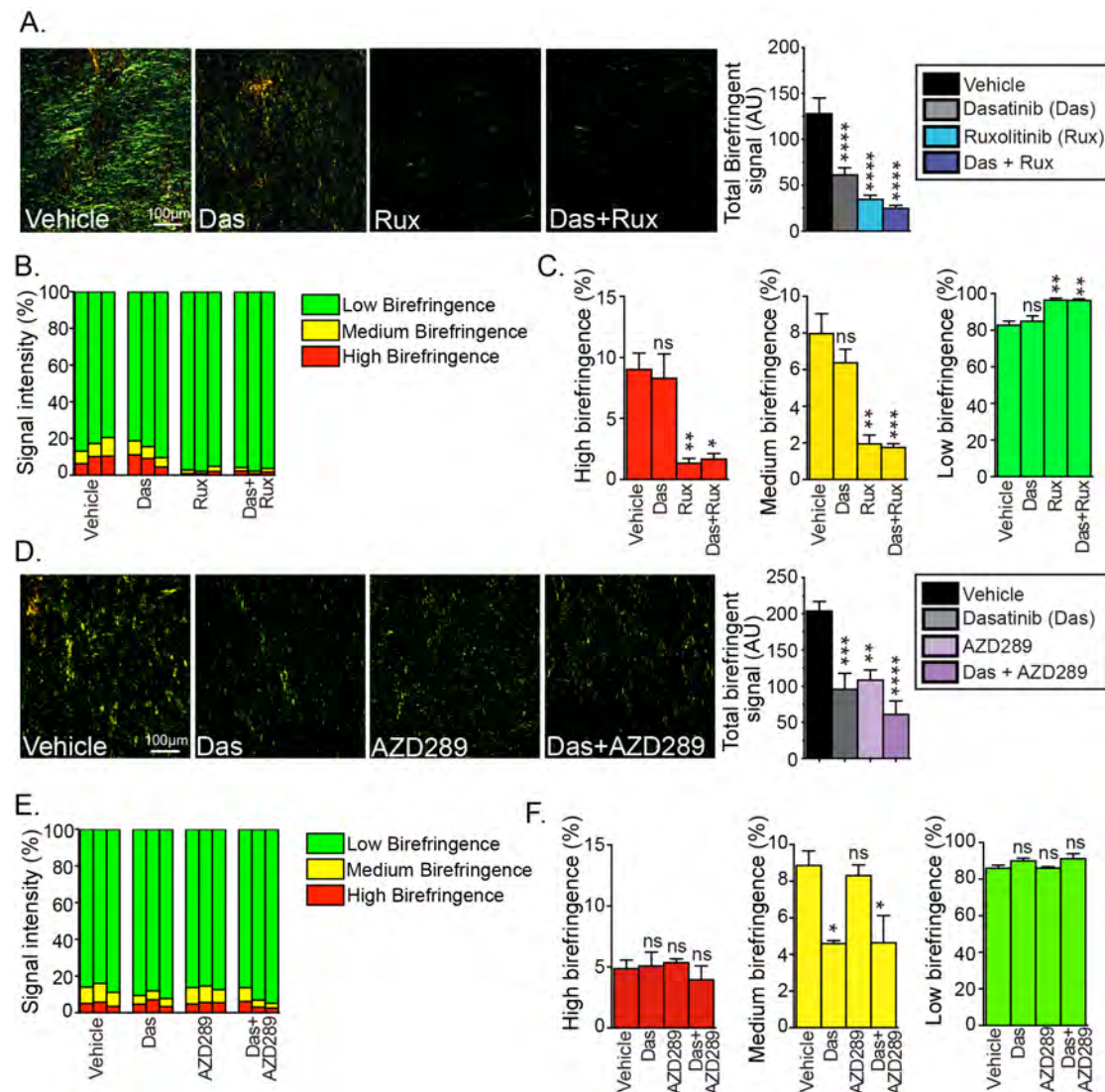


Figure 4.2.7 JAK1/2 inhibition disrupts collagen remodelling. Quantification of total collagen content measured as intensity of the signal acquired via polarised light and representative polarised light images of Picrosirius Red-stained TIF-collagen matrices following treatment with (A) dasatinib and ruxolitinib (JAK1/2 inhibitor), and (D) dasatinib and AZD289 (JAK1-inhibitor). Contribution and quantification of signal emitted from fibres with high, medium and low birefringence normalised to total signal acquired via polarised imaging of Picrosirius Red-stained collagen matrices treated with (B+C) dasatinib and ruxolitinib and (E+F) dasatinib and AZD289. Data are presented as mean \pm SEM (n=3 independent experiments, performed in triplicate matrices per condition, per repeat). Significance was determined using nonparametric ANOVA test with a Tukey multiple comparisons test where *p<0.05, **p<0.01, ***p<0.001 and ****p<0.0001.

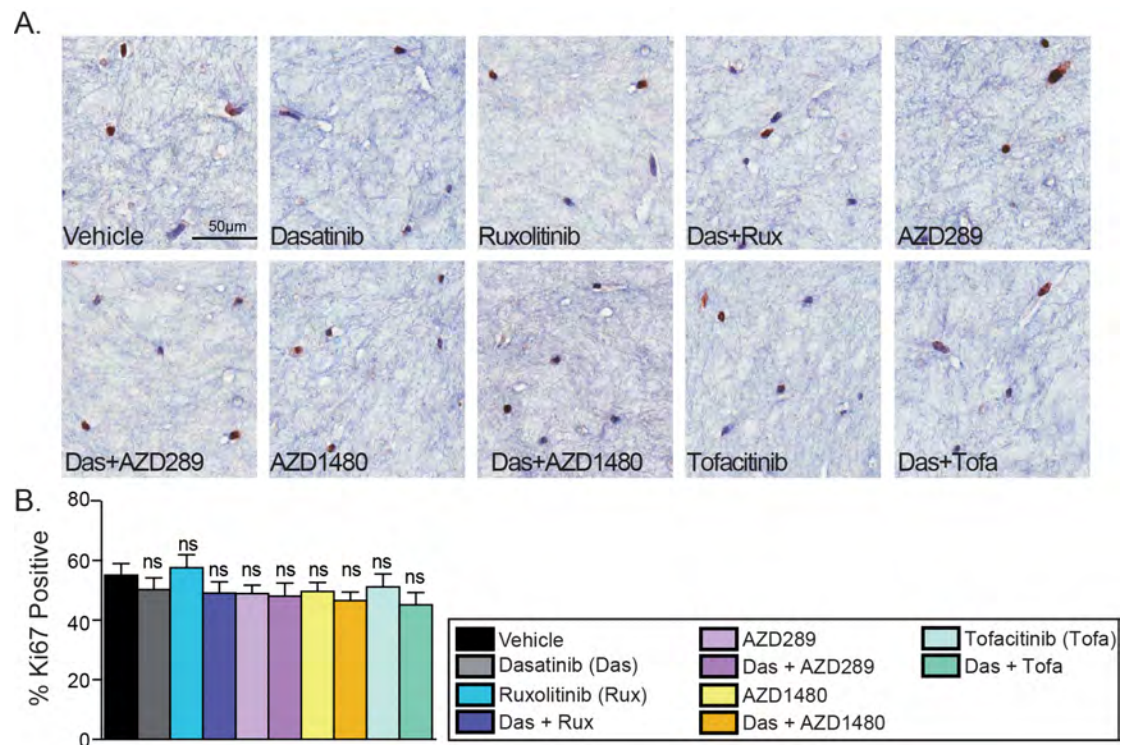


Figure 4.2.8 The effect of SRC and JAK inhibition on the proliferative capacity of fibroblasts in 3D. (A) Representative images of Ki67 staining in collagen matrices. (B) Quantification of TIF proliferation, via Ki67 staining, in collagen matrices after 12-day contraction assay following treatment with dasatinib, ruxolitinib, AZD289, AZD1480, tofacitinib and combinations of dasatinib and JAK-inhibitors. Data are presented as mean \pm SEM (n=3 independent experiments, performed in triplicate matrices per condition, per repeat). Significance was determined using nonparametric ANOVA test with a Tukey multiple comparisons test where *p<0.05, **p<0.01, ***p<0.001 and ****p<0.0001. Unless specifically indicated, significance is compared against vehicle.

4.2.2 Assessing the anti-invasive potential of the combined inhibition of SRC and JAK in three-dimensional organotypic assays

Three-dimensional topology and mechanical cues provided by the stroma can actively shape and drive invasive tumour behaviour [617]. As our findings indicate that inhibition of JAK1/2 alters extracellular matrix integrity, next, we sought to assess the effects of extracellular matrix manipulation via JAK and SRC inhibition on cancer cell invasion, a key event in pancreatic cancer progression. To evaluate the effect of SRC and JAK inhibition on cancer cell invasion, 3D organotypic invasion assays were utilised (Figure 4.2.1). We examined the invasion of three PDAC cell lines, selected based on their P53 mutant, phospho-STAT3-‘high’ status, using the established 3D organotypic assay of invasion (Figure 4.2.1; as per [83, 149], and described in methods section 2.8), in the presence or absence of SRC and JAK inhibitors. To quantify cell invasion, organotypic matrices were fixed and processed for immunohistochemical analyses, and were stained with a pan-cytokeratin antibody (to identify KPC cells), or a GFP antibody (to identify green-fluorescent protein (eGFP)-luciferase-labelled patient-derived cell lines). Treatment with dasatinib (SRC-inhibitor) and ruxolitinib (JAK1/2-inhibitor) monotherapies significantly impaired invasion of KPC cells (Figure 4.2.9A), as well as two patient-derived cell lines TKCC-05 (Figure 4.2.9B) and TKCC-10 cells (Figure 4.2.9C). Moreover, the combination of dasatinib and ruxolitinib was markedly superior to each monotherapy in all P53-mutant, phospho-STAT3 “high” pancreatic cancer cell lines examined.

To elucidate if the effects seen on cellular invasion are dependent on dual JAK1/2 targeting, three more selective JAK inhibitors were included in the organotypic assays for comparison. JAK1 (AZD289) and JAK2 (AZD1480) inhibitors both decreased the invasive potential of all 3 cell lines (Figure 4.2.10 and Figure 4.2.11), and when either inhibitor was combined with dasatinib there was a further decrease in invasion. In contrast, the JAK3 inhibitor (tofacitinib) showed no effect on invasion in all 3 cell lines. Taken together, this suggests that combined dasatinib and ruxolitinib treatment synergistically inhibits cancer cell invasion.

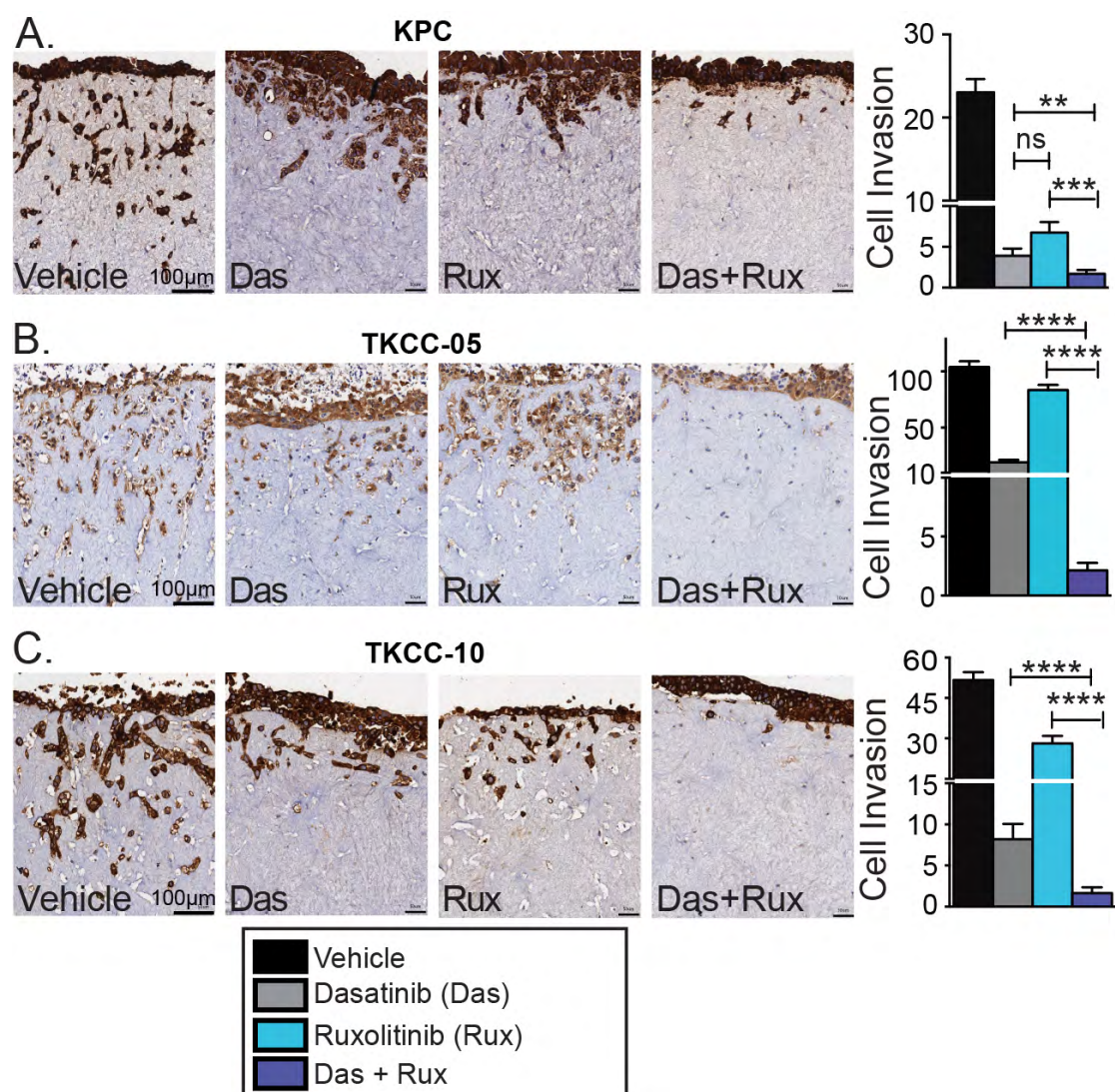


Figure 4.2.9 Combined dasatinib and ruxolitinib treatment impairs the invasive potential of PDAC cell lines. Quantification and representative images of cell invasion (number of cells that have invaded between 100 μ m – 400 μ m) through 3D organotypic matrices, of vehicle-treated, and dasatinib + ruxolitinib-treated (A) KPC (Pdx1-Cre; KrasLSL.G12D/+; p53R172H/+) cells, as indicated by multi-cytokeratin staining. (B) Green-fluorescent protein (eGFP)-luciferase-labelled TKCC-05 cells, and (C) green-fluorescent protein (eGFP)-luciferase-labelled TKCC-10 cells, as indicated by GFP immunohistochemistry. Data are presented as mean \pm SEM (n=3 independent experiments, performed in triplicate matrices per condition, per repeat). Significance was determined using nonparametric ANOVA test with a Tukey multiple comparisons test where *p<0.05, **p<0.01, ***p<0.001 and ****p<0.0001.

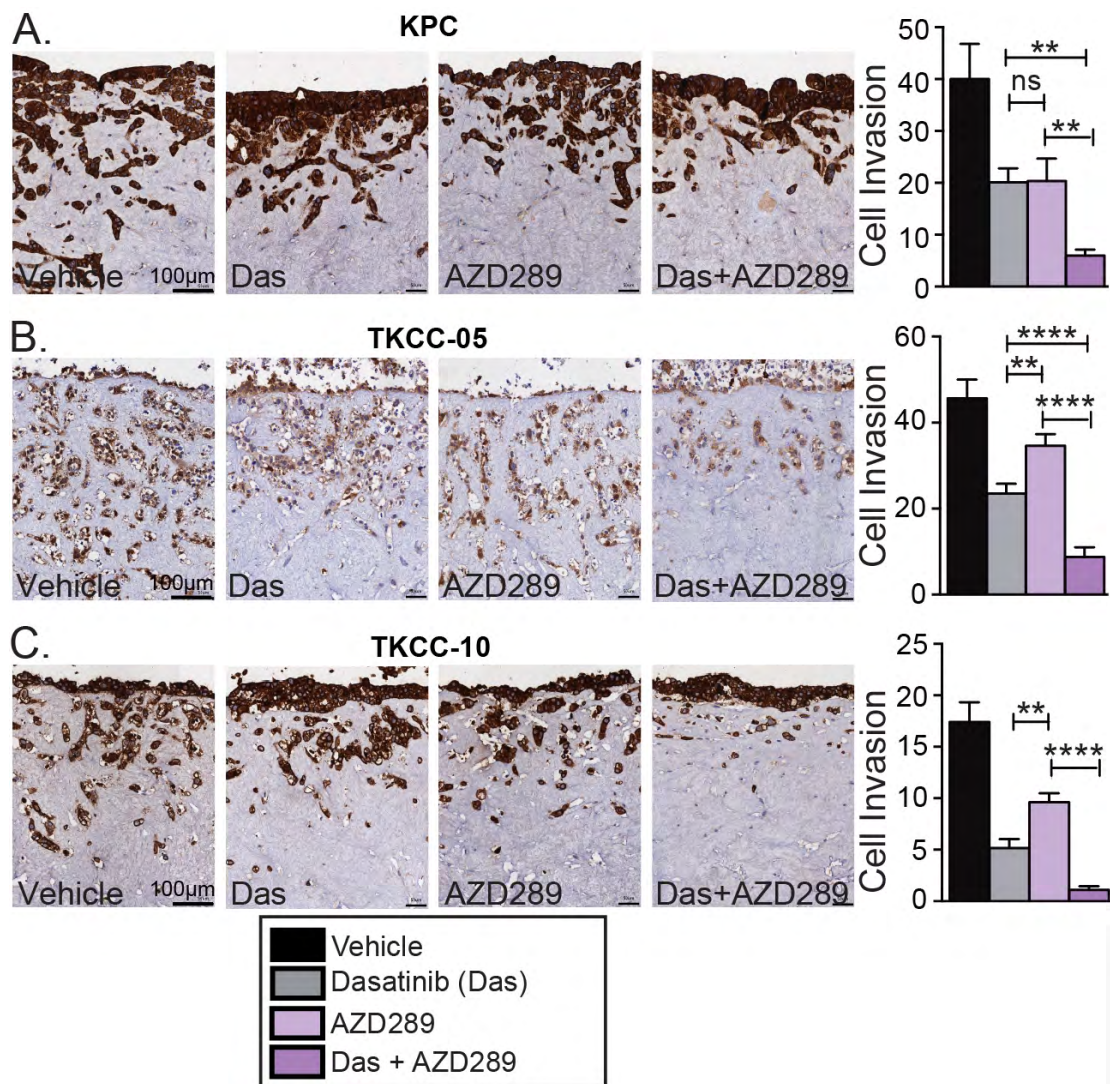


Figure 4.2.10 Combined dasatinib and AZD289 treatment impairs the invasive potential of PDAC cell lines. Quantification and representative images of cell invasion (number of cells that have invaded between 100 μ m – 400 μ m) through 3D organotypic matrices, of vehicle-treated, and dasatinib + AZD289-treated (A) KPC (Pdx1-Cre; KrasLSL.G12D/+; p53R172H/+) cells, as indicated by multi-cytokeratin staining. (B) Green-fluorescent protein (eGFP)-luciferase-labelled TKCC-05 cells, and (C) green-fluorescent protein (eGFP)-luciferase-labelled TKCC-10 cells, as indicated by GFP immunohistochemistry. Data are presented as mean \pm SEM (n=3 independent experiments, performed in triplicate matrices per condition, per repeat). Significance was determined using nonparametric ANOVA test with a Tukey multiple comparisons test where *p<0.05, **p<0.01, ***p<0.001 and ****p<0.0001.

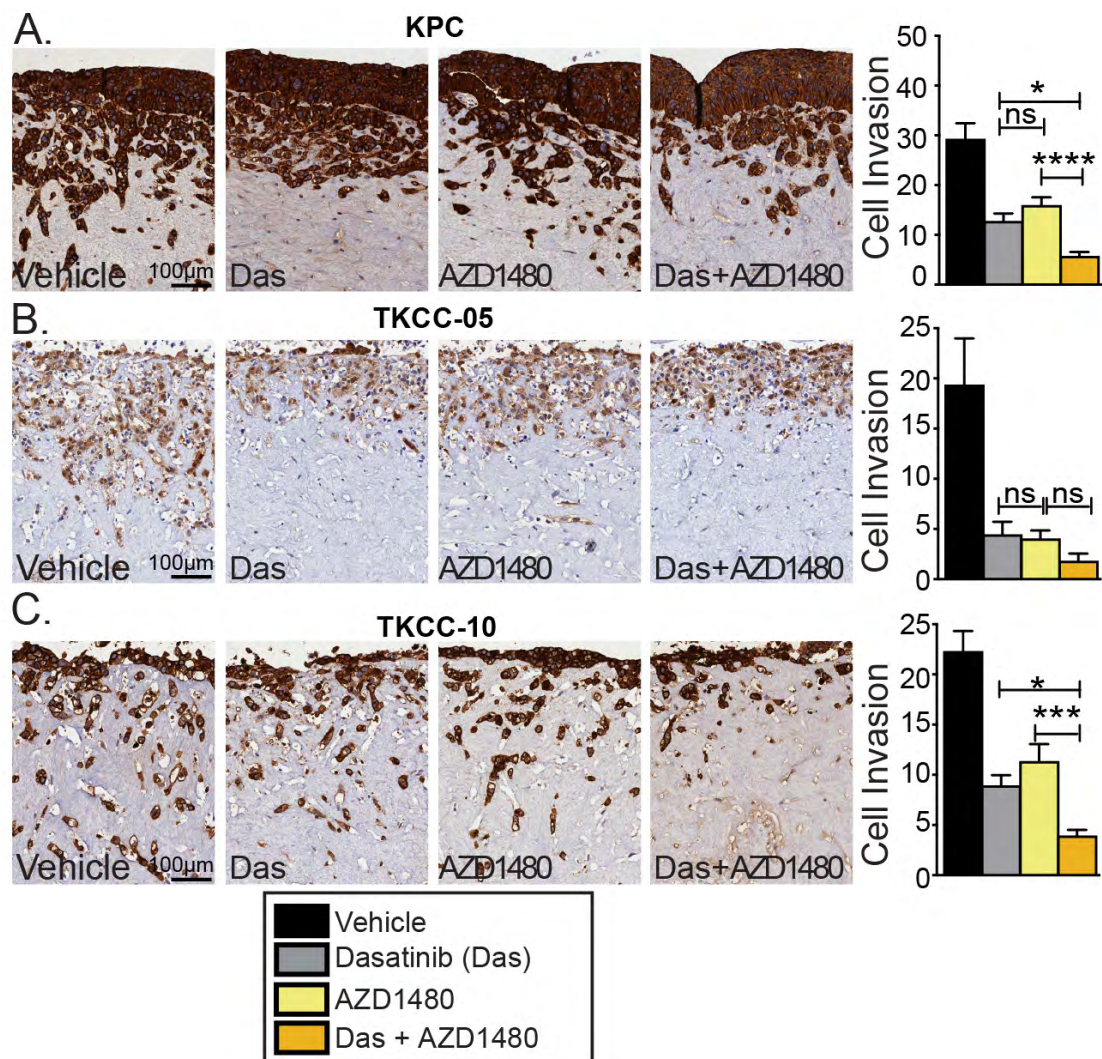


Figure 4.2.11 Combined dasatinib and AZD1480 impairs the invasive potential of PDAC cell lines. Quantification and representative images of cell invasion (number of cells that have invaded between 100 μ m – 400 μ m) through 3D organotypic matrices, of vehicle-treated, and dasatinib + AZD1480-treated (A) KPC (Pdx1-Cre; KrasLSL.G12D/+; p53R172H/+) cells, as indicated by multi-cytokeratin staining. (B) Green-fluorescent protein (eGFP)-luciferase-labelled TKCC-05 cells, and (C) green-fluorescent protein (eGFP)-luciferase-labelled TKCC-10 cells, as indicated by GFP immunohistochemistry. Data are presented as mean \pm SEM (n=3 independent experiments, performed in triplicate matrices per condition, per repeat). Significance was determined using nonparametric ANOVA test with a Tukey multiple comparisons test where *p<0.05, **p<0.01, ***p<0.001 and ****p<0.0001.

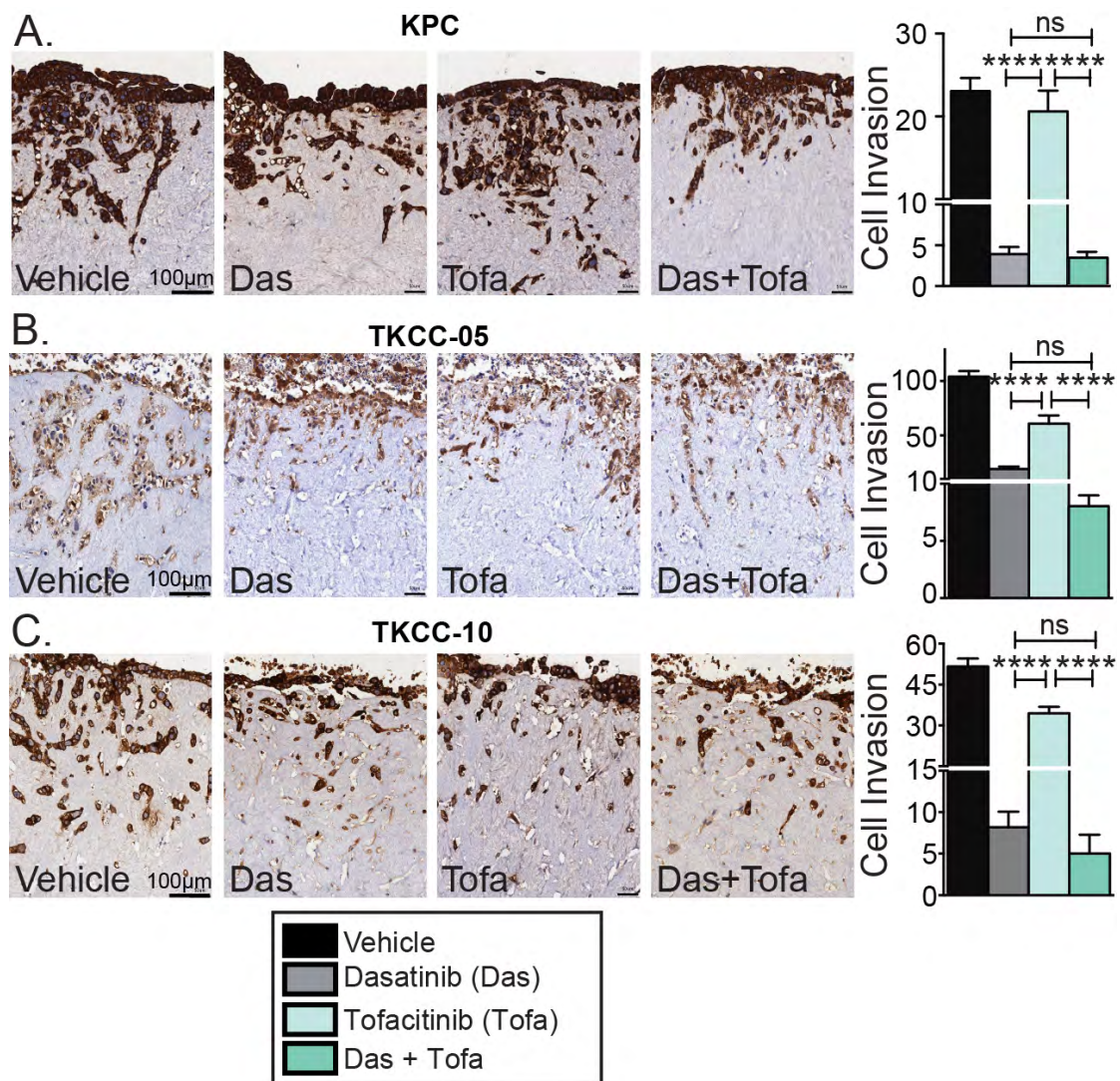


Figure 4.2.12 Combined dasatinib and tofacitinib impairs the invasive potential of PDAC cell lines and is no better than dasatinib monotherapy. Quantification and representative images of cell invasion (number of cells that have invaded between 100 μ m – 400 μ m) through 3D organotypic matrices, of vehicle-treated, and dasatinib + tofacitinib-treated (A) KPC (Pdx1-Cre; KrasLSL.G12D/+; p53R172H/+) cells, as indicated by multi-cytokeratin staining. (B) Green-fluorescent protein (eGFP)-luciferase-labelled TKCC-05 cells, and (C) green-fluorescent protein (eGFP)-luciferase-labelled TKCC-10 cells, as indicated by GFP immunohistochemistry. Data are presented as mean \pm SEM (n=3 independent experiments, performed in triplicate matrices per condition, per repeat). Significance was determined using nonparametric ANOVA test with a Tukey multiple comparisons test where *p<0.05, **p<0.01, ***p<0.001 and ****p<0.0001.

To directly compare each treatment and the associated effect on cancer cell invasion, data was normalised to the vehicle control of each individual experiment (Figure 4.2.13). Ruxolitinib (JAK1/2-inhibitor) and AZD289 (JAK1-inhibitor) equally decreased the invasive capacity of all 3 cell lines, and overall, were both more effective when compared to AZD1480 (JAK2-inhibitor) and tofacitinib (JAK3-inhibitor). Moreover, the combination of dasatinib and ruxolitinib was the most effective at inhibiting invasion of all 3 cell lines.

Taken together, these data demonstrate that inhibition of JAK1/2 and SRC kinases has a potent inhibitory effect on pancreatic cancer cell invasion through three-dimensional matrices, simultaneously disrupting the integrity and organisation of the extracellular matrix. Importantly, the combination of dasatinib and ruxolitinib treatment was the most efficacious, when compared to other SRC and JAK-inhibitor combinations. Consequently, the combination of dasatinib and ruxolitinib was selected for further studies investigating the intricacies of SRC/JAK/STAT3 targeting of tumour cells within the complex microenvironment.

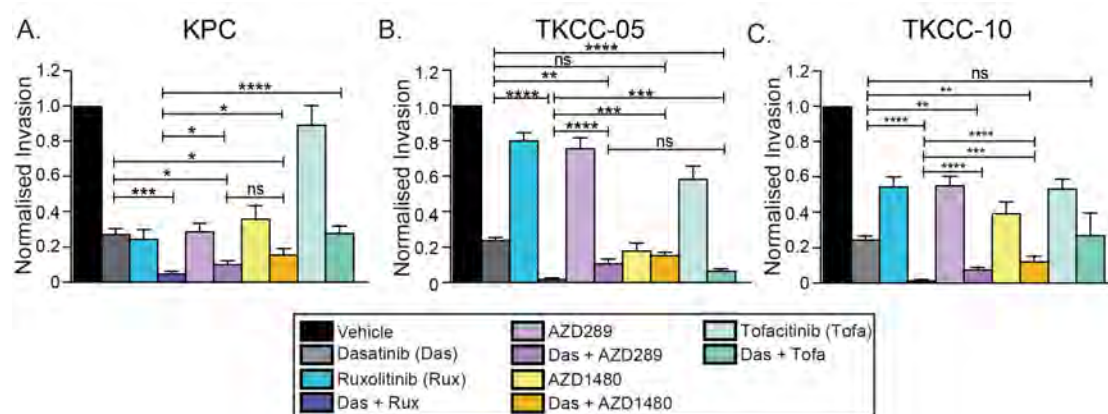


Figure 4.2.13 Ruxolitinib is the most effective at impairing the invasive potential of PDAC cell lines when compared to AZD289, AZD1480 and Tofacitinib. Normalised quantification of cell invasion (100 μ m – 400 μ m) through 3D organotypic matrices, treated with either vehicle, dasatinib, ruxolitinib, AZD289, AZD1480, tofacitinib and combinations of dasatinib and JAK-inhibitors in (A) KPC (Pdx1-Cre; KrasLSL.G12D/+; p53R172H/+) cells, (B) green-fluorescent protein (eGFP)-luciferase-labelled TKCC-05 cells and (C) green-fluorescent protein (eGFP)-luciferase-labelled TKCC-10 cells. Data are presented as mean \pm SEM (n=3 independent experiments, performed in triplicate matrices per condition, per repeat). Significance was determined using nonparametric ANOVA test with a Tukey multiple comparisons test where *p<0.05, **p<0.01, ***p<0.001 and ****p<0.0001.

To assess whether the observed inhibitory effects of dasatinib and ruxolitinib treatment on PDAC cell invasion were accompanied with changes in cell proliferation and apoptosis, sections of the organotypic matrices were stained with Ki67 (Figure 4.2.14) and cleaved-caspase-3 (Figure 4.2.15). Following treatment with dasatinib, the proportion of cancer cells positive for Ki67 was significantly decreased in both the invading and non-invading KPC (Figure 4.2.14 A+B), TKCC-05 (Figure 4.2.14C+D) and TKCC-10 (Figure 4.4.14 E+F) cell lines. Moreover, this decrease in cell proliferation was maintained in the dasatinib and ruxolitinib combination, and in contrast, no change was seen following ruxolitinib monotherapy. Furthermore, there was no change in the proportion of cells positive for cleaved-caspase-3 following treatment with dasatinib, ruxolitinib or the combination of dasatinib and ruxolitinib in all three cell lines examined (Figure 4.2.15).

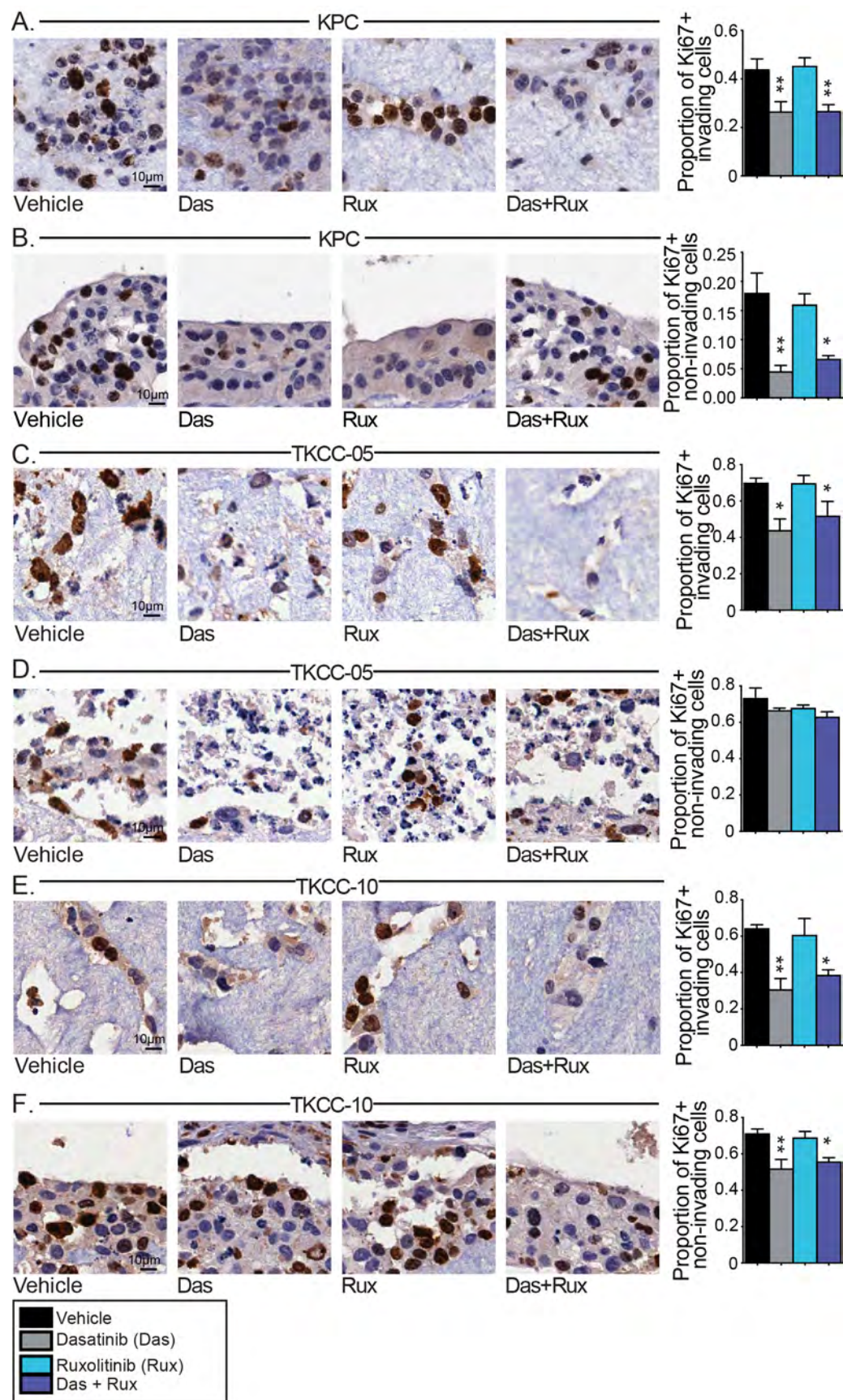


Figure 4.2.14 >>>

>>> **Figure 4.2.14** SRC inhibition impairs cancer cell proliferation *in vitro* in 3D organotypic assays. Quantification and representative images of Ki67 staining in matrices treated with vehicle, dasatinib, ruxolitinib or dasatinib + ruxolitinib in (A) invading KPC cells, (B) non-invading KPC cells, (C) invading TKCC-05 cells, (D) non-invading TKCC-05 cells, (E) invading TKCC-10 cells and (F) non-invading TKCC-10 cells. Data are presented as mean \pm SEM (n=3 independent experiments, performed in triplicate matrices per condition, per repeat). Significance was determined using nonparametric ANOVA test with a Tukey multiple comparisons test where *p<0.05, **p<0.01, ***p<0.001 and ****p<0.0001. Das: dasatinib; Rux: ruxolitinib; Das+Rux: dasatinib and ruxolitinib.

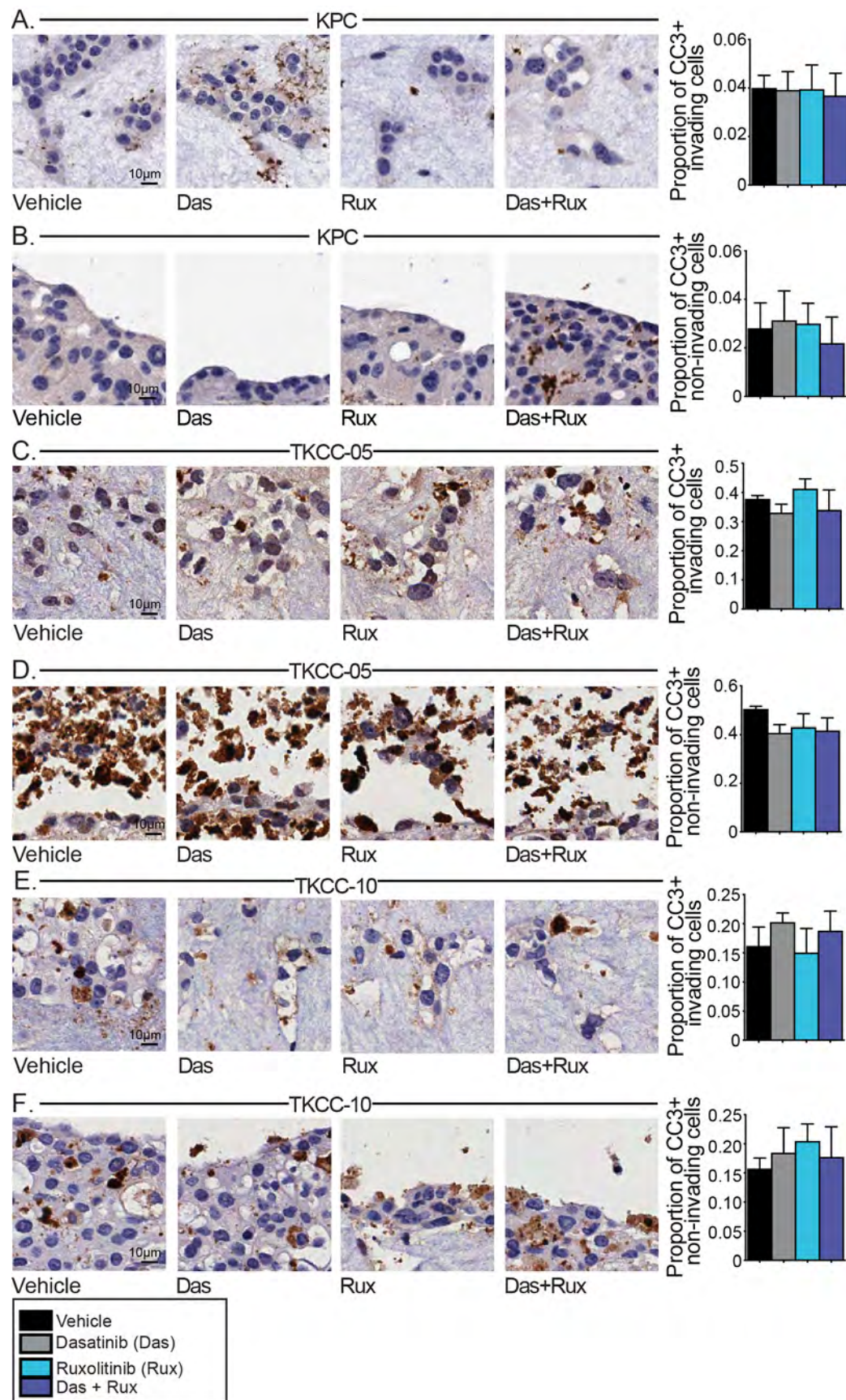


Figure 4.2.15 >>>

>>> Figure 4.2.15 Dasatinib and ruxolitinib does not promote cancer cell apoptosis *in vitro* in 3D organotypic assays. Quantification and representative images of cleaved-caspase-3 staining in matrices treated with vehicle, dasatinib, ruxolitinib, dasatinib + ruxolitinib in (A) invading KPC cells, (B) non-invading KPC cells, (C) invading TKCC-05 cells, (D) non-invading TKCC-05 cells, (E) invading TKCC-10 cells and (F) non-invading TKCC-10 cells. Data are presented as mean \pm SEM (n=3 independent experiments, performed in triplicate matrices per condition, per repeat). Significance was determined using nonparametric ANOVA test with a Tukey multiple comparisons test where *p<0.05, **p<0.01, ***p<0.001 and ****p<0.0001. Das: dasatinib; Rux: ruxolitinib; Das+Rux: dasatinib and ruxolitinib; CC3: cleaved-caspase-3.

4.2.3 Examining the effect of dasatinib and ruxolitinib treatment on inter-cellular signalling in three-dimensional co-culture organoids

Paracrine signalling between cancer cells and cancer-associated fibroblasts (CAFs) can influence cancer cell behaviour and is known to promote tumour cell invasion, metastasis and survival [135, 136]. Moreover, over-activation of pro-inflammatory, pro-fibrotic and pro-tumourigenic signalling networks is largely driven by the SRC/JAK/STAT3 pathway [188, 416], and can influence the development of the immunosuppressive tumour microenvironment that defines PDAC [150]. To examine whether dasatinib and ruxolitinib disrupts the intercellular crosstalk that occurs within the tumour microenvironment, we adapted established methodology for 3D co-culture organoids (Figure 4.2.16) (described in methods section 2.10, based on Ohlund *et al.* 2017). These co-cultures accurately recapitulate physiologically relevant aspects of pancreatic tumours *in vitro*, and have been used previously to assess pancreatic tumour heterogeneity [141], as well as biomarker identification and therapeutic testing in other cancer types [618]. Organoid co-cultures were treated for 24 or 48h with pre-defined concentrations of dasatinib or ruxolitinib monotherapies (IC_{10}), and the dasatinib and ruxolitinib combination. Culture media (supernatant) was collected and analysed using multiplex cytokine arrays that simultaneously measures the concentration of 32 cytokines (Bio-Plex Pro™ Mouse Cytokine 9-plex and 23-plex assays).

Subsequently, we applied the same approach to examine treatment-induced alterations in paracrine signalling within patient-derived TKCC-10 co-culture organoids. In this context, we used multiplex cytokine arrays that simultaneously measure the concentration of 77 human cytokines (Bio-Plex Pro™ Human Chemokine 40-plex and Human Inflammation 37-plex assays).

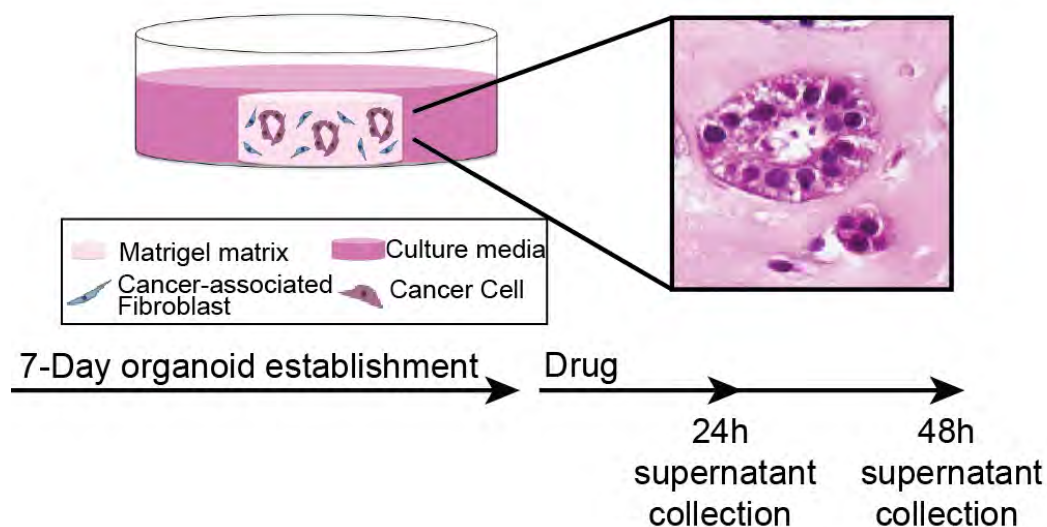


Figure 4.2.16 Schematic of co-culture organoid set-up. Organoids were allowed to establish over 7 days, and subsequently treated with the drug of interested. Supernatants were collected at 24h and 48h post treatment.

In the KPC organoids (comprising KPC tumour cells and KPC tumour-derived cancer-associated fibroblasts), treatment with dasatinib significantly reduced secretion of 5 signalling factors (Figure 4.2.17), and these included the SRC-promoting chemokines CCL2 [305], CCL5 (RANTES; [619]), CCL3, CCL4, and growth factor M-CSF. Conversely, inhibition of SRC with dasatinib led to increased secretion of G-CSF (negatively regulated by SRC [620]), GM-CSF, IL-5 and STAT3-activating cytokine IL-10. However when dasatinib was combined with ruxolitinib the concentration of G-CSF decreased, the concentration of GM-CSF and Th-2 cytokine IL-5 returned to baseline (vehicle-treated) levels, while the cytokine IL-10, with complex pleiotropic roles in immunoregulation remained significantly elevated.

Ruxolitinib treatment significantly inhibited secretion of 19 factors examined including the STAT3-regulated chemokines CCL2, CCL3, CCL4, CCL5, CXCL1 and CXCL2. Additionally there was decreased production of interleukin 1 family members IL-1 α , IL-1 β and IL-18, STAT3-activating cytokines (IL-6 and IL-9), class I cytokines IL-2, IL-3, IL-13, G-CSF, GM-CSF, as well as IL-17A, secreted TNF- α and growth factors M-CSF, FGF and

VEGF. In contrast, IL-10 was the only factor identified to be elevated following ruxolitinib treatment.

Combined dasatinib and ruxolitinib treatment enforced the inhibitory effect of ruxolitinib on 17 secreted factors including interleukin 1 family members IL-1 α and IL-1 β , class I cytokines IL-2, IL-3, IL-6, IL-13 and G-CSF, as well as IL-17A, CXCL2 and TNF- α . Moreover, 7/17 factors were further significantly reduced following dasatinib and ruxolitinib treatment when compared to either monotherapy alone. These included chemokines CCL2, CCL3, CCL4 and CCL5, as well as pro-tumourigenic growth factors FGF, M-CSF and VEGF.

In order to elucidate the functional effects of these changes in secreted signalling factors following treatment with dasatinib and ruxolitinib, factors were grouped based on their function and are displayed in a schematic (Figure 4.2.18). Significant among the factors reduced by dasatinib and ruxolitinib were those involved in tumour-associated macrophage (TAM) recruitment, activation and polarisation which included CCL2, CCL3, CCL4, CCL5 and M-CSF [621, 622]. Moreover, CCL2/CCL5 promote Th17 and T-regulatory cell recruitment as well as granulocyte recruitment and myeloid-derived suppressor cell (MDSC) recruitment [159, 623]. These results suggest that inhibition of pro-inflammatory cytokines and chemokines by dasatinib and ruxolitinib aids in reversing the immunosuppressive tumour microenvironment. This is reinforced by the presence of IFN- γ , IL-18 and IL-12, key factors involved in cytotoxic T-cell recruitment [624]. In addition, CCL5 promotes basement membrane degradation, and this process is inhibited by IL-10 [625, 626], a cytokine that is upregulated following treatment with dasatinib and ruxolitinib. This is further reinforced by the decrease in the STAT3-activating cytokine IL-6, in addition to IL-13 and IL-9, all of which are known to promote proliferation and survival, migration and metastasis of cancer cells [411, 627]. Furthermore, dasatinib and ruxolitinib significantly inhibited release of pro-angiogenic factors VEGF and FGF, along with IL-3, IL-6 and IL-17A [628-632].

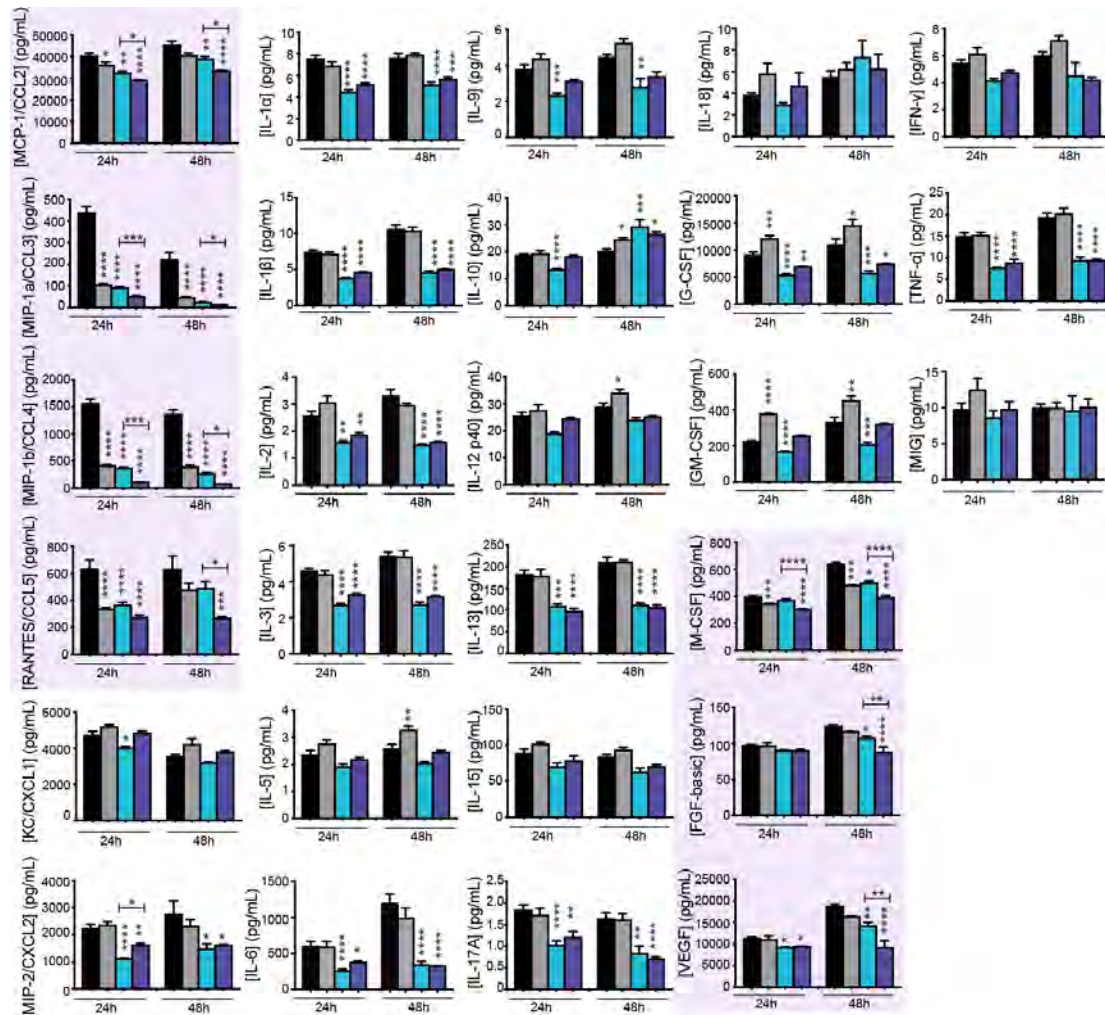


Figure 4.2.17 Dasatinib and ruxolitinib alter cytokine profiles in KPC co-culture organoids. Concentration of various mouse cytokines and chemokines present in the conditioned media of KPC co-culture organoids treated with vehicle, dasatinib, ruxolitinib or the combination of ruxolitinib and dasatinib for 24 and 48 hours. Graphs highlighted in pink depict superior efficacy of the dasatinib and ruxolitinib combination at inhibiting mediator release into the medium, compared with either monotherapy alone. Data are presented as mean \pm SEM (n=3 biological replicates, with three technical replicates per condition). Significance was determined using nonparametric ANOVA test with a Tukey multiple comparisons test where *p<0.05, **p<0.01, ***p<0.001

and **** $p < 0.0001$. Das: dasatinib; Rux: ruxolitinib; Das+Rux: dasatinib and ruxolitinib.

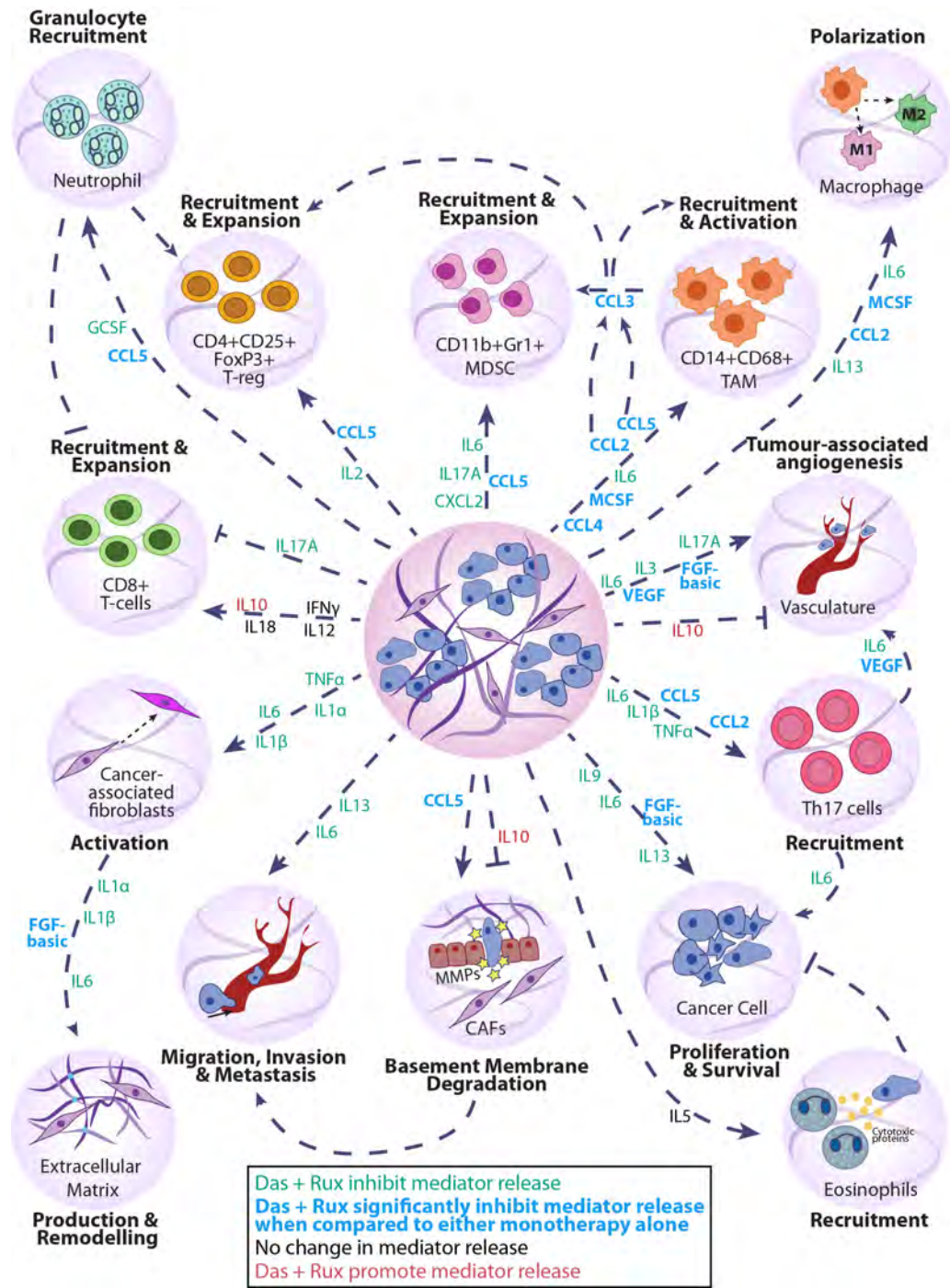


Figure 4.2.18 Cytokine profile schematic of KPC co-culture organoids following treatment with dasatinib and ruxolitinib (data summarised from figure 4.2.17). Factors highlighted in green depict efficacy of dasatinib and ruxolitinib combination in inhibiting mediator release, factors highlighted in blue depict

superior efficacy of the combination treatment compared to either monotherapy alone. Black depicts no change and red depicts increased mediator release. TAM: tumour-associated macrophage; MDSC: myeloid-derived suppressor cell; CAF: cancer-associated fibroblast; T-reg: T-regulatory cell.

Subsequent analysis of cytokine profiles from the drug-treated human PDAC (TKCC-10) organoids revealed interesting alterations in the immunoregulatory signalling. Secretion of 26 human signalling factors were significantly reduced following dasatinib treatment (Figure 4.2.19). These included chemokines CCL1, CCL3, CCL21, CCL22, CCL23, CXCL2, CXCL13, CXCL16 and CX3CL1, STAT3-activating class I cytokines IL-6, IL-27 and GM-CSF, class II cytokines (IL-20, IL-28), and interleukin 1 family member IL-1 β . Moreover, we saw decreased secretion of SRC-regulated matrix metalloproteinase MMP-2 [633] and IL-1/SRC-induced MMP-3 [634], tumour necrosis factor superfamily members (TNF α and TNFSF12), as well as other pro-inflammatory factors including IL-34, MIF, CD163 and Chi3L1.

Ruxolitinib treatment resulted in the reduction of 34 secreted factors. These included numerous chemokines CCL1, CCL3, CCL7, CCL8, CCL11, CCL15, CCL17, CCL20, CCL21, CCL25 and CCL26, as well as CXCL2, CXCL13 and CXCL16. Furthermore there was decreased production of the STAT3-activating cytokine IL-6, IL-6-associated receptors gp130 and sIL-6R, as well as IL-6 related cytokine IL-27. We also observed decreased concentration of the class I cytokine GM-CSF, class II cytokines (IFN-2, IFN- β , IL-20 and IL-29), interleukin 1 family member IL-1 β , as well as IL-34 and IL-35. Similar to the observed dasatinib-induced effects, inhibition of JAK1/2 led to a robust decrease in the secretion of tumour necrosis factor superfamily members TNF α and TNFSF12, matrix metalloproteinases (MMP-2, MMP-3 and in addition MMP-1), MIF, CD163 and Chi3L1, with associated increased production of the potentially immunostimulatory CCL11 (Eotaxin; [635]).

Combination of dasatinib and ruxolitinib significantly blocked a wide range of pro-tumourigenic signalling factors, with robust suppression of 42 mediators. These significantly reduced factors included broad CC and CXC chemokines

(CCL1, CCL2, CCL3, CCL7, CCL8, CCL15, CCL17, CCL20, CCL21, CCL22, CCL23, CCL25, CCL26, CCL27, CXCL2, CXCL5, CXCL12, CXCL13, CXCL16, CX3CL1), STAT3-regulated IL-1 β , class I cytokines (IL-2, IL-4, IL-6, IL-27 and GM-CSF), class II cytokines (IL-20 and IL-28), the IL-6 receptors gp130 and sIL-6R, as well as TNF α , TNFSF12 and the TNF-inducible factor Pentraxin 3, along with matrix metalloproteinases (MMP-1, MMP-2, and MMP-3), IL-34, MIF, chi3L1, TSLP and CD163. Moreover, CCL11 was the only chemokine identified to be upregulated following dasatinib and ruxolitinib treatment.

Further investigation into the potential functional effects of dasatinib and ruxolitinib treatment on paracrine signalling (Figure 4.2.20) revealed similar effects to those seen in the KPC organoids. The combination treatment resulted in a significant reduction in factors involved in tumour-associated macrophage (TAM) recruitment, activation and polarisation. These included CCL2, CCL3, CCL7, GM-CSF and IL-6 [621, 622, 636]. Moreover, myeloid-derived suppressor cell (MDSC) recruitment factors (IL-6, MIF and CXCL2) [637-639], granulocyte recruitment factors (GM-CSF) [640], T-regulatory cell recruitment factors (CCL1 and CCL17, MIF, IL2 and IL4) [641-644], and Th17 cell recruitment factors (IL-1 and IL-6, CCL2 and CCL20, and TNF- α) were decreased following treatment with dasatinib and ruxolitinib [623]. In parallel, release of potentially immunostimulatory factors IFN- α , IFN- β , IFN- γ , IL-10, IL-12, IL-28 and IL-29, which are involved in cytotoxic T-cell recruitment [624], remained unaltered post-treatment, and was further associated with increased secretion of CCL11 (Eotaxin), a key factor for eosinophil-mediated anti-tumour responses [645, 646]. Furthermore, dasatinib and ruxolitinib combination therapy significantly inhibited release of pro-angiogenic factors (CCL21, CCL23, CCL24, CCL27, CXCL5, CXCL12, MMP-2, IL-6 and MIF) [628, 647, 648], pro-survival factors (CCL12, CCL13, CCL17, CCL21, CCL24, CCL25, Pentraxin3, MIF and IL-6) [649], pro-migratory factors (CCL7, CCL8, CCL20, CCL25, CXCL5, CXCL13, IL-6 and MMP2) [650], as well as a decrease in pro-fibrotic factors, and cytokines involved in CAF-activation and extracellular matrix remodelling including IL-1 β , IL-6 and TNF- α [141, 479, 651].

Taken together, these data suggest that inhibition of the SRC/JAK/STAT3 networks may alter the dynamics of intercellular communication that occurs within the pancreatic tumour microenvironment and can modulate pro-inflammatory, pro-fibrotic and pro-tumourigenic cross-talk that has been shown to promote cancer progression and immunosuppression in PDAC.

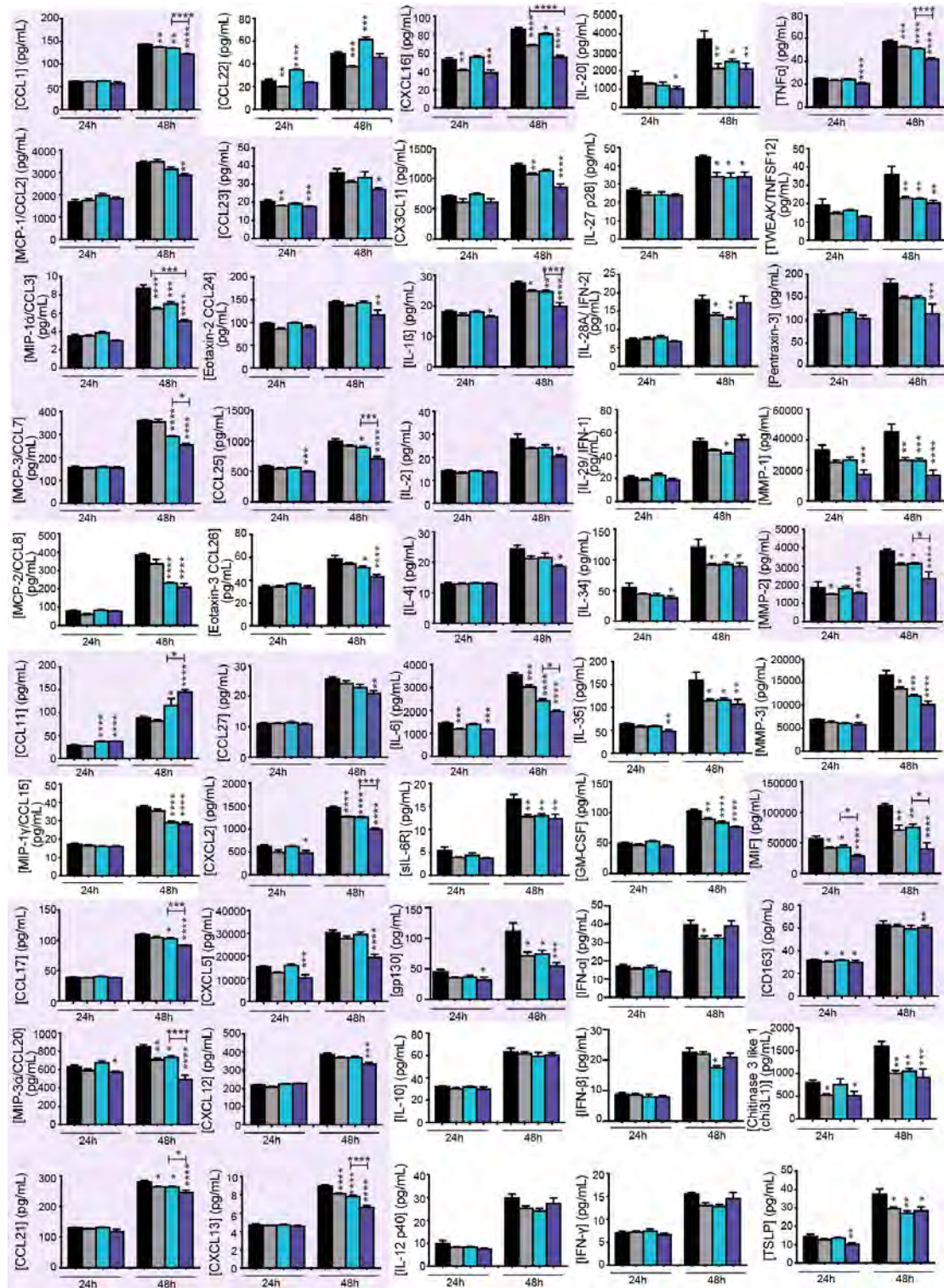


Figure 4.2.19 >>>

>>> Figure 4.2.19 Dasatinib and ruxolitinib alter cytokine profiles in TKCC-10 co-culture organoids. Concentration of various human cytokines and chemokines present in the conditioned media of TKCC-10 co-culture organoids treated with vehicle, dasatinib, ruxolitinib or the combination of ruxolitinib and dasatinib for 24 and 48 hours. Graphs highlighted in pink depict superior efficacy of the dasatinib and ruxolitinib combination at inhibiting mediator release into the medium, compared with either monotherapy alone. Data are presented as mean \pm SEM (n=3 biological replicates, with three technical replicates per condition). Significance was determined using nonparametric ANOVA test with a Tukey multiple comparisons test where *p<0.05, **p<0.01, ***p<0.001 and ****p<0.0001. Das: dasatinib; Rux: ruxolitinib; Das+Rux: dasatinib and ruxolitinib.

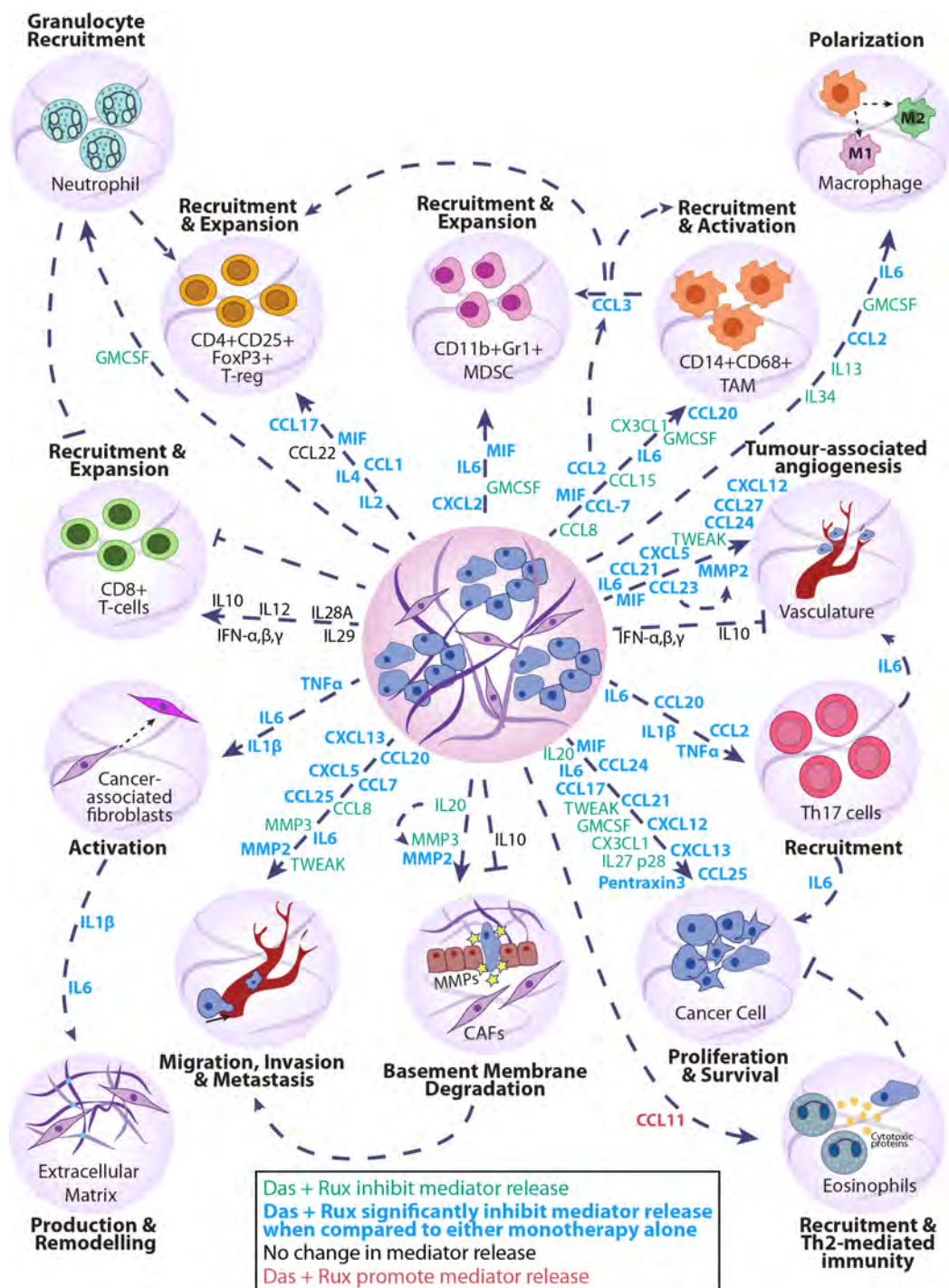


Figure 4.2.20 Cytokine profile schematic of TKCC-10 co-culture organoids following treatment with dasatinib and ruxolitinib (data summarised from figure 4.2.19). Factors highlighted in green depict efficacy of dasatinib and ruxolitinib combination in inhibiting mediator release, factors highlighted in blue depict superior efficacy of the combination treatment compared to either monotherapy alone. Black depicts no change and red depicts increased mediator release. TAM: tumour-associated macrophage; MDSC: myeloid-derived suppressor cell; CAF: cancer-associated fibroblast; T-reg: T-regulatory cell.

4.2.4 Identifying transcriptional signatures associated with dasatinib and ruxolitinib treatment in three-dimensional co-culture organoids

4.2.4.1 Characterising the cellular composition of KPC co-culture organoids using single-cell transcriptomics

In order to further understand the molecular mechanisms underlying the efficacy of dasatinib, ruxolitinib and combination therapy on various cell populations in 3D culture, highly efficient and massively-parallel single cell RNA-sequencing was performed. KPC co-culture organoids were treated with dasatinib and ruxolitinib monotherapies and in combination, at a pre-determined non-toxic (IC_{10}) concentration for 24h. Organoids were then dissociated into a single-cell suspension and captured using 10x Chromium technology. Single-cell RNA sequencing profiles were generated using NovaSeq for 5000 cells per treatment group.

Principal component analysis (PCA) was performed using highly variable genes with significant components (1 to 16) selected via heatmaps and elbow plot (Appendix E), where the majority of the total variation of the system was defined by the first 16 principal components (PCs). These top 16 PCs were used to model the cellular composition of organoids using UMAP (uniform manifold approximation and projection for dimension reduction) [652]. The UMAP algorithm was utilised to convert high dimensionality of transcriptomics in single cells to two-dimensional space for data visualisation of each sample (Appendix F). From this analysis, 6 clusters were identified at resolution 0.1 (Appendix G: cluster tree), and these clusters show distinct spatial distribution. Low quality, doublets or dying cells were excluded (as defined as <500 genes per cell, >8500 genes per cell, less than 3 cells per gene and >12.5% mitochondrial counts) (Appendix H and Appendix I), and when individual sample quality was compared between treatment groups, there was no significant difference. Next, data from each sample were combined, and integrated UMAP analysis was performed (Figure 4.2.21A). To compare how well the biological replicates overlaid we performed a correlation analysis (Appendix J), and from this analysis one replicate (dasatinib-treated) was

removed due to poor correlation. All remaining replicates displayed a high level of correlation (correlation values >0.97), and hence were suitable for further analyses. Moreover, cells from biological replicates contributed to all cell clusters (Figure 4.2.21B), confirming that the defined principle components weren't driven by technical batch effects.

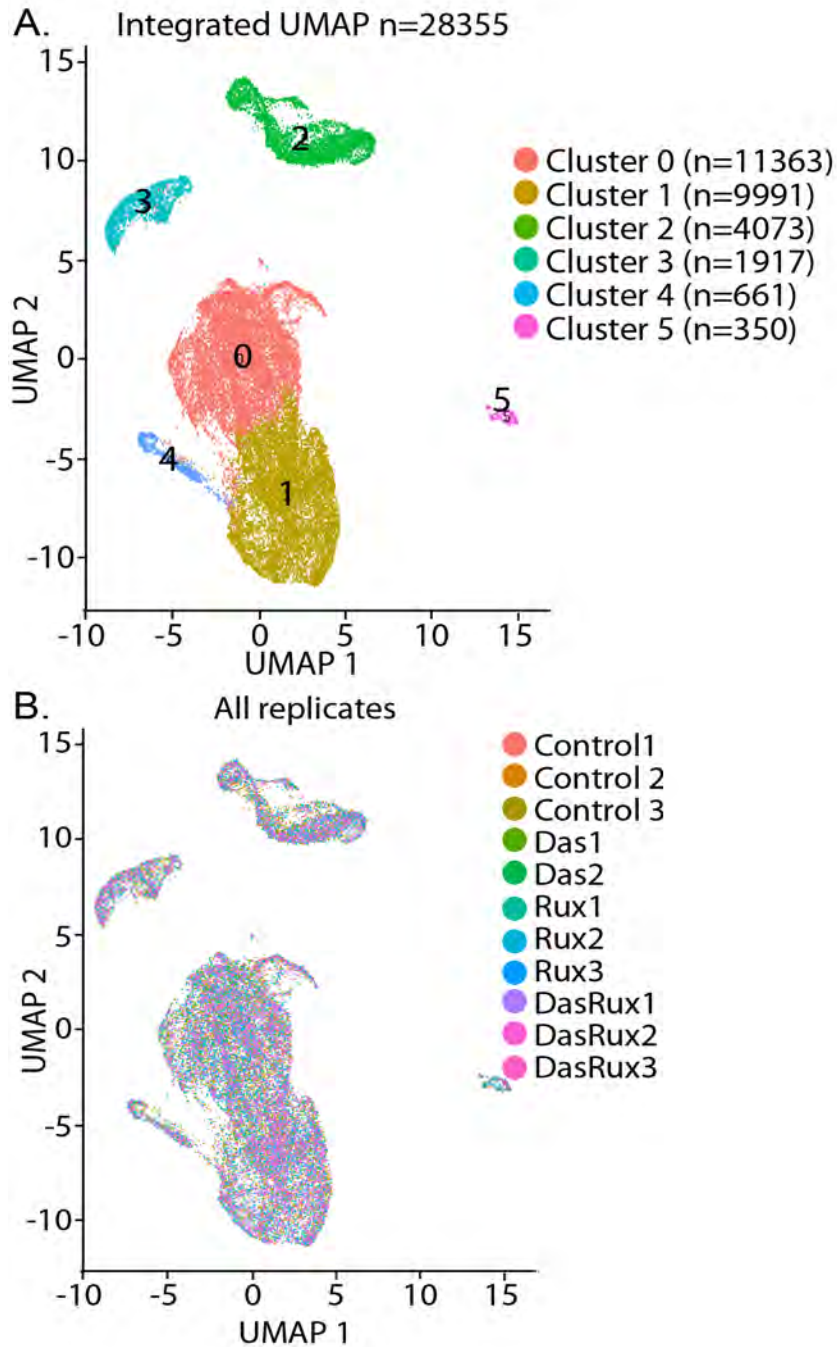


Figure 4.2.21 (A) Integrated UMAP plot of KPC co-culture organoids displaying 28355 cells comprising 6 distinct cell populations. (B) UMAP plot of individual replicates reveals no treatment bias within clusters.

To define the identity of individual cell clusters we first inferred large-scale chromosomal copy-number variations (CNVs) in each single cell based on average expression profiles along chromosomal intervals (Figure 4.2.22). These inferred CNVs separated malignant cells (clusters 0, 1, 3 and 4) from non-malignant cells with normal karyotypes (clusters 2 and 5). Secondly, we employed an epithelial score, generated from the expression of key epithelial marker genes (*Krt8*, *Krt18*, and *Krt19*) (Figure 4.2.23). This analysis has classified our cells into two major classes: malignant epithelial cells (clusters 0, 1, 3 and 4) and non-epithelial stromal cells or fibroblasts (clusters 2 and 5), with the majority of cells being defined as epithelial (84.4%). Importantly we showed significant concordance between cells with epithelial marker expression and aberrant karyotypes.

To further classify the malignant epithelial cells we annotated clusters by the expression of key marker genes previously identified by Tuveson *et al.* [145], (Figure 4.2.23). We identified genes belonging to ductal cluster 2 (*Bax*, *Hbegf*, *Cd81*, *Ctsd*) expressed specifically in cluster 0. Genes belonging to ductal cluster 3 (*S100a4*, *Krt8* and *Ecm1*) were expressed specifically in cluster 1. Moreover cluster 3 contained genes that matched to ductal cluster 1 (*Tsc22d1*, *Socs2*, *Slc16a3*, *Msmo1*, *Ldha*, *Lgfbp3*, *Ier3*, *Id2*, *Dusp5*, *Btc*, *Areg*, *Aldh1a3*, *Cadm1*, *Cd44* and *Gatm*). Lastly, cluster 4 contained genes that matched with ductal cluster 4 including *Tff1*, *Tff2*, *Spint2*, *S100a6*, *Ociad2*, *Muc1* and *Lgals4*.

We also examined the 4 malignant epithelial clusters for marker genes of the classical and quasi-mesenchymal PDAC subtypes described by Collisson *et al.* [7]. Cluster 4 expressed genes belonging to the classical subtype of human PDAC (*GPX2*, *LGALS4*, *TSPAN8*, *TFF1* and *TFF2*), characterised by intrinsic gemcitabine resistance. Accordingly, *Muc1* and *Fbp2*, key chemoresistance-associated genes, were also identified in this cluster [7]. Moreover, genes that characterise the quasi-mesenchymal phenotype, a phenotype associated with poorer survival, were identifiable in cancer clusters 0, 1 and 3 (*Ahnak2*, *Cav1*, *Cks2*, *Fermt1* and *Phlda1*). These clusters also comprised genes associated with cell-cycle regulation and proliferation (*Cks1b*, *Cks2*, *Cdk6*, *Ccna2*, *Birc5*)

[653], as well as cell motility and invasion (*Ecm1*, *Hspb1*, *Lbp*) [654-656], further reinforcing the aggressive nature of this subtype.

Lastly, we compared clusters with marker genes from the 4 PDAC subtypes described by Bailey *et al.* (squamous, ADEX, progenitor and immunogenic subtypes) [3]. Cluster 0 comprised characteristic squamous subtype genes, including those associated with cell proliferation (*Aurka*, *Aurkb*, *Cdca8*, *Birc5*, *Cenpa*, *Nsun2*, *Racgap1*, *Smc2*, *Smc4*, *Ccna2*, *Rfc3*, *Rfc2*) [657]. Moreover, cluster 0 also comprised genes associated with RNA processing (*Ncl*, *Cks1b* and *Ruvbl2*), another defining characteristic of the squamous subtype. In contrast, cluster 4 comprised genes associated with xenobiotic metabolism (*Gsta1*, *Mgst3*) and O-linked glycosylation of mucins (*Gcnt3*, *Muc5ac* and *Muc1*), key features of the progenitor subtype.

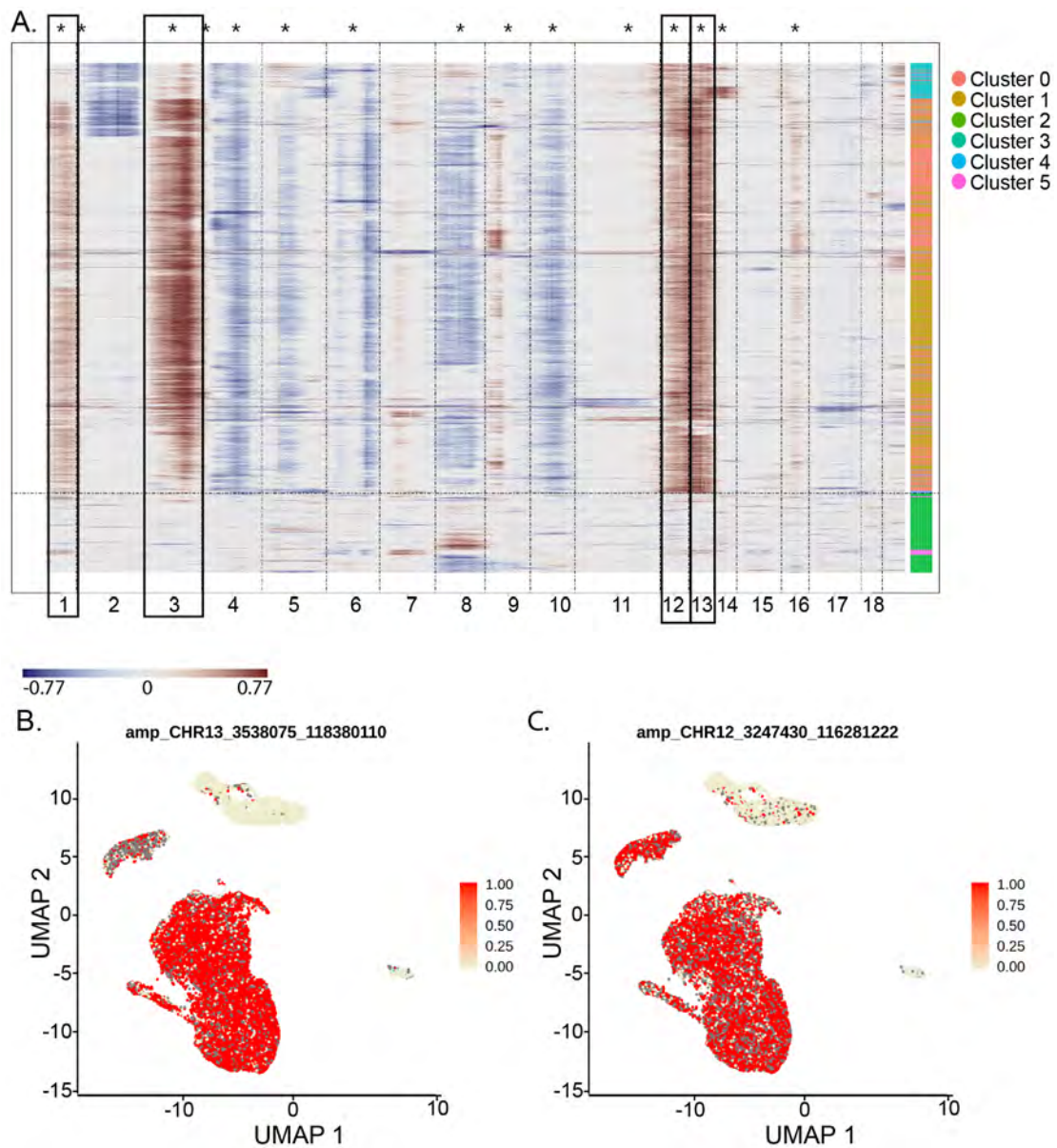


Figure 4.2.22 Cells are classified as malignant and non-malignant based on CNVs. (A) Heatmap shows large-scale CNVs for individual cells (rows) along the genome, separated by chromosomal position (columns). Brown= copy number gain, Blue= copy number loss. UMAP plots with cells coloured based on the amplification (red) of chromosome 13 (B) and chromosome 12 (C).

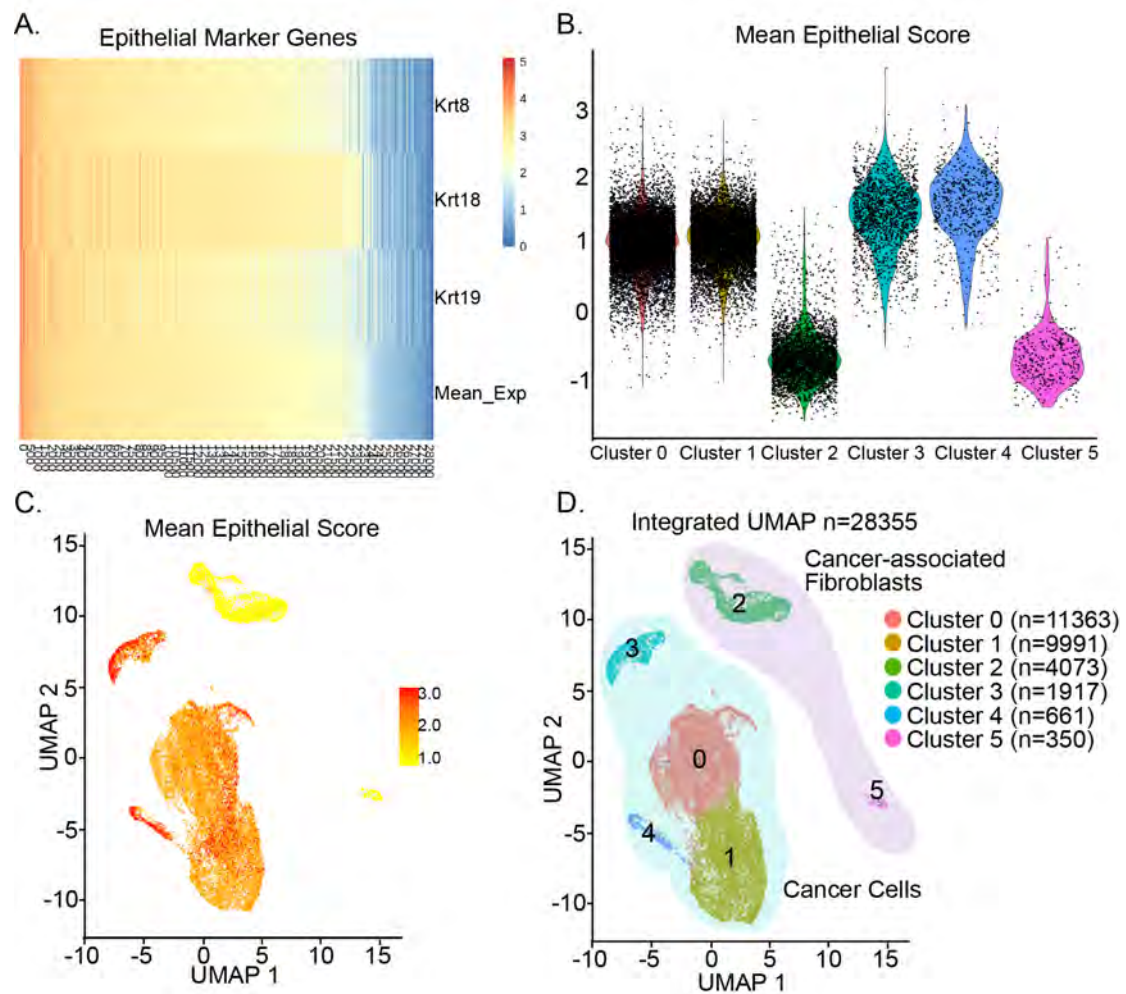


Figure 4.2.23 Cells are classified as epithelial and non-epithelial based on epithelial marker expression. (A) Heatmap showing expression of epithelial marker genes (*Krt8*, *Krt18* and *Krt19*) across 28355 single cells (columns), sorted by the average expression of each gene. (B) Violin plot showing distributions of epithelial scores (average expression of epithelial marker genes) for cells in each cluster. (C) UMAP visualisation of mean epithelial score. (D) Integrated UMAP plot annotated with two different cell types based on epithelial score.

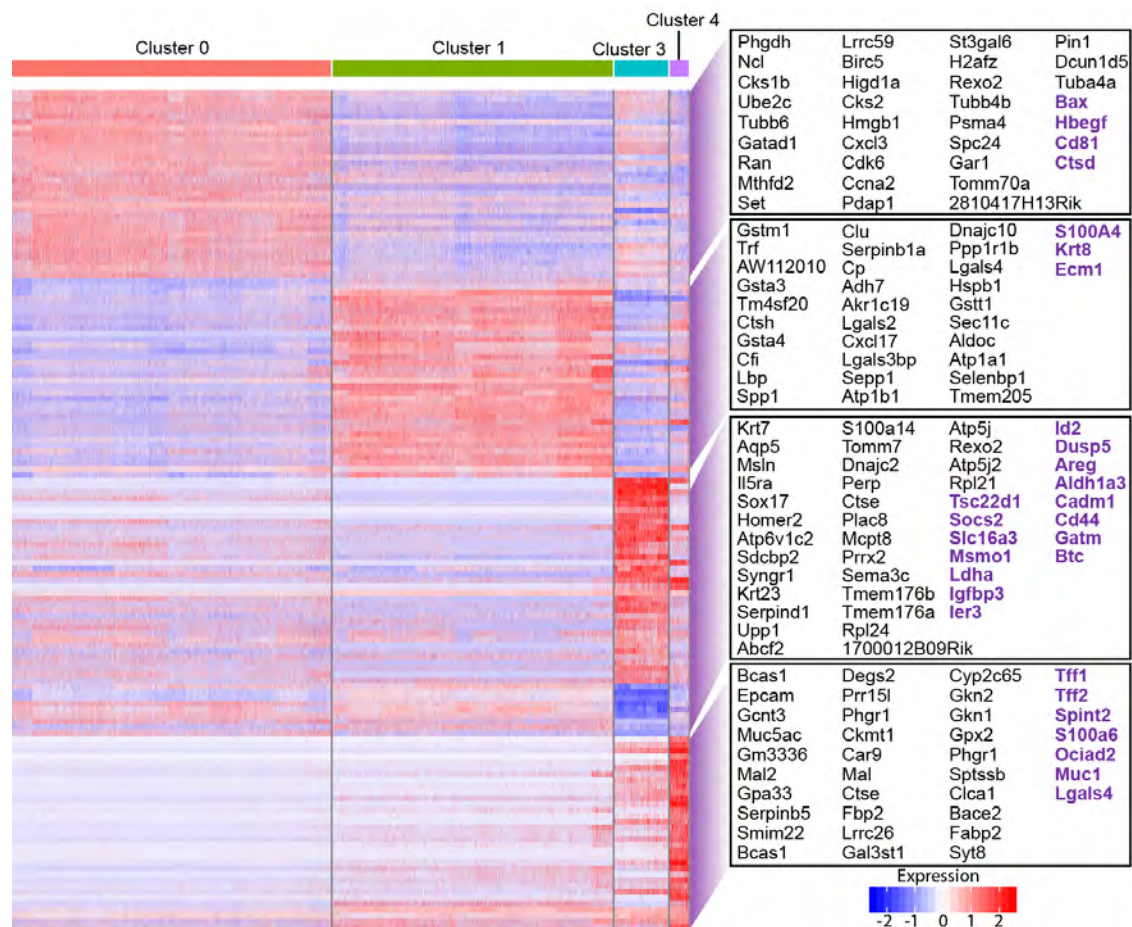


Figure 4.2.24 Single cell profiling heatmap of epithelial cancer clusters (clusters 0,1,3,4) displaying top differentially expressed genes between each population. Gene names are listed in the boxes, with genes highlighted in purple indicating marker genes of ductal clusters previously identified by Elyada and Tuveson *et al.* [145], and Ohlund and Tuveson *et al.* [141]. Each column represents an individual cell and each row displays the gene expression value for an individual gene.

The non-epithelial, stromal cells partitioned into 2 distinct clusters (clusters 2 and 5), and these were annotated with key marker genes previously identified by Tuveson *et al.* to define distinct cancer-associated fibroblast (CAF) populations [145, 147] (Figure 4.2.25). Cluster 5 expressed genes specifically associated with inflammatory CAFs (iCAFs) (*S100a8*, *Gpr84*, *Adamtsl5*, *Apoe*, *Ccl7*, *Ifi27l2a*), characterised by their pro-inflammatory and immunosuppressive phenotype. Whereas cluster 2 expressed genes specifically associated with myofibroblasts (myCAFs) (*Acta2*, *Col15a1*, *Col1a1*, *Serpine2*, *Sparc*, *Tagln*, *Thbs2* and *Tnc*), characterised by their ability to produce extracellular matrix proteins [145, 147]. Furthermore we have identified novel unique genes that define clusters 2 and 5. Cluster 5 comprised several genes involved in chemokine signalling (*Ccl2*, *Ccl3*, *Ccl4*, *Ccl6*, *Ccl9*, *Ccl12*, and *Rac2*), and cluster 2 comprised additional extracellular matrix genes (*Mmp3*, *Fn1*, *Dcn*, *Bgn*, *Col1a2*, *Col6a1*, *Fbln2* and *Ccdc80*). We were unable to identify the third CAF population previously described by Tuveson *et al.* (antigen-presenting CAFs; apCAFs) [145, 147]. Antigen-presenting CAFs (apCAFs) are another dynamic cell state that can differentiate into myCAFs under different environmental cues, therefore limiting their presence to particular environmental conditions. This may explain our inability to identify this apCAF population in organoid cultures.

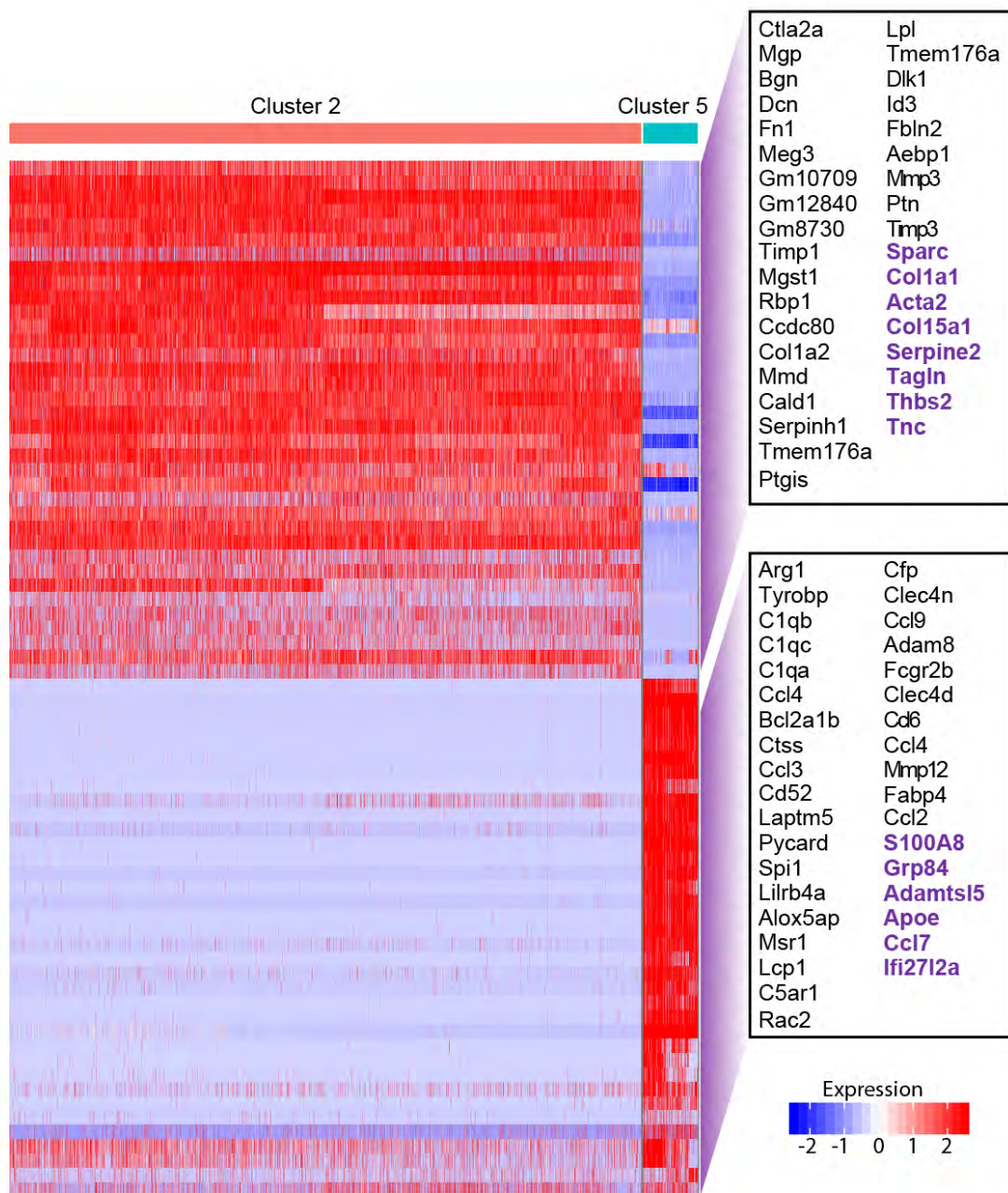


Figure 4.2.25 Single cell profiling heatmap of non-epithelial fibroblast clusters (clusters 2 and 5) displaying top differentially expressed genes between each population. Gene names are listed in the boxes, with genes highlighted in purple indicating marker genes of CAF clusters previously identified by Elyada and Tuveson *et al.* [145], and Ohlund and Tuveson *et al.* [141]. Each column represents an individual cell and each row displays the gene expression value for an individual gene.

4.2.4.2 Identifying molecular mechanisms associated with dasatinib and ruxolitinib treatment in KPC organoids using single cell transcriptomics.

To understand the mechanisms associated with dasatinib and ruxolitinib treatment on various cell populations in KPC organoids, we examined differential gene expression (DEG) patterns in each cluster following treatment with dasatinib, ruxolitinib, and the combination of dasatinib and ruxolitinib (Tables 4.2.1-4.2.3). Pathway enrichment analysis based on Gene Ontology (GO) was also performed to identify enriched gene signatures (Figures 4.2.26 - 4.2.28).

Dasatinib treatment resulted in the downregulation of key SRC-regulated genes and SRC downstream targets (*Atp1a1* in QM-PDA/squamous-like cluster 0; *Cxcl12*, *Sdc2*, *Timp1* and *Anxa2* in ECM-producing myCAF cluster 2) (Table 4.2.1), known for their role in promoting cancer cell survival, migration and invasion [658-663]. SRC is also known to facilitate cell cycle progression and cellular proliferation [664], and inhibition of SRC resulted in the downregulation of key cell cycle regulators including *Ccnd1* (cluster 3) [665], *Id1* and *Id3* (cluster 1) [666], *Ube2s*, *Ranbp1* and *Cks1b* (cluster 2) [667-669], as well as *Ccl2* (cluster 5) [670]. These findings are strengthened by the gene ontology (GO) analyses that revealed enrichment of signatures associated with protein synthesis and cellular metabolism (Figure 4.2.26), key processes involved in the cellular proliferation and survival of cancer cells [671, 672]. Moreover, we also observed that SRC-inhibition modulates characteristic myCAF genes (cluster 2), including *Col1a2* and *Col3a1*, major ECM proteins that contribute to the fibrotic tumour microenvironment of PDAC [114, 673]. In addition, SRC kinase targeting decreased expression of characteristic iCAF genes (*Ccl2*, *Ccl3* and *Ccl4*) in the stromal cluster 5, involved in the recruitment and activation of immunosuppressive cell populations, including tumour-associated macrophages, myeloid-derived suppressor cells and regulatory T cells [159, 623, 674].

Table 4.2.1 Top downregulated and upregulated genes in KPC co-culture organoids following treatment with dasatinib.

	List of most downregulated and upregulated genes following dasatinib treatment											
	Cluster 0		Cluster 1		Cluster 2		Cluster 3		Cluster 4		Cluster 5	
	Gene ID	Fold change	Gene ID	Fold change	Gene ID	Fold change	Gene ID	Fold change	Gene ID	Fold change	Gene ID	Fold change
Top 20 downregulated genes	Gm26917	0.75	Gm26917	0.72	Gm26917	0.73	Gm26917	0.74	Gm26917	0.72	Ccl7	0.20
	Gm42418	0.83	Gm42418	0.80	Gm42418	0.82	Gm42418	0.81	Gm42418	0.78	Ccl4	0.24
	Ppp1r14b	0.85	Ras11a	0.86	Cebpb	0.85	Ppp1r14b	0.86	AY036118	0.86	Ccl2	0.25
	AY036118	0.88	Ttr	0.87	Cks1b	0.86	Stra6	0.87			Ccl12	0.26
	Ras11a	0.89	AY036118	0.88	Sparrc	0.87	AY036118	0.89			Mmp12	0.28
	Gm8730	0.90	Serpina1a	0.89	Cxcl12	0.87	Fkbp11	0.90			Spp1	0.33
	St3gal6	0.90	Ppp1r14b	0.89	Tuba1b	0.87	Gm10073	0.91			Ccl3	0.37
	Alp1a1	0.91	Id3	0.89	AY036118	0.88	Gm8730	0.91			Cond1	0.40
	Stard10	0.91	C3	0.90	Timp1	0.88	Ccnd1	0.92			Id1	0.43
	Ube2m	0.91	Smm6	0.90	Dynl1	0.88	Ube2m	0.92			AA467197	0.50
	Hdgf	0.92	Lgals4	0.90	Col3a1	0.88	Gm9493	0.93			Lpl	0.50
	Gm10073	0.92	Lbp	0.91	Col1a2	0.88	Elf5	0.93			Zranb3	0.53
	Hrsp12	0.92	Id1	0.91	Fam162a	0.89					Ch25h	0.54
	Hspb1	0.92	Akr1c19	0.91	Scd2	0.89					Tuba1b	0.57
	Csrp2	0.93	Cebpb	0.92	Pcolce	0.89					Ranbp1	0.57
	mt-Co2	0.93	Gm8730	0.92	Ube2s	0.89					Adam8	0.58
	Akr1c19	0.93	Gm9493	0.92	Anxa2	0.90					Dok2	0.63
	Gm9493	0.93	Hspa5	0.92	Ranbp1	0.90					Lat2	0.64
	mt-Co3	0.93	Gm10073	0.92	Mrpl42	0.90					St3gal5	0.65
	Vnn1	0.93	Hist1h1c	0.92	Hmg1	0.90					Nans	0.66
Top 20 upregulated genes	Rps27	1.19	Rps28	1.18	Snrpg	1.26	Mt1	1.27	Ndufa3	1.13	Saa3	6.03
	Rps28	1.19	Crip1	1.17	Clu	1.26	Mt2	1.26	Usmg5	1.15	Thbs1	2.16
	Rpl38	1.19	Tmsb10	1.17	Rps28	1.23	Rps28	1.25	Rpl38	1.16	Sod2	1.85
	Usmg5	1.18	Mt1	1.17	Lcn2	1.23	Usmg5	1.25	Rpl39	1.19	Cybb	1.77
	Sprr1a	1.17	Mt2	1.16	Rps27	1.21	Rpl35	1.22	Rps28	1.20	Clec4d	1.76
	Rpl35	1.17	Rpl38	1.16	Mt1	1.19	Rpl38	1.22	Rps27	1.22	Ypel3	1.69
	Rps29	1.17	Rpl41	1.15	Rpl38	1.19	Rpl39	1.22			Ifitm2	1.64
	Gm12840	1.15	S100a6	1.15	Usmg5	1.18	Rps27	1.20			Tnfrsf2	1.63
	Rpl39	1.15	Rps27	1.15	Mmd	1.16	Tomm7	1.20			Blg1	1.63
	Snrpg	1.15	Usmg5	1.15	Gm8186	1.18	Atp5k	1.18			Lst1	1.63
	Tmsb10	1.15	Rpl35	1.15	Neat1	1.17	Rps29	1.19			Mgst1	1.62
	Rpl41	1.15	Rps29	1.15	Gm12840	1.17	Rpl37	1.18			Eva1b	1.61
	S100a11	1.15	Snrpg	1.14	Rpl36	1.17	Rps21	1.18			Cox7a2l	1.58
	2010107E04Rik	1.15	Rpl39	1.14	Rpl37	1.16	Rpl37a	1.18			Itim2b	1.53
	Rpl27	1.14	2010107E04Rik	1.14	Rpl37a	1.16	Rpl41	1.17			Blvrh	1.53
	Rpl37	1.14	Rpl27	1.13	Blg1	1.16	S100a6	1.17			Gclm	1.50
	Rps21	1.14	Rpl37	1.13	Rpl39	1.16	Rpl36	1.16			Marcksf1	1.49
	Rpl38	1.13	Tomm7	1.12	Cd24a	1.16	Rpl27	1.16			Smpd3a	1.48
	Crip1	1.13	Rps21	1.12	Procr	1.15	Cox7c	1.15			Fcgr3	1.43
	Rpl37a	1.13	Rpl36	1.12	Rpl35	1.15	2010107E04Rik	1.15			Gltscr2	1.41

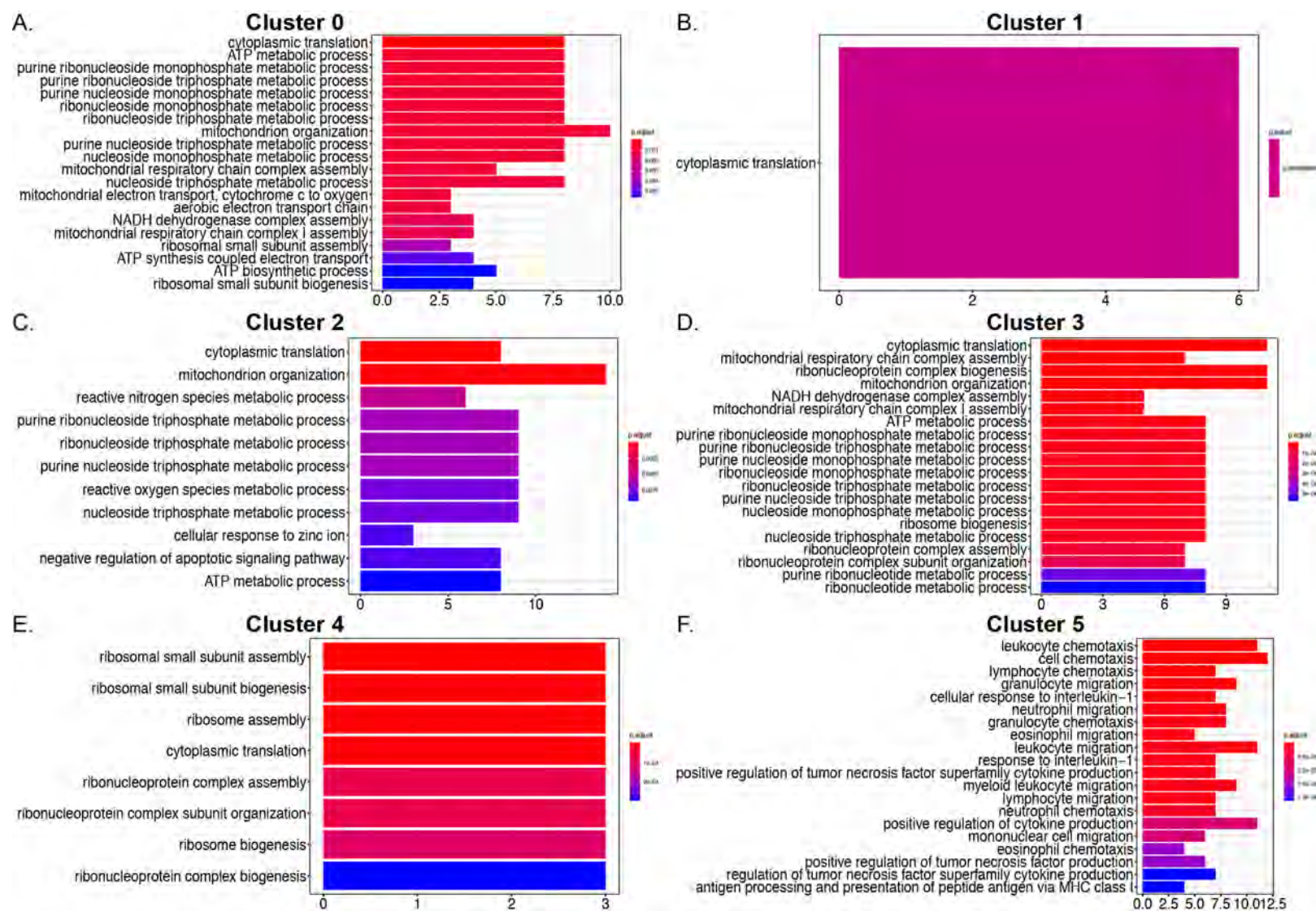


Figure 4.2.26 Gene ontology (GO) analysis for KPC organoids showing enriched pathways following treatment with dasatinib.

JAK1/2 inhibition via ruxolitinib treatment resulted in the downregulation of key pro-tumourigenic STAT3-target genes known to regulate cancer cell migration, invasion and metastasis including *Tubb6* (QM-PDA-like cancer clusters 0 and 3), *Anxa2* (clusters 0 and 1) and *Ccl20* (cluster 1) [675-678], as well as *Lcn2* (all clusters) (Table 4.2.2). Importantly *Lcn2* is frequently overexpressed in cancer, and is associated with increased pancreatic tumour cell invasion as well as gemcitabine resistance [479, 679]. Furthermore, STAT3 activation has previously been shown to prevent apoptosis of pancreatic cancer cells [680], accordingly we have shown that ruxolitinib treatment downregulates important negative regulators of apoptosis including *Clu* (cancer clusters 0, 1 and stromal cluster 2) [681] and *Spp1* (clusters 2 and 3) [682], findings that are supported by the GO analyses (cluster 2) (Figure 4.2.27C). Analogous to that of dasatinib treatment, ruxolitinib treatment resulted in the modulation of characteristic myCAF genes involved in extracellular matrix organisation (*Sdc1* and *Spp1*; cluster 2) [683-685], as well as distinctive iCAF genes that promote an immunosuppressive tumour microenvironment, including various tumour-promoting chemokines (*Ccl2*, *Ccl3*, *Ccl4*, *Ccl6*, *Ccl7*, *Ccl9*, *Ccl12*; cluster 5) involved in tumour-associated macrophage chemotaxis and activation [159, 623, 674, 686]. Additionally, we observed modulation of *Cxcl1* (stromal cluster 2), a STAT3-activating paracrine signalling factor that regulates tumour-stromal interactions and enhances the motility and invasive potential of cancer cells [687], as well as several genes associated with the activation and accumulation of CAFs (*Saa3*, *Timp1* and *Sod2*; cluster 2) [688-690], suggesting that JAK inhibition impedes the recruitment and differentiation of CAFs as well as their phenotype.

Table 4.2.2 Top downregulated and upregulated genes in KPC co-culture organoids following treatment with ruxolitinib.

	List of most downregulated and upregulated genes following ruxolitinib treatment											
	Cluster 0		Cluster 1		Cluster 2		Cluster 3		Cluster 4		Cluster 5	
	Gene ID	Fold change	Gene ID	Fold change	Gene ID	Fold change	Gene ID	Fold change	Gene ID	Fold change	Gene ID	Fold change
Top 20 downregulated genes	Gm26917	0.74	Lcn2	0.48	Lcn2	0.45	Spp1	0.68	Gm26917	0.74	Ccl7	0.22
	Lcn2	0.75	Spp1	0.71	Saa3	0.46	Gm26917	0.74	Gm42418	0.86	Ccl2	0.24
	Spp1	0.81	Gm26917	0.72	Timp1	0.46	Serpind1	0.76	Mgp	0.88	Ccl12	0.27
	Slpi	0.85	Ifi27	0.77	Ifitm3	0.49	Plat	0.76	Saa3	0.88	Arg1	0.31
	Cliu	0.85	Rbp4	0.77	Cliu	0.50	Ier3	0.77	Ctla2a	0.91	Mmp12	0.34
	Tm4sf1	0.85	Ifitm3	0.77	Spp1	0.51	Phgdh	0.80	Lcn2	0.92	Ccl4	0.37
	Tnfrsf12a	0.86	Ccl20	0.79	Timp3	0.53	Ankrd1	0.81			Ccl3	0.40
	Plat	0.87	Cfi	0.81	Hp	0.56	Lcn2	0.82			Ccl6	0.41
	Tubb6	0.87	C3	0.81	Sod2	0.57	Tuba1a	0.82			Ccl9	0.50
	Anxa2	0.87	Ly6a	0.81	Spr2b	0.59	Tpm4	0.83			Clec4n	0.57
	Gm42418	0.87	Cliu	0.81	Cp	0.63	Tubb6	0.84			Ch25h	0.56
	Eil4a1	0.88	Tnfrsf12a	0.82	Spr2e	0.63	Tm4sf1	0.84			Bcl2a1a	0.63
	Nup56	0.88	Slpi	0.82	Fth1	0.67	Anxa5	0.84			Il1rn	0.63
	Eil6	0.88	Cp	0.83	Sdc1	0.67	Tagln2	0.85			Fabp4	0.66
	Lyar	0.88	Gda	0.84	Gda	0.69	Rtn4	0.85			Pycard	0.67
	Ier3	0.89	Tifa	0.84	Tnfrsf9	0.71	Ctsl	0.85			Mgl2	0.68
	Tagln2	0.89	Plat	0.84	Slpi	0.71	Upp1	0.85			Pla2r	0.68
	Ly6a	0.89	Anxa2	0.84	Ifitm2	0.72	Eil4a1	0.85			Cd300lf	0.69
	Ifitm3	0.89	Trf	0.84	Rbp1	0.73	Mcpt8	0.86			Msr1	0.69
	Lmna	0.90	Sltm2	0.85	Cxcl1	0.73	Angptl4	0.86			Socs2	0.69
Top 20 upregulated genes	Rps28	1.24	Mt2	1.33	Angptl7	1.72	Rps28	1.30	Tomm7	1.11	Gas6	1.54
	Rps27	1.23	Mt1	1.31	Ifi2712a	1.38	Rps27	1.26	2010107E04Rik	1.12	Sepp1	1.54
	Rpl38	1.20	Rps28	1.24	Igf1bp6	1.36	Rps29	1.26	Rps26	1.13	Aif1	1.51
	Rps21	1.20	Rps27	1.23	Smim1	1.35	Tspan13	1.24	Atp5e	1.13	Lipa	1.44
	Rps29	1.20	mt-Nd3	1.23	Gstm1	1.34	Mt2	1.24	Alp5k	1.13	Ctla2b	1.43
	Rpl39	1.19	Ttr	1.22	Meg3	1.33	Rps21	1.23	Cox7c	1.14	Smpd3a	1.39
	Mt2	1.19	Gstm1	1.22	Col6a1	1.31	Rpl38	1.22	Rps29	1.15	Ptpn18	1.37
	mt-Nd3	1.18	Blg2	1.21	Sdpr	1.31	Rpl41	1.22	Rpl38	1.15	Caf1r	1.37
	Rpl41	1.17	Rps21	1.19	Gsta4	1.31	Rpl37	1.22	Rps27rt	1.15	Serpinb6a	1.36
	Rpl37	1.17	Rpl38	1.19	Rps28	1.29	Mt1	1.21	mt-Nd3	1.16	Sirpa	1.35
	Rpl37a	1.17	Rps27rt	1.19	Gata6	1.28	mt-Nd3	1.21	Rpl39	1.16	Adgre1	1.33
	Usmg5	1.16	Hes1	1.19	Rps27	1.28	Rpl36	1.21	Rps27	1.17	Lst1	1.33
	Rps27rt	1.16	Rpl39	1.19	Ces2g	1.25	Rpl39	1.21	Rps28	1.19	Ypel3	1.33
	Rpl36	1.16	Hsd17b14	1.18	Zfos1	1.25	Usmg5	1.19			Rps29	1.33
	Rpl27	1.15	Rps29	1.18	Ptn	1.24	Rpl35	1.19			Rps27	1.32
	Rpl35	1.15	Rpl36	1.17	Maoa	1.24	Ccnd2	1.19			Itim2b	1.32
	Gstm1	1.15	Crip1	1.18	Oik1	1.24	Gsta4	1.18			Ompk	1.31
	2010107E04Rik	1.15	Rpl37	1.16	Nfib	1.24	Rpl37a	1.18			Hexa	1.30
	Rps26	1.14	Cmb1	1.16	Snhg18	1.24	Nm1	1.18			Rgs10	1.30
	Alp5k	1.14	Rpl41	1.16	Thbs1	1.23	Rps26	1.18			Cox7a2l	1.29

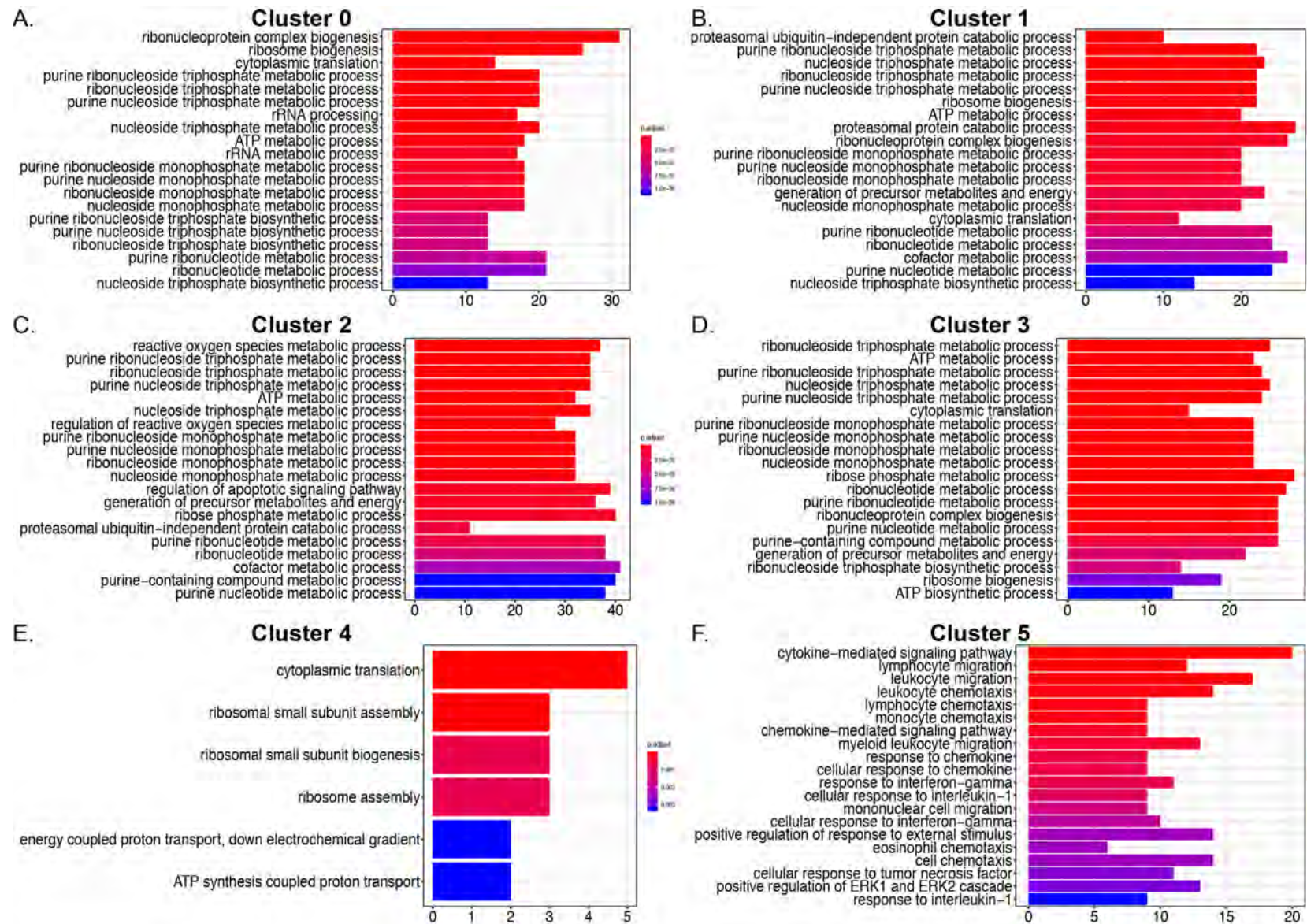


Figure 4.2.27 Gene ontology (GO) analysis for KPC organoids showing enriched pathways following treatment with ruxolitinib.

Examination of transcriptomic signatures following treatment with the combination of dasatinib and ruxolitinib (Table 4.2.3) revealed an amalgamation of both SRC- and STAT3-mediated effects. These included the downregulation of the STAT3-target gene *Lcn2* (QM-PDA-like clusters 0, 1 and 3, and stromal ‘myCAF’ cluster 2), the STAT3-activating gene *Cxcl1* (cluster 2), as well as the SRC-target gene *Timp1* (cluster 2); genes with previously described pro-tumourigenic functions. Furthermore we observed enhanced inhibitory effects on cell cycle regulatory genes across the tumour (*Cdk6*, cluster 0; *Cks1b*, cluster 1; *Mif*, cluster 4) and stromal subpopulations (*Mif*, cluster 2; *Ccnd1*, cluster 5) [669, 691, 692] as well as genes associated with cancer cell proliferation and survival (*Lyar*, cluster 0; *Phgdh*, cluster 3; *Hdgf*, cluster 0, 3 and 4; *Mmp12*, *Id1*; iCAF stromal cluster 5) [693-697]. Moreover, we observed inhibitory effects on genes associated with the negative regulation of apoptosis (*Clu*, *Sod2*; myCAF stromal cluster 2) [681, 698], as well as key genes involved in the chemoresistance and metastasis of PDAC (*Tuba1a* and *Tubb6*; cancer cluster 3) [699]. Furthermore, dasatinib and ruxolitinib treatment modulated the extracellular matrix-associated genes *Mmp3* and *Timp1* in the myCAFs (cluster 2) [700], as well as typical iCAF genes previously described for their role in the recruitment and activation of immunosuppressive cell populations, (*Ccl2*, *Ccl3*, *Ccl4*, *Ccl6*, *Ccl7*, *Ccl9*, *Ccl12*; iCAF stromal cluster 5) [686, 701]. Interestingly, only the combination of dasatinib and ruxolitinib treatment resulted in the upregulation of genes associated with the positive regulation of T-cell mediated cytotoxicity (*H2-K1* and *H2-D1*; iCAF stromal cluster 5), (*B2m*, *H2-D1* and *Ifngr2*; “classical”-type cancer cluster 4) [702-704]. This finding is reinforced by the accompanied enrichment of gene signatures associated with antigen processing and presentation, as well as immune cell migration (Figure 4.2.28E+F). These results suggest that this therapeutic strategy may alter the expression of specific immunomodulatory genes in subpopulations of CAFs and cancer cells, which with associated changes in cytokine signalling (as presented in section 4.2.3), may collectively alter the immunosuppressive tumour microenvironment that defines PDAC.

To further assess the molecular mechanisms specifically associated with the synergy between dasatinib and ruxolitinib we also examined the DEGs in each cluster that were unique to the combination treatment, and were not identified in any other treatment group (Figure 4.2.29). From this analysis we have identified 162 unique DEGs for cluster 0, 170 unique DEGs for cluster 1, 366 DEGs for cluster 2, 243 DEGs for cluster 3, 72 DEGs for cluster 4, and 264 DEGs for cluster 5. Of particular interest, we have identified the downregulation of several SRC/JAK/STAT3-regulated genes associated with cell cycle regulation in QM-PDA-like clusters (*Cdk6*, *Cks1b*, *Rdx*, *Npm1*, *Gnb2l1*; cluster 0), (*Cdk4*, *Bin1*, *Sox4*; cluster 3), and stromal clusters (*Cdk4*, *Hras*, *Birc5*, *Ube2c*; myCAF stromal cluster 2), (*Ube2s*, *Anp32b*, *Calm3*, *Calm1*, *Ccnd2*, *Cdk6*; iCAF stromal cluster 5) [691, 705-707]. Moreover, we have shown that dasatinib and ruxolitinib treatment modulates genes involved in antigen processing and presentation (*Tapbp*, *H2-T23*, *H2-D1* and *B2m*; “classical”-type cancer cluster 4) [702-704], and lymphocyte activation (*Itgam*, *Trem12*, *Lcp1*, *Rhoh* and *Lgals1*; iCAF stromal cluster 5) [708-710], further reinforcing the immunoregulatory mechanisms of this treatment combination. Furthermore, we have identified the downregulation of genes involved in RNA translation and protein synthesis in QM-PDA-like clusters (*Rpl12*, *Rpl7*, *Rpl8*, *Rps20* and *Eif5* in cancer cluster 0; *Rpl5*, *Rpl13a*, *Rps3*, *Rpl12* in cancer cluster 1) [711, 712], a key process involved in the pathogenesis of cancer [671]. Moreover we observed upregulation of genes associated with stress response (*Cd9*, *B2m*, *Tapbp*, *Gstp1*, *Dusp1*, *Glul*; “classical” cancer cluster 4) [713-715], and glutathione metabolism (*Gsta1*, *Gstm1*, *Gsta4*; QM-PDA-like clusters 0, 1 and 3), key processes involved in the detoxification of carcinogens as well as the modulation of T-cell functions including cytotoxic T-cell activation [716, 717].

Taken together, our single cell transcriptomic analysis of KPC organoid cultures following treatment with dasatinib and ruxolitinib has revealed modulation of complex gene networks regulated by both SRC and JAK/STAT3 signalling, and associated negative regulation of select pro-tumourigenic, pro-survival cues in distinct cancer and stromal cell subpopulations. Moreover, we have shown specific effects of the proposed

combination therapy on genes that are key determinants of specific CAF phenotypes, thus potentially playing a role in reprogramming of CAF subtypes, findings that are in agreement with our previously observed effects on reduced extracellular matrix production and remodelling (section 4.2.1), as well as alterations in immunomodulatory signalling (section 4.2.3).

Table 4.2.3 Top downregulated and upregulated genes in KPC co-culture organoids following treatment with dasatinib and ruxolitinib.

	List of most downregulated and upregulated genes following dasatinib and ruxolitinib treatment											
	Cluster 0		Cluster 1		Cluster 2		Cluster 3		Cluster 4		Cluster 5	
	Gene ID	Fold change	Gene ID	Fold change	Gene ID	Fold change	Gene ID	Fold change	Gene ID	Fold change	Gene ID	Fold change
Top 20 downregulated genes	Lcn2	0.75	Lcn2	0.46	Saa3	0.41	Spp1	0.72	Ppp1r14b	0.78	Ccl7	0.09
	Gm26917	0.80	Ifitm3	0.73	Timp1	0.45	Serpind1	0.74	Odc1	0.79	Ccl2	0.10
	Hdgf	0.82	Ifi27	0.76	Ifitm3	0.46	Ankrdf1	0.75	Gm26917	0.80	Ccl4	0.19
	Ppp1r14b	0.83	Spp1	0.77	Lcn2	0.50	Ier3	0.77	Hdgf	0.80	Ccl12	0.20
	Lyar	0.84	Cfi	0.79	Clu	0.53	Phgdh	0.77	Rpl12	0.82	Arg1	0.26
	Odc1	0.85	Rbp4	0.80	Timp3	0.54	Gm26917	0.79	Gm42418	0.82	Pf4	0.31
	Fam213a	0.85	Rbp1	0.80	Sod2	0.58	1700012B09RIK	0.81	Nhp2	0.82	Mmp12	0.32
	Gm42418	0.87	C3	0.80	Spr2e	0.58	Lcn2	0.81	Tnfrsf12a	0.82	Ccl3	0.32
	Npm3	0.88	Gm26917	0.81	Spr2b	0.59	Odc1	0.82	Set	0.84	Ccl6	0.33
	Ube2s	0.88	Cp	0.81	Cp	0.64	Mcp1b	0.82	Hnmpab	0.85	Spp1	0.35
	Gstm5	0.88	Trf	0.81	Fth1	0.66	Tnfrsf12a	0.83	Npm3	0.85	Id1	0.39
	Tspan4	0.88	Pcolce	0.82	Gda	0.67	Tubb6	0.84	Ybx3	0.85	Ccnd1	0.40
	Srm	0.89	Ly6a	0.83	Hp	0.67	Plat	0.84	Mif	0.86	Dab2	0.41
	Nhp2	0.89	Gstm5	0.84	Fam162a	0.69	Ccl2	0.84	Ube2m	0.87	Ccl9	0.45
	Rpl12	0.89	Wfdc2	0.84	Cxcl5	0.69	Ppp1r14b	0.85	Zfp91	0.87	Msr1	0.47
	Ifitm3	0.89	Barx2	0.84	Cxcl1	0.69	Slc16a3	0.85	P4hb	0.87	AA467197	0.46
	Cdk6	0.89	Cks1b	0.84	Slc25a5	0.72	Hdgf	0.85	Hras	0.88	Tuba1b	0.50
	Mtdh	0.89	Tnfrsf12a	0.84	Ivi	0.72	Marcks1	0.85	Erf5	0.88	Zranb3	0.50
	Tnfrsf12a	0.89	Gda	0.85	Mmp3	0.73	Tuba1a	0.85	Rps12-ps3	0.89	Glrx	0.52
	Pcolce	0.90	Ccl20	0.85	Mif	0.73	Fkbp11	0.85	Pcbp1	0.89	Actb	0.52
Top 20 upregulated genes	Gsta1	1.66	Gsta1	1.49	Gstm1	1.51	Adh7	1.53	Adh7	1.49	Apoe	12.59
	Crip1	1.36	Gstm1	1.34	Dlk1	1.45	Gsta1	1.47	Gstm1	1.45	Saa3	4.56
	Gstm1	1.31	Mt1	1.30	Angptl7	1.45	Gsta4	1.46	Gsta1	1.40	Ypel3	2.60
	Gsta4	1.30	Crip1	1.30	Gsta4	1.38	Gstm1	1.46	Rhoc	1.34	Itm2b	2.53
	Adh7	1.27	Lgals4	1.29	Meg3	1.35	Cmb1	1.29	Cd9	1.30	Thbs1	2.36
	Lgals2	1.26	Mt2	1.27	Cpe	1.33	Lgals2	1.29	Cbr3	1.29	Sepp1	2.23
	Lgals4	1.25	Lgals2	1.25	Tmem158	1.32	Tm4sf4	1.29	Tm4sf20	1.29	Fxyd2	2.11
	Akr1c19	1.22	Car2	1.24	Csrp1	1.32	Dpcr1	1.29	Gstp1	1.28	H2-D1	2.07
	Cbr3	1.19	Adh7	1.24	Phoc	1.31	Tspan13	1.29	Itm2b	1.28	Lsl1	2.03
	Sqstm1	1.19	Car8	1.22	Mmd	1.30	Mt2	1.28	Id3	1.27	Ms4a7	2.02
	Cyb5a	1.19	Sepp1	1.21	Sepp1	1.30	Mt1	1.26	Btg2	1.27	Adgre1	1.98
	Mgst3	1.18	Rhoc	1.21	Sl3gal5	1.29	Crip1	1.26	B2m	1.26	Csf1r	1.97
	Tm4sf4	1.18	Uap111	1.21	Lamp2	1.29	Foxq1	1.24	Ifngr2	1.21	Pla2g7	1.94
	S100a13	1.18	Ugdh	1.20	Hexa	1.27	Hsd17b14	1.24	Foxq1	1.21	Junb	1.88
	Rps27	1.17	Jun	1.20	Zfos1	1.27	Fam101b	1.22	H2-D1	1.21	Hexa	1.86
	Prr13	1.17	Eps8l3	1.20	Crip1	1.27	Car6	1.22	Serpinb6a	1.20	Tnfrsf2	1.87
	Ugdh	1.17	Rps27	1.19	Ypel3	1.26	Nm1	1.21	Cmb1	1.19	Glpr1	1.86
	Serpinb6a	1.17	Tm4sf4	1.18	Itm2b	1.26	Fli1	1.21	Cyb5a	1.19	Ctss	1.83
	Mt2	1.17	Akr1c19	1.18	Aldh2	1.26	Gipc2	1.21	Piscr1	1.19	Cybb	1.81
	Uap111	1.17	Cbr3	1.18	Prnp	1.25	Id3	1.21	Glul	1.19	H2-K1	1.81

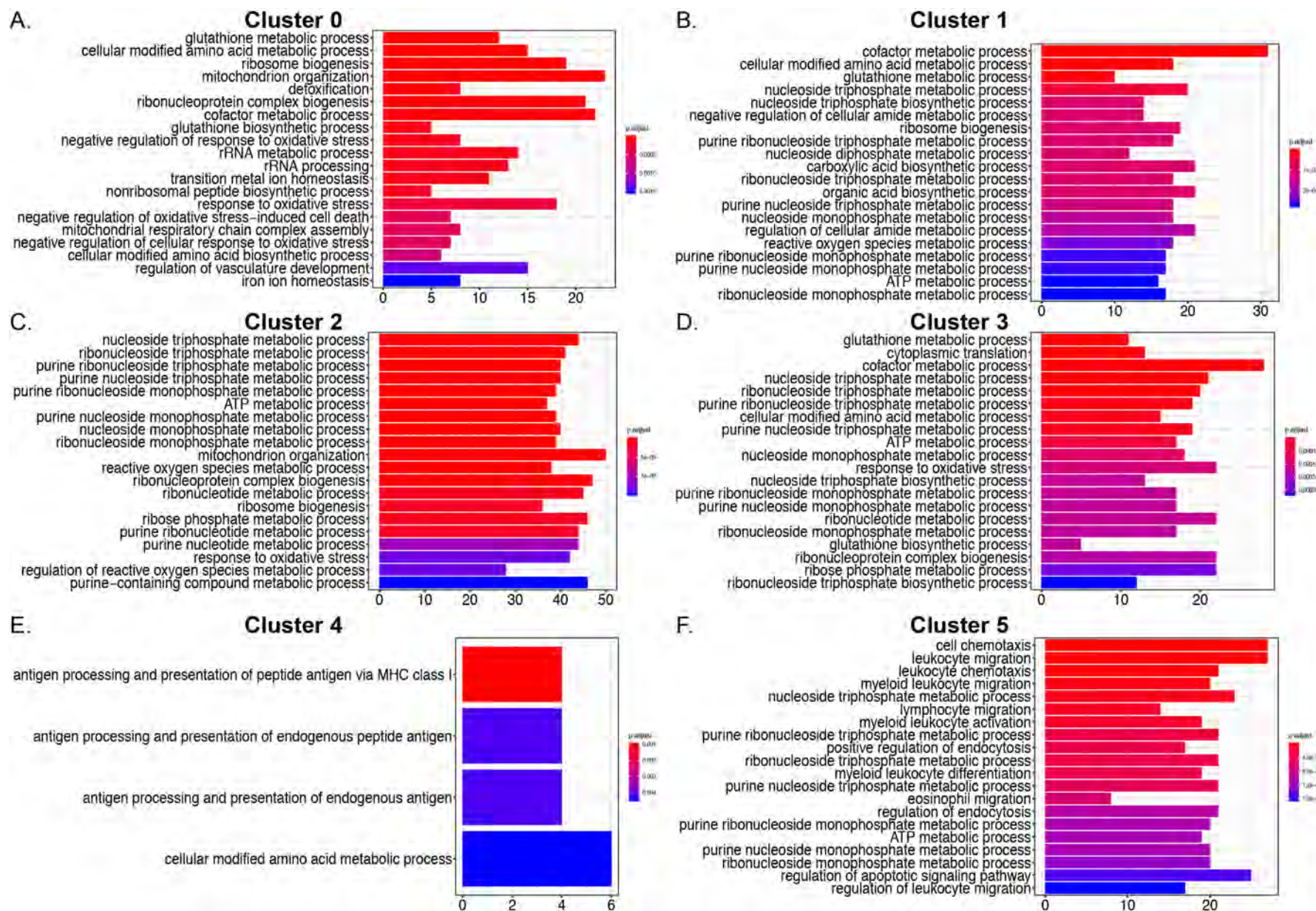


Figure 4.2.28 Gene ontology (GO) analysis for KPC organoids following treatment with dasatinib + ruxolitinib.

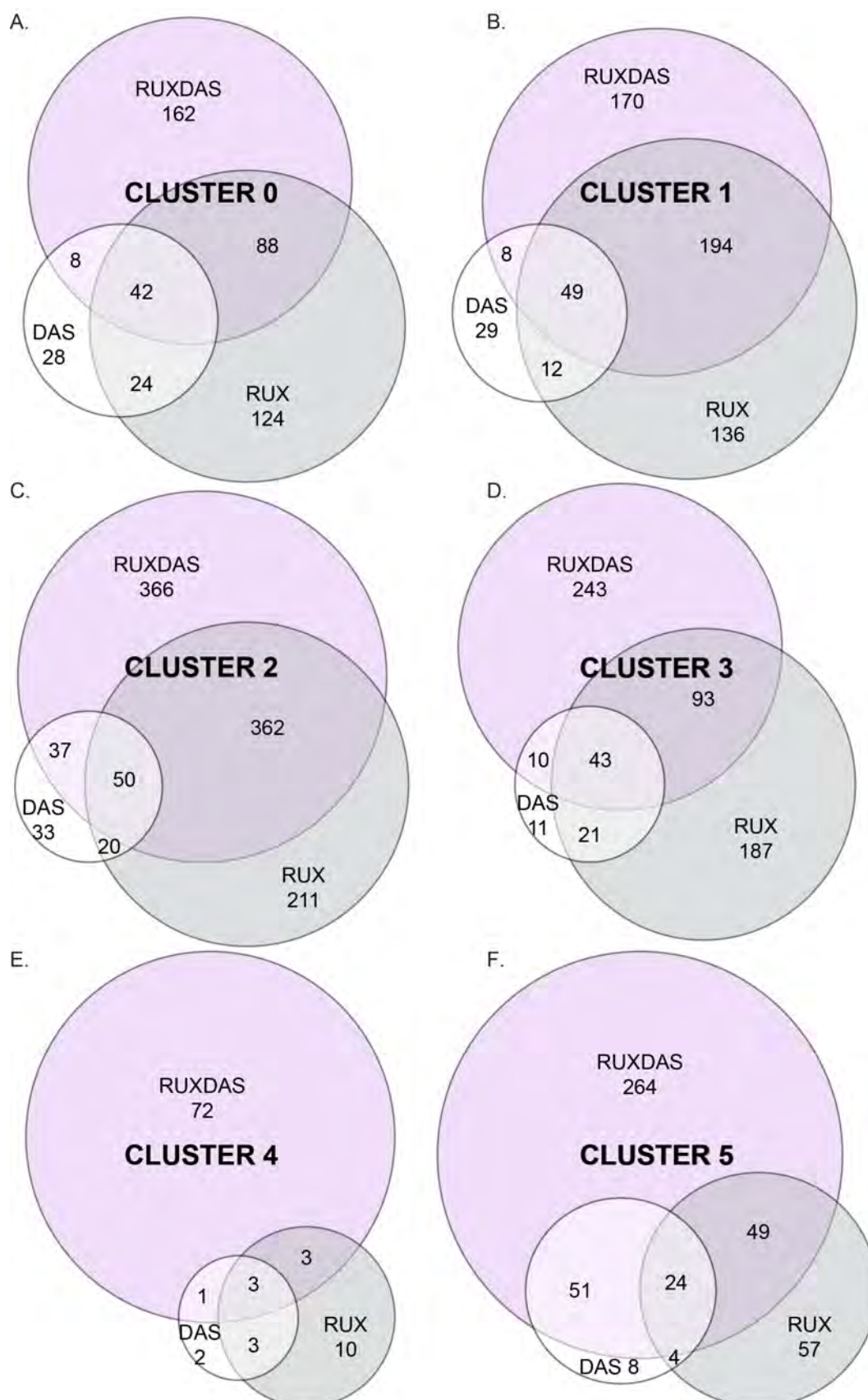


Figure 4.2.29 Venn diagrams displaying the number of differentially expressed genes following treatment with dasatinib (DAS), ruxolitinib (RUX), dasatinib and ruxolitinib (DASRUX) in each cluster.

4.3 Discussion

The pancreatic tumour microenvironment is a complex system comprising heterogeneous cellular populations as well as significant desmoplasia. The mechanical and biochemical properties of the extracellular matrix, along with dynamic paracrine signalling directly influences cell behaviour, and consequently leads to tumour progression and impaired response to chemotherapy [119, 201, 202, 205]. The SRC/JAK/STAT3 pathway has been previously shown to play a role in this process by promoting fibrosis and increasing tissue tension [321], and by regulating the intercellular crosstalk that occurs between cancer cells and stromal cells [114]. Hence, targeting this pathway has significant potential to prevent PDAC disease progression and improve chemotherapeutic efficacy. The aim of the work described in this chapter was therefore to assess the effects of dasatinib and ruxolitinib on the (i) physical properties of the extracellular matrix, (ii) cancer cell invasion and (iii) intercellular crosstalk, as well as to identify transcriptional changes associated with dasatinib and ruxolitinib treatment in cancer cell and stromal cell populations in a 3D co-culture setting. In comparison with 2D *in vitro* assays, the 3D organotypic assays [83, 149, 604, 605, 612], and organoid co-cultures [141, 718] utilised in this chapter, are robust models which better recapitulate the biochemical and physical properties of the extracellular matrix and the cellular interactions that occur within PDAC tumours.

We have established that ruxolitinib treatment impairs the ability of fibroblasts to engage with the surrounding matrix, decreases fibrillar collagen I abundance, and promotes a highly disorganised extracellular matrix network. Moreover, our study is the first to demonstrate that inhibition of the extracellular matrix ultrastructure appears to be a JAK1-dependent mechanism, and that combined JAK1/2 inhibition is most effective at disrupting extracellular matrix integrity compared to JAK1, JAK2 and JAK3 inhibition alone. We do however acknowledge that some off-target activity may have contributed to this effect. These results are consistent with previous findings where genetic disruption of STAT3 was shown to reduce fibrosis in PDAC [122, 321], and specific JAK2-inhibition via AZD1480 was ineffective [443]. Importantly we have shown that JAK1/2 inhibition can manipulate the

extracellular matrix without significantly altering fibroblast proliferation, therefore avoiding the potential adverse effects of stromal targeting as described by Ozdemir *et al.* [538].

Extracellular matrix deposition, fibrosis and paracrine signalling networks play an important role in regulating the phenotype of pancreatic cancer cells. Moreover, SRC and STAT3 downstream signalling pathways control cell motility and invasion via regulation of the actin cytoskeleton [719, 720], as well as regulate cell-extracellular matrix interactions, and can promote the transmission of pro-survival and pro-proliferative signals [180, 721]. By using three-dimensional organotypic assays, we have demonstrated that targeting the SRC/JAK/STAT3 signalling pathway can significantly inhibit the invasive potential of 'P53 mutant', 'phospho-STAT3-high' pancreatic cancer cell lines. Although it has been previously shown that inhibition of SRC can reduce the migratory and invasive capacity of pancreatic cancer cells [177], JAK inhibition has never been assessed in three-dimensional models of pancreatic cancer. Moreover, we are the first to demonstrate that the combination of dasatinib and ruxolitinib has a synergistic effect, that is associated with decreased cellular proliferation, and that JAK1/2 inhibition with ruxolitinib is superior at inhibiting invasive potential when compared to more selective JAK inhibitors. However, we acknowledge that diverse selectivity of these compounds (ie. SRC, ABL and c-MET targeting) may also contribute to the demonstrated activity.

From identifying different cellular populations in KPC organoids we were then able to examine the mechanisms associated with dasatinib and ruxolitinib treatment. We have shown that this therapeutic strategy downregulates downstream pro-tumourigenic, pro-survival targets such as *Lcn2*. Lipocalin-2 (*Lcn2*) is a STAT3-target gene specifically downregulated in cancer clusters 0, 1 and 3, which share a number of genes with the previously characterised, poor prognosis QM-PDA subtype [7]. *Lcn2* has previously been shown to enhance metastasis via MMP-9 regulation [722], promote cell survival [723], increase migration and invasion of gastric and oesophageal cancers [724], as well as prevent apoptosis [725]. Moreover, in PDAC Lipocalin-2 is overexpressed and associated with key characteristics of the aggressive QM-

PDA subtype, including increased proliferation and invasion. Lipocalin-2 is also associated with gemcitabine resistance [679], and is a critical regulator of energy metabolism and glucose homeostasis [726], key ontologies identified in our analyses. Importantly, constitutively active STAT3 is a master regulator of cellular metabolism and can induce aerobic glycolysis and downregulate mitochondrial activity, protecting cancer cells from apoptosis and making them highly sensitive to glucose deprivation [727, 728]. In line with this, we have demonstrated an effect of dasatinib and ruxolitinib on key metabolic gene signatures in QM-PDA-like cancer clusters, including upregulation of *Dusp1*, known to increase cancer cell susceptibility to oxidative damage leading to cell death [715]. Moreover, we observed elevated expression of genes associated with glutathione metabolism (*Gsta1*, *Gstm1*, *Gsta4*; clusters 0, 1 and 3), a metabolic process involved in the detoxification of carcinogens as well as the modulation of the immune response via cytotoxic T-cell activation [716, 717].

The SRC/JAK/STAT3 pathway is also known to control cancer pathogenesis by regulating cell cycle progression and proliferation [664], as well as prevent apoptosis [680], and we have demonstrated that dasatinib and ruxolitinib downregulate these pathways in QM-PDA-like cancer clusters. More specifically, we identified inhibition of cell cycle regulators including cyclins and cyclin-dependent kinases (Cdk4, Cdk6, Cks1b; cluster 0 and 3) [705], as well as negative regulators of apoptosis, osteopontin (cluster 3) [682], and clusterin (clusters 0 and 1) [681]. In line with this, we have demonstrated that in QM-PDA-like cancer cells (clusters 0 and 1), dasatinib and ruxolitinib effectively downregulated expression of genes associated with protein synthesis, including eukaryotic initiating factors (eIF) and ribosomal proteins (Rps). Protein initiation factors such as eIF4E control ribosome recruitment at the mRNA 5' end, and inhibition via STAT3 can decrease eIF4E binding to 7-methyl-guanosine-triphosphate, therefore preventing ribosome binding and mRNA translation, an essential process required for the survival and growth of cancer cells [729]. JAK inhibition has previously been shown to inhibit protein synthesis of Gp130 specifically, therefore desensitizing cellular response to the cytokine IL-6 by reducing the amount of signal transducing receptor for IL-

6, and in turn deactivating downstream STAT3 signalling [730]. Further, JAK inhibition can induce phosphorylation of eIF-2 α by promoting ER stress, thereby preventing eIF-2 α from initiating protein translation [730]. Taken together, these findings demonstrate the ability of this therapeutic strategy to target tumour cells characterised as QM-PDA, and reveal the potential to improve prognosis and survival rates for patients diagnosed with this PDAC subtype.

The previously characterised “classical” gemcitabine-resistant PDAC subtype [7] is also represented in our KPC organoids, with a number of genes being shared with cancer cluster 4. In this cluster we observed elevated expression of key genes involved in antigen processing and presentation (Table 4.2.3 and Figure 4.2.28; *β 2-m*, *H2-D1*, *Tapbp*, *H2-T23*), post-treatment with dasatinib and ruxolitinib. Upregulation of these MHC-I class molecules in tumour cells has been previously shown to promote recruitment of CD8+ (cytotoxic) T cells to the microenvironment [731], and along with other components involved in immunosurveillance (*Ifngr2*), may potentially help stimulate anti-tumour immunity.

Recent evidence also suggests that cancer-associated fibroblasts (CAFs) are a heterogeneous population, and can be separated into many subtypes. The inflammatory CAFs (iCAFs) and the myfibroblasts (myCAFs) are two reversible, and mutually exclusive subtypes [141]. The iCAF population express inflammatory markers including IL-6, and their formation is dependent on IL-1 secretion which induces LIF expression and JAK/STAT activation [141, 147]. In contrast, myCAFs are a population that express myfibroblast markers such as α -smooth muscle actin, and fibroblast activation protein (FAP), and are associated with extensive extracellular matrix deposition [141, 147]. TGF- β antagonizes IL-1 activity and JAK/STAT signalling to promote differentiation of iCAFs into myCAFs [141, 147]. Antigen-presenting CAFs (apCAFs), are another recent population defined by their expression of MHCII molecules, and their ability to present a model antigen to CD4+ T cells [145]. ApCAFs lack the costimulatory molecules to induce T-cell proliferation, so it is hypothesised that MHCII acts as a decoy receptor and deactivates CD4+ T cells by potentially inducing regulatory T cell differentiation, thereby

restraining antitumour immunity. From our single cell transcriptomic analyses of KPC organoids we have identified two of these CAF subtypes the iCAFs (cluster 5) and myCAFs (cluster 2) based on their expression of key marker genes defined by Elyada and Tuveson *et al.* [145], however we were unable to isolate apCAFs potentially due to the environmental conditions in which the organoids were cultured. Our assessment of the differentially expressed genes in CAF populations following dasatinib and ruxolitinib treatment revealed significant downregulation of characteristic myCAF genes, including extracellular matrix-associated genes including collagens (*Col1a2* and *Col3a1*) and matrix metalloproteinases (*Mmp3*, *Timp1*) that help create the desmoplastic microenvironment that promotes the survival and proliferation of pancreatic cancer cells [732, 733]. Moreover, we have shown specific modulation of typical iCAF genes, including chemokines (*Ccl2*, *Ccl3*, *Ccl4*), associated with the infiltration and activation of immune cells responsible for promoting the immunosuppressive tumour microenvironment that defines PDAC [145, 734]. Moreover, the considerable upregulation (~12.5 fold) of *Apoe* mRNA levels observed in the iCAF population (stromal cluster 5), has previously been associated with induction of apoptosis and increased caspase-3 activity in fibroblasts [735], further accompanied by increased levels of pro-apoptotic *Itm2b* [736], senescence-inducing *Ypel3* [737] and acute stress response gene *Saa3*.

The SRC/JAK/STAT3 pathway drives complex intercellular signalling cascades that occur between different cellular populations within tumours and alter their behaviour. These signalling cascades lead to the proliferation and survival of tumour cells, the activation of stromal cells, as well as the recruitment, expansion and activation of various immune cells [153, 416]. IL-6 (through its receptor Gp130), can directly and indirectly (via soluble IL-6R) [411, 430, 431] act on tumour cells by inducing expression of STAT3 and its target genes including those involved in tumour proliferation and survival [411, 627], as well as neovascularisation and angiogenesis [738]. We have demonstrated that dasatinib and ruxolitinib treatment can reduce the production of IL-6, Gp130 and sIL-6R, as well as several other pro-proliferative and pro-survival factors, including IL-9 [739] IL-13 [740], CCL21

[741], CCL24 [742], CXCL13 [743] and Pentraxin 3 [744]. Moreover, we have identified a reduction in CCL25 production following dasatinib and ruxolitinib, which is supported by prior studies in metastatic melanoma [745], and breast cancer [746], where reduced CCL25 production was observed following downregulation of the integrin signalling pathway. Furthermore we see decreased production of CXCL12, a multifaceted chemokine that not only acts on cancer cells to promote tumour growth but also acts on endothelial cells to promote angiogenesis [747].

Angiogenesis is an important event in pancreatic tumour growth and metastasis and is highlighted by poor vasculature and dense stroma. Vascular endothelial growth factor (VEGF) and matrix metalloproteinases (MMPs) are key regulators that stimulate blood vessel growth, extracellular matrix degradation, and endothelial cell migration resulting in angiogenesis [628]. Tumour cells secrete pro-angiogenic factors including MMP-2, TWEAK, FGF, IL-3, IL-6 and IL-17 [628-631], that act by potentiating VEGF expression and activity, resulting in increased blood vessel formation that leads to metastasis and a poorer prognosis in PDAC patients [632, 647, 748-750]. Several other chemokines have also been shown to promote angiogenesis including CCL23 (via enhanced expression of MMP-2) [647], CXCL12 [751], CCL24 [752], CXCL5 [753], CCL21 [754]. Importantly the upregulation of VEGF via these various pro-angiogenic factors is largely STAT3-mediated, and it has been previously demonstrated that targeting STAT3 in models of gastric cancer may inhibit angiogenesis [631]. Consistent with this, we have demonstrated that combined dasatinib and ruxolitinib treatment is effective at decreasing production of these pro-angiogenic factors. Moreover, interferon- α and IL-10 have anti-angiogenic activity due to their ability to inhibit VEGF and MMP2, respectively. We have also shown that dasatinib and ruxolitinib increased production of IL-10 in the KPC organoid model, while IL-10 remained unchanged in the TKCC-10 organoid model. In addition, the interferons remained unchanged in both organoid models following treatment, suggesting that combined dasatinib and ruxolitinib treatment restores the balance between pro- and anti-angiogenic signals, and has the potential to restrain the

formation of aberrant blood vessels, tumour cell circulation, neovascularisation and metastasis [628].

As mentioned previously, transformation of the pancreatic tumour microenvironment is largely a result of activation of pancreatic stellate cells (PSCs) into cancer associated fibroblasts (CAFs), which then perpetuate their activation state via autocrine signalling networks that involve IL-1, IL-6, and FGF, following which they acquire proliferative capabilities and upregulate the production of matrix metalloproteinases (MMPs), as well as extracellular matrix proteins [160]. This leads to increased basement membrane degradation and cancer cell migration as well as extensive extracellular matrix production and remodelling [755]. Our results demonstrate that combined dasatinib and ruxolitinib treatment can effectively reduce the signalling associated with PSC activation, as well as the resultant autocrine signalling that promotes extracellular matrix production and remodelling (via decreased production of IL-1, IL-6, TNF- α and FGF). Moreover we have shown that this treatment combination can decrease production of factors associated with basement membrane degradation and the subsequent promotion of cancer cell invasion and metastasis including MMP-1, MMP-2 and MMP-3 [756] and chemokines including CXCL13 [757], CCL25 [745], CXCL5 [758], CCL20 [759] and CCL7 [760].

Macrophages are the dominant leukocyte population in human PDAC and autochthonous models [761], and they infiltrate both pre-invasive pancreatic tumour lesions and invasive pancreatic cancer [160]. Tumour-associated macrophages (TAMs) promote tumour growth not only via inhibition of immunity but also via induction of angiogenesis, remodelling of the extracellular matrix and stimulation of cancer cell proliferation [762]. Moreover, the increased presence of TAMs is a hallmark of developing chemoresistance and correlates with poor clinical outcomes [763, 764]. Treatment of KPC co-culture organoids with the combination of dasatinib and ruxolitinib downregulated several pro-inflammatory chemokines involved in macrophage recruitment and polarisation including CCL2, CCL3, CCL4 and CCL5. The relationship between these chemokines is complex, and involves a mechanism called 'chemokine-induced chemokine secretion', where CCL5

increases the secretion of CCL2, resulting in the recruitment of TAMs to the tumour, as well as CD11b+Gr1+ monocytes (myeloid derived suppressor cells), where they then differentiate into tumour-associated macrophages (TAMs) [621]. Moreover, CCL3 signalling enhances and stabilises the interaction between cancer cells and TAMs, partly through integrin binding to VCAM1 which is expressed on the tumour cell surface [765], resulting in the retention of TAMs that further promote the metastatic spread of cancer cells through conferring survival signals [621]. Consistent with our observations, CCL2 inhibition has previously been shown to reduce the accumulation of TAMs in breast cancer [621]. Furthermore, we also observed a significant decrease in the production of M-CSF, a key factor involved in the recruitment, extravasation, proliferation and maturation of Ly6C-high monocytes [622]. M-CSF signalling is critical for TAM differentiation into M1/M2 phenotypes. M2-polarised TAMs drive multiple pro-tumourigenic processes including immunosuppression, angiogenesis, metastasis, survival and cancer cell stemness [763, 764, 766]. In addition, PDAC cancer-associated fibroblasts (CAFs) have been shown to overproduce M-CSF, and induce M2 polarisation via increased reactive oxygen species production in monocytes [767]. Consistent with our findings, it has been previously shown using the KPC mouse model, that inhibition of M-CSF drives a shift in phenotype from a pro-tumoural M2-like TAM phenotype, to an anti-tumoural M1-like TAM phenotype [622], and is associated with smaller tumours and improved survival [768].

Furthermore, the effect of dasatinib and ruxolitinib on macrophage recruitment and differentiation is reinforced through the reduced secretion of GM-CSF in our TKCC-10 organoid model. GM-CSF is a growth and differentiation factor for granulocyte and macrophage populations [640], and can enhance the synthesis of IL8, a chemoattractant for neutrophils as well as CCL3, to further enhance the recruitment of TAMs and MDSCs [621]. Moreover, GM-CSF can mediate mesenchymal-epithelial cross talk of PDAC cells, as well as enhance their growth, invasion and metastatic potential [769]. While a review of the literature reveals that GM-CSF can also act as an anti-inflammatory cytokine, the function of GM-CSF is dependent on the dose and presence of other relevant cytokines in the context of an immune response. Consistent with the

pro-inflammatory role of GM-CSF, secretion by tumour cells can lead to the development of an inhibitory population of CD11b+Gr1+ myeloid-derived suppressor cells, resulting in functional impairment of CD8+ T-cells [770], and suppression of T-cell functions through expression of arginase in a suppressor myeloid subpopulation [771]. Furthermore, following treatment we observe a significant reduction in CD163 and Chi2L1, markers of pro-tumoural M2-macrophage activation [772-774]. As well as IL-34, a pro-survival cytokine that enhances the immunosuppressive function of TAMs through a C/EBP-beta-mediated mechanism [775]. Moreover, both IL-34 and IL-35 are overexpressed in PDAC [768, 776], however IL-35 facilitates the recruitment of TAMs by promoting ICAM1 overexpression [776]. Additional factors involved in macrophage recruitment and polarisation include TSLP [777], CXCL16 [778, 779], IL-13 [740], and MIF [780], all of which were modulated following dasatinib and ruxolitinib treatment.

Myeloid-derived suppressor cells (MDSCs) are immature myeloid cells that play an immunosuppressive role in pancreatic cancer. As mentioned previously, the proliferation and migration of MDSCs into the tumour microenvironment is induced by granulocyte macrophage colony-stimulating factor (GM-CSF) [160], and we have demonstrated modulation of GM-CSF following dasatinib and ruxolitinib treatment. MDSCs are also capable of suppressing the antitumour activity of CD8+ T cells, can promote the expansion of immunosuppressive regulatory T cells, and can promote M2 macrophage polarisation [781]. Moreover, we have demonstrated decreased production of CXCL2, an MDSC (CD11b+GR1+) chemoattractant, following dasatinib and ruxolitinib treatment. Interestingly, CXCL2 has previously been shown to play a role in chemoresistance in multiple tumour types including breast and lung, via a mechanism involving amplified MDSC cytokine production including S100A8/9 [637]. These findings reveal the potential of dasatinib and ruxolitinib to not only decrease MDSC infiltration, but may also improve chemotherapeutic efficacy and prevent metastasis by blocking multiple stages of the MDSC molecular cycle.

Regulatory T cells suppress the adaptive immune response and are associated with tumour progression and a poor prognosis for PDAC patients

[157, 158]. CCL5, previously discussed for its role in macrophage recruitment, is an important chemokine that encourages the migration of regulatory T cells (CD4⁺CD25⁺FoxP3⁺, or T-regs) into the tumour microenvironment (due to their expression of CCR5) [159]. We have demonstrated a significant decrease in CCL5 production following dasatinib and ruxolitinib treatment. Consistent with this result, neutralisation of CCL5 has previously been shown to inhibit T-regulatory cell recruitment and inhibit the growth of PDAC [782]. Moreover, we observed decreased secretion of CCL1 and CCL17, both of which play a major role in the recruitment of T-regulatory cells via the CCR8, and CCR4 receptors respectively [641, 642]. Further, CCL17 production is induced by IL-4 signalling [643], and we observed decreased IL-4 production following dasatinib and ruxolitinib treatment. Importantly, IL-4 neutralisation has previously been shown to enhance anti-tumour immunity and delay tumour progression by reducing the generation of immunosuppressive M2 macrophages, myeloid-derived suppressor cells, regulatory T cells, and enhance tumour-specific cytotoxic T cells [783]. We also observed a decrease in IL-2 production, the function of which is dependent on the immunological context. Increasing evidence suggests that IL-2 maintains a balance between promoting proliferation and differentiation of effector T cells, and mediating the survival of T-regs [644], therefore supporting the role of this treatment combination in improving the immunosuppressive tumour microenvironment.

T helper 17 (Th17) cells are another immune cell population with a pro-tumourigenic role. Th17 cells express IL-17, and are dependent on IL-6, IL-21, IL-23 and TGF- β for their differentiation [623]. Moreover, the pro-tumourigenic activity of Th17 cells is largely due to induction of IL-6, leading to the promotion of cancer cell proliferation and survival as well as angiogenesis, and macrophage recruitment [623]. In addition, IL-1, STAT3 and TNF- α are important for inducing Th17 cell generation and expansion [623], while CCL2 and CCL5 are strong Th17 chemoattractants that are essential for Th17 cell migration [623]. We have demonstrated that combined dasatinib and ruxolitinib treatment is capable of reducing the production of Th17-associated cytokines in both the mouse organoid model (CCL2, CCL5, IL-6, IL-1 β and

TNF-alpha), and human TKCC10 organoid model (CCL2, CCL20, IL-6, IL-1 β , and TNF-alpha).

Effector or Cytotoxic CD8⁺ T cells are the predominant T-cell subset and are associated with favourable clinical outcomes and prolonged survival in pancreatic cancer [156]. CD8⁺ T cells eliminate tumour cells via IFN- γ -mediated direct tumouricidal activity, and via induction of macrophage tumouricidal activity [156]. Factors involved in CD8⁺ T cell recruitment include IL-12, IL-18, IL-28A, IL-29, interferons, all of which remained unchanged following dasatinib and ruxolitinib treatment. Moreover, IL-10 is an anti-inflammatory cytokine that inhibits IL-6 and IL-12/IL-23, and stimulates cytotoxicity of CD8⁺ T cells and expression of interferon-gamma in CD8⁺ T cells [784]. As mentioned previously IL10 production remained unchanged in the TKCC-10 organoid model, and was increased in the mouse organoid model. Further, we demonstrated a decrease in the production of IL-17A, a pro-tumourigenic cytokine that blocks the entry of cytotoxic CD8⁺ T cells whilst increasing MDSC recruitment [785]. Taken together, these results suggest that dasatinib and ruxolitinib decrease T regulatory cell recruitment, and prevents blocking of cytotoxic/effector T cell infiltration.

In summary, these data have established that there is potent efficacy of combined dasatinib and ruxolitinib in 3D models of pancreatic cancer that are defined by p53 mutations and high phospho-STAT3 expression, and that this efficacy occurs via a complex mechanism involving deregulation of tumour cell and stromal cell signalling, as well as the disruption of the surrounding extracellular matrix, and inhibitory effects on pro-tumourigenic, immunosuppressive mediators released from these cells. Given the promising preliminary data of the dasatinib and ruxolitinib combination in select 2D and 3D *in vitro* models of PDAC, the remaining chapter of this thesis aimed to assess the efficacy of this therapeutic combination in well-established, realistic immunocompetent and immunocompromised *in vivo* models of pancreatic cancer.

Chapter 5. *In vivo* efficacy of dasatinib and ruxolitinib in models of pancreatic cancer

5.1 Introduction

Assessment of the combined inhibition of dasatinib and ruxolitinib in *in vitro* three-dimensional models has demonstrated that this therapeutic strategy inhibits the invasive and proliferative capacity of tumour cells, disrupts collagen remodelling and extracellular matrix integrity, interferes with paracrine signalling and may have strong immunomodulatory effects (Chapter 4). Based on these promising findings, and given known limitations associated with two-dimensional and three-dimensional *in vitro* models [83, 149, 612], we next utilised a range of *in vivo* orthotopic xenograft models to examine the effects of dasatinib and ruxolitinib in the context of a more complex tumour microenvironment.

Considering the significant inhibitory effects of dasatinib and ruxolitinib treatment on pancreatic cancer cell lines characterised by high phospho-STAT3 expression and *TP53* mutations, it is reasonable to hypothesise that this therapeutic combination should have significant *in vivo* anti-tumour activity, in tumours stratified using these markers. SRC and JAK inhibitor monotherapies have previously been shown to control disease progression and improve survival in *in vivo* pancreatic cancer models [177, 533, 534], however the combination of SRC and JAK inhibitors is novel in this disease setting. Accordingly, we selected three ‘on-phenotype’ patient-derived models with high phospho-STAT3 expression and *TP53* mutations to assess the therapeutic efficacy of the SRC inhibitor dasatinib and the JAK1/2 inhibitor ruxolitinib in combination. Previous evidence suggests that SRC [199, 279, 285] and JAK inhibitors [443, 553, 554], have the potential to improve response to chemotherapies such as gemcitabine. Therefore, we also examined whether dual-targeting of tumour cell-stromal cell cross-talk by dasatinib and ruxolitinib could further improve response to standard of care chemotherapy (gemcitabine and Abraxane) for metastatic disease [9].

First, syngeneic KPC xenografts were orthotopically implanted in immunocompetent C57BL6 mice in order to assess the effect of combined

dasatinib and ruxolitinib on tumour growth and metastatic spread, in the context of an intact tumour microenvironment. Since the cellular elements of the pancreatic tumour microenvironment are diverse and comprise a heterogeneous population of cancer, stromal and immune cells [114, 141], we examined the tumours post-treatment for cancer-cell and stromal-cell autonomous effects using immunohistochemistry (IHC) and immunofluorescent antibody staining.

Given the known role of the SRC/JAK/STAT3 pathway in promoting matricellular fibrosis and increasing tissue tension in PDAC [122, 321, 443], and based on our observations of JAK inhibitor-mediated effects on extracellular matrix remodelling (Chapter 4), we also evaluated the impact of dasatinib and ruxolitinib on the tumour extracellular matrix *in vivo*. Furthermore, the desmoplastic stroma that envelops pancreatic cancer cells in growing tumours, not only presents a physical barrier that reduces therapeutic efficacy, but also presents an environment that actively produces pro-tumourigenic, immunosuppressive signals that further drive pancreatic tumourigenesis [10, 11]. Building on the established potent immunomodulatory functions of SRC and JAK/STAT3 pathway inhibition in diverse cancers including pancreas [301, 321], and our observed immunomodulatory effects (Chapter 4), we next assessed the effects of therapeutic strategies involving dasatinib and ruxolitinib treatment on the immunosuppressive pancreatic tumour microenvironment using the syngeneic KPC (Pdx1-Cre, LSL-KRasG12D/+, LSL-TrP53R172H/+) mouse model.

Finally, we also examined the effects of dasatinib and ruxolitinib on tumour growth and metastasis using two 'on-phenotype' (P53 mutant, phospho-STAT3 high), immunocompromised, orthotopic patient-derived models.

This chapter aims to:

- Assess the therapeutic efficacy of dasatinib and ruxolitinib treatment in both immunocompetent and immunocompromised mouse models of pancreatic cancer characterised by high phospho-STAT3 expression and *TP53* mutations.
- Determine if this treatment strategy can sensitize pancreatic tumours to chemotherapy.
- Assess the cancer-cell autonomous effects of dasatinib and ruxolitinib.
- Assess the effects on stromal cell populations.
- Examine the effects of dasatinib and ruxolitinib on extracellular matrix composition and the fibrotic tumour microenvironment.
- Examine the effects of dasatinib and ruxolitinib on the immunosuppressive tumour microenvironment using the syngeneic KPC model.
- Examine the efficacy (overall survival) of this treatment strategy in the syngeneic KPC orthotopic and patient-derived orthotopic TKCC-05 model of pancreatic cancer.

5.2 Results

5.2.1 Expression of phospho-STAT3 (Tyr705) in selected patient-derived xenograft and KPC models of pancreatic cancer

Based on our *in vitro* findings (Chapter 2), which indicate that the synergistic efficacy of dasatinib and ruxolitinib is predominant in P53-mutant pancreatic cancer lines harbouring high phospho-STAT3 (Tyr705) levels, we analysed tumours from The Kinghorn Cancer Centre (TKCC) patient-derived xenograft cohort (n=54) for phospho-STAT3 (Tyr705) expression using IHC (Figure 5.2.1 A+B). This cohort of PDXs have previously been whole genome sequenced as part of the ICGC [3], and have a P53 mutation rate of 67%. In contrast with the *in vitro* data (Figure 3.2.10; Chapter 3), high phospho-STAT3 expression correlated with P53 mutation status, when expression was assessed using H-score (Figure 5.2.1C), and a semi-quantitative scoring system (0= absent nuclear stain, 1= weakly positive nuclear stain, 2= moderate-strongly positive nuclear stain) (Figure 5.2.1D+E). The correlation was maintained even when comparing scores of 0 and 2 (Figure 5.2.1D). Furthermore, this analysis identified a significant proportion of tumours (24%, 13/54) that were of potential interest for targeting with SRC and JAK1/2 inhibitors, due to their characterisation as pSTAT3-high and P53 mutant.

Following this, we next selected three 'on-phenotype' (pSTAT3-high, P53 mutant) orthotopic models of pancreatic cancer which we had previously assessed *in vitro* (KPC, TKCC-05 and TKCC-10) for *in vivo* therapeutic efficacy evaluation (Figure 5.2.2A). Outside the scope of this thesis we have also identified three interesting 'off-phenotype' (P53 wildtype and low pSTAT3-expression) tumour models (Figure 5.2.2B) which will be used for future validation of our personalised medicine approach and potential examination of any 'off-target' effects.

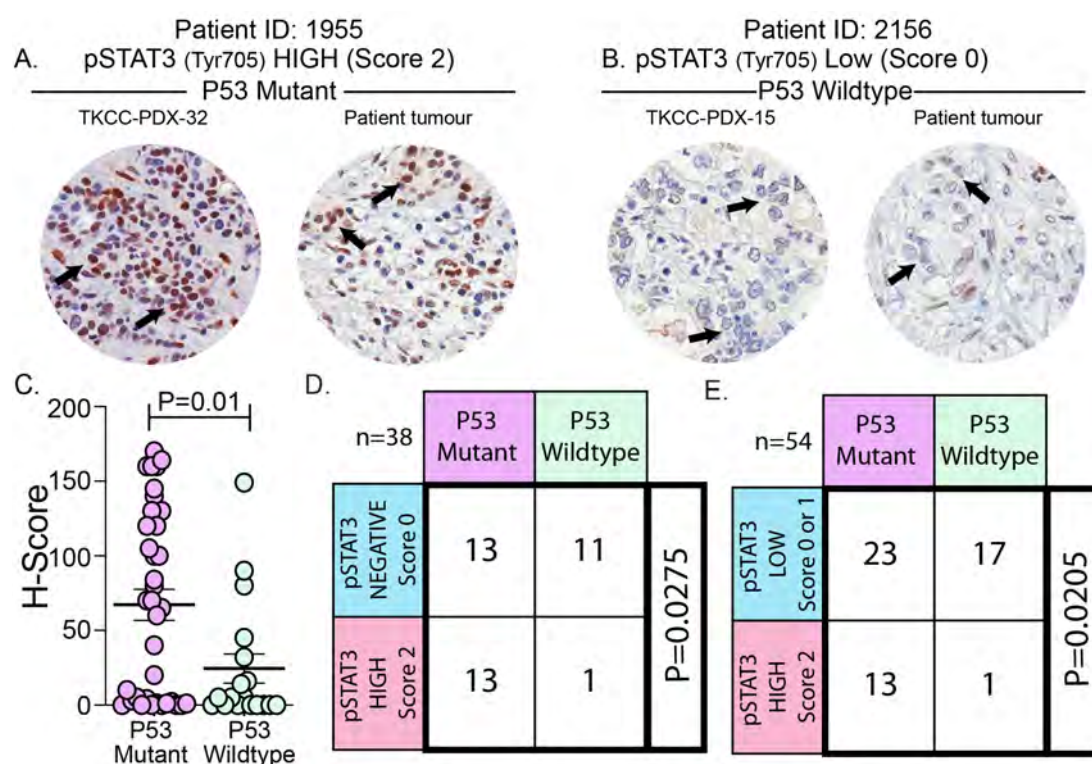


Figure 5.2.1 Expression of phospho-STAT3 (pSTAT3; Tyr705) in The Kinghorn Cancer Centre (TKCC) pancreatic cancer patient-derived xenograft cohort (n=54). (A) Representative PDX and matched patient tumour characterised by high pSTAT3 expression (score 2) (indicated by arrows) and P53 mutation. (B) Representative PDX and matched patient tumour characterised by low pSTAT3 expression (score 0) (indicated by arrows) and P53 wildtype. (C) pSTAT3 IHC H-scores for PDX cohort with known P53 mutation status (n=54). Correlation of P53 mutation status with (D) pSTAT3 expression defined as high (score 2) and negative (score 0), and (E) pSTAT3 expression defined as high (score 2) and low (score 0 or 1). Significance was determined by non-parametric t-test (C) and Fischers exact test (D-E), where *p<0.05, **p<0.01, ***p<0.001 and ****p<0.0001.

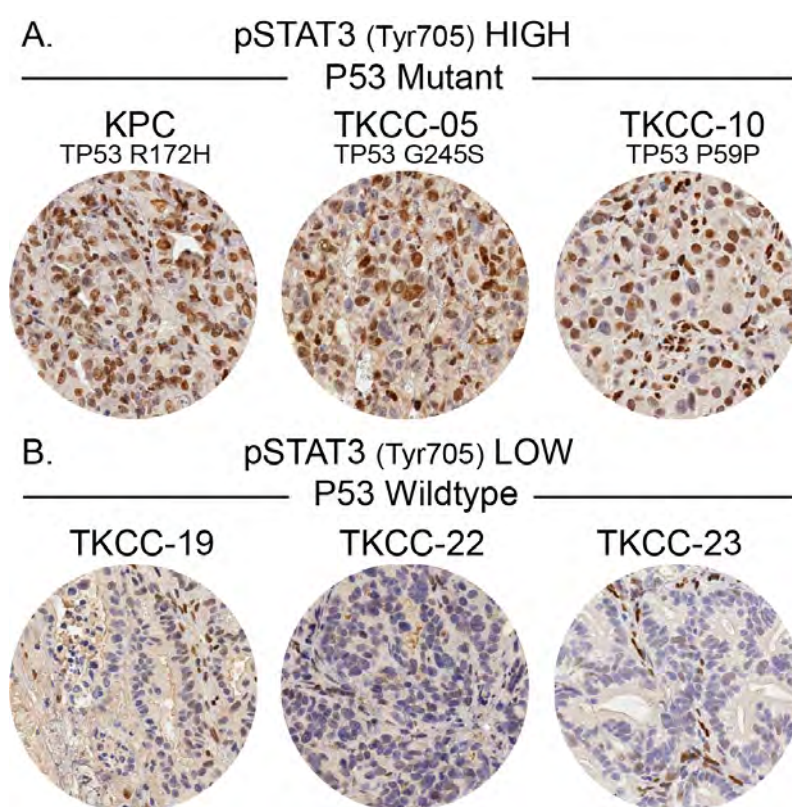


Figure 5.2.2 Expression of phospho-STAT3 (pSTAT3; Tyr705) in selected *in vivo* models of pancreatic cancer. (A) Tumours with high-pSTAT3 and P53 mutations: the genetically engineered KPC model of pancreatic cancer, and two patient-derived xenograft models, TKCC-05 and TKCC-10. (B) Tumours with low-pSTAT3 expression and P53 wildtype: three patient-derived xenograft models TKCC-19, TKCC-22 and TKCC-23.

5.2.2 Efficacy of dual dasatinib and ruxolitinib treatment in the immunocompetent (syngeneic) KPC orthotopic model of pancreatic cancer

5.2.2.1 Effect of dasatinib and ruxolitinib treatment on tumour growth and metastasis

To assess the *in vivo* efficacy of dasatinib and ruxolitinib in the context of an intact tumour microenvironment, syngeneic primary KPC cancer cells were orthotopically injected into the pancreas of immuno-competent C57BL6 mice (Figure 5.2.3A, outlined in methods section 2.17). Tumours were allowed to establish for one week, until they reached a palpable size. Mice were subsequently randomised into treatment groups comprising vehicle control, dasatinib monotherapy, ruxolitinib monotherapy, and dasatinib and ruxolitinib combination therapy. To examine the ability of our dual SRC/JAK targeting approach to improve chemoresponsiveness *in vivo*, additional treatment arms included dasatinib/ruxolitinib plus gemcitabine/Abraxane, compared with gemcitabine/Abraxane alone. Targeted therapies were administered 5 days/week via oral gavage, and chemotherapy was administered twice weekly via intraperitoneal injection, based on published findings (Chapter 2, Table 2.10). Following 30 days of treatment, mice were euthanised and organs were collected for further analysis. Importantly, the treatment regimen combining dasatinib, ruxolitinib and gemcitabine and Abraxane was well tolerated in all studies performed in this thesis.

Examination of *in vivo* efficacy of dasatinib and ruxolitinib as monotherapies showed a non-significant trend towards a decrease in tumour weight when compared to vehicle control (Figure 5.2.3B). In comparison, the combination of dasatinib and ruxolitinib significantly decreased tumour weight compared to vehicle control, and this decrease was similar to that of gemcitabine/Abraxane (Figure 5.2.3B). Moreover, the combination of dasatinib and ruxolitinib with gemcitabine and Abraxane reduced tumour weight significantly compared to gemcitabine and Abraxane alone, with treatment being well tolerated as indicated by no change in mouse weight (Figure 5.2.3C).

To investigate the effects of dasatinib and ruxolitinib on metastatic burden, tissues were collected (liver, spleen, lung, and diaphragm), and metastases were scored in haemotoxylin and eosin-stained sections (Figure 5.2.3D). Examining for the presence or absence of metastases in mice demonstrated that following dasatinib and ruxolitinib combination treatment, 80% of mice presented with metastases compared to 100% in vehicle controls and dasatinib and ruxolitinib monotherapies (Figure 5.2.3D). Moreover, when treated with a combination of dasatinib and ruxolitinib with gemcitabine and Abraxane only 20% of mice presented with metastases, compared with 90% of mice treated with gemcitabine and Abraxane alone (Figure 5.2.3D). In line with this, quantification of metastases in the liver (Figure 5.2.3E), spleen (Figure 5.2.3F), lung (Figure 5.2.3G) and diaphragm (Figure 5.2.3H) revealed a significant reduction in the proportion of mice that presented with metastases following treatment with dasatinib and ruxolitinib, with 80% of mice presenting with liver metastases and 60% of mice presenting with metastases in the spleen, lungs and diaphragm. Furthermore, the combination of dasatinib and ruxolitinib with gemcitabine and Abraxane resulted in even fewer mice presenting with metastases, with only 10% of mice with liver metastases (Figure 5.2.3E), and no mice with spleen, lung and diaphragm metastases (Figure 5.2.3F-H respectively). Taken together, these data demonstrate that combined dasatinib and ruxolitinib treatment can reduce primary tumour size and metastatic burden in the orthotopic KPC model, as well as significantly improve response to chemotherapy, following completion of a full (30-day) treatment cycle.

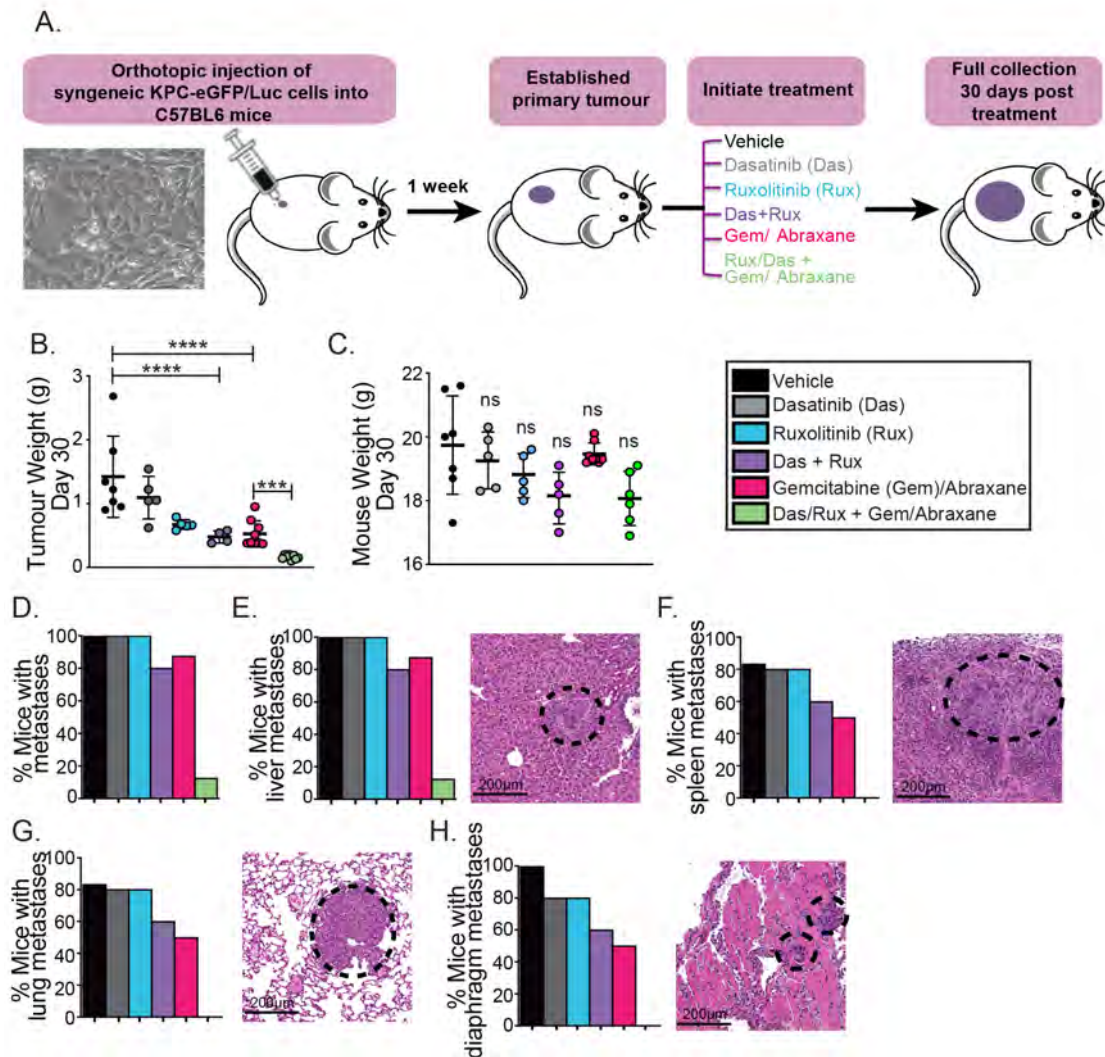


Figure 5.2.3 Effects of dasatinib and ruxolitinib on tumour weight and metastasis in the syngeneic and orthotopic KPC model of pancreatic cancer. (A) Schematic representation of orthotopic injection and treatment timeline. (B) Tumour weight at 30 days post treatment. (C) Mouse weight at 30 days post treatment. (D) Proportion of mice with metastases at 30 days post treatment. Proportion of mice with metastases and representative images of tumours found in the (E) liver, (F) spleen, (G) lung and (H) diaphragm. Data are presented as mean \pm SEM (n= 5-7 mice/ treatment group). Significance was determined using nonparametric ANOVA test with a Tukey multiple comparisons test where * p <0.05, ** p <0.01, *** p <0.001 and **** p <0.0001. Das: dasatinib (10mg/kg daily); rux: ruxolitinib (60mg/kg twice daily); das+rux: dasatinib and ruxolitinib; gem: gemcitabine (60mg/kg twice weekly), Abraxane (30mg/kg twice weekly).

5.2.2.2 Effects of dasatinib and ruxolitinib treatment on cellular proliferation and apoptosis in KPC tumours

To determine if dasatinib and ruxolitinib are effective at modulating their molecular targets *in vivo*, tumour sections were immunohistochemically examined for activation of the STAT3 and SRC networks, using antibodies binding phospho-STAT3 (Tyr705) and phospho-SRC (Tyr416) (Figure 5.2.4). Dasatinib and ruxolitinib monotherapy treatments blocked phosphorylation of specific SRC and STAT3 sites, respectively (Figure 5.2.4). Further, the combination of dasatinib and ruxolitinib resulted in a reduction in both phospho-STAT3 and phospho-SRC levels, which was maintained when these agents were combined with gemcitabine and Abraxane.

Dysregulation of proliferation and apoptosis plays an important role in the pathogenesis of pancreatic cancer, therefore we next wanted to determine if this treatment strategy could inhibit proliferation and induce apoptosis in KPC tumours. To do this, we examined treated tumours for cleaved-caspase-3, and Ki67, using immunohistochemistry (Figure 5.2.5). No change was seen in the proportion of cleaved-caspase-3 positive cells following treatment with dasatinib, ruxolitinib or a combination of dasatinib and ruxolitinib. However the combination of dasatinib and ruxolitinib with gemcitabine and Abraxane significantly potentiated the apoptosis-inducing effects of chemotherapy (Figure 5.2.5C). Moreover, upon treatment with dasatinib, ruxolitinib and the combination of dasatinib and ruxolitinib there was a significant decrease in the proportion of Ki67 positive cells, and this result was maintained when combined with gemcitabine and Abraxane (Figure 5.2.5D).

Together, these analyses demonstrate that dasatinib and ruxolitinib when combined with chemotherapy has superior pro-apoptotic effects when compared to chemotherapy alone. Moreover, this combination has significant anti-proliferative effects, building on our *in vitro* results (Figure 4.2.14 and Figure 4.2.15; Chapter 4).

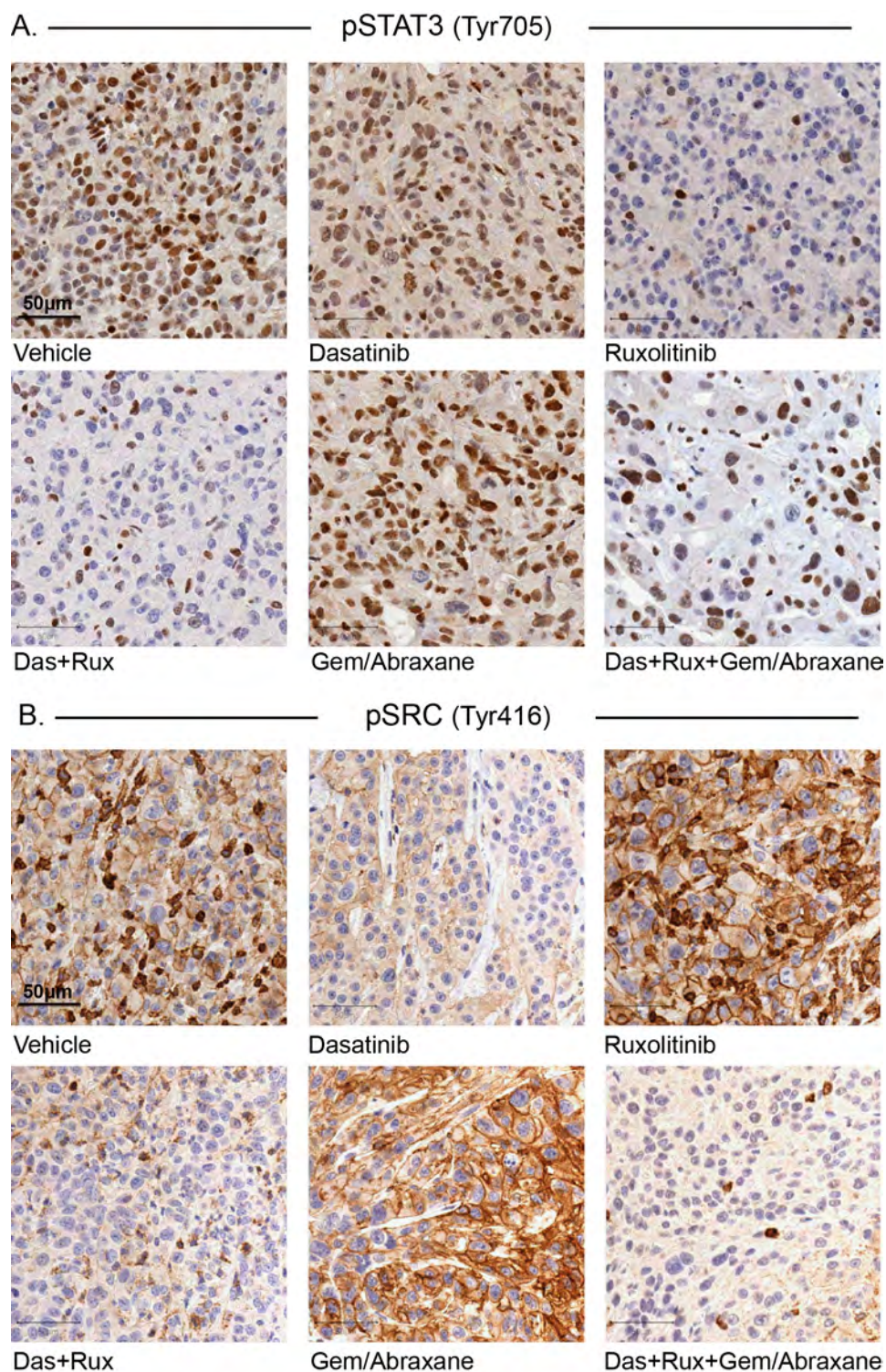


Figure 5.2.4 Effects of dasatinib and ruxolitinib treatment on phospho-STAT3 and phospho-SRC protein levels in KPC tumours. (A) pSTAT3 (Tyr705) and (B) pSRC (Tyr416) IHC staining on KPC tumours 30 days post-treatment. Das: dasatinib; rux: ruxolitinib; das+rux: dasatinib and ruxolitinib; gem: gemcitabine.

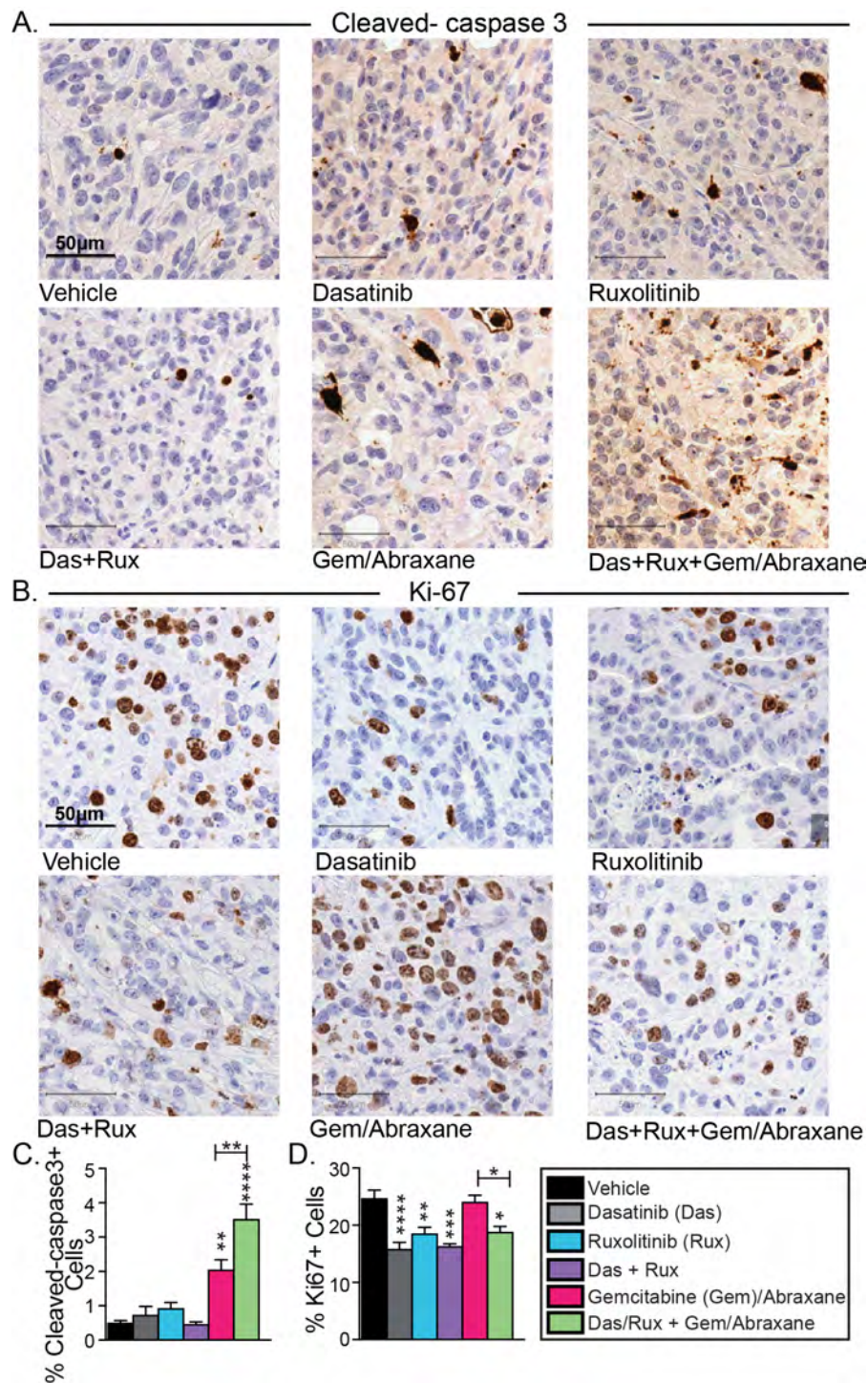


Figure 5.2.5 Effects of dasatinib and ruxolitinib treatment on cancer cell apoptosis and proliferation. Representative images of (A) cleaved-caspase-3 and (B) Ki67 IHC staining and quantification (C-D) of KPC tumours 30 days post-treatment. Data are presented as mean \pm SEM (n= 4 tumours/ treatment, with 6 fields of view (FOV) analysed per tumour per treatment group). Significance was determined using nonparametric ANOVA test with a Tukey

multiple comparisons test where * $p < 0.05$, ** $p < 0.01$, *** $p < 0.001$ and **** $p < 0.0001$.

5.2.2.3 Effect of dasatinib and ruxolitinib treatment on regulating pancreatic stellate cell activation *in vivo*

An abundant stromal reaction is characteristic of pancreatic cancer, and pancreatic cancer-associated fibroblasts are the main cell type responsible for this reaction [786]. To assess the effects of our proposed dual JAK/SRC targeting treatment approach on this cell population, treated tumours were processed using immunohistochemistry for alpha-smooth muscle actin (α -SMA), a prototypical marker of activated cancer-associated fibroblasts [124, 138] (Figure 5.2.6). Of all examined therapies, dasatinib and ruxolitinib in combination led to a 3-fold decrease in α SMA-positivity, and this significant decrease was maintained when dasatinib and ruxolitinib was combined with chemotherapy. This suggests that dual dasatinib and ruxolitinib treatment impedes activation of pancreatic cancer-associated fibroblasts, which drive extensive fibrosis typically observed in PDAC [124, 138]. To examine the effects of treatment on pancreatic stellate cell activity, we next assessed pancreatic stellate cell-secreted proteins within the tumour microenvironment (5.2.2.4).

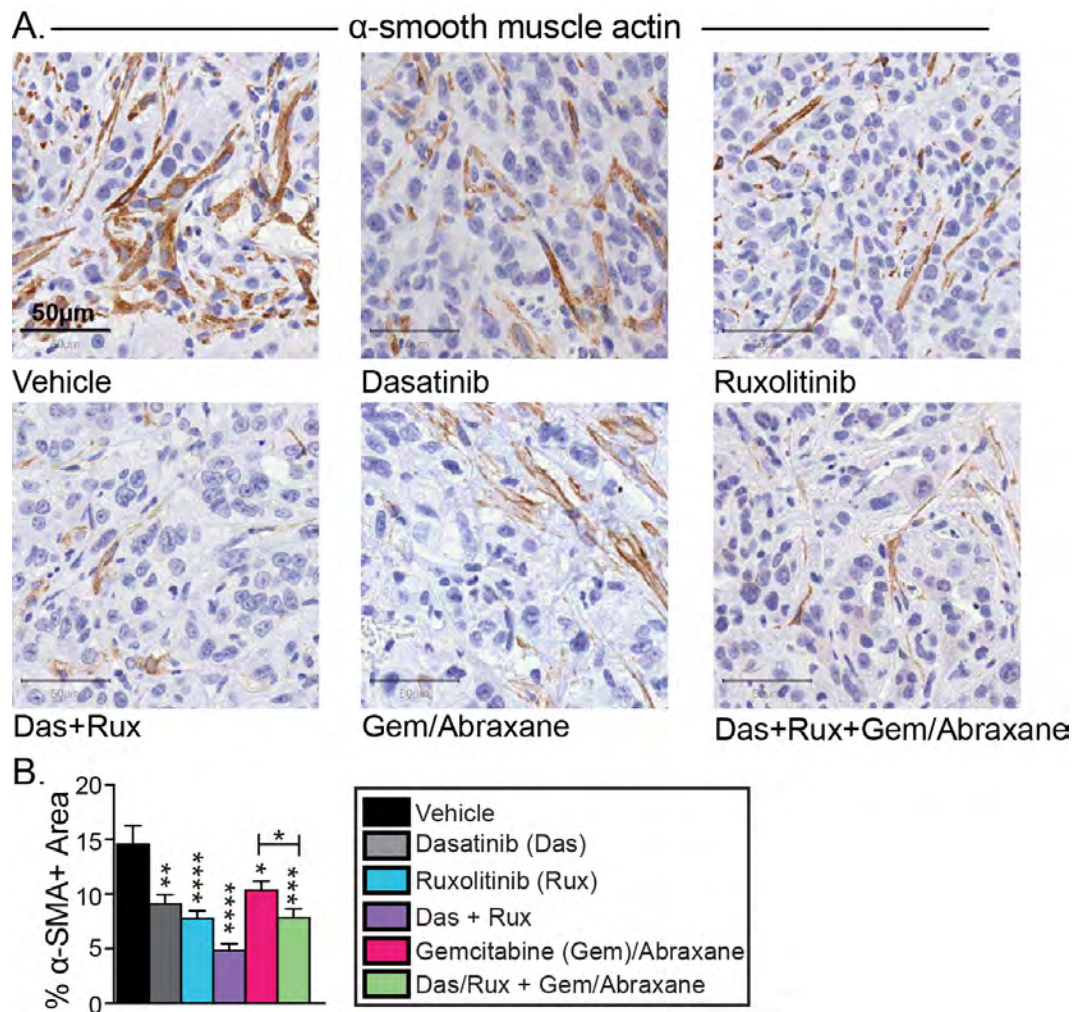


Figure 5.2.6 Effects of dasatinib and ruxolitinib treatment on activated cancer-associated fibroblasts. Representative images (A) and quantification (B) of α -smooth muscle actin IHC staining on KPC tumours 30 days post treatment. Data are presented as mean α SMA-positive staining area \pm SEM (n= 4 tumours per treatment group, with 6 fields of view (FOV) analysed per tumour per treatment group). Significance was determined using nonparametric ANOVA test with a Tukey multiple comparisons test where *p<0.05, **p<0.01, ***p<0.001 and ****p<0.0001. Das: dasatinib; rux: ruxolitinib; das+rux: dasatinib and ruxolitinib; gem: gemcitabine.

5.2.2.4 Effects of dasatinib and ruxolitinib treatment on remodelling the fibrotic tumour microenvironment.

Pancreatic stellate cells secrete a range of extracellular matrix proteins including collagen type I, fibronectin and periostin, and excessive secretion of these proteins leads to the desmoplastic stroma that defines PDAC [787]. We assessed the effects of dasatinib and ruxolitinib on the levels of key extracellular matrix proteins using a variety of methodologies. Second harmonic generation imaging and Picrosirius Red staining was performed on tumour sections following various treatments (Figure 5.2.7) to examine collagen I deposition and extracellular matrix integrity. Following treatment with ruxolitinib collagen content was significantly reduced (Figure 5.2.7 A-F), and similar results were seen when ruxolitinib was combined with dasatinib, and when these targeted agents were combined with chemotherapy. Furthermore, birefringence analysis of collagen organisation within tumours revealed that ruxolitinib-based treatments reduced the proportion of highly-crosslinked collagen fibres defined by high and medium birefringence, and this was associated with an increase in less remodelled collagen fibres defined by low birefringence (Figure 5.2.7G-J).

We next examined effects of treatment on other components of the extracellular matrix including fibronectin and periostin, two key proteins with structural and functional roles in maintaining tissue density and regulating cellular signalling cascades [202]. Immunofluorescence staining revealed that ruxolitinib-based treatments significantly decreased the positive area of both periostin (Figure 5.2.8A+C) and fibronectin (Figure 5.2.8B+D). We also assessed tumours for effects on tumour vasculature, another key component of the fibrotic tumour microenvironment. Using CD31 staining (Figure 5.2.7 B+E), we observed no change in CD31 positive area following treatment with dasatinib and ruxolitinib. Taken together, this data demonstrates that JAK1/2 inhibition leads to decreased deposition of extracellular matrix proteins including fibrillar collagen, periostin and fibronectin, and promotes a significantly disorganised extracellular matrix network in KPC tumours.

Moreover, combining JAK1/2 inhibition with SRC inhibition and chemotherapy produces a similar effect.

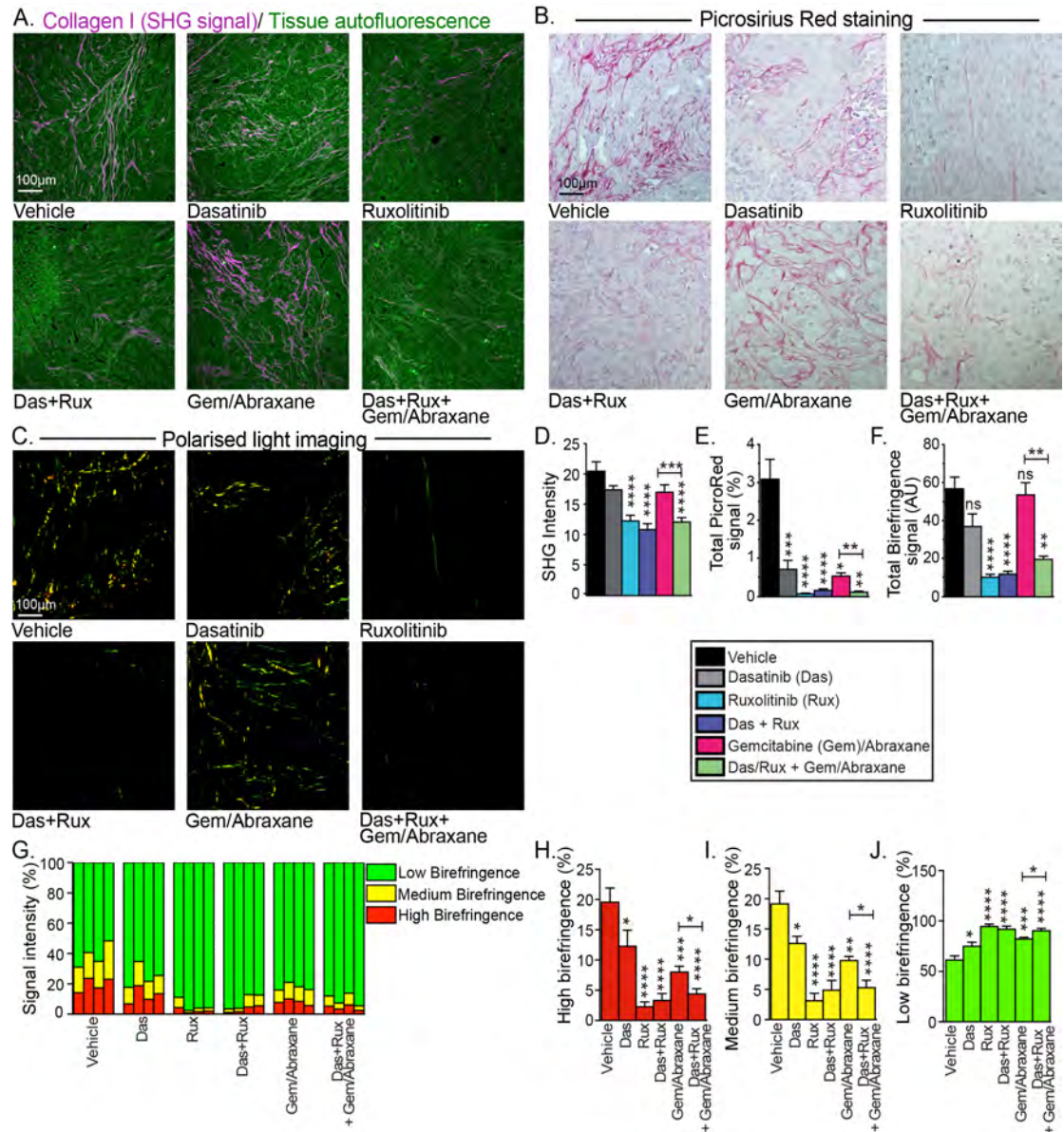


Figure 5.2.7 Effects of dasatinib and ruxolitinib treatment on the extracellular matrix. (A) Second-harmonic generation (SHG) maximum intensity images of KPC tumours 30 days post treatment, with quantification of peak signal intensity in (D). (B) Brightfield and (C) polarised light imaging of Picrosirius Red-stained sections and quantification of total collagen content (E+F). (G-J) Quantification of signal emitted from fibres with high (red), medium (yellow) and low (green) birefringence normalised to total signal acquired via polarised imaging. Data are presented as mean \pm SEM (n= 4 tumours per treatment group, with 6 FOV per tumour). Significance was determined using

nonparametric ANOVA test with a Tukey multiple comparisons test where * $p < 0.05$, ** $p < 0.01$, *** $p < 0.001$ and **** $p < 0.0001$.

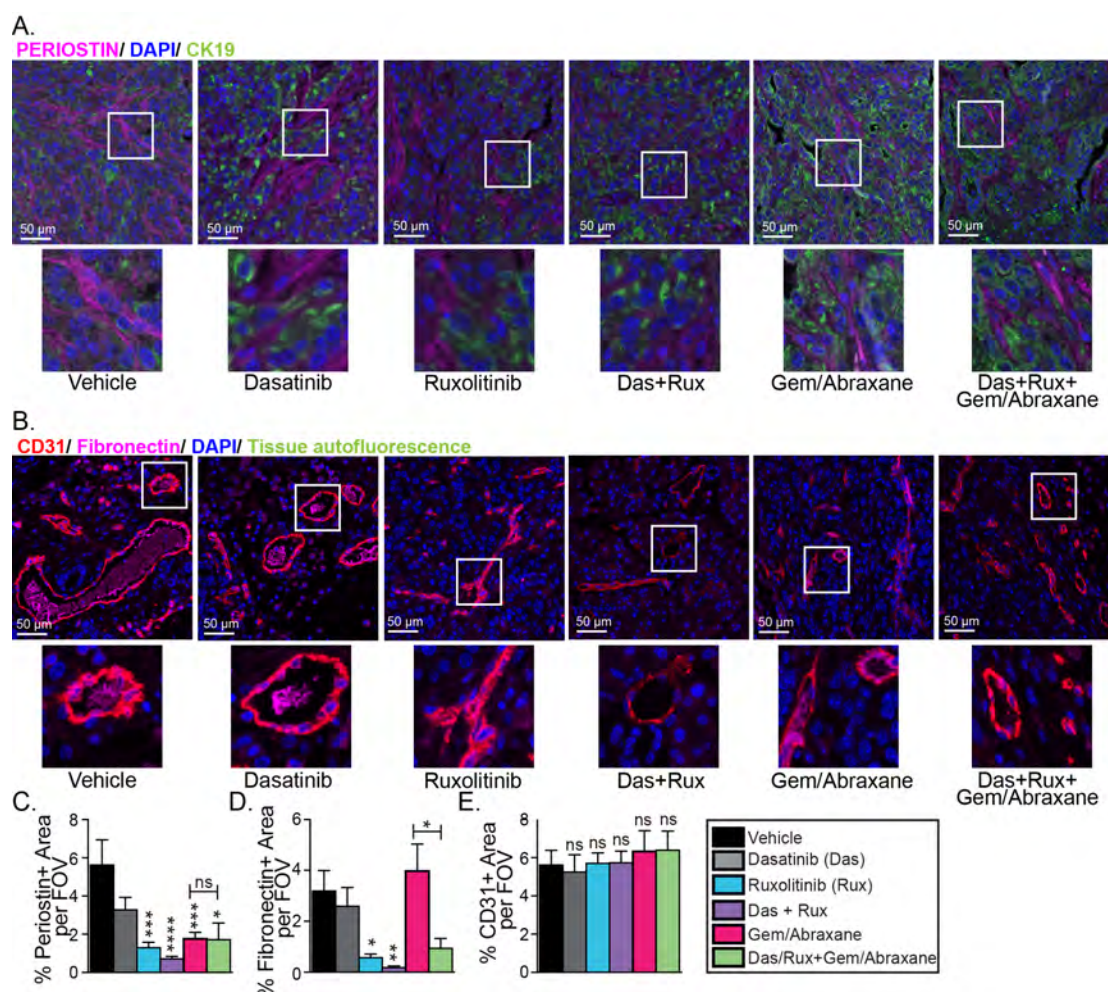


Figure 5.2.8 Effects of dasatinib and ruxolitinib treatment on additional components of the extracellular matrix and tumour vasculature. Representative images of immunofluorescence analysis of (A) Periostin+ (pink) and CK19 (green) (used to visualise cancer cells). (B) CD31+ (red) and fibronectin+ (pink), in KPC tumours 30 days post-treatment. Percentage area positive per field of view (FOV) are quantified in (C-E). Data are presented as mean \pm SEM (n=4 tumours per treatment group, with 6 FOV analysed per tumour per treatment group). Significance was determined using non-parametric ANOVA test with a Tukey multiple comparisons test where * $p < 0.05$, ** $p < 0.01$, *** $p < 0.001$ and **** $p < 0.0001$. Das: dasatinib; rux: ruxolitinib; das+rux: dasatinib and ruxolitinib; gem: gemcitabine.

5.2.2.5 Effects of dual SRC/JAK targeting on altering the immunosuppressive tumour microenvironment

Overactivation of pro-inflammatory signalling networks is largely driven by the SRC/JAK/STAT3 pathway and can influence the development of the immunosuppressive tumour microenvironment that is characteristic of PDAC [188, 416]. To examine whether dasatinib and ruxolitinib treatment alters the immunosuppressive tumour microenvironment, immunohistochemistry and immunofluorescence staining was used to examine infiltrating immune-cell populations within KPC tumours post-therapy (Figure 5.2.9 and Figure 5.2.10).

Following treatment with dasatinib and ruxolitinib there was a significant decrease in the proportion of CD4⁺ T cells (Figure 5.2.9A+D), an increase in CD8⁺ T cells (Figure 5.2.9B+E), and a significant decrease in FoxP3⁺ regulatory T cells (Figure 5.2.9C+F), as well as F4/80⁺ macrophages (Figure 5.2.10A+C). Moreover, the combination of dasatinib and ruxolitinib with gemcitabine and Abraxane also resulted in significant decreases in the proportion of CD4⁺ T cells (Figure 5.2.9A+D), FoxP3⁺ T cells (Figure 5.2.9C+F) and F4/80⁺ macrophages (Figure 5.2.10C), when compared to gemcitabine and Abraxane alone. Interestingly, effects on CD8⁺ T cells appear to be ruxolitinib-mediated, and were unaffected following treatment with the combination of dasatinib, ruxolitinib and chemotherapy. We next assessed the effect of treatment on macrophage polarisation and found that the combination of dasatinib and ruxolitinib significantly decreased the number of pro-tumourigenic M2 macrophages, while numbers of anti-tumourigenic M1 macrophages remained unchanged (Figure 5.2.10A-E). Moreover, when the proportion of M1:M2 macrophages was compared the combination of dasatinib and ruxolitinib showed a significantly higher ratio, and these results were increased further when dasatinib and ruxolitinib were combined with chemotherapy (Figure 5.2.10F).

These findings demonstrate that the combination of dasatinib and ruxolitinib treatment can significantly impair pro-inflammatory immune cell infiltration, while promoting CD8⁺ T cell infiltration, suggesting that this therapeutic

combination may improve the immunosuppressive tumour microenvironment of pancreatic cancer by reducing the presence of populations associated with immune evasion.

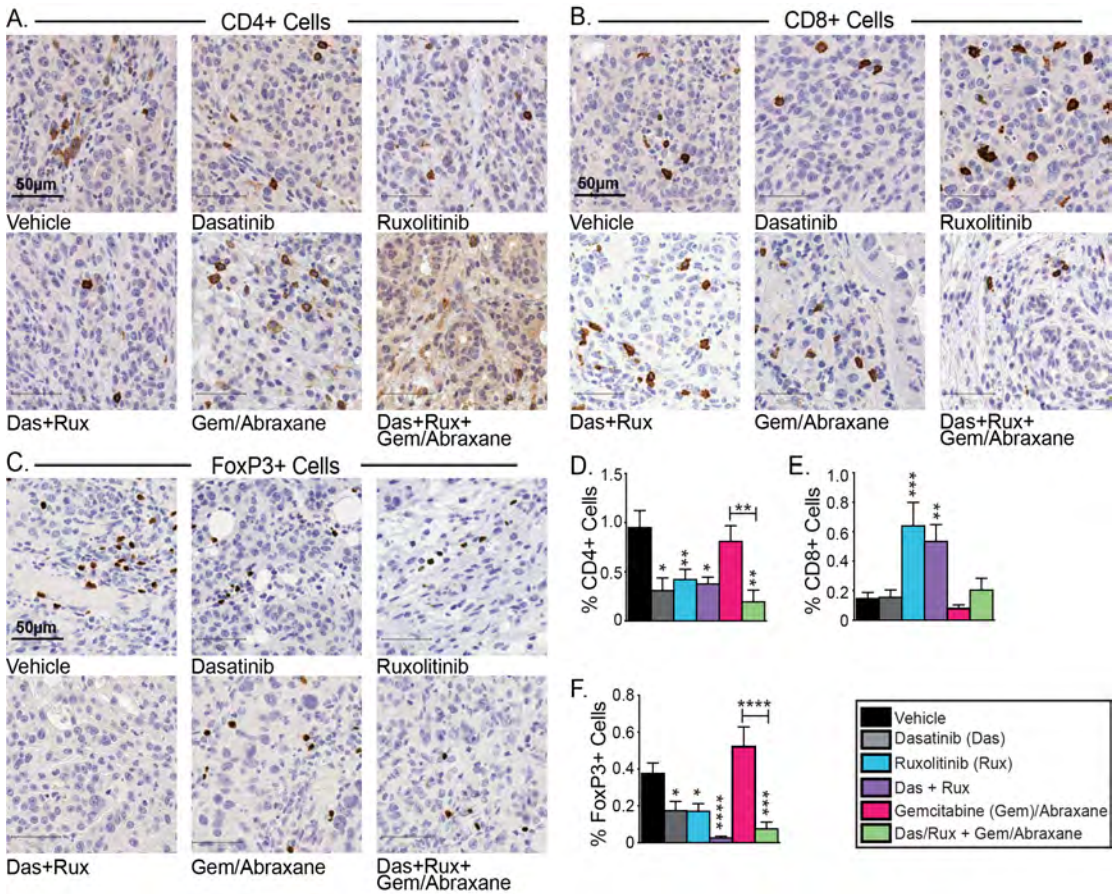


Figure 5.2.9 Effects of dasatinib and ruxolitinib treatment on the immunosuppressive tumour microenvironment. Representative images of (A) CD4+ cells, (B) CD8+ cells (marker for cytotoxic T-cells) and (C) FoxP3+ cells (marker for T-regulatory cells), in KPC tumours 30 days post treatment. Percentage positive cells are quantified in (D-F). Data are presented as mean \pm SEM (n=4 tumours per treatment group, with 6 FOV analysed per tumour per treatment group). Significance was determined using nonparametric ANOVA test with a Tukey multiple comparisons test where *p<0.05, **p<0.01, ***p<0.001 and ****p<0.0001. Das: dasatinib; rux: ruxolitinib; das+rux: dasatinib and ruxolitinib; gem: gemcitabine.

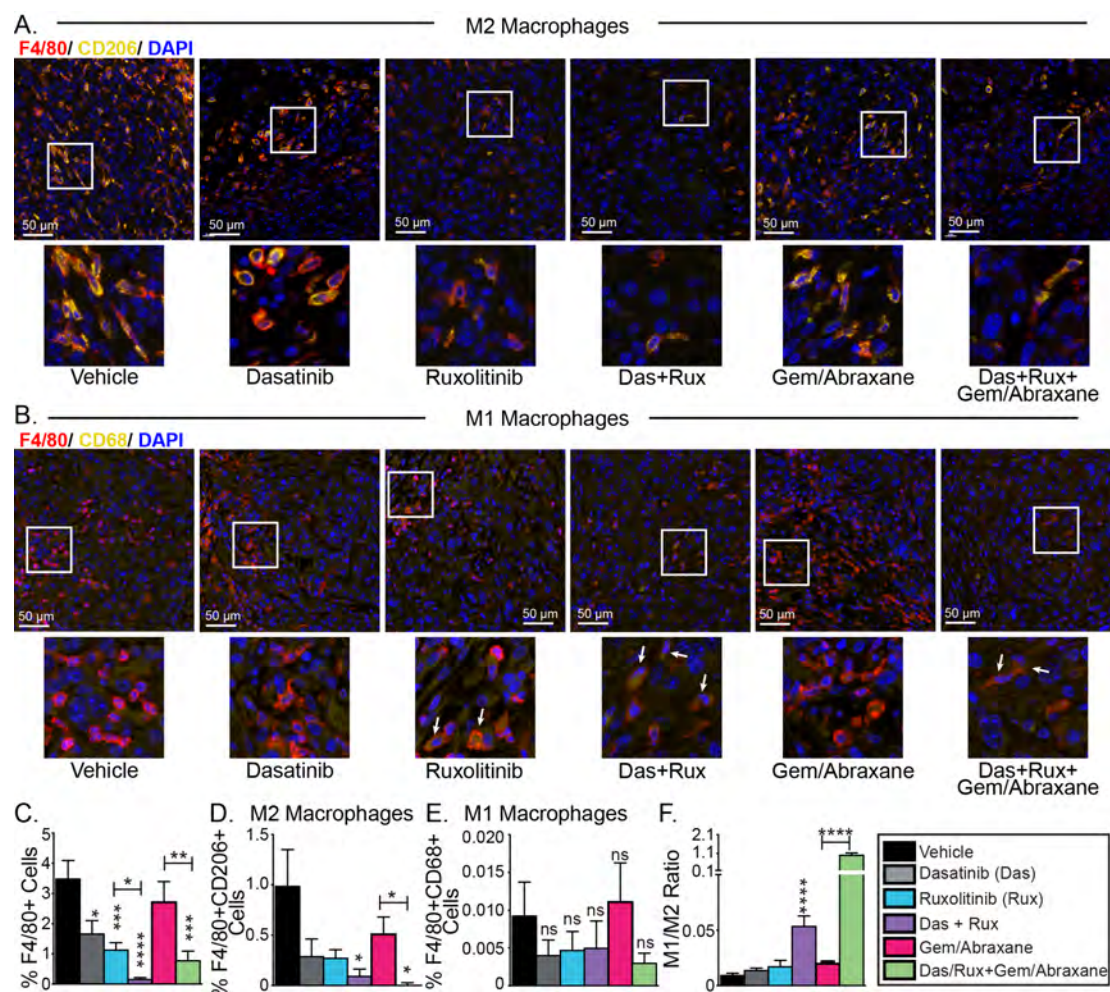


Figure 5.2.10 Effects of dasatinib and ruxolitinib treatment on tumour-associated macrophages. Representative images of immunofluorescence analysis of (A) F4/80+ (red) and CD206+ (yellow) M2-polarised tumour-associated macrophages, and (B) F4/80+ (red) and CD68+ (yellow) M1-polarised tumour-associated macrophages, in KPC tumours 30 days post-treatment. Percentage of positive cells as a total of all cells per field of view (FOV) are quantified in (C-E), and the proportion of M1-macrophages and M2 macrophages following treatment is compared using the ratio M1/M2 (F). Data are presented as mean \pm SEM (n=4 tumours per treatment group, with 6 FOV analysed per tumour per treatment group). Significance was determined using nonparametric ANOVA test with a Tukey multiple comparisons test where *p<0.05, **p<0.01, ***p<0.001 and ****p<0.0001. Das: dasatinib; rux: ruxolitinib; das+rux: dasatinib and ruxolitinib; gem: gemcitabine.

5.2.2.6 Effect of dasatinib and ruxolitinib treatment on prolonging survival in the highly aggressive and metastatic syngeneic KPC model of pancreatic cancer

To examine the effects of dual dasatinib and ruxolitinib treatment on tumour progression and survival in the context of an intact tumour microenvironment the same syngeneic KPC orthotopic mouse model was utilised, as per 5.2.2.1, with the model treated until ethical endpoint (defined in Chapter 2). Kaplan-Meier survival analyses revealed that dasatinib and ruxolitinib therapy significantly prolonged overall survival of treated mice (median survival= 41 days, $p=0.0125$; vs vehicle median survival= 36 days), as well as gemcitabine and Abraxane (median survival = 65 days, $p=0.0011$; Figure 5.2.11B). Of note, the combination of dasatinib, ruxolitinib plus gemcitabine and Abraxane chemotherapy proved to be the best therapeutic approach (median survival= 78.5 days $p<0.0001$; compared with vehicle control median survival of 36 days), and importantly, when compared to gemcitabine and Abraxane alone ($p=0.0007$). No difference in tumour weight or mouse weight was observed at endpoint (Figure 5.2.11C+D), indicating ethical endpoints were appropriately applied across all treatment groups and there were no obvious signs of treatment-induced toxicity.

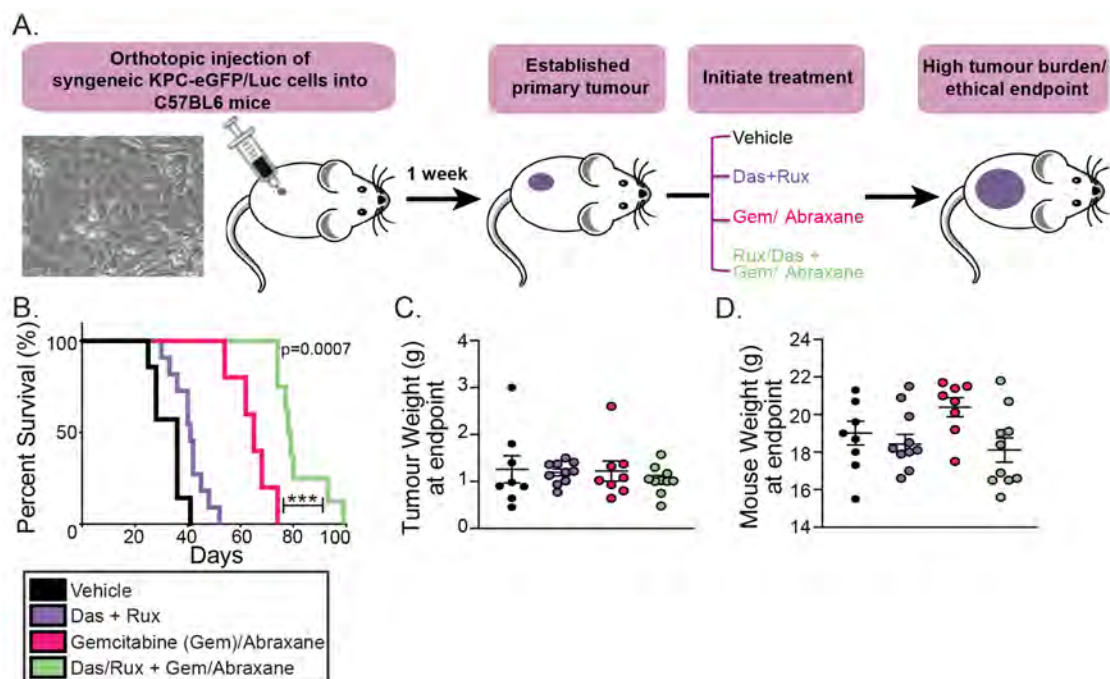


Figure 5.2.11 Effects of dasatinib and ruxolitinib treatment on survival in the syngeneic and orthotopic KPC model of pancreatic cancer. (A) Schematic representation of orthotopic injection and treatment timeline. (B) Kaplan-Meier survival analyses of dasatinib and ruxolitinib combination, also combined with gemcitabine (Gem) and Abraxane, compared with Gem/Abraxane alone. Log-rank analysis where * $p < 0.05$, ** $p < 0.01$, *** $p < 0.001$ and **** $p < 0.0001$. (C) Tumour weight at endpoint and (D) mouse weight at endpoint. Data are presented as mean \pm SEM ($n = 8-10$ mice/treatment group). Das: dasatinib (10mg/kg daily); rux: ruxolitinib (60mg/kg twice daily); das+rux: dasatinib and ruxolitinib; gem: gemcitabine (60mg/kg twice weekly), Abraxane (30mg/kg twice weekly).

5.2.3 Efficacy of dual dasatinib and ruxolitinib treatment in immunocompromised, patient-derived, orthotopic models of pancreatic cancer

5.2.3.1 Effect of dasatinib and ruxolitinib treatment on tumour growth and metastasis

Building on the thus far observed significant *in vivo* anti-tumour efficacy of our proposed treatment approach, next we systematically examined the *in vivo* therapeutic potential of dasatinib and ruxolitinib in two “on-phenotype” (P53 mutant, pSTAT3-high) orthotopic eGFP/Luciferase-tagged patient-derived models of pancreatic cancer (TKCC-05-eGFP/Luc; TKCC-10-eGFP/Luc). Patient-derived cells were orthotopically injected into the pancreas of immunocompromised NSG mice (Figure 5.2.12A and Figure 5.2.13A). Once primary tumours reached palpable size (measurable using IVIS imaging, starting Flux = $\sim 1.5 \times 10^8$ p/s for the TKCC-05 model, and $\sim 5.0 \times 10^8$ p/s for the TKCC-10 model), mice were randomised into treatment groups. For the TKCC-05 model treatment groups included vehicle control, dasatinib and ruxolitinib, plus a combination of dasatinib, ruxolitinib and gemcitabine/Abraxane chemotherapy as well as chemotherapy alone. For the TKCC-10 model only the combination of dasatinib and ruxolitinib, plus a combination of dasatinib, ruxolitinib and gemcitabine/Abraxane chemotherapy as well as chemotherapy alone was used as these were the most effective treatment strategies identified from the KPC and TKCC-05 studies. Mice were monitored weekly using bioluminescent live imaging (IVIS Spectrum) to detect tumour burden and metastatic spread.

30-day timepoint analyses of both models revealed interesting modulation of primary tumour size by the dasatinib and ruxolitinib combination, compared to vehicle control, and this decrease was similar to that of gemcitabine and Abraxane (Figure 5.2.12B and Figure 5.2.13B). Moreover, the combination of dasatinib and ruxolitinib with gemcitabine and Abraxane reduced tumour weight significantly compared to the combination of dasatinib and ruxolitinib alone, or gemcitabine and Abraxane alone, with treatment being well tolerated in immunocompromised settings (Figure 5.2.12C and Figure 5.2.13C).

Examining for the presence of metastases in mice demonstrated that the extent of metastatic spread was significantly reduced following treatment with dasatinib and ruxolitinib, in both the TKCC-05 (Figure 5.2.12D-H) and TKCC-10 (Figure 5.2.13D-H) models. Liver metastases were present in 80% and 70% of dasatinib and ruxolitinib-treated mice with TKCC-05 and TKCC-10 tumours respectively, compared to 100% of control mice. Moreover, spleen metastases were identified in 30% (TKCC-05) and 80% (TKCC-10) of mice. Lung metastases were present in 50% (TKCC-05) and 80% (TKCC-10) of mice, while 60% (TKCC-05) and 30% (TKCC-10) showed diaphragm metastases. Interestingly, when mice were treated with a combination of dasatinib and ruxolitinib with gemcitabine and Abraxane there was no evidence of metastases in the liver, spleen, lung or diaphragm of the TKCC-05 model. Moreover, there were no metastases in the spleen or diaphragm of the TKCC-10 model, and only 20% of mice presented with liver and lung metastases. In comparison 40% (TKCC-05) and 80% (TKCC-10) of mice treated with chemotherapy alone (gemcitabine and Abraxane) presented with metastases, with 20% (TKCC-05) and 40% (TKCC-10) having liver metastases, and 40% (TKCC-05) and 60% (TKCC-10) having spleen metastases. In concordance with the above, live animal bioluminescent imaging (IVIS imaging) over time revealed similar effects of treatment on tumour growth and metastatic spread in both models (Figure 5.2.14 and Figure 5.2.15). Taken together, these data demonstrate that combined dasatinib and ruxolitinib treatment can reduce primary tumour growth and metastatic burden of patient-derived TKCC-05 and TKCC-10 tumours, as well as significantly improving response to chemotherapy.

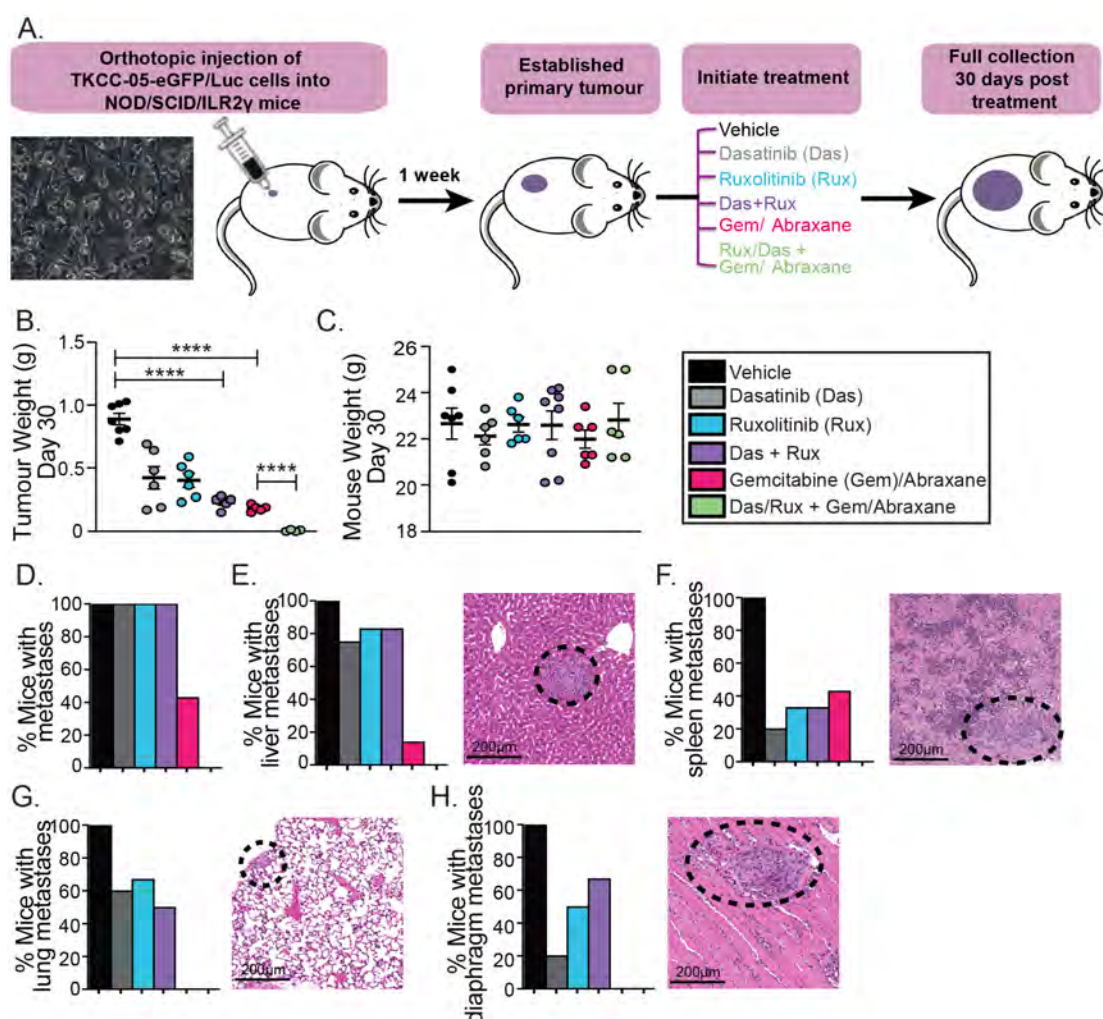


Figure 5.2.12 Effects of dasatinib and ruxolitinib treatment on tumour weight and metastasis in the immunocompromised, patient-derived TKCC-05 orthotopic model of pancreatic cancer. (A) Schematic representation of orthotopic injection and treatment timeline. (B) Tumour weight at 30 days post treatment. (C) Mouse weight at 30 days post treatment. (D) Proportion of mice with metastases at 30 days post-treatment. Proportion of mice with metastases and representative image of tumours found in the (E) liver, (F) spleen, (G) lung and (H) diaphragm. Data are presented as mean \pm SEM (n= 5-7 mice/treatment group). Significance was determined using nonparametric ANOVA test with a Tukey multiple comparisons test where * $p < 0.05$, ** $p < 0.01$, *** $p < 0.001$ and **** $p < 0.0001$. Das: dasatinib (10mg/kg daily); rux: ruxolitinib (60mg/kg twice daily); das+rux: dasatinib and ruxolitinib; gem: gemcitabine (100mg/kg weekly), Abraxane (30mg/kg weekly).

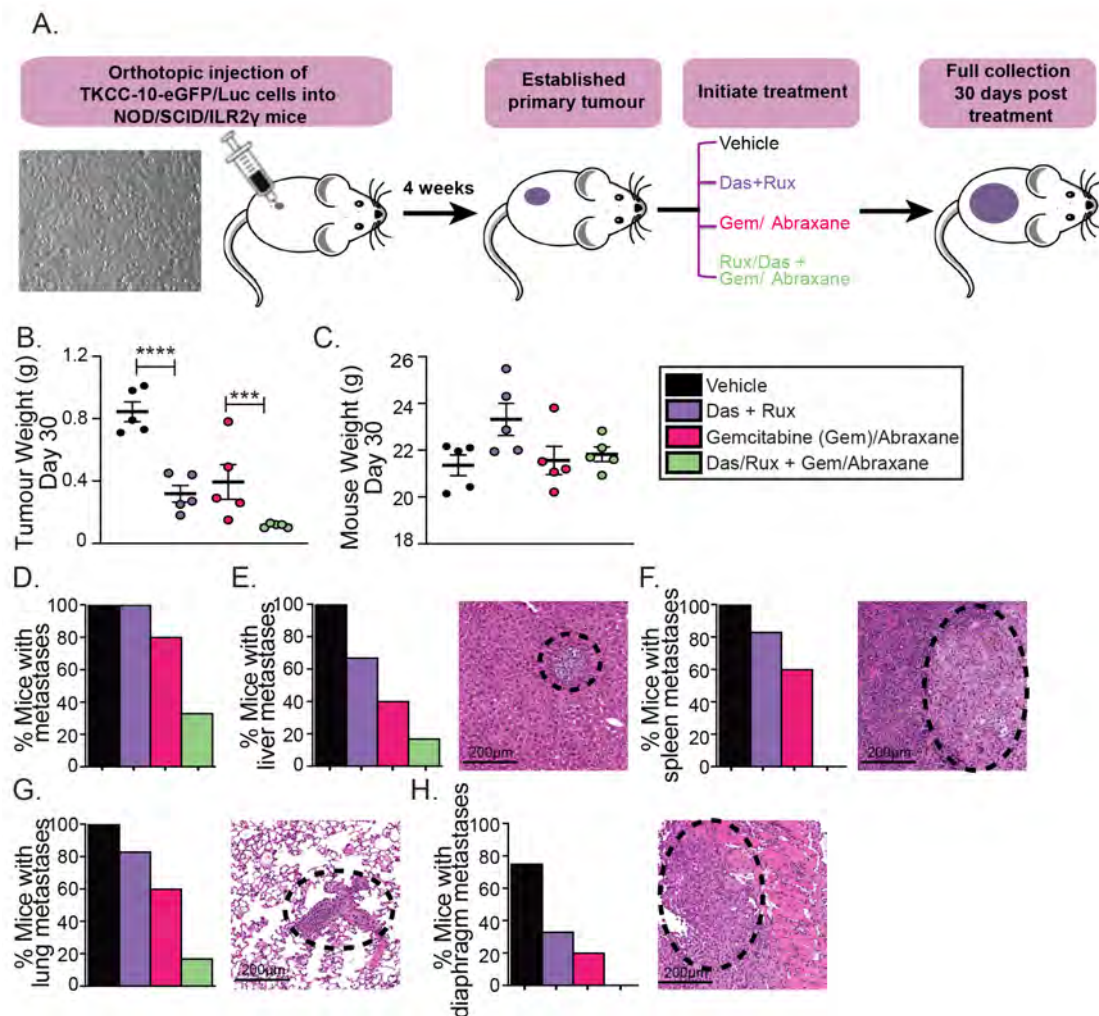


Figure 5.2.13 Effects of dasatinib and ruxolitinib treatment on tumour weight and metastasis in the immunocompromised, patient-derived TKCC-10 orthotopic model of pancreatic cancer. (A) Schematic representation of orthotopic injection and treatment timeline. (B) Tumour weight at 30 days post treatment. (C) Mouse weight at 30 days post treatment. (D) Proportion of mice with metastases at 30 days post-treatment. Proportion of mice with metastases and representative image of tumours found in the (E) liver, (F) spleen, (G) lung and (H) diaphragm. The most efficacious treatment strategies from our prior mouse models were selected for this study. These included the dasatinib and ruxolitinib combination, gemcitabine and Abraxane, and dasatinib and ruxolitinib in combination with gemcitabine and Abraxane. Data are presented as mean \pm SEM (n= 5 mice/treatment group). Significance was determined using nonparametric ANOVA test with a Tukey multiple comparisons test where * p <0.05, ** p <0.01, *** p <0.001 and **** p <0.0001. Das: dasatinib (10mg/kg daily); rux: ruxolitinib (60mg/kg twice daily); das+rux:

dasatinib and ruxolitinib; gem: gemcitabine (100mg/kg weekly), Abraxane (30mg/kg weekly).

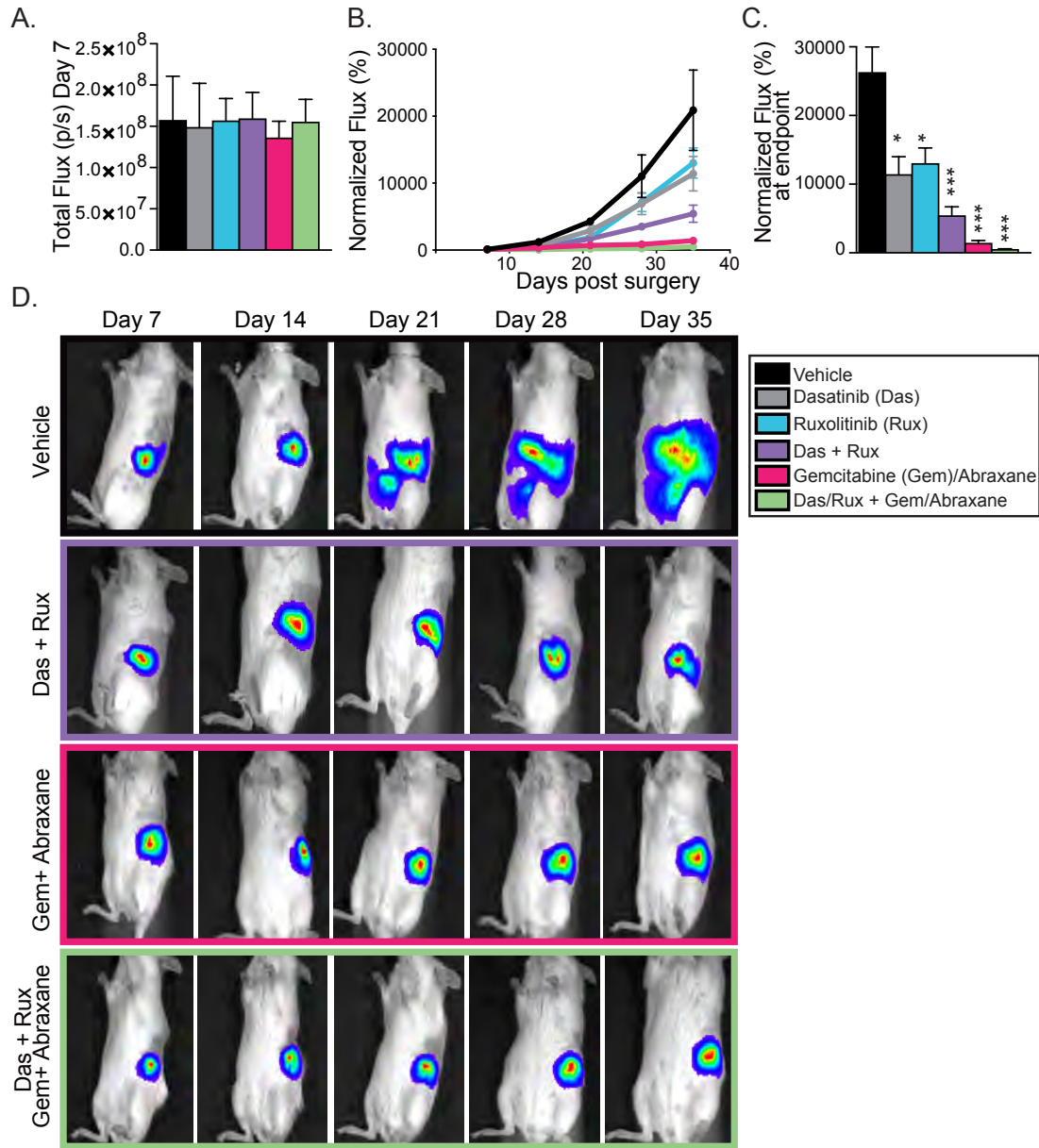


Figure 5.2.14 Effects of dasatinib and ruxolitinib treatment on metastatic spread using bioluminescence imaging, in the immunocompromised, patient-derived TKCC-05 orthotopic model of pancreatic cancer. (A) Analysis of luciferase total flux (photons/sec) on day 7 post-surgery shows no significant difference in tumour size once mice were randomised to treatment groups. (B+D) Whole body imaging of mice was performed weekly, and normalised flux (% of the initial signal, day 7 post-surgery) was calculated weekly. (C) Normalised flux calculated at endpoint. Data are presented as mean \pm SEM (n= 5-7 mice/treatment group). Significance was determined using

nonparametric ANOVA test with a Tukey multiple comparisons test where * $p < 0.05$, ** $p < 0.01$, *** $p < 0.001$ and **** $p < 0.0001$.

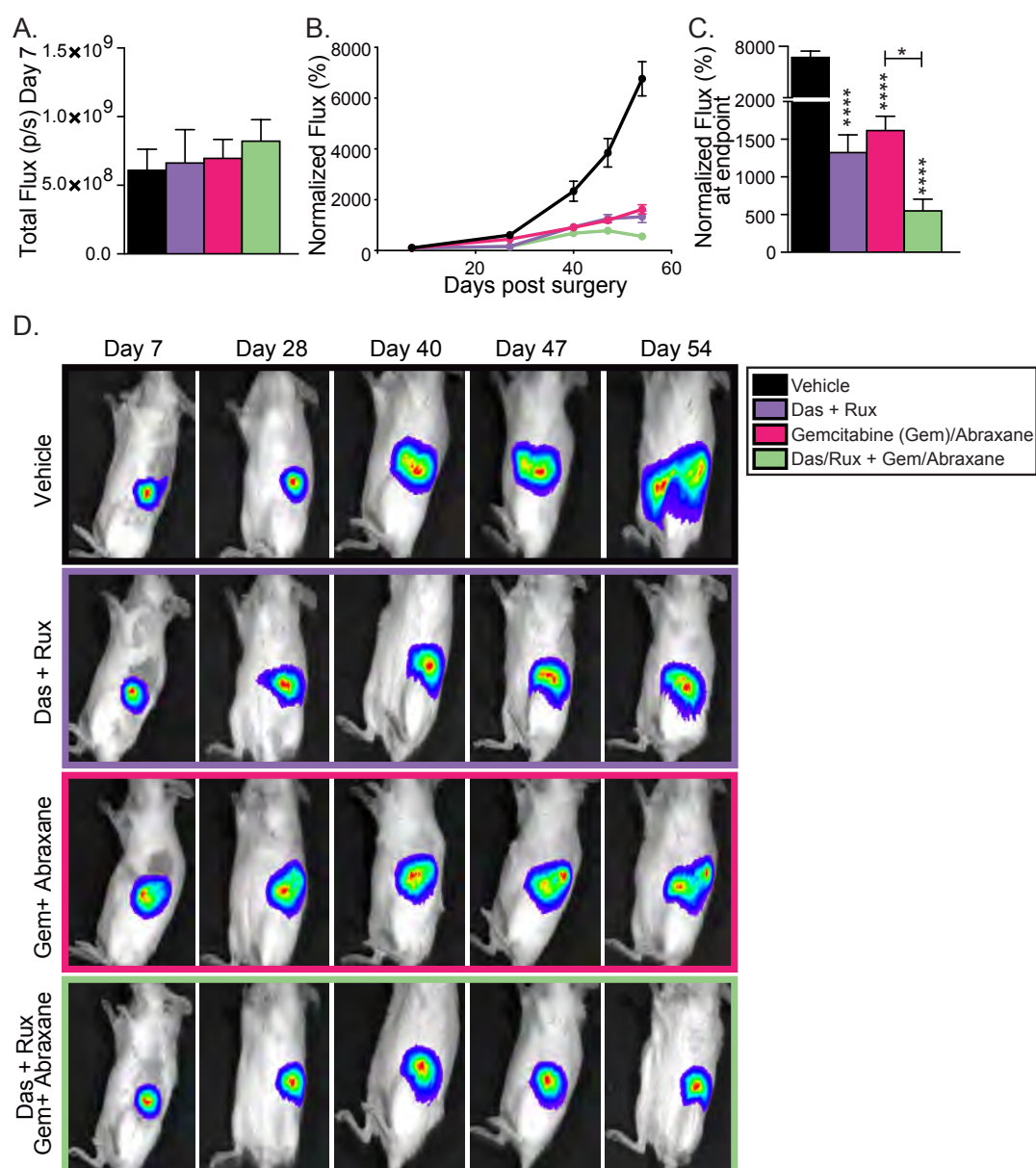


Figure 5.2.15 Effects of dasatinib and ruxolitinib treatment on metastatic spread using bioluminescence imaging, in the immunocompromised, patient-derived TKCC-10 orthotopic model of pancreatic cancer. (A) Analysis of luciferase total flux (photons/sec) on day 7 post-surgery shows no significant difference in tumour size once mice were randomised to treatment groups. (B+D) Whole body imaging of mice was performed weekly, and normalised flux (% of the initial signal, day 7 post-surgery) was calculated weekly (C) Normalised flux calculated at endpoint. Data are presented as mean \pm SEM (n= 5-7 mice/ treatment group). Significance was determined using

nonparametric ANOVA test with a Tukey multiple comparisons test where * $p < 0.05$, ** $p < 0.01$, *** $p < 0.001$ and **** $p < 0.0001$.

5.2.3.2 Effect of dasatinib and ruxolitinib treatment on cellular proliferation and apoptosis, in patient-derived models of pancreatic cancer

Building on our findings using the KPC model, we aimed to examine the effect of dasatinib and ruxolitinib treatment on cellular proliferation and apoptosis in the patient-derived setting (Figure 5.2.16 and Figure 5.2.17). Immunohistochemical analysis of collected patient-derived tumours for markers of apoptosis (cleaved-caspase-3) revealed a significant increase in the proportion of apoptotic cells following treatment with dasatinib and ruxolitinib, effects further enhanced in the combined dasatinib/ruxolitinib plus chemotherapy group in both tumour models (Figure 5.2.16A+C and Figure 5.2.17A+C). Unlike with the KPC model, there was no change in the number of Ki67 positive cells following treatment with dasatinib and ruxolitinib, even when combined with gemcitabine and Abraxane in the TKCC-05 model (Figure 5.2.16B+D). However, similarly to the KPC model, there was a decrease in the number of Ki67 positive cells following dasatinib and ruxolitinib treatment, and this was further reduced when combined with chemotherapy in the TKCC-10 model (Figure 5.2.17B+D).

Collectively, these analyses demonstrate that the observed significant inhibition of primary tumour growth and metastasis in “on-phenotype” patient-derived orthotopic models, following dasatinib and ruxolitinib treatment is robustly associated with induction of apoptotic signalling and variable inhibitory effects on proliferation.

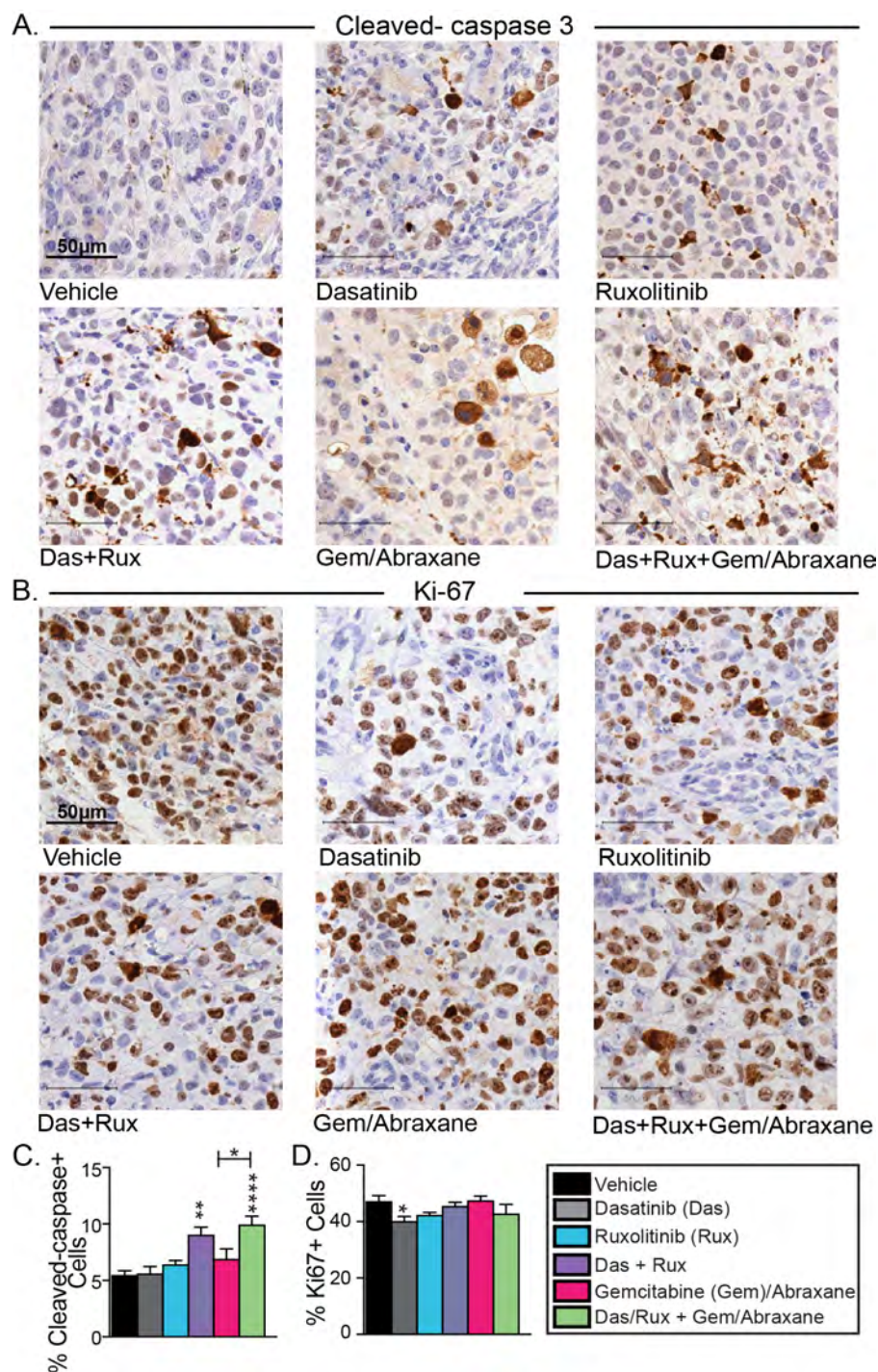


Figure 5.2.16 Effects of dasatinib and ruxolitinib treatment on cancer cell apoptosis and proliferation in the TKCC-05 model of pancreatic cancer. Representative images of (A) cleaved-caspase-3 and (B) Ki67 IHC staining, and quantification (C-D) of tumours 30 days post-treatment. Data are presented as mean \pm SEM (n= 4 tumours/ treatment, with 6 FOV analysed/ tumour/ treatment). Significance was determined using nonparametric

ANOVA test with a Tukey multiple comparisons test where * $p < 0.05$, ** $p < 0.01$, *** $p < 0.001$ and **** $p < 0.0001$.

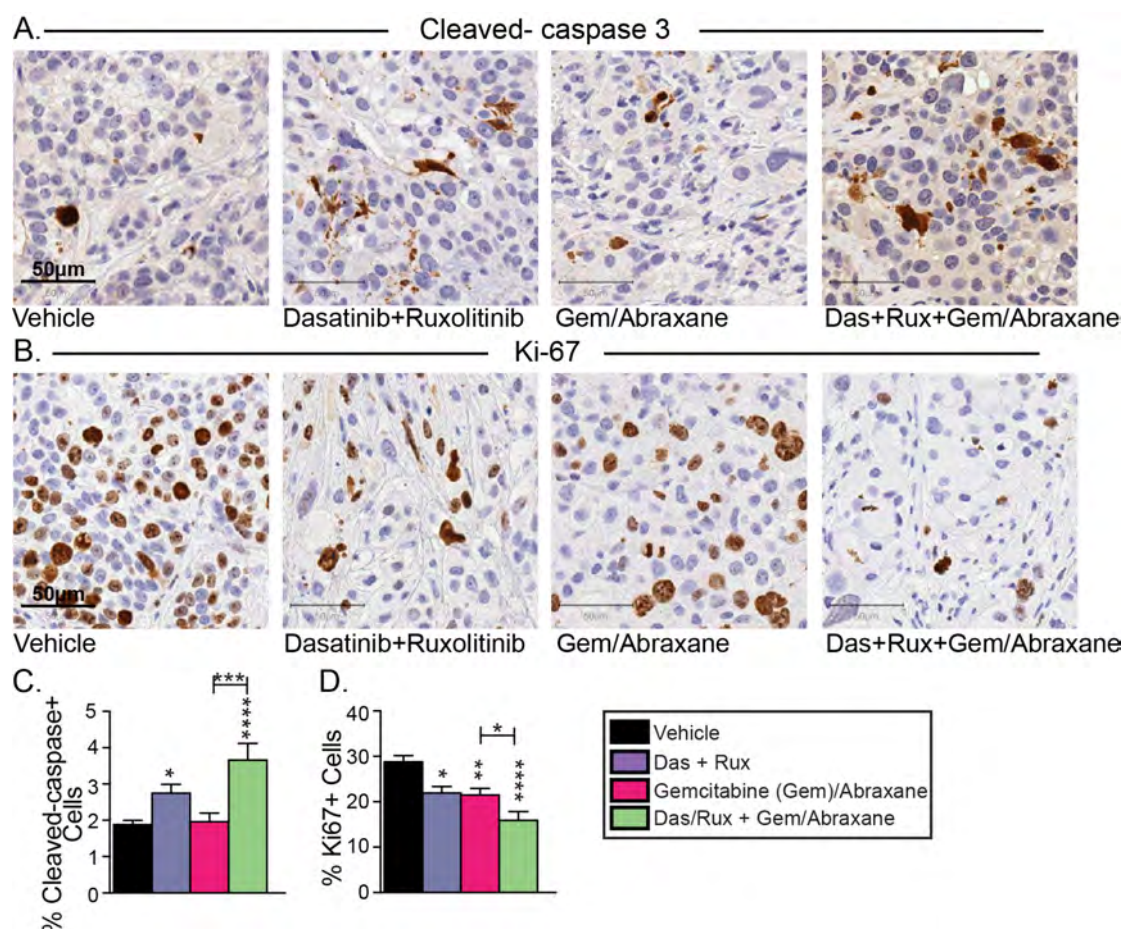


Figure 5.2.17 Effects of dasatinib and ruxolitinib treatment on cancer cell apoptosis and proliferation in the patient-derived TKCC-10 model of pancreatic cancer. Representative images of (A) cleaved-caspase-3 and (B) Ki67 IHC staining and quantification (C-D) of KPC tumours 30 days post-treatment. Data are presented as mean \pm SEM ($n=4$ tumours per treatment group, with 6 FOV analysed per tumour per treatment group). Significance was determined using nonparametric ANOVA test with a Tukey multiple comparisons test where * $p < 0.05$, ** $p < 0.01$, *** $p < 0.001$ and **** $p < 0.0001$.

5.2.3.3 Effect of dasatinib and ruxolitinib treatment on regulating pancreatic stellate cell activation in patient-derived models of pancreatic cancer

As dasatinib and ruxolitinib combination significantly altered the levels of cancer-associated fibroblast (CAF) marker, α -smooth muscle actin (α -SMA) in the syngeneic KPC model, next we assessed the effect of our promising treatment approach on CAF activation in the TKCC-05 and TKCC-10 patient-derived orthotopic pancreatic cancer models. Following treatment with ruxolitinib, or ruxolitinib-based combination therapies, the proportion of α -SMA-positive cells decreased 2-fold (TKCC-05) and 1.5-fold (TKCC-10) in examined tumours (Figure 5.2.18 and Figure 5.2.19). This suggests that JAK1/2 inhibition is sufficient to effectively impede activation of pancreatic cancer-associated fibroblasts in multiple patient-derived models of pancreatic cancer.

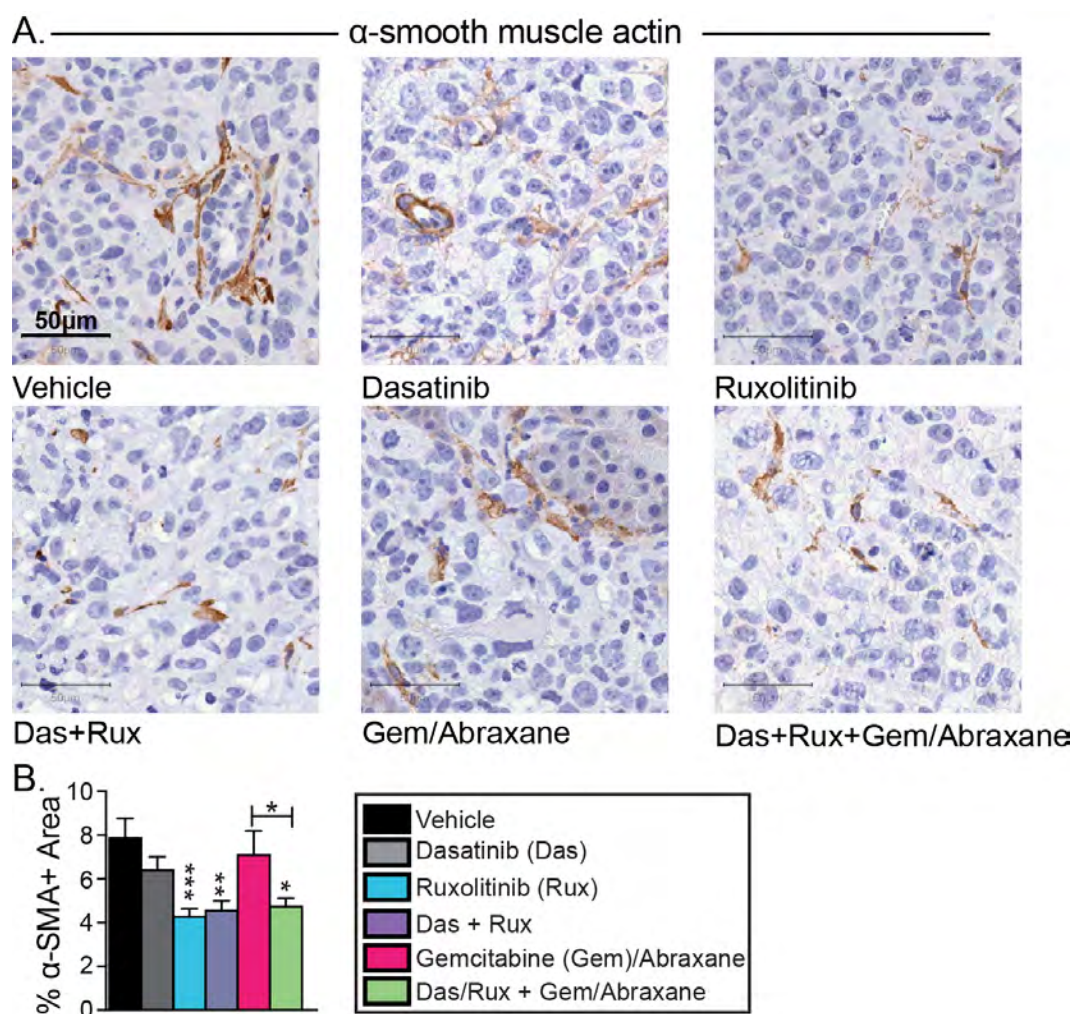


Figure 5.2.18 Effects of dasatinib and ruxolitinib treatment on activated cancer-associated fibroblasts in TKCC-05 tumours. Representative images (A) and quantification (B) of α -smooth muscle actin IHC staining on TKCC-05 tumours 30 days post-treatment. Data are presented as mean SMA-positive staining area \pm SEM ($n=4$ tumours per treatment group, with 6 FOV analysed per tumour per treatment group). Significance was determined using non-parametric ANOVA test with a Tukey multiple comparisons test where $*p<0.05$, $**p<0.01$, $***p<0.001$ and $****p<0.0001$. Das: dasatinib; rux: ruxolitinib; das+rux: dasatinib and ruxolitinib; gem: gemcitabine.

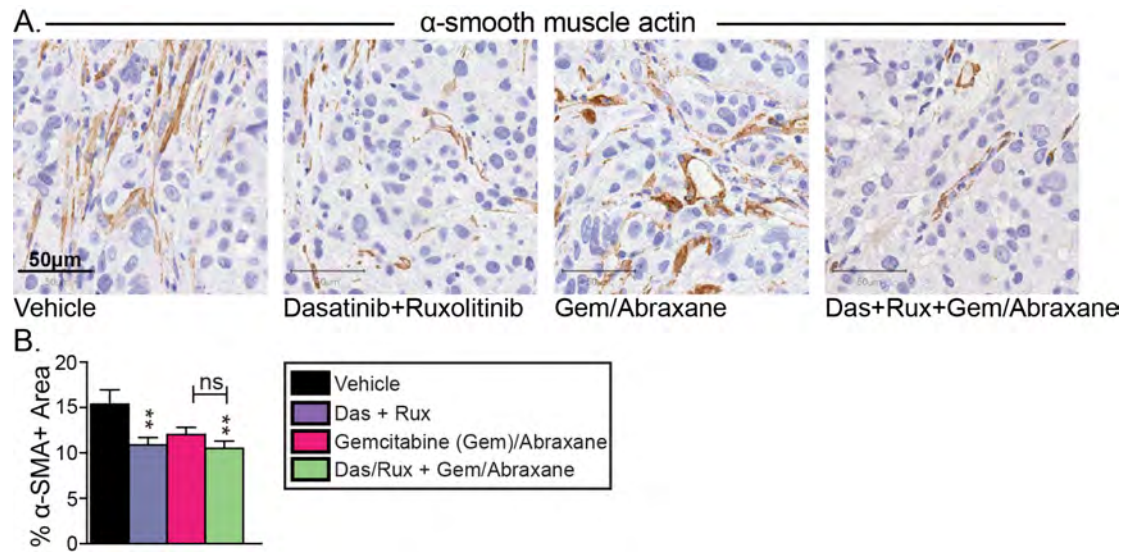


Figure 5.2.19 Effects of dasatinib and ruxolitinib treatment on activated cancer-associated fibroblasts in TKCC-10 tumours. Representative images and quantification of α-smooth muscle actin IHC staining on TKCC-05 tumours 30 days post treatment. Data are presented as mean SMA-positive staining area \pm SEM (n= 4 tumours per treatment group, with 6 FOV analysed per tumour per treatment group). Significance was determined using nonparametric ANOVA test with a Tukey multiple comparisons test where *p<0.05, **p<0.01, ***p<0.001 and ****p<0.0001. Das: dasatinib; rux: ruxolitinib; das+rux: dasatinib and ruxolitinib; gem: gemcitabine.

5.2.3.4 Effects of dasatinib and ruxolitinib treatment on remodelling the fibrotic tumour microenvironment

Previously we observed significant effects of JAK inhibition on tumour fibrosis and extracellular matrix integrity in the immunocompetent KPC model (chapter 5.2.2). Next we wanted to assess these effects in the context of immunocompromised patient-derived models (Figure 5.2.20 and Figure 5.2.21). In the TKCC-05 model, collagen content was significantly reduced following treatment with ruxolitinib, (Figure 5.2.20 D-F). Similar results were seen when ruxolitinib was combined with dasatinib, and also when combined with chemotherapy, in both TKCC-05 and TKCC-10 models (Figures 5.2.20E-F and 5.2.21D-F). Moreover, in both models, birefringence analysis of collagen organisation revealed that ruxolitinib-based treatments reduced the proportion of highly-crosslinked collagen fibres and this was associated with an increase in less remodelled collagen fibres (Figures 5.2.20 G-J and Figures 5.2.21 G-J).

Taken together, these findings support our previous 3D *in vitro* and *in vivo* data (KPC model), confirming that JAK1/2 inhibition robustly leads to decreased fibrillar collagen content, and promotes a significantly disorganised extracellular matrix network in patient-derived settings.

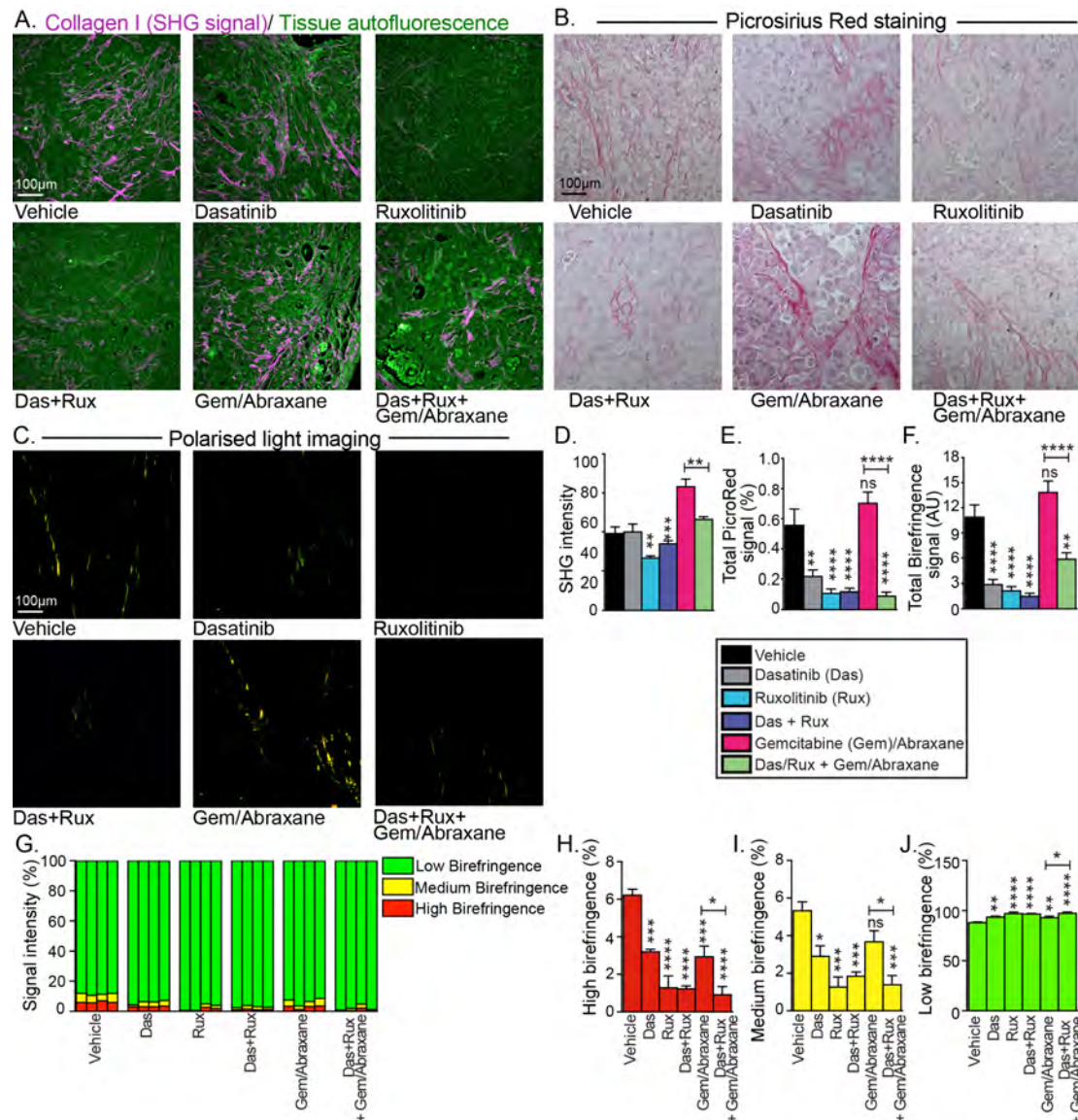


Figure 5.2.20 Effects of dasatinib and ruxolitinib treatment on the extracellular matrix in TKCC-05 tumours. (A) Second-harmonic generation (SHG) maximum intensity images of TKCC-05 tumours 30 days post-treatment, with quantification of signal intensity at peak in (D). (B) Brightfield and (C) polarised light imaging of Picrosirius Red-stained sections and quantification of total collagen content (E+F). (G-J) Quantification of signal emitted from fibres with high (red), medium (yellow) and low (green) birefringence normalised to total signal acquired via polarised imaging. Data are presented as mean \pm SEM ($n=4$ tumours per treatment group, with 6 FOV per tumour). Significance was determined using nonparametric ANOVA test with a Tukey multiple comparisons test where * $p<0.05$, ** $p<0.01$, *** $p<0.001$ and **** $p<0.0001$.

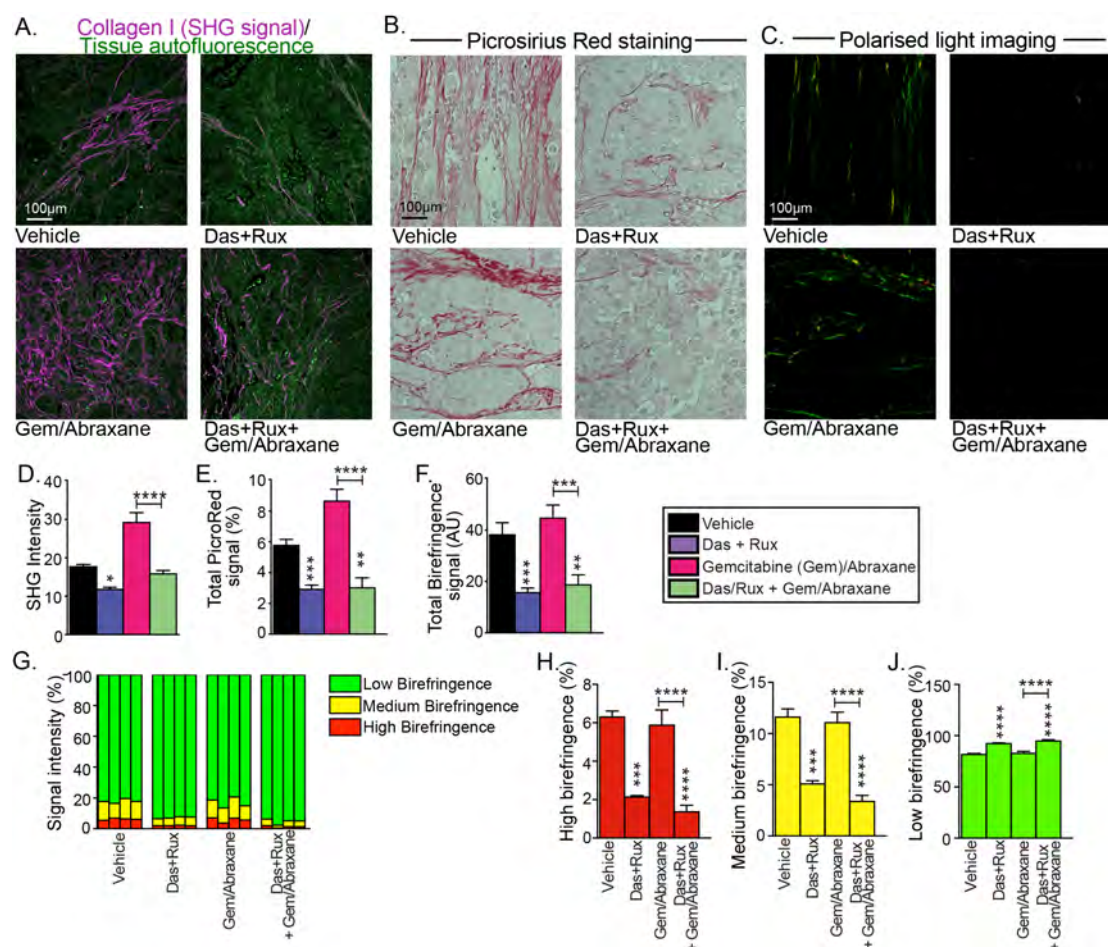


Figure 5.2.21 Effects of dasatinib and ruxolitinib treatment on the extracellular matrix in TKCC-10 tumours. (A) Second-harmonic generation (SHG) maximum intensity images of TKCC-10 tumours 30 days post-treatment, with quantification of signal intensity at peak in (D). (B) Brightfield and (C) polarised light imaging of Picrosirius Red-stained sections and quantification of total collagen content (E+F). (G-J) Quantification of signal emitted from fibres with high (red), medium (yellow) and low (green) birefringence normalised to total signal acquired via polarised imaging. Data are presented as mean \pm SEM ($n = 4$ tumours per treatment group, with 6 FOV per tumour). Significance was determined using nonparametric ANOVA test with a Tukey multiple comparisons test where * $p < 0.05$, ** $p < 0.01$, *** $p < 0.001$ and **** $p < 0.0001$.

5.2.3.5 Effect of dasatinib and ruxolitinib treatment on prolonging survival in metastatic patient-derived models of pancreatic cancer

To examine the effects of dual dasatinib and ruxolitinib treatment on tumour progression and survival in the patient-derived and immunocompromised setting, the orthotopic patient-derived pSTAT3-high, P53 mutant TKCC-05 model was utilised. Mice were monitored using bioluminescent imaging (IVIS) until ethical endpoint as defined by high tumour burden and/or the presence of ascites (Figure 5.2.22A). Kaplan-Meier survival analyses revealed that dasatinib and ruxolitinib in combination prolonged overall survival (median survival = 43 days, $p=0.00001$; vs vehicle median survival = 31 days). Gemcitabine and Abraxane also extended survival (median survival = 64 days, $p=0.0001$) (Figure 5.2.22B). Moreover, the dasatinib and ruxolitinib with gemcitabine and Abraxane combination extended survival further (median survival= 73 days $p<0.0001$; vs vehicle = 31 days) versus gemcitabine and Abraxane alone ($p=0.0009$; Figure 5.2.22B). No significant difference in tumour weight or mouse weight was observed at endpoint (Figure 5.2.22C+D), indicating ethical endpoints were appropriately applied across all treatment groups and there were no obvious signs of treatment-induced toxicity. In line with these results, IVIS imaging over time revealed similar effects of treatment on tumour growth and metastatic spread (Figure 5.2.23).

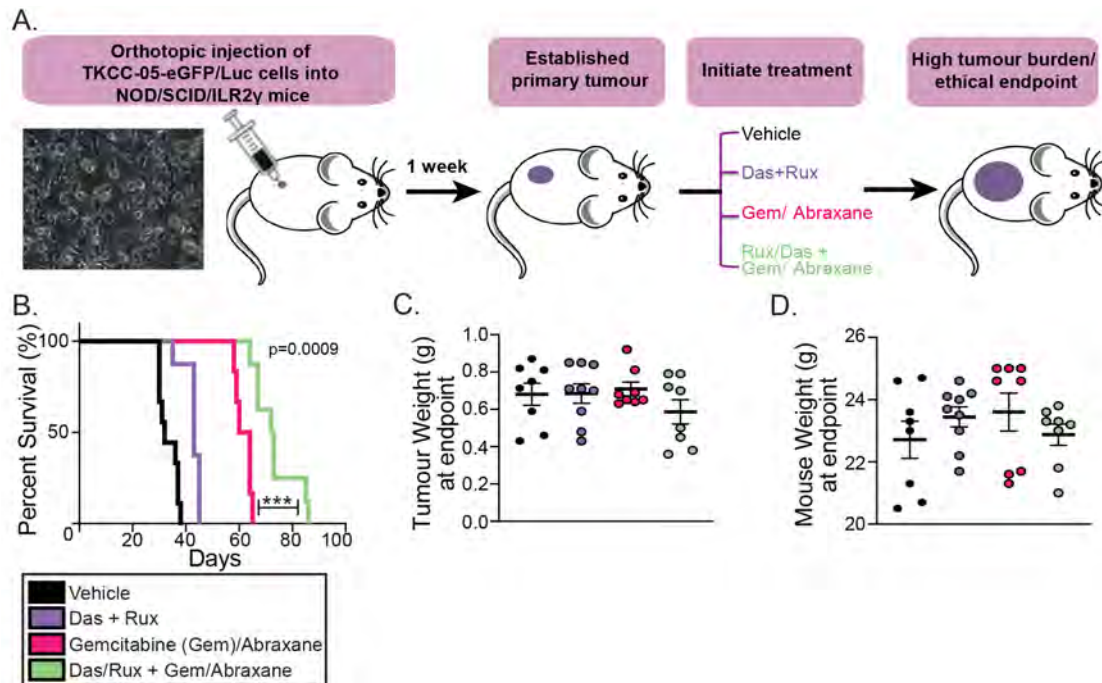


Figure 5.2.22 Effects of dasatinib and ruxolitinib treatment on survival in the immunocompromised, patient-derived TKCC-05 orthotopic model of pancreatic cancer. (A) Schematic representation of orthotopic injection and treatment timeline. (B) Kaplan-Meier survival analyses of dasatinib and ruxolitinib combination, also combined with gemcitabine (gem) and Abraxane, compared with gem/Abraxane alone. Log-rank analysis where * $p < 0.05$, ** $p < 0.01$, *** $p < 0.001$ and **** $p < 0.0001$. (C) Tumour weight at endpoint and (D) mouse weight at endpoint. Data are presented as mean \pm SEM ($n = 8-10$ mice/treatment group). Das+rux: dasatinib and ruxolitinib.

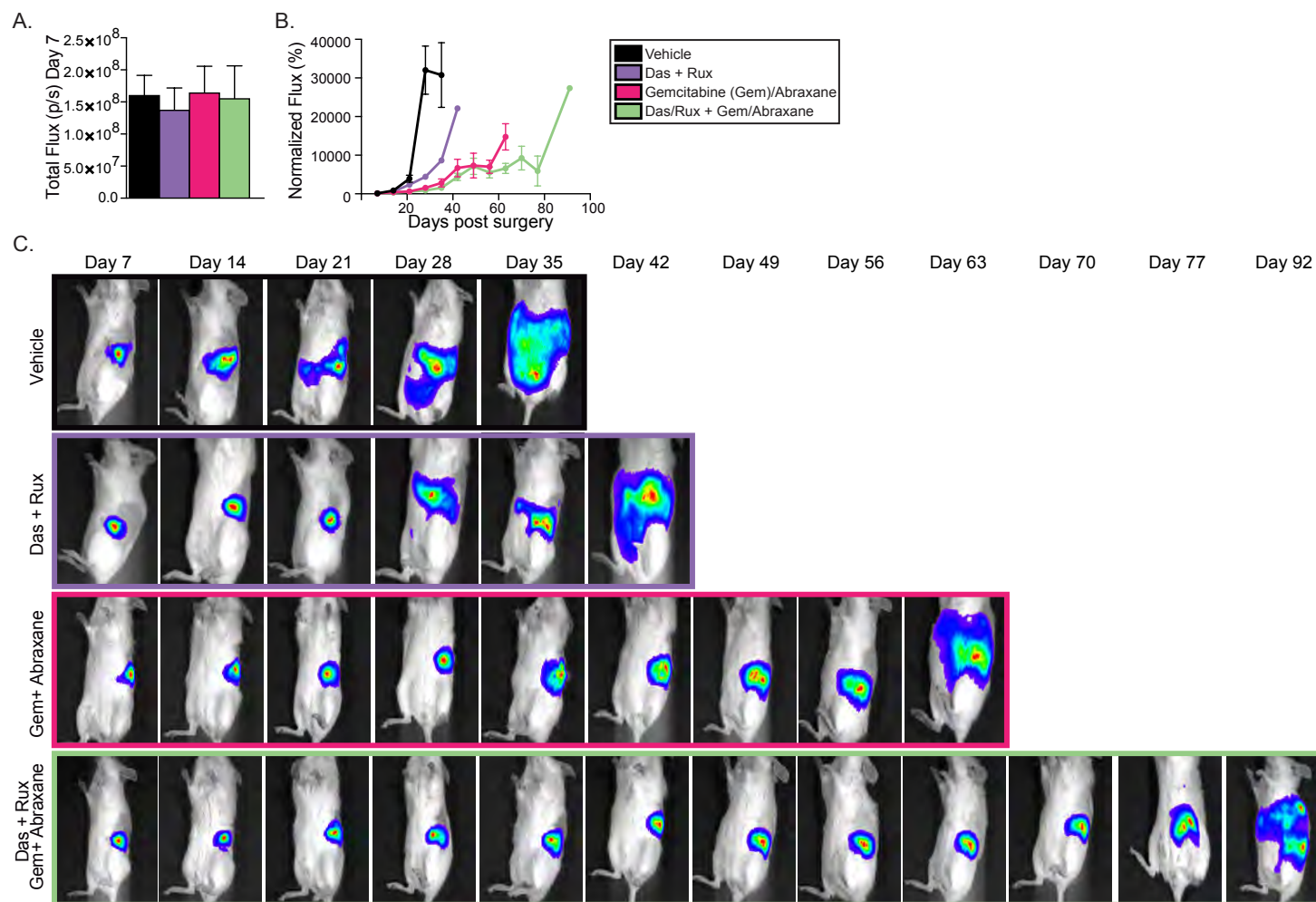


Figure 5.2.23 Effects of dasatinib and ruxolitinib treatment on metastatic spread in the TKCC-05 model. (A) Analysis of luciferase total flux (photons/sec) on day 7 post-surgery. (B+C) Normalised flux (% of the initial signal on day 7 post-surgery) was calculated weekly. Data are presented as mean \pm SEM (n= 8-10 mice/group).

5.3 Discussion

Despite recent progress developing novel treatment combinations, chemotherapy remains the standard of care for most patients with advanced pancreatic cancer, despite modest improvements in survival [9, 788]. Given the limitations associated with two-dimensional and three-dimensional *in vitro* models [83, 149, 612], *in vivo* models are essential tools for assessing the ability of new treatment combinations to improve chemosensitivity. Based on our promising findings in chapter 3 and chapter 4, we explored the efficacy of dual dasatinib and ruxolitinib treatment in the context of the complex tumour microenvironment *in vivo*. *In vivo* models were used to investigate the ability of SRC/JAK inhibition to delay tumour progression, improve response to chemotherapy, and also to examine broad mechanisms of action.

The effect of combined dasatinib and ruxolitinib treatment was examined in three selected pancreatic cancer models characterised by high phospho-STAT3 expression and *TP53* mutations. Importantly, all three models displayed enhanced sensitivity to the combination of dasatinib and ruxolitinib, as evidenced by reduced primary tumour weight, decreased metastatic burden and improved survival. Previous studies have combined SRC and JAK monotherapies with chemotherapies such as gemcitabine and have demonstrated improved chemotherapeutic efficacy [443, 553, 554]. However, we are the first to demonstrate that dual dasatinib and ruxolitinib treatment in combination with standard of care chemotherapy (gemcitabine and Abraxane) is a viable therapeutic approach for pancreatic tumours that have been molecularly stratified. We have shown significantly inhibited tumour progression, improved survival while delaying the development of metastasis in both immunocompetent and immunocompromised *in vivo* models of pancreatic cancer. Building on our promising *in vitro* findings, we have also shown that combined dasatinib and ruxolitinib therapy robustly enhanced the apoptotic effect of chemotherapy in all three “on-phenotype” *in vivo* models examined, with significant anti-proliferative effects on cancer cells in two of these models.

As discussed previously (Chapter 4), pancreatic tumours comprise a heterogeneous population of cancer-associated fibroblasts, the inflammatory CAFs (iCAFs) and the myofibroblasts (myCAFs) collectively referred to as 'pancreatic stellate cells', which play a significant role in promoting pancreatic tumourigenesis via the secretion of pro-inflammatory factors (iCAFs) and extracellular matrix (ECM) deposition (myCAFs) [141]. Despite several studies observing that modulation of the JAK/STAT3 pathway can alter stromal remodelling and decrease extracellular matrix deposition [443, 553, 554], Tuveson *et al.* have shown that JAK2 inhibition significantly increases the myCAF/iCAF ratio, reducing the secretion of tumour-promoting cytokines and chemokines, and shifting the CAF population to a myofibroblastic state, associated with increased extracellular matrix deposition and tumour fibrosis that is known to impede drug delivery [141, 147]. Our study has demonstrated that modulation of both JAK1 and JAK2 leads to effective disruption of collagen organisation (associated with myCAF activity), decreased overall CAF activation (assessed by α -smooth muscle actin staining), as well as significant decrease in signalling from the iCAF population (Chapter 4), suggesting that dual JAK1/JAK2 disruption can alter both CAF populations. In parallel, this therapeutic strategy can disrupt tumour-stromal interactions by inhibiting IL-4, IL-13, FGF and TNF- α signalling *in vitro* (Chapter 4) and the *in vivo* deposition of periostin, a matricellular protein induced by these pro-inflammatory mediators [789]. Fibronectin, a STAT3 target and extracellular matrix protein with a role in regulating tumour architecture, as well as in promoting cell migration and transformation [790, 791] was also significantly modulated by dasatinib and ruxolitinib therapy. Notably, the major extracellular matrix components collagen, periostin and fibronectin, affected by the combination of dasatinib and ruxolitinib in this study, have all previously been shown to promote significant desmoplasia and lead to pancreatic tumour progression [787]. As the desmoplastic stroma of pancreatic tumours can impede chemotherapy delivery and promote chemoresistance [144, 792], and manipulation of the stroma has already shown significant success in improving chemosensitivity [149, 321, 793] [555], the novel therapeutic combination presented in this thesis highlights a tailored approach at targeting

diverse but distinct tumour cell and stromal cell components, to delay disease progression in this highly lethal malignancy.

Pancreatic tumours are also defined by an immunosuppressive tumour microenvironment [153, 416], and inhibition of the SRC/JAK/STAT3 pathway has previously shown potent immunomodulatory effects in cancers including pancreas [149, 301, 321]. We have demonstrated (Chapter 4) that combined dasatinib and ruxolitinib treatment significantly decreases the production of secreted factors, including chemokines and cytokines, that play a role in promoting an immunosuppressive tumour microenvironment. In concordance with this, we have now demonstrated that this treatment strategy significantly impairs the infiltration of pro-inflammatory, tumour-promoting immune-cell populations, including regulatory T cells. Regulatory T cells are a population of immune cells that are associated with a poor prognosis in PDAC [157, 158] and are known to suppress the adaptive immune response by inhibiting effector T cell functions [160, 321]. In line with this, we observed a significant increase in the proportion of effector T cells following treatment with dasatinib and ruxolitinib. Effector T cells (CD8+) work by eliminating tumour cells via IFN- γ -mediated direct tumouricidal activity and induction of macrophage tumouricidal activity [156], and are associated with favourable clinical outcomes in PDAC [156]. Although increased CD8+ T cell infiltration has previously been shown following downregulation of SRC alone or STAT3 alone [149, 301, 321], we are the first to demonstrate that combined inhibition with clinically-used agents is more effective. Moreover, we observed decreased infiltration of pro-tumourigenic (M2) macrophages that promote pancreatic cancer progression by secreting matrix proteins and proteases that modify the extracellular matrix, as well as pro-angiogenic and pro-invasive factors [156]. Importantly, we also observed decreased infiltration of pro-inflammatory and pro-tumourigenic immune cell populations and increased infiltration of effector T-cells when dasatinib and ruxolitinib treatment was combined with chemotherapy.

Collectively, these data establish potent efficacy of dual dasatinib and ruxolitinib treatment in tumours characterised by high phospho-STAT3 levels and *TP53* mutations, particularly when combined with standard-of-care

treatment. The observed efficacy is associated with complex deregulation of tumour cell and stromal cell signalling as well as the disruption of the surrounding extracellular matrix and immunosuppressive tumour microenvironment.

Chapter 6. General discussion

Despite significant efforts in developing new therapeutic strategies for pancreatic cancer, prognosis remains poor, with only 8% of patients surviving 5-years post diagnosis. Moreover, these statistics have remained largely unchanged for the past 5 decades, indicating the importance of further research in this field. Pancreatic cancer is a complex and molecularly heterogeneous disease [3], making it difficult to treat with a 'one-size fits all' therapeutic strategy. Currently, most fields of medicine including oncology are transitioning towards the paradigm of 'precision medicine', where an individual patient is offered personalised care with an available treatment that targets the specific biology of an individual tumour. This approach has recently showed success in treating cancers with high microsatellite instability (MSI-high) and mismatch repair (MMR) deficiency, with programmed death receptor-1 (PD-1) blockade (Pembrolizumab) [48]. Importantly, this trial assessed 12 different tumour types including pancreatic tumours, and showed measurable clinical responses. These results led to accelerated FDA approval, and set a precedent for the approval of biomarker-driven pancreatic cancer therapy [794]. Furthermore, these 'proof of principle' findings indicate that histology-independent, biomarker-selected 'basket' trials are feasible for developing personalised medicine strategies, and have already shown promising results in other cancers (Table 6.1). Moreover, other 'basket' trials are currently underway including the TAPUR study, [795] and NCI-MATCH [796].

To date, precision oncology trials have been focused on molecular matching with predetermined monotherapies [797-802], however many of these trials experience low matching rates due to limited gene panels and poor response rates [88]. A new paradigm for precision medicine has emerged that involves treating molecularly complex and heterogeneous cancers with combinations of customised agents. Results from the I-PREDICT study revealed that targeting tumours with multiple molecular alterations with molecular recommendation-based therapeutic combination(s) significantly improved disease-free and overall survival in patients with advanced cancer [88].

Accordingly, this study has employed a novel multimodal personalised medicine strategy that involves combining SRC and JAK inhibitors to target pancreatic tumours characterised by high phospho-STAT3 (Tyr705) expression and *TP53* mutations. The SRC/JAK/STAT3 network is a major oncogenic signalling cascade that is frequently deregulated in PDAC [122, 177, 321], presenting an attractive target for the development of tailored treatment strategies.

In this study, using patient-derived and genetically engineered *in vitro* models of pancreatic cancer, we have demonstrated that dasatinib and ruxolitinib synergise in molecular subtypes defined by high phospho-STAT3 (Tyr705) expression and P53 mutations. We have also demonstrated that the combination of dasatinib and ruxolitinib treatment is the most effective at inhibiting the invasive, and proliferative capacity of 'on-phenotype' tumour cells in 3D organotypic models, and significantly disrupts extracellular matrix remodelling and collagen crosslinking (summarised in Figure 6.1) .

In line with previous studies by Elyada *et al.* [145], Collisson *et al.* [7], and Bailey *et al.* [3], that have established that PDAC tumours are molecularly heterogeneous, we have demonstrated inter-tumoural heterogeneity in KPC co-culture organoids using single cell transcriptomics. We have identified 4 ductal cancer clusters as well as 2 cancer-associated fibroblast clusters: the iCAFs and myCAFs, previously described by Ohlund *et al.* [141]. Moreover, by examining cluster-specific transcriptomic signatures, we have begun to unravel the mechanisms behind dasatinib and ruxolitinib treatment. In cancer clusters this therapeutic strategy downregulates a number of important SRC and STAT3 target genes that promote pancreatic tumour progression. Additionally we have shown an effect of treatment on key processes that are significantly deregulated in cancer including the proliferation, apoptosis, cell cycle, protein synthesis [803], and metabolic processes such as glucose and glutathione metabolism [727, 728]. Dysregulation of these processes are a frequent feature of most cancers, therefore targeting them holds the promise of overcoming therapeutic issues associated with intra-tumoural heterogeneity. Furthermore we have demonstrated that dasatinib and ruxolitinib treatment downregulates key processes that are essential for the

production of a desmoplastic microenvironment, including extracellular matrix production by myCAFs. At the same time, this therapeutic combination appeared to 're-program' or modulate specific gene signatures within iCAFs, namely pro-inflammatory pathways associated with chemokine production and secretion, that enable iCAFs to promote an immunosuppressive and pro-metastatic tumour microenvironment.

Assessment of the effects of dasatinib and ruxolitinib treatment on intercellular signalling within KPC organoids confirmed that this treatment strategy significantly modulates the secretion of immunomodulatory and pro-fibrotic mediators (cytokines, chemokines and growth factors). In particular, we observed that dual JAK and SRC targeting decreased the concentration of key mediators associated with the infiltration, activation and differentiation of immunosuppressive cell populations including tumour-associated macrophages, myeloid-derived suppressor cells, regulatory T-cells and T-helper-17 cells. We have also shown effects of dasatinib and ruxolitinib on the secretion of pro-tumourigenic signals including IL-6 and its receptor Gp130, key factors that induce expression of STAT3 and promote tumour cell proliferation and survival [411, 627]. Moreover we have demonstrated that this treatment combination can modulate the secretion of factors that control the activation of pancreatic stellate cells, and can interfere with the autocrine signalling that promotes extracellular matrix production and remodelling (including IL-1, IL-6, TNF- α , and FGF) [160]. Furthermore, this treatment strategy is effective at dampening pro-metastatic signals including matrix metalloproteinases [756].

Lastly, using various 'on-phenotype' patient-derived and genetically engineered *in vivo* models of PDAC, we have demonstrated that this novel therapeutic strategy robustly reduced tumour weight, decreased metastatic burden and significantly improved survival. Moreover, we are the first to demonstrate that dual dasatinib and ruxolitinib treatment in combination with standard of care chemotherapy (gemcitabine and Abraxane), is a viable therapeutic approach for pancreatic tumours that have been molecularly stratified. This therapeutic strategy significantly enhanced the apoptotic and anti-proliferative effects of chemotherapy and significantly inhibited tumour

progression. Moreover, in line with our *in vitro* findings, we have shown significant modulation of extracellular matrix protein deposition and extracellular matrix remodelling, as well as impaired infiltration of pro-inflammatory, tumour-promoting immune-cell populations. These results are consistent with previously published work from Wormann *et al.* [321], who showed that genetic disruption of STAT3 *in vivo* reduces fibrosis by decreasing collagen content and the number of pancreatic stellate cells, and alters the proportion of immunosuppressive cell populations including tumour-associated macrophages and regulatory T-cells. Finally, by examining our cohort of patient-derived xenograft tumour tissues, we have demonstrated a correlation between high phospho-STAT3 expression and P53 mutations, and have identified a significant proportion of tumours (24%) defined by this molecular phenotype that are of potential interest for targeting with this therapeutic strategy.

6.1 Limitations and future studies

Given the limitations of preclinical models, particularly their inability to fully recapitulate the complex human tumour microenvironment, this study has attempted to reduce these limitations by utilising a diverse range of both *in vitro* and *in vivo* mouse and patient-derived models characterised by high phospho-STAT3 expression and *TP53* mutations. Importantly, this study has revealed similar effects of treatment in all models tested, suggesting that the combination of dasatinib and ruxolitinib is an effective therapeutic strategy and is likely to be consistent in this specific molecular context. This molecular context will need further *in vivo* exploration, as our *in vitro* data suggest that dasatinib and ruxolitinib have additional molecular targets that may be important for explaining the mechanism of action. These molecular targets may include downstream SRC/JAK/STAT3 pathway components such as AKT, MLC2 and MYPT. In addition, these results are limited to the 3 'on-phenotype' models selected, and would benefit from further biomarker validation via characterisation of additional 'on-phenotype' models, as well as 'off-phenotype' models that are characterised by low phospho-STAT3 expression and P53-wildtype status. 'Off-phenotype' models will help determine the specificity and selectivity of our personalised medicine strategy,

and we would expect the combination of dasatinib and ruxolitinib to be ineffective in these models.

Moreover, while orthotopic *in vivo* models were selected to explore the effects of dasatinib and ruxolitinib on metastatic spread, analysis of the distinct stages of metastasis (invasion, intravasation, dissemination, extravasation and colonization) is needed to better understand the associated mechanisms. Intrasplenic injection of cancer cells can be used to mimic the early stages of liver colonisation, and to assess systemic targeting with dasatinib and ruxolitinib in the presence of circulating tumour cells [804]. Additionally, analysis of cell survival in the blood circulation via collection of circulating tumour cells *in vivo*, or via shear stress assays *in vitro*, could provide further insight into the effects of treatment on tumour cells in circulation. Moreover transendothelial migration assays [805] could be used to identify anti-extravasation effects. Furthermore, examination of extracellular matrix integrity in the liver will determine whether JAK inhibition can remodel the extracellular matrix in metastatic sites as well as primary tumours.

An additional limitation of this work is that although we have used single cell transcriptomics to assess the mechanisms associated with dasatinib and ruxolitinib in distinct cellular populations, we have yet to functionally validate all the identified mechanisms. In particular, we are yet to validate effects seen on metabolic pathways. Future studies may include assessment of glucose metabolism using glucose tolerance tests *in vivo* [806], measuring glycolysis and oxidative phosphorylation in live cells using Seahorse XF24 extracellular flux analyser *in vitro* [807], or performing high throughput metabolomics studies *in vitro* and *in vivo* [411]. Moreover, isolation of individual cancer and stromal cell clusters would enable more refined functional validation, and could be used to identify sensitive and resistant populations to the combination therapy. Furthermore, we will examine the transcriptomic mechanisms associated with the combination of dasatinib and ruxolitinib with gemcitabine and Abraxane, as this therapeutic combination showed the most efficacy *in vivo*.

Lastly, we plan to examine patient cohorts to determine the prevalence of high phospho-STAT3 expression and *TP53* mutations in the patient setting. To do this we will utilise patient tumour microarrays (TMAs) from the ICGC primary operable patient PDAC cohort (n= 200) [3], as well as the Royal North Shore Hospital metastatic cohort (RNSH; n= 54) [83].

In regards to future clinical implementation, dasatinib and ruxolitinib are both clinically approved drugs for use in other cancers [282, 528], and the combination of dasatinib and ruxolitinib is currently showing promising results in phase I/II trials for acute lymphoblastic leukaemia (NCT02494882), and chronic myelogenous leukemia (NCT03654768). However this combination has yet to be combined with chemotherapy in the clinic. Although we see no signs of toxicity *in vivo*, the dosing schedule may need to be optimized to accommodate for side effects of combinations involving more toxic chemotherapies. The use of innovative treatment schedules such as a 'priming regimen' [149] or sequential administration as 'maintenance' therapy [294], may assist in limiting toxicity. We envisage that a future phase I trial combining dasatinib and ruxolitinib with gemcitabine and Abraxane would be performed in the neoadjuvant setting, in order to attain safety and tolerability data, as well as collect tumour tissue for further biomarker validation. Application of the I-PREDICT [88], TARGET [808], study protocols in a similar manner to test clinical efficacy of a molecular recommendation-based treatment involving dasatinib, ruxolitinib and modern chemotherapy, presents the next logical step in order to translate this precision medicine strategy into clinical practice.

In summary, we propose that dasatinib and ruxolitinib deregulates tumour cell and stromal cell signalling, manipulates the extracellular matrix and associated tissue fibrosis, reprograms the immunosuppressive tumour microenvironment, and renders pancreatic tumours more sensitive to cytotoxic drugs while delaying metastatic spread. Collectively, these findings contribute to a better understanding of mechanisms associated with SRC and JAK inhibitors in pancreatic cancer, and may help to develop personalised precision medicine strategies involving combinations of customised agents. Moreover, we hope that the long-term outcomes of this study include

improving the quality of life of patients with pancreatic cancer by minimising side effects, the impacts of ineffective treatment, and by ensuring that appropriate therapy is tailored specifically to the biology of each tumour.

Table 6.1 Overview of clinical studies focused on testing the precision medicine paradigm (adapted from Zimmer *et al.* [809]).

Profiling mode	Author/Trial	Study design	Cancer type	Methods	Median survival (months) matched vs. unmatched	Response (in %)
Next generation sequencing	Rothwell <i>et al.</i> (TARGET) 2019 [810]	prospective matched vs. unmatched	solid	NGS/Foundati on One		PR: 36 vs 0; SD > 3 months: 64 vs 23
	Schwaederle <i>et al.</i> (PREDICT) 2016 [800]	Retrospective	solid	NGS	PFS: 4.0 vs 3.0 $p = .05$;	SD > 6 months/PR/CR: 34.5 vs. 16.1
	Wheler <i>et al.</i> 2016 [811]	prospective matched vs. unmatched	solid	NGS	TTF 2.8 vs 1.9, $p = .001$;	SD > 6 months/PR/CR 19 vs 5 $p = .061$
	Stockley <i>et al.</i> (IMPACT/COMPACT) 2016 [812]	prospective	solid	NGS	OS: 16 vs 13 $p = .10$	ORR: 19 vs 9 $p = .026$
Multi-platform profiling	Tsimberidou <i>et al.</i> 2012 [798]	prospective	solid	PCR, FISH	TTF: 5.2 vs 2.2 $p < .0001$; OS: 13.4 vs. 9.0 $p = .017$	ORR: 27 vs 5 $p < .0001$, SD > 6 months: 23 vs. 10
	Tsimberidou <i>et al.</i> 2014 [813]	prospective	solid	PCR, FISH	PFS: 3.9 vs 2.2 $p = .001$; OS: 11.4 vs. 8.6 $p = .04$	ORR: 12 vs 5 $p < .0001$, SD > 6 months: 16.4 vs 12.3
	Massard <i>et al.</i> (MOSCATO-01) 2017 [814]	prospective	solid	targeted sequencing, aCGH, RNA-seq, WGS	OS: 11.9	ORR: 11, SD: 52; PFS2/PFS1 > 1.3 33
	Bryce <i>et al.</i> 2017 [815]	prospective	hematologic and solid	NGS, CGH, WES		ORR: 8
	Tredan <i>et al.</i> (PROFILER) 2017 [816]	prospective	solid	Targeted exon sequencing, CGH	PFS: 2.8	PR: 13 (0.9% of overall cohort); ORR: 43
	Rodon <i>et al.</i> (WINTHER) 2018 [817]	prospective	solid	NGS, Oligo-arrays	PFS: 2.1	SD > 6 months/P R/CR: 26.2
Meta-analysis	Schwaederle <i>et al.</i> 2015 [818]	meta-analysis (phase I)	hematologic and solid tumours		PFS: 5.9 vs. 2.7 $p < .001$; OS: 13.7 vs. 8.9 $p < .001$	SD: 29.2 vs 6.2 $p < .001$
	Schwaederle <i>et al.</i> 2016 [819]	meta-analysis (phase II)	hematologic and solid tumours		PFS: 5.7 vs. 2.95 $p < .001$	SD: 30.6 vs 4.9 $p < .001$

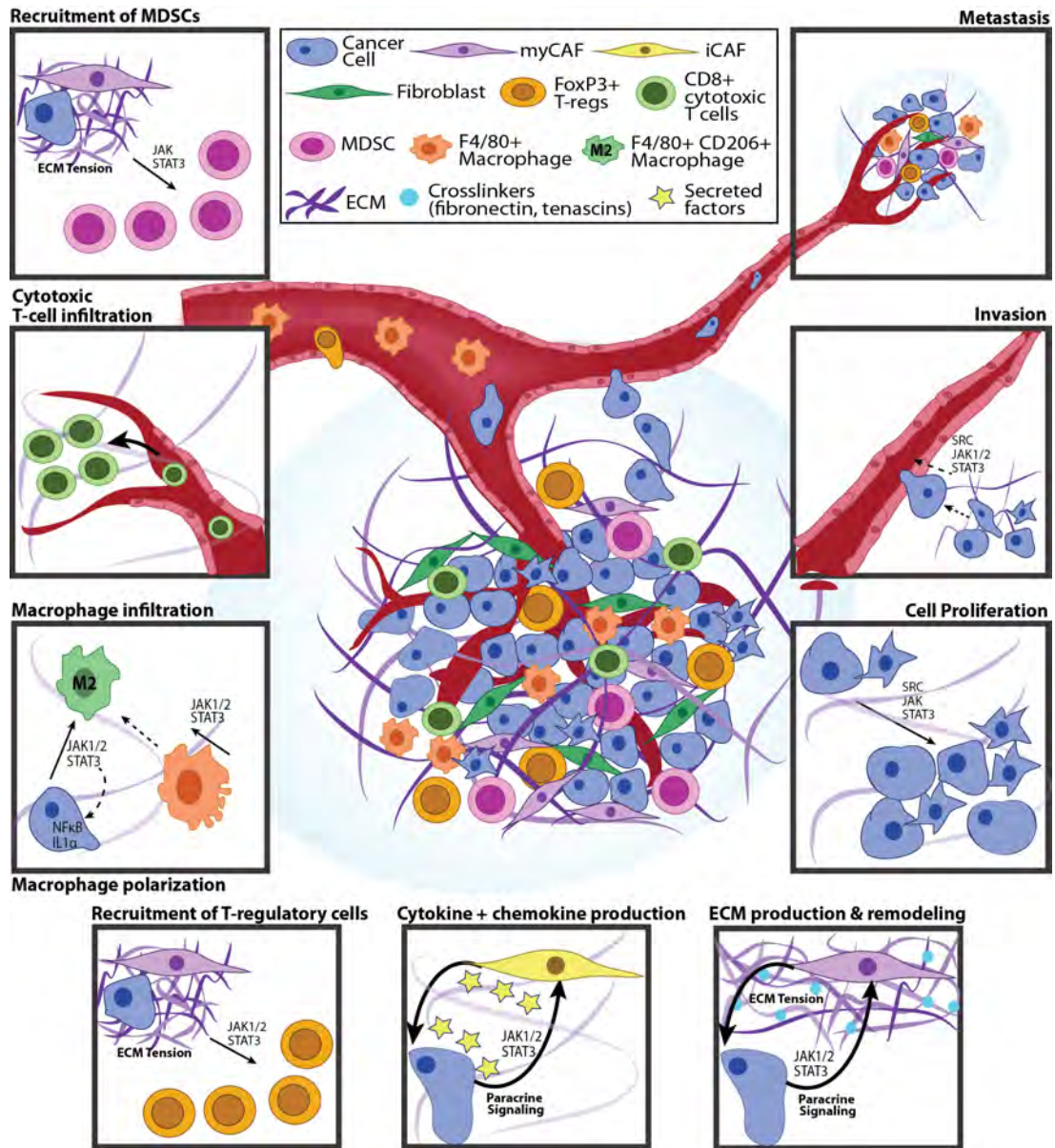
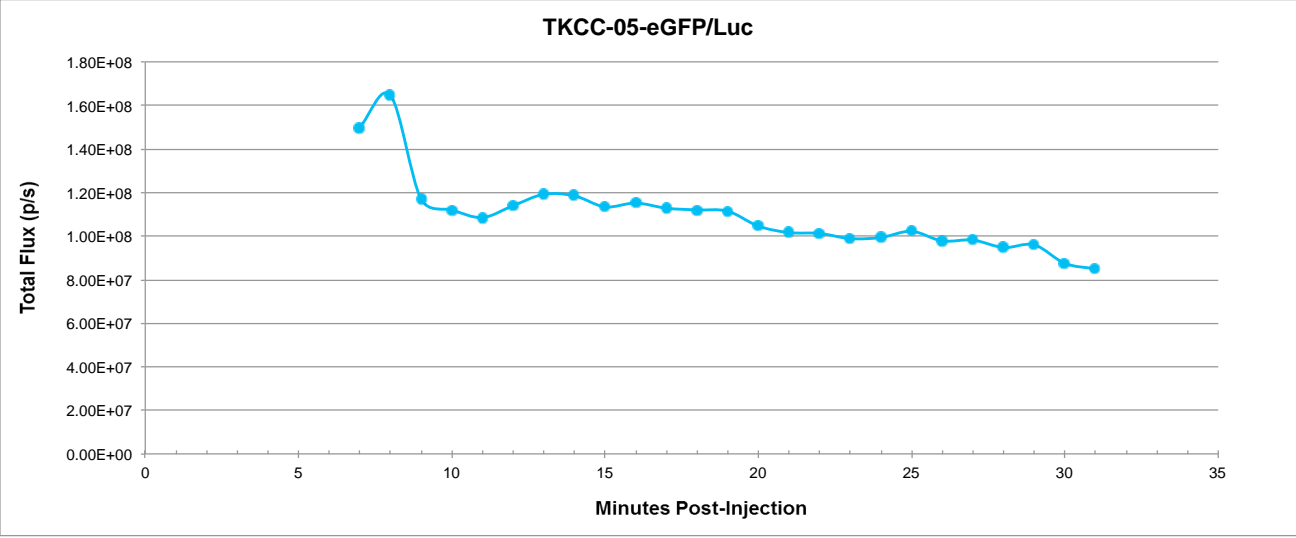


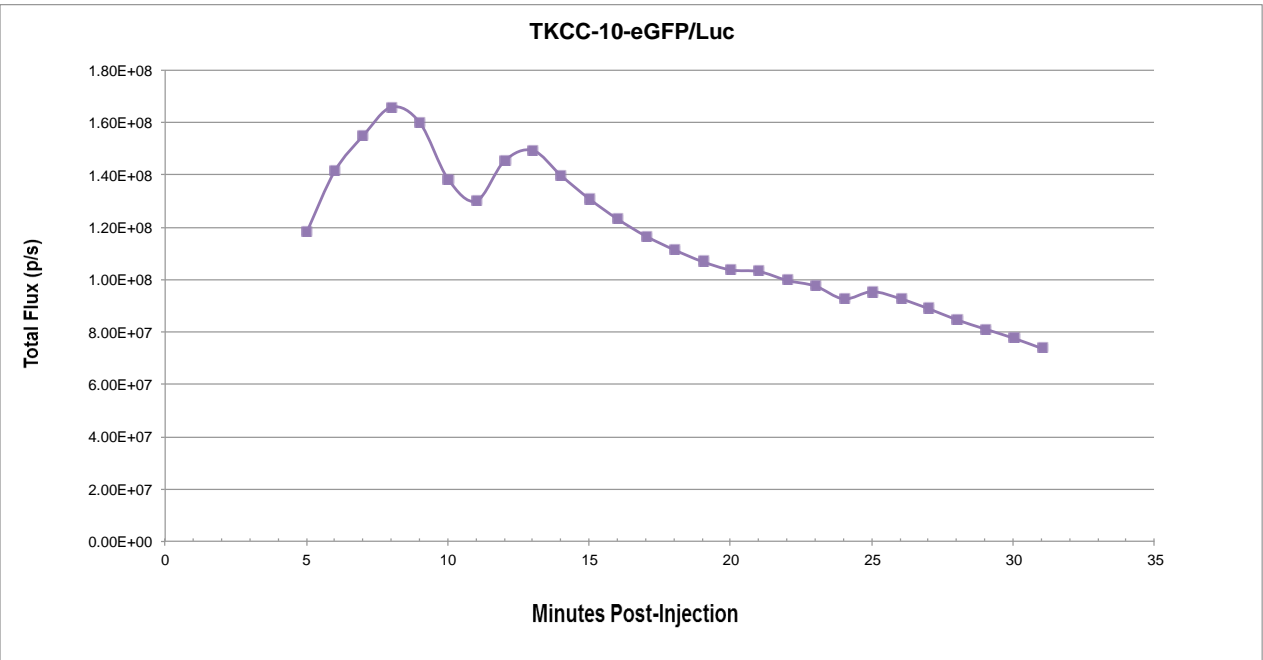
Figure 6.1 Schematic summary of the effects of dasatinib and ruxolitinib on pancreatic tumours and their microenvironment.

Appendix

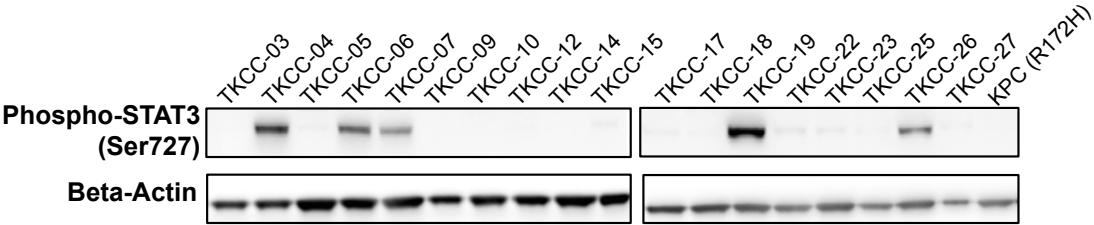
Appendix A: Luciferin kinetics curve for TKCC-05-eGFP/Luc



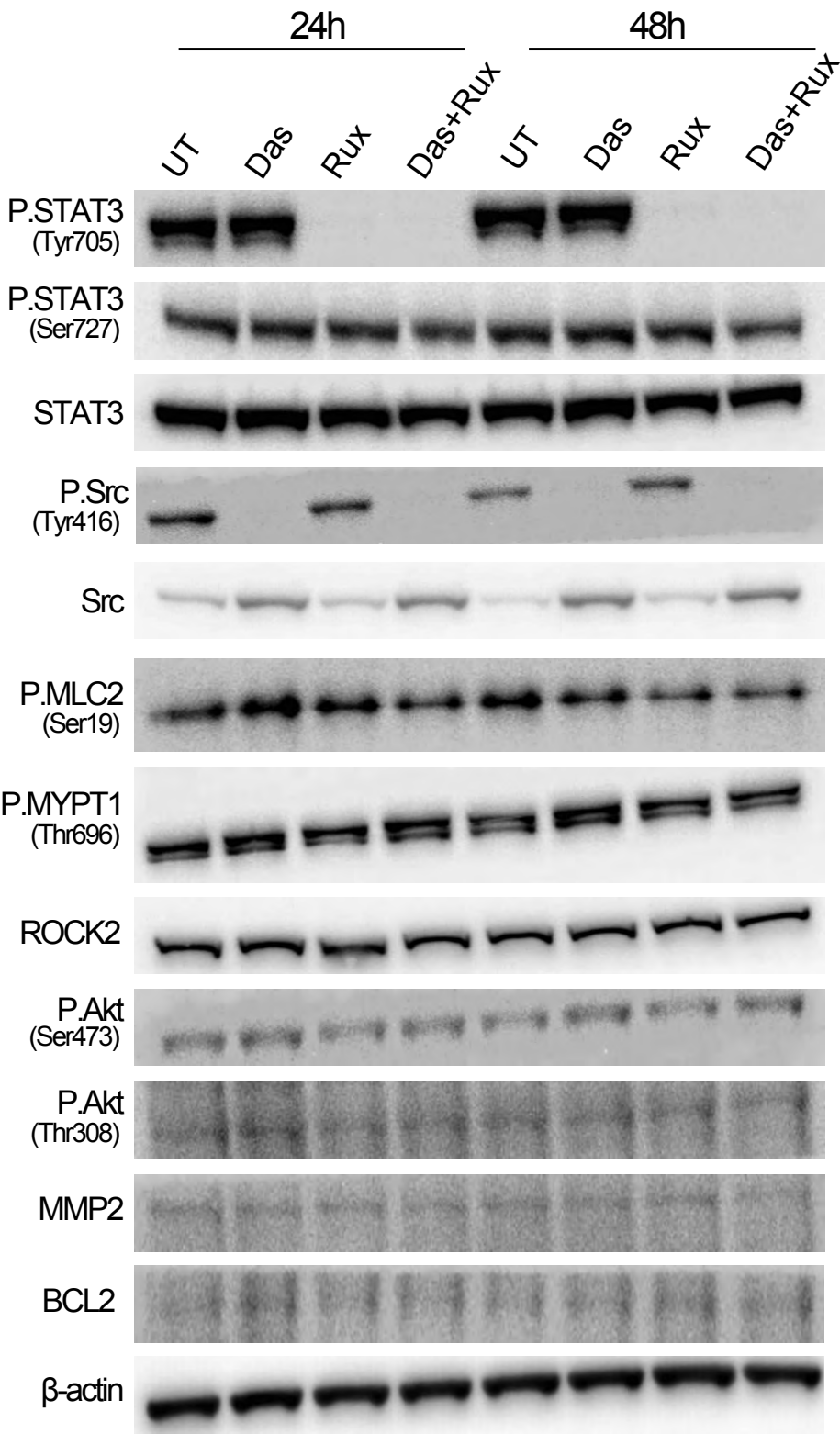
Appendix B: Luciferin kinetics curve for TKCC-10-eGFP/Luc



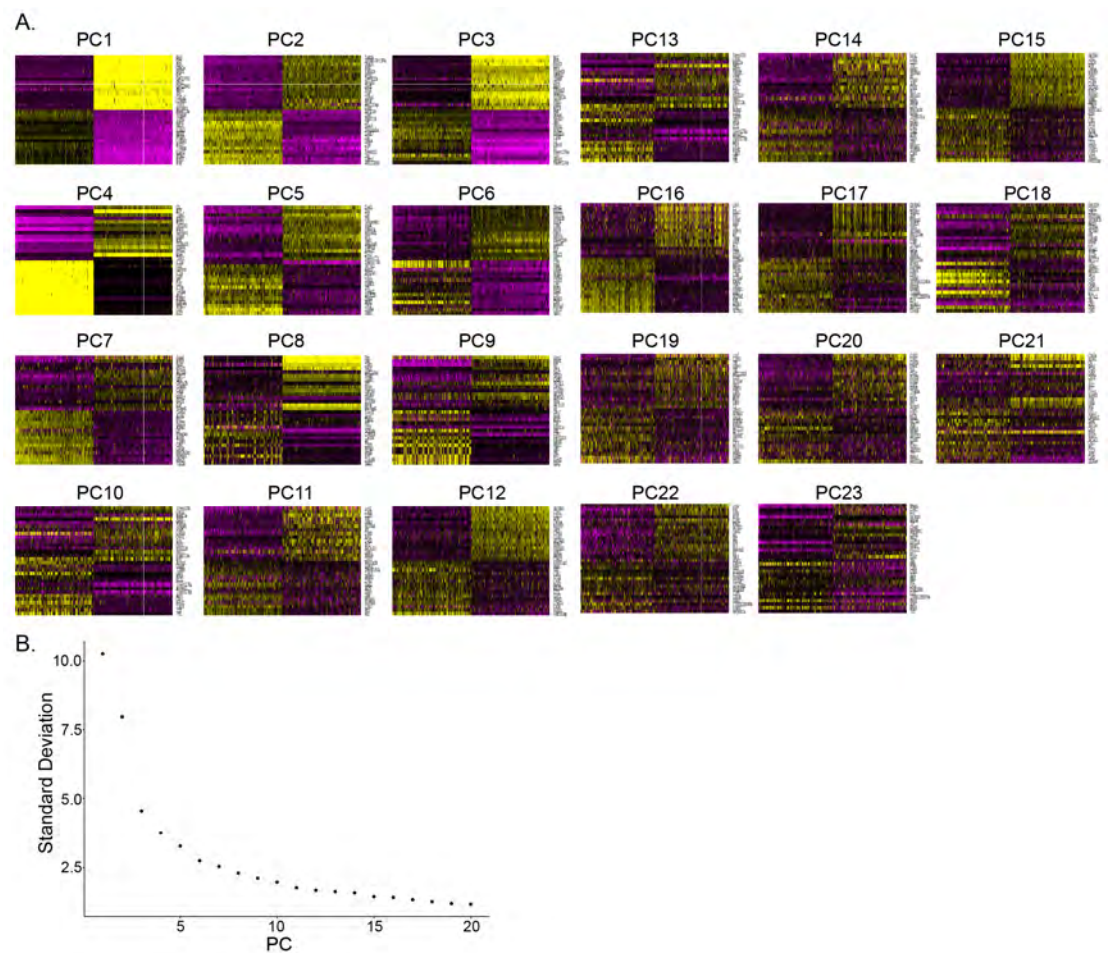
Appendix C: Western blot showing phosphorylated STAT3 (phospho-STAT3 Ser727) and beta-actin levels in pancreatic cancer patient-derived cell lines (TKCC) and cells from the KPC mouse model of pancreatic cancer (KPC R172H).



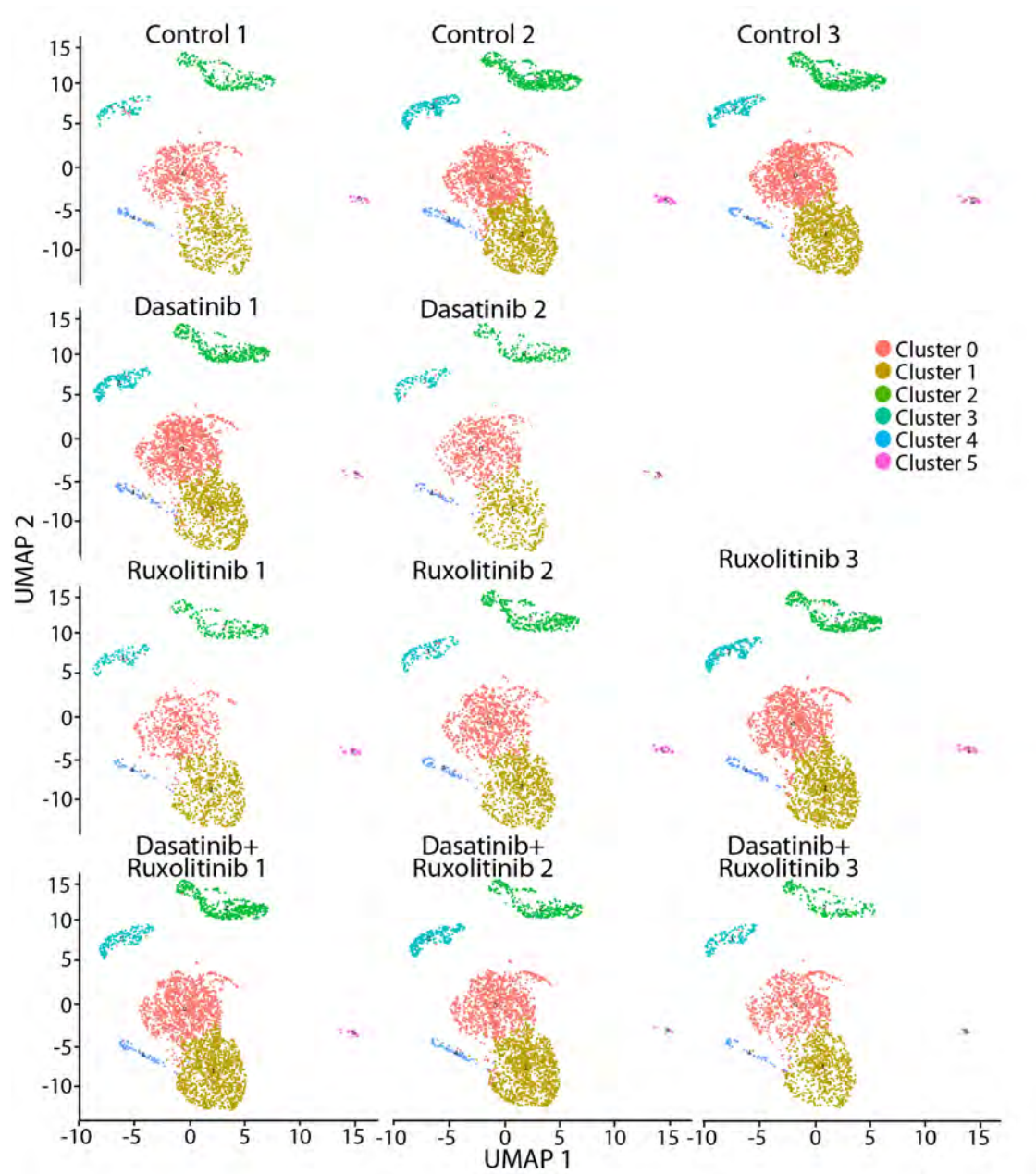
Appendix D: Western blot showing time-dependent effects of dasatinib, ruxolitinib and combination treatment on levels of SRC/STAT3 downstream effectors in TKCC-05 cells.



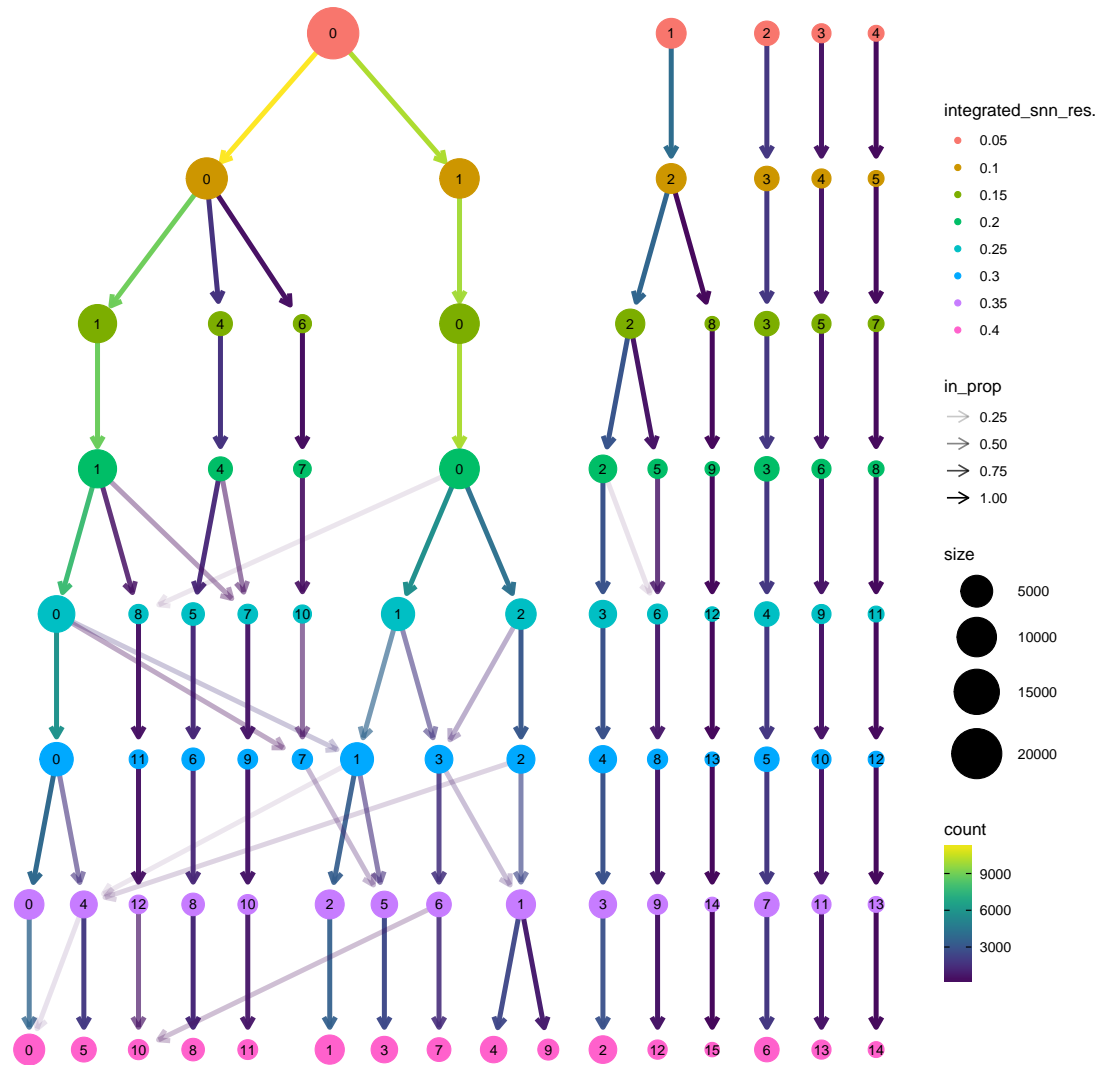
Appendix E: (A) Principal components analysis (PCA) heatmaps of the most differentially expressed genes in KPC organoids. (B) Elbow plot that ranks the principle components based on the percentage variance of each PC.



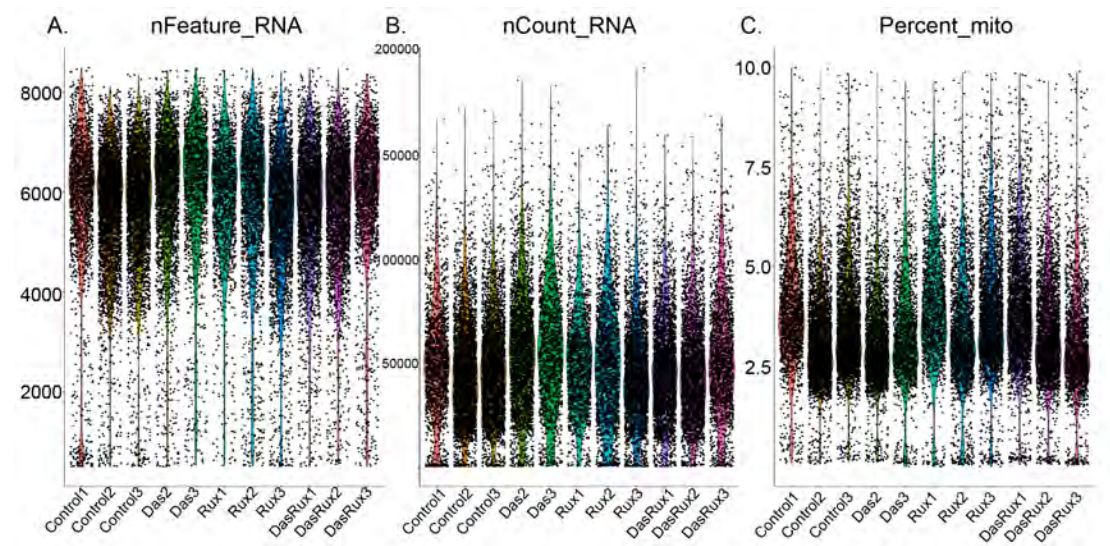
Appendix F: UMAP plots for individual replicates showing the same 6 clusters in each replicate.



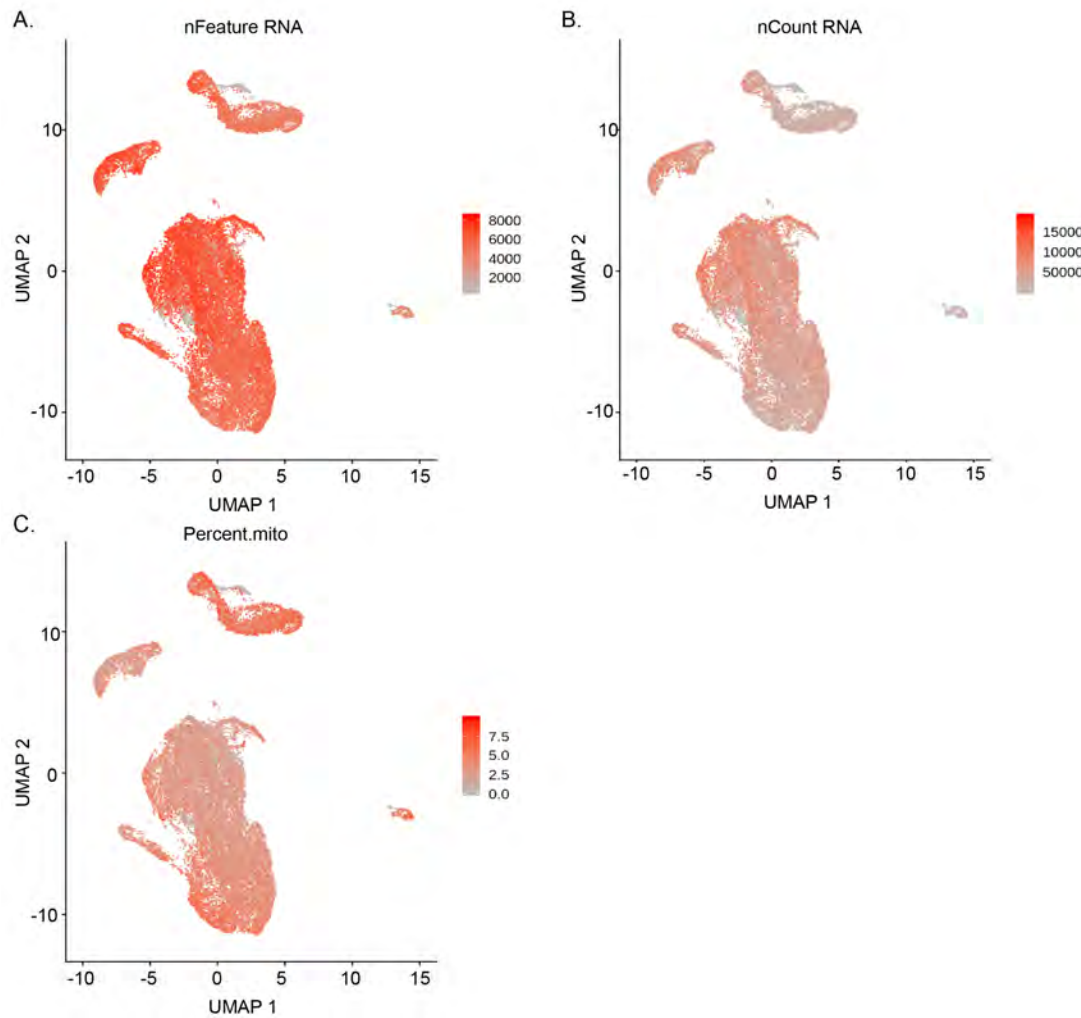
Appendix G: Cluster tree modelling the phylogenic relationship of different clusters at different clustering resolutions.



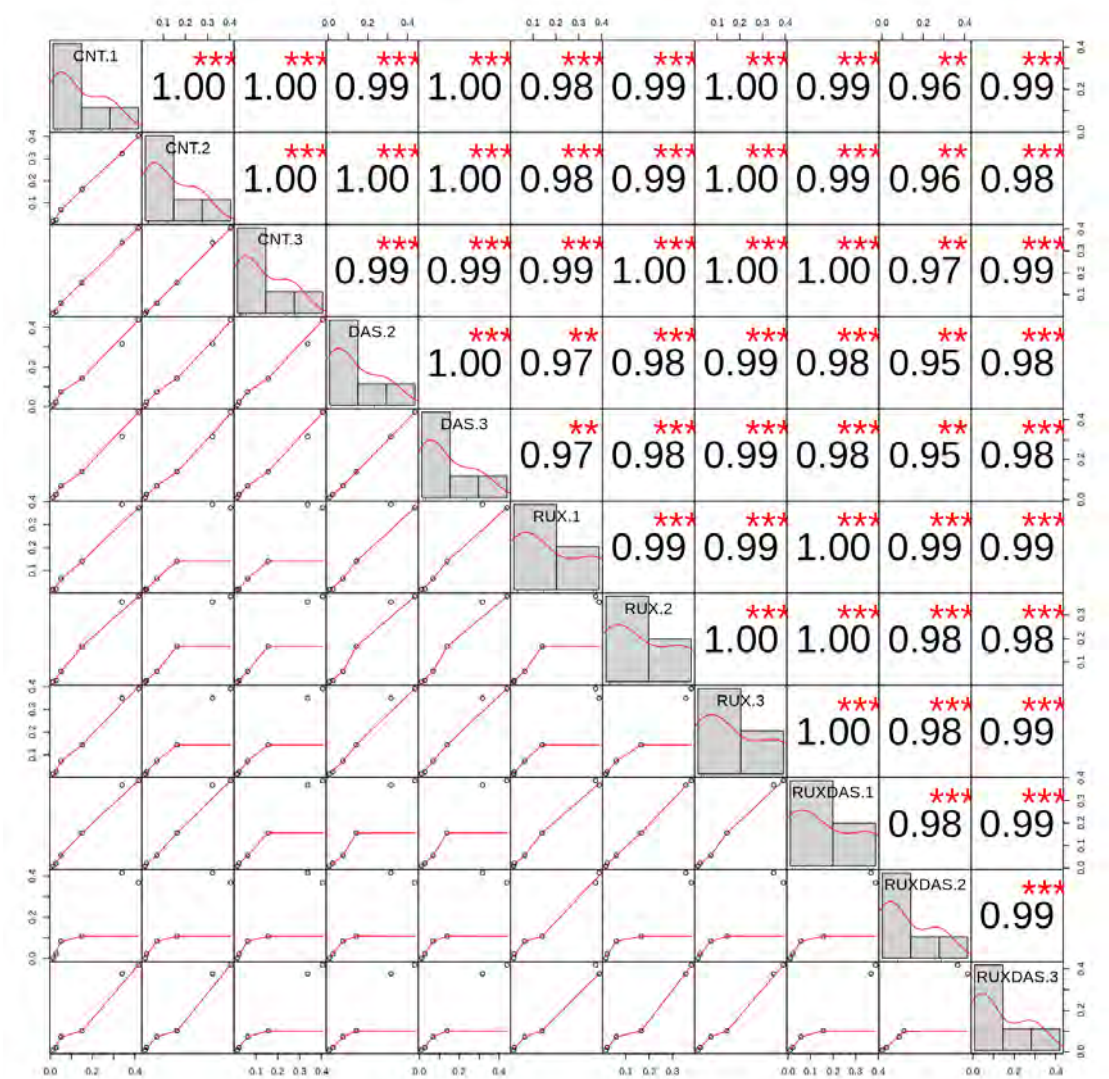
Appendix H: Violin plots of (A) number of unique genes per cell. (B) Total number of molecules detected within a cell. (C) Percentage of reads that map to the mitochondrial genome.



Appendix I: UMAP plots to visualise (A) number of unique genes per cell. (B) Total number of molecules detected within a cell. (C) Percentage of reads that map to the mitochondrial genome.



Appendix J: Pearson's correlation matrix comparing the association between individual replicates. (Pearson's correlation coefficient of 1.0 indicates a perfect positive relationship).



References

1. Rahib, L., et al., *Projecting cancer incidence and deaths to 2030: the unexpected burden of thyroid, liver, and pancreas cancers in the United States*. Cancer Res, 2014. **74**(11): p. 2913-21.
2. Siegel, R.L., K.D. Miller, and A. Jemal, *Cancer Statistics, 2017*. CA Cancer J Clin, 2017. **67**(1): p. 7-30.
3. Bailey, P., et al., *Genomic analyses identify molecular subtypes of pancreatic cancer*. Nature, 2016. **531**(7592): p. 47-52.
4. Waddell, N., et al., *Whole genomes redefine the mutational landscape of pancreatic cancer*. Nature, 2015. **518**(7540): p. 495-501.
5. Witkiewicz, A.K., et al., *Whole-exome sequencing of pancreatic cancer defines genetic diversity and therapeutic targets*. Nat Commun, 2015. **6**: p. 6744.
6. Biankin, A.V., et al., *Pancreatic cancer genomes reveal aberrations in axon guidance pathway genes*. Nature, 2012. **491**(7424): p. 399-405.
7. Collisson, E.A., et al., *Subtypes of pancreatic ductal adenocarcinoma and their differing responses to therapy*. Nat Med, 2011. **17**(4): p. 500-3.
8. Conroy, T., et al., *FOLFIRINOX versus gemcitabine for metastatic pancreatic cancer*. N Engl J Med, 2011. **364**(19): p. 1817-25.
9. Von Hoff, D.D., et al., *Increased survival in pancreatic cancer with nab-paclitaxel plus gemcitabine*. N Engl J Med, 2013. **369**(18): p. 1691-703.
10. Hruban, R.H., et al., *Pancreatic intraepithelial neoplasia: a new nomenclature and classification system for pancreatic duct lesions*. Am J Surg Pathol, 2001. **25**(5): p. 579-86.
11. Hruban, R.H., et al., *Progression model for pancreatic cancer*. Clin Cancer Res, 2000. **6**(8): p. 2969-72.
12. Neuzillet, C., et al., *Pancreatic cancer: French clinical practice guidelines for diagnosis, treatment and follow-up (SNFGE, FFCD, GERCOR, UNICANCER, SFCD, SFED, SFRO, ACHBT, AFC)*. Dig Liver Dis, 2018.
13. Modolell, I., L. Guarner, and J.R. Malagelada, *Vagaries of clinical presentation of pancreatic and biliary tract cancer*. Ann Oncol, 1999. **10 Suppl 4**: p. 82-4.
14. Bakkevold, K.E., B. Arnesjo, and B. Kambestad, *Carcinoma of the pancreas and papilla of Vater: presenting symptoms, signs, and diagnosis related to stage and tumour site. A prospective multicentre trial in 472 patients. Norwegian Pancreatic Cancer Trial*. Scand J Gastroenterol, 1992. **27**(4): p. 317-25.
15. Li, J., et al., *The bidirectional interation between pancreatic cancer and diabetes*. World J Surg Oncol, 2012. **10**: p. 171.
16. Guillén-Ponce, C., et al., *Diagnosis and staging of pancreatic ductal adenocarcinoma*. Clinical and Translational Oncology, 2017. **19**(10): p. 1205-1216.
17. Cohen, J.D., et al., *Combined circulating tumor DNA and protein biomarker-based liquid biopsy for the earlier detection of pancreatic cancers*. Proceedings of the National Academy of Sciences, 2017. **114**(38): p. 10202-10207.
18. Cohen, J.D., et al., *Detection and localization of surgically resectable cancers with a multi-analyte blood test*. Science, 2018. **359**(6378): p. 926-930.

19. Tkach, M. and C. Thery, *Communication by Extracellular Vesicles: Where We Are and Where We Need to Go*. Cell, 2016. **164**(6): p. 1226-1232.
20. Yang, S., et al., *Detection of mutant KRAS and TP53 DNA in circulating exosomes from healthy individuals and patients with pancreatic cancer*. Cancer Biol Ther, 2017. **18**(3): p. 158-165.
21. Allen, P.J., et al., *Multi-institutional Validation Study of the American Joint Commission on Cancer (8th Edition) Changes for T and N Staging in Patients With Pancreatic Adenocarcinoma*. Ann Surg, 2017. **265**(1): p. 185-191.
22. Kamarajah, S.K., et al., *Validation of the American Joint Commission on Cancer (AJCC) 8th Edition Staging System for Patients with Pancreatic Adenocarcinoma: A Surveillance, Epidemiology and End Results (SEER) Analysis*. Ann Surg Oncol, 2017. **24**(7): p. 2023-2030.
23. Bilimoria, K.Y., et al., *Validation of the 6th edition AJCC Pancreatic Cancer Staging System: report from the National Cancer Database*. Cancer, 2007. **110**(4): p. 738-44.
24. Cascinu, S., et al., *Pancreatic cancer: ESMO Clinical Practice Guidelines for diagnosis, treatment and follow-up*. Ann Oncol, 2010. **21 Suppl 5**: p. v55-8.
25. Ammori, B.J. and S. Baghdadi, *Minimally invasive pancreatic surgery: the new frontier?* Curr Gastroenterol Rep, 2006. **8**(2): p. 132-42.
26. Katz, M.H., et al., *Long-term survival after multidisciplinary management of resected pancreatic adenocarcinoma*. Ann Surg Oncol, 2009. **16**(4): p. 836-47.
27. Winter, J.M., et al., *1423 pancreaticoduodenectomies for pancreatic cancer: A single-institution experience*. J Gastrointest Surg, 2006. **10**(9): p. 1199-210; discussion 1210-1.
28. Li, D., et al., *Pancreatic cancer*. Lancet, 2004. **363**(9414): p. 1049-57.
29. Wolfgang, C.L., et al., *Recent progress in pancreatic cancer*. CA Cancer J Clin, 2013. **63**(5): p. 318-48.
30. Dreyer, S.B., et al., *Precision Oncology in Surgery: Patient Selection for Operable Pancreatic Cancer*. Ann Surg, 2018.
31. Dimitrakopoulos, C., et al., *Identification and Validation of a Biomarker Signature in Patients With Resectable Pancreatic Cancer via Genome-Wide Screening for Functional Genetic Variants*. JAMA Surg, 2019: p. e190484.
32. Cunningham, D., et al., *Phase III randomized comparison of gemcitabine versus gemcitabine plus capecitabine in patients with advanced pancreatic cancer*. J Clin Oncol, 2009. **27**(33): p. 5513-8.
33. Khorana, A.A., et al., *Potentially Curable Pancreatic Adenocarcinoma: ASCO Clinical Practice Guideline Update*. Journal of Clinical Oncology, 2019. **0**(0): p. JCO.19.00946.
34. White, R.R. and A.M. Lowy, *Clinical Management: Resectable Disease*. Cancer J, 2017. **23**(6): p. 343-349.
35. Burris, H.A., 3rd, et al., *Improvements in survival and clinical benefit with gemcitabine as first-line therapy for patients with advanced pancreas cancer: a randomized trial*. J Clin Oncol, 1997. **15**(6): p. 2403-13.
36. Poplin, E., et al., *Phase III, randomized study of gemcitabine and oxaliplatin versus gemcitabine (fixed-dose rate infusion) compared with gemcitabine (30-minute infusion) in patients with pancreatic carcinoma E6201: a trial*

- of the Eastern Cooperative Oncology Group. *J Clin Oncol*, 2009. **27**(23): p. 3778-85.
37. Bria, E., et al., *Gemcitabine-based combinations for inoperable pancreatic cancer: have we made real progress? A meta-analysis of 20 phase 3 trials*. *Cancer*, 2007. **110**(3): p. 525-33.
 38. Chin, V., et al., *Chemotherapy and radiotherapy for advanced pancreatic cancer*. *Cochrane Database of Systematic Reviews*, 2018(3).
 39. Sultana, A., et al., *Meta-analyses of chemotherapy for locally advanced and metastatic pancreatic cancer*. *J Clin Oncol*, 2007. **25**(18): p. 2607-15.
 40. Kim, S., et al., *Comparative Effectiveness of nab-Paclitaxel Plus Gemcitabine vs FOLFIRINOX in Metastatic Pancreatic Cancer: A Retrospective Nationwide Chart Review in the United States*. *Adv Ther*, 2018.
 41. Sohal, D.P., P.B. Mangu, and D. Laheru, *Metastatic Pancreatic Cancer: American Society of Clinical Oncology Clinical Practice Guideline Summary*. *J Oncol Pract*, 2017. **13**(4): p. 261-264.
 42. Sohal, D.P.S., et al., *Metastatic Pancreatic Cancer: ASCO Clinical Practice Guideline Update*. *J Clin Oncol*, 2018. **36**(24): p. 2545-2556.
 43. Reni, M., et al., *Nab-paclitaxel plus gemcitabine with or without capecitabine and cisplatin in metastatic pancreatic adenocarcinoma (PACT-19): a randomised phase 2 trial*. *Lancet Gastroenterol Hepatol*, 2018. **3**(10): p. 691-697.
 44. Jones, S., et al., *Core signaling pathways in human pancreatic cancers revealed by global genomic analyses*. *Science*, 2008. **321**(5897): p. 1801-6.
 45. Biankin, A.V., et al., *Genomic Analysis Reveals Aberrations in Chromatin Modification and Axon Guidance Pathway Genes in Pancreatic Cancer*. *Nature*, 2012. **491**: p. 399-405.
 46. Alexandrov, L.B., et al., *Signatures of mutational processes in human cancer*. *Nature*, 2013. **500**(7463): p. 415-21.
 47. Connor, A.A., et al., *Association of Distinct Mutational Signatures With Correlates of Increased Immune Activity in Pancreatic Ductal Adenocarcinoma*. *JAMA Oncol*, 2017. **3**(6): p. 774-83.
 48. Le, D.T., et al., *Mismatch repair deficiency predicts response of solid tumors to PD-1 blockade*. *Science*, 2017. **357**(6349): p. 409-413.
 49. Krishnamurthy, N. and R. Kurzrock, *Targeting the Wnt/beta-catenin pathway in cancer: Update on effectors and inhibitors*. *Cancer Treat Rev*, 2018. **62**: p. 50-60.
 50. Conway, J.R.W., et al., *Combating pancreatic cancer with PI3K pathway inhibitors in the era of personalized medicine*. *Gut*, 2018.
 51. Boyiadzis, M.M., et al., *Significance and implications of FDA approval of pembrolizumab for biomarker-defined disease*. *Journal for ImmunoTherapy of Cancer*, 2018. **6**(1): p. 35.
 52. Gara, R.K., et al., *Slit/Robo pathway: a promising therapeutic target for cancer*. *Drug Discov Today*, 2015. **20**(1): p. 156-64.
 53. Hingorani, S.R., et al., *HALO 202: Randomized Phase II Study of PEGPH20 Plus Nab-Paclitaxel/Gemcitabine Versus Nab-Paclitaxel/Gemcitabine in Patients With Untreated, Metastatic Pancreatic Ductal Adenocarcinoma*. *J Clin Oncol*, 2018. **36**(4): p. 359-366.
 54. Mendt, M., et al., *Generation and testing of clinical-grade exosomes for pancreatic cancer*. *JCI Insight*, 2018. **3**(8).

55. Parkin, A., et al., *The Evolving Understanding of the Molecular and Therapeutic Landscape of Pancreatic Ductal Adenocarcinoma*. Diseases, 2018. **6**(4).
56. Ihle, N.T., et al., *Effect of KRAS oncogene substitutions on protein behavior: implications for signaling and clinical outcome*. J Natl Cancer Inst, 2012. **104**(3): p. 228-39.
57. Cox, A.D., C.J. Der, and M.R. Philips, *Targeting RAS Membrane Association: Back to the Future for Anti-RAS Drug Discovery?* Clin Cancer Res, 2015. **21**(8): p. 1819-27.
58. Cox, A.D., et al., *Drugging the undruggable RAS: Mission possible?* Nat Rev Drug Discov, 2014. **13**(11): p. 828-51.
59. Fakih, M., et al., *Phase 1 study evaluating the safety, tolerability, pharmacokinetics (PK), and efficacy of AMG 510, a novel small molecule KRASG12C inhibitor, in advanced solid tumors*. Journal of Clinical Oncology, 2019. **37**(15_suppl): p. 3003-3003.
60. Jackson, J.H., et al., *Farnesol modification of Kirsten-ras exon 4B protein is essential for transformation*. Proc Natl Acad Sci U S A, 1990. **87**(8): p. 3042-6.
61. Macdonald, J.S., et al., *A phase II study of farnesyl transferase inhibitor R115777 in pancreatic cancer: a Southwest oncology group (SWOG 9924) study*. Invest New Drugs, 2005. **23**(5): p. 485-7.
62. Van Cutsem, E., et al., *Phase III trial of gemcitabine plus tipifarnib compared with gemcitabine plus placebo in advanced pancreatic cancer*. J Clin Oncol, 2004. **22**(8): p. 1430-8.
63. Kazi, A., et al., *Dual farnesyl and geranylgeranyl transferase inhibitor thwarts mutant KRAS-driven patient-derived pancreatic tumors*. Clin Cancer Res, 2019.
64. Blasco, M.T., et al., *Complete Regression of Advanced Pancreatic Ductal Adenocarcinomas upon Combined Inhibition of EGFR and C-RAF*. Cancer Cell, 2019. **35**(4): p. 573-587 e6.
65. Ruess, D.A., et al., *Mutant KRAS-driven cancers depend on PTPN11/SHP2 phosphatase*. Nat Med, 2018. **24**(7): p. 954-960.
66. Waters, A.M. and C.J. Der, *KRAS: The Critical Driver and Therapeutic Target for Pancreatic Cancer*. Cold Spring Harb Perspect Med, 2018. **8**(9).
67. Adhikari, H. and C.M. Counter, *Interrogating the protein interactomes of RAS isoforms identifies PIP5K1A as a KRAS-specific vulnerability*. Nat Commun, 2018. **9**(1): p. 3646.
68. Moore, M.J., et al., *Erlotinib plus gemcitabine compared with gemcitabine alone in patients with advanced pancreatic cancer: a phase III trial of the National Cancer Institute of Canada Clinical Trials Group*. J Clin Oncol, 2007. **25**(15): p. 1960-6.
69. Sinn, M., et al., *CONKO-005: Adjuvant Chemotherapy With Gemcitabine Plus Erlotinib Versus Gemcitabine Alone in Patients After R0 Resection of Pancreatic Cancer: A Multicenter Randomized Phase III Trial*. J Clin Oncol, 2017. **35**(29): p. 3330-3337.
70. Van Cutsem, E., et al., *Phase III trial of bevacizumab in combination with gemcitabine and erlotinib in patients with metastatic pancreatic cancer*. J Clin Oncol, 2009. **27**(13): p. 2231-7.

71. Heinemann, V., et al., *Gemcitabine plus erlotinib followed by capecitabine versus capecitabine plus erlotinib followed by gemcitabine in advanced pancreatic cancer: final results of a randomised phase 3 trial of the 'Arbeitsgemeinschaft Internistische Onkologie' (AIO-PK0104)*. Gut, 2013. **62**(5): p. 751-9.
72. Haas, M., et al., *Efficacy of gemcitabine plus erlotinib in rash-positive patients with metastatic pancreatic cancer selected according to eligibility for FOLFIRINOX: A prospective phase II study of the 'Arbeitsgemeinschaft Internistische Onkologie'*. Eur J Cancer, 2018. **94**: p. 95-103.
73. Boeck, S., et al., *EGFR pathway biomarkers in erlotinib-treated patients with advanced pancreatic cancer: translational results from the randomised, crossover phase 3 trial AIO-PK0104*. Br J Cancer, 2013. **108**(2): p. 469-76.
74. Schultheis, B., et al., *Gemcitabine combined with the monoclonal antibody nimotuzumab is an active first-line regimen in KRAS wildtype patients with locally advanced or metastatic pancreatic cancer: a multicenter, randomized phase IIb study*. Annals of Oncology, 2017. **28**(10): p. 2429-2435.
75. O'Leary, B., R.S. Finn, and N.C. Turner, *Treating cancer with selective CDK4/6 inhibitors*. Nat Rev Clin Oncol, 2016. **13**(7): p. 417-30.
76. Schutte, M., et al., *Abrogation of the Rb/p16 tumor-suppressive pathway in virtually all pancreatic carcinomas*. Cancer Res, 1997. **57**(15): p. 3126-30.
77. Cristofanilli, M., et al., *Fulvestrant plus palbociclib versus fulvestrant plus placebo for treatment of hormone-receptor-positive, HER2-negative metastatic breast cancer that progressed on previous endocrine therapy (PALOMA-3): final analysis of the multicentre, double-blind, phase 3 randomised controlled trial*. Lancet Oncol, 2016. **17**(4): p. 425-39.
78. Finn, R.S., et al., *Results of a randomized phase 2 study of PD 0332991, a cyclin-dependent kinase (CDK) 4/6 inhibitor, in combination with letrozole vs letrozole alone for first-line treatment of ER+/HER2- advanced breast cancer (BC) in Thirty-Fifth Annual CTRC-AACR San Antonio Breast Cancer Symposium-- Dec 4-8, 2012*. 2012, Cancer Research: San Antonio, Texas. p. Supplement 3
79. Patnaik, A., et al., *Efficacy and Safety of Abemaciclib, an Inhibitor of CDK4 and CDK6, for Patients with Breast Cancer, Non-Small Cell Lung Cancer, and Other Solid Tumors*. Cancer Discov, 2016. **6**(7): p. 740-53.
80. Franco, J., et al., *Metabolic Reprogramming of Pancreatic Cancer Mediated by CDK4/6 Inhibition Elicits Unique Vulnerabilities*. Cell Rep, 2016. **14**(5): p. 979-90.
81. Franco, J., A.K. Witkiewicz, and E.S. Knudsen, *CDK4/6 inhibitors have potent activity in combination with pathway selective therapeutic agents in models of pancreatic cancer*. Oncotarget, 2014. **5**(15): p. 6512-25.
82. Chiorean, E.G., et al., *A phase II study of abemaciclib as a monotherapy and in combination with other agents in patients with previously treated metastatic pancreatic ductal adenocarcinoma (PDAC)*. Journal of Clinical Oncology, 2017. **35**(15_suppl): p. TPS4150-TPS4150.
83. Chou, A., et al., *Tailored first-line and second-line CDK4-targeting treatment combinations in mouse models of pancreatic cancer*. Gut, 2018. **67**(12): p. 2142-2155.

84. Liu, T., et al., *CDK4/6-dependent activation of DUB3 regulates cancer metastasis through SNAIL1*. Nat Commun, 2017. **8**: p. 13923.
85. Goel, S., et al., *CDK4/6 inhibition triggers anti-tumour immunity*. Nature, 2017.
86. Deng, J., et al., *CDK4/6 Inhibition Augments Antitumor Immunity by Enhancing T-cell Activation*. Cancer Discov, 2018. **8**(2): p. 216-233.
87. Pishvaian, M.J. and E. Petricoin, 3rd, *Molecular Profiling of Pancreatic Cancer Patients-Response*. Clin Cancer Res, 2018. **24**(24): p. 6612.
88. Sicklick, J.K., et al., *Molecular profiling of cancer patients enables personalized combination therapy: the I-PREDICT study*. Nat Med, 2019. **25**(5): p. 744-750.
89. Lord, C.J. and A. Ashworth, *PARP inhibitors: Synthetic lethality in the clinic*. Science, 2017. **355**(6330): p. 1152-1158.
90. Ford, D., et al., *Risks of cancer in BRCA1-mutation carriers*. Breast Cancer Linkage Consortium. Lancet, 1994. **343**(8899): p. 692-5.
91. Greer, J.B. and D.C. Whitcomb, *Role of BRCA1 and BRCA2 mutations in pancreatic cancer*. Gut, 2007. **56**(5): p. 601-5.
92. Sehdev, A., et al., *Germline and Somatic DNA Damage Repair Gene Mutations and Overall Survival in Metastatic Pancreatic Adenocarcinoma Patients Treated with FOLFIRINOX*. Clin Cancer Res, 2018.
93. Villarroel, M.C., et al., *Personalizing cancer treatment in the age of global genomic analyses: PALB2 gene mutations and the response to DNA damaging agents in pancreatic cancer*. Mol Cancer Ther, 2011. **10**(1): p. 3-8.
94. Heinemann, V., et al., *Randomized phase III trial of gemcitabine plus cisplatin compared with gemcitabine alone in advanced pancreatic cancer*. J Clin Oncol, 2006. **24**(24): p. 3946-52.
95. Heinemann, V., et al., *Gemcitabine and cisplatin in the treatment of advanced or metastatic pancreatic cancer*. Ann Oncol, 2000. **11**(11): p. 1399-403.
96. Heinemann, V., et al., *Increased survival using platinum analog combined with gemcitabine as compared to single-agent gemcitabine in advanced pancreatic cancer: pooled analysis of two randomized trials, the GERCOR/GISCAD intergroup study and a German multicenter study*. Ann Oncol, 2007. **18**(10): p. 1652-9.
97. Sonnenblick, A., et al., *Complete remission, in BRCA2 mutation carrier with metastatic pancreatic adenocarcinoma, treated with cisplatin based therapy*. Cancer Biol Ther, 2011. **12**(3): p. 165-8.
98. Golan, T., et al., *Overall survival and clinical characteristics of pancreatic cancer in BRCA mutation carriers*. Br J Cancer, 2014. **111**(6): p. 1132-8.
99. Kaufman, B., et al., *Olaparib monotherapy in patients with advanced cancer and a germline BRCA1/2 mutation*. J Clin Oncol, 2015. **33**(3): p. 244-50.
100. Golan, T., et al., *Maintenance Olaparib for Germline BRCA-Mutated Metastatic Pancreatic Cancer*. N Engl J Med, 2019. **381**(4): p. 317-327.
101. *Maintenance Rucaparib Controls Some Pancreatic Cancers*. Cancer Discovery, 2019. **9**(6): p. OF4-OF4.
102. Lowery, M.A., et al., *Phase II trial of veliparib in patients with previously treated BRCA-mutated pancreas ductal adenocarcinoma*. Eur J Cancer, 2018. **89**: p. 19-26.

103. Murai, J., et al., *Trapping of PARP1 and PARP2 by Clinical PARP Inhibitors*. Cancer Res, 2012. **72**(21): p. 5588-99.
104. Tempero, M.A., et al., *Pancreatic Adenocarcinoma, Version 2.2017, NCCN Clinical Practice Guidelines in Oncology*. J Natl Compr Canc Netw, 2017. **15**(8): p. 1028-1061.
105. Kindler, H.L., et al., *Olaparib as maintenance treatment following first-line platinum-based chemotherapy (PBC) in patients (pts) with a germline BRCA mutation and metastatic pancreatic cancer (mPC): Phase III POLO trial*. Journal of Clinical Oncology, 2019. **37**(18_suppl): p. LBA4-LBA4.
106. Brahmer, J., et al., *Nivolumab versus Docetaxel in Advanced Squamous-Cell Non-Small-Cell Lung Cancer*. N Engl J Med, 2015. **373**(2): p. 123-35.
107. Wolchok, J.D., et al., *Nivolumab plus ipilimumab in advanced melanoma*. N Engl J Med, 2013. **369**(2): p. 122-33.
108. Royal, R.E., et al., *Phase 2 trial of single agent Ipilimumab (anti-CTLA-4) for locally advanced or metastatic pancreatic adenocarcinoma*. J Immunother, 2010. **33**(8): p. 828-33.
109. Aglietta, M., et al., *A phase I dose escalation trial of tremelimumab (CP-675,206) in combination with gemcitabine in chemotherapy-naïve patients with metastatic pancreatic cancer*. Ann Oncol, 2014. **25**(9): p. 1750-5.
110. Brahmer, J.R., et al., *Safety and activity of anti-PD-L1 antibody in patients with advanced cancer*. N Engl J Med, 2012. **366**(26): p. 2455-65.
111. Le, D.T., et al., *PD-1 Blockade in Tumors with Mismatch-Repair Deficiency*. N Engl J Med, 2015. **372**(26): p. 2509-20.
112. Baretti, M. and D.T. Le, *DNA mismatch repair in cancer*. Pharmacol Ther, 2018. **189**: p. 45-62.
113. Hu, Z.I., et al., *Evaluating Mismatch Repair Deficiency in Pancreatic Adenocarcinoma: Challenges and Recommendations*. Clin Cancer Res, 2018. **24**(6): p. 1326-1336.
114. Vennin, C., et al., *Reshaping the Tumor Stroma for Treatment of Pancreatic Cancer*. Gastroenterology, 2018. **154**(4): p. 820-838.
115. Thomas, D. and P. Radhakrishnan, *Tumor-stromal crosstalk in pancreatic cancer and tissue fibrosis*. Mol Cancer, 2019. **18**(1): p. 14.
116. Byron, A., J.D. Humphries, and M.J. Humphries, *Defining the extracellular matrix using proteomics*. Int J Exp Pathol, 2013. **94**(2): p. 75-92.
117. van der Rest, M. and R. Garrone, *Collagen family of proteins*. FASEB J, 1991. **5**(13): p. 2814-23.
118. Frantz, C., K.M. Stewart, and V.M. Weaver, *The extracellular matrix at a glance*. J Cell Sci, 2010. **123**(Pt 24): p. 4195-200.
119. Levental, K.R., et al., *Matrix crosslinking forces tumor progression by enhancing integrin signaling*. Cell, 2009. **139**(5): p. 891-906.
120. Lu, P., V.M. Weaver, and Z. Werb, *The extracellular matrix: a dynamic niche in cancer progression*. J Cell Biol, 2012. **196**(4): p. 395-406.
121. Rice, A.J., et al., *Matrix stiffness induces epithelial-mesenchymal transition and promotes chemoresistance in pancreatic cancer cells*. Oncogenesis, 2017. **6**(7): p. e352.
122. Laklai, H., et al., *Genotype tunes pancreatic ductal adenocarcinoma tissue tension to induce matricellular fibrosis and tumor progression*. Nat Med, 2016. **22**(5): p. 497-505.

123. Kalluri, R. and M. Zeisberg, *Fibroblasts in cancer*. Nat Rev Cancer, 2006. **6**(5): p. 392-401.
124. Apte, M.V., et al., *Desmoplastic reaction in pancreatic cancer: role of pancreatic stellate cells*. Pancreas, 2004. **29**(3): p. 179-87.
125. Bachem, M.G., et al., *Pancreatic carcinoma cells induce fibrosis by stimulating proliferation and matrix synthesis of stellate cells*. Gastroenterology, 2005. **128**(4): p. 907-21.
126. Vonlaufen, A., et al., *Pancreatic stellate cells: partners in crime with pancreatic cancer cells*. Cancer Res, 2008. **68**(7): p. 2085-93.
127. Bhowmick, N.A., E.G. Neilson, and H.L. Moses, *Stromal fibroblasts in cancer initiation and progression*. Nature, 2004. **432**(7015): p. 332-7.
128. McAnulty, R.J., *Fibroblasts and myofibroblasts: their source, function and role in disease*. Int J Biochem Cell Biol, 2007. **39**(4): p. 666-71.
129. Hayward, S.W., et al., *Malignant transformation in a nontumorigenic human prostatic epithelial cell line*. Cancer Res, 2001. **61**(22): p. 8135-42.
130. Olumi, A.F., et al., *Carcinoma-associated fibroblasts direct tumor progression of initiated human prostatic epithelium*. Cancer Res, 1999. **59**(19): p. 5002-11.
131. Schor, S.L., A.M. Schor, and G. Rushton, *Fibroblasts from cancer patients display a mixture of both foetal and adult-like phenotypic characteristics*. J Cell Sci, 1988. **90 (Pt 3)**: p. 401-7.
132. Schor, S.L., et al., *Adult, foetal and transformed fibroblasts display different migratory phenotypes on collagen gels: evidence for an isoformic transition during foetal development*. J Cell Sci, 1985. **73**: p. 221-34.
133. Watanabe, I., et al., *Advanced pancreatic ductal cancer: fibrotic focus and beta-catenin expression correlate with outcome*. Pancreas, 2003. **26**(4): p. 326-33.
134. Xing, F., J. Saidou, and K. Watabe, *Cancer associated fibroblasts (CAFs) in tumor microenvironment*. Front Biosci (Landmark Ed), 2010. **15**: p. 166-79.
135. Phillips, P., *Pancreatic stellate cells and fibrosis*, in *Pancreatic Cancer and Tumor Microenvironment*, P.J. Grippo and H.G. Munshi, Editors. 2012: Trivandrum (India).
136. Kalluri, R., *The biology and function of fibroblasts in cancer*. Nat Rev Cancer, 2016. **16**(9): p. 582-98.
137. Sato, N., N. Maehara, and M. Goggins, *Gene expression profiling of tumor-stromal interactions between pancreatic cancer cells and stromal fibroblasts*. Cancer Res, 2004. **64**(19): p. 6950-6.
138. Apte, M.V., et al., *A starring role for stellate cells in the pancreatic cancer microenvironment*. Gastroenterology, 2013. **144**(6): p. 1210-9.
139. Menke, A. and G. Adler, *TGFbeta-induced fibrogenesis of the pancreas*. Int J Gastrointest Cancer, 2002. **31**(1-3): p. 41-6.
140. Chu, G.C., et al., *Stromal biology of pancreatic cancer*. J Cell Biochem, 2007. **101**(4): p. 887-907.
141. Ohlund, D., et al., *Distinct populations of inflammatory fibroblasts and myofibroblasts in pancreatic cancer*. J Exp Med, 2017. **214**(3): p. 579-596.
142. Olive, K.P., et al., *Inhibition of Hedgehog signaling enhances delivery of chemotherapy in a mouse model of pancreatic cancer*. Science, 2009. **324**(5933): p. 1457-61.

143. Jacobetz, M.A., et al., *Hyaluronan impairs vascular function and drug delivery in a mouse model of pancreatic cancer*. Gut, 2013. **62**(1): p. 112-20.
144. Provenzano, P.P., et al., *Enzymatic targeting of the stroma ablates physical barriers to treatment of pancreatic ductal adenocarcinoma*. Cancer Cell, 2012. **21**(3): p. 418-29.
145. Elyada, E., et al., *Cross-Species Single-Cell Analysis of Pancreatic Ductal Adenocarcinoma Reveals Antigen-Presenting Cancer-Associated Fibroblasts*. Cancer Discov, 2019. **9**(8): p. 1102-1123.
146. Duluc, C., et al., *Pharmacological targeting of the protein synthesis mTOR/4E-BP1 pathway in cancer-associated fibroblasts abrogates pancreatic tumour chemoresistance*. EMBO Mol Med, 2015. **7**(6): p. 735-53.
147. Biffi, G., et al., *IL1-Induced JAK/STAT Signaling Is Antagonized by TGFbeta to Shape CAF Heterogeneity in Pancreatic Ductal Adenocarcinoma*. Cancer Discov, 2019. **9**(2): p. 282-301.
148. Shang, B., et al., *Deciphering the Key Features of Malignant Tumor Microenvironment for Anti-cancer Therapy*. Cancer Microenviron, 2012. **5**(3): p. 211-23.
149. Vennin, C., et al., *Transient tissue priming via ROCK inhibition uncouples pancreatic cancer progression, sensitivity to chemotherapy, and metastasis*. Sci Transl Med, 2017. **9**(384).
150. Feig, C., et al., *Targeting CXCL12 from FAP-expressing carcinoma-associated fibroblasts synergizes with anti-PD-L1 immunotherapy in pancreatic cancer*. Proc Natl Acad Sci U S A, 2013. **110**(50): p. 20212-7.
151. Mitchem, J.B., et al., *Targeting tumor-infiltrating macrophages decreases tumor-initiating cells, relieves immunosuppression, and improves chemotherapeutic responses*. Cancer Res, 2013. **73**(3): p. 1128-41.
152. Yako, Y.Y., et al., *Cytokines as Biomarkers of Pancreatic Ductal Adenocarcinoma: A Systematic Review*. PLoS One, 2016. **11**(5): p. e0154016.
153. Steele, C.W., et al., *CXCR2 inhibition suppresses acute and chronic pancreatic inflammation*. J Pathol, 2015. **237**(1): p. 85-97.
154. Goedegebuure, P., et al., *Myeloid-derived suppressor cells: general characteristics and relevance to clinical management of pancreatic cancer*. Curr Cancer Drug Targets, 2011. **11**(6): p. 734-51.
155. Er, J.L., et al., *Identification of inhibitors synergizing gemcitabine sensitivity in the squamous subtype of pancreatic ductal adenocarcinoma (PDAC)*. Apoptosis, 2018.
156. Wormann, S.M., et al., *The immune network in pancreatic cancer development and progression*. Oncogene, 2014. **33**(23): p. 2956-67.
157. Moo-Young, T.A., et al., *Tumor-derived TGF-beta mediates conversion of CD4+Foxp3+ regulatory T cells in a murine model of pancreas cancer*. J Immunother, 2009. **32**(1): p. 12-21.
158. Tang, Y., et al., *An increased abundance of tumor-infiltrating regulatory T cells is correlated with the progression and prognosis of pancreatic ductal adenocarcinoma*. PLoS One, 2014. **9**(3): p. e91551.
159. Daniel, S.K., et al., *Hypoxia as a barrier to immunotherapy in pancreatic adenocarcinoma*. Clin Transl Med, 2019. **8**(1): p. 10.

160. Looi, C.K., et al., *Therapeutic challenges and current immunomodulatory strategies in targeting the immunosuppressive pancreatic tumor microenvironment*. J Exp Clin Cancer Res, 2019. **38**(1): p. 162.
161. Gabrilovich, D.I. and S. Nagaraj, *Myeloid-derived suppressor cells as regulators of the immune system*. Nat Rev Immunol, 2009. **9**(3): p. 162-74.
162. Sinha, S. and S.D. Leach, *New insights in the development of pancreatic cancer*. Curr Opin Gastroenterol, 2016.
163. Liu, C., et al., *Expansion of spleen myeloid suppressor cells represses NK cell cytotoxicity in tumor-bearing host*. Blood, 2007. **109**(10): p. 4336-42.
164. Casazza, A., et al., *Tumor stroma: a complexity dictated by the hypoxic tumor microenvironment*. Oncogene, 2014. **33**(14): p. 1743-54.
165. Gajewski, T.F., H. Schreiber, and Y.X. Fu, *Innate and adaptive immune cells in the tumor microenvironment*. Nat Immunol, 2013. **14**(10): p. 1014-22.
166. Lesina, M., et al., *Stat3/Socs3 activation by IL-6 transsignaling promotes progression of pancreatic intraepithelial neoplasia and development of pancreatic cancer*. Cancer Cell, 2011. **19**(4): p. 456-69.
167. Jiang, G.M., et al., *The application of the fibroblast activation protein alpha-targeted immunotherapy strategy*. Oncotarget, 2016. **7**(22): p. 33472-82.
168. Arnold, J.N., et al., *Tumoral immune suppression by macrophages expressing fibroblast activation protein-alpha and heme oxygenase-1*. Cancer Immunol Res, 2014. **2**(2): p. 121-6.
169. Weizman, N., et al., *Macrophages mediate gemcitabine resistance of pancreatic adenocarcinoma by upregulating cytidine deaminase*. Oncogene, 2014. **33**(29): p. 3812-9.
170. Chiossone, L., et al., *Natural killer cell immunotherapies against cancer: checkpoint inhibitors and more*. Semin Immunol, 2017. **31**: p. 55-63.
171. Van Audenaerde, J.R.M., et al., *Natural killer cells and their therapeutic role in pancreatic cancer: A systematic review*. Pharmacol Ther, 2018. **189**: p. 31-44.
172. Janakiram, N.B., et al., *Loss of natural killer T cells promotes pancreatic cancer in LSL-Kras(G12D/+) mice*. Immunology, 2017. **152**(1): p. 36-51.
173. Davis, M., et al., *Effect of pemetrexed on innate immune killer cells and adaptive immune T cells in subjects with adenocarcinoma of the pancreas*. J Immunother, 2012. **35**(8): p. 629-40.
174. Stehelin, D., et al., *DNA related to the transforming gene(s) of avian sarcoma viruses is present in normal avian DNA*. Nature, 1976. **260**(5547): p. 170-3.
175. Chen, Z., et al., *EGFR family and Src family kinase interactions: mechanics matters?* Curr Opin Cell Biol, 2018. **51**: p. 97-102.
176. Chen, Z., et al., *Spatially modulated ephrinA1:EphA2 signaling increases local contractility and global focal adhesion dynamics to promote cell motility*. Proc Natl Acad Sci U S A, 2018. **115**(25): p. E5696-E5705.
177. Morton, J.P., et al., *Dasatinib inhibits the development of metastases in a mouse model of pancreatic ductal adenocarcinoma*. Gastroenterology, 2010. **139**(1): p. 292-303.
178. Je, D.W., et al., *The inhibition of SRC family kinase suppresses pancreatic cancer cell proliferation, migration, and invasion*. Pancreas, 2014. **43**(5): p. 768-76.

179. Ischenko, I., et al., *Effect of Src kinase inhibition on metastasis and tumor angiogenesis in human pancreatic cancer*. *Angiogenesis*, 2007. **10**(3): p. 167-82.
180. Frame, M.C., *Src in cancer: deregulation and consequences for cell behaviour*. *Biochim Biophys Acta*, 2002. **1602**(2): p. 114-30.
181. Thomas, S.M. and J.S. Brugge, *Cellular functions regulated by Src family kinases*. *Annu Rev Cell Dev Biol*, 1997. **13**: p. 513-609.
182. Ishizawar, R. and S.J. Parsons, *c-Src and cooperating partners in human cancer*. *Cancer Cell*, 2004. **6**(3): p. 209-14.
183. Yeatman, T.J., *A renaissance for SRC*. *Nat Rev Cancer*, 2004. **4**(6): p. 470-80.
184. Serrels, A., et al., *Identification of potential biomarkers for measuring inhibition of Src kinase activity in colon cancer cells following treatment with dasatinib*. *Mol Cancer Ther*, 2006. **5**(12): p. 3014-22.
185. Zhang, J., et al., *c-Src phosphorylation and activation of hexokinase promotes tumorigenesis and metastasis*. *Nat Commun*, 2017. **8**: p. 13732.
186. Parkin, A., et al., *Targeting the complexity of Src signalling in the tumour microenvironment of pancreatic cancer: from mechanism to therapy*. *The FEBS Journal*, 2019. **0**(ja).
187. Carragher, N.O., et al., *Calpain 2 and Src dependence distinguishes mesenchymal and amoeboid modes of tumour cell invasion: a link to integrin function*. *Oncogene*, 2006. **25**(42): p. 5726-40.
188. Liu, S.T., et al., *Src as the link between inflammation and cancer*. *Front Physiol*, 2013. **4**: p. 416.
189. Yokoi, K., et al., *Identification and validation of SRC and phospho-SRC family proteins in circulating mononuclear cells as novel biomarkers for pancreatic cancer*. *Transl Oncol*, 2011. **4**(2): p. 83-91.
190. Ramnath, R.D., J. Sun, and M. Bhatia, *Involvement of SRC family kinases in substance P-induced chemokine production in mouse pancreatic acinar cells and its significance in acute pancreatitis*. *J Pharmacol Exp Ther*, 2009. **329**(2): p. 418-28.
191. Lutz, M.P., et al., *Overexpression and activation of the tyrosine kinase Src in human pancreatic carcinoma*. *Biochem Biophys Res Commun*, 1998. **243**(2): p. 503-8.
192. Hakam, A., et al., *Coexpression of IGF-1R and c-Src proteins in human pancreatic ductal adenocarcinoma*. *Dig Dis Sci*, 2003. **48**(10): p. 1972-8.
193. Nuche-Berenguer, B., I. Ramos-Alvarez, and R.T. Jensen, *Src kinases play a novel dual role in acute pancreatitis affecting severity but no role in stimulated enzyme secretion*. *Am J Physiol Gastrointest Liver Physiol*, 2016. **310**(11): p. G1015-27.
194. Aleshin, A. and R.S. Finn, *SRC: a century of science brought to the clinic*. *Neoplasia*, 2010. **12**(8): p. 599-607.
195. Ito, H., et al., *Inhibition of tyrosine kinase Src suppresses pancreatic cancer invasiveness*. *Surgery*, 2003. **134**(2): p. 221-6.
196. Nagaraj, N.S., et al., *Targeted inhibition of SRC kinase signaling attenuates pancreatic tumorigenesis*. *Mol Cancer Ther*, 2010. **9**(8): p. 2322-32.
197. Trevino, J.G., et al., *Inhibition of SRC expression and activity inhibits tumor progression and metastasis of human pancreatic adenocarcinoma cells in an orthotopic nude mouse model*. *Am J Pathol*, 2006. **168**(3): p. 962-72.

198. Yezhelyev, M.V., et al., *Inhibition of SRC tyrosine kinase as treatment for human pancreatic cancer growing orthotopically in nude mice*. Clin Cancer Res, 2004. **10**(23): p. 8028-36.
199. Duxbury, M.S., et al., *Inhibition of SRC tyrosine kinase impairs inherent and acquired gemcitabine resistance in human pancreatic adenocarcinoma cells*. Clin Cancer Res, 2004. **10**(7): p. 2307-18.
200. Desgrosellier, J.S. and D.A. Cheresh, *Integrins in cancer: biological implications and therapeutic opportunities*. Nat Rev Cancer, 2010. **10**(1): p. 9-22.
201. Samuel, M.S., et al., *Actomyosin-mediated cellular tension drives increased tissue stiffness and beta-catenin activation to induce epidermal hyperplasia and tumor growth*. Cancer Cell, 2011. **19**(6): p. 776-91.
202. Ibbetson, S.J., et al., *Mechanotransduction pathways promoting tumor progression are activated in invasive human squamous cell carcinoma*. Am J Pathol, 2013. **183**(3): p. 930-7.
203. Timpson, P., et al., *Coordination of cell polarization and migration by the Rho family GTPases requires Src tyrosine kinase activity*. Curr Biol, 2001. **11**(23): p. 1836-46.
204. Hamidi, H., M. Pietila, and J. Ivaska, *The complexity of integrins in cancer and new scopes for therapeutic targeting*. Br J Cancer, 2016. **115**(9): p. 1017-1023.
205. Paszek, M.J., et al., *Tensional homeostasis and the malignant phenotype*. Cancer Cell, 2005. **8**(3): p. 241-54.
206. Carter, A., *Integrins as Target: First Phase III Trial Launches, but Questions Remain*. JNCI: Journal of the National Cancer Institute, 2010. **102**(10): p. 675-677.
207. Tod, J., et al., *Pro-migratory and TGF-beta-activating functions of alphavbeta6 integrin in pancreatic cancer are differentially regulated via an Eps8-dependent GTPase switch*. J Pathol, 2017. **243**(1): p. 37-50.
208. Krebs, A.M., et al., *The EMT-activator Zeb1 is a key factor for cell plasticity and promotes metastasis in pancreatic cancer*. Nat Cell Biol, 2017. **19**(5): p. 518-529.
209. David, C.J., et al., *TGF-beta Tumor Suppression through a Lethal EMT*. Cell, 2016. **164**(5): p. 1015-30.
210. Moore, K.M., et al., *Therapeutic targeting of integrin alphavbeta6 in breast cancer*. J Natl Cancer Inst, 2014. **106**(8).
211. Croucher, D.R., et al., *Revisiting the biological roles of PAI2 (SERPINB2) in cancer*. Nat Rev Cancer, 2008. **8**(7): p. 535-45.
212. Harris, N.L.E., et al., *SerpinaB2 regulates stromal remodelling and local invasion in pancreatic cancer*. Oncogene, 2017. **36**(30): p. 4288-4298.
213. Zhu, G.H., et al., *Expression and prognostic significance of CD151, c-Met, and integrin alpha3/alpha6 in pancreatic ductal adenocarcinoma*. Dig Dis Sci, 2011. **56**(4): p. 1090-8.
214. Franco-Barraza, J., et al., *Matrix-regulated integrin alphavbeta5 maintains alpha5beta1-dependent desmoplastic traits prognostic of neoplastic recurrence*. Elife, 2017. **6**.
215. Seguin, L., et al., *Integrins and cancer: regulators of cancer stemness, metastasis, and drug resistance*. Trends Cell Biol, 2015. **25**(4): p. 234-40.

216. Hsia, D.A., et al., *Differential regulation of cell motility and invasion by FAK*. J Cell Biol, 2003. **160**(5): p. 753-67.
217. Jiang, H., et al., *Targeting focal adhesion kinase renders pancreatic cancers responsive to checkpoint immunotherapy*. Nat Med, 2016. **22**(8): p. 851-60.
218. Sulzmaier, F.J., C. Jean, and D.D. Schlaepfer, *FAK in cancer: mechanistic findings and clinical applications*. Nat Rev Cancer, 2014. **14**(9): p. 598-610.
219. Kong, D.B., F. Chen, and N. Sima, *Focal adhesion kinases crucially regulate TGFbeta-induced migration and invasion of bladder cancer cells via Src kinase and E-cadherin*. Onco Targets Ther, 2017. **10**: p. 1783-1792.
220. Schlaepfer, D.D. and S.K. Mitra, *Multiple connections link FAK to cell motility and invasion*. Curr Opin Genet Dev, 2004. **14**(1): p. 92-101.
221. Timpson, P., et al., *Spatial regulation of RhoA activity during pancreatic cancer cell invasion driven by mutant p53*. Cancer Res, 2011. **71**(3): p. 747-57.
222. Nobis, M., et al., *A RhoA-FRET Biosensor Mouse for Intravital Imaging in Normal Tissue Homeostasis and Disease Contexts*. Cell Rep, 2017. **21**(1): p. 274-288.
223. Serrels, A. and M.C. Frame, *FAK goes nuclear to control antitumor immunity-a new target in cancer immuno-therapy*. Oncoimmunology, 2016. **5**(4): p. e1119356.
224. Kanteti, R., et al., *Focal adhesion kinase a potential therapeutic target for pancreatic cancer and malignant pleural mesothelioma*. Cancer Biol Ther, 2018. **19**(4): p. 316-327.
225. Stokes, J.B., et al., *Inhibition of focal adhesion kinase by PF-562,271 inhibits the growth and metastasis of pancreatic cancer concomitant with altering the tumor microenvironment*. Mol Cancer Ther, 2011. **10**(11): p. 2135-45.
226. Tavora, B., et al., *Endothelial-cell FAK targeting sensitizes tumours to DNA-damaging therapy*. Nature, 2014. **514**(7520): p. 112-6.
227. Zhao, X.K., et al., *Focal Adhesion Kinase Regulates Fibroblast Migration via Integrin beta-1 and Plays a Central Role in Fibrosis*. Sci Rep, 2016. **6**: p. 19276.
228. Serrels, A., et al., *Nuclear FAK controls chemokine transcription, Tregs, and evasion of anti-tumor immunity*. Cell, 2015. **163**(1): p. 160-73.
229. Burridge, K., *Focal adhesions: a personal perspective on a half century of progress*. FEBS J, 2017. **284**(20): p. 3355-3361.
230. Romanova, L.Y. and J.F. Mushinski, *Central role of paxillin phosphorylation in regulation of LFA-1 integrins activity and lymphocyte migration*. Cell Adh Migr, 2011. **5**(6): p. 457-62.
231. Chin, V.T., et al., *Rho-associated kinase signalling and the cancer microenvironment: novel biological implications and therapeutic opportunities*. Expert Rev Mol Med, 2015. **17**: p. e17.
232. Pajic, M., et al., *The dynamics of Rho GTPase signaling and implications for targeting cancer and the tumor microenvironment*. Small GTPases, 2015. **6**(2): p. 123-33.
233. Rath, N., et al., *ROCK signaling promotes collagen remodeling to facilitate invasive pancreatic ductal adenocarcinoma tumor cell growth*. EMBO Mol Med, 2017. **9**(2): p. 198-218.

234. Kagawa, Y., et al., *Cell cycle-dependent Rho GTPase activity dynamically regulates cancer cell motility and invasion in vivo*. PLoS One, 2013. **8**(12): p. e83629.
235. Rodriguez-Hernandez, I., et al., *Rho, ROCK and actomyosin contractility in metastasis as drug targets*. F1000Res, 2016. **5**.
236. Rath, N., et al., *Rho Kinase Inhibition by AT13148 Blocks Pancreatic Ductal Adenocarcinoma Invasion and Tumor Growth*. Cancer Res, 2018. **78**(12): p. 3321-3336.
237. Huveneers, S. and E.H. Danen, *Adhesion signaling - crosstalk between integrins, Src and Rho*. J Cell Sci, 2009. **122**(Pt 8): p. 1059-69.
238. Joshi, B., et al., *Phosphorylated caveolin-1 regulates Rho/ROCK-dependent focal adhesion dynamics and tumor cell migration and invasion*. Cancer Res, 2008. **68**(20): p. 8210-20.
239. Sadok, A., et al., *Rho kinase inhibitors block melanoma cell migration and inhibit metastasis*. Cancer Res, 2015. **75**(11): p. 2272-84.
240. Massihnia, D., et al., *Triple negative breast cancer: shedding light onto the role of pi3k/akt/mtor pathway*. Oncotarget, 2016. **7**(37): p. 60712-60722.
241. Liu, P., et al., *Targeting the phosphoinositide 3-kinase pathway in cancer*. Nat Rev Drug Discov, 2009. **8**(8): p. 627-44.
242. Conway, J.R., et al., *Combating pancreatic cancer with PI3K pathway inhibitors in the era of personalised medicine*. Gut, 2018: p. gutjnl-2018-316822.
243. Mayer, I.A. and C.L. Arteaga, *The PI3K/AKT Pathway as a Target for Cancer Treatment*. Annu Rev Med, 2016. **67**: p. 11-28.
244. Schlieman, M.G., et al., *Incidence, mechanism and prognostic value of activated AKT in pancreas cancer*. Br J Cancer, 2003. **89**(11): p. 2110-5.
245. Garrido-Laguna, I., et al., *N of 1 case reports of exceptional responders accrued from pancreatic cancer patients enrolled in first-in-man studies from 2002 through 2012*. Oncoscience, 2015. **2**(3): p. 285-93.
246. Dancey, J., *mTOR signaling and drug development in cancer*. Nat Rev Clin Oncol, 2010. **7**(4): p. 209-19.
247. Manning, B.D. and L.C. Cantley, *AKT/PKB signaling: navigating downstream*. Cell, 2007. **129**(7): p. 1261-74.
248. Murthy, D., K.S. Attri, and P.K. Singh, *Phosphoinositide 3-Kinase Signaling Pathway in Pancreatic Ductal Adenocarcinoma Progression, Pathogenesis, and Therapeutics*. Front Physiol, 2018. **9**: p. 335.
249. Thillai, K., et al., *Deciphering the link between PI3K and PAK: An opportunity to target key pathways in pancreatic cancer?* Oncotarget, 2017. **8**(8): p. 14173-14191.
250. Baer, R., et al., *Implication of PI3K/Akt pathway in pancreatic cancer: When PI3K isoforms matter?* Adv Biol Regul, 2015. **59**: p. 19-35.
251. Kennedy, A.L., et al., *Activation of the PIK3CA/AKT pathway suppresses senescence induced by an activated RAS oncogene to promote tumorigenesis*. Mol Cell, 2011. **42**(1): p. 36-49.
252. Conway, J.R.W., et al., *Intravital Imaging to Monitor Therapeutic Response in Moving Hypoxic Regions Resistant to PI3K Pathway Targeting in Pancreatic Cancer*. Cell Rep, 2018. **23**(11): p. 3312-3326.
253. Irby, R.B., et al., *Activating SRC mutation in a subset of advanced human colon cancers*. Nat Genet, 1999. **21**(2): p. 187-90.

254. Daigo, Y., et al., *Absence of genetic alteration at codon 531 of the human c-src gene in 479 advanced colorectal cancers from Japanese and Caucasian patients*. Cancer Res, 1999. **59**(17): p. 4222-4.
255. Laghi, L., et al., *Lack of mutation at codon 531 of SRC in advanced colorectal cancers from Italian patients*. Br J Cancer, 2001. **84**(2): p. 196-8.
256. Siveen, K.S., et al., *Role of Non Receptor Tyrosine Kinases in Hematological Malignances and its Targeting by Natural Products*. Mol Cancer, 2018. **17**(1): p. 31.
257. Cerami, E., et al., *The cBio cancer genomics portal: an open platform for exploring multidimensional cancer genomics data*. Cancer Discov, 2012. **2**(5): p. 401-4.
258. Gao, J., et al., *Integrative analysis of complex cancer genomics and clinical profiles using the cBioPortal*. Sci Signal, 2013. **6**(269): p. pl1.
259. Ku, M., et al., *Src family kinases and their role in hematological malignancies*. Leuk Lymphoma, 2015. **56**(3): p. 577-86.
260. Donahue, T.R., et al., *Integrative survival-based molecular profiling of human pancreatic cancer*. Clin Cancer Res, 2012. **18**(5): p. 1352-63.
261. Kelber, J.A., et al., *KRas induces a Src/PEAK1/ErbB2 kinase amplification loop that drives metastatic growth and therapy resistance in pancreatic cancer*. Cancer Res, 2012. **72**(10): p. 2554-64.
262. Malric, L., et al., *Interest of integrins targeting in glioblastoma according to tumor heterogeneity and cancer stem cell paradigm: an update*. Oncotarget, 2017. **8**(49): p. 86947-86968.
263. Ren, B., et al., *Analysis of integrin alpha7 mutations in prostate cancer, liver cancer, glioblastoma multiforme, and leiomyosarcoma*. J Natl Cancer Inst, 2007. **99**(11): p. 868-80.
264. Burkin, D.J. and T.M. Fontelonga, *Mesothelioma cells breaking bad: loss of integrin alpha7 promotes cell motility and poor clinical outcomes in patients*. J Pathol, 2015. **237**(3): p. 282-4.
265. Laszlo, V., et al., *Epigenetic down-regulation of integrin alpha7 increases migratory potential and confers poor prognosis in malignant pleural mesothelioma*. J Pathol, 2015. **237**(2): p. 203-14.
266. International Cancer Genome, C., et al., *International network of cancer genome projects*. Nature, 2010. **464**(7291): p. 993-8.
267. Ben-David, U., et al., *Genetic and transcriptional evolution alters cancer cell line drug response*. Nature, 2018. **560**(7718): p. 325-330.
268. Stewart, R.L. and K.L. O'Connor, *Clinical significance of the integrin alpha6beta4 in human malignancies*. Lab Invest, 2015. **95**(9): p. 976-86.
269. Lee, B.Y., et al., *FAK signaling in human cancer as a target for therapeutics*. Pharmacol Ther, 2015. **146**: p. 132-49.
270. Zhang, Y., et al., *A Pan-Cancer Proteogenomic Atlas of PI3K/AKT/mTOR Pathway Alterations*. Cancer Cell, 2017. **31**(6): p. 820-832 e3.
271. Zhou, B., et al., *Somatic Mutations and Splicing Variants of Focal Adhesion Kinase in Non-Small Cell Lung Cancer*. J Natl Cancer Inst, 2018. **110**(2).
272. Payne, S.N., et al., *PIK3CA mutations can initiate pancreatic tumorigenesis and are targetable with PI3K inhibitors*. Oncogenesis, 2015. **4**: p. e169.
273. Ying, H., et al., *PTEN is a major tumor suppressor in pancreatic ductal adenocarcinoma and regulates an NF-kappaB-cytokine network*. Cancer Discov, 2011. **1**(2): p. 158-69.

274. Soria, J.C., et al., *A phase I, pharmacokinetic and pharmacodynamic study of GSK2256098, a focal adhesion kinase inhibitor, in patients with advanced solid tumors*. Ann Oncol, 2016. **27**(12): p. 2268-2274.
275. Quan, M., et al., *Merlin/NF2 Suppresses Pancreatic Tumor Growth and Metastasis by Attenuating the FOXM1-Mediated Wnt/beta-Catenin Signaling*. Cancer Res, 2015. **75**(22): p. 4778-4789.
276. Yu, I.S. and W.Y. Cheung, *A Contemporary Review of the Treatment Landscape and the Role of Predictive and Prognostic Biomarkers in Pancreatic Adenocarcinoma*. Can J Gastroenterol Hepatol, 2018. **2018**: p. 1863535.
277. Patel, A., et al., *Novel roles of Src in cancer cell epithelial-to-mesenchymal transition, vascular permeability, microinvasion and metastasis*. Life Sci, 2016. **157**: p. 52-61.
278. Rajeshkumar, N.V., et al., *Antitumor effects and biomarkers of activity of AZD0530, a Src inhibitor, in pancreatic cancer*. Clin Cancer Res, 2009. **15**(12): p. 4138-46.
279. George, T.J., Jr., J.G. Trevino, and C. Liu, *Src inhibition is still a relevant target in pancreatic cancer*. Oncologist, 2014. **19**(2): p. 211.
280. Messersmith, W.A., et al., *Efficacy and pharmacodynamic effects of bosutinib (SKI-606), a Src/Abl inhibitor, in freshly generated human pancreas cancer xenografts*. Mol Cancer Ther, 2009. **8**(6): p. 1484-93.
281. Demetri, G.D., et al., *Phase I dose-escalation and pharmacokinetic study of dasatinib in patients with advanced solid tumors*. Clin Cancer Res, 2009. **15**(19): p. 6232-40.
282. Khoury, H.J., et al., *Dasatinib treatment for Philadelphia chromosome-positive leukemias: practical considerations*. Cancer, 2009. **115**(7): p. 1381-94.
283. Lombardo, L.J., et al., *Discovery of N-(2-chloro-6-methyl- phenyl)-2-(6-(4-(2-hydroxyethyl)- piperazin-1-yl)-2-methylpyrimidin-4- ylamino)thiazole-5-carboxamide (BMS-354825), a dual Src/Abl kinase inhibitor with potent antitumor activity in preclinical assays*. J Med Chem, 2004. **47**(27): p. 6658-61.
284. Nam, S., et al., *Action of the Src family kinase inhibitor, dasatinib (BMS-354825), on human prostate cancer cells*. Cancer Res, 2005. **65**(20): p. 9185-9.
285. Montero, J.C., et al., *Inhibition of SRC family kinases and receptor tyrosine kinases by dasatinib: possible combinations in solid tumors*. Clin Cancer Res, 2011. **17**(17): p. 5546-52.
286. Park, S.I., et al., *Targeting SRC family kinases inhibits growth and lymph node metastases of prostate cancer in an orthotopic nude mouse model*. Cancer Res, 2008. **68**(9): p. 3323-33.
287. Abbas, R., et al., *A phase I ascending single-dose study of the safety, tolerability, and pharmacokinetics of bosutinib (SKI-606) in healthy adult subjects*. Cancer Chemother Pharmacol, 2012. **69**(1): p. 221-7.
288. Campone, M., et al., *Phase II study of single-agent bosutinib, a Src/Abl tyrosine kinase inhibitor, in patients with locally advanced or metastatic breast cancer pretreated with chemotherapy*. Ann Oncol, 2012. **23**(3): p. 610-7.

289. Mayer, E.L., et al., *A phase 2 trial of dasatinib in patients with advanced HER2-positive and/or hormone receptor-positive breast cancer*. Clin Cancer Res, 2011. **17**(21): p. 6897-904.
290. Pusztai, L., et al., *Gene signature-guided dasatinib therapy in metastatic breast cancer*. Clin Cancer Res, 2014. **20**(20): p. 5265-71.
291. Reddy, S.M., et al., *Phase II study of saracatinib (AZD0530) in patients with previously treated metastatic colorectal cancer*. Invest New Drugs, 2015. **33**(4): p. 977-84.
292. Chee, C.E., et al., *Phase II study of dasatinib (BMS-354825) in patients with metastatic adenocarcinoma of the pancreas*. Oncologist, 2013. **18**(10): p. 1091-2.
293. Hong, D.S., et al., *A phase 1 study of gemcitabine combined with dasatinib in patients with advanced solid tumors*. Invest New Drugs, 2013. **31**(4): p. 918-26.
294. Reni, M., et al., *Maintenance sunitinib or observation in metastatic pancreatic adenocarcinoma: a phase II randomised trial*. Eur J Cancer, 2013. **49**(17): p. 3609-15.
295. Renouf, D.J., et al., *A phase I/II study of the Src inhibitor saracatinib (AZD0530) in combination with gemcitabine in advanced pancreatic cancer*. Invest New Drugs, 2012. **30**(2): p. 779-86.
296. Hsyu, P.H., et al., *Population pharmacokinetic and pharmacodynamic analysis of bosutinib*. Drug Metab Pharmacokinet, 2014. **29**(6): p. 441-8.
297. Evans, T.R.J., et al., *Phase 2 placebo-controlled, double-blind trial of dasatinib added to gemcitabine for patients with locally-advanced pancreatic cancer*. Ann Oncol, 2017. **28**(2): p. 354-361.
298. Isakoff, S.J., et al., *Bosutinib plus capecitabine for selected advanced solid tumours: results of a phase 1 dose-escalation study*. Br J Cancer, 2014. **111**(11): p. 2058-66.
299. Dosch, A.R., et al., *Src kinase inhibition restores E-cadherin expression in dasatinib-sensitive pancreatic cancer cells*. Oncotarget, 2019. **10**(10): p. 1056-1069.
300. Evans, T.R.J., et al., *Dasatinib combined with gemcitabine (Gem) in patients (pts) with locally advanced pancreatic adenocarcinoma (PaCa): Design of CA180-375, a placebo-controlled, randomized, double-blind phase II trial*. Journal of Clinical Oncology, 2012. **30**(15_suppl): p. TPS4134-TPS4134.
301. Hekim, C., et al., *Dasatinib Changes Immune Cell Profiles Concomitant with Reduced Tumor Growth in Several Murine Solid Tumor Models*. Cancer Immunol Res, 2017. **5**(2): p. 157-169.
302. Najima, Y., et al., *Regulatory T cell inhibition by dasatinib is associated with natural killer cell differentiation and a favorable molecular response-The final results of the D-first study*. Leuk Res, 2018. **66**: p. 66-72.
303. Christiansson, L., et al., *The tyrosine kinase inhibitors imatinib and dasatinib reduce myeloid suppressor cells and release effector lymphocyte responses*. Mol Cancer Ther, 2015. **14**(5): p. 1181-91.
304. Kreutzman, A., et al., *Dasatinib promotes Th1-type responses in granzyme B expressing T-cells*. Oncoimmunology, 2014. **3**: p. e28925.
305. Mao, L., et al., *Inhibition of SRC family kinases reduces myeloid-derived suppressor cells in head and neck cancer*. Int J Cancer, 2017. **140**(5): p. 1173-1185.

306. Ozanne, J., A.R. Prescott, and K. Clark, *The clinically approved drugs dasatinib and bosutinib induce anti-inflammatory macrophages by inhibiting the salt-inducible kinases*. *Biochem J*, 2015. **465**(2): p. 271-9.
307. Yu, G.T., et al., *Inhibition of SRC family kinases facilitates anti-CTLA4 immunotherapy in head and neck squamous cell carcinoma*. *Cell Mol Life Sci*, 2018. **75**(22): p. 4223-4234.
308. D'Angelo, S.P., et al., *Combined KIT and CTLA-4 Blockade in Patients with Refractory GIST and Other Advanced Sarcomas: A Phase Ib Study of Dasatinib plus Ipilimumab*. *Clin Cancer Res*, 2017. **23**(12): p. 2972-2980.
309. Wu, A.A., E. Jaffee, and V. Lee, *Current Status of Immunotherapies for Treating Pancreatic Cancer*. *Curr Oncol Rep*, 2019. **21**(7): p. 60.
310. Gotwals, P., et al., *Prospects for combining targeted and conventional cancer therapy with immunotherapy*. *Nat Rev Cancer*, 2017. **17**(5): p. 286-301.
311. Luttrell, D.K., L.M. Luttrell, and S.J. Parsons, *Augmented mitogenic responsiveness to epidermal growth factor in murine fibroblasts that overexpress pp60c-src*. *Molecular and Cellular Biology*, 1988. **8**(1): p. 497-501.
312. Amos, S., et al., *Phorbol 12-myristate 13-acetate induces epidermal growth factor receptor transactivation via protein kinase Cdelta/c-Src pathways in glioblastoma cells*. *J Biol Chem*, 2005. **280**(9): p. 7729-38.
313. Fischgrabe, J., et al., *Targeting endothelin A receptor enhances anti-proliferative and anti-invasive effects of the HER2 antibody trastuzumab in HER2-overexpressing breast cancer cells*. *Int J Cancer*, 2010. **127**(3): p. 696-706.
314. Sooro, M.A., N. Zhang, and P. Zhang, *Targeting EGFR-mediated autophagy as a potential strategy for cancer therapy*. *Int J Cancer*, 2018.
315. Lemmon, M.A. and J. Schlessinger, *Cell signaling by receptor tyrosine kinases*. *Cell*, 2010. **141**(7): p. 1117-34.
316. Zhang, H., et al., *ErbB receptors: from oncogenes to targeted cancer therapies*. *J Clin Invest*, 2007. **117**(8): p. 2051-8.
317. Sheahan, A.V., et al., *Targeted therapies in the management of locally advanced and metastatic pancreatic cancer: a systematic review*. *Oncotarget*, 2018. **9**(30): p. 21613-21627.
318. Moore, M.J., et al., *Erlotinib plus gemcitabine compared with gemcitabine alone in patients with advanced pancreatic cancer: a phase III trial of the National Cancer Institute of Canada Clinical Trials Group*. *J Clin Oncol*, 2007. **25**(15): p. 1960-6.
319. Fornier, M.N., et al., *A phase I study of dasatinib and weekly paclitaxel for metastatic breast cancer*. *Ann Oncol*, 2011. **22**(12): p. 2575-81.
320. Nagaraj, N.S., M.K. Washington, and N.B. Merchant, *Combined blockade of Src kinase and epidermal growth factor receptor with gemcitabine overcomes STAT3-mediated resistance of inhibition of pancreatic tumor growth*. *Clin Cancer Res*, 2011. **17**(3): p. 483-93.
321. Wormann, S.M., et al., *Loss of P53 Function Activates JAK2-STAT3 Signaling to Promote Pancreatic Tumor Growth, Stroma Modification, and Gemcitabine Resistance in Mice and Is Associated With Patient Survival*. *Gastroenterology*, 2016. **151**(1): p. 180-193 e12.

322. Cardin, D.B., et al., *Dual Src and EGFR inhibition in combination with gemcitabine in advanced pancreatic cancer: phase I results : A phase I clinical trial*. Invest New Drugs, 2018. **36**(3): p. 442-450.
323. Pan, Y., et al., *A preclinical evaluation of SKLB261, a multikinase inhibitor of EGFR/Src/VEGFR2, as a therapeutic agent against pancreatic cancer*. Mol Cancer Ther, 2015. **14**(2): p. 407-18.
324. El Touny, L.H., et al., *Combined SFK/MEK inhibition prevents metastatic outgrowth of dormant tumor cells*. J Clin Invest, 2014. **124**(1): p. 156-68.
325. Gomes, E.G., S.F. Connelly, and J.M. Summy, *Targeting the yin and the yang: combined inhibition of the tyrosine kinase c-Src and the tyrosine phosphatase SHP-2 disrupts pancreatic cancer signaling and biology in vitro and tumor formation in vivo*. Pancreas, 2013. **42**(5): p. 795-806.
326. Fedele, C., et al., *SHP2 Inhibition Prevents Adaptive Resistance to MEK Inhibitors in Multiple Cancer Models*. Cancer Discov, 2018. **8**(10): p. 1237-1249.
327. Trarbach, T., et al., *Phase I open-label study of cediranib, an oral inhibitor of VEGF signalling, in combination with the oral Src inhibitor saracatinib in patients with advanced solid tumours*. Invest New Drugs, 2012. **30**(5): p. 1962-71.
328. Zhang, J., et al., *A small molecule FAK kinase inhibitor, GSK2256098, inhibits growth and survival of pancreatic ductal adenocarcinoma cells*. Cell Cycle, 2014. **13**(19): p. 3143-9.
329. Begum, A., et al., *The extracellular matrix and focal adhesion kinase signaling regulate cancer stem cell function in pancreatic ductal adenocarcinoma*. PLoS One, 2017. **12**(7): p. e0180181.
330. Hingorani, S.R., et al., *Preinvasive and invasive ductal pancreatic cancer and its early detection in the mouse*. Cancer Cell, 2003. **4**(6): p. 437-50.
331. Hingorani, S.R., et al., *Trp53R172H and KrasG12D cooperate to promote chromosomal instability and widely metastatic pancreatic ductal adenocarcinoma in mice*. Cancer Cell, 2005. **7**(5): p. 469-83.
332. Jiang, H., et al., *Development of resistance to FAK inhibition in pancreatic cancer is linked to stromal depletion*. Gut, 2019.
333. Aung, K.L., et al., *A phase II trial of GSK2256098 and trametinib in patients with advanced pancreatic ductal adenocarcinoma (PDAC) (MOBILITY-002 Trial, NCT02428270)*. Journal of Clinical Oncology, 2018. **36**(4_suppl): p. 409-409.
334. Infante, J.R., et al., *Safety, pharmacokinetic, and pharmacodynamic phase I dose-escalation trial of PF-00562271, an inhibitor of focal adhesion kinase, in advanced solid tumors*. J Clin Oncol, 2012. **30**(13): p. 1527-33.
335. Shapiro, I.M., et al., *Merlin deficiency predicts FAK inhibitor sensitivity: a synthetic lethal relationship*. Sci Transl Med, 2014. **6**(237): p. 237ra68.
336. Shah, N.R., et al., *Analyses of merlin/NF2 connection to FAK inhibitor responsiveness in serous ovarian cancer*. Gynecol Oncol, 2014. **134**(1): p. 104-11.
337. Kato, T., et al., *E-cadherin expression is correlated with focal adhesion kinase inhibitor resistance in Merlin-negative malignant mesothelioma cells*. Oncogene, 2017. **36**(39): p. 5522-5531.

338. Mak, G., et al., *A phase Ib dose-finding, pharmacokinetic study of the focal adhesion kinase inhibitor GSK2256098 and trametinib in patients with advanced solid tumours*. Br J Cancer, 2019. **120**(10): p. 975-981.
339. Fennell, D.A., et al., *Maintenance Defactinib Versus Placebo After First-Line Chemotherapy in Patients With Merlin-Stratified Pleural Mesothelioma: COMMAND-A Double-Blind, Randomized, Phase II Study*. J Clin Oncol, 2019. **37**(10): p. 790-798.
340. Jones, S.F., et al., *A phase I study of VS-6063, a second-generation focal adhesion kinase inhibitor, in patients with advanced solid tumors*. Invest New Drugs, 2015. **33**(5): p. 1100-7.
341. Papadatos-Pastos, D., et al., *A first-in-human study of the dual ROCK I/II inhibitor, AT13148, in patients with advanced cancers*. Journal of Clinical Oncology, 2015. **33**(15_suppl): p. 2566-2566.
342. Zhang, Y., et al., *Novel agents for pancreatic ductal adenocarcinoma: emerging therapeutics and future directions*. J Hematol Oncol, 2018. **11**(1): p. 14.
343. Morran, D.C., et al., *Targeting mTOR dependency in pancreatic cancer*. Gut, 2014. **63**(9): p. 1481-9.
344. Garrido-Laguna, I., et al., *Integrated preclinical and clinical development of mTOR inhibitors in pancreatic cancer*. Br J Cancer, 2010. **103**(5): p. 649-55.
345. Rozengurt, E., H.P. Soares, and J. Sinnett-Smith, *Suppression of feedback loops mediated by PI3K/mTOR induces multiple overactivation of compensatory pathways: an unintended consequence leading to drug resistance*. Mol Cancer Ther, 2014. **13**(11): p. 2477-88.
346. Chandarlapaty, S., *Negative feedback and adaptive resistance to the targeted therapy of cancer*. Cancer Discov, 2012. **2**(4): p. 311-9.
347. Basu, B., et al., *First-in-Human Pharmacokinetic and Pharmacodynamic Study of the Dual m-TORC 1/2 Inhibitor AZD2014*. Clin Cancer Res, 2015. **21**(15): p. 3412-9.
348. Driscoll, D.R., et al., *mTORC2 Signaling Drives the Development and Progression of Pancreatic Cancer*. Cancer Res, 2016. **76**(23): p. 6911-6923.
349. Hassan, Z., et al., *MTOR inhibitor-based combination therapies for pancreatic cancer*. Br J Cancer, 2018. **118**(3): p. 366-377.
350. Chiron, D., et al., *Cell-cycle reprogramming for PI3K inhibition overrides a relapse-specific C481S BTK mutation revealed by longitudinal functional genomics in mantle cell lymphoma*. Cancer Discov, 2014. **4**(9): p. 1022-35.
351. Noel, M.S., et al., *Phase II trial of SM-88 in patients with metastatic pancreatic cancer: Preliminary results of the first stage*. Journal of Clinical Oncology, 2019. **37**(4_suppl): p. 200-200.
352. Stega, J., et al., *A first-in-human study of the novel metabolism-based anti-cancer agent SM-88 in subjects with advanced metastatic cancer*. Invest New Drugs, 2019.
353. Fruman, D.A. and C. Rommel, *PI3K and cancer: lessons, challenges and opportunities*. Nat Rev Drug Discov, 2014. **13**(2): p. 140-56.
354. Bean, G.R., et al., *PUMA and BIM are required for oncogene inactivation-induced apoptosis*. Sci Signal, 2013. **6**(268): p. ra20.

355. Engelman, J.A., et al., *Effective use of PI3K and MEK inhibitors to treat mutant Kras G12D and PIK3CA H1047R murine lung cancers*. Nat Med, 2008. **14**(12): p. 1351-6.
356. Abel, E.V., et al., *Melanoma adapts to RAF/MEK inhibitors through FOXD3-mediated upregulation of ERBB3*. J Clin Invest, 2013. **123**(5): p. 2155-68.
357. Pettazzoni, P., et al., *Genetic events that limit the efficacy of MEK and RTK inhibitor therapies in a mouse model of KRAS-driven pancreatic cancer*. Cancer Res, 2015. **75**(6): p. 1091-101.
358. Shimizu, T., et al., *The clinical effect of the dual-targeting strategy involving PI3K/AKT/mTOR and RAS/MEK/ERK pathways in patients with advanced cancer*. Clin Cancer Res, 2012. **18**(8): p. 2316-25.
359. Simpkins, F., et al., *Dual Src and MEK Inhibition Decreases Ovarian Cancer Growth and Targets Tumor Initiating Stem-Like Cells*. Clin Cancer Res, 2018. **24**(19): p. 4874-4886.
360. Bedard, P.L., et al., *A phase Ib dose-escalation study of the oral pan-PI3K inhibitor buparlisib (BKM120) in combination with the oral MEK1/2 inhibitor trametinib (GSK1120212) in patients with selected advanced solid tumors*. Clin Cancer Res, 2015. **21**(4): p. 730-8.
361. Chung, V., et al., *Effect of Selumetinib and MK-2206 vs Oxaliplatin and Fluorouracil in Patients With Metastatic Pancreatic Cancer After Prior Therapy: SWOG S1115 Study Randomized Clinical Trial*. JAMA Oncol, 2017. **3**(4): p. 516-522.
362. Tolcher, A.W., et al., *Phase I study of the MEK inhibitor trametinib in combination with the AKT inhibitor afuresertib in patients with solid tumors and multiple myeloma*. Cancer Chemother Pharmacol, 2015. **75**(1): p. 183-9.
363. Yan, C., Q. Yang, and Z. Gong, *Activation of Hepatic Stellate Cells During Liver Carcinogenesis Requires Fibrinogen/Integrin alphavbeta5 in Zebrafish*. Neoplasia, 2018. **20**(5): p. 533-542.
364. Zhao, W., et al., *Galectin-3 Mediates Tumor Cell-Stroma Interactions by Activating Pancreatic Stellate Cells to Produce Cytokines via Integrin Signaling*. Gastroenterology, 2018. **154**(5): p. 1524-1537 e6.
365. Smith, J.W., *Cilengitide Merck*. Curr Opin Investig Drugs, 2003. **4**(6): p. 741-5.
366. Gilbert, M.R., et al., *Cilengitide in patients with recurrent glioblastoma: the results of NABTC 03-02, a phase II trial with measures of treatment delivery*. J Neurooncol, 2012. **106**(1): p. 147-53.
367. Nabors, L.B., et al., *A safety run-in and randomized phase 2 study of cilengitide combined with chemoradiation for newly diagnosed glioblastoma (NABTT 0306)*. Cancer, 2012. **118**(22): p. 5601-7.
368. Stupp, R., et al., *Cilengitide combined with standard treatment for patients with newly diagnosed glioblastoma with methylated MGMT promoter (CENTRIC EORTC 26071-22072 study): a multicentre, randomised, open-label, phase 3 trial*. Lancet Oncol, 2014. **15**(10): p. 1100-8.
369. Reardon, D.A., et al., *Randomized phase II study of cilengitide, an integrin-targeting arginine-glycine-aspartic acid peptide, in recurrent glioblastoma multiforme*. J Clin Oncol, 2008. **26**(34): p. 5610-7.
370. Friess, H., et al., *A randomized multi-center phase II trial of the angiogenesis inhibitor Cilengitide (EMD 121974) and gemcitabine*

- compared with gemcitabine alone in advanced unresectable pancreatic cancer. *BMC Cancer*, 2006. **6**: p. 285.
371. Massabeau, C., et al., *Continuous Infusion of Cilengitide Plus Chemoradiotherapy for Patients With Stage III Non-Small-cell Lung Cancer: A Phase I Study*. *Clin Lung Cancer*, 2018. **19**(3): p. e277-e285.
 372. Pandolfi, F., et al., *Integrins: Integrating the Biology and Therapy of Cell-cell Interactions*. *Clin Ther*, 2017. **39**(12): p. 2420-2436.
 373. Ricart, A.D., et al., *Volociximab, a chimeric monoclonal antibody that specifically binds alpha5beta1 integrin: a phase I, pharmacokinetic, and biological correlative study*. *Clin Cancer Res*, 2008. **14**(23): p. 7924-9.
 374. Elez, E., et al., *Abituzumab combined with cetuximab plus irinotecan versus cetuximab plus irinotecan alone for patients with KRAS wild-type metastatic colorectal cancer: the randomised phase I/II POSEIDON trial*. *Ann Oncol*, 2015. **26**(1): p. 132-40.
 375. Hussain, M., et al., *Differential Effect on Bone Lesions of Targeting Integrins: Randomized Phase II Trial of Abituzumab in Patients with Metastatic Castration-Resistant Prostate Cancer*. *Clin Cancer Res*, 2016. **22**(13): p. 3192-200.
 376. Paez-Ribes, M., et al., *Antiangiogenic therapy elicits malignant progression of tumors to increased local invasion and distant metastasis*. *Cancer Cell*, 2009. **15**(3): p. 220-31.
 377. Ebos, J.M., et al., *Accelerated metastasis after short-term treatment with a potent inhibitor of tumor angiogenesis*. *Cancer Cell*, 2009. **15**(3): p. 232-9.
 378. Reynolds, A.R., et al., *Stimulation of tumor growth and angiogenesis by low concentrations of RGD-mimetic integrin inhibitors*. *Nat Med*, 2009. **15**(4): p. 392-400.
 379. Carmeliet, P. and R.K. Jain, *Principles and mechanisms of vessel normalization for cancer and other angiogenic diseases*. *Nat Rev Drug Discov*, 2011. **10**(6): p. 417-27.
 380. Webb, T., *Vascular normalization: study examines how antiangiogenesis therapies work*. *J Natl Cancer Inst*, 2005. **97**(5): p. 336-7.
 381. Wong, P.P., et al., *Dual-action combination therapy enhances angiogenesis while reducing tumor growth and spread*. *Cancer Cell*, 2015. **27**(1): p. 123-37.
 382. Muller, P.A., et al., *Mutant p53 drives invasion by promoting integrin recycling*. *Cell*, 2009. **139**(7): p. 1327-41.
 383. Hingorani, S.R., et al., *Phase Ib Study of PEGylated Recombinant Human Hyaluronidase and Gemcitabine in Patients with Advanced Pancreatic Cancer*. *Clin Cancer Res*, 2016. **22**(12): p. 2848-54.
 384. Clift, R., et al., *Abstract 1743: Rationale for evaluating PEGylated recombinant human hyaluronidase PH20 (pegvorhyaluronidase alfa; PEGPH20) in patients with hyaluronan (HA)-accumulating colorectal cancer*. *Cancer Research*, 2018. **78**(13 Supplement): p. 1743-1743.
 385. Ko, A.H., et al., *Perioperative stromal depletion by PEGPH20 in pancreatic ductal adenocarcinoma*. *Journal of Clinical Oncology*, 2016. **34**(4_suppl): p. TPS476-TPS476.
 386. Yu, K.H., et al., *Pilot study of gemcitabine, nab-paclitaxel, PEGPH20, and rivaroxaban for advanced pancreatic adenocarcinoma: An interim analysis*. *Journal of Clinical Oncology*, 2018. **36**(4_suppl): p. 405-405.

387. Ramanathan, R.K., et al., *A phase IB/II randomized study of mFOLFIRINOX (mFFOX) + pegylated recombinant human hyaluronidase (PEGPH20) versus mFFOX alone in patients with good performance status metastatic pancreatic adenocarcinoma (mPC): SWOG S1313 (NCT #01959139)*. Journal of Clinical Oncology, 2018. **36**(4_suppl): p. 208-208.
388. Ramanathan, R.K., et al., *Phase IB/II Randomized Study of FOLFIRINOX Plus Pegylated Recombinant Human Hyaluronidase Versus FOLFIRINOX Alone in Patients With Metastatic Pancreatic Adenocarcinoma: SWOG S1313*. J Clin Oncol, 2019. **37**(13): p. 1062-1069.
389. Wang, S., et al., *Extracellular matrix (ECM) circulating peptide biomarkers as potential predictors of survival in patients (pts) with untreated metastatic pancreatic ductal adenocarcinoma (mPDA) receiving pegvorhyaluronidase alfa (PEGPH20), nab-paclitaxel (A), and gemcitabine (G)*. Journal of Clinical Oncology, 2018. **36**((suppl; abstr 12030)).
390. Cao, J., et al., *Dynamic Contrast-enhanced MRI Detects Responses to Stroma-directed Therapy in Mouse Models of Pancreatic Ductal Adenocarcinoma*. Clin Cancer Res, 2019. **25**(7): p. 2314-2322.
391. Wong, K.M., et al., *Targeting the Tumor Stroma: the Biology and Clinical Development of Pegylated Recombinant Human Hyaluronidase (PEGPH20)*. Curr Oncol Rep, 2017. **19**(7): p. 47.
392. Hammel, P., et al., *Effect of Chemoradiotherapy vs Chemotherapy on Survival in Patients With Locally Advanced Pancreatic Cancer Controlled After 4 Months of Gemcitabine With or Without Erlotinib: The LAP07 Randomized Clinical Trial*. JAMA, 2016. **315**(17): p. 1844-53.
393. Semrad, T., et al., *Pharmacodynamic separation of gemcitabine and erlotinib in locally advanced or metastatic pancreatic cancer: therapeutic and biomarker results*. Int J Clin Oncol, 2015. **20**(3): p. 518-24.
394. Boeck, S., et al., *Cytokeratin 19-fragments (CYFRA 21-1) as a novel serum biomarker for response and survival in patients with advanced pancreatic cancer*. Br J Cancer, 2013. **108**(8): p. 1684-94.
395. Philip, P.A., et al., *Phase III study comparing gemcitabine plus cetuximab versus gemcitabine in patients with advanced pancreatic adenocarcinoma: Southwest Oncology Group-directed intergroup trial S0205*. J Clin Oncol, 2010. **28**(22): p. 3605-10.
396. Strumberg, D., et al., *Gemcitabine combined with the monoclonal antibody nimotuzumab is an active first-line regimen in KRAS wildtype patients with locally advanced or metastatic pancreatic cancer: a multicenter, randomized phase IIb study*. Annals of Oncology, 2017. **28**(10): p. 2429-2435.
397. Wang-Gillam, A., et al., *Phase I study of defactinib combined with pembrolizumab and gemcitabine in patients with advanced cancer*. Journal of Clinical Oncology, 2018. **36**(4_suppl): p. 380-380.
398. Thompson, D.S., et al., *A phase I dose-escalation study of IMG388 in patients with solid tumors*. Journal of Clinical Oncology, 2010. **28**(15_suppl): p. 3058-3058.
399. Hingorani, S.R., et al., *High response rate and PFS with PEGPH20 added to nab-paclitaxel/gemcitabine in stage IV previously untreated pancreatic cancer patients with high-HA tumors: interim results of a randomized phase 2 study*. ASCO Annual Meeting, 2015.

400. Ko, A.H., et al., *A Multicenter, Open-Label Phase II Clinical Trial of Combined MEK plus EGFR Inhibition for Chemotherapy-Refractory Advanced Pancreatic Adenocarcinoma*. Clin Cancer Res, 2016. **22**(1): p. 61-8.
401. Ettrich, T.J., et al., [ASCO- and ESMO-update 2017 - highlights of the 53. meeting of the American Society of Clinical Oncology/ASCO 2017 and European Society for Medical Oncology/ESMO congress 2017]. Z Gastroenterol, 2018. **56**(4): p. 384-397.
402. Marsh Rde, W., et al., *A phase II trial of perifosine in locally advanced, unresectable, or metastatic pancreatic adenocarcinoma*. Am J Clin Oncol, 2007. **30**(1): p. 26-31.
403. Javle, M.M., et al., *Inhibition of the mammalian target of rapamycin (mTOR) in advanced pancreatic cancer: results of two phase II studies*. BMC Cancer, 2010. **10**: p. 368.
404. Wolpin, B.M., et al., *Oral mTOR inhibitor everolimus in patients with gemcitabine-refractory metastatic pancreatic cancer*. J Clin Oncol, 2009. **27**(2): p. 193-8.
405. Bjerregaard, J.K., et al., *A randomized phase I/II study of everolimus, irinotecan, and cetuximab versus capecitabine and oxaliplatin in gemcitabine-resistant patients with pancreatic cancer*. Journal of Clinical Oncology, 2014. **32**(3_suppl): p. 337-337.
406. Kordes, S., et al., *A phase I/II, non-randomized, feasibility/safety and efficacy study of the combination of everolimus, cetuximab and capecitabine in patients with advanced pancreatic cancer*. Invest New Drugs, 2013. **31**(1): p. 85-91.
407. Joka, M., et al., *Combination of antiangiogenic therapy using the mTOR-inhibitor everolimus and low-dose chemotherapy for locally advanced and/or metastatic pancreatic cancer: a dose-finding study*. Anticancer Drugs, 2014. **25**(9): p. 1095-101.
408. Tan, B.R., et al., *Phase I study of X-82, an oral dual anti-VEGFR/PDGFR tyrosine kinase inhibitor, with everolimus in solid tumors*. Journal of Clinical Oncology, 2016. **34**(15_suppl): p. 2588-2588.
409. Koumarianou, A., et al., *1326PEvaluation of the efficacy and safety of everolimus as a first-line treatment in newly diagnosed patients with advanced gastroenteropancreatic neuroendocrine tumors*. Annals of Oncology, 2018. **29**(suppl_8).
410. Toyonaga, T., et al., *Blockade of constitutively activated Janus kinase/signal transducer and activator of transcription-3 pathway inhibits growth of human pancreatic cancer*. Cancer Lett, 2003. **201**(1): p. 107-16.
411. Johnson, D.E., R.A. O'Keefe, and J.R. Grandis, *Targeting the IL-6/JAK/STAT3 signalling axis in cancer*. Nat Rev Clin Oncol, 2018. **15**(4): p. 234-248.
412. Jones, S.A. and B.J. Jenkins, *Recent insights into targeting the IL-6 cytokine family in inflammatory diseases and cancer*. Nat Rev Immunol, 2018. **18**(12): p. 773-789.
413. Balic, J.J., et al., *Interleukin-11-driven gastric tumourigenesis is independent of trans-signalling*. Cytokine, 2017. **92**: p. 118-123.
414. Putoczki, T.L., et al., *Interleukin-11 is the dominant IL-6 family cytokine during gastrointestinal tumorigenesis and can be targeted therapeutically*. Cancer Cell, 2013. **24**(2): p. 257-71.

415. Huynh, J., et al., *The JAK/STAT3 axis: A comprehensive drug target for solid malignancies*. Semin Cancer Biol, 2017. **45**: p. 13-22.
416. Yu, H., M. Kortylewski, and D. Pardoll, *Crosstalk between cancer and immune cells: role of STAT3 in the tumour microenvironment*. Nat Rev Immunol, 2007. **7**(1): p. 41-51.
417. Zhong, Z., Z. Wen, and J.E. Darnell, Jr., *Stat3: a STAT family member activated by tyrosine phosphorylation in response to epidermal growth factor and interleukin-6*. Science, 1994. **264**(5155): p. 95-8.
418. Ruff-Jamison, S., et al., *Epidermal growth factor and lipopolysaccharide activate Stat3 transcription factor in mouse liver*. J Biol Chem, 1994. **269**(35): p. 21933-5.
419. Catlett-Falcone, R., et al., *Constitutive activation of Stat3 signaling confers resistance to apoptosis in human U266 myeloma cells*. Immunity, 1999. **10**(1): p. 105-15.
420. Yu, C.L., et al., *Enhanced DNA-binding activity of a Stat3-related protein in cells transformed by the Src oncoprotein*. Science, 1995. **269**(5220): p. 81-3.
421. Yu, H. and R. Jove, *The STATs of cancer--new molecular targets come of age*. Nat Rev Cancer, 2004. **4**(2): p. 97-105.
422. Bromberg, J.F., et al., *Stat3 as an oncogene*. Cell, 1999. **98**(3): p. 295-303.
423. Niu, G., et al., *Roles of activated Src and Stat3 signaling in melanoma tumor cell growth*. Oncogene, 2002. **21**(46): p. 7001-10.
424. Grandis, J.R., et al., *Constitutive activation of Stat3 signaling abrogates apoptosis in squamous cell carcinogenesis in vivo*. Proc Natl Acad Sci U S A, 2000. **97**(8): p. 4227-32.
425. Dang, C.V., *c-Myc target genes involved in cell growth, apoptosis, and metabolism*. Mol Cell Biol, 1999. **19**(1): p. 1-11.
426. Prendergast, G.C., *Mechanisms of apoptosis by c-Myc*. Oncogene, 1999. **18**(19): p. 2967-87.
427. Niu, G., et al., *Constitutive Stat3 activity up-regulates VEGF expression and tumor angiogenesis*. Oncogene, 2002. **21**(13): p. 2000-8.
428. Wei, D., et al., *Stat3 activation regulates the expression of vascular endothelial growth factor and human pancreatic cancer angiogenesis and metastasis*. Oncogene, 2003. **22**(3): p. 319-29.
429. Darnell, J.E., Jr., *Studies of IFN-induced transcriptional activation uncover the Jak-Stat pathway*. J Interferon Cytokine Res, 1998. **18**(8): p. 549-54.
430. Garbers, C., et al., *Interleukin-6: designing specific therapeutics for a complex cytokine*. Nat Rev Drug Discov, 2018. **17**(6): p. 395-412.
431. Garbers, C. and S. Rose-John, *Dissecting Interleukin-6 Classic- and Trans-Signaling in Inflammation and Cancer*. Methods Mol Biol, 2018. **1725**: p. 127-140.
432. Walter, M., et al., *Interleukin 6 secreted from adipose stromal cells promotes migration and invasion of breast cancer cells*. Oncogene, 2009. **28**(30): p. 2745-55.
433. Campbell, I.L., et al., *Trans-signaling is a dominant mechanism for the pathogenic actions of interleukin-6 in the brain*. J Neurosci, 2014. **34**(7): p. 2503-13.

434. Neurath, M.F. and S. Finotto, *IL-6 signaling in autoimmunity, chronic inflammation and inflammation-associated cancer*. Cytokine Growth Factor Rev, 2011. **22**(2): p. 83-9.
435. Lui, V.W., et al., *Frequent mutation of receptor protein tyrosine phosphatases provides a mechanism for STAT3 hyperactivation in head and neck cancer*. Proc Natl Acad Sci U S A, 2014. **111**(3): p. 1114-9.
436. Corcoran, R.B., et al., *STAT3 plays a critical role in KRAS-induced pancreatic tumorigenesis*. Cancer Res, 2011. **71**(14): p. 5020-9.
437. Miyatsuka, T., et al., *Persistent expression of PDX-1 in the pancreas causes acinar-to-ductal metaplasia through Stat3 activation*. Genes Dev, 2006. **20**(11): p. 1435-40.
438. Scholz, A., et al., *Activated signal transducer and activator of transcription 3 (STAT3) supports the malignant phenotype of human pancreatic cancer*. Gastroenterology, 2003. **125**(3): p. 891-905.
439. Jaganathan, S., P. Yue, and J. Turkson, *Enhanced sensitivity of pancreatic cancer cells to concurrent inhibition of aberrant signal transducer and activator of transcription 3 and epidermal growth factor receptor or Src*. J Pharmacol Exp Ther, 2010. **333**(2): p. 373-81.
440. Fukuda, A., et al., *Stat3 and MMP7 contribute to pancreatic ductal adenocarcinoma initiation and progression*. Cancer Cell, 2011. **19**(4): p. 441-55.
441. Huang, C., et al., *Inhibition of STAT3 activity with AG490 decreases the invasion of human pancreatic cancer cells in vitro*. Cancer Sci, 2006. **97**(12): p. 1417-23.
442. Arpin, C.C., et al., *Applying Small Molecule Signal Transducer and Activator of Transcription-3 (STAT3) Protein Inhibitors as Pancreatic Cancer Therapeutics*. Mol Cancer Ther, 2016. **15**(5): p. 794-805.
443. Nagathihalli, N.S., et al., *Signal Transducer and Activator of Transcription 3, Mediated Remodeling of the Tumor Microenvironment Results in Enhanced Tumor Drug Delivery in a Mouse Model of Pancreatic Cancer*. Gastroenterology, 2015. **149**(7): p. 1932-1943 e9.
444. Ioannou, N., et al., *Acquired resistance of pancreatic cancer cells to treatment with gemcitabine and HER-inhibitors is accompanied by increased sensitivity to STAT3 inhibition*. Int J Oncol, 2016. **48**(3): p. 908-18.
445. Zhang, Z., et al., *Gemcitabine treatment promotes pancreatic cancer stemness through the Nox/ROS/NF-kappaB/STAT3 signaling cascade*. Cancer Lett, 2016. **382**(1): p. 53-63.
446. Glienke, W., E. Hausmann, and L. Bergmann, *Downregulation of STAT3 signaling induces apoptosis but also promotes anti-apoptotic gene expression in human pancreatic cancer cell lines*. Tumour Biol, 2011. **32**(3): p. 493-500.
447. Satoh, K., et al., *Expression of survivin is correlated with cancer cell apoptosis and is involved in the development of human pancreatic duct cell tumors*. Cancer, 2001. **92**(2): p. 271-8.
448. Huang, C., et al., *Down-regulation of STAT3 expression by vector-based small interfering RNA inhibits pancreatic cancer growth*. World J Gastroenterol, 2011. **17**(25): p. 2992-3001.

449. Gansauge, S., et al., *Overexpression of cyclin D1 in human pancreatic carcinoma is associated with poor prognosis*. Cancer Res, 1997. **57**(9): p. 1634-7.
450. Hessmann, E., et al., *MYC in pancreatic cancer: novel mechanistic insights and their translation into therapeutic strategies*. Oncogene, 2016. **35**(13): p. 1609-18.
451. Chen, Z., et al., *miR-204 mediated loss of Myeloid cell leukemia-1 results in pancreatic cancer cell death*. Mol Cancer, 2013. **12**(1): p. 105.
452. Modica, C., et al., *MET/HGF Co-Targeting in Pancreatic Cancer: A Tool to Provide Insight into the Tumor/Stroma Crosstalk*. Int J Mol Sci, 2018. **19**(12).
453. Shukla, S.K., et al., *MUC1 and HIF-1alpha Signaling Crosstalk Induces Anabolic Glucose Metabolism to Impart Gemcitabine Resistance to Pancreatic Cancer*. Cancer Cell, 2017. **32**(1): p. 71-87 e7.
454. Ellenrieder, V., et al., *Role of MT-MMPs and MMP-2 in pancreatic cancer progression*. International Journal of Cancer, 2000. **85**(1): p. 14-20.
455. Grunwald, B., et al., *Matrix metalloproteinase-9 (MMP-9) as an activator of nanosystems for targeted drug delivery in pancreatic cancer*. J Control Release, 2016. **239**: p. 39-48.
456. Booy, S., et al., *IFN-beta is a potent inhibitor of insulin and insulin like growth factor stimulated proliferation and migration in human pancreatic cancer cells*. Am J Cancer Res, 2015. **5**(6): p. 2035-46.
457. Detjen, K.M., et al., *Interferon gamma inhibits growth of human pancreatic carcinoma cells via caspase-1 dependent induction of apoptosis*. Gut, 2001. **49**(2): p. 251-62.
458. Lunardi, S., et al., *IP-10/CXCL10 induction in human pancreatic cancer stroma influences lymphocytes recruitment and correlates with poor survival*. Oncotarget, 2014. **5**(22): p. 11064-80.
459. Ebrahimi, S., et al., *Targeting the Akt/PI3K Signaling Pathway as a Potential Therapeutic Strategy for the Treatment of Pancreatic Cancer*. Curr Med Chem, 2017. **24**(13): p. 1321-1331.
460. Pop, V.V., et al., *IL-6 roles - Molecular pathway and clinical implication in pancreatic cancer - A systemic review*. Immunol Lett, 2017. **181**: p. 45-50.
461. Batchu, R.B., et al., *Inhibition of Interleukin-10 in the tumor microenvironment can restore mesothelin chimeric antigen receptor T cell activity in pancreatic cancer in vitro*. Surgery, 2018. **163**(3): p. 627-632.
462. Truty, M.J. and R. Urrutia, *Basics of TGF-beta and pancreatic cancer*. Pancreatology, 2007. **7**(5-6): p. 423-35.
463. Wang, P., et al., *Re-designing Interleukin-12 to enhance its safety and potential as an anti-tumor immunotherapeutic agent*. Nat Commun, 2017. **8**(1): p. 1395.
464. Sato, T., et al., *An apoptosis-inducing gene therapy for pancreatic cancer with a combination of 55-kDa tumor necrosis factor (TNF) receptor gene transfection and mutein TNF administration*. Cancer Res, 1998. **58**(8): p. 1677-83.
465. Lapteva, N. and X.F. Huang, *CCL5 as an adjuvant for cancer immunotherapy*. Expert Opin Biol Ther, 2010. **10**(5): p. 725-33.

466. Bengsch, F., et al., *CTLA-4/CD80 pathway regulates T cell infiltration into pancreatic cancer*. *Cancer Immunol Immunother*, 2017. **66**(12): p. 1609-1617.
467. Wen, Z., et al., *alpha-Solanine inhibits vascular endothelial growth factor expression by down-regulating the ERK1/2-HIF-1alpha and STAT3 signaling pathways*. *Eur J Pharmacol*, 2016. **771**: p. 93-8.
468. Mano, Y., et al., *Tumor-associated macrophage promotes tumor progression via STAT3 signaling in hepatocellular carcinoma*. *Pathobiology*, 2013. **80**(3): p. 146-54.
469. Koscsó, B., et al., *Adenosine augments IL-10-induced STAT3 signaling in M2c macrophages*. *J Leukoc Biol*, 2013. **94**(6): p. 1309-15.
470. Fernando, M.R., et al., *The pro-inflammatory cytokine, interleukin-6, enhances the polarization of alternatively activated macrophages*. *PLoS One*, 2014. **9**(4): p. e94188.
471. Sumida, K., et al., *IL-11 induces differentiation of myeloid-derived suppressor cells through activation of STAT3 signalling pathway*. *Sci Rep*, 2015. **5**: p. 13650.
472. Mace, T.A., et al., *Pancreatic cancer-associated stellate cells promote differentiation of myeloid-derived suppressor cells in a STAT3-dependent manner*. *Cancer Res*, 2013. **73**(10): p. 3007-18.
473. Zorn, E., et al., *IL-2 regulates FOXP3 expression in human CD4+CD25+ regulatory T cells through a STAT-dependent mechanism and induces the expansion of these cells in vivo*. *Blood*, 2006. **108**(5): p. 1571-9.
474. Yang, X., et al., *FAP Promotes Immunosuppression by Cancer-Associated Fibroblasts in the Tumor Microenvironment via STAT3-CCL2 Signaling*. *Cancer Res*, 2016. **76**(14): p. 4124-35.
475. Wang, T., et al., *Regulation of the innate and adaptive immune responses by Stat-3 signaling in tumor cells*. *Nat Med*, 2004. **10**(1): p. 48-54.
476. Gabrilovich, D.I., et al., *Production of vascular endothelial growth factor by human tumors inhibits the functional maturation of dendritic cells*. *Nat Med*, 1996. **2**(10): p. 1096-103.
477. Yang, A.S. and E.C. Lattime, *Tumor-induced interleukin 10 suppresses the ability of splenic dendritic cells to stimulate CD4 and CD8 T-cell responses*. *Cancer Res*, 2003. **63**(9): p. 2150-7.
478. Hanahan, D. and R.A. Weinberg, *Hallmarks of cancer: the next generation*. *Cell*, 2011. **144**(5): p. 646-74.
479. Hamada, S., et al., *IL-6/STAT3 Plays a Regulatory Role in the Interaction Between Pancreatic Stellate Cells and Cancer Cells*. *Dig Dis Sci*, 2016. **61**(6): p. 1561-71.
480. Ligorio, M., et al., *Stromal Microenvironment Shapes the Intratumoral Architecture of Pancreatic Cancer*. *Cell*, 2019. **178**(1): p. 160-175 e27.
481. Wu, P., et al., *Prognostic role of STAT3 in solid tumors: a systematic review and meta-analysis*. *Oncotarget*, 2016. **7**(15): p. 19863-83.
482. Denley, S.M., et al., *Activation of the IL-6R/Jak/stat pathway is associated with a poor outcome in resected pancreatic ductal adenocarcinoma*. *J Gastrointest Surg*, 2013. **17**(5): p. 887-98.
483. Thomas, S.J., et al., *The role of JAK/STAT signalling in the pathogenesis, prognosis and treatment of solid tumours*. *Br J Cancer*, 2015. **113**(3): p. 365-71.

484. Shahmarvand, N., et al., *Mutations in the signal transducer and activator of transcription family of genes in cancer*. Cancer Sci, 2018. **109**(4): p. 926-933.
485. Koskela, H.L., et al., *Somatic STAT3 mutations in large granular lymphocytic leukemia*. N Engl J Med, 2012. **366**(20): p. 1905-13.
486. Pilati, C., et al., *Somatic mutations activating STAT3 in human inflammatory hepatocellular adenomas*. J Exp Med, 2011. **208**(7): p. 1359-66.
487. Roskoski, R., Jr., *Janus kinase (JAK) inhibitors in the treatment of inflammatory and neoplastic diseases*. Pharmacol Res, 2016. **111**: p. 784-803.
488. Lupardus, P.J., et al., *Structure of the pseudokinase-kinase domains from protein kinase TYK2 reveals a mechanism for Janus kinase (JAK) autoinhibition*. Proc Natl Acad Sci U S A, 2014. **111**(22): p. 8025-30.
489. Kocher, H.M., et al., *JAK V617F missense mutation is absent in pancreatic cancer*. Gut, 2007. **56**(8): p. 1174-5.
490. Kiel, M.J., et al., *Integrated genomic sequencing reveals mutational landscape of T-cell prolymphocytic leukemia*. Blood, 2014. **124**(9): p. 1460-72.
491. Buchert, M., C.J. Burns, and M. Ernst, *Targeting JAK kinase in solid tumors: emerging opportunities and challenges*. Oncogene, 2016. **35**(8): p. 939-51.
492. Cancer Genome Atlas Research, N., *Comprehensive molecular characterization of gastric adenocarcinoma*. Nature, 2014. **513**(7517): p. 202-9.
493. Quintas-Cardama, A. and S. Verstovsek, *Molecular pathways: Jak/STAT pathway: mutations, inhibitors, and resistance*. Clin Cancer Res, 2013. **19**(8): p. 1933-40.
494. Looyenga, B.D., et al., *STAT3 is activated by JAK2 independent of key oncogenic driver mutations in non-small cell lung carcinoma*. PLoS One, 2012. **7**(2): p. e30820.
495. Crescenzo, R., et al., *Convergent mutations and kinase fusions lead to oncogenic STAT3 activation in anaplastic large cell lymphoma*. Cancer Cell, 2015. **27**(4): p. 516-32.
496. Kumari, N., et al., *Role of interleukin-6 in cancer progression and therapeutic resistance*. Tumour Biol, 2016. **37**(9): p. 11553-11572.
497. Rebouissou, S., et al., *Frequent in-frame somatic deletions activate gp130 in inflammatory hepatocellular tumours*. Nature, 2009. **457**(7226): p. 200-4.
498. Fishman, D., et al., *The effect of novel polymorphisms in the interleukin-6 (IL-6) gene on IL-6 transcription and plasma IL-6 levels, and an association with systemic-onset juvenile chronic arthritis*. J Clin Invest, 1998. **102**(7): p. 1369-76.
499. Tartaglia, M., et al., *Somatic mutations in PTPN11 in juvenile myelomonocytic leukemia, myelodysplastic syndromes and acute myeloid leukemia*. Nat Genet, 2003. **34**(2): p. 148-50.
500. Yue, P. and J. Turkson, *Targeting STAT3 in cancer: how successful are we?* Expert Opin Investig Drugs, 2009. **18**(1): p. 45-56.
501. Oh, D.Y., et al., *Phase I Study of OPB-31121, an Oral STAT3 Inhibitor, in Patients with Advanced Solid Tumors*. Cancer Res Treat, 2015. **47**(4): p. 607-15.

502. Wong, A.L., et al., *Phase I and biomarker study of OPB-51602, a novel signal transducer and activator of transcription (STAT) 3 inhibitor, in patients with refractory solid malignancies*. Ann Oncol, 2015. **26**(5): p. 998-1005.
503. Angevin, E., et al., *A phase I/II, multiple-dose, dose-escalation study of siltuximab, an anti-interleukin-6 monoclonal antibody, in patients with advanced solid tumors*. Clin Cancer Res, 2014. **20**(8): p. 2192-204.
504. Ogura, M., et al., *Phase I study of OPB-51602, an oral inhibitor of signal transducer and activator of transcription 3, in patients with relapsed/refractory hematological malignancies*. Cancer Sci, 2015. **106**(7): p. 896-901.
505. Sen, M., et al., *Systemic administration of a cyclic signal transducer and activator of transcription 3 (STAT3) decoy oligonucleotide inhibits tumor growth without inducing toxicological effects*. Mol Med, 2014. **20**: p. 46-56.
506. Sen, M., et al., *First-in-human trial of a STAT3 decoy oligonucleotide in head and neck tumors: implications for cancer therapy*. Cancer Discov, 2012. **2**(8): p. 694-705.
507. Reilley, M.J., et al., *STAT3 antisense oligonucleotide AZD9150 in a subset of patients with heavily pretreated lymphoma: results of a phase 1b trial*. J Immunother Cancer, 2018. **6**(1): p. 119.
508. Hong, D., et al., *AZD9150, a next-generation antisense oligonucleotide inhibitor of STAT3 with early evidence of clinical activity in lymphoma and lung cancer*. Sci Transl Med, 2015. **7**(314): p. 314ra185.
509. Shastri, A., et al., *Antisense STAT3 inhibitor decreases viability of myelodysplastic and leukemic stem cells*. J Clin Invest, 2018. **128**(12): p. 5479-5488.
510. Li, Y., et al., *Suppression of cancer relapse and metastasis by inhibiting cancer stemness*. Proc Natl Acad Sci U S A, 2015. **112**(6): p. 1839-44.
511. Zhang, Y., et al., *Suppression of prostate cancer progression by cancer cell stemness inhibitor napabucasin*. Cancer Med, 2016. **5**(6): p. 1251-8.
512. Rose-John, S. and P.C. Heinrich, *Soluble receptors for cytokines and growth factors: generation and biological function*. Biochem J, 1994. **300 (Pt 2)**: p. 281-90.
513. van Rhee, F., et al., *Siltuximab for multicentric Castleman's disease: a randomised, double-blind, placebo-controlled trial*. Lancet Oncol, 2014. **15**(9): p. 966-74.
514. Kurzrock, R., et al., *A phase I, open-label study of siltuximab, an anti-IL-6 monoclonal antibody, in patients with B-cell non-Hodgkin lymphoma, multiple myeloma, or Castleman disease*. Clin Cancer Res, 2013. **19**(13): p. 3659-70.
515. van Rhee, F., et al., *Siltuximab, a novel anti-interleukin-6 monoclonal antibody, for Castleman's disease*. J Clin Oncol, 2010. **28**(23): p. 3701-8.
516. Coward, J., et al., *Interleukin-6 as a therapeutic target in human ovarian cancer*. Clin Cancer Res, 2011. **17**(18): p. 6083-96.
517. Cavarretta, I.T., et al., *Mcl-1 is regulated by IL-6 and mediates the survival activity of the cytokine in a model of late stage prostate carcinoma*. Adv Exp Med Biol, 2008. **617**: p. 547-55.
518. Song, L., et al., *Antitumor efficacy of the anti-interleukin-6 (IL-6) antibody siltuximab in mouse xenograft models of lung cancer*. J Thorac Oncol, 2014. **9**(7): p. 974-82.

519. Goumas, F.A., et al., *Inhibition of IL-6 signaling significantly reduces primary tumor growth and recurrences in orthotopic xenograft models of pancreatic cancer*. Int J Cancer, 2015. **137**(5): p. 1035-46.
520. Hemmann, U., et al., *Differential activation of acute phase response factor/Stat3 and Stat1 via the cytoplasmic domain of the interleukin 6 signal transducer gp130. II. Src homology SH2 domains define the specificity of stat factor activation*. J Biol Chem, 1996. **271**(22): p. 12999-3007.
521. Gerhartz, C., et al., *Differential activation of acute phase response factor/STAT3 and STAT1 via the cytoplasmic domain of the interleukin 6 signal transducer gp130. I. Definition of a novel phosphotyrosine motif mediating STAT1 activation*. J Biol Chem, 1996. **271**(22): p. 12991-8.
522. Krause, D.S. and R.A. Van Etten, *Tyrosine kinases as targets for cancer therapy*. N Engl J Med, 2005. **353**(2): p. 172-87.
523. Ikezoe, T., et al., *Expression of p-JAK2 predicts clinical outcome and is a potential molecular target of acute myelogenous leukemia*. Int J Cancer, 2011. **129**(10): p. 2512-21.
524. Gozgit, J.M., et al., *Effects of the JAK2 inhibitor, AZ960, on Pim/BAD/BCL-xL survival signaling in the human JAK2 V617F cell line SET-2*. J Biol Chem, 2008. **283**(47): p. 32334-43.
525. Thompson, J.E., et al., *Photochemical preparation of a pyridone containing tetracycle: a Jak protein kinase inhibitor*. Bioorg Med Chem Lett, 2002. **12**(8): p. 1219-23.
526. Verstovsek, S., et al., *Safety and efficacy of INCB018424, a JAK1 and JAK2 inhibitor, in myelofibrosis*. N Engl J Med, 2010. **363**(12): p. 1117-27.
527. Vannucchi, A.M., et al., *A pooled analysis of overall survival in COMFORT-I and COMFORT-II, 2 randomized phase III trials of ruxolitinib for the treatment of myelofibrosis*. Haematologica, 2015. **100**(9): p. 1139-45.
528. Bose, P. and S. Verstovsek, *JAK2 inhibitors for myeloproliferative neoplasms: what is next?* Blood, 2017. **130**(2): p. 115-125.
529. Verstovsek, S., et al., *Phase 1/2 study of pacritinib, a next generation JAK2/FLT3 inhibitor, in myelofibrosis or other myeloid malignancies*. J Hematol Oncol, 2016. **9**(1): p. 137.
530. Hu, Y., et al., *Inhibition of the JAK/STAT pathway with ruxolitinib overcomes cisplatin resistance in non-small-cell lung cancer NSCLC*. Apoptosis, 2014. **19**(11): p. 1627-36.
531. Wen, W., et al., *Synergistic anti-tumor effect of combined inhibition of EGFR and JAK/STAT3 pathways in human ovarian cancer*. Mol Cancer, 2015. **14**: p. 100.
532. Judd, L.M., et al., *Inhibition of the JAK2/STAT3 pathway reduces gastric cancer growth in vitro and in vivo*. PLoS One, 2014. **9**(5): p. e95993.
533. Gore, J., et al., *TCGA data and patient-derived orthotopic xenografts highlight pancreatic cancer-associated angiogenesis*. Oncotarget, 2015. **6**(10): p. 7504-21.
534. Koblisch, H.K., et al., *Abstract 1336: Novel immunotherapeutic activity of JAK and PI3K δ inhibitors in a model of pancreatic cancer*. Cancer Research, 2015. **75**(15 Supplement): p. 1336-1336.

535. Mace, T.A., et al., *Single agent BMS-911543 Jak2 inhibitor has distinct inhibitory effects on STAT5 signaling in genetically engineered mice with pancreatic cancer*. *Oncotarget*, 2015. **6**(42): p. 44509-22.
536. Komar, H.M., et al., *Inhibition of Jak/STAT signaling reduces the activation of pancreatic stellate cells in vitro and limits caerulein-induced chronic pancreatitis in vivo*. *Sci Rep*, 2017. **7**(1): p. 1787.
537. Rhim, A.D., et al., *Stromal elements act to restrain, rather than support, pancreatic ductal adenocarcinoma*. *Cancer Cell*, 2014. **25**(6): p. 735-47.
538. Ozdemir, B.C., et al., *Depletion of carcinoma-associated fibroblasts and fibrosis induces immunosuppression and accelerates pancreas cancer with reduced survival*. *Cancer Cell*, 2014. **25**(6): p. 719-34.
539. Shi, Y., et al., *Targeting LIF-mediated paracrine interaction for pancreatic cancer therapy and monitoring*. *Nature*, 2019. **569**(7754): p. 131-135.
540. Neesse, A., et al., *Stromal biology and therapy in pancreatic cancer*. *Gut*, 2011. **60**(6): p. 861-8.
541. Hanna, D.M., et al., *A unique case of refractory primary mediastinal B-cell lymphoma with JAK3 mutation and the role for targeted therapy*. *Haematologica*, 2014. **99**(9): p. e156-8.
542. Meyer, D.M., et al., *Anti-inflammatory activity and neutrophil reductions mediated by the JAK1/JAK3 inhibitor, CP-690,550, in rat adjuvant-induced arthritis*. *J Inflamm (Lond)*, 2010. **7**: p. 41.
543. Koo, G.C., et al., *Janus kinase 3-activating mutations identified in natural killer/T-cell lymphoma*. *Cancer Discov*, 2012. **2**(7): p. 591-7.
544. Dymock, B.W. and C.S. See, *Inhibitors of JAK2 and JAK3: an update on the patent literature 2010 - 2012*. *Expert Opin Ther Pat*, 2013. **23**(4): p. 449-501.
545. Flanagan, M.E., et al., *Discovery of CP-690,550: a potent and selective Janus kinase (JAK) inhibitor for the treatment of autoimmune diseases and organ transplant rejection*. *J Med Chem*, 2010. **53**(24): p. 8468-84.
546. Manshouri, T., et al., *The JAK kinase inhibitor CP-690,550 suppresses the growth of human polycythemia vera cells carrying the JAK2V617F mutation*. *Cancer Sci*, 2008. **99**(6): p. 1265-73.
547. Farrow, B., et al., *Inflammatory mechanisms contributing to pancreatic cancer development*. *Ann Surg*, 2004. **239**(6): p. 763-9; discussion 769-71.
548. Dvorak, H.F., *Tumors: wounds that do not heal. Similarities between tumor stroma generation and wound healing*. *N Engl J Med*, 1986. **315**(26): p. 1650-9.
549. Simon, N., et al., *Tofacitinib enhances delivery of antibody-based therapeutics to tumor cells through modulation of inflammatory cells*. *JCI Insight*, 2019. **4**(5).
550. Neubauer, H., et al., *Jak2 deficiency defines an essential developmental checkpoint in definitive hematopoiesis*. *Cell*, 1998. **93**(3): p. 397-409.
551. Komrokji, R.S., et al., *Results of a phase 2 study of pacritinib (SB1518), a JAK2/JAK2(V617F) inhibitor, in patients with myelofibrosis*. *Blood*, 2015. **125**(17): p. 2649-55.
552. Plimack, E.R., et al., *AZD1480: a phase I study of a novel JAK2 inhibitor in solid tumors*. *Oncologist*, 2013. **18**(7): p. 819-20.

553. Nagaraju, G.P., et al., *Targeting the Janus-activated kinase-2-STAT3 signalling pathway in pancreatic cancer using the HSP90 inhibitor ganetespib*. Eur J Cancer, 2016. **52**: p. 109-19.
554. Seavey, M.M. and P. Dobrzanski, *The many faces of Janus kinase*. Biochem Pharmacol, 2012. **83**(9): p. 1136-45.
555. Bauer, T.M., et al., *A Phase Ib study of ruxolitinib + gemcitabine +/- nab-paclitaxel in patients with advanced solid tumors*. Onco Targets Ther, 2018. **11**: p. 2399-2407.
556. Hurwitz, H.I., et al., *Randomized, Double-Blind, Phase II Study of Ruxolitinib or Placebo in Combination With Capecitabine in Patients With Metastatic Pancreatic Cancer for Whom Therapy With Gemcitabine Has Failed*. J Clin Oncol, 2015. **33**(34): p. 4039-47.
557. Tavallai, M., et al., *Rationally Repurposing Ruxolitinib (Jakafi ((R))) as a Solid Tumor Therapeutic*. Front Oncol, 2016. **6**: p. 142.
558. Machado-Neto, J.A., et al., *Stathmin 1 inhibition amplifies ruxolitinib-induced apoptosis in JAK2V617F cells*. Oncotarget, 2015. **6**(30): p. 29573-84.
559. Assi, R., et al., *A phase II trial of ruxolitinib in combination with azacytidine in myelodysplastic syndrome/myeloproliferative neoplasms*. Am J Hematol, 2018. **93**(2): p. 277-285.
560. Fiskus, W., et al., *Heat shock protein 90 inhibitor is synergistic with JAK2 inhibitor and overcomes resistance to JAK2-TKI in human myeloproliferative neoplasm cells*. Clin Cancer Res, 2011. **17**(23): p. 7347-58.
561. Monaghan, K.A., et al., *The novel JAK inhibitor CYT387 suppresses multiple signalling pathways, prevents proliferation and induces apoptosis in phenotypically diverse myeloma cells*. Leukemia, 2011. **25**(12): p. 1891-9.
562. Derenzini, E., et al., *The JAK inhibitor AZD1480 regulates proliferation and immunity in Hodgkin lymphoma*. Blood Cancer J, 2011. **1**(12): p. e46.
563. Wang, Y., et al., *Cotreatment with panobinostat and JAK2 inhibitor TG101209 attenuates JAK2V617F levels and signaling and exerts synergistic cytotoxic effects against human myeloproliferative neoplastic cells*. Blood, 2009. **114**(24): p. 5024-33.
564. Evrot, E., et al., *JAK1/2 and Pan-deacetylase inhibitor combination therapy yields improved efficacy in preclinical mouse models of JAK2V617F-driven disease*. Clin Cancer Res, 2013. **19**(22): p. 6230-41.
565. Fiskus, W., et al., *Dual PI3K/AKT/mTOR inhibitor BEZ235 synergistically enhances the activity of JAK2 inhibitor against cultured and primary human myeloproliferative neoplasm cells*. Mol Cancer Ther, 2013. **12**(5): p. 577-88.
566. Choong, M.L., et al., *Combination treatment for myeloproliferative neoplasms using JAK and pan-class I PI3K inhibitors*. J Cell Mol Med, 2013. **17**(11): p. 1397-409.
567. Harir, N., et al., *Constitutive activation of Stat5 promotes its cytoplasmic localization and association with PI3-kinase in myeloid leukemias*. Blood, 2007. **109**(4): p. 1678-86.
568. Will, B., et al., *Apoptosis induced by JAK2 inhibition is mediated by Bim and enhanced by the BH3 mimetic ABT-737 in JAK2 mutant human erythroid cells*. Blood, 2010. **115**(14): p. 2901-9.

569. Joungh, Y.H., et al., *Combination of AG490, a Jak2 inhibitor, and methylsulfonylmethane synergistically suppresses bladder tumor growth via the Jak2/STAT3 pathway*. *Int J Oncol*, 2014. **44**(3): p. 883-95.
570. Appelmann, I., et al., *Janus kinase inhibition by ruxolitinib extends dasatinib- and dexamethasone-induced remissions in a mouse model of Ph+ ALL*. *Blood*, 2015. **125**(9): p. 1444-51.
571. Quintarelli, C., et al., *Selective strong synergism of Ruxolitinib and second generation tyrosine kinase inhibitors to overcome bone marrow stroma related drug resistance in chronic myelogenous leukemia*. *Leuk Res*, 2014. **38**(2): p. 236-42.
572. Lue, H.W., et al., *Src and STAT3 inhibitors synergize to promote tumor inhibition in renal cell carcinoma*. *Oncotarget*, 2015. **6**(42): p. 44675-87.
573. Hurwitz, H., et al., *Ruxolitinib + capecitabine in advanced/metastatic pancreatic cancer after disease progression/intolerance to first-line therapy: JANUS 1 and 2 randomized phase III studies*. *Invest New Drugs*, 2018. **36**(4): p. 683-695.
574. Al-Ejeh, F., et al., *Gemcitabine and CHK1 inhibition potentiate EGFR-directed radioimmunotherapy against pancreatic ductal adenocarcinoma*. *Clin Cancer Res*, 2014. **20**(12): p. 3187-97.
575. Rubio-Viqueira, B., et al., *An in vivo platform for translational drug development in pancreatic cancer*. *Clin Cancer Res*, 2006. **12**(15): p. 4652-61.
576. Munro, J., et al., *Human fibroblast replicative senescence can occur in the absence of extensive cell division and short telomeres*. *Oncogene*, 2001. **20**(27): p. 3541-52.
577. Dull, T., et al., *A third-generation lentivirus vector with a conditional packaging system*. *J Virol*, 1998. **72**(11): p. 8463-71.
578. Johnsson, A.K., et al., *The Rac-FRET Mouse Reveals Tight Spatiotemporal Control of Rac Activity in Primary Cells and Tissues*. *Cell Rep*, 2014. **6**(6): p. 1153-64.
579. Nobis, M., et al., *Intravital FLIM-FRET imaging reveals dasatinib-induced spatial control of src in pancreatic cancer*. *Cancer Res*, 2013. **73**(15): p. 4674-86.
580. Stuart, T., et al., *Comprehensive Integration of Single-Cell Data*. *Cell*, 2019. **177**(7): p. 1888-1902 e21.
581. Hafemeister, C. and R. Satija, *Normalization and variance stabilization of single-cell RNA-seq data using regularized negative binomial regression*. *bioRxiv*, 2019: p. 576827.
582. McInnes, L., *UMAP: Uniform Manifold Approximation and Projection for Dimension Reduction*. *arXiv*, 2018. **1802**(03426v2).
583. Finak, G., et al., *MAST: a flexible statistical framework for assessing transcriptional changes and characterizing heterogeneity in single-cell RNA sequencing data*. *Genome Biology*, 2015. **16**(1): p. 278.
584. Sergushichev, A.A., *An algorithm for fast preranked gene set enrichment analysis using cumulative statistic calculation*. *bioRxiv*, 2016: p. 060012.
585. Yu, G., et al., *clusterProfiler: an R package for comparing biological themes among gene clusters*. *OMICS*, 2012. **16**(5): p. 284-7.

586. Muller, S., et al., *CONICS integrates scRNA-seq with DNA sequencing to map gene expression to tumor sub-clones*. Bioinformatics, 2018. **34**(18): p. 3217-3219.
587. Law, A.M.K., et al., *Andy's Algorithms: new automated digital image analysis pipelines for Fiji*. Sci Rep, 2017. **7**(1): p. 15717.
588. Fedchenko, N. and J. Reifenrath, *Different approaches for interpretation and reporting of immunohistochemistry analysis results in the bone tissue - a review*. Diagnostic pathology, 2014. **9**: p. 221-221.
589. Nones, K., et al., *Genome-wide DNA methylation patterns in pancreatic ductal adenocarcinoma reveal epigenetic deregulation of SLIT-ROBO, ITGA2 and MET signaling*. Int J Cancer, 2014.
590. Chou, T.-C., *Drug Combination Studies and Their Synergy Quantification Using the Chou-Talalay Method*. Cancer Research, 2010. **70**(2): p. 440-446.
591. Yang, W., et al., *Genomics of Drug Sensitivity in Cancer (GDSC): a resource for therapeutic biomarker discovery in cancer cells*. Nucleic Acids Res, 2013. **41**(Database issue): p. D955-61.
592. Noll, E.M., et al., *CYP3A5 mediates basal and acquired therapy resistance in different subtypes of pancreatic ductal adenocarcinoma*. Nat Med, 2016. **22**(3): p. 278-87.
593. Du, Y., et al., *Molecular Subtyping of Pancreatic Cancer: Translating Genomics and Transcriptomics into the Clinic*. J Cancer, 2017. **8**(4): p. 513-522.
594. Jain, N., et al., *Ruxolitinib or Dasatinib in Combination with Chemotherapy for Patients with Relapsed/Refractory Philadelphia (Ph)-like Acute Lymphoblastic Leukemia: A Phase I-II Trial*. Blood, 2017. **130**(Suppl 1): p. 1322-1322.
595. Li, N., S.I. Grivennikov, and M. Karin, *The unholy trinity: inflammation, cytokines, and STAT3 shape the cancer microenvironment*. Cancer Cell, 2011. **19**(4): p. 429-31.
596. Reid, T., et al., *Modulation of Janus kinase 2 by p53 in ovarian cancer cells*. Biochem Biophys Res Commun, 2004. **321**(2): p. 441-7.
597. Lin, J., et al., *p53 regulates Stat3 phosphorylation and DNA binding activity in human prostate cancer cells expressing constitutively active Stat3*. Oncogene, 2002. **21**(19): p. 3082-8.
598. Bloomston, M., E.E. Zervos, and A.S. Rosemurgy, 2nd, *Matrix metalloproteinases and their role in pancreatic cancer: a review of preclinical studies and clinical trials*. Ann Surg Oncol, 2002. **9**(7): p. 668-74.
599. Yu, H., et al., *Revisiting STAT3 signalling in cancer: new and unexpected biological functions*. Nat Rev Cancer, 2014. **14**(11): p. 736-46.
600. Phillips, R.M., M.C. Bibby, and J.A. Double, *A critical appraisal of the predictive value of in vitro chemosensitivity assays*. J Natl Cancer Inst, 1990. **82**(18): p. 1457-68.
601. Cox, T.R. and J.T. Erler, *Fibrosis and Cancer: Partners in Crime or Opposing Forces?* Trends Cancer, 2016. **2**(6): p. 279-282.
602. Calvo, F., et al., *Mechanotransduction and YAP-dependent matrix remodelling is required for the generation and maintenance of cancer-associated fibroblasts*. Nat Cell Biol, 2013. **15**(6): p. 637-46.

603. Sanz-Moreno, V., et al., *ROCK and JAK1 signaling cooperate to control actomyosin contractility in tumor cells and stroma*. Cancer Cell, 2011. **20**(2): p. 229-45.
604. Herrmann, D., et al., *Three-dimensional cancer models mimic cell-matrix interactions in the tumour microenvironment*. Carcinogenesis, 2014. **35**(8): p. 1671-9.
605. Madsen, C.D., et al., *Hypoxia and loss of PHD2 inactivate stromal fibroblasts to decrease tumour stiffness and metastasis*. EMBO Rep, 2015. **16**(10): p. 1394-408.
606. Marei, H., et al., *Differential Rac1 signalling by guanine nucleotide exchange factors implicates FLII in regulating Rac1-driven cell migration*. Nat Commun, 2016. **7**: p. 10664.
607. Alexander, S. and P. Friedl, *Cancer invasion and resistance: interconnected processes of disease progression and therapy failure*. Trends Mol Med, 2012. **18**(1): p. 13-26.
608. Gaggioli, C., et al., *Fibroblast-led collective invasion of carcinoma cells with differing roles for RhoGTPases in leading and following cells*. Nat Cell Biol, 2007. **9**(12): p. 1392-400.
609. Kai, F., H. Laklai, and V.M. Weaver, *Force Matters: Biomechanical Regulation of Cell Invasion and Migration in Disease*. Trends Cell Biol, 2016. **26**(7): p. 486-497.
610. Cassereau, L., et al., *A 3D tension bioreactor platform to study the interplay between ECM stiffness and tumor phenotype*. J Biotechnol, 2015. **193**: p. 66-9.
611. Friedl, P. and K. Wolf, *Tumour-cell invasion and migration: diversity and escape mechanisms*. Nat Rev Cancer, 2003. **3**(5): p. 362-74.
612. Erami, Z., et al., *Intravital FRAP Imaging using an E-cadherin-GFP Mouse Reveals Disease- and Drug-Dependent Dynamic Regulation of Cell-Cell Junctions in Live Tissue*. Cell Rep, 2016. **14**(1): p. 152-67.
613. Baslan, T. and J. Hicks, *Unravelling biology and shifting paradigms in cancer with single-cell sequencing*. Nat Rev Cancer, 2017. **17**(9): p. 557-569.
614. Timpson, P., et al., *Organotypic collagen I assay: a malleable platform to assess cell behaviour in a 3-dimensional context*. J Vis Exp, 2011(56): p. e3089.
615. Cicchi, R., et al., *Scoring of collagen organization in healthy and diseased human dermis by multiphoton microscopy*. J Biophotonics, 2010. **3**(1-2): p. 34-43.
616. Arun Gopinathan, P., et al., *Study of Collagen Birefringence in Different Grades of Oral Squamous Cell Carcinoma Using Picrosirius Red and Polarized Light Microscopy*. Scientifica (Cairo), 2015. **2015**: p. 802980.
617. Rath, N. and M.F. Olson, *Regulation of pancreatic cancer aggressiveness by stromal stiffening*. Nat Med, 2016. **22**(5): p. 462-3.
618. Broutier, L., et al., *Human primary liver cancer-derived organoid cultures for disease modeling and drug screening*. Nat Med, 2017. **23**(12): p. 1424-1435.
619. Fang, H., et al., *PAI-1 induces Src inhibitor resistance via CCL5 in HER2-positive breast cancer cells*. Cancer Sci, 2018. **109**(6): p. 1949-1957.

620. Sampson, M., Q.S. Zhu, and S.J. Corey, *Src kinases in G-CSF receptor signaling*. Front Biosci, 2007. **12**: p. 1463-74.
621. Kitamura, T. and J.W. Pollard, *Therapeutic potential of chemokine signal inhibition for metastatic breast cancer*. Pharmacol Res, 2015. **100**: p. 266-70.
622. Van Overmeire, E., et al., *M-CSF and GM-CSF Receptor Signaling Differentially Regulate Monocyte Maturation and Macrophage Polarization in the Tumor Microenvironment*. Cancer Res, 2016. **76**(1): p. 35-42.
623. Ye, J., R.S. Livergood, and G. Peng, *The role and regulation of human Th17 cells in tumor immunity*. Am J Pathol, 2013. **182**(1): p. 10-20.
624. Oelkrug, C. and J.M. Ramage, *Enhancement of T cell recruitment and infiltration into tumours*. Clin Exp Immunol, 2014. **178**(1): p. 1-8.
625. Stearns, M.E., J. Rhim, and M. Wang, *Interleukin 10 (IL-10) inhibition of primary human prostate cell-induced angiogenesis: IL-10 stimulation of tissue inhibitor of metalloproteinase-1 and inhibition of matrix metalloproteinase (MMP)-2/MMP-9 secretion*. Clin Cancer Res, 1999. **5**(1): p. 189-96.
626. Chabot, V., et al., *CCL5-enhanced human immature dendritic cell migration through the basement membrane in vitro depends on matrix metalloproteinase-9*. J Leukoc Biol, 2006. **79**(4): p. 767-78.
627. Tsukamoto, H., et al., *Soluble IL6R Expressed by Myeloid Cells Reduces Tumor-Specific Th1 Differentiation and Drives Tumor Progression*. Cancer Res, 2017. **77**(9): p. 2279-2291.
628. Zhang, Z., et al., *Role of angiogenesis in pancreatic cancer biology and therapy*. Biomed Pharmacother, 2018. **108**: p. 1135-1140.
629. Dentelli, P., et al., *IL-3 is a novel target to interfere with tumor vasculature*. Oncogene, 2011. **30**(50): p. 4930-40.
630. Feurino, L.W., et al., *IL-6 stimulates Th2 type cytokine secretion and upregulates VEGF and NRP-1 expression in pancreatic cancer cells*. Cancer Biol Ther, 2007. **6**(7): p. 1096-100.
631. Wu, X., et al., *IL-17 promotes tumor angiogenesis through Stat3 pathway mediated upregulation of VEGF in gastric cancer*. Tumour Biol, 2016. **37**(4): p. 5493-501.
632. Seo, Y., et al., *High expression of vascular endothelial growth factor is associated with liver metastasis and a poor prognosis for patients with ductal pancreatic adenocarcinoma*. Cancer, 2000. **88**(10): p. 2239-45.
633. Kuo, L., et al., *Src oncogene activates MMP-2 expression via the ERK/Sp1 pathway*. J Cell Physiol, 2006. **207**(3): p. 729-34.
634. Wang, Q., et al., *Importance of protein-tyrosine phosphatase-alpha catalytic domains for interactions with SHP-2 and interleukin-1-induced matrix metalloproteinase-3 expression*. J Biol Chem, 2010. **285**(29): p. 22308-17.
635. Munitz, A. and S.P. Hogan, *Alarming eosinophils to combat tumors*. Nat Immunol, 2019. **20**(3): p. 250-252.
636. Allavena, P., et al., *The inflammatory micro-environment in tumor progression: the role of tumor-associated macrophages*. Crit Rev Oncol Hematol, 2008. **66**(1): p. 1-9.
637. Acharyya, S., et al., *A CXCL1 paracrine network links cancer chemoresistance and metastasis*. Cell, 2012. **150**(1): p. 165-78.

638. Chen, M.F., et al., *IL-6-stimulated CD11b+ CD14+ HLA-DR- myeloid-derived suppressor cells, are associated with progression and poor prognosis in squamous cell carcinoma of the esophagus*. *Oncotarget*, 2014. **5**(18): p. 8716-28.
639. Simpson, K.D. and J.V. Cross, *MIF: metastasis/MDSC-inducing factor?* *OncImmunology*, 2013. **2**(3): p. e23337.
640. Bhattacharya, P., et al., *Dual Role of GM-CSF as a Pro-Inflammatory and a Regulatory Cytokine: Implications for Immune Therapy*. *J Interferon Cytokine Res*, 2015. **35**(8): p. 585-99.
641. Xu, Y., et al., *Sox2 Communicates with Tregs Through CCL1 to Promote the Stemness Property of Breast Cancer Cells*. *Stem Cells*, 2017. **35**(12): p. 2351-2365.
642. Kuehnemuth, B., et al., *CCL1 is a major regulatory T cell attracting factor in human breast cancer*. *BMC Cancer*, 2018. **18**(1): p. 1278.
643. Rawal, S., et al., *Role of IL-4 in Inducing Immunosuppressive Tumor Microenvironment in Follicular Lymphoma*. *Blood*, 2011. **118**(21): p. 771-771.
644. Letourneau, S., et al., *IL-2- and CD25-dependent immunoregulatory mechanisms in the homeostasis of T-cell subsets*. *J Allergy Clin Immunol*, 2009. **123**(4): p. 758-62.
645. Mattes, J., et al., *Immunotherapy of Cytotoxic T Cell-resistant Tumors by T Helper 2 Cells. An Eotaxin and STAT6-dependent Process*, 2003. **197**(3): p. 387-393.
646. Hollande, C., et al., *Inhibition of the dipeptidyl peptidase DPP4 (CD26) reveals IL-33-dependent eosinophil-mediated control of tumor growth*. *Nat Immunol*, 2019. **20**(3): p. 257-264.
647. Son, K.N., et al., *Human CC chemokine CCL23 enhances expression of matrix metalloproteinase-2 and invasion of vascular endothelial cells*. *Biochem Biophys Res Commun*, 2006. **340**(2): p. 498-504.
648. Szekanecz, Z. and A.E. Koch, *Chemokines and angiogenesis*. *Curr Opin Rheumatol*, 2001. **13**(3): p. 202-8.
649. Karnoub, A.E. and R.A. Weinberg, *Chemokine networks and breast cancer metastasis*. *Breast Dis*, 2006. **26**: p. 75-85.
650. O'Hayre, M., et al., *Chemokines and cancer: migration, intracellular signalling and intercellular communication in the microenvironment*. *Biochemical Journal*, 2008. **409**(3): p. 635-649.
651. Masamune, A., et al., *Roles of pancreatic stellate cells in pancreatic inflammation and fibrosis*. *Clin Gastroenterol Hepatol*, 2009. **7**(11 Suppl): p. S48-54.
652. Becht, E., et al., *Dimensionality reduction for visualizing single-cell data using UMAP*. *Nat Biotechnol*, 2018.
653. Bendris, N., B. Lemmers, and J.M. Blanchard, *Cell cycle, cytoskeleton dynamics and beyond: the many functions of cyclins and CDK inhibitors*. *Cell Cycle*, 2015. **14**(12): p. 1786-98.
654. Filipe, E.C., J.L. Chitty, and T.R. Cox, *Charting the unexplored extracellular matrix in cancer*. *Int J Exp Pathol*, 2018. **99**(2): p. 58-76.
655. Harmey, J.H., et al., *Lipopolysaccharide-induced metastatic growth is associated with increased angiogenesis, vascular permeability and tumor cell invasion*. *Int J Cancer*, 2002. **101**(5): p. 415-22.

656. Gibert, B., et al., *Targeting heat shock protein 27 (HspB1) interferes with bone metastasis and tumour formation in vivo*. British Journal Of Cancer, 2012. **107**: p. 63.
657. Feitelson, M.A., et al., *Sustained proliferation in cancer: Mechanisms and novel therapeutic targets*. Seminars in cancer biology, 2015. **35 Suppl(Suppl)**: p. S25-S54.
658. Conley-LaComb, M.K., et al., *Pharmacological targeting of CXCL12/CXCR4 signaling in prostate cancer bone metastasis*. Mol Cancer, 2016. **15**(1): p. 68.
659. Zhang, X.H., et al., *Latent bone metastasis in breast cancer tied to Src-dependent survival signals*. Cancer Cell, 2009. **16**(1): p. 67-78.
660. Lee, S.J., et al., *TIMP-1 inhibits apoptosis in breast carcinoma cells via a pathway involving pertussis toxin-sensitive G protein and c-Src*. Biochem Biophys Res Commun, 2003. **312**(4): p. 1196-201.
661. De Oliveira, T., et al., *Syndecan-2 promotes perineural invasion and cooperates with K-ras to induce an invasive pancreatic cancer cell phenotype*. Mol Cancer, 2012. **11**: p. 19.
662. Rocha, M.R., et al., *Annexin A2 overexpression associates with colorectal cancer invasiveness and TGF- α induced epithelial mesenchymal transition via Src/ANXA2/STAT3*. Sci Rep, 2018. **8**(1): p. 11285.
663. Yu, Y., et al., *ATP1A1 Integrates AKT and ERK Signaling via Potential Interaction With Src to Promote Growth and Survival in Glioma Stem Cells*. Front Oncol, 2019. **9**: p. 320.
664. Mitra, S.K. and D.D. Schlaepfer, *Integrin-regulated FAK-Src signaling in normal and cancer cells*. Curr Opin Cell Biol, 2006. **18**(5): p. 516-23.
665. Wang, J.C., et al., *Inhibition of pancreatic cancer cell growth in vivo using a tetracycline-inducible cyclin D1 antisense expression system*. Pancreas, 2013. **42**(1): p. 141-8.
666. Roschger, C. and C. Cabrele, *The Id-protein family in developmental and cancer-associated pathways*. Cell Commun Signal, 2017. **15**(1): p. 7.
667. Rensen, W.M., et al., *RanBP1 downregulation sensitizes cancer cells to taxol in a caspase-3-dependent manner*. Oncogene, 2009. **28**(15): p. 1748-58.
668. Garnett, M.J., et al., *UBE2S elongates ubiquitin chains on APC/C substrates to promote mitotic exit*. Nat Cell Biol, 2009. **11**(11): p. 1363-9.
669. Ganoth, D., et al., *The cell-cycle regulatory protein Cks1 is required for SCF(Skp2)-mediated ubiquitinylation of p27*. Nat Cell Biol, 2001. **3**(3): p. 321-4.
670. Yao, M., et al., *CCR2 Chemokine Receptors Enhance Growth and Cell-Cycle Progression of Breast Cancer Cells through SRC and PKC Activation*. Mol Cancer Res, 2019. **17**(2): p. 604-617.
671. Vadivel Gnanasundram, S. and R. Fahraeus, *Translation Stress Regulates Ribosome Synthesis and Cell Proliferation*. Int J Mol Sci, 2018. **19**(12).
672. Vander Heiden, M.G. and R.J. DeBerardinis, *Understanding the Intersections between Metabolism and Cancer Biology*. Cell, 2017. **168**(4): p. 657-669.
673. Shields, M.A., et al., *Biochemical role of the collagen-rich tumour microenvironment in pancreatic cancer progression*. Biochem J, 2012. **441**(2): p. 541-52.

674. Ruytinx, P., et al., *Chemokine-Induced Macrophage Polarization in Inflammatory Conditions*. Front Immunol, 2018. **9**: p. 1930.
675. Walker, S.R., et al., *Microtubule-targeted chemotherapeutic agents inhibit signal transducer and activator of transcription 3 (STAT3) signaling*. Mol Pharmacol, 2010. **78**(5): p. 903-8.
676. Wang, T., et al., *Anxa2 binds to STAT3 and promotes epithelial to mesenchymal transition in breast cancer cells*. Oncotarget, 2015. **6**(31): p. 30975-92.
677. Muscella, A., C. Vetrugno, and S. Marsigliante, *CCL20 promotes migration and invasiveness of human cancerous breast epithelial cells in primary culture*. Mol Carcinog, 2017. **56**(11): p. 2461-2473.
678. Rubie, C., et al., *CCL20/CCR6 expression profile in pancreatic cancer*. Journal of Translational Medicine, 2010. **8**(1): p. 45.
679. Leung, L., et al., *Lipocalin2 promotes invasion, tumorigenicity and gemcitabine resistance in pancreatic ductal adenocarcinoma*. PLoS One, 2012. **7**(10): p. e46677.
680. Greten, F.R., et al., *Stat3 and NF-kappaB activation prevents apoptosis in pancreatic carcinogenesis*. Gastroenterology, 2002. **123**(6): p. 2052-63.
681. Zhang, H., et al., *Clusterin inhibits apoptosis by interacting with activated Bax*. Nat Cell Biol, 2005. **7**(9): p. 909-15.
682. Rangaswami, H., A. Bulbule, and G.C. Kundu, *Osteopontin: role in cell signaling and cancer progression*. Trends Cell Biol, 2006. **16**(2): p. 79-87.
683. Hrabar, D., et al., *Epithelial and stromal expression of syndecan-2 in pancreatic carcinoma*. Anticancer Res, 2010. **30**(7): p. 2749-53.
684. Koopmann, J., et al., *Evaluation of Osteopontin as Biomarker for Pancreatic Adenocarcinoma*. Cancer Epidemiology Biomarkers & Prevention, 2004. **13**(3): p. 487-491.
685. Yang, N., et al., *Syndecan-1 in breast cancer stroma fibroblasts regulates extracellular matrix fiber organization and carcinoma cell motility*. Am J Pathol, 2011. **178**(1): p. 325-35.
686. Powell, D., et al., *Chemokine Signaling and the Regulation of Bidirectional Leukocyte Migration in Interstitial Tissues*. Cell reports, 2017. **19**(8): p. 1572-1585.
687. Wei, Z.W., et al., *CXCL1 promotes tumor growth through VEGF pathway activation and is associated with inferior survival in gastric cancer*. Cancer Lett, 2015. **359**(2): p. 335-43.
688. Djurec, M., et al., *Saa3 is a key mediator of the protumorigenic properties of cancer-associated fibroblasts in pancreatic tumors*. Proceedings of the National Academy of Sciences, 2018. **115**(6): p. E1147-E1156.
689. Yoshida, S., et al., *Pancreatic cancer stimulates pancreatic stellate cell proliferation and TIMP-1 production through the MAP kinase pathway*. Biochem Biophys Res Commun, 2004. **323**(4): p. 1241-5.
690. Hurt, E.M., et al., *Molecular consequences of SOD2 expression in epigenetically silenced pancreatic carcinoma cell lines*. Br J Cancer, 2007. **97**(8): p. 1116-23.
691. Sun, F., et al., *Downregulation of CCND1 and CDK6 by miR-34a induces cell cycle arrest*. FEBS Lett, 2008. **582**(10): p. 1564-8.
692. Denz, A., et al., *Inhibition of MIF leads to cell cycle arrest and apoptosis in pancreatic cancer cells*. J Surg Res, 2010. **160**(1): p. 29-34.

693. Sun, Y., et al., *Upregulation of LYAR induces neuroblastoma cell proliferation and survival*. Cell Death Differ, 2017. **24**(9): p. 1645-1654.
694. Song, Z., et al., *PHGDH is an independent prognosis marker and contributes cell proliferation, migration and invasion in human pancreatic cancer*. Gene, 2018. **642**: p. 43-50.
695. Li, M., et al., *Downregulated expression of hepatoma-derived growth factor (HDGF) reduces gallbladder cancer cell proliferation and invasion*. Med Oncol, 2013. **30**(2): p. 587.
696. Noel, A., M. Jost, and E. Maquoi, *Matrix metalloproteinases at cancer tumor-host interface*. Semin Cell Dev Biol, 2008. **19**(1): p. 52-60.
697. Wong, Y.C., X. Wang, and M.T. Ling, *Id-1 expression and cell survival*. Apoptosis, 2004. **9**(3): p. 279-89.
698. Drane, P., et al., *Reciprocal down-regulation of p53 and SOD2 gene expression-implication in p53 mediated apoptosis*. Oncogene, 2001. **20**(4): p. 430-9.
699. McCarroll, J.A., et al., *betatubulin: a novel mediator of chemoresistance and metastases in pancreatic cancer*. Oncotarget, 2015. **6**(4): p. 2235-49.
700. Bourboulia, D. and W.G. Stetler-Stevenson, *Matrix metalloproteinases (MMPs) and tissue inhibitors of metalloproteinases (TIMPs): Positive and negative regulators in tumor cell adhesion*. Semin Cancer Biol, 2010. **20**(3): p. 161-8.
701. Balkwill, F., *Cancer and the chemokine network*. Nat Rev Cancer, 2004. **4**(7): p. 540-50.
702. Koliesnik, I.O., et al., *RelB regulates Th17 differentiation in a cell-intrinsic manner*. Immunobiology, 2018. **223**(2): p. 191-199.
703. Zanetti, M., et al., *The role of relB in regulating the adaptive immune response*. Ann N Y Acad Sci, 2003. **987**: p. 249-57.
704. Zaidi, M.R. and G. Merlino, *The two faces of interferon-gamma in cancer*. Clin Cancer Res, 2011. **17**(19): p. 6118-24.
705. Kar, S., *Unraveling Cell-Cycle Dynamics in Cancer*. Cell Syst, 2016. **2**(1): p. 8-10.
706. Ma, X., et al., *[Stat3 signal transduction pathway orchestrates G1 to S cell cycle transition in colon cancer cells]*. Beijing Da Xue Xue Bao Yi Xue Ban, 2003. **35**(1): p. 50-3.
707. Otto, T. and P. Sicinski, *Cell cycle proteins as promising targets in cancer therapy*. Nature Reviews Cancer, 2017. **17**: p. 93.
708. Ripperger, T., et al., *The heteromeric transcription factor GABP activates the ITGAM/CD11b promoter and induces myeloid differentiation*. Biochim Biophys Acta, 2015. **1849**(9): p. 1145-54.
709. Dubovsky, J.A., et al., *Lymphocyte cytosolic protein 1 is a chronic lymphocytic leukemia membrane-associated antigen critical to niche homing*. Blood, 2013. **122**(19): p. 3308-16.
710. Mino, A., et al., *RhoH participates in a multi-protein complex with the zinc finger protein kaiso that regulates both cytoskeletal structures and chemokine-induced T cells*. Small GTPases, 2018. **9**(3): p. 260-273.
711. Pelletier, J., G. Thomas, and S. Volarevic, *Ribosome biogenesis in cancer: new players and therapeutic avenues*. Nat Rev Cancer, 2018. **18**(1): p. 51-63.

712. Ali, M.U., et al., *Eukaryotic translation initiation factors and cancer*. Tumor Biology, 2017. **39**(6): p. 1010428317709805.
713. Tew, K.D. and Z. Ronai, *GST function in drug and stress response*. Drug Resist Updat, 1999. **2**(3): p. 143-147.
714. Kitajima, S., et al., *Hypoxia-inducible factor-1alpha promotes cell survival during ammonia stress response in ovarian cancer stem-like cells*. Oncotarget, 2017. **8**(70): p. 114481-114494.
715. Liu, Y.-X., et al., *DUSP1 Is Controlled by p53 during the Cellular Response to Oxidative Stress*. Molecular Cancer Research, 2008. **6**(4): p. 624-633.
716. Multhoff, G., et al., *Differential effects of ifosfamide on the capacity of cytotoxic T lymphocytes and natural killer cells to lyse their target cells correlate with intracellular glutathione levels*. Blood, 1995. **85**(8): p. 2124-31.
717. Balendiran, G.K., R. Dabur, and D. Fraser, *The role of glutathione in cancer*. Cell Biochem Funct, 2004. **22**(6): p. 343-52.
718. Boj, S.F., et al., *Organoid models of human and mouse ductal pancreatic cancer*. Cell, 2015. **160**(1-2): p. 324-38.
719. Rath, N. and M.F. Olson, *Rho-associated kinases in tumorigenesis: re-considering ROCK inhibition for cancer therapy*. EMBO Rep, 2012. **13**(10): p. 900-8.
720. Olson, M.F. and E. Sahai, *The actin cytoskeleton in cancer cell motility*. Clin Exp Metastasis, 2009. **26**(4): p. 273-87.
721. Schwartz, M.A., *Integrins and extracellular matrix in mechanotransduction*. Cold Spring Harb Perspect Biol, 2010. **2**(12): p. a005066.
722. Yang, J., et al., *Lipocalin 2 promotes breast cancer progression*. Proc Natl Acad Sci U S A, 2009. **106**(10): p. 3913-8.
723. Lin, H.H., et al., *Lipocalin-2-induced cytokine production enhances endometrial carcinoma cell survival and migration*. Int J Biol Sci, 2011. **7**(1): p. 74-86.
724. Du, Z.P., et al., *Lipocalin 2 promotes the migration and invasion of esophageal squamous cell carcinoma cells through a novel positive feedback loop*. Biochim Biophys Acta, 2015. **1853**(10 Pt A): p. 2240-50.
725. Devireddy, L.R., et al., *A cell-surface receptor for lipocalin 24p3 selectively mediates apoptosis and iron uptake*. Cell, 2005. **123**(7): p. 1293-305.
726. Abella, V., et al., *The potential of lipocalin-2/NGAL as biomarker for inflammatory and metabolic diseases*. Biomarkers, 2015. **20**(8): p. 565-71.
727. Demaria, M., et al., *A STAT3-mediated metabolic switch is involved in tumour transformation and STAT3 addiction*. Aging (Albany NY), 2010. **2**(11): p. 823-42.
728. Grasso, C., G. Jansen, and E. Giovannetti, *Drug resistance in pancreatic cancer: Impact of altered energy metabolism*. Crit Rev Oncol Hematol, 2017. **114**: p. 139-152.
729. Zuo, D., et al., *Inhibition of STAT3 blocks protein synthesis and tumor metastasis in osteosarcoma cells*. J Exp Clin Cancer Res, 2018. **37**(1): p. 244.
730. Seo, I.A., et al., *Janus Kinase 2 Inhibitor AG490 Inhibits the STAT3 Signaling Pathway by Suppressing Protein Translation of gp130*. Korean J Physiol Pharmacol, 2009. **13**(2): p. 131-8.

731. Luo, N., et al., *DNA methyltransferase inhibition upregulates MHC-I to potentiate cytotoxic T lymphocyte responses in breast cancer*. Nat Commun, 2018. **9**(1): p. 248.
732. Richards, K.E., et al., *Cancer-associated fibroblast exosomes regulate survival and proliferation of pancreatic cancer cells*. Oncogene, 2017. **36**(13): p. 1770-1778.
733. Korc, M., *Pancreatic cancer-associated stroma production*. Am J Surg, 2007. **194**(4 Suppl): p. S84-6.
734. Rollins, B.J., *Inflammatory chemokines in cancer growth and progression*. Eur J Cancer, 2006. **42**(6): p. 760-7.
735. Quinn, C.M., et al., *Induction of fibroblast apolipoprotein E expression during apoptosis, starvation-induced growth arrest and mitosis*. Biochem J, 2004. **378**(Pt 3): p. 753-61.
736. Fleischer, A., et al., *Proapoptotic activity of ITM2B(s), a BH3-only protein induced upon IL-2-deprivation which interacts with Bcl-2*. Oncogene, 2002. **21**(20): p. 3181-9.
737. Kelley, K.D., et al., *YPEL3, a p53-regulated gene that induces cellular senescence*. Cancer Res, 2010. **70**(9): p. 3566-75.
738. Lo, C.W., et al., *IL-6 trans-signaling in formation and progression of malignant ascites in ovarian cancer*. Cancer Res, 2011. **71**(2): p. 424-34.
739. Hu, B., et al., *Interleukin-9 Promotes Pancreatic Cancer Cells Proliferation and Migration via the miR-200a/Beta-Catenin Axis*. Biomed Res Int, 2017. **2017**: p. 2831056.
740. Suzuki, A., et al., *Targeting of IL-4 and IL-13 receptors for cancer therapy*. Cytokine, 2015. **75**(1): p. 79-88.
741. Lu, L.L., et al., *CCL21 Facilitates Chemoresistance and Cancer Stem Cell-Like Properties of Colorectal Cancer Cells through AKT/GSK-3beta/Snail Signals*. Oxid Med Cell Longev, 2016. **2016**: p. 5874127.
742. Cheadle, E.J., et al., *Eotaxin-2 and colorectal cancer: a potential target for immune therapy*. Clin Cancer Res, 2007. **13**(19): p. 5719-28.
743. Zhu, Z., et al., *CXCL13-CXCR5 axis promotes the growth and invasion of colon cancer cells via PI3K/AKT pathway*. Mol Cell Biochem, 2015. **400**(1-2): p. 287-95.
744. Ying, T.H., et al., *Knockdown of Pentraxin 3 suppresses tumorigenicity and metastasis of human cervical cancer cells*. Sci Rep, 2016. **6**: p. 29385.
745. Amersi, F.F., et al., *Activation of CCR9/CCL25 in cutaneous melanoma mediates preferential metastasis to the small intestine*. Clin Cancer Res, 2008. **14**(3): p. 638-45.
746. Zhang, Z., et al., *CCL25/CCR9 Signal Promotes Migration and Invasion in Hepatocellular and Breast Cancer Cell Lines*. DNA Cell Biol, 2016. **35**(7): p. 348-57.
747. Orimo, A., et al., *Stromal fibroblasts present in invasive human breast carcinomas promote tumor growth and angiogenesis through elevated SDF-1/CXCL12 secretion*. Cell, 2005. **121**(3): p. 335-48.
748. Ikeda, N., et al., *Prognostic significance of angiogenesis in human pancreatic cancer*. Br J Cancer, 1999. **79**(9-10): p. 1553-63.
749. Niedergethmann, M., et al., *High expression of vascular endothelial growth factor predicts early recurrence and poor prognosis after curative resection*

- for ductal adenocarcinoma of the pancreas. *Pancreas*, 2002. **25**(2): p. 122-9.
750. Hu, G., W. Zeng, and Y. Xia, *TWEAK/Fn14 signaling in tumors*. *Tumour Biol*, 2017. **39**(6): p. 1010428317714624.
 751. Matsuo, Y., et al., *CXCL8/IL-8 and CXCL12/SDF-1 α co-operatively promote invasiveness and angiogenesis in pancreatic cancer*. *International Journal of Cancer*, 2009. **124**(4): p. 853-861.
 752. Jin, L., et al., *CCL24 contributes to HCC malignancy via RhoB- VEGFA- VEGFR2 angiogenesis pathway and indicates poor prognosis*. *Oncotarget*, 2017. **8**(3): p. 5135-5148.
 753. Chen, C., et al., *CXCL5 induces tumor angiogenesis via enhancing the expression of FOXD1 mediated by the AKT/NF-kappaB pathway in colorectal cancer*. *Cell Death Dis*, 2019. **10**(3): p. 178.
 754. Xiong, Y., et al., *CCL21/CCR7 interaction promotes cellular migration and invasion via modulation of the MEK/ERK1/2 signaling pathway and correlates with lymphatic metastatic spread and poor prognosis in urinary bladder cancer*. *Int J Oncol*, 2017. **51**(1): p. 75-90.
 755. McCarroll, J.A., et al., *Role of pancreatic stellate cells in chemoresistance in pancreatic cancer*. *Front Physiol*, 2014. **5**: p. 141.
 756. Koikawa, K., et al., *Basement membrane destruction by pancreatic stellate cells leads to local invasion in pancreatic ductal adenocarcinoma*. *Cancer Lett*, 2018. **425**: p. 65-77.
 757. Garg, R., et al., *Protein Kinase C Epsilon Cooperates with PTEN Loss for Prostate Tumorigenesis through the CXCL13-CXCR5 Pathway*. *Cell Rep*, 2017. **19**(2): p. 375-388.
 758. Li, A., et al., *Overexpression of CXCL5 is associated with poor survival in patients with pancreatic cancer*. *The American journal of pathology*, 2011. **178**(3): p. 1340-1349.
 759. Liu, B., et al., *Tumor-associated macrophage-derived CCL20 enhances the growth and metastasis of pancreatic cancer*. *Acta Biochimica et Biophysica Sinica*, 2016. **48**(12): p. 1067-1074.
 760. Lee, Y.S., et al., *Crosstalk between CCL7 and CCR3 promotes metastasis of colon cancer cells via ERK-JNK signaling pathways*. *Oncotarget*, 2016. **7**(24): p. 36842-36853.
 761. Habtezion, A., M. Edderkaoui, and S.J. Pandol, *Macrophages and pancreatic ductal adenocarcinoma*. *Cancer Lett*, 2016. **381**(1): p. 211-6.
 762. Qian, B.Z. and J.W. Pollard, *Macrophage diversity enhances tumor progression and metastasis*. *Cell*, 2010. **141**(1): p. 39-51.
 763. Noy, R. and J.W. Pollard, *Tumor-associated macrophages: from mechanisms to therapy*. *Immunity*, 2014. **41**(1): p. 49-61.
 764. Ruffell, B. and L.M. Coussens, *Macrophages and therapeutic resistance in cancer*. *Cancer Cell*, 2015. **27**(4): p. 462-72.
 765. Chen, Q., X.H. Zhang, and J. Massague, *Macrophage binding to receptor VCAM-1 transmits survival signals in breast cancer cells that invade the lungs*. *Cancer Cell*, 2011. **20**(4): p. 538-49.
 766. De Palma, M. and C.E. Lewis, *Cancer: Macrophages limit chemotherapy*. *Nature*, 2011. **472**(7343): p. 303-4.

767. Zhang, A., et al., *Cancer-associated fibroblasts promote M2 polarization of macrophages in pancreatic ductal adenocarcinoma*. *Cancer Med*, 2017. **6**(2): p. 463-470.
768. Candido, J.B., et al., *CSF1R(+) Macrophages Sustain Pancreatic Tumor Growth through T Cell Suppression and Maintenance of Key Gene Programs that Define the Squamous Subtype*. *Cell Rep*, 2018. **23**(5): p. 1448-1460.
769. Waghray, M., et al., *GM-CSF Mediates Mesenchymal-Epithelial Cross-talk in Pancreatic Cancer*. *Cancer Discov*, 2016. **6**(8): p. 886-99.
770. Gallina, G., et al., *Tumors induce a subset of inflammatory monocytes with immunosuppressive activity on CD8+ T cells*. *J Clin Invest*, 2006. **116**(10): p. 2777-90.
771. Kohanbash, G., et al., *GM-CSF promotes the immunosuppressive activity of glioma-infiltrating myeloid cells through interleukin-4 receptor-alpha*. *Cancer Res*, 2013. **73**(21): p. 6413-23.
772. Shiraishi, D., et al., *CD163 Is Required for Protumoral Activation of Macrophages in Human and Murine Sarcoma*. *Cancer Res*, 2018. **78**(12): p. 3255-3266.
773. Kawada, M., et al., *Chitinase 3-like 1 promotes macrophage recruitment and angiogenesis in colorectal cancer*. *Oncogene*, 2012. **31**(26): p. 3111-23.
774. Cohen, N., et al., *Fibroblasts drive an immunosuppressive and growth-promoting microenvironment in breast cancer via secretion of Chitinase 3-like 1*. *Oncogene*, 2017. **36**(31): p. 4457-4468.
775. Baghdadi, M., et al., *Chemotherapy-Induced IL34 Enhances Immunosuppression by Tumor-Associated Macrophages and Mediates Survival of Chemoresistant Lung Cancer Cells*. *Cancer Res*, 2016. **76**(20): p. 6030-6042.
776. Huang, C., et al., *Tumour-derived Interleukin 35 promotes pancreatic ductal adenocarcinoma cell extravasation and metastasis by inducing ICAM1 expression*. *Nat Commun*, 2017. **8**: p. 14035.
777. De Monte, L., et al., *Intratumor T helper type 2 cell infiltrate correlates with cancer-associated fibroblast thymic stromal lymphopoietin production and reduced survival in pancreatic cancer*. *J Exp Med*, 2011. **208**(3): p. 469-78.
778. Allaoui, R., et al., *Cancer-associated fibroblast-secreted CXCL16 attracts monocytes to promote stroma activation in triple-negative breast cancers*. *Nat Commun*, 2016. **7**: p. 13050.
779. Liang, K., et al., *High CXC Chemokine Ligand 16 (CXCL16) Expression Promotes Proliferation and Metastasis of Lung Cancer via Regulating the NF-kappaB Pathway*. *Med Sci Monit*, 2018. **24**: p. 405-411.
780. Soumoy, L., et al., *Role of Macrophage Migration Inhibitory Factor (MIF) in Melanoma*. *Cancers (Basel)*, 2019. **11**(4).
781. Sinha, P., et al., *Cross-talk between myeloid-derived suppressor cells and macrophages subverts tumor immunity toward a type 2 response*. *J Immunol*, 2007. **179**(2): p. 977-83.
782. Wang, X., et al., *Cancer-FOXP3 directly activated CCL5 to recruit FOXP3(+)Treg cells in pancreatic ductal adenocarcinoma*. *Oncogene*, 2017. **36**(21): p. 3048-3058.
783. Ito, S.E., et al., *IL-4 blockade alters the tumor microenvironment and augments the response to cancer immunotherapy in a mouse model*. *Cancer Immunol Immunother*, 2017. **66**(11): p. 1485-1496.